



**Isolation and characterisation of novel
non-ribosomal peptide synthetase genes from the entomopathogenic
Xenorhabdus bovienii T228**

Rebecca A. Pinyon, B. Sc. (Hons)



A Thesis submitted for the Degree of Doctor of Philosophy

Discipline of Microbiology and Immunology

Department of Molecular Biosciences

Adelaide University

Adelaide, SA, 5005

Australia

January, 2002

Abstract

Xenorhabdus spp. are entomopathogenic bacteria grouped within the family Enterobacteriaceae. These bacteria exhibit a colony pleiomorphism, termed phase variation in which phase 1 and phase 2 forms differ in expression of a variety phenotypic characteristics. The main aim of this thesis was to identify and characterise genes involved in the expression of phase variant characteristics. A secondary aim was the construction of a RecA mutant of *X. bovienii* to facilitate genetic complementation analysis and the introduction of foreign DNA. This construct was also used to determine a possible role for *recA* in phase variation and virulence.

The *recA* gene of *Xenorhabdus bovienii* was cloned and sequenced. Phylogenetic analysis of *recA* sequence data confirmed the placement of *Xenorhabdus* within Enterobacteriaceae. A *recA* insertion mutant of *X. bovienii* was constructed using allelic exchange mutagenesis. The *recA* mutant displayed phase variation and did not show any differences in expression of the phase dependent characteristics phospholipase C, lipase, haemolysin, protease, antimicrobial activity or Congo Red binding. No differences in the virulence of *X. bovienii*, or the *recA* mutant, for *Galleria mellonella* were observed. These results suggest *recA* is unlikely to be involved in phase variation, or the expression of phase dependent characteristics.

Transposon mutagenesis was used to identify regions of the *X. bovienii* chromosome involved in expression of phase variant characteristics. Five transposon insertion mutants showing a disruption in the expression of phospholipase C, Congo Red, haemolytic and antimicrobial activity were further characterised. *X. bovienii* chromosomal DNA flanking each transposon insertion was mapped, cloned and sequenced. Three transposon insertion mutants; XB26(20), XB29(45) and XB34(45) inserted into a common 15,582 bp region of DNA showing significant homology at the amino acid level to non-ribosomal peptide synthetases (NRPSs). Two partial open reading frames (ORFs) (*xpsD* and *xpsC*) and two complete ORFs (*xpsA* and *xpsB*) were identified. ORF *xpsD* is 653 bp and shows significant homology at the amino acid level to ATP-binding cassette transporters required for the secretion of NRPSs pyoverdine and syringomycin. 788 bp downstream of *xpsD*, ORF *xpsA* has the potential to encode a protein of 1089 amino acids with a predicted *Mr* value of 122,980. 37 bp downstream of *xpsA*, ORF *xpsB* has the potential to encode a 3316 amino acid protein with a predicted *Mr* value of 368,263. The stop codon (ATGA) of *xpsB* overlaps the initiation codon (ATGA) of the 1177 bp ORF *xpsC*. ORFs *xpsA*, *xpsB* and *xpsC* are predicted to have an operon arrangement. BLASTX analysis of the *xpsABC* region shows

homology at the amino acid level to NRPSs such as the plant toxin syringomycin (*Pseudomonas syringae* pv. *syringae*) (Guenzi *et al.*, 1998), tumor suppressing cryptophycins (*Nostoc* sp. GSV224) (Subbaraju *et al.*, 1997) and the peptide antibiotic tyrocidine (Mootz & Marahiel, 1997b). The portion of *X. bovienii* NRPS identified to date is predicted to activate the amino acids serine, 6-*N*-hydroxylysine and glutamine. On the basis of this analysis, this NRPS is predicted to be a siderophore antibiotic.

To investigate regulation of the *X. bovienii* NRPS an *xpsA-lacZ* transcriptional fusion was constructed and introduced into the *X. bovienii* chromosome by transposon mutagenesis. Over a 96 hr incubation period the level of β -galactosidase activity increase 2 - 3 fold in *X. bovienii* broth cultures. This is in comparison to an *E. coli* based *xpsA-lacZ* construct, where levels of β -galactosidase activity remained constant over the 96 hr incubation period. These results suggest the expression of *X. bovienii* NRPS may be linked to a cell density dependent mechanism. The levels of β -galactosidase expression in *xpsA-lacZ* transcriptional fusion mutant cultures did not change when cultures were grown in 20% (v/v) conditioned culture medium. This result suggests a quorum sensing mechanism similar to that observed in *Serratia liquefaciens* (Lindum *et al.*, 1998) is not involved in expression of *X. bovienii* NRPS. Attempts to detect XpsA expression in *X. bovienii* whole cell lysates using an XpsA antiserum were unsuccessful, and this may reflect an extremely low level of XpsA expression.

To determine a function for *X. bovienii* NRPS, inframe deletion mutants in *xpsA*, *xpsB* and *xpsAB* were constructed by allelic exchange mutagenesis. Culture supernatants were tested for cytotoxic activity against cultured Schneider's cells. Also, whole bacterial cells were injected into *Galleria mellonella* to assess subsequent haemocyte damage by transmission electron microscopy. No significant difference in cytotoxic activity was observed between wild type and inframe deletion mutant strains.

The antimicrobial activity of phase 1 *X. bovienii* and in-frame deletion mutant supernatants against the indicator organism *M. luteus* was tested using a microtitre tray bioassay. Surprisingly, both the single and double in-frame deletion mutants showed a greater level of antimicrobial activity than the wild type *X. bovienii* supernatant. This result may be explained by the modular nature of NRPS. Deletion of one or more modules may result in production of a modified antimicrobial peptide. However, this observation can only be resolved by purification of the bioactive peptide and structural comparison of the wild type and mutant derived compounds in the absence of other background bacterial compounds.

Statement

This work contains no material that has been accepted for the award of any other degree or diploma in any university or other tertiary institution. To the best of my knowledge and belief, this thesis contains no material previously published or written by another person, except where due reference is made in the text.

When accepted for the award of the degree I give consent for this thesis to be made available for photocopying and loan.

Rebecca A. Pinyon
January, 2002.

Abbreviations

Ω	ohms
μF	microFarad
μg	microgram(s)
μl	microlitre(s)
$\times\text{g}$	relative centrifugal force
A_{260}	absorbance at 260 nm
A_{410}	absorbance at 410 nm
A_{570}	absorbance at 570 nm
A_{600}	absorbance at 600 nm
aa	amino acid(s)
Amp	ampicilin
APS	ammonium persulphate
ATP	adenosine 5'-triphosphate
bp	base pair(s)
cfu	colony forming units
Ci	curie
cm	centimetre(s)
Cm	chloramphenicol
CTP	cytosine 5'-triphosphate
ddNTP	dideoxyribonucleotide triphosphate
DIG	digoxigenin
DIG-11-dUTP	digoxigenin -11- uridine 5' triphosphate
DMPC	dimethyl pyrocarbonate
DMSO	dimethyl sulphoxide
DNA	deoxyribonucleic acid
dNTP	deoxyribonucleotide triphosphate
dsDNA	double stranded deoxyribonucleic acid
DTT	dithiothreitol
<i>E. coli</i>	<i>Escherichia coli</i>
EDTA	ethylene-diamine-tetra-acetic-acid disodium salt
EtBr	ethidium bromide
FCS	foetal calf serum
g/L	grams per litre
<i>G. mellonella</i>	<i>Galleria mellonella</i>
GTP	guanosine 5'-triphosphate
hr	hour(s)
HCl	hydrochloric acid
IP	intra-peritoneal
IPTG	isopropyl- β -D-thio-galactopyranoside
kb	kilobase(s)

kDa	kilodalton(s)
Km	kanamycin
L	litre(s)
LA	Luria Bertani agar
LB	Luria Bertani broth
LD ₅₀	lethal dose to 50% of the population
M	molar
mA	milliampre(s)
mg	milligram(s)
mg/ml	milligram(s)/millilitre
min	minute(s)
ml	millilitre(s)
<i>M. luteus</i>	<i>Micrococcus luteus</i>
mm	millimetre(s)
mM	millimolar
MOPS	3-[N-Morpholino]propane-sulfonic acid
mRNA	messenger ribonucleic acid
MCS	multiple cloning site
NA	Nutrient agar
NB	Nutrient broth
NBT	4-Nitroblue tetrazolium chloride
ng	nanogram(s)
nm	nanometre(s)
O/N	overnight
OD	optical density
ONPG	o-Nitrophenyl-β-D-galactopyranoside
ORF	open reading frame
P1	phase 1
P2	phase 2
PAGE	polyacrylamide gel electrophoresis
PBS	phosphate buffered saline
PCR	Polymerase Chain Reaction
pmol	picomole(s)
R	resistant
rbs	ribosome binding site
RNA	ribonucleic acid
RNase	ribonuclease
Rif	rifampicin
RT	room temperature
RT-PCR	reverse transcription polymerase chain reaction
s	sensitive
SDS	sodium dodecyl sulphate
sec	second(s)

SIP	shrimp alkaline phosphatase
Sm	streptomycin
SSC	standard saline citrate
TAE	tris-acetate EDTA buffer
TBS	tris buffered saline
Tc	tetracycline
TE	tris-EDTA buffer
TEMED	N,N,N',N'-Tetramethyl-ethylenediamine
Tn	transposon
Tp	trimethoprim
Tris	tris[hydroxymethyl]amino-methane
TTBS	tween tris buffered saline
TTP	thymine 5'-triphosphate
UTP	uridine 5' triphosphate
UV	ultraviolet light
V	volt(s)
v/v	volume per volume
vol	volume(s)
w/v	weight per volume
<i>X. bovienii</i>	<i>Xenorhabdus bovienii</i>
X-gal	5-Bromo-4-chloro-3-indolyl- β -D-galactopyranoside
XMM	<i>Xenorhabdus</i> minimal media
X-pho	5-Bromo-4-chloro-3-indolyl-phosphate

NOTE

Wherever possible, this thesis refers to *Bacillus brevis* strains as *Brevibacillus brevis* as proposed by Shida, *et al.* (1997).

References:

Shida, O.; Takagi, H.; Kadowaki, K. and K. Komagata (1995). Proposal for two new genera, *Brevibacillus* gen. nov. and *Aneurinibacillus* gen. nov. *International Journal of Systematic Bacteriology*. **46**: 939-946.

Acknowledgements

Firstly I would like to thank my supervisor Dr. Connor Thomas for giving me the opportunity to do a PhD in his laboratory. Thankyou for your supervision, advice and encouragement through the more difficult times of my study. Thankyou to Dr. Jacques Ravel (The Johns Hopkins University, Baltimore) for useful discussion, CEMMSA for invaluable help with transmission electron microscopy studies and Professor Otto Schmidt (Adelaide University, Waite Campus) for providing stocks of *Galleria mellonella* larvae.

Thankyou to everyone that works and studies in the Microbiology and Immunology discipline for making this department a friendly and welcoming place to be. I would especially like to acknowledge the friendship and encouragement of past and present laboratory members. We have shared many memorable experiences together that can only make us stronger people. In particular thankyou to Dr. Tony Focareta, Rebecca Fitzsimmons, Leanne Purins and past department member Dr. Monica Ogierman. A special thankyou goes to Dr Jamie Botton for helping me with countless computer hassles.

To everyone at Gribbles Pathology thankyou for you encouragement, friendship and endless conversation. I have had the privilege to work several nights a week with a group of amazing women, who have enlightened me on various aspects of life. You have all certainly supplemented my education!

Alex Lech, what can I say? You have gone from my teacher to my friend. Thank you for your support and sarcasm through my more forgettable times. I cherish our friendship and hope you will be part of the next chapter of my life.

Thank you to my family for their support and encouragement, and to long time friends Nicole, Liz and Sharon – we've all come a long way.

Peter, your friendship and love have been an enormous source of support. I look forward to spending the rest of our lives together – I love you.

Permanence, perseverance and persistence in spite of all obstacles, discouragements, and impossibilities:

It is this, that in all things distinguishes the strong soul from the weak.

~Thomas Carlyle~

Part 1

Table of Contents

Abstract	i
Statement	iii
Abbreviations	iv
Note	vii
Acknowledgements	viii
Quotation	ix

Chapter 1 Introduction

1.1	Introduction	1
1.2	Classification	1
1.2.1	Reclassification of <i>X. luminescens</i>	2
1.3	Placement of <i>Xenorhabdus</i> and <i>Photorhabdus</i> within Enterobacteriaceae	5
1.3.1	Reasons for and against placement of <i>Xenorhabdus</i> and <i>Photorhabdus</i> within Enterobacteriaceae	5
1.4	Basic biology of <i>Xenorhabdus</i> and <i>Photorhabdus</i> spp.	6
1.5	Lifecycle of the bacteria and nematode symbiotic complex	7
1.5.1	Entry of the symbiotic complex into the insect haemocoel	7
1.5.1.1	Insect physical and behavioral barriers to nematode infection	10
1.5.1.2	<i>Heterorhabditis</i> and <i>Steinernema</i> display different mechanisms for invasion of insect haemocoels	10
1.5.2	Release of bacterial into the insect host haemocoel	11
1.5.3	The role of antimicrobial agents in maintenance of <i>Xenorhabdus</i> and <i>Photorhabdus</i> monoxenies after insect host death	11
1.5.3.1	Antimicrobial agents expressed by <i>Xenorhabdus</i>	12
1.5.3.1.1	Xenorhabdins	12
1.5.3.1.2	Xenocoumacins	15
1.5.3.1.3	Indole derivatives	15
1.5.3.2	Antimicrobial agents expressed by <i>Photorhabdus</i>	15

	1.5.3.2.1	Hydroxystilbenes	15
	1.5.3.2.2	Non-ribosomal peptide synthetases (NRPSs)	16
	1.5.3.3	Bacteriocins (Defective Phages)	17
1.5.4	Evidence against antimicrobial compounds produced by <i>Xenorhabdus</i> having a role in prevention of secondary invasion of insect carcasses by contaminating bacteria		20
1.5.5	Re-association of the symbiotic complex		22
	1.5.5.1	Specificity of bacteria/nematode symbiotic interaction	22
1.5.6	Transmission of <i>Xenorhabdus</i> and <i>Photorhabdus</i> spp.		23
	1.5.6.1	Establishment of <i>Xenorhabdus</i> and <i>Photorhabdus</i> in the nematode intestine	26
	1.5.6.1.1	Host-symbiont specificity in Steinernematidae	26
	1.5.6.1.2	Host-symbiont specificity in Heterorhabditidae	26
1.6	Insect defence mechanisms		27
1.6.1	Timing of <i>Xenorhabdus</i> and <i>Photorhabdus</i> release into the insect haemocoel		28
1.6.2	Insect opsonin mediated immunity		28
1.6.3	Nematode interaction with insect haemolymph		28
1.6.4	Insect inducible antibacterial peptide mediated immunity		29
1.6.5	<i>Xenorhabdus</i> interactions with insect haemolymph		29
	1.6.5.1	<i>Xenorhabdus</i> lipopolysaccharide (LPS)	30
	1.6.5.2	Inhibition of prophenoloxidase cascade	31
1.7	Current Field Use		33
	1.7.1	Entomopathogenic nematode application to crops	33
1.8	Molecular manipulation of <i>Xenorhabdus</i> and <i>Photorhabdus</i> spp.		35
	1.8.1	Transformation	35
	1.8.2	Conjugation	36
	1.8.3	Transduction	37
1.9	Phase Variation		37
	1.9.1	The role of phase variation and significance of P2 bacteria	38
	1.9.2	Differences in nutrient assimilation by phase variants	41
	1.9.3	Nematode preferential selection of P1 bacteria	41
	1.9.4	Induction and repression of phase variation by environmental signaling	42

1.9.5	The molecular basis of phase variation in both <i>Xenorhabdus</i> and <i>Photorhabdus</i> spp.	42
1.9.5.1	Plasmid based regulation of phase variation	43
1.9.5.1.1	Megaplasmids	43
1.9.5.2	Regulation of phase variant characteristics by post-translational modifications	44
1.9.5.2.1	<i>P.luminescens</i> lipase (<i>lip-1</i>)	44
1.9.5.2.2	<i>P.luminescens</i> protease	44
1.9.6	The proposed role of repressor molecules in phase variation	45
1.9.6.1	Regulation of the <i>P.luminescens lux</i> operon by a proposed repressor	46
1.9.6.2	Identity of the <i>lux</i> operon repressor	47
1.9.7	Homoserine lactone autoinducers	47
1.9.7.1	<i>N</i> - β -Hydroxybutanoyl homoserine lactone (HBHL) autoinducer	48
1.9.7.2	Experimental evidence for a homoserine lactone autoinducer using the <i>V. harveyi lux</i> operon	48
1.9.8	Repression or induction of the <i>lux</i> operon	49
1.9.9	Independent regulation of a collection of phase variant characteristics	49
1.10	Project Aims	50

Chapter 2 Materials and Methods

2.1	Bacterial strains and plasmids	52
2.2	Bacterial growth media	52
2.3	Maintenance of bacterial strains	67
2.4	Animals	67
2.5	Chemicals and reagents	67
2.6	Enzymes and antibodies	68
2.7	DNA extraction procedures	68
2.7.1	Plasmid DNA isolation	68
2.7.2	Preparation of bacterial genomic DNA	70
2.8	Analysis and manipulation of DNA	70
2.8.1	DNA quantitation	70
2.8.2	Restriction endonuclease digestion of DNA	70

2.8.3	Agarose gel electrophoresis of DNA	70
2.8.4	Determination of restriction fragment size	71
2.8.5	Extraction of DNA fragments from agarose gels	71
2.8.6	Dephosphorylation of DNA using shrimp alkaline phosphatase (SIP)	71
2.8.7	End-filling of linear DNA by T4 polymerase	72
2.8.8	<i>In vitro</i> cloning	72
2.9	Construction of uni-directional deletions of cloned DNA	72
2.9.1	Plasmid pCT406 and pCT407 top strands	73
2.9.2	Plasmid pCT406 complementary strand	73
2.9.3	Plasmid pCT407 complementary strand	73
2.10	High efficiency electrotransformation of <i>E. coli</i>	74
2.10.1	Preparation of competent cells	74
2.10.2	Electroporation procedure	74
2.11	Bacterial conjugation	74
2.12	Non-radioactive probe construction	75
2.12.1	Labeling of double stranded DNA	75
2.12.2	End labeled oligonucleotide probe	75
2.12.3	Digoxigenin labeling of DNA probes using PCR	75
2.13	Southern hybridisation	76
2.13.1	Southern transfer	76
2.13.2	Hybridisation	76
2.13.2.1	Double stranded DNA probes	76
2.13.2.2	Oligonucleotide probes	76
2.13.2.3	Detection	77
2.14	Oligonucleotide synthesis	77
2.15	Polymerase Chain Reaction	77
2.15.1	Standard PCR reaction conditions	77
2.15.2	Rapid screening of chromosomal mutations and plasmid libraries	84
2.15.3	Plasmid Assisted PCR Rescue (PAPCR)	84
2.15.3.1	PCR amplification of 5' <i>X. bovienii recA</i> DNA	84
2.15.3.2	PCR amplification of 3' <i>X. bovienii xpsC</i> DNA	86
2.16	Sequence analysis	86
2.16.1	Dye-primer sequencing	86
2.16.2	Dye-terminator sequencing	87
2.17	Analysis of sequence data	87

2.18	RNA Analysis	88
2.18.1	RNA extraction	88
2.18.2	RNA quantitation	88
2.18.3	Primer extension analysis	88
2.18.3.1	Oligonucleotide labeling	88
2.18.3.2	Primer extension reaction	89
2.18.4	Northern Analysis	89
2.18.4.1	DNA probe preparation for use in Northern hybridisation analysis	89
2.18.4.2	Separation of RNA on denaturing agarose gels	89
2.18.4.3	Northern transfer	90
2.18.4.4	Hybridisation	90
2.18.4.5	Detection	90
2.18.5	Reverse transcription polymerase chain reaction (RT-PCR)	90
2.19	Isolation of XpsA expressed in <i>E. coli</i>	91
2.19.1	Construction of plasmids for over-expression of XpsA	91
2.19.2	Over-expression of XpsA	91
2.20	Preparation of whole cell lysates	91
2.21	Sodium dodecyl sulphate-polyacrylamide gel electrophoresis (SDS-PAGE)	92
2.22	Purification of truncated XpsA	92
2.23	Production of antisera against unprocessed <i>X. bovienii</i> T228 XpsA	93
2.24	Western Immunoblotting	93
2.25	Rearing of <i>Galleria mellonella</i> larvae cultures	94
2.26	LD ₅₀ analysis of <i>X. bovienii recA</i> mutants for <i>G. mellonella</i>	94
2.27	UV sensitivity studies	95
2.28	Recombination proficiency assay to demonstrate RecA function	95
2.29	Antimicrobial bioassays	95
2.30	Transmission Electron Microscopy studies of haemocytes from <i>G. mellonella</i> infected with <i>X. bovienii</i> XB3444, XB6246 and XB92388	96
2.31	Schneider's cell cytotoxicity assays	97
2.32	β -galactosidase assays	98
2.32.1	β -galactosidase activity using conditioned growth media	99

Chapter 3 Analysis of the role of RecA in *X. bovienii* phase variation

3.1	Introduction	100
3.2	Results	101
3.2.1	Cloning and sequence analysis of <i>X. bovienii</i> <i>recA</i>	101
3.2.1.1	Generation of degenerate oligonucleotides for the amplification of an internal <i>recA</i> sequence	101
3.2.1.2	Identification of <i>recA</i> DNA sequence located 5' and 3' of the 363bp <i>recA</i> internal fragment	103
3.2.1.3	Plasmid Assisted PCR Rescue (PAPCR) to identify DNA sequences 5' of <i>recA</i>	103
3.2.1.4	Analysis of the <i>X. bovienii</i> <i>recA</i> gene sequence	109
3.2.1.5	Phylogenetic analysis of <i>recA</i> from <i>Xenorhabdus</i> spp.	111
3.2.2	Assessment of <i>X. bovienii</i> <i>recA</i> function in <i>E. coli</i>	111
3.2.2.1	Recombination proficiency assay to demonstrate RecA function	111
3.2.3	Construction of a <i>X. bovienii</i> <i>recA</i> insertion mutant	113
3.2.3.1	Construction of a suicide delivery vector for allelic-exchange mutagenesis	116
3.2.3.2	Confirmation of a kanamycin-resistance gene cartridge insertion into <i>X. bovienii</i> <i>recA</i>	116
3.2.3.3	Theoretical expression of a truncated RecA by <i>X. bovienii</i> XB001	120
3.2.4	Complementation analysis of <i>X. bovienii</i> <i>recA</i> insertion mutant XB001	120
3.2.5	Phenotypic comparison of <i>X. bovienii</i> T228, XB001 and XB002 with respect to <i>recA</i> function	126
3.2.5.1	Expression of phase dependent phenotypic characteristics by the <i>recA</i> insertion mutant (XB001) and the <i>recA</i> complemented strain (XB002)	126
3.2.6	Analysis of virulence of <i>recA</i> mutants for <i>Galleria mellonella</i>	127
3.3	Discussion	129

Chapter 4 Transposon mutagenesis of *X. bovienii* T228, and identification of non-ribosomal peptide synthetase (NRPS) homologous DNA

4.1	Introduction	134
4.2	Results	136
4.2.1	Construction of a <i>X. bovienii</i> mini-Tn5 Km based transposon mutant bank	136
4.2.1.1	Conjugal transfer of pUTKm into <i>X. bovienii</i> T228	136
4.2.1.2	Southern hybridisation analysis of <i>X. bovienii</i> mini-Tn5 Km insertion mutants	136
4.2.2	Characterisation of mini-Tn5 Km induced transposon insertion mutants of <i>X. bovienii</i> T228	140
4.2.2.1	Phenotypic characterisation of <i>X. bovienii</i> transposon insertion mutants	140
4.2.2.2	Southern hybridisation analysis of <i>X. bovienii</i> mini-Tn5 Km insertion mutants XB26(20), XB29(45), XB33(21), XB34(45) and XB41(23)	142
4.2.3	Identification of <i>X. bovienii</i> DNA flanking transposon insertion mutants XB26(20), XB29(45), XB33(21), XB34(45) and XB41(23)	142
4.2.3.1	Cloning of <i>X. bovienii</i> chromosomal DNA flanking transposon insertion mutants XB26(20), XB29(45), XB33(21), XB34(45) and XB41(23)	142
4.2.3.2	Sequence analysis of mini-Tn5 Km	145
4.2.3.3	Identification and cloning of <i>X. bovienii</i> DNA flanking mini-Tn5 Km	147
4.2.4	Analysis of <i>X. bovienii</i> DNA flanking clones pCT401, pCT402, pCT403, pCT404 and pCT405	155
4.2.4.1	BLASTX 2.1.1 analysis of <i>X. bovienii</i> DNA sequence flanking clones pCT401, pCT402, pCT403, pCT404 and pCT405	155
4.2.4.2	Mapping of transposon insertion mutants XB26(20), XB29(45) and XB34(45)	156
4.2.5	Nucleotide sequence analysis of pCT400	157

4.2.5.1	Confirmation pCT400 and pCT403 are from the same mini-Tn5 Km insertion located in XB34(45)	159
4.2.5.2	BLASTX 2.1.1 analysis of <i>X. bovienii</i> DNA distal to the mini-Tn5 Km insertion cloned into pCT400	160
4.2.5.3	Restriction enzyme and nested deletion analysis of pCT400	160
4.2.5.4	Identification of DNA sequence junctions between pCT406, pCT407 and pCT403a	163
4.2.5.5	Analysis of pCT403 O end DNA sequence	163
4.2.5.6	Plasmid Assisted PCR (PAPCR) to generate further non-ribosomal peptide synthetase homologous sequence	163
4.2.6	Preliminary analysis of compiled nucleotide sequence data from pCT400, pCT403 and pCT408	172
4.2.6.1	Partial ORF <i>xpsD</i>	172
4.2.6.2	ORFs <i>xpsA</i> , <i>xpsB</i> (complete) and <i>xpsC</i> (partial)	172
4.2.6.3	Mapping transposon insertion mutants XB26(20), XB29(45), XB33(21), XB34(45) and XB41(23) to the 15,582 bp <i>X. bovienii</i> nucleotide region	179
4.3	Discussion	179

Part 2

Chapter 5 Computer analysis of the 15.5 kb region of DNA encoding a putative non-ribosomal peptide synthetase from *X. bovienii* T228

5.1	Introduction	184
5.2	Results	184
5.2.1	Gene organisation and general features	184
5.2.1.1	Comparison of the mol% (G+C) of <i>X. bovienii</i> <i>xpsABC</i> and <i>xpsD</i> with the <i>P. syringae</i> syringomycin synthesis and export region	199
5.2.1.2	Analysis of nucleotide regulatory sequences flanking <i>xpsABC</i> and <i>xpsD</i>	199
5.2.1.3	Northern hybridisation analysis to determine the <i>xpsABC</i> operon transcript size	203
5.2.2	Analysis of DNA translation products	207
5.2.2.1	Comparison of partial ORF <i>xpsD</i> to sequences contained within protein databases	207
5.2.2.2	Comparison of ORF XpsA, XpsB and XpsC polypeptides to sequence contained within protein databases	210
5.2.3	Organisation of the XpsA, XpsB and XpsC polypeptide modules and domains	214
5.2.3.1	Alignment of XpsA, XpsB and XpsC domain core sequences with the published core consensus sequence	214
5.2.4	Predictive, structure-based modelling of amino acid recognition by the XpsA and XpsB NRPS A domains	219
5.2.4.1	Alignment of XpsA and XpsB module adenylation domains with the adenylation domain of GrsA	224
5.2.4.2	BLAST analysis of the XpsA and XpsB adenylation domain signature sequences	224
5.2.5	Hydrophobicity analysis and amino acid composition of <i>X. bovienii</i> XpsA M1, XpsB M1, XpsB M2, XpsB M3 and other serine activating domains	227

5.2.5.1	Module hydrophobicity analysis	227
5.2.5.2	Module amino acid composition analysis	231
5.2.6	Phylogenetic analysis of the <i>X. bovienii</i> NRPS operon	231
5.3	Discussion	239

Chapter 6 Regulation of expression of the non-ribosomal peptide synthetase gene *xpsA*

6.1	Introduction	246
6.2	Results	247
6.2.1	PCR amplification of RP4 <i>mob</i> and subsequent cloning into transcriptional fusion vector pMU575	247
6.2.1.1	Conjugal transfer of pCT410.1 from <i>E. coli</i> SM10 λ <i>pir</i> to <i>X. bovienii</i>	251
6.2.2	Transfer of an <i>xpsA-lacZ</i> transcriptional fusion into <i>X. bovienii</i> T228 facilitated by mini-Tn5 <i>xylE</i>	252
6.2.2.1	PCR amplification and cloning of the <i>xpsA</i> promoter region	252
6.2.2.2	Cloning the <i>xpsA-lacZ</i> transcriptional fusion into mini-Tn5 <i>xylE</i>	255
6.2.2.3	Mobilisation of pCT414 from <i>E. coli</i> SM10 λ <i>pir</i> to <i>X. bovienii</i> T228 by conjugal transfer	258
6.2.2.4	Confirmation of an <i>xpsA-lacZ</i> insertion in XB414.1, XB414.2 and XB414.3	261
6.2.3	Influence of culture conditions on expression of <i>xpsA-lacZ</i> fusions by XB414.1, XB414.2 and XB414.3	265
6.2.3.1	Refinement of β -galactosidase assay conditions	265
6.2.3.2	Growth of wild type <i>X. bovienii</i> , XB414.1, XB414.2 and XB414.3 on Luria bertani medium (LB) and <i>Xenorhabdus</i> minimal medium (XMM) and expression of the <i>xpsA-lacZ</i> fusions	268
6.2.3.3	β -galactosidase expression by XB414.1, XB414.2 and XB414.3 at different cell culture densities over a 96 hr time period	271

6.2.3.4	β -galactosidase expression by XB414.1, XB414.2 and XB414.3 at different initial cell culture densities over a 96 hr time period in 20% (v/v) conditioned LB broth	273
6.2.4	Translation of XpsA	273
6.2.4.1	Construction of XpsA expression vectors pCT445 and pCT446	275
6.2.4.2	Over-expression of XpsA in <i>E. coli</i> BL21	275
6.2.4.3	Detection of XpsA in <i>X. bovienii</i> T228	280
6.3	Discussion	283

Chapter 7 Construction and analysis of *X. bovienii* non-ribosomal peptide synthetase in-frame deletion mutants

7.1	Introduction	289
7.2	Results	290
7.2.1	Construction of the <i>xpsA</i> in-frame deletion mutant XB6246	290
7.2.1.1	Cloning of DNA generated by PCR amplification of <i>X. bovienii</i> chromosomal DNA, using oligonucleotide pairs P6054/P6247 and P6246/P6256	290
7.2.1.2	Construction of plasmid pCT421 and pCT422	291
7.2.1.3	Construction of <i>xpsA</i> deletion mutant XB6246	295
7.2.2	Construction of the <i>xpsB</i> in-frame deletion mutant XB3444	298
7.2.2.1	Cloning of DNA generated by PCR amplification of <i>X. bovienii</i> chromosomal DNA, using oligonucleotide pairs P6248/P6257 and P5292/P6249	298
7.2.2.2	Construction of plasmids pCT423 and pCT424	301
7.2.2.3	Construction of plasmids pCT425, pCT426 and pCT427	301
7.2.2.4	Construction of <i>xpsB</i> deletion mutant XB3444	304
7.2.3	Construction of the <i>xpsA/xpsB</i> double in-frame deletion mutant XB92388	309
7.2.3.1	Construction of plasmids pCT430 and pCT431	309

7.2.3.2	Construction of plasmids pCT432, pCT433 and pCT434	314
7.2.3.3	Construction of <i>xpsA/xpsB</i> double deletion mutant XB92388	317
7.2.3.4	Summary of modules and domains deleted in XB3444, XB6246 and XB92388	320
7.2.4	Phenotypic characterisation of deletion mutants XB3444, XB6246 and XB92388	320
7.2.4.1	Expression of phase dependent characteristics by XB3444, XB6246 and XB92388	325
7.2.4.2	Quantitation of XB3444, XB6246 and XB92388 antimicrobial activity against <i>M. luteus</i>	329
7.2.4.3	<i>In vivo</i> effects of <i>X. bovienii</i> T228, XB3444, XB6246 and XB92388 on <i>Galleria mellonella</i> haemocytes	332
7.2.4.4	Cytotoxicity of <i>X. bovienii</i> T228, XB3444, XB6246 and XB92388 culture supernatants for Schneider's cells	335
7.3	Discussion	335

Chapter 8 General Discussion

8.1	Introduction	345
8.2	RecA is not required for <i>X. bovienii</i> phase variation	345
8.3	Transposon mutagenesis of <i>X. bovienii</i> T228 and identification of non-ribosomal peptide synthetase (NRSP) homologous DNA	347
8.4	Sequence analysis of 15,582 bp of cloned <i>X. bovienii</i> chromosomal DNA identifies ORFs <i>xpsA</i> , <i>xpsB</i> , <i>xpsC</i> and <i>xpsD</i>	347
8.5	<i>X. bovienii</i> NRPS is predicted to encode a siderophore antibiotic	348
8.6	Motifs found in XpsD suggest an ABC transport function	349
8.7	<i>X. bovienii</i> NRPS transcription is cell culture density dependent	350
8.8	XpsA levels could not be detected using α -XpsA antisera	351
8.9	Antimicrobial activity of <i>X. bovienii</i> NRPS	352

Appendices

Appendix A: <i>X. bovienii</i> DNA sequence flanking transposon insertion mutants XB26(20), XB29(45), XB33(21), XB34(45) and XB41(23).	355
Appendix B: Listing of adenylation modules used for phylogenetic analysis.	357
Chapter 9 Bibliography	363

Chapter 1

Introduction

Xe. No. rhab' dus. Gr. noun *xenos* unwanted guest (pathogen); Gr. noun *rhabdus* (rod-shaped bacterium associated with rhabditoid nematodes in the superfamily *Rhabditoidea*) (Thomas & Poinar, 1979).

1.1 Introduction

Bacteria belonging to the genus *Xenorhabdus* are symbiotically associated with entomopathogenic nematodes of the family Steinernema (Akhurst, 1980; Boemare & Akhurst, 1988). These bacterium/nematode complexes are able to invade and kill the larval stage of several insect species (Akhurst & Boemare, 1990).

1.2 Classification

Xenorhabdus are Gram negative, nonsporeforming, facultative anaerobes and motile by means of peritrichous flagella (Boemare & Akhurst, 1988). Microscopically, *Xenorhabdus* appear as straight rods of approximately 1.5 to 3.0 by 0.8 to 1.1 μm . Older cultures (3 to 5 days) contain bacilli of varying sizes (up to 8 μm long) and spheroplasts 1.4 to 2 μm in diameter (Thomas & Poinar, 1979; Grimont *et al.*, 1984). *Xenorhabdus* nutrition is chemoorganotrophic; metabolism is respiratory and fermentative (Thomas & Poinar, 1979). *Xenorhabdus* biochemical reactions are sluggish, and characteristically, acid production from D-glucose and other carbohydrates is weak or delayed. *Xenorhabdus* are mesophilic bacteria, where the optimum growth temperature is approximately 25°C. However some species may grow poorly at 36°C (Buchanan & Gibbons, 1974).

Xenorhabdus are very fragile under standard laboratory conditions, where colony-forming units (CFU) after dilution plating is often dramatically reduced compared to the number of cells observed by microscopic examination (Poinar & Thomas, 1967; Xu & Hurlbert, 1990). Experimental evidence suggests *Xenorhabdus* spp. are extremely sensitive to photoproducts produced in several common media irradiated by fluorescent light (Xu & Hurlbert, 1990).

The production of toxic photoproducts in bacterial media by near-UV (NUV) visible light has been previously reported (Webb & Lorenz, 1972; Hoffman *et al.*, 1983). H₂O₂ can be responsible for toxicity (Waterworth, 1969; Fridovich, 1978; Hoffman *et al.*, 1983;) and is formed by the action of visible light on tryptophan (Hartman & Eisenstark, 1980), riboflavin and its derivatives (Xu & Hurlbert, 1990). Photodynamic action of biological chromophores has been shown to produce other oxygen species (hydroxyl radical [OH]; superoxide radical [O₂⁻]; and singlet oxygen [¹O₂]) that are toxic to bacteria (Fridovich, 1978; Kramer & Ames, 1987). Refined techniques can increase *Xenorhabdus* plating efficiency eg; preparing and storing plates in dim light, adding the H₂O₂ scavengers catalase or pyruvate to growth media, diluting bacteria in growth media, and using gentle plating methods (Xu & Hurlbert, 1990).

Oligonucleotide cataloguing (Ehlers *et al.*, 1988) and 16S rRNA sequence analysis (Rainey *et al.*, 1995) have placed *Xenorhabdus* within the gamma subdivision of the purple bacteria (proteobacteria). When describing the genus *Xenorhabdus*, Thomas and Poinar reported the DNA G+C content to be 43 - 44 mol% for the nine isolates examined (Thomas & Poinar, 1979). Previously, the genus *Xenorhabdus* contained seven species of bacteria: *X. beddingii*, *X. bovienii*, *X. feltiae*, *X. japonicus*, *X. luminescens*, *X. nematophilus* and *X. poinarii* (Akhurst, 1986; Boemare & Akhurst, 1988; Boemare *et al.*, 1993; Nishimura *et al.*, 1994). Prior to 1993, *X. beddingii*, *X. bovienii* and *X. poinarii* were considered to be subspecies of *X. nematophilus*. However, DNA-DNA hybridisation studies (Boemare *et al.*, 1993) and differences in morphological properties (Akhurst, 1983; Akhurst & Boemare, 1986; Boemare & Akhurst, 1988) confirmed they were significantly different enough to be elevated to individual species.

1.2.1 **Reclassification of *X. luminescens***

Luminous isolates of *Xenorhabdus* (*X. luminescens*) are associated with heterorhabditid nematodes (Thomas & Poinar, 1979). On the basis of DNA-DNA hybridisation studies and phenotypic analysis Grimont (Grimont *et al.*, 1984) first suggested *Xenorhabdus luminescens* should be placed in a separate genus. Almost a decade later Boemare (Boemare *et al.*, 1993) proposed a formal separation, and suggested a change to the genus name *Photorhabdus*.

Akhurst (Akhurst, 1993), Forst (Forst & Neelson, 1996) and Boemare (Boemare *et al.*, 1997) have suggested the similarities between *Photorhabdus* and *Xenorhabdus* may be the result of

convergent evolution between two different bacterial genera associated with the two phylogenetically distinct nematode genera, *Heterorhabditis* and *Steinernema* respectively. This concept is supported by Liu (Liu *et al.*, 1997) who noted that partial 16S rRNA gene sequences of *Photorhabdus* spp. were found to closely parallel taxonomic grouping of their nematode associates and their geographic origins. Liu (Liu *et al.*, 1997) also found two well-supported taxonomic groups in *Photorhabdus* spp., and suggested the genus *Photorhabdus* coevolved with the nematodes.

The main reasons for the exclusion of *Photorhabdus luminescens* from the genus *Xenorhabdus* were low interspecies reassociation values (Grimont *et al.*, 1984; Farmer *et al.*, 1989; Suzuki *et al.*, 1990; Boemare *et al.*, 1993) phenotypic (Boemare & Akhurst, 1988; Boemare *et al.*, 1993) and chemotaxonomic properties (Suzuki *et al.*, 1990). Numerical taxonomic studies based on fatty acid analysis showed *P. luminescens* strains form discrete clusters regardless of datum set or clustering strategy (Suzuki *et al.*, 1990). Interspecies DNA reassociation values of <20% for the type strains of *X. nematophilus* and *P. luminescens* were considered sufficient justification for genus separation, even though reassociation values for type strains of other *Xenorhabdus* species ranged between 20 and 40% (Rainey *et al.*, 1995). DNA-DNA hybridisation methods are well defined for species separation, but not at the genus level, therefore raising questions regarding the validity of these results (Stackebrandt & Goebel, 1994).

Whereas taxonomic studies have defined clear groups for *Xenorhabdus* spp., *Photorhabdus* appears overall to be a more homogeneous genus (Akhurst *et al.*, 1996). On the basis of 16S rRNA studies and distance matrix methods Rainey (Rainey *et al.*, 1995) argues there may not be a sufficient separation of *Xenorhabdus* and *Photorhabdus* to warrant a new genus. Comparative analysis was carried out using the 16S rRNA sequences, and a close phylogenetic relationship was determined. Although the data set used for their analysis was small, and this result was dependent on the statistical analyses used (Rainey *et al.*, 1995). Nevertheless, this study outlined the importance of the species used for out-grouping when determining relationships.

Among other differentiating characteristics of *Xenorhabdus* and *Photorhabdus* (outlined in Table 1.1), bioluminescence and catalase activity are both physiologically very significant.

Table 1.1 Characteristics distinguishing *Xenorhabdus* from *Photorhabdus* spp.

Character	<i>Xenorhabdus</i> spp.	<i>Photorhabdus</i> spp.
Nematode host	<i>Steinernema</i> spp.	<i>Heterorhabditis</i> spp.
Bioluminescence	-	+
Catalase	-	+
Pigment ^a	Unknown	Anthraquinone
Antimicrobials ^b	Xenorhabdins, xenocoumacins, indoles	Hydroxystilbenes, anthraquinones
Intracellular crystal size (kDa) ^c	22, 24	10, 11
Protease ^d	Unknown	Serine protease
Lipase ^e	Unknown	Lip-1
Insecticidal toxin (kDa)	31 ^f	>700 ^g
Entomopathogenicity ^h	d	+
Urease ^h	-	d
Indole ^h	-	d

^a While some *Xenorhabdus* strains are pigmented, the yellow or red colour characteristic of *Photorhabdus* spp. is not seen, and no anthraquinones have been isolated.

^b Antimicrobial production is a group trait, but the compounds produced are very different between *Xenorhabdus* spp. (xenocoumacins, xenorhabdins, and indole derivatives) and *Photorhabdus* spp. (hydroxystilbene derivatives).

^c Bintrim (Bintrim, 1995) has shown that the crystalline protein genes from *Photorhabdus* spp. are not homologous with those from *Xenorhabdus* spp.

^d Patterns of protease activity and expression (Boemare & Akhurst, 1988) suggest that these proteins are probably different between the two genera. The *Photorhabdus* protease is metalloprotease (Bowen *et al.*, 2000).

^e (Wang & Dowds, 1993).

^f Akhurst 1995 unpublished results, referenced by Forst (Forst & Neelson, 1996).

^g (Bowen, 1995).

^h d = varies with strain or biovar (Boemare *et al.*, 1997).

Table 1.1 is a compilation of information reproduced from Boemare (Boemare *et al.*, 1997) and Forst (Forst & Neelson, 1996)..

P. luminescens is the only terrestrial bioluminescent bacterium, however not all strains of *Photorhabdus* are luminescent (Akhurst & Boemare, 1988). Furthermore, the absence of catalase activity in *Xenorhabdus* spp. is very unusual for Enterobacteriaceae, however this phenotype is also observed in some strains of *Shigella dysenteriae* O group 1 (Boemare *et al.*, 1997). Since all *Xenorhabdus* and *Photorhabdus* strains occupy very similar environmental niches, major physiological differences are significant taxonomic indicators (Boemare *et al.*, 1993).

1.3 Placement of *Xenorhabdus* and *Photorhabdus* within Enterobacteriaceae

All oxidase negative, Gram negative, facultative anaerobic rods fall into one of two families, the Enterobacteriaceae or the Vibrionaceae (Buchanan & Gibbons, 1974). Oligonucleotide cataloguing estimated *Xenorhabdus* and *Photorhabdus* each constitute a taxonomic unit equivalent to, and possibly distinct from, the family Enterobacteriaceae (Ehlers *et al.*, 1988). Whilst the placement of the genera *Xenorhabdus* and *Photorhabdus* within Enterobacteriaceae seems firm, there is still uncertainty on this issue.

When compared to the enterobacterial reference strain database, 16S rRNA sequence analysis showed the similarity to *Xenorhabdus* strains (*X. nematophilus* DSM 3370^T, *X. beddingii* DSM 4764^T, *X. poinarii* DSM 4768^T, and *X. bovienii* 4766^T) ranged between 96.0 and 97.7% (Rainey *et al.*, 1995). When the same reference strains were compared with *P. luminescens* strains (*P. luminescens* DSM 3368^T and DSM 3369, *P. luminescens* HSH2) the similarities ranged between 94.1 and 96.6 % (Rainey *et al.*, 1995). With a 16S rRNA similarity of 92.3 to 95.2% the inclusion of *Xenorhabdus* and *Photorhabdus* within the family Enterobacteriaceae is in agreement with prior studies (Ehlers *et al.*, 1988). *Proteus vulgaris* is considered the closest phylogenetic neighbour (between 93.5 and 95.1% similarity).

1.3.1 Reasons for and against placement of *Xenorhabdus* and *Photorhabdus* within Enterobacteriaceae

Rainey (Rainey *et al.*, 1995) discussed the appropriateness of including *Xenorhabdus* and *Photorhabdus* within Enterobacteriaceae based on;

1. 16S rRNA data show a close relationship with other members of the gamma proteobacteria.
2. This data included other organisms that specialise as symbionts and/or pathogens of eukaryotes.

However as previously mentioned, the data set used for this analysis was small, and results dependent on statistical analyses used (Rainey *et al.*, 1995).

The fact that *Xenorhabdus* spp. are unable to reduce nitrate or produce catalase has been cited as reason to question their inclusion within Enterobacteriaceae (Farmer, 1984; Farmer *et al.*, 1989). However it should be noted that some strains of *Erwinia* and *Yersinia* are nitrate-reductase negative, whilst as previously mentioned some strains of *Shigella dysenteriae* O group 1 are catalase negative (Boemare *et al.*, 1997a). *Photorhabdus* spp. are nitrate-reductase negative and produce characteristic red and yellow pigments not commonly produced by Enterobacteriaceae. Furthermore, *Photorhabdus* are luminescent, a trait which is unknown within Enterobacteriaceae (Farmer, 1984; Farmer *et al.*, 1989).

Whilst the enterobacterial common antigen has been demonstrated in *Xenorhabdus* spp. (Ramia *et al.*, 1982), *Xenorhabdus* and *Photorhabdus* are not easy to identify due to their biochemically inactive nature when compared to many other members of the Enterobacteriaceae. Many of the traits used to distinguish the genera from the Enterobacteriaceae are negative for the *Xenorhabdus* and *Photorhabdus* groups. This difficulty is even more apparent when the conversion of these bacteria between the pleiomorphic forms; phase 1 (P1) and phase 2 (P2); is considered. In this case, some of the traits labelled positive or variable in P1 forms can be negative for P2 variants.

1.4 Basic biology of symbiotic *Xenorhabdus* and *Photorhabdus* spp.

As mentioned above, *Xenorhabdus* and *Photorhabdus* demonstrate colony pleiomorphism (Akhurst, 1980). One form, designated the P1 variant, is isolated from infective dauer juveniles (Boemare & Akhurst, 1988). P1 bacteria are characterised by the production of antibiotic substances and the adsorption of dyes (Akhurst, 1980). Depending on the species and strain P1 bacteria can be pigmented, bioluminescent, produce phospholipase C and protease (Akhurst & Boemare, 1988). P1 cells are larger than P2 cells, and may show pleiomorphism in cell shape. Generally a P1 culture will consist of 80-90% rods and 10-20%

spheroplasts (Givaudan *et al.*, 1995). P1 cultures develop paracrystalline inclusions and fimbriae (Binnington & Brooks, 1993; Brehelin *et al.*, 1993; Moureaux *et al.*, 1995).

P2 variants of *Xenorhabdus* appear spontaneously during stationary phase of *in vitro* culture or during the rearing of nematodes on artificial diets. Pure P2 cultures either do not express, or only weakly express, P1 characteristics outlined above. Both forms are equally pathogenic and share all other bacteriological properties (Akhurst, 1980; Akhurst & Boemare, 1990; Pinyon *et al.*, 2000). DNA relatedness studies confirm that P1 and P2 forms of *Xenorhabdus* and *Photorhabdus* are variations and not culture contaminants (Boemare *et al.*, 1993).

1.5 Lifecycle of the bacteria and nematode symbiotic complex

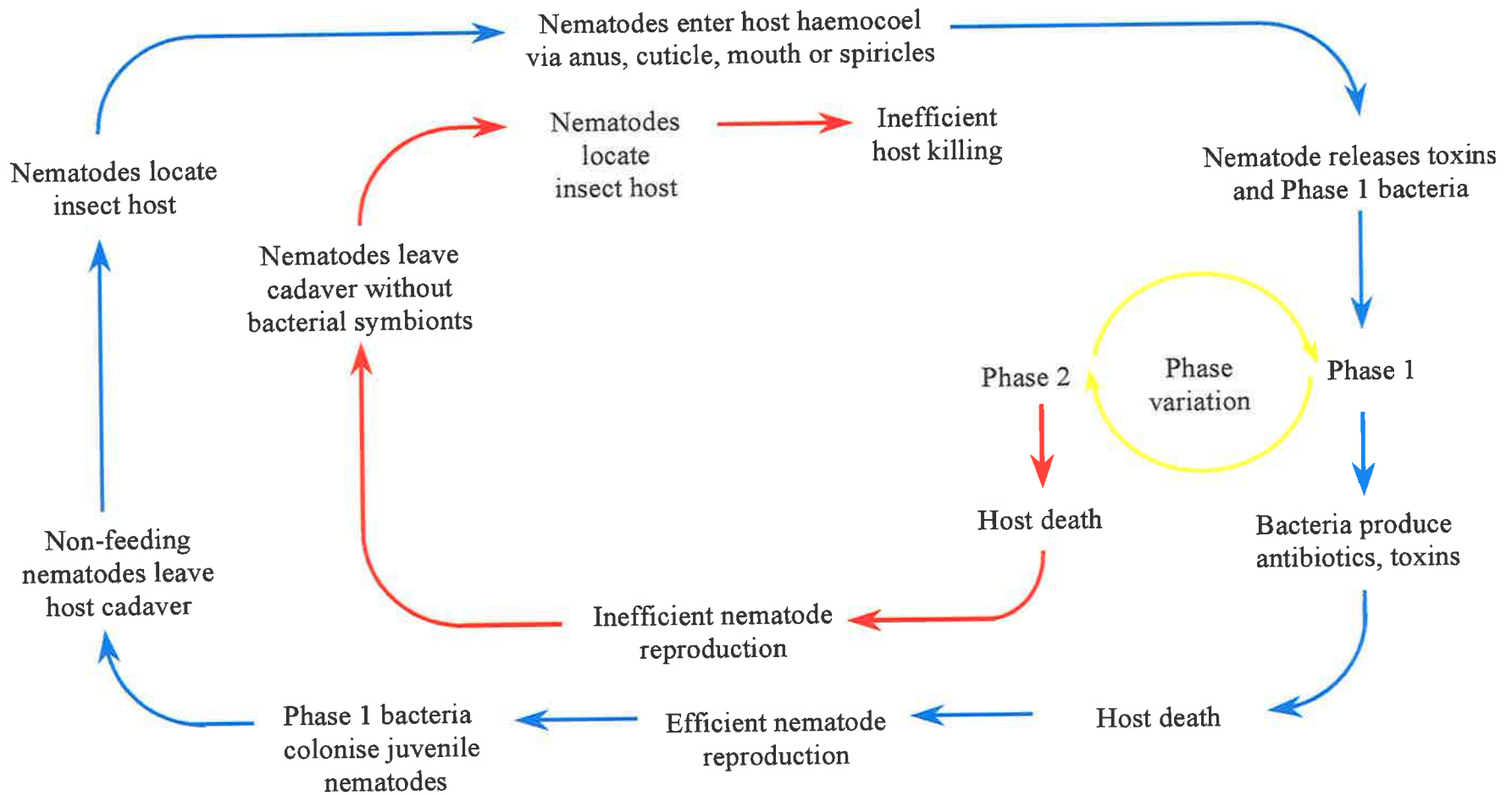
Xenorhabdus and *Photorhabdus* spp. are carried as symbionts in the intestine of infective juvenile stage nematodes belonging to the genus' *Steinernematidae* (Bird & Akhurst, 1983) and *Heterorhabditidae* (Akhurst, 1983) respectively. *Xenorhabdus* spp. are carried in specialised vesicles formed by outpocketing of the *Steinernema* nematode gut, whilst *Photorhabdus* spp. are located throughout the gut of *Heterorhabditis* nematodes. The nematodes are of fundamental importance as they carry their symbiont into the haemocoel of an insect host where the bacteria may rapidly multiply, kill the host by septicaemia and serve as an essential food source for reproducing nematodes (Figure 1.1) (Akhurst & Boemare, 1990).

1.5.1 Entry of the symbiotic complex into the insect haemocoel

Infective juvenile nematodes of *Steinernema* exist as amphimictic males and females (Poinar, 1990). For development to proceed both a male and female must infect the insect host. *Heterorhabditis* nematodes develop into hermaphroditic females and subsequently into amphimictic males and females (Zioni *et al.*, 1992). Therefore only one hermaphroditic nematode is required to initiate a successful infection. Variation in the susceptibility of insect species, or instars, to nematode infection is associated with the nematodes ability to gain access to the insect haemocoel. This is a two-stage problem as the infective juvenile nematode will enter the insect via the mouth, anus or spiracles; before traversing the gut or tracheal lumen to invade the haemocoel (Poinar & Thomas, 1966; Poinar, 1979).

Figure 1.1 Life cycle of the nematode-bacterium infection complex. The consequence of nematodes symbiotically associating with P1 or P2 *Xenorhabdus* is indicated by the blue and red lines respectively.

This figure is reproduced with the permission of Dr C. J. Thomas (<http://www.microbiology.adelaide.edu.au>).



1.5.1.1 Insect physical and behavioural barriers to nematode infection

Initial entry into the haemocoel will be affected by insect behavioural or physical barriers, whilst further progress from the gut or tracheal lumen will be affected purely by physical barriers. The early instars of mosquito larvae (Dadd, 1971) and blackfly larvae (Gaugler & Molloy, 1981) were shown not to be susceptible to the nematode *S. carpocapsae* until later stages of development. Observations show these insects are only infected via the mouth, and that the physical factor of small mouthpart sizes of the earlier instars either prevented nematode entry, or lethally damaged the nematodes during ingestion. Other physical factors hypothesised to retard or prevent invasion of the insect host are the silken lining of the cocoon of some hymenopterous pupae (Akhurst & Dunphy, 1993) and sieve plates on scarabaeids (Bedding & Molyneux, 1982). Scarabaeid larvae are postulated to have defence mechanisms that include the use of anterior legs to push nematodes away from the mouth-parts. Penetration from the gut or trachea to the haemocoel is a physical process and may be inhibited by factors such as anoxia (e.g., the hindgut of scarabaeids), and the high rate of food passage that occurs in some lepidopteran larvae (Bedding & Molyneux, 1982).

1.5.1.2 *Heterorhabditis* and *Steinernema* display different mechanisms for invasion of insect haemocoels

Heterorhabditis spp. are generally more efficient at invading the insect haemocoel than *Steinernema* spp. This observation may be related to the fact that *Heterorhabditis* spp. possess an anterior tooth like structure which enables infective juveniles to penetrate the external cuticle of insects providing an additional route of entry (Bedding & Molyneux, 1982). Penetration of the external cuticle has an advantage over penetration of the hindgut, as the latter may allow for additional bacterial flora to be carried into the insect haemocoel, providing extra competition for the *Photorhabdus* symbiont. In this case *Photorhabdus* may be unable to dominate the insect host haemocoel, and as a consequence, nematode reproduction is inhibited (Bedding & Molyneux, 1982). Poinar (Poinar, 1979) demonstrated bacteria could be carried on the outer cuticle of infective juvenile nematodes. However *Heterorhabditis* species shed the cuticle before or during penetration, hence the infective juvenile may enter with a surface that is largely free of bacteria (Poinar, 1979). As a result nematodes are able to release their symbiotic bacteria into the host haemocoel in a relatively aseptic manner.

In contrast *Steinernema* spp. juveniles have minute heads ranging from 8 – 15 µm, and this combined with the high internal hydrostatic pressure characteristic of nematodes facilitates puncturing the insect cuticle in a syringe-like action (Bedding & Molyneux, 1982).

1.5.2 Release of bacteria into the insect host haemocoel

Entomopathogenic nematodes release *Xenorhabdus* or *Photorhabdus* spp. into the insect host haemocoel, where the bacteria grow to stationary phase, induce septicaemia and death of the insect (Poinar & Thomas, 1967; Poinar, 1979). As *Xenorhabdus* or *Photorhabdus* enter stationary phase they secrete (into the insect haemolymph) a variety of extracellular products including a lipase(s), phospholipase(s), protease(s) and several broad-spectrum antibiotics (Akhurst, 1982; Boemare & Akhurst, 1988; Akhurst & Boemare, 1990; Neilson *et al.*, 1990). Macromolecules of the insect cadaver (broken down by bacterial degradative enzymes) and crystalline inclusion bodies produced by the symbiotic bacteria are thought to provide a nutrient supply for the developing nematodes. Nematodes need a special "menu", and the most suitable for their reproduction is a medium conditioned by their bacterial symbionts. Like many other rhabditids, *Steinernema* and *Heterorhabditis* are microbivorous. Axenic rearing of *Steinernema* on artificial diet produces a low level of progeny. Axenic *Steinernema* are able to kill their insect host, but do not multiply (Poinar, 1990), they are unable to utilise the host tissues and fluids as food sources without bacterial bioconversion. Although some non-symbiotic bacteria can provide the essential nutrients, none are as suitable as those produced by the natural symbionts (Wilkinson & Hay, 1997). Furthermore, nematode reproduction is most successful when the natural symbiont (*Xenorhabdus* or *Photorhabdus* spp.) dominates the microbial flora (Akhurst & Boemare, 1990; Akhurst & Dunphy, 1993; Poinar, 1990). This suggests the bacteria can serve as a food source and/or provide essential nutrients required for efficient nematode proliferation.

1.5.3 The role of antimicrobial agents in maintenance of *Xenorhabdus* and *Photorhabdus* monoxenies after insect host death

Monoxenic cultures of *Xenorhabdus* or *Photorhabdus* are maintained after insect death. Normally other microorganisms would be expected to enter the insect cadaver resulting in putrefaction. *Xenorhabdus* and *Photorhabdus* produce *in vitro*, particularly during the last third part of the log period and the beginning of the stationary period, several antimicrobial

compounds such as bacteriocins and antibiotics possessing a large activity against different bacteria, fungi and yeasts (Akhurst, 1982). Antimicrobial production by *Xenorhabdus* and *Photorhabdus* is common (Akhurst, 1982; Richardson *et al.*, 1988; McInerney *et al.*, 1991; McInerney *et al.*, 1991a; Sundar & Chang, 1993; Bowen *et al.*, 1998; Morgan *et al.*, 2001). It is widely speculated that at the time of insect death the gut microflora cannot invade the insect body cavity because;

1. The niche is occupied by a large symbiont population.
2. The antimicrobials produced during the septicaemia can inhibit most of the insect holoxenic micro-organisms.

The role of antimicrobials is only speculative and has yet to be proven experimentally. Defined mutants lacking antimicrobial activity may help to resolve/support this issue, although these are unlikely to be produced given the wide array of antimicrobials produced by a single strain.

1.5.3.1 Antimicrobial agents expressed by *Xenorhabdus*

Uncertainty exists as to whether the different antimicrobials isolated by different groups from *Xenorhabdus* and *Photorhabdus* spp. are the result of differences in extraction method, growth media or bacterial strains used. Nevertheless, the following classes of antibiotic substances have been isolated and characterised.

1.5.3.1.1 Xenorhabdins

There are five related compounds designated xenorhabdins, which are previously unreported members of the pyrrothine family of antibiotics, and can be isolated from P1 *Xenorhabdus* spp. (McInerney *et al.*, 1991). The chemical structure of xenorhabdins was elucidated using X-ray crystallography, NMR, and mass spectral analyses. They are all *N*-acyl derivatives of either 6-amino-4,5-dihydro-5-oxo-1,2-dithiolo [4,3-*b*] pyrrole (compounds 1-3) (Figure 1.2 and Table 1.2) or 6-amino-4,5-dihydro-4-methyl-5-oxo-1,2-dithiolo[4,3-*b*] pyrrole (compounds 4 and 5) (Figure 1.2 and Table 1.2) (McInerney *et al.*, 1991). Xenorhabdins are particularly effective against Gram positive bacteria, and to a lesser extent inhibit Gram negative bacteria. Moreover, these compounds show insecticidal activity.

Table 1.2 Antimicrobial compounds expressed by *Xenorhabdus* and *Photorhabdus* spp.

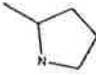
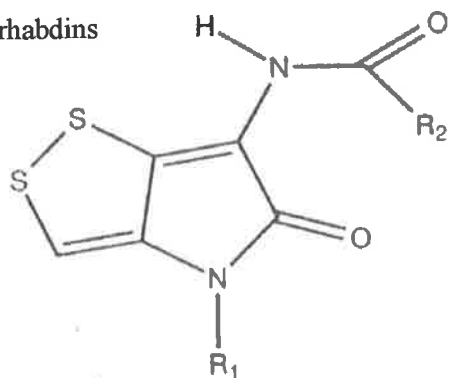
Antimicrobial Family	Activity	R Groups	Reference
Xenorhabdins	Antimicrobial and insecticidal activity	R ₁ R ₂	(McInerney <i>et al.</i> , 1991)
		1. H n-pentyl	
		2. H 4-methylpentyl	
		3. H n-heptyl	
		4. CH ₃ n-pentyl	
5. CH ₃ 4-methylpentyl			
Xenocoumacins	Antibacterial, antifungal and antiulcer activity	$R = \text{CH}_3(\text{CH}_2)_3\text{-NH-C=NH}$ <div style="text-align: center;"> $\begin{array}{c} \\ \text{NH}_2 \end{array}$ </div> R = 	(McInerney <i>et al.</i> , 1991a)
Hydroxystilbenes	Antifungal activity	R = H R = CH ₃	(Paul <i>et al.</i> , 1981; Richardson <i>et al.</i> , 1988; Sundar & Chang, 1992; Li <i>et al.</i> , 1995)
Indole Derivatives	Inhibition of RNA and protein synthesis in Gram positive and Gram negative bacteria	R ₁ R ₂ 1. H CH ₃ 2. H CH ₂ CH ₃ 3. Ac CH ₃ 4. Ac CH ₂ CH ₃	(Paul <i>et al.</i> , 1981; Sundar & Chang, 1993)

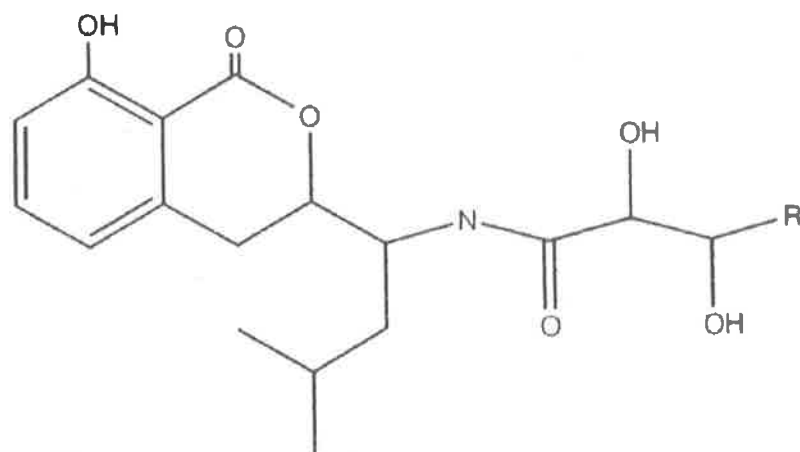
Table 1.2 is reproduced from Forst & Neilson, 1996.

Figure 1.2 Structures of antimicrobial compounds produced by *Xenorhabdus* and *Photorhabdus* species.

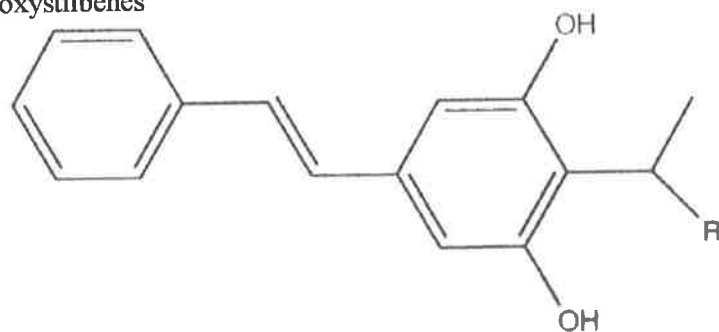
Xenorhabdins



Xenocoumacins



Hydroxystilbenes



Indole Derivatives

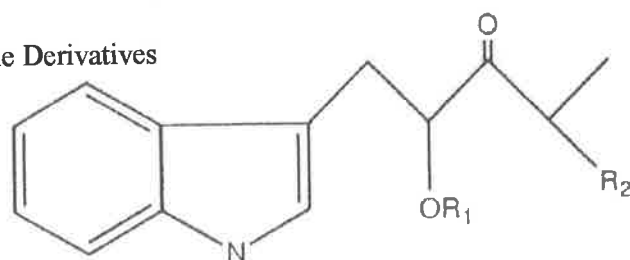


Figure 1.2 is reproduced from Forst & Neilson, 1996.

Xenorhabdins were initially prepared by sequential ethyl acetate and acetone extraction of an original ethanol extract of *Xenorhabdus* cells grown on chicken offal on polyurethane foam (McInerney *et al.*, 1991a). *Micrococcus luteus* was used as the test organism to identify active (yellow) fractions with a characteristic UV-visible spectrum, from the extract.

1.5.3.1.2 Xenocoumacins

Xenocoumacins were extracted from the water-soluble fraction of P1 *Xenorhabdus* spp. strain Q-1 and *X. nematophilus* A11. They are colourless with no UV-visible spectrum and show antibacterial, antifungal and antiulcer activity (McInerney *et al.*, 1991a) (Figure 1.2 and Table 1.2).

1.5.3.1.3 Indole derivatives

Antibiotic activity derived from complex synthetic growth media extracted with ethyl acetate was due to hydroxyl- and acetoxy- bearing indole derivatives found in P1 *X. nematophilus* (Sundar & Chang, 1993) (Figure 1.2 and Table 1.2). These potent antibiotics (Paul *et al.*, 1981) were found to inhibit RNA synthesis in Gram negative and Gram positive bacteria by enhancing the regulatory nucleotide ppGpp (guanosine 3',5'-bispyrophosphate) synthesis, therefore inhibiting RNA synthesis (Sundar & Chang, 1993). Maximum production of indole derivatives occurs in the late log phase, and production is increased by the addition of tryptophan to growth media (Sundar & Chang, 1993).

1.5.3.2 Antimicrobial agents expressed by *Photorhabdus*

1.5.3.2.1 Hydroxystilbenes

P. luminescens produce 4-ethyl- and 4-isopropyl-3,5-dihydroxy-*trans*-stilbenes that are presumed to have arisen from polyketide pathways (Paul, *et al.*, 1981) (Figure 1.2 and Table 1.2). This observation was confirmed by Richardson (Richardson *et al.*, 1988) and Li (Li *et al.*, 1995). Richardson (Richardson *et al.*, 1988) was unable to detect any antimicrobial activity by these compounds, however Li (Li *et al.*, 1995) established these compounds disappear in very late log phase and show activity against several fungi of medical and agricultural importance. The disappearance in late log phase probably accounts for

Richardson (Richardson *et al.*, 1988) failing to identify antimicrobial action. Nothing is known of polyketide antimicrobials in *Xenorhabdus* spp.

1.5.3.2.2 Non-ribosomal peptide synthetases (NRPSs)

DNA sequence encoding NRPSs have been identified in *P. luminescens* (Ffrench-Constant *et al.*, 2000), suggesting these bacteria may express another class of antimicrobial compound. Using a *P. luminescens* DNA library, 2000 random sequence reactions were analysed by comparison to BLASTN and BLASTX. 3.7% (80 out of 2000) of hits revealed significant homology to NRPS gene sequences. Most of these hits (31 out of 80) were to syringomycin from *P. syringae* pv. *syringae*. McClelland and Wilson (McClelland & Wilson, 1998) suggest sequencing the 4.78 Mbp *Salmonella typhi* genome once would require 12,000 sequence reactions of 400 nucleotides each. Whilst Ffrench-Constant has only achieved a fraction of this, peptide synthetases do appear to constitute a significant portion of the *P. luminescens* genome.

NRPS are multienzyme complexes, which range in size between 100 > 1600 kDa (Stachelhaus & Marahiel, 1995), and catalyse the non-ribosomal synthesis of a family of diverse bioactive peptides in both prokaryotes and lower eukaryote species. Examples of the final peptide products include; the immunosuppressant cyclosporin; cell toxin syringomycin; the surfactant surfactin; the siderophore enterobactin and antibiotics such as penicillin, vancomycin and bacitracin. A comprehensive list of bacterial and fungal peptide synthetases has been compiled by Konz and Marahiel (Konz & Marahiel, 1999) and Challis (Challis *et al.*, 2000).

NRPS often incorporate unusual nonproteinogenic residues. More than 300 residues have been identified, including D-configured and N-methylated amino acids or a variety of hydroxy acids. These can be further modified by acylation, glycosylation or heterocyclic ring formation. The final peptide products have either a linear, branched linear or cyclic structure and are synthesized by a thio-template multienzyme mechanism (Kleinkauf & von Döhren, 1990).

The thiotemplate mechanism (Figure 1.3) involves peptide synthetases activating their acyl substrates by ATP-hydrolysis, as acyl adenylates. These intermediates are tethered covalently to enzyme bound 4'-phosphopantetheinyl (4'-PP) cofactors as thioesters. The incorporation of each residue into the peptide is carried out by specific modules on the peptide synthetase that contain all of the information required for recognition, activation, thiolation, and in some cases, modification (epimerization or *N*-methylation) of a single substrate. The modules generate the peptide product by stepwise incorporation of the thioesterified residues in a series of amino- to carboxy-terminal directed transpeptidations (Lipmann, 1980; Stein & Morris, 1996; Marahiel, 1997). The order of modules in the peptide synthetase amino acid sequence directs the residue order of the final peptide product. However non-linear processing has been shown for the biosynthesis of syringomycin (Guenzi *et al.*, 1998a), yersiniabactin (Gehring *et al.*, 1998) and microcystin (Tillett *et al.*, 2000).

1.5.3.3 Bacteriocins (Defective Phages)

The term "Bacteriocin" was coined by Jacob (as referenced by Thaler (Thaler *et al.*, 1997)), for the proteinaceous antibacterial agents that were synthesised by bacteria and required specific receptors (Ackermann & Dubow, 1987). Defective phage particles produced by P1 and P2 *Xenorhabdus/Photorhabdus* spp. were first reported by Poinar in 1980 (as referenced by Forst & Neelson, 1996). Boemare (Boemare *et al.*, 1992) used mitomycin and high temperature to induce lytic phage in *Xenorhabdus* spp., the lysates contained detectable levels of a bacteriocin. Transmission electron microscopy (TEM) showed the presence of rigid phage tail-like particles, empty head phages, and a few intact phage particles. Most of the phage tails are helical with six-fold symmetry (Baghdiguian *et al.*, 1993), and are very similar to bacteriocins associated with lysogenic strains of Enterobacteriaceae and Pseudomonadaceae (Thaler *et al.*, 1997). *Photorhabdus* were found to produce very low levels of bacteriocins, but could not induce production by use of high temperatures or mitomycin. Both *Xenorhabdus* and *Photorhabdus* continually produce low levels of defective phage and have different sensitivities and susceptibilities to phage induction by mitomycin and temperature (Boemare *et al.*, 1992; Baghdiguian *et al.*, 1993).

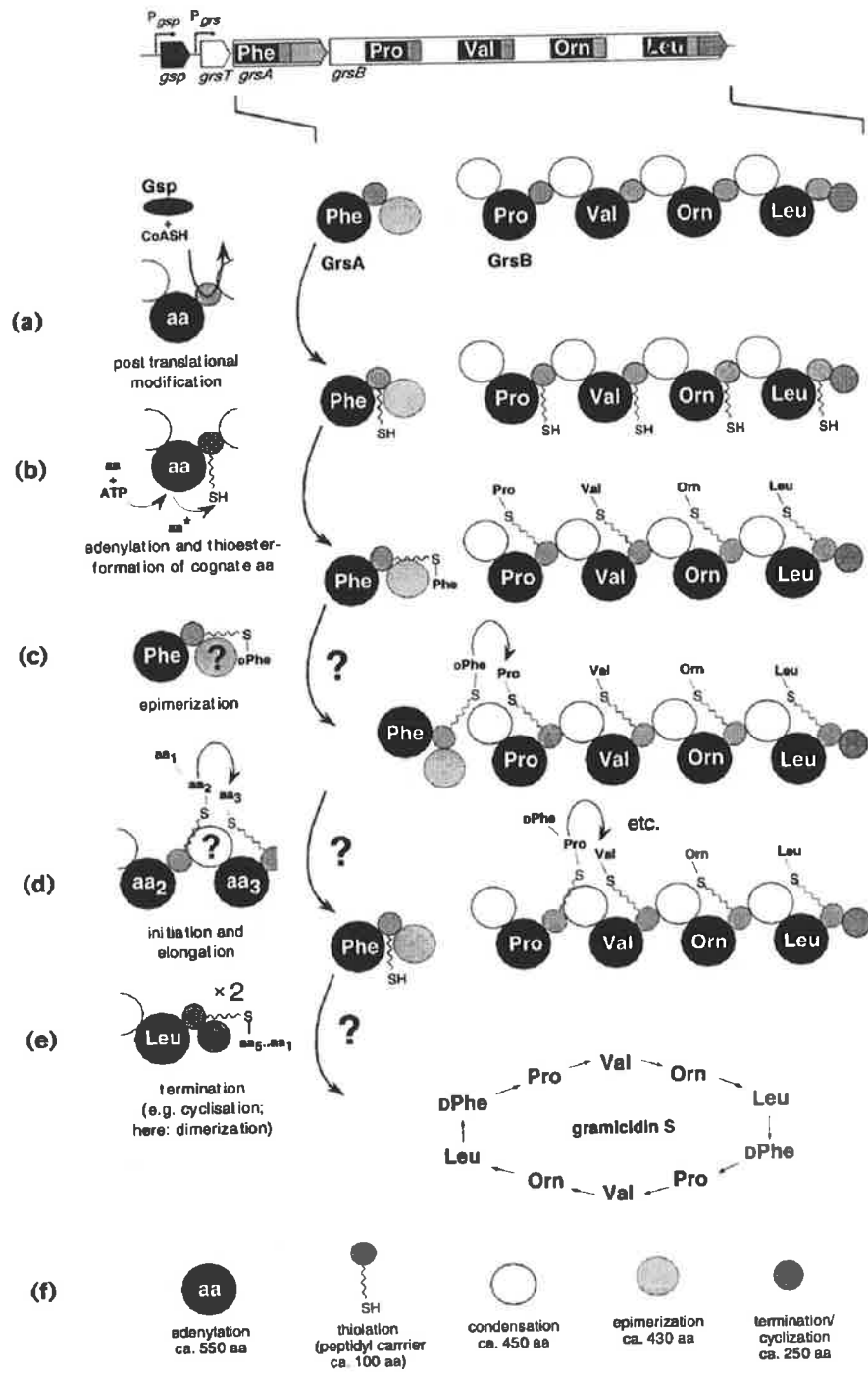
Figure 1.3 Thiotemplate mechanism of peptide synthetase synthesis.

The gramicidin S biosynthesis gene cluster from *Bacillus brevis* and the thiotemplate multiple carrier model. Gramicidin S synthetases GrsA and GrsB are illustrated. The zigzagged line at the thiolation domain represents the bound cofactor 4'-phosphopantetheine. Question marks indicate reactions that are poorly understood.

- [a], Post translational modification of the peptide synthetases at their thiolation domains with the P-pant cofactor by action of Gsp;
- [b], Loading of each module with its cognate amino acid;
- [c], Epimerisation of the GrsA substrate L-phenylalanine;
- [d], Initiation and elongation of the peptide chain;
- [e], Termination by head to tail condensation of two pentapeptides;
- [f], Key to the different domains represented as circles (aa = amino acids, CoASH = Coenzyme A).

Figure 1.3 and figure legend 1.3 are reproduced from (Mootz & Marahiel, 1997a).

grsT, encodes 29 kDa protein of unknown function homologous to fatty-acid thioesterases (Conti *et al.*, 1997).



Bacteriocins produced by *X. nematophilus* A24 inhibits *P. luminescens*, *X. beddingii* and some *Proteus* spp., but not other *X. nematophilus* strains (Boemare *et al.*, 1992). These bacteriocins are thought to inhibit closely related species of bacteria that may be resistant to antibiotics produced by the infecting *Xenorhabdus/Photorhabdus* spp. Therefore preventing infections of larvae resulting in suboptimal conditions for nematode reproduction and development (Thaler *et al.*, 1995).

Phage DNA used as a probe for Southern hybridisation analysis of restriction enzyme digested chromosomal DNA from *Xenorhabdus* phage producer strains, and closely related species as a control, showed strong hybridisation to producer strain chromosomal DNA only (Boemare *et al.*, 1992). These results suggest a specific prophage located on the genome of each *Xenorhabdus* strain (Boemare *et al.*, 1992).

The term xenorhabdycin describes the phage tail-like bacteriocin and phage head particles of *X. nematophilus*. Electrophoresis of xenorhabdycin showed two major subunits of 43 and 20 kDa that represent the sheath and inner core respectively. Five other minor subunits were also characterised 67, 54, 35, 28 and 16 kDa (Thaler *et al.*, 1995). Electrophoresis of the phage head showed a major 40 kDa subunit and two minor 50 and 34 kDa subunits. *X. nematophilus* bacteriocins are similar in structure to rigid bacteriophage tails that are made up of a contractile sheath, a core and a base plate with six caudal fibres (Baghdiguian *et al.*, 1993). Rigid tail-like particles have been shown to be different from the flexible tails of the entire phage particles accompanying bacteriocinogeny (Boemare *et al.*, 1992).

1.5.4 Evidence against antimicrobial compounds produced by *Xenorhabdus* having a role in prevention of secondary invasion of insect carcasses by contaminating bacteria

Work by Jarosz (Jarosz, 1996) on *X. nematophilus* suggests production of antibiotic compounds by these bacteria does not play a role in cadaver preservation. Jarosz found that inhibitory substances were not present in all developmental stages of the nematode/bacterial complex, and that when present had low potency and narrow spectrum of activity. Laboratory based bioassays confirmed that P1 *X. nematophilus* were able to produce antibiotics on nutrient agar, preferentially inhibiting micrococci and bacilli species. Moderate inhibition of Gram negative bacteria such as *Enterobacter cloacae*, *E. coli* and *P. aeruginosa* was also

observed. Dead or moribund insects, representing each stage of nematode development, were blended in distilled water or phosphate buffer (pH 6.4, 6.8 and 7.6) and the extracts tested for antimicrobial activity. Both filtered (Schot G-5 filter) and unfiltered extracts were tested. The extracts showed little or no antibiotic activity when tested against the same range of bacteria used for the nutrient agar based assays, this is despite the fact that the infected *G. mellonella* retained a fresh body typical of insects killed by *Steinernema* spp. Jarosz noted that the inhibition zones produced by *X. nematophilus* disappeared after extended incubation, and suggested a bacteriostatic rather than bacteriocidal activity. Based on this observation Jarosz suggested that bacteriocins do not have a significant role in the cadaver, as they are involved in lysis (a bacteriocidal activity) of bacteria such as the indicator organism *B. cereus*. Furthermore, Jarosz suggested a competition mechanism other than antibiotic activity operates, where by rapid proliferation of *Xenorhabdus* in the insect cadaver would create unfavourable conditions for the growth of contaminating microflora. Further work by Jarosz (Jarosz, 1998) suggested a specific extracellular protease selectively degrades the cecropin-based immune defence system of *G. mellonella*. This protease is secreted into the larval body by the *H. bacteriophora*/*P. luminescens* complex and by P1 bacteria. P2 variants of bacteria were shown to be proteolytically inactive, however bacteria were still able to kill *G. mellonella* larvae. The titre of proteinase in larvae parasitised with the bacterium/nematode complex is approximately 4-5 fold higher than when larvae are infected with bacteria alone. When cecropin-family peptides of *G. mellonella* were treated with P1 infected larvae extracts all antibiotic activity against the indicator organism *E. coli* was depressed. Conversely, untreated cecropins retained their antibiotic activity.

P1 or P2 *Xenorhabdus*/*Photorhabdus* injected into the haemocoel of susceptible larvae are equally pathogenic (Akhurst, 1980; Akhurst & Boemare, 1990; Pinyon *et al.*, 2000), however production of infective juvenile nematodes is significantly reduced when accompanied by a P2 infection. Thus, the protease identified by Jarosz (Jarosz, 1998) may be involved in the reassociation of the nematode/bacteria symbiotic complex. Whilst Jarosz submits compelling evidence to suggest an alternative mechanism for the preservation of the insect cadaver, identification of the protease gene sequence and mutant construction is required to further corroborate the findings.

1.5.5 Re-association of the symbiotic complex

In the final stages of development, nematodes and bacteria reassociate, and the nematodes then develop into non-feeding infective juveniles. Within 2 weeks post infection with a bacteria/nematode symbiotic complex, thousands of newly formed infective non-feeding juveniles emerge in search of a new insect host. *Xenorhabdus* and *Photorhabdus* are never found as a free-living entity, suggesting the symbiotic association may be essential for survival of the bacteria in the soil environment. In the absence of fresh hosts, infective juveniles can survive in soil for many months without feeding (Poinar, 1979).

1.5.5.1 Specificity of bacteria/nematode symbiotic interaction

The specificity of a symbiotic interaction refers to the taxonomically distinct partners with which an organism can form an association (Wilkinson & Hay, 1997). When establishing a symbiotic relationship, several processes may be involved to select or reject various organisms. These processes are collectively termed recognition and may include specific chemical interactions; tolerance or suppression of host defences; and metabolic, morphological or behavioural interactions (Wilkinson & Hay, 1997).

Specificity and recognition are closely linked. Recognition mechanisms determine the specificity of an association, and therefore play a significant role in determining how the symbiotic interaction is maintained throughout the generations. However, the degree of importance of specificity and recognition will depend on the source symbionts are obtained from at each host generation. If symbionts are free-living the mechanism of specificity and recognition must be firm, allowing selection between numerous taxonomically distinct partners (Wilkinson & Hay, 1997). For entomopathogenic nematodes, symbiont transmission is functionally analogous to vertical transmission, where the symbiont population is transmitted from a monoculture within the parent directly to the offspring (Wilkinson & Hay, 1997). It is widely accepted that the metabolic activities of the symbiont, most notably the production of antimicrobial compounds, inhibit the growth of other organisms and thereby maintaining the monoculture.

Taxonomic studies confirm each entomopathogenic species has a specific natural association with only one *Xenorhabdus* or *Photorhabdus* spp. However a *Xenorhabdus* or *Photorhabdus*

species may be associated with more than one nematode species (Akhurst & Boemare, 1988) (Table 1.3).

The specificity of the bacteria/nematode symbiotic association exists at two levels:

1. Acquisition of essential nutrients for the nematode by the bacterium.
2. Retention of bacteria within the intestine of the non-feeding infective juvenile nematode.

Nematode nutrient requirements vary in their specificity. For example, the nematode *S. carpocapsae* can be propagated in culture with bacterial species other than *Xenorhabdus* (Akhurst & Boemare, 1990). However, no steinernematid or heterorhabditid can be cultured monoxenically with all other *Xenorhabdus* or *Photorhabdus* spp. suggesting a degree of specificity (Akhurst, 1983). *Steinernema feltiae* (= *bibionis*) can be successfully cultured monoxenically with the symbiont of any of five other *Steinernema* spp., but not with *P. luminescens*. Furthermore, some artificial growth media provide better growth conditions; eg. *S. glaseri* reproduces faster on lipid fortified agar when cultured with *X. bovienii* rather than *X. nematophilus*, or the natural symbiont *X. poinarii* (Dunphy *et al.*, 1985).

1.5.6 Transmission of *Xenorhabdus* and *Photorhabdus* spp.

The transmission of *Xenorhabdus* and *Photorhabdus* species by a nematode host is very specific. The symbionts of all *Heterorhabditis* spp. are classified as *P. luminescens*. Studies show significant differences in the ability of various strains of *P. luminescens* to support cultures of non-host *Heterorhabditis* spp., and the ability of the nematodes to retain the bacteria in the infective juvenile intestine (Akhurst & Boemare, 1990). Even though *Steinernema* spp. can be cultured with bacteria other than their natural symbionts, they cannot retain non-*Xenorhabdus* bacteria within their intestine, and retain limited numbers of the symbiont of other *Steinernema* spp. (Akhurst, 1983). For example, the *S. carpocapsae*/*X. nematophilus* symbiosis is very specific. Infective juveniles do not retain the symbiont of any other bacterial species (Akhurst, 1983). However, *S. feltiae* (= *bibionis*) and *S. glaseri* infective juveniles are capable of inefficiently carrying the symbionts of some other *Steinernema* spp. (Akhurst, 1983; Dunphy *et al.*, 1985). The retention rate of both *S. carpocapsae* and *S. feltiae* (= *bibionis*) for their natural symbiont is 90%, whilst the *S. glaseri* retention rate is 50% (Akhurst, 1983; Dunphy *et al.*, 1985). No morphological basis for the differences in retention rate has been observed (Bird & Akhurst, 1983).

Table 1.3 *Xenorhabdus* and *Photorhabdus* spp. associated nematodes

<i>Xenorhabdus</i> or <i>Photorhabdus</i> spp.	Associated nematode species	Reference
<i>X. nematophilus</i>	<i>Steinernema carpocapsae</i>	(Thomas & Poinar, 1979; Akhurst, 1983; Boemare & Akhurst <i>et al.</i> , 1988; Akhurst <i>et al.</i> , 1989)
<i>P. luminescens</i> ^a	All <i>Heterorhabditis</i> spp.	(Thomas & Poinar, 1979; Akhurst, 1983; Boemare & Akhurst <i>et al.</i> , 1988; Akhurst <i>et al.</i> , 1989)
<i>X. bovienii</i>	<i>S. feltiae</i> (= <i>bibionis</i>)	(Akhurst, 1983; Boemare & Akhurst, 1988; Akhurst <i>et al.</i> , 1989)
	<i>S. kraussei</i>	(Akhurst, 1982a; Boemare & Akhurst, 1988; Akhurst <i>et al.</i> , 1989)
	<i>S. affinis</i>	(Boemare & Akhurst, 1988)
	<i>S. intermedia</i>	(Poinar, 1985; Akhurst <i>et al.</i> , 1989)

Table 1.3 continued

	undescribed <i>Steinernema</i> spp. F3	(Boemare & Akhurst, 1988; Akhurst <i>et al.</i> , 1989)
	undescribed <i>Steinernema</i> spp. F9	(Boemare & Akhurst, 1988)
<i>X. poinarii</i>	<i>S. glaseri</i>	(Akhurst, 1983; Akhurst, 1986a; Akhurst <i>et al.</i> , 1989)
	<i>Steinernema</i> spp. NC513	(Akhurst, 1986a; Curran, 1989)
<i>X. beddingii</i>	undescribed <i>Steinernema</i> spp. M	(Akhurst, 1983; Akhurst, 1986; Boemare & Akhurst, 1988; Akhurst <i>et al.</i> , 1989)
	undescribed <i>Steinernema</i> spp. N	(Akhurst, 1983; Akhurst, 1986)
<i>Xenorhabdus</i> spp.	<i>S. rara</i>	(Poinar <i>et al.</i> , 1988; Akhurst <i>et al.</i> , 1989)
<i>Xenorhabdus</i> spp.	<i>S. anomali</i>	(Akhurst <i>et al.</i> , 1989)

^a *P. luminescens* is a multispecies taxon (Fischer-LeSaux *et al.*, 1999).

Table 1.3 is reproduced from Akhurst & Boemare, 1990.

However imbalances in the proportions of bacteria and nematode populations may be one possible explanation (Akhurst & Boemare, 1990).

1.5.6.1 Establishment of *Xenorhabdus* or *Photorhabdus* in the nematode intestine

The mechanism for establishment of *Xenorhabdus* or *Photorhabdus* in the juvenile nematode intestine is unknown. Two possible steps may be;

1. Colonisation, followed by;
2. Removal or destruction of foreign microorganisms.

Colonisation may be facilitated by fimbriae and glycocalyxes expressed by the bacteria. Both have been observed in two strains of *X. nematophilus* (Binnington & Brooks, 1993; Brehelin *et al.*, 1993; Moureaux *et al.*, 1995). P1 bacteria express fimbriae and are preferentially maintained by the nematode host, however P2 bacteria can also colonise the intestine in the absence of P1 bacteria (Akhurst, 1980) and do not express fimbriae (Moureaux *et al.*, 1995). Therefore fimbriae are not likely to be the only determinant of colonisation. Removal or destruction of other foreign microorganisms may occur after attachment of the symbiont to the foregut, and might be achieved by physical removal due to out growth of the natural symbiont, or enzymatically destroying the foreign bacterial cell.

1.5.6.1.1 Host-symbiont specificity in Steinernematidae

There is some evidence that host-symbiont specificity is relatively low in the Steinernematidae. Ehlers, referenced by Wilkinson (Wilkinson & Hay, 1997), showed diets consisting of yeast, peptone and cholesterol sustain growth of *S. carpocapse* when supplemented with cells of *Escherichia coli*. Isolates from *S. carpocapse* include *Ochrobactrum anthropi*, *Paracoccus dentrificans*, and *Xanthomonas maltophili* in addition to various *Xenorhabdus* species (Aguillera *et al.*, 1993).

1.5.6.1.2 Host-symbiont specificity in Heterorhabditidae

Specificity is more significant in the Heterorhabditidae than the Steinernematidae. Whilst various isolates of *Heterorhabditis* spp. have been cultured on diets consisting of bacteria derived from other heterorhabditid nematodes, most experimental recombinations have been

unsuccessful (Han *et al.*, 1991; Gerritsen & Smits, 1993). In rare cases where growth and reproduction does occur, the infective dauer juvenile stage fails to retain the bacteria and the symbiosis is unsuccessful (Gerritsen & Smits, 1993). This suggests that the ability of *Xenorhabdus* or *Photorhabdus* to colonise the nematode host intestine is an important factor for determining symbiotic persistence through successive generations (Akhurst & Boemare, 1990).

The exchange of symbionts in nature is very unlikely for several reasons. Two *Xenorhabdus* species are unable to exist in the one insect cadaver except in rare situations where they are partitioned. (Alatorre-Rosas & Kaya, 1990). In a mixed culture of P1 and P2 bacteria the P1 bacteria will be preferentially taken up by the juvenile nematodes (Akhurst, 1980). Therefore P1 cells are able to out compete P2 cells for putative binding sites in the juvenile nematode intestine. Thus it is very unlikely that a foreign symbiont could out compete the normal P1 bacteria for binding sites and subsequently be transmitted (Akhurst, 1993).

1.6 Insect defence mechanisms

Insects are capable of recognising foreign objects in their haemolymph. Defence mechanisms include structural and passive barriers (e.g., cuticle, gut physiochemical properties and peritrophic membrane (Dunn, 1986)), constitutive cellular and humoral factors in the haemolymph, and inducible antibacterial proteins (Boman & Hultmark, 1987). The insect response varies depending on the combination of nematode and bacteria used, the insect species and physiological status of the insect. For example, most *Xenorhabdus* spp. are highly pathogenic for *Galleria mellonella* larvae when introduced into the haemocoel (the LD₅₀ usually being less than 50 cells) (Akhurst & Boemare, 1990). However, *X. nematophilus* is less pathogenic for pupae of lepidopteran *Hyalophora cecropia* (LD₅₀ = 500 cells), (Akhurst & Boemare, 1990) and not at all pathogenic for the dipteran *Chironomus* (Avisé *et al.*, 1987). Only 20 *X. nematophilus* cells are required to kill more than 90% of *Manduca sexta* larvae, emphasising the pathogenicity of this bacteria (Forst *et al.*, 1997). For contrast, the LD₅₀ of *Pseudomonas aeruginosa* strain P11-1 towards *Manduca sexta* is 10⁵ bacteria/larvae, whereas less than 100 cells are sufficient to kill *G. mellonella* (Dunphy, 1995).

1.6.1 Timing of *Xenorhabdus* or *Photorhabdus* release into the insect haemocoel

The timing of release of *Xenorhabdus* and *Photorhabdus* species from either steinernematid or heterorhabditid nematodes respectively, and cues triggering release *in vivo*, are unknown. There is little published work that addresses these questions. One limited approach to this problem has been to measure the time taken for an immune response to the presence of infectious complexes to be detected. Matha (Matha & Mracek, 1984) showed that elevated haemocyte counts were detected within 4 hours of a *Steinernema* spp. (isolated from sawfly *Cephalcia abietis*) gaining access to the *G. mellonella* gut tissue. Injection of surface sterilised monoxenic *H. bacteriophora* into *G. mellonella* induced haemocytopenia within 5 hours post injection. Both of these immune responses were directed towards the bacteria, and therefore suggest the bacteria are released from the nematode vesicle within 5 hours postparasitism.

1.6.2 Insect opsonin mediated immunity

Recognition of foreign bodies in the insect proceeds the production of some humoral factors which act as opsonins. These opsonins are probably lectin like molecules, and different factors produced by the phenol-oxidase system. They direct the recruitment of haemocytes for phagocytosis and encapsulation (Brehelin *et al.*, 1990). The phenol-oxidase system is triggered by endotoxins (eg. LPS) and some glucans or serine proteases such as trypsin. However, entomopathogenic organisms are able to either evade or depress the immune reactions of some insect species. The evasion systems can be grouped as;

1. Tolerating the host's defensive mechanisms;
2. Destroying the recognition and/or response systems;
3. Avoiding the immune responses either by evading recognition or by suppressing the host's non-self recognition or response systems (Dunphy & Thurston, 1990).

1.6.3 Nematode interaction with insect haemolymph

Humoral encapsulation of steinernematids in a polyphenol/protein capsule by aquatic dipteran larvae (e.g. *Aedes* spp.) does not always prevent insect host death. In this case, *X. nematophilus* is released from its nematode host before encapsulation is complete. Thus

pathogenic bacteria are not affected by the insect immune response and are able to multiply and kill the mosquitoes (Akhurst, 1993).

Neither *S. carpocapsae* or *H. bacteriophora* elicit a humoral or cellular immune response in *G. mellonella* larval haemolymph (Dunphy & Thurston, 1990). This observation is also true for *S. carpocapsae* in *Locusta migratoria* larval haemolymph (Brehelin *et al.*, 1990). This phenomenon has been attributed to the nematode cuticle not being recognised as non-self rather than the inhibition of humoral factors or haemocyte activity (Brehelin *et al.*, 1990). The nematode is in an advantageous position as the host can repair damaged tissue and contain the bacteria introduced by the nematode during initial haemocoel invasion. Evasion of recognition as non-self may occur by possession of nonreactive surfaces, innate molecular mimicry or possession of heterophile antigens (Dunphy & Thurston, 1990). Within 4-6 hours of *G. mellonella* invasion, *S. carpocapsae* and *H. bacteriophora* suppress an increase in haemocyte counts and changes to haemocyte differential counts, suggesting impairment of haemocyte activity (Dunphy & Thurston, 1990). This suppression occurred slightly before or at the time bacteria were believed to be released. The cause of haemocyte suppression is unknown.

1.6.4 Insect inducible antibacterial peptide mediated immunity

Some insects use a defence system consisting of inducible antibacterial peptides (e.g. cecropins, attacins and dipterocins) that the bacterial symbiont is unable to withstand (Akhurst, 1993). Under these circumstances the nematode/bacteria complex is a success because the nematodes produce a proteinaceous inhibitor of the inducible antibacterial peptides as they recommence development from the infective juvenile stage, therefore protecting their symbiont (Akhurst, 1993). This phenomenon is exemplified by the fact that injection of 1150 *X. poinarii* cells into each *G. mellonella* larvae is not lethal, whilst co-injection of 115 *X. poinarii* cells with one *S. glaseri* infective juvenile killed 75% of the *G. mellonella* larvae (Akhurst, 1986a).

1.6.5 *Xenorhabdus* interactions with insect haemolymph

In both *G. mellonella* (Dunphy & Webster, 1985) and *Locusta migratoria* (Brehelin *et al.*, 1990), *X. nematophilus* does not avoid immune recognition and is initially bound by

haemocytes. However, *X. nematophilus* is able to subsequently deactivate the haemocytes and escape back into the haemolymph (Dunphy & Thurston, 1990). This is an example of tolerance of the insect immune response, as less than 10 cells injected into the haemocoel of *G. mellonella* are needed to induce insect death (Poinar & Thomas, 1967).

1.6.5.1 *Xenorhabdus* lipopolysaccharide (LPS)

The lipopolysaccharide (LPS) of *Xenorhabdus* spp. is toxic for the haemocytes of *G. mellonella*. Dunphy (Dunphy & Webster, 1988) concluded LPS was a haemocytotoxin based on several observations;

1. A phenol-water extract of serum from *Xenorhabdus* infected *G. mellonella* (where the bacteria had been removed) elevated haemocyte counts when re-injected into *G. mellonella*.
2. The similarity in SDS-PAGE profile between LPS from the species of infecting *Xenorhabdus* and the extracts of haemolymph from infected larvae.
3. The ability of LPS from *Xenorhabdus* spp. to elevate haemocyte counts.
4. The induction of gelation of a *Limulus* amoebocyte lysate (an indicator of LPS in biological fluids).

Using the amoebocyte lysate assay a correlation between the appearance of LPS from *X. nematophilus* and *P. luminescens in vivo*, bacterial re-emergence into the haemolymph and elevation of haemocyte levels was detected. It was therefore concluded that endotoxin was significant for virulence (Dunphy & Webster, 1988). Dunphy (Dunphy & Webster, 1988) concluded the toxic moiety of the endotoxin was lipid A for LPS species from *Xenorhabdus* spp. The electrophoretic profiles of the endotoxin from *X. nematophilus* strains DD-136 and Breton differed, despite both strains being equally pathogenic. This observation suggested the oligosaccharide side chain (O-side chains) and core were not toxic to insect haemocytes (Dunphy & Webster, 1988). Lipid A injections were shown to elevate haemocyte counts, this effect could be abolished by the co-injection of lipid A and polymixin B (an antibiotic which binds to lipid A), suggesting lipid A may bind to haemocytes. Further work established lipid A probably bound to glucosaminyl receptors on the haemocytes, as formation of granular cells by injection of LPS and lipid A from *X. nematophilus* DD-136 and *P. luminescens* was blocked by low concentrations of *N*-acetylated and nonacetylated glucosamine (Dunphy & Webster, 1984; Dunphy & Webster, 1988). Total fatty acids extracts from the glucosaminyl

glucosamine disaccharide backbone of lipid A were as toxic to the haemocytes as the corresponding amount of lipid A and LPS. The major fatty acids detected in Enterobacteriaceae lipid A vary in their haemocytic toxicity in *G. mellonella* with 3-hydroxy tetradecanoic acid and *n*-tetradecanoic acid being the most toxic (Dunphy & Webster, 1984).

1.6.5.2 Inhibition of the prophenoloxidase cascade

In the Greater Wax Moth, *Galleria mellonella*, five haemocyte types have been identified: plasmatocytes, granular haemocytes, spherule cells, oenocytoids and prohaemocytes. Oenocytoids and granular cells contain components of the prophenoloxidase system and are capable of melanin production (Schmidt & Ratcliffe, 1977). Haemolymph coagulation is initiated by rapid release of material from the granular cells (Rowley & Ratcliffe, 1976), whilst the plasmatocyte is the main phagocytic cell type (Ratcliffe, 1985). Studies indicate *G. mellonella*, recognition, and the subsequent cellular defences elicited, involve interaction of granular cells with plasmatocytes (Ratcliffe & Gagen, 1977; Schmidt & Ratcliffe, 1977).

Several theories have been proposed to account for the differential responsiveness of haemocytes to non-self, including the concept that the surface charge of the foreign material may or may not favour haemocyte attachment *in vivo*. However there is no convincing experimental evidence to support this theory. In mammals, surface charge and van der Waals forces are not considered to play a significant role in cell adhesion during tissue differentiation and development (Soderhall & Smith, 1986). However, the concept of the prophenoloxidase system being required for arthropod cellular defence has gained momentum.

The prophenoloxidase activating system is a complex cascade of enzymes responsible for the initiation of melanin synthesis by the host, and is present in the granular species of haemocyte (Soderhall & Smith, 1986). Pye (Pye, 1974) and Unestam (Unestam & Soderhall, 1977) demonstrated yeasts or their constituent β -1,3-glucans initiated melanisation reactions in arthropod haemolymph by activating prophenoloxidase, the key enzyme in melanisation reactions. Subsequent work established that along with the β -1,3-glucans, bacterial cell walls and their associated LPS will specifically activate the prophenoloxidase system that constitutes a multitude of intermediate proteins such as serine proteases and a coagulogen (Soderhall & Smith, 1986).

Melanisation is a common feature of both the humoral and cellular immune responses of insects and other arthropods, with the substrates and enzymes involved in melanin synthesis perhaps playing an important role in immune recognition (Taylor, 1969). Tyrosine, as well as its derivatives dopa and dopamine, are precursors of quinones which are required as cross-linking agents in the sclerotisation and melanisation of the integument during pre-adult molting, pupariation, adult eclosion, and wound healing of cuticle abrasions. The enzymes involved in these processes (i.e., monophenoloxidases and diphenoloxidases, decarboxylases, and dopamine N-acetyltransferases) may be localised intracellularly and sequestered from their substrates, and/or exist in inactive states (proenzymes) (Nappi & Christensen, 1986). On a functional level the prophenoloxidase cascade provides opsonins, initiates nodule formation, participates in coagulation, facilitates microbial killing and mediates communication/cooperation between various haemocyte populations.

Cellular encapsulation, or nodulation, is an important process in insect immunity. It involves aggregation of host haemocytes around the foreign particle present in the haemocoel resulting in the formation of a multi-layered cellular sheath (Soderhall & Smith, 1986). Nodule formation has been shown to begin within five minutes of introduction of foreign tissue into the haemocoel of *Galleria mellonella* (Schmidt & Ratcliffe, 1977). Plasmatocytes were found to form the structural element of the capsule, however they are not responsible for the initial identification of the foreign object, (fragments of nerve cord from the locust *Schistocerca gregaria*) within the haemocoel. This role is played by the granular cells and their lysis on the foreign surface appears to be necessary for plasmatocyte adhesion, as granular cell debris is always found between these cells and the implant. Melanisation occurs between the foreign object and haemocytes. During the second stage of nodulation successive layers of plasmatocytes build up around the melanised core, and in the case of bacteria some have been shown to be intracellularly located within the plasmatocytes (Ratcliffe & Gagen, 1977). A mature nodule has formed by 12-24 hours, and the sheath is divided into an outer region of newly attached cells, a middle region of extremely flattened cells and an inner region of partially flattened cells containing melanised inclusions. If capsule build-up occurs by purely physical means, all haemocyte types, (i.e., plasmatocytes, granular cells, spherule cells, prohaemocytes and oenocytoids) are incorporated into the structure. As only plasmatocytes adhere, there is an element of specificity, and the cells may be responding to a chemotactic stimulus. Such a stimulus is unlikely to come from the foreign entity as observations show inert objects such as glass and araldite are encapsulated by *G. mellonella*. Therefore it seems

likely the initial breakdown of granular cells releases some factor(s) that specifically attract plasmatocytes to the site of encapsulation, and may also cause the continuing release of granular cell proteins enabling the cells to stick together (Ratcliffe & Gagen, 1977).

1.7 Current Field Use

Insect parasitic nematodes have been known since the 17th century, however it wasn't until the 1930s that significant attention was given to using entomopathogenic nematodes for the control of insect pests (Smart Jr, 1995). Now in the 21st century entomopathogenic nematodes are being used throughout a number of countries to control insect pests (Table 1.4). However these biocontrol agents represent less than 1% of the pest control market (Smart Jr, 1995). One major reason for this is likely to be cost. In 1991 production of nematode-bacteria infectious complexes was estimated to cost 10 - 60% more than chemical products (Smart Jr, 1995). Over the last decade improvements in production, formulation, packaging and shelf life have been encouraging, however prices will need to fall further to entice primary producers who will not accept biological agents that do not provide similar results to standard chemical pesticides.

1.7.1 Entomopathogenic nematode application to crops

Although entomopathogenic nematodes are lethal to target soil insect pests, they are safe for plants and animals. Nematode applications do not require masks or other safety equipment, also re-entry time, residues, groundwater contamination, chemical trespass and pollinators are not an issue (Gaugler, 1999). Nematodes can be applied with standard agrochemical equipment including pressurised, mist, electrostatic, fan and aerial sprayers (Gaugler, 1999). One billion nematodes per acre (250,000 per m²) is the suggested application rate against most soil insects, however containerised and greenhouse soils are generally treated at a higher rate (Gaugler, 1999). The bacterial/nematode symbiotic complex kills insects within 24 - 48 hours, and thousands of infective juvenile nematodes emerge in search of fresh host within a few days.

Table 1.4 Current use of entomopathogenic nematodes as bioinsecticides

Commodity	Insect Pest	Nematode Species
Artichokes	Artichoke plume moth	<i>S. carpocapsae</i>
Berries	Root weevils	<i>H. bacteriophora</i>
Blackcurrant ^a	Blackcurrant borer	<i>S. feltiae</i>
Citrus	Root weevils	<i>S. riobravis</i>
Cranberries	Root weevils	<i>H. bacteriophora, S. carpocapsae</i>
	Cranberry girdler	<i>S. carpocapsae</i>
Mushrooms	Sciarids	<i>S. feltiae</i>
Ornamentals	Root weevils	<i>H. bacteriophora, H. megidis</i>
	Wood borers	<i>S. carpocapsae, H. bacteriophora</i>
	Fungus gnats	<i>S. feltiae</i>
Turf	Scarabs	<i>H. bacteriophora</i>
	Mole crickets	<i>S. riobravis, S. scapterisci</i>
	Billbugs	<i>H. bacteriophora, S. carpocapsae</i>
	Armyworm, Cutworm,	<i>S. carpocapsae</i>
	Webworm	

Table 1.4 is reproduced from Gaugler, 1999, ^aBedding & Miller, 1981.

Apart from the aforementioned cost considerations the main disadvantage of using entomopathogenic nematodes is the requirement for more management, planning, education and training to use the biological agent safely and effectively. Furthermore, whilst entomopathogenic nematodes are very pathogenic for the insect host; the process takes time and killing is not rapid or dramatic as that caused by chemical insecticides. Whilst the entomopathogenic nematodes are very specific for the host insect, this may prove to be a disadvantage in comparison to broad range insecticides if a number different insect species infect a crop.

1.8 Molecular manipulation of *Xenorhabdus* and *Photorhabdus* spp.

Genetic engineering of *Xenorhabdus* and *Photorhabdus* spp. could facilitate improving their pathogenicity and host specificity for insect species. To genetically engineer a bacterial species, requirements for DNA uptake; availability of suitably maintained and selectable cloning vectors and for incoming DNA not being affected by restriction modification systems must be met.

1.8.1 Transformation

Xenorhabdus spp. have a restriction modification system that affects the transformation of different plasmids. *X. nematophilus* ATCC 19061 can be transformed with the broad-host-range vector pHK17 if the plasmid is first passaged through *Xenorhabdus* cells (Xu *et al.*, 1989). MgCl₂, RbCl₂ and KCl were found to inhibit transformation efficiency. The transformation buffer giving best results consisted of 0.01M Tris-HCl buffer [pH 6.5] and 0.06M CaCl₂. Addition of DMSO to a final concentration of 7% (v/v) increased transformation efficiency 3 - 5 fold. Maximum transformation was achieved over a pH range of 6.5 - 7.0 and the best cell to DNA ratio was approximately 2.4×10^8 total cells, per 2 ng of plasmid, per standard transformation mixture. The bacterial cells/DNA mixture is heated for 3 min at 37°C or 1.5 min at 42°C, maximum transformation was achieved when cells were grown to mid-to-late logarithmic phase (total counts 2.5×10^8 to 5×10^8 cells per ml) within 4.5 to 5.5 hours of inoculation of the starter culture (Xu *et al.*, 1989). Using this method approximately 10^5 to 10^6 transformants per µg of pHK17 could be obtained. This is in

contrast to pHK17 initially isolated from *E. coli*, resulting in a 250-fold reduced transformation efficiency (Xu *et al.*, 1989).

The fact that transforming plasmid DNA isolated from *E. coli* showed a reduced transformation efficiency is consistent with the notion of a restriction modification system active in *X. nematophilus*. Other supporting evidence comes from observations that digestion of *X. nematophilus* chromosomal DNA with several common enzymes is often difficult and requires excessive amounts of enzyme (Boemare *et al.*, 1993). Furthermore, there are differences in the ability of particular strains to be transformed. Whilst *X. nematophilus* ATCC 19061 could be transformed using the DMSO method, *X. nematophilus* IM/1 could not. The reason for this variability is unknown (Xu *et al.*, 1989), but may be related to the presence/absence of capsular materials that inhibit DNA uptake.

P. luminescens is more readily transformed than *Xenorhabdus*, using a modification of the CaCl₂/RbCl₂ procedure commonly used for *E. coli* cells (Kushner, 1978). The modifications were;

1. The addition of 0.5% NaCl to transformation buffers to prevent cell lysis of *P. luminescens*;
2. Changing the temperature and duration of the heat shock from 43 - 44°C for 30 sec to 37°C for 2 min.

P1 and P2 *P. luminescens* variants transformed with pBR322, pACYC184 and pSF60 were maintained extrachromosomally and in high copy number (Frackman *et al.*, 1990; Frackman & Nealson, 1990).

1.8.2 Conjugation

Development of a negative-selection vector, pHX1, was used for construction of *X. nematophilus* ATCC 19061 transposon mutants by conjugation (Xu *et al.*, 1991). Plasmid pHX1 contains the *sacB* (levansucrase) gene from *Bacillus subtilis* that is lethal to Gram-negative bacteria in the presence of sucrose. The plasmid also contains the transfer (*tra*) and mobilisation (*mob*) regions, and the Tn5 (kanamycin resistance) transposon. Only bacteria that have lost the plasmid and inserted the Tn5 transposon into their genome are viable on kanamycin/sucrose plates (Xu *et al.*, 1991). A similar *sacB* based system was used to

insertionally inactivate the crystalline proteins of *cipA* and *cipB* of *P. luminescens* (Bintrim & Ensign, 1998), and the *envZ* gene from *X. nematophilus* (Forst & Tabatabai, 1997).

Conjugation using Tn5 derived minitransposons (De Lorenzo *et al.*, 1990) has successfully been used to create stable insertion mutants in *X. bovienii* T228 (Pinyon *et al.*, 1996). The delivery system for the mini-Tn5 transposons is the pUT plasmid (Herrero *et al.*, 1990) that has as its origin of replication the π protein-dependent origin of plasmid R6K (Kolter *et al.*, 1978). The plasmid is only maintained in π protein-producing bacteria, and carries the origin of transfer *oriT* of plasmid RP4 that results in conjugal transfer to recipient strains from donor strains expressing RP4-conjugative functions. Plasmid pUT carries a mutant *tnp* gene of IS50R that encodes the transposase needed for transposition of the mini-Tn5 elements (De Lorenzo *et al.*, 1990).

1.8.3 Transduction

A lambda delivery system has been used to introduce copies of Tn10 mutants into *X. bovienii* by transduction (Francis *et al.*, 1993). As *X. bovienii* does not normally express the receptor for lambda, a prerequisite for infection is expression of LamB from an introduced plasmid. Conjugative transfer of a plasmid encoding *lamB* (pTROY) into *X. bovienii* T228 resulted in the constitutive expression of LamB on the bacterial cell surface. Subsequent infection of *X. bovienii*/pTROY with λ bacteriophage carrying the Tn10-derived transposon resulted in enhanced phage absorption over the wild type strain. Auxotrophic, haemolytic, Congo Red binding, DNase, protease, lipase and phospholipase C mutants were obtained by this technique.

1.9 Phase Variation

Xenorhabdus and *Photorhabdus* spp. exhibit a cellular dimorphism termed phase variation (Akhurst, 1980). The P1, form is usually isolated from the intestines of L3 stage infective juvenile nematodes. P1 cells are unstable *in vitro*, and occasionally *in vivo*, producing the P2 form during stationary phase. Generally P1 cells differ from P2 cells in colony morphology, adsorption of dyes from agar, the ability to provide a superior nutrient source for nematodes and in the production of antimicrobial factors (Akhurst, 1980; Dunphy *et al.*, 1985; Akhurst, 1993). P1 cells reduce triphenyltetrazolium chloride to red coloured formazan and adsorb

bromothymol blue (BTB) from nutrient agar containing 0.004% (w/v) triphenyltetrazolium chloride and 0.0025% (w/v) BTB. Therefore P1 cells form blue colonies surrounded by a decolourised zone after 3 to 5 days incubation at 28°C. P2 cells do not adsorb BTB, but form red colonies due to the reduction of triphenyltetrazolium chloride (Akhurst, 1980).

There can be considerable variation between P1 cells, whilst some *Xenorhabdus* strains do not show variation in all characteristics (Akhurst & Boemare, 1990). An internationally accepted standard assay and criteria for characterisation of P1 and P2 phenotypes is required to generate consistency within and between research groups. Table 1.5 outlines phenotypic characteristics of *Xenorhabdus* and *Photorhabdus* that are affected by phase variation.

1.9.1 The role of phase variation and significance of P2 bacteria

The role of *Xenorhabdus* P2 variants is unknown, and there is no convincing data to explain their presence. This becomes more complex when the differences between strains with regard to the specific phenotypes characteristic of this variation are considered (Couche *et al.*, 1987; Bleakley & Neilson, 1988; Boemare & Akhurst, 1988). Generally, P2 bacteria are less able to provide appropriate nutrient conditions for nematode growth and reproduction within the insect host (Akhurst, 1980). Recent studies have defined this further, demonstrating axenic eggs of *S. carpocapsae* can grow to adult stage on P2 cells of *X. nematophilus* and continue developing into infective juvenile nematodes (Volgyi *et al.*, 1998). However, nematodes were unable to grow on heat killed P2 *Xenorhabdus*. Overall these *in vitro* results suggest viable P2 cells provide a nutrient base that allows efficient nematode development (Volgyi *et al.*, 1998). *In vivo* however, low numbers of infective *S. carpocapsae* juveniles are produced when *G. mellonella* larvae are infected with P2 cells of *X. nematophilus* (Akhurst, 1982). The difference between the *in vitro* and *in vivo* situations may reflect an *in vivo* requirement for the stationary-phase products that are produced by P1 and not P2 cells (Volgyi *et al.*, 1998).

Phase dependent phenotypic differences are displayed in stationary phase cultures. The stability of P1 cultures varies from strain to strain, some producing P2 forms at a high frequency and some producing multiple form variants (Hurlbert *et al.*, 1989; Gerritsen *et al.*, 1992). *Xenorhabdus* phase changes occur during the *in vitro* stationary period in an extremely unpredictable manner (Boemare & Akhurst, 1990). The ability to quickly change metabolic properties should allow the symbiont to adapt to different niches. The distinct environmental

Table 1.5. Phenotypic characters of *Xenorhabdus* and *Photorhabdus* affected by phase variation

Colony Properties	P1	P2	References
Morphology	mucoid	smooth	
Stickiness	+	-	
Dye adsorption	+	-	(Akhurst, 1980; Boemare <i>et al.</i> , 1997a)
Pigmentation ^a	+	d	(Boemare & Akhurst, 1988; Neilson <i>et al.</i> , 1990; Boemare <i>et al.</i> , 1997a)
Swarming ^b	+	-	(Givaudan <i>et al.</i> , 1995)
Ultrastructural elements and cytological properties			
Protoplasmic inclusions	+	w/-	(Neilson <i>et al.</i> , 1990)
Flagella ^b	+	-	(Givaudan <i>et al.</i> , 1995)
OpnA, OpnB ^c	+	-	(Leisman <i>et al.</i> , 1995)
Fimbriae ^d	+	-	(Binnington & Brooks, 1993; Brehelin <i>et al.</i> , 1993)
Glycocalyx thickness ^d	+	w	(Brehelin <i>et al.</i> , 1993)
Insect hemocytes	+	-	(Moureaux <i>et al.</i> , 1995)
Agglutination ^d			
Erythrocytes agglutination ^d	+	-	(Binnington & Brooks, 1993; Moureaux <i>et al.</i> , 1995)
Enzymatic activities			
Respiratory enzymes ^e	w	+	(Smigielski <i>et al.</i> , 1994)
Bioluminescence ^f	+	w/-	(Grimont <i>et al.</i> , 1984)

Table 1.5. continued

Antimicrobials ^g	+	w/-	(Akhurst, 1982; Boemare <i>et al.</i> , 1997a)
Phospholipase(s) ^h	d	w/-	(Boemare & Akhurst, 1988; Boemare <i>et al.</i> , 1997a)
Protease(s) ^a	+	d	(Akhurst, 1980; Boemare <i>et al.</i> , 1997a)
Lipase(s) ⁱ	d	d	(Boemare & Akhurst, 1988; Boemare <i>et al.</i> , 1997a)

Table 1.5 is reproduced from Boemare *et al.*, 1997.

+ = positive; - = negative; d = according to strain or biovar; w = weak

^a no pigmentation for *X. nematophilus*; negative for other *Xenorhabdus* P2 variants; differential pigmentation for *Photorhabdus* variants.

^b for *X. nematophilus*, few exceptions for other *Xenorhabdus* spp; according to strain for *Photorhabdus*.

^c Outer membrane proteins of *X. nematophilus*.

^d For *X. nematophilus*.

^e For *P. luminescens* and *X. nematophilus*.

^f For *Photorhabdus*, little light can be detected in a scintillator counter from P2 variant cultures.

^g Some P2 variants can produce a weak antibiosis.

^h Some negative results in both variants of *Xenorhabdus* and *Photorhabdus*. It is checked as “weak lecithinase” when opacity is recorded below the colonies.

ⁱ Sometimes P2 variants are more lipolytic than P1 variants, but they give generally negative or weak responses.

biotypes encountered when firstly entering a starvation period in the infective juvenile nematode gut, and secondly the growth period in the insect haemolymph, probably forces adaptive responses where phase variation might take place.

1.9.2 Differences in nutrient assimilation by phase variants

Phase variants differ in their assimilation of nutrients and their vitamin requirements. P2 variants show poor growth on complex media previously utilised by P1 variants (Boemare and Akhurst, 1990). Differences in the respiratory activity have been detected between the two phases of *X. nematophilus* (Smigielski *et al.*, 1994). After periods of starvation P2 cells recommenced growth within 2-4 hours from addition of nutrients; compared with 14 hours for P1 cells. This indicates P2 cells show a more efficient nutrient uptake. The shorter lag period for P2 cells after addition of nutrients would give P2 cells a greater chance than P1 cells if they have to compete with other free-living microorganisms outside the insects. An increase in P2 bacteria membrane potentials was noted which reflects the ability of the P2 variant to respond to nutrients, both through growth and nutrient uptake. These experiments suggest that while P1 cells are better adapted to conditions in the insect, P2 cells may be better adapted to other conditions (Smigielski *et al.*, 1994). While the environmental conditions favouring P2 forms have yet to be defined, one important ramification is that if P2 bacteria were common in soils or other environments they may be easily missed as detection methods strongly favour P1 characteristics (Forst & Nealson, 1996).

1.9.3 Nematode preferential selection of P1 bacteria

Xenorhabdus P1 to P2 conversion is not detected *in vivo* during the period of nematode reproduction, however this observation may be biased by the small range of insect hosts tested (Akhurst, 1980). Nematodes strongly select for P1 cells (Akhurst, 1980), suggesting a mechanism has evolved to remove the undesirable P2 variants. As P2 cells appear *in vitro* when bacterial growth has stopped or significantly slowed (Akhurst & Dunphy, 1993), P2 bacteria may be found in insects that provide a poor nutrient basis for P1 bacteria. As the two phases show different metabolic activity (Bleakley & Nealson, 1988; Boemare & Akhurst, 1988; Boemare & Akhurst, 1990) phase changes could facilitate a mechanism for exploitation of different insect species (Akhurst & Dunphy, 1993). The phase change may occur in insect species where P1 forms are unable to grow or cease growth before the nematodes have been

able to mature. The change would therefore result in a different bacterial metabolic system operating to utilise the insect cadaver. As the phase shift is not 100% when the culture is initially pure P1, the remaining P1 cells could colonise the nematode intestine to ensure the next generation of infective juveniles carry only the P1 bacteria (Akhurst, 1980).

Overall, as phase variation is a common property in both *Xenorhabdus* and *Photorhabdus* spp., (Boemare & Akhurst, 1988; Nealson *et al.*, 1990) it may indicate phase variation is a key factor required for a successful symbiotic relationship and killing of host insects.

1.9.4 Induction and repression of phase variation by environmental signalling.

Stress experiments, where environmental conditions are altered, have been reported to induce phase variation. The lack of NaCl in the culture medium causes *Photorhabdus* to phase shift (Krasomil-Osterfeld, 1995). Several other environmental conditions were also tested; low oxygen levels, light, extreme pH values and temperature change, however none of these had any affect on phase variation (Krasomil-Osterfeld, 1995). Both microaerophilic pressure in unshaken broth for *Xenorhabdus* and *Photorhabdus* spp., and culturing in *Xenorhabdus* anaerobically (requiring the use of fermentative pathways) induce phase variation (Boemare & Akhurst, 1990). These experiments demonstrate phase variation may be a response to environmental changes that occur during stationary phase where requirements for one phase are consumed or not permitted. However they cannot explain the mechanism(s) of phase variation, or the likelihood of a single common control mechanism regulating a number of different phenotypes that use different metabolic pathways.

1.9.5 The molecular basis of phase variation in both *Xenorhabdus* and *Photorhabdus* spp.

The common properties expressed by *Xenorhabdus* and *Photorhabdus* spp. are probably examples of a convergent evolution necessary for the association with two phylogenetically different nematodes (Forst & Nealson, 1996). The mechanism(s) of phase variation is/are probably different between *Xenorhabdus* and *Photorhabdus* spp. as the result of a complex genetic and metabolic cascade of events starting from environmental signals via membrane transports, gene regulation and protein synthesis for each appropriate metabolism. Whilst

neither the function nor mechanism of phase variation is understood, molecular genetics has provided some answers regarding the mechanism.

1.9.5.1 Plasmid based regulation of phase variation

Studies of the nature of symbiotic relationships between bacteria and higher organisms (e.g. *Rhizobium* spp. and leguminous plants) has revealed a significant amount of genetic information necessary for these symbioses is located on megaplasmids (Coplin, 1989). Megaplasmids can be defined as extrachromosomal DNA (plasmid) contained within the bacteria that are larger than 45 kb (Brock & Madigan, 1988). Pathogenicity traits have also been found to be megaplasmid associated. The δ -endotoxin of entomopathogenic *Bacillus thuringiensis* (Gonzalez *et al.*, 1982) and genes for *Agrobacterium tumefaciens* causing crown gall in plants (Brock & Madigan, 1988; Coplin, 1989) are located on megaplasmids.

In *Xenorhabdus* spp. plasmids have been reported (Couche *et al.*, 1987), and studies conducted to determine if phase variation is linked to plasmid-encoded genes (Leclerc & Boemare, 1991). Three strains of *X. nematophilus* (A24, F1, NC116) and strain Dan of *X. bovienii* were evaluated to determine if phase variation was linked to plasmid content. No difference was observed between the undigested or digested plasmid DNA patterns of the two phases from the three *X. nematophilus* strains, whilst no plasmids were detected in either phase of *X. bovienii* strain Dan. Probes were prepared from restriction enzyme digested *X. nematophilus* A24 plasmid DNA, and attempts to hybridise plasmid probes with either undigested or digested chromosomal DNA from the two phases of strain A24 were unsuccessful. The results suggest that neither a difference in plasmid content nor a plasmid recombination with the chromosome is involved in phase variation. However, hybridisation patterns revealed homologous DNA sequences among the three plasmids of strain A24 and among the plasmids of strains such as A24 and NC116. Each *X. nematophilus* strain was isolated from geographically distant countries, suggesting the plasmids may encode similar proteins. DNA sequence analysis will be required to provide evidence for this hypothesis.

1.9.5.1.2 Megaplasmids

Smigielski (Smigielski & Akhurst, 1994) examined 18 strains of *Xenorhabdus* and *Photorhabdus* spp. for the presence of megaplasmids. All contained either one or two

megaplasms, ranging from 48 to > 680 kb. No cross hybridisation between megaplasms from different species, or differences in plasmid profiles between P1 and P2 bacteria, was observed. Again these results suggest phase variation is not due to plasmid loss.

The *Xenorhabdus* and *Photorhabdus* genomes were estimated to be approximately 4.2×10^6 bp (the size of the *E. coli* genome (Brock & Madigan, 1988)) to assess the information input of these megaplasms (Smigielski & Akhurst, 1994). The percentage of total DNA contained in these molecules ranges from 2.5 to 20%. These numbers suggest an importance of megaplasms to *Xenorhabdus* and *Photorhabdus* spp., as the energy requirement for the replication of these plasmids is significant when considering the overall energy requirement for cell growth and division. Analysis of these plasmids through curing and transfer studies might reveal whether megaplasms are involved in the symbiotic relationship between *Xenorhabdus* and *Photorhabdus* spp. and entomopathogenic nematodes (Smigielski & Akhurst, 1994).

1.9.5.2 Regulation of phase variant characteristics by post-translational modifications

1.9.5.2.1 *P. luminescens* lipase (*lip-1*)

The lipase gene of *P. luminescens*, known as *lip-1*, has been cloned and sequenced (Wang & Dowds, 1993). The *lip-1* gene can be expressed off of its own promoter in *E. coli* and encodes a protein of 645 amino acids (Wang & Dowds, 1993). Two possible promoters were identified by primer extension analysis, a σ^{70} like sequence starting at -4, and a less conserved promoter starting at -9. Lipase gene transcription is initiated at the same site in the two phases of bacteria, and Northern analysis revealed mRNA accumulates to the same extent in the two *P. luminescens* phases (Wang & Dowds, 1993). Western analysis with antisera against the 66 kDa protein revealed that both P1 and P2 forms were secreting the lipase protein, and expressing lipase in equal amounts. Lipase was inactive when expressed by P2 bacteria, however lipase was activated by treatment with SDS (Wang & Dowds, 1993). This data suggests lipase gene expression in P2 cells is repressed at a post-translational level.

1.9.5.2.2 *P. luminescens* protease

The protease of *P. luminescens* Hm has been characterised as a monomeric alkaline metalloprotease, with an approximate molecular weight of 61 kDa, a pH optimum near 8, and

an isoelectric point of 4.2 ± 0.2 (Schmidt *et al.*, 1988; Bowen *et al.*, 2000). Protease is also phase regulated, with activity being 10 times greater in P1 than in P2 cells. The protease gene has not been isolated, nor has antiserum been raised against this protein (Forst *et al.*, 1997). However, it has been shown that protease activity is almost as high in P2 as in P1 extracellular extracts after SDS treatment (Forst *et al.*, 1997). This suggests protease is probably inactivated in the same way as lipase since the P2 forms of both enzymes can be activated by SDS treatment *in vitro* (Wang & Dowds, 1993).

The combined data from lipase and protease studies suggest a common post-translational control mechanism, for these proteins in *P. luminescens*. Neither the lipase or protease genes, nor their gene products have been isolated from *Xenorhabdus* spp.

1.9.6 The proposed role of repressor molecules in phase variation

Frackman and Nealson (Frackman *et al.*, 1990) suggest P2 forms of bacteria may either lack an activator needed for expression of phase variant characteristics or produce a repressor of these characteristics. This hypothesis was investigated using the *lux* genes for bioluminescence cloned from *P. luminescens*. The *lux* genes have been isolated from four different strains of *P. luminescens* by screening *E. coli* banks for light emission (Frackman *et al.*, 1990; Szittner & Meighen, 1990; Wang & Dowds, 1991; Xi *et al.*, 1991). The *lux* gene sequence and arrangement in *P. luminescens* is similar to Vibrionaceae and Photobacterium genera of marine bacteria suggesting a common evolutionary origin (Szittner & Meighen, 1990). Vibrionaceae are phylogenetically separate from *P. luminescens*, suggesting the genes were acquired by horizontal gene transfer. This gene transfer has probably occurred more than once as the chromosomal location of the *lux* genes differs between a strain of *P. luminescens* isolated from a human wound and two nematode symbiont strains, however the gene sequences were 80-95% identical (Meighen & Szittner, 1992). Marine luminous bacteria are subject to gene regulation by a variety of different factors including autoinduction, catabolite repression, iron concentration, osmolarity and oxygen concentration (Nealson *et al.*, 1990). Most bioluminescent bacteria are found in marine environments either living saprophytically or in symbiotic association with marine organisms (Nealson & Hastings, 1979). *P. luminescens* has been found only in terrestrial environments, usually in association with nematodes. Therefore *P. luminescens* has evolved mechanisms to regulate

bioluminescence in response to its environment and the needs of a terrestrial nematode, which would vary from that of marine luminous bacteria (Nealson *et al.*, 1990).

1.9.6.1 Regulation of the *P. luminescens lux* operon by a proposed repressor

The regulatory genes of the *P. luminescens lux* gene system have not been identified. However an 11 kb region of DNA has been cloned (pCGLS1) that encodes *lux* and regulates the expression of this system in a similar manner to the wild type (Frackman *et al.*, 1990). As the luminous system is also expressed in *E. coli* this suggests that either the genes that regulate the luminous system are present in *E. coli*, or that the regulatory genes are present on the 11 kb DNA insert. Further study suggested the presence of a closely linked transcriptional unit, found on pCGLS1, which encodes a positive regulatory gene (Frackman *et al.*, 1990).

When *P. luminescens* is grown in a rich medium such as L-broth, bioluminescence remains low until the cells reach the late logarithmic or early stationary phase of growth. The bioluminescence increases after the culture reaches an A_{560} of 2.0 or more; whilst maximal light production occurs after the culture reaches a stationary phase A_{560} greater than 4.0. *E. coli* carrying a plasmid pCGLS1 carrying genes for bioluminescence shows a similar pattern of development to *P. luminescens* (Frackman *et al.*, 1990). Two significant differences in the pattern of bioluminescence expression were noted. The *E. coli* strain produced 10 - 15 fold more light than *P. luminescens*, whilst the magnitude of increase in light production in late growth phase was approximately 10 - fold smaller in the *E. coli* strain than in *P. luminescens*. These differences are likely to be due to a gene dosage effect, as pCGLS1 (based on pUC18) is present at a high copy number in the cell. Cultures were grown at 28 - 30°C for these experiments where the copy number for pUC18 is < 25 copies per cell. The *E. coli* host strain used was DH α 5F'I^Q which carries the *lacI*^Q repressor gene on an F' episome producing 10 - fold more repressor than is found in most host strains. The combination of the low copy number at 28°C and the *lacI*^Q gene should maintain the *lac* promoter present on pUC18 in a repressed state unless an inducer is present. Therefore expression of *lux* is not likely to be due to plasmid promoter activity (Frackman *et al.*, 1990).

When P1 and P2 *P. luminescens* were transformed with pCGLS1, carrying the *P. luminescens lux* genes, the amount of light emitted by the two forms was equivalent. Furthermore the production of light, as a function of growth, by these strains was similar to that for *E. coli* carrying the cloned *lux* genes. Light production was found to be approximately 10 times

higher in the transformed strains than in the non-recombinant P1 cultures. Earlier induction of light in the recombinant strains is probably due to plasmid copy number (Frackman & Neelson, 1990). Dowds (Dowds, 1997) suggests P2 bacteria produce a repressor of bioluminescence that was diluted out by the excess of *lux* gene products formed from the multicopy plasmid. The proposed repressor may have a partial effect or be unstable as light emission occurred slightly later in the growth cycle of transformed P2 cultures (Dowds, 1997).

1.9.6.2 Identity of the *lux* operon repressor

Experimentation by Hosseini (Hosseini & Neelson, 1995) to identify the nature of the proposed *lux* repressor concluded;

1. Light emission from P1 cells begins late in the growth cycle at a density of approximately 4 A₅₆₀ units, however light emission occurs earlier in the presence of transcription inhibitors such as rifampicin.
2. Rifampicin derepresses bioluminescence in the P2 cultures so that it occurs at the same time and to the same extent as P1 cultures treated with rifampicin.

Hosseini noted that an inhibitor of protein synthesis did not have the same effect as rifampicin, and argued that the repressor may be an RNA molecule, presumably an antisense RNA that inhibits translation of the *lux* mRNA. In the absence of the putative antisense RNA, the *lux* mRNA would be more abundant, resulting in the increased synthesis of lux proteins.

1.9.7 Homoserine lactone autoinducers

A putative homoserine lactone based autoinducer involved in the regulation of *Xenorhabdus* virulence has been identified (Dunphy *et al.*, 1997). Chloroform extraction of media conditioned with wild type *X. nematophilus* led to the isolation of a compound with the same chromatographic mobility as *N*- β -Hydroxybutanoyl homoserine lactone (HBHL), as well as the ability to stimulate the luminescence of a dim autoinducer-dependent mutant of *V. harveyi* (Dunphy *et al.*, 1997).

1.9.7.1 *N*- β -Hydroxybutanoyl homoserine lactone (HBHL) autoinducer

HBHL is an autoinducer of the luminescent system of *Vibrio harveyi*, and restored virulence to transposon induced avirulent strains of *X. nematophilus* (Dunphy *et al.*, 1997). HBHL was shown to increase levels of mutant lipase excretion by 175%, and lowered phenoloxidase activity 80% in the haemolymph of insects infected with *X. nematophilus* (Dunphy *et al.*, 1997). Mortality of insects infected with *X. nematophilus* was restored by injection of HBHL into the haemolymph, whilst HBHL injection alone did not kill the *G. mellonella* (Dunphy *et al.*, 1997). As insect mortality occurs at a critical concentration of *X. nematophilus* (Dunphy & Webster, 1991), a density-dependent global regulator may initiate the release of toxic factors (Dunphy & Hurlbert, 1995).

1.9.7.2 Experimental evidence for a homoserine lactone autoinducer using the *V. harveyi lux* operon

The *V. harveyi lux* operon was transferred into avirulent and wild type *X. nematophilus* by conjugation, generating dim and bright luminescent strains respectively. These strains responded to HBHL, an agonist (β -hydroxyvaleryl homoserine lactone), and antagonist (β -hydroxyhexanoyl homoserine lactone) in a similar fashion to the luminescence of dim autoinducer-deficient and bright wild-type strains of *V. harveyi*. These results suggest a similar HBHL-dependent regulatory system in *X. nematophilus* and *V. harveyi* (Dunphy *et al.*, 1997).

The light emission by *X. nematophilus* containing the *V. harveyi lux* genes was 50 times brighter than that for *E. coli* cells containing the same plasmid. The luminescent intensity of *X. nematophilus* was observed to be growth dependent and exhibited a lag effect characteristic of light emission in the native *V. harveyi* strain. Expression lag in *V. harveyi* is due to excretion of *lux* autoinducer, HBHL, which accumulates in the media and triggers the induction of luminescence at higher cell densities (Dunphy *et al.*, 1997).

Conjugation of the *V. harveyi lux* operon into the avirulent *X. nematophilus* strain generated a dim phenotype that only increased at much higher cell density than the transconjugated wild type *X. nematophilus*. When synthetic HBHL was added to the transconjugated wild type and avirulent strains of *X. nematophilus* there was a shift in the induction of light to an earlier

stage of growth, a large increase in the luminescence of the avirulent strain and a small increase in the wildtype strain. HBHL had no effect on the luminescence of *E. coli* containing *V. harveyi lux* operon or *V. fischeri* that has a closely related homoserine lactone autoinducer. These results indicate HBHL or a very closely related molecule is the regulatory factor in *X. nematophilus* (Dunphy *et al.*, 1997).

1.9.8 Repression or induction of the *lux* operon

When comparing the work of Frackman (Frackman *et al.*, 1990) and Dunphy (Dunphy *et al.*, 1997) an obvious difference in *lux* expression patterns in an *E. coli* host is observed. Frackman (Frackman *et al.*, 1990) found *E. coli* carrying plasmid based *P. luminescens lux* genes (pCGLS1) was able to express *lux* comparably to wild type *P. luminescens*, whilst Dunphy (Dunphy *et al.*, 1997) found a 50 fold difference in the expression of plasmid based *V. harveyi lux* genes by *X. nematophilus*. These differences may be due to methods of data collection, data measurement, or amount of *lux* related DNA contained on the plasmid being studied. Frackman (Frackman *et al.*, 1990) suggests the presence of a positive regulatory element encoded by the 11 kb region of cloned DNA (pCGLS1) containing the *P. luminescens lux* genes, citing this as a reason why P1 and P2 *P. luminescens* are equally luminescent when transformed with the cloned *P. luminescens lux* genes. This is in direct conflict with Dowds suggestion that the equal luminescence of P1 and P2 bacteria is due to a repressor molecule being sequestered in the presence of a moderate copy number plasmid (Dowds, 1997). Dunphy (Dunphy *et al.*, 1997) suggests the homoserine lactone autoinducer stimulates another molecule to stimulate *lux*, the reasoning for this being that addition of HBHL to avirulent *X. nematophilus* carrying the *lux* operon induces luminescence, whereas addition of HBHL to *E. coli* carrying the *lux* operon has no effect on luminescence. The Dunphy (Dunphy *et al.*, 1997) construct must be lacking the proposed putative positive regulatory region encoded on pCGLS1, otherwise *E. coli* carrying pCGLS1 would have a similar luminescence to wild type *P. luminescens*.

1.9.9 Independent regulation of a collection of phase variant characteristics

Much of the evidence regarding the regulation of phase variant characteristics suggests independent types of regulation of different collections of phenotypes. The following list of evidence is provided by Dowds (Dowds, 1997).

1. Intermediate phases have been isolated that display protease activity typical of P1 *P. luminescens*, lipase and antibiotic activity typical of P2 and intermediate degrees of pigmentation and bioluminescence.
2. A mutant isolated by Hosseini (Hosseini & Neilson, 1995) over-expressed pigment, light and antibiotics. These were also produced earlier in growth cycle than in wild type.
3. Krasomil-Osterfeld and Ehlers (Krasomil-Osterfeld & Ehlers, 1994) found a decrease in osmolarity could induce a P1 to P2 shift, and that increased osmolarity reversed this shift for *P. luminescens*.
4. Phase variant characteristics expressed by *P. luminescens* that respond to changes in osmolarity are cell morphology, inclusion bodies, pigmentation, luminescence and antibiotic production (Krasomil-Osterfeld & Ehlers, 1994).
5. Low osmolarity failed to reduce lipase and protease to the low levels seen in P2 cultures and a variety of different pigment colours were produced under different conditions (Krasomil-Osterfeld & Ehlers, 1994). This implies that different characteristics are controlled separately.

All the available data strongly suggests it is unlikely that phase variant characteristics are controlled independently of each other. It is probable there is a master switch that differentially affects a number of regulatory systems that in turn control one or a small number of phase variant characteristics.

1.10 Project Aims

X. bovienii are entomopathogenic bacteria that form a symbiotic relationship with nematodes from the family Steinernematidae. This symbiotic complex is able to seek out and invade a range of insect species. Upon invasion of an insect host by a bacteria-nematode complex, the bacteria are released from the nematode gut directly into the insect haemocoel. At this stage the bacteria are thought to release a variety of potential virulence factors, however most of the information about these virulence factors is based on observations regarding the secretion of factors into the bacterial culture supernatants.

An interesting hypothesis suggests some of these virulence factors could be phase variant characteristics that are differentially expressed in P1 and P2 bacteria. This seems reasonable as nematodes preferentially take up P1 bacteria, and the process of infection of insect hosts is

more efficient when P1 bacteria are present. Studies examining the role of virulence factors, and genetic engineering of *Xenorhabdus* strains, are uncommon. Thus, while much is known about infection and killing at a primary level, little is known of the molecular mechanisms driving these processes.

The primary aim of this thesis was to identify and characterise the expression of a phase variant characteristic in an attempt to contribute to the body of knowledge relating to this subset of genes. This involved the following steps:

- a. Construction of a bank of *X. bovienii* Tn5 transposon insertion mutants.
- b. Screen for mutants showing altered expression of one or more phase variant characteristics.
- c. Map selected transposon insertion mutants.
- d. Sequence and characterize DNA flanking the transposon insertions.
- e. Examine the regulation of gene(s) identified at the transcriptional and translational level.
- f. Construct in-frame deletion mutants to establish/confirm a function for the gene(s) identified.

A second aim of this work was the construction of a RecA mutant of *X. bovienii*. This is justified by the fact that:

- a. RecA deficient mutants are well known to allow increased stability of recombinant plasmids and facilitate genetic complementation analysis.
- b. In other unrelated bacteria, differential expression of virulence determinants and the process of phase variation are known to be dependent on expression of a functional RecA protein (Kooimey *et al.*, 1987; Ball *et al.*, 1990; Zagaglia *et al.*, 1991).

Thus while construction of a RecA deficient strain would allow genetic analysis of virulence factors and other aspects of bacterial physiology identified in the first aim, this work would also allow a study of the role of RecA function on phase variation and expression of potential virulence factors.

Chapter 2

Materials and Methods

2.1 Bacterial strains and plasmids

All *Xenorhabdus* spp. used in this study are listed in Table 2.1. *Escherichia coli* and *Micrococcus luteus* strains are listed in Table 2.2. Plasmid vectors and clones constructed in this study are listed with their relevant characteristics in Table 2.3.1 – 2.3.10.

2.2 Bacterial growth media

All strains of *Xenorhabdus*, *E. coli* and *M. luteus* were routinely cultivated on Nutrient Agar (NA) and in Nutrient Broth (NB) (Oxoid Ltd., London, England). Luria Bertani Broth (LB) and Luria Bertani Agar (LA) were prepared as described by Miller (Miller, 1972). Modified *Xenorhabdus* minimal media (mXMM) consisted of 10% (w/v) 10x M9 salts [Na_2HPO_4 (60g/L), KH_2PO_4 (30g/L), NH_4Cl (10g/L) and NaCl (5g/L)], 1% casamino acids (Difco) and 0.5% (v/v) filter sterilised glucose. BTB agar [NA + Bromothymol Blue 0.0025% (v/v) (Sigma Chemical Company, St Louis, Missouri, USA) and Tetrazolium Chloride 0.004% (v/v) (Sigma Chemical Company, St Louis, Missouri, USA)] was used to differentiate Phase 1 (P1) and Phase 2 (P2) *Xenorhabdus* variants. Media to determine expression of phase dependent characteristics was prepared and incubated as previously described (Boemare *et al.*, 1997a). SOC medium used in electro-transformation studies of *E. coli* contained 2% (w/v) Bacto tryptone (Difco), 0.5% (w/v) Bacto yeast extract (Difco), 10 mM NaCl, 2.5 mM KCl, 10 mM MgCl_2 , 10 mM MgSO_4 and 20 mM glucose. Antibiotics were added to broth and solid media, where required, at the following final concentrations: ampicillin (Amp), 100 $\mu\text{g/ml}$; chloramphenicol (Cm), 25 50 $\mu\text{g/ml}$; kanamycin (Km), 50 $\mu\text{g/ml}$; rifampicin (Rif), 100 $\mu\text{g/ml}$; streptomycin (Sm), 100 $\mu\text{g/ml}$; tetracycline (Tc), 5 $\mu\text{g/ml}$ and trimethoprim (Tp), 10 - 100 $\mu\text{g/ml}$.

All bacterial species were incubated at their optimum growth temperature (*Xenorhabdus* spp. at 28°C, *E. coli* and *M. luteus* at 37°C) unless otherwise indicated.

Table 2.1 *X. bovienii* strains used in this study

Strain	Description	Reference/Source
T228	Amp ^R , Sm ^R	R.J. Akhurst
XB001	Amp ^R , Km ^R :: <i>recA</i> , Sm ^R , T228	This study
XB002	XB001[pCT303]	This study
XB26(20)	Amp ^R , <i>xpsB</i> ::Tn5-Km ^R , Sm ^R , T228	This study
XB29(45)	Amp ^R , <i>xpsA</i> ::Tn5-Km ^R , Sm ^R , T228	This study
XB33(21)	Amp ^R , Tn5-Km ^R , Sm ^R , T228	This study
XB34(45)	Amp ^R , <i>xpsA</i> ::Tn5-Km, Sm ^R , T228	This study
XB41(23)	Amp ^R , Tn5-Km ^R , Sm ^R , T228	This study
XB3444	Amp ^R , Sm ^R , Δ <i>xpsB</i> , T228	This study
XB6246	Amp ^R , Sm ^R , Δ <i>xpsA</i> , T228	This study
XB92388	Amp ^R , Sm ^R , Δ <i>xpsA</i> , Δ <i>xpsB</i> , T228	This study
XB414.1	Amp ^R , Tn5- <i>xpsA-lacZ</i> -Km ^R , Sm ^R , T228	This study
XB414.2	Amp ^R , Tn5- <i>xpsA-lacZ</i> -Km ^R , Sm ^R , T228	This study
XB414.3	Amp ^R , Tn5- <i>xpsA-lacZ</i> -Km ^R , Sm ^R , T228	This study

Table 2.2 *Escherichia coli* and *Micrococcus luteus* strains used in this study

Strain	Description	Reference/Source
<i>E. coli</i> BL21(DE3)	F, <i>ompT</i> , <i>hsdS_B</i> , (<i>r_B⁻ m_B⁻</i>), <i>gal</i> , <i>dcm</i> , (DE3)	Novagen
<i>E. coli</i> DK1	Δ (<i>sr1-recA</i>)	(Casadaban & Cohen, 1980)
<i>E. coli</i> DH5 α	F, ϕ 80 <i>lacZ</i> Δ M15, Δ (<i>lacZYA-argF</i>) U169, <i>endA-1</i> , <i>recA-1</i> , <i>hsdR-17</i> (<i>r_k⁻ m_k⁺</i>), <i>deoR</i> , <i>thi-1</i> , <i>supE-44</i> , <i>gyrA-96</i> , <i>relA-1</i> , λ	B.R.L (Gibco)
<i>E. coli</i> JC14604	F, <i>lac⁻</i> , <i>hsdR</i> , Δ (<i>sr1-recA</i>)306	(Clark, 1973)
<i>E. coli</i> SM10 λ pir	<i>thi-1</i> , <i>thr</i> , <i>leu</i> , <i>tonA</i> , <i>lacY</i> , <i>supE</i> , <i>recA::RP4-2-Tc::Mu</i> , Km ^R , λ pir	(Miller & Mekalanos, 1998)
<i>E. coli</i> SY327 λ pir	Δ (<i>lac-pro</i>), <i>argE</i> (Am), <i>rif</i> , <i>nalA</i> , <i>recA56</i>	(Donnenberg & Kaper, 1991)
<i>Micrococcus luteus</i>		IMVS, Adelaide, South Australia

Table 2.3.1 General purpose plasmids used in this study

Plasmid	Description	Reference /Source
pBR322	Amp ^R , Tc ^R .	NEB
pBSL15	Source of Km ^R cassette.	(Alexegev, 1995)
pBSL86	Source of Km ^R cassette.	(Alexegev, 1995)
pCVD442	Suicide vector, Amp ^R , <i>sacB</i> , <i>mobRP4</i> , replication dependent on λ <i>pir</i> .	(Donnenberg & Kaper, 1991)
pET29a(+)	IPTG induced expression vector, Km ^R .	Novagen
pGEM-7zf(+)	Cloning vector, Amp ^R .	Promega
pGEM-T	PCR fragment cloning vector, Amp ^R .	Promega
pGEM-T Easy	PCR fragment cloning vector, Amp ^R .	Promega
pMU575	Transcriptional fusion vector, carrying <i>lacZ</i> 'YA', Tp ^R .	(Praszkier <i>et al.</i> , 1989)
pSUP201.1	Mobilisable vector, Amp ^R , Cm ^R .	(Simon <i>et al.</i> , 1983)
pSUP203	Mobilisable vector, Amp ^R , Cm ^R , Tc ^R .	(Simon <i>et al.</i> , 1983)
pUT mini-Tn5 Km	Suicide vector, λ <i>pir</i> dependent, carries Tn5, Amp ^R , Km ^R .	(De Lorenzo <i>et al.</i> , 1990)
pUT mini-Tn5 Km <i>xylE</i>	Suicide vector, λ <i>pir</i> dependent, carries Tn5 containing promoterless <i>xylE</i> gene, Amp ^R , Km ^R .	(De Lorenzo <i>et al.</i> , 1990)
pWKS130	Cloning vector, Km ^R .	(Wang & Kushner, 1991)

Table 2.3.2 Plasmids associated with *X. bovienii recA* mutants XB001 and XB002

Plasmid	Description	Source
pCT300	pGEM-T with a 850 bp PCR product insert containing part of <i>X. bovienii recA</i> gene.	This study
pCT301.1	pCT301 with a Km ^R cassette inserted into the unique <i>EcoRI</i> site.	This study
pCT301.2	pCVD442 with the 850 bp <i>recA</i> fragment containing a Km ^R cassette, removed from pCT301.1 as an <i>SphI/SalI</i> fragment.	This study
pCT302	pGEM-T with the <i>recA</i> gene cloned as a 2064 bp PCR product.	This study
pCT302.1	pWKS130 containing the <i>recA</i> gene, cloned as a <i>NotI</i> fragment, in the same orientation as the <i>lacZ</i> promoter.	This study
pCT302.2	pWKS130 containing the <i>recA</i> gene, cloned as a <i>NotI</i> fragment, in the opposite orientation as the <i>lacZ</i> promoter.	This study
pCT303	pSUP203 containing the <i>recA</i> gene cloned as a <i>PstI/NotI</i> fragment.	This study

Table 2.3.3 Plasmids associated with the cloning and sequencing of *xtg*, *xpsA*, *xpsB* and *xpsC*

Plasmid	Description	Source
pCT400	pGEM7zf(+) containing mini-Tn5 Km and O end flanking chromosomal DNA from XB34(45) as a 13 kb <i>EcoRI</i> fragment.	This study
pCT400a	1000 bp <i>DraI</i> fragment containing XB34(45) chromosomal DNA and flanking O end DNA from pCT400, cloned into <i>SmaI</i> digested pGEM-7zf(+).	This study
pCT400b	1300 bp <i>DraI</i> fragment containing flanking I end DNA from pCT400, cloned into <i>SmaI</i> digested pGEM7zf(+).	This study
pCT401	pBR322 containing mini-Tn5 Km and flanking chromosomal DNA from XB26(20) as a 4.19 kb <i>ClaI</i> fragment.	This study
pCT401a	2.5 kb fragment derived from <i>DraI</i> digestion and Southern hybridisation analysis of pCT401 using DIG labelled oligonucleotide probe P2066. Cloned into <i>SmaI</i> digested pGEM7zf(+).	This study
pCT401b	1.6 kb fragment derived from <i>DraI</i> digestion and Southern hybridisation analysis of pCT401 using DIG labelled oligonucleotide probe P2066. Cloned into <i>SmaI</i> digested pGEM7zf(+).	This study
pCT402	pBR322 containing mini-Tn5 Km and flanking chromosomal DNA from XB29(45) as a 3.27 kb <i>ClaI</i> fragment.	This study
pCT402a	3.7 kb fragment derived from <i>DraI</i> digestion and Southern hybridisation analysis of pCT402 using DIG labelled oligonucleotide probe P2066. Cloned into <i>SmaI</i> digested pGEM7zf(+).	This study
pCT402b	1.1 kb fragment derived from <i>DraI</i> digestion and Southern hybridisation analysis of pCT402 using DIG labelled oligonucleotide probe P2066. Cloned into <i>SmaI</i> digested pGEM7zf(+).	This study
pCT403	pBR322 containing mini-Tn5 Km and flanking chromosomal DNA from XB34(45) as a 5.31 kb <i>ClaI</i> fragment.	This study

Table 2.3.3 continued

pCT403a	1.16 kb fragment derived from <i>DraI</i> digestion and Southern hybridisation analysis of pCT403 using DIG labelled oligonucleotide probe P2066. Cloned into <i>SmaI</i> digested pGEM7zf(+).	This study
pCT403b	0.5 kb fragment derived from <i>DraI</i> digestion and Southern hybridisation analysis of pCT403 using DIG labelled oligonucleotide probe P2066. Cloned into <i>SmaI</i> digested pGEM7zf(+).	This study
pCT404	pBR322 containing mini-Tn5 Km and flanking chromosomal DNA from XB33(21) as a 8.5 kb <i>EcoRV</i> fragment.	This study
pCT404a	0.7 kb fragment derived from <i>DraI</i> digestion and Southern hybridisation analysis of pCT404 using DIG labelled oligonucleotide probe P2066. Cloned into <i>SmaI</i> digested pGEM7zf(+).	This study
pCT404b	0.35 kb fragment derived from <i>DraI</i> digestion and Southern hybridisation analysis of pCT404 using DIG labelled oligonucleotide probe P2066. Cloned into <i>SmaI</i> digested pGEM7zf(+).	This study
pCT405	pBR322 containing mini-Tn5 Km and flanking chromosomal DNA from XB41(23) as a 7.1 kb <i>EcoRV</i> fragment.	This study
pCT405a	2.3 kb fragment derived from <i>DraI</i> digestion and Southern hybridisation analysis of pCT405 using DIG labelled oligonucleotide probe P2066. Cloned into <i>SmaI</i> digested pGEM7zf(+).	This study
pCT405b	0.48 kb fragment derived from <i>DraI</i> digestion and Southern hybridisation analysis of pCT405 using DIG labelled oligonucleotide probe P2066. Cloned into <i>SmaI</i> digested pGEM7zf(+).	This study
pCT406	7.4 kb <i>DraI</i> fragment containing XB34(45) DNA derived from pCT400, cloned into <i>SmaI</i> digested pGEM7zf(+).	This study
pCT407	4.5 kb <i>EcoRI/DraI</i> fragment containing XB34(45) DNA derived from pCT400, cloned into <i>EcoRI/SmaI</i> digested pGEM7zf(+).	This study
pCT408	pGEM-T containing a 1.5 kb PCR product derived from PAPCR of <i>X. bovienii</i> chromosomal DNA using oligonucleotides P5292 and P2177. PCR product cloned into the <i>EcoRI</i> site of pBR322.	This study

Table 2.3.4 Plasmids associated with uni-directional deletion analysis of pCT406

Plasmid	Description	Source
pCT2.1.3	Plasmid derived from 1 min exonuclease III digestion of pCT406. Sequenced with M13F oligonucleotide. See section 2.9.1 and Figure 4.11b.	This study
pCT2.1.7	Plasmid derived from 1 min exonuclease III digestion of pCT406. Sequenced with M13F oligonucleotide. See section 2.9.1 and Figure 4.11a.	This study
pCT5.1.2	Plasmid derived from 2.5 min exonuclease III digestion of pCT406. Sequenced with M13F oligonucleotide. See section 2.9.1 and Figure 4.11a.	This study
pCT5.1.5	Plasmid derived from 2.5 min exonuclease III digestion of pCT406. Sequenced with M13F oligonucleotide. See section 2.9.1 and Figure 4.11a.	This study
pCT8.1.3	Plasmid derived from 4 min exonuclease III digestion of pCT406. Sequenced with M13F oligonucleotide. See section 2.9.1 and Figure 4.11b.	This study
pCT9.1.6	Plasmid derived from 4.5 min exonuclease III digestion of pCT406. Sequenced with M13F oligonucleotide. See section 2.9.1 and Figure 4.11b.	This study
pCT11.1.1	Plasmid derived from 5.5 min exonuclease III digestion of pCT406. Sequenced with M13F oligonucleotide. See section 2.9.1 and Figure 4.11a.	This study
pCT14.1.2	Plasmid derived from 7 min exonuclease III digestion of pCT406. Sequenced with M13F oligonucleotide. See section 2.9.1 and Figure 4.11a.	This study
pCT4.1R.1	Plasmid derived from 2 min exonuclease III digestion of pCT406. Sequenced with M13R oligonucleotide. See section 2.9.2 and Figure 4.11b	This study
pCT5.1R.1	Plasmid derived from 2.5 min exonuclease III digestion of pCT406. Sequenced with M13R oligonucleotide. See section 2.9.2 and Figure 4.11b.	This study

Table 2.3.4 continued

pCT6.1R.5	Plasmid derived from 3 min exonuclease III digestion of pCT406. Sequenced with M13R oligonucleotide. See section 2.9.2 and Figure 4.11b.	This study
pCT6.1R.7	Plasmid derived from 3 min exonuclease III digestion of pCT406. Sequenced with M13R oligonucleotide. See section 2.9.2 and Figure 4.11b.	This study
pCT8.1R.9	Plasmid derived from 4 min exonuclease III digestion of pCT406. Sequenced with M13R oligonucleotide. See section 2.9.2 and Figure 4.11b.	This study
pCT9.1R.2	Plasmid derived from 4.5 min exonuclease III digestion of pCT406. Sequenced with M13R oligonucleotide. See section 2.9.2 and Figure 4.11b.	This study

Table 2.3.5 Plasmids associated with uni-directional deletion analysis of pCT407

Plasmid	Description	Source
pCT1.2.1	Plasmid derived from 30 sec exonuclease III digestion of pCT406. Sequenced with M13F oligonucleotide. See section 2.9.3 and Figure 4.12.	This study
pCT5.2.2	Plasmid derived from 2.5 min exonuclease III digestion of pCT406. Sequenced with M13F oligonucleotide. See section 2.9.3 and Figure 4.12.	This study
pCT10.2.1	Plasmid derived from 5 min exonuclease III digestion of pCT406. Sequenced with M13F oligonucleotide. See section 2.9.3 and Figure 4.12.	This study
pCT7.2R.4	Plasmid derived from 3.5 min exonuclease III digestion of pCT406. Sequenced with M13R oligonucleotide. See section 2.9.4 and Figure 4.12.	This study
pCT10.2R.2	Plasmid derived from 5 min exonuclease III digestion of pCT406. Sequenced with M13R oligonucleotide. See section 2.9.4 and Figure 4.12.	This study

Table 2.3.6 Plasmids associated with construction of *xpsA* transcriptional fusion transposon insertions XB414.1, XB414.2 and XB414.3

Plasmids	Description	Source
pCT410	pGEM-T containing 1.9 kb <i>mob</i> fragment PCR amplified from pSUP201.1 using oligonucleotides P3537/P3538.5.	This study
pCT410.1	pMU575 containing <i>mob</i> from pCT410 cloned into a unique <i>XhoI</i> site.	This study
pCT411	pGEM-T Easy containing a 438 bp PCR product generated by amplification of <i>X. bovienii</i> chromosomal DNA using oligonucleotides P3679/P6247.	This study
pCT412	0.45 kb <i>EcoRI</i> fragment from pCT411 cloned into similarly digested pGEM7zf(+).	This study
pCT413	0.45 kb <i>HindIII/XbaI</i> fragment from pCT412 cloned into similarly digested pMU575.	This study
pCT414	3.5 kb <i>DraI</i> fragment from pCT413 cloned into the unique <i>SfiI</i> site of mini-Tn5 Km <i>xylE</i> . <i>xylE</i> was removed as an <i>SfiI</i> fragment and the 5' protruding <i>SfiI</i> ends filled with T4 DNA polymerase.	This study

Table 2.3.7 Plasmids associated with construction of *xpsA* inframe deletion mutant $\Delta 6246$

Plasmid	Description	Source
pCT420	1208 bp and 1399 bp PCR products generated by amplification of <i>X. bovienii</i> chromosomal DNA, by oligonucleotide pairs P6054/P6247 and P6246/P6256 respectively, were <i>EcoRI</i> digested, ligated together and further ligated to pGEM-T.	This study
pCT421	2.6 kb <i>SalI/SphI</i> fragment from pCT420 cloned into similarly digested pCVD442.	This study
pCT422	1.2 kb Km ^R cassette from pBSL86 cloned into a unique <i>SacI</i> site of pCT421. <i>SacI</i> site is located in pCVD442 derived DNA.	This study

Table 2.3.8 Plasmids associated with construction of *xpsB* inframe deletion mutant $\Delta 3444$

Plasmid	Description	Source
pCT423	1622 bp PCR product generated by amplification of pCT408 plasmid DNA, using oligonucleotides P5292/P6249, cloned into pGEM-T.	This study
pCT424	2083 bp PCR product generated by amplification of <i>X. bovienii</i> chromosomal DNA, using oligonucleotides P6248/P6257, cloned into pGEM-T.	This study
pCT425	1.6 kb <i>EcoRI/SalI</i> fragment from pCT423 cloned into similarly digested pGEM7zf(+).	This study
pCT426	2.1 kb <i>EcoRI/SphI</i> fragment from pCT424 cloned into similarly digested pCT425.	This study
pCT427	3.7 kb <i>SalI/SphI</i> fragment from pCT426 cloned into similarly digested pCVD442.	This study
pCT428	1.2 kb Km ^R cassette from pBSL86 cloned into a unique <i>SacI</i> site of pCT427. <i>SacI</i> site is located in pCVD422 derived DNA.	This study

Table 2.3.9 Plasmids associated with construction of *xpsA*, *xpsB* inframe deletion mutant $\Delta 92388$

Plasmid	Description	Source
pCT429	1207 bp PCR product generated by amplification of <i>X. bovienii</i> chromosomal DNA, with oligonucleotides P6054/P6247, cloned into pGEM-T.	This study
pCT430	209 bp PCR product generated by amplification of <i>X. bovienii</i> chromosomal DNA, with oligonucleotides P6246/P92388, cloned into pGEM-T.	This study
pCT431	1.22 kb <i>EcoRI/SalI</i> fragment from pCT429 cloned into similarly digested pGEM7zf(+).	This study
pCT432	0.23 kb <i>EcoRI/SphI</i> fragment from pCT430 cloned into similarly digested pCT431.	This study
pCT433	1.5 kb <i>SalI/SphI</i> fragment from pCT432 cloned into similarly digested pCVD442.	This study
pCT434	1.2 kb Km ^R cassette from pBSL86 cloned into a unique <i>SacI</i> site of pCT433. <i>SacI</i> site is located on pCVD442 derived DNA.	This study

Table 2.3.10 Plasmids associated with the over-expression of *xpsA*

Plasmid	Description	Source
pCT445	3209 bp PCR product generated by amplification of <i>X. bovienii</i> chromosomal DNA, using oligonucleotides P3412/P5435, cloned into pGEM-T	This study
pCT446	3.2 kb <i>NdeI/NotI</i> fragment from pCT445 cloned into similarly digested pET29a(+).	This study

2.3 Maintenance of bacterial strains

All strains were stored in Wheaton vials (Millville, New Jersey, USA) in a 1 ml solution of 32% (v/v) glycerol and 0.6% (w/v) Bacto peptone (Difco) at -70°C . Lyophilised stocks (see below) were stored *in vacuo* in sealed glass ampoules at 4°C . Fresh single colonies of *Xenorhabdus*, *E. coli* and *M. luteus* strains were prepared by streaking a loopful of glycerol stock onto the appropriate media and incubated for the appropriate time at the correct temperature. For routine use, cultures were maintained on agar plates at 4°C .

Lyophilisation of bacterial cultures was performed by suspending several colonies in 300 μl of 10% (w/v) sterile skim milk. Approximately 200 μl of each bacterial suspension was dispensed into sterile 0.25 x 4 inch freeze-drying ampoules and plugged with cotton wool. The samples were then lyophilised in a Dynavac engineering freezer drier at -50°C . After releasing the vacuum the cotton wool plugs were pushed well down the ampoule and a constriction was made just above the level of the plug. The ampoules were evacuated to a partial pressure of 30 microns, sealed at the constriction without releasing the vacuum and stored at 4°C .

2.4 Animals

Pathogen free BALB/C female mice were obtained from the Animal Services Branch (Adelaide University, Adelaide, South Australia, Australia), for use in raised polyclonal antibodies. All mice were handled and used in accordance with the University Ethics Committee guidelines.

2.5 Chemicals and reagents

Chemicals were Analar grade. Unless otherwise stated, all chemicals used in this study were purchased from either Ajax Chemicals (Auburn, New South Wales, Australia), BDH Laboratory Supplies (Poole, Dorset, England) or Sigma Chemical Company (St Louis, Missouri, USA). Acetic acid, HCl, phenol, EDTA, SDS, sodium chloride, sodium acetate, and sucrose were purchased from BDH Laboratory Supplies. Ethanol, methanol, propan-2-ol, chloroform and formaldehyde were obtained from Ajax Chemicals. Congo Red, Coomassie brilliant blue R250, deionised formamide, TEMED, ONPG, and X-pho were obtained from

Sigma Chemical Company. X-gal was purchased from Progen Industries Ltd. (Darra, Queensland, Australia). DIG DNA labelling and detection kits, DIG-11-dUTP, Tris base, IPTG, NBT, glycogen, herring sperm DNA, glycine, and Amp were purchased from Roche. All other antibiotics were purchased from Sigma Chemical Company. dNTP's were purchased from Amersham Pharmacia Biotech.

The following electrophoresis grade reagents were obtained from the sources indicated: DNA grade agarose (Progen Industries Ltd.), acrylamide and (APS) ammonium persulphate (BioRad, Richmond, California, USA), and ultra pure N,N-methylene bis acrylamide and urea (Bethesda Research Laboratories, Grand Island, New York, USA). Pre-made acrylamide and bis acrylamide stock solutions were purchased from BioRad.

Milli-Q H₂O was used to prepare all buffers and reagents for DNA and RNA manipulation. Additional reagents and buffers were prepared with deionised water.

2.6 Enzymes and antibodies

Restriction endonucleases were routinely purchased from either Roche, New England Biolabs (Beverly, Massachusetts, USA) or Progen Industries Ltd and used according to the manufacturers instructions. Lysozyme, pronase, T4 DNA ligase, terminal transferase, shrimp alkaline phosphatase (SIP) and Klenow fragment of *E. coli* DNA polymerase I were obtained from Roche. *TaqBead*TM Hot Start Polymerase was purchased from Promega and MLV reverse transcriptase was purchased from Gibco. Horseradish peroxidase-conjugated sheep anti-mouse IgG was obtained from Amersham Pharmacia Biotech. Anti-digoxigenin-AP (Fab fragments) was obtained from Roche. Nucleotide sequencing kits using either dye-labelled primer or dye-labelled terminators were purchased from Applied Biosystems. Double-stranded Nested Deletion kits (Erase-a-Base kit) were purchased from (Promega).

2.7 DNA extraction procedures

2.7.1 Plasmid DNA isolation

Plasmid DNA was extracted by one of the three following procedures.

Method 1: Small scale quantities of plasmid DNA (3 to 5 µg per ml) were purified from *E. coli* by a modification of the three step alkali lysis method (Sambrook *et al.*, 1989). An

O/N culture (1.5 ml), was collected in a 1.5 ml reaction tube (Sarstedt) by centrifugation (30 sec, 20 000×g, Eppendorf) and the pellet resuspended in 100 µl of Solution 1 [50 mM glucose, 25 mM Tris-HCl (pH 8.0), 10 mM EDTA]. After the addition of 200 µl Solution 2 [200 mM NaOH, 1% (w/v) SDS], the sample was incubated on ice for 5 min. 150 µl of Solution 3 [3M potassium acetate, 2M acetic acid (pH 4.8)] was further added, followed by a 5 min incubation on ice. Cell debris was collected by centrifugation (5 min, 20 000×g, Eppendorf), and the supernatant was extracted with an equal volume of TE-equilibrated phenol:chloroform (1:1) in a fresh tube. The aqueous phase was transferred to a fresh reaction tube, plasmid DNA was precipitated in 2 vol of absolute ethanol, collected by centrifugation (10 min, 20 000×g, Eppendorf), washed with 70% (v/v) ethanol and dried *in vacuo*. The DNA pellet was resuspended in 50 µl Milli-Q H₂O and stored at 4°C.

Method 2: Small scale plasmid DNA purification for use as a template in nucleotide sequence analysis was prepared using a modified alkaline/SDS lysis method. O/N bacterial cell cultures (10 ml) were pelleted by centrifugation (10 min, 12 000×g, JA20 rotor using a Beckman J2-21M ultracentrifuge). The cell pellets were resuspended in 300 µl Solution P1 [50 mM glucose, 25 mM Tris-HCl (pH 8.0), 10 mM EDTA]. Cells were lysed by the addition of 300 µl Solution P2 [200 mM NaOH, 1.0% SDS (w/v)] and gently mixed until the lysate was homogenous. The cell lysate was incubated for 5 min at room temperature (RT) prior to the addition of 300 µl Solution P3 [3.2 M potassium acetate, adjusted with acetic acid to pH 5.0]. The tube was inverted several times and left on ice for 15 min. The cellular debris was removed by centrifugation (15 min, 20 000×g, Eppendorf). The supernatant was extracted twice with 400 µl of chloroform. Plasmid DNA was precipitated by the addition of 700 µl of iso-propanol and incubated at -70°C for 30 min. Plasmid DNA was collected by centrifugation (15 min, 20 000×g, Eppendorf), washed with 70% ethanol, and dried *in vacuo*. The DNA pellet was resuspended in Milli-Q H₂O and stored at 4°C.

Method 3: Qiagen-tip 20, -tip 100 and Plasmid-mega kit (QIAGEN GmbH; Hilden, Germany) were used to isolate plasmid DNA according the manufacturers instructions.

2.7.2 Preparation of bacterial genomic DNA

Genomic DNA from *X. bovienii* was isolated by modification of a previously described method (Manning *et al.*, 1986). Bacterial cells were incubated O/N in NB, pelleted in 20 ml McCartney bottles (10 min 6 000×g, MSE Minor S centrifuge), washed in normal saline and re-pelleted. Cell pellets were resuspended in 2 ml 25% (w/v) sucrose, 0.05 M Tris-HCl (pH 8.0). Lysozyme (10 mg/ml) in 1 ml of 0.25 M EDTA (pH 8.0) was added and the cell solution incubated on ice for 20 min, followed by the addition of 750 µl TE buffer, 250 µl lysis solution [5% (w/v) sarkosyl, 50 mM Tris-HCl (pH 8.0), 62.5 mM EDTA], and 1 mg solid pronase. After incubating at 56°C for 1 hr, the DNA was gently extracted twice with phenol, twice with phenol:chloroform and twice with chloroform. The genomic DNA solution was then dialysed against 5 L of TE buffer O/N at 4°C.

2.8 Analysis and manipulation of DNA

2.8.1 DNA quantitation

DNA concentration was determined using a Pharmacia LKB Ultraspec Plus Spectrophotometer, assuming that A_{260} of 1 is equal to 50 µg dsDNA/ml (Miller, 1972).

2.8.2 Restriction endonuclease digestion of DNA

Cleavage reactions with restriction endonuclease enzymes were performed using restriction buffers and reaction conditions specified by the manufacturer. 2 units of restriction endonuclease per 0.1-0.5 µg of DNA were incubated at the appropriate temperature for a minimum of 2 hr. Each digestion reaction varied depending on the concentration of DNA and the volume of digested sample required. Prior to loading onto an agarose gel, 0.1 vol of tracking dye [15% (w/v) Ficoll, 0.1% (w/v) bromophenol blue, 0.1 mg/ml RNase A] was added.

2.8.3 Agarose gel electrophoresis of DNA

Electrophoresis was performed at RT on horizontal 0.7% to 2.0% (w/v) agarose gels. The concentration of agarose depended on the expected size of the DNA fragments to be analysed. Gels were electrophoresed in Easy-CastTM gel tanks (OWL Scientific Inc.) at a maximum of 120 V for 1 - 3 hr in 1x TAE buffer [40 mM Tris, 1.5 mM EDTA, 0.012% (v/v) glacial acetic

acid], followed by staining in 1 x TAE containing 2 µg/ml EtBr for 10-15 min. DNA fragments were visualised by trans-illumination using a UV transilluminator (UVP Inc., Upland, California USA) and documented with a Tractel Gel Documentation System (Vision Systems, Salisbury, South Australia, Australia).

2.8.4 Determination of restriction fragment size

The size of DNA fragments and PCR products were calculated by comparing their relative mobility to *EcoR1* digested *Bacillus subtilis* bacteriophage SPP1 DNA. The calculated sizes of the SPP1 *EcoR1* fragments used were (in kb): 8.51; 7.35; 6.11; 4.84; 3.59; 2.81; 1.95; 1.86; 1.51; 1.39; 1.16; 0.98; 0.72; 0.49; 0.36. The size of small restriction enzyme fragments and PCR products were calculated by comparing their relative mobility with that of DNA ladder markers (DMW-100M) purchased from GeneWorks. DMW-100M ranges from 100 bp to 3 kb in exact 100 bp increments, with brighter reference bands at 1 kb and 3 kb. The computer software package DNAFRAG (Rood & Gawthorne, 1984) was used to calculate unknown fragment sizes compared to known reference markers.

2.8.5 Extraction of DNA fragments from agarose gels

The required DNA fragment was extracted from an agarose gel slice using the BRESAclean DNA Purification Kit (GeneWorks) according to the manufacturer's instructions.

2.8.6 Dephosphorylation of DNA using shrimp alkaline phosphatase (SIP)

To 0.1-0.5 µg of restriction endonuclease digested DNA 1 unit of SIP and 0.1 vol of 10x phosphatase buffer (supplied by the manufacturer) were added. The reaction was incubated for 10 min at 37°C for sticky end fragments (60 min for blunt ends), followed by inactivating SIP at 65°C for 15 min. To the contents of this reaction, 0.1 vol of tracking dye was added prior to electrophoresis on a 1% (w/v) agarose gel. The linearised dephosphorylated DNA fragment was then gel extracted as described in section 2.8.5.

2.8.7 End-filling of linear DNA by T4 DNA polymerase

Protruding 3' ends created by cleavage with restriction endonuclease were filled using T4 DNA polymerase. Approximately 1 µg of digested DNA was heated to 65°C to inactivate the restriction endonuclease. A mixture of 2 mM dNTPs to a final concentration of 40 µM was added with 2 units of T4 DNA polymerase, 0.1 vol 10x T4 DNA polymerase buffer, and incubated at 37°C for 30 min. The reaction was terminated by heating at 65°C for 30 min and the mixture extracted with phenol:chloroform. DNA was precipitated by the addition of 0.1 vol 3 M sodium acetate pH 3.2, 20 µg of glycogen, 3 vol cold absolute ethanol and incubated at -70°C for 30 min. DNA was recovered by centrifugation (20 000×g, 15 min, Eppendorf), washed in 70% ethanol and dried *in vacuo*. DNA was resuspended in an appropriate volume of Milli-Q H₂O and stored at -20°C.

2.8.8 *In vitro* cloning

DNA to be cloned was mixed with the appropriately cleaved vector DNA at an insert to vector molar ratio of 3:1. Milli-Q H₂O was used to bring the final ligation reaction volume up to 16 µl. The tube was heated to 45°C for 5 min to melt cohesive termini, cooled on ice for 1 min. To the contents of the tube, 2 µl of 10x ligation buffer (supplied by the manufacturer) and T4 DNA ligase (2 units) were added. Sticky end ligation reactions were incubated O/N at RT. For blunt end ligations, 4 units T4 DNA ligase was used in a reaction, and the incubation period was O/N at 4°C. The ratio of vector to insert DNA was modified to 1:1 when cloning chromosomal DNA fragments. Before electroporation into *E. coli*, the reaction was phenol:chloroform extracted, the top layer absolute ethanol precipitated, washed in 70% (v/v) ethanol, dried *in vacuo* and resuspended in 10 µl Milli-Q H₂O.

2.9 Construction of uni-directional deletions of cloned DNA

Uni-directional deletions of pCT406 (see Section 4.2.5.3, Figures 4.11a and 4.11b) and pCT407 (see Section 4.2.5.3, Figure 4.12), were constructed using the Erase-a-Base kit (Promega) in exact accordance with the manufacturers instructions. Specific restriction enzyme digests and oligonucleotides used to construct and generate nucleotide sequence from each nested deletion are outlined below.

2.9.1 Plasmid pCT406 and pCT407 top strands

Plasmids pCT406 and pCT407 were individually digested with *SphI* to generate a 4 nucleotide - 3' protrusion, resistant to exonuclease III digestion. Plasmid DNA was further digested with *EcoRI*, producing a 5' protrusion adjacent to the cloned insert, from which deletions could proceed (nesting site). Four to six clones from each time point were linearised with *XbaI* to determine extent of DNA deletion. Subsequent clones were sequenced with the M13 forward oligonucleotide, and gaps in the sequence were filled by oligonucleotide walking, using pCT406 as template DNA. Oligonucleotides used for sequence analysis of pCT406 are outlined in Table 2.5, Figures 4.11a and 4.11b. Oligonucleotides used for sequence analysis of pCT407 are outlined in Table 2.5 and Figure 4.12.

2.9.2 Plasmid pCT406 complementary strand

Plasmid pCT406 was digested with *SacI* to generate a 4 nucleotide - 3' protrusion, resistant to exonuclease III digestion. Plasmid DNA was further digested with *HindIII*, producing a 5' protrusion adjacent to the cloned insert, from which deletions could proceed (nesting site). Four to six clones from each time point were linearised with *NsiI* to determine extent of DNA deletion. Subsequent clones were sequenced with the M13 reverse oligonucleotide, and gaps in the sequence were filled by oligonucleotide walking, using pCT406 as the template DNA. Oligonucleotides used are outlined in Table 2.5, Figures 4.11a and 4.11b.

2.9.3 Plasmid pCT407 complementary strand

Plasmid pCT407 was digested with *NsiI* to generate a 4 nucleotide - 3' protrusion, resistant to exonuclease III digestion. Plasmid DNA was further digested with *BamHI*, producing a 5' protrusion adjacent to the cloned insert, from which deletions could proceed (nesting site). Four to six clones from each time point were linearised with *ApaI* to determine extent of DNA deletion. Subsequent clones were sequenced with the M13 reverse oligonucleotide, and gaps in the sequence were filled by oligonucleotide walking, using pCT407 as the template DNA. Oligonucleotides used are outlined in Table 2.5 and Figure 4.12.

2.10 High efficiency electrotransformation of *E. coli*

2.10.1 Preparation of competent cells

100 ml NB was inoculated with 0.1 vol of an O/N *E. coli* culture and grown to middle to late log phase with agitation at 37°C. The culture was chilled for 20 min in an ice/water slurry, and centrifuged (7 400×g, 10 min, in a JA14 rotor using a Beckman J2-21M ultracentrifuge) at 4°C. The pellet was consecutively washed in 100 ml and 20 ml sterile ice cold H₂O, followed by a 20 ml ice cold 10% (v/v) glycerol wash. The bacteria were resuspended in 2 ml ice cold 10% (v/v) glycerol and 100 µl aliquots frozen in a dry ice/ethanol bath and stored at -70°C.

2.10.2. Electroporation procedure

Electrocompetent *E. coli* were thawed on ice prior to the addition of plasmid DNA contained in a maximum volume of 10 µl H₂O. The *E. coli* Pulser™ transformation apparatus (Bio-Rad), set to 2000 V, 25 µF capacitance and 200 Ω resistance. Cold 0.2 cm electrode gap cuvettes (Bio-Rad) were used to pulse bacteria. Bacteria were immediately recovered in 1 ml of SOC medium, and incubated at 37°C for 1 hr prior to plating appropriate dilutions onto selective media.

2.11 Bacterial conjugation

Donor *E. coli* bacterial cultures grown O/N in NB were diluted 1:20 in NB and grown to early exponential phase with slow agitation to avoid damaging the sex pili. O/N *X. bovienii* cultures were used as recipient cells without subculturing. All cells were washed in NB to remove any excess antibiotic and resuspended in an appropriate volume of NB, such that approximately 1 x 10⁶ bacteria/ml of the donor organism was mixed with 1 x 10⁷ bacteria/ml of recipient. A total volume of 400 µl of cell suspension was evenly spread onto a 5 cm diameter, 0.2 µm nitrocellulose membrane filter (Millipore, USA), placed on the surface of a pre-warmed NA plate, and incubated for 16 hr at 28°C. Bacteria were then resuspended in 3 ml NB, and samples plated onto selective agar and incubated for at least 48 hr at 28°C.

2.12 Non-radioactive probe construction

2.12.1 Labelling of double stranded DNA

Purified DNA fragments from either restriction endonuclease fragments or DNA from PCR products was labelled by random primed incorporation of DIG-11-dUTP. Components of the DIG DNA labelling kit (Roche) and the method of Feinberg and Vogelstein (Feinberg & Vogelstein, 1983) were used. In a final volume of 17 μ l, purified linear DNA template (10 ng to 3 μ g), and 2 μ l 10x hexanucleotide mix (random primers), were denatured at 95°C for 10 min, and chilled immediately on ice. To this sample, 2 μ l 10x dNTP labelling mix and 1 unit Klenow were added and incubated at 37°C for 20 hr. The reaction was terminated by the addition of 0.1 vol 0.25 M EDTA, pH 8.0. Unincorporated DIG-11-dUTP was removed by precipitating the labelled DNA with 2.5 μ l 4M LiCl and 75 μ l cold absolute ethanol. After a minimum of 1 hr at -70°C, labelled DNA was collected by centrifugation (12 000 \times g, 10 min, Eppendorf) at 4°C. The DNA pellet was washed with 50 μ l cold 70% (v/v) ethanol, dried *in vacuo* and resuspended in 20 μ l 10 mM Tris -HCl, 1 mM EDTA, pH 8.0. Labelled DNA probes were stored at -20°C until required.

2.12.2 End labelled oligonucleotide probe

To 200 ng of oligonucleotide, 1 μ l 400 mM CoCl₂, 2.5 μ l tailing buffer [1.4 mM potassium cacodylate, 300 mM Tris-HCl (pH 7.2), 1 mM DTT], 2.5 μ l DIG-11-dUTP and 1 μ l terminal transferase were added, and made up to a reaction volume of 25 μ l with Milli-Q H₂O. The reaction was incubated for 1 hr at 37°C and stored at -20°C until required.

2.12.3 Digoxigenin labelling of DNA probes using PCR

Digoxigenin labelled PCR products were generated by incorporation of DIG-11-dUTP. To a PCR tube 5 μ l of PCR buffer [100 mM Tris-HCl, 500 mM KCl, pH 8.3], 4 μ l of 25 mM MgCl₂, 1 μ M of the appropriate upstream and downstream primer, 5 μ l dNTPS [2 mM dATP, 2 mM dCTP, 2 mM dGTP, 1.3 mM dTTP, 0.7 mM alkali-labile DIG-11-dUTP, pH 7.0], 50 μ g of template DNA and 1 unit of *TaqBead*TM Hot Start polymerase (Promega). Milli-Q H₂O was added to the reaction to make a final volume of 50 μ l. The thermocycling profile consisted of an initial denaturation at 95°C for 7 min, followed by 30 cycles of 95°C for 45

sec, 60°C for 1 min, 72°C for 2 min and a final extension of 72°C for 2 min. PCR products were visualised on a 1% TAE agarose gel after EtBr staining and extracted using a BRESAclean DNA Purification Kit as described in section 2.8.5.

2.13 Southern hybridisation

2.13.1 Southern transfer

Unidirectional transfers of DNA from 1.0% agarose gels to nylon membranes (Nylon membrane, positively charged, Roche) were performed as described by Southern (Southern, 1975) and modified by Reed (Reed, 1990), using capillary transfer. DNA was irreversibly bound to the membrane after either UV-crosslinking (254 nm, 5 min) or washing for 20 min in 0.4M NaOH.

2.13.2 Hybridisation

2.13.2.1 Double stranded DNA probes

Nylon membranes were incubated in a prehybridisation solution [50% (v/v) formamide, 5x SSPE (0.75 M NaCl, 0.44 M sodium phosphate buffer, 5 mM EDTA, pH 7.4), 1% (w/v) skim milk, 7% (w/v) SDS, and 250 µg/ml single stranded herring sperm DNA (Roche)] for a minimum of 2 hr at 42°C. The denatured double stranded DNA probes were combined with fresh prehybridisation solution and incubated with filters O/N at 42°C in an Extron HI 2001 hybridisation oven (Bartelt Instruments). Filters were washed 2x 5 min in 2x SSC [60 mM NaCl, 60 mM sodium citrate, pH 7.0] and 0.1% (w/v) SDS at RT, followed by 2x 20 min washes with 0.1x SSC, 0.1% (w/v) SDS at 68°C.

2.13.2.2 Oligonucleotide probes

Nylon membranes were incubated in a prehybridisation solution [1 M NaCl, 0.1 M Tris-HCl pH (7.6), 10 mM EDTA, 5x Denhardt's reagent (0.1% (w/v) Ficoll, 0.1% (w/v) polyvinylpyrrolidone, 0.1% (w/v) BSA), 0.1 mg/ml single stranded herring sperm DNA, 0.05% (w/v) SDS] for a minimum of 1 hr at 5°C to 10°C below the melting temperature of the oligonucleotide probe [$T_m = 67.5 + 34(G+C/\text{primer length}) - (395/\text{primer length})$]. Membranes were incubated in the presence of probe DNA O/N in fresh prehybridisation

solution at the calculated temperature. Stringency washes (3x 10 min) were performed at the hybridisation temperature with 5x SSC.

2.13.2.3 Detection

After a 2 min in Buffer 1 [0.1 M Tris-HCl, 0.15 M NaCl (pH 7.5)], membranes were incubated in Buffer 2 [5% (w/v) skim milk in Buffer 1] for 1 hr prior to a 30 min incubation with anti-DIG-AP Fab fragments, diluted in fresh Buffer 2 (1:5000). Membranes were washed for 2x 15 min in Buffer 1 and then neutralised with Buffer 3 [0.1 M Tris-HCl, 0.1 M NaCl, 50 mM MgCl₂ (pH 9.5)]. Colourimetric detection of target DNA was performed using 0.34 mg/ml NBT and 0.18 mg/ml X-pho in Buffer 3.

2.14 Oligonucleotide synthesis

Oligonucleotides used in this study were purchased from either the Sequencing Centre of the Institute of Medical and Veterinary Science (I.M.V.S.) Adelaide South Australia or GeneWorks Adelaide South Australia. All oligonucleotides used in this study are listed in Table 2.4, sections 2.4.1 - 2.4.4.

2.15 Polymerase Chain Reaction

2.15.1 Standard PCR reaction conditions

All PCRs performed in this study followed the general reaction conditions described. In a final volume of 50 µl, the PCR reaction contained 5 µl 10x PCR buffer [500 mM KCl, 100 mM Tris-HCl (pH 8.3)], 4 µl 25 mM MgCl₂, 3.5 µg/ml of each primer, 2.0 mM of each dNTP, 2 µl chromosomal DNA [0.5 µl plasmid DNA or 5 µl boiled lysate (see section 2.15.2)], and 1 unit *TaqBead*[™] Hot Start Polymerase (Promega). The reaction mixture was overlaid with sterile mineral oil (Sigma) prior to thermal cycling in either an FTS-320 Thermal Sequencer (Corbett Research) or a GeneAmp PCR System 2400 (Perkin Elmer). The annealing temperature for a PCR was set at 2°C lower than the lowest T_m°C of the oligonucleotide pair. Thermocycling parameters (unless otherwise stated) were 1 min at 94°C; 30 cycles of 1 min at 94°C, 30 sec at the set annealing temperature, 1 min per kb of

Table 2.4.1 General purpose oligonucleotides used in this study. Nucleotides that deviate from the normal sequence are underlined.

Oligonucleotide	Oligonucleotide sequence 5'→3'	T _m [°] C	Reference/Source
pUC/M13 Forward	GTT TTC CCA GTC ACG AC	60	Promega
pUC/M13 Reverse	CAG GAA ACA GCT ATG AC	55	Promega
P364 (anneals to deoxyribonucleotides 364 – 384 of <i>lacZ</i> carried by pMU575)	GGT TGT TAC TCG CTC ACA TT	62	This study
P735 (anneals to deoxyribonucleotides 735 – 712 of <i>lacZ</i> carried by pMU575)	AAC TTC AGC CTC CAG TAC AG	62	This study
P2177 (anneals to nucleotides 468 - 451 of pBR322)	TCT TCC CCA TCG GTG ATG	69	This study
P3537 (anneals to nucleotides 334 - 353 of pBR325)	<u>CTC</u> <u>GAG</u> CGA CTA CGC GAT CA	54	This study
P3538.5 (anneals to nucleotides 450 - 432 of pBR325)	<u>CTC</u> <u>GAG</u> GAT ATA GGC GCC AG	52	This study
P6249 (anneals to nucleotides 4274 - 4294 of pBR322)	AGT GCC ACC TGA CGT CTA AG	68	This study

Table 2.4.2 *recA* associated oligonucleotides

Oligonucleotide	Oligonucleotide sequence 5'→3'	T _m °C	Reference
PRecA1	CAC AGC AGG TTA TCA ATA TC	61	This study
PRecA2	TTA TCA ACC AGA TCC GTA TG	64	This study
PRecAF	AGG TTC TAT CAT GCG TCT GG	68	This study
PRecAR	ATA GCT GTA CCA TGC ACC TG	66	This study
P01	CAG ACG CAT GAT AGA ACC	53	This study
P02	GGT ACA GCT ATA ACG GAG	53	This study
P227	CAG CTT AGT ATT GAA CTT GG	61	This study
P1067	TTT ATT GAT GCT GAA CAT GC C C C C G C A A G		This study
P1068	CCA CCA GGA GTA GTC TCA GG T T TT T T T C		This study
P2293	AGT GAA CTG CTT GGT ACT AT	59	This study
P4958	AGT GAG CCA GTA GAG ATA GT	58	This study
P5021	CAG CTT AGT ATT GAA CTT GG	61	This study
P5022	AGT GAA CTG CTT GGT ACT AT	59	This study
P5278	CAG TGC ATT ACC ACC TGT TG	67	This study
P5285	ATA CCG TGA CAT ATC GCC AG	69	This study
P5286	TAC AGG TGA ACA GGC ACT GG	69	This study

Table 2.4.3 Oligonucleotides associated with sequence analysis of mini-Tn5 Km

Oligonucleotide	Oligonucleotide sequence 5'→3'	T _m °C	Source
P2020	GCA ATC CAT CTT GTT CAA T	65	This study
P2021	GCC TTC TTG ACG AGT TCT TC	67	This study
P2033	TTC TTG TTA TCG CAA TAG TT	61	This study
P2061	GGG TCA AGG ATC TGG ATT	64	This study
P2066	AGC TTG CTC AAT CAA TCA CC	68	This study
P2090	TTG CTC AAT CAA TCA CCG GA	72	This study

Table 2.4.4. *xtg*, *xpsA*, *xpsB* and *xpsC* associated oligonucleotides. Nucleotides that deviate from the normal sequence are underlined.

Oligonucleotide	Oligonucleotide sequence 5'→3'	Tm°C	Source
P1208C	ATA TTG AAA CCA ACG GCT GC	71	This study
P3412	ATC <u>ATA</u> TGA ACC ACC CTG AA	65	This study
P3533	ATT GAG CAA GGA ACC ATA GG	67	This study
P3679	ACA ACG CAG ATA CAC ATT AC	61	This study
P4344	GGC AGA TCC ACG ATA CTG AA	69	This study
P4345	AAC CAA CTG GCA CAT CAC CT	70	This study
P4346	GGC CAT ACA GGT TGT GAA GT	68	This study
P4347	CTC TGG CTC AAC AGG CTT AC	70	This study
P4541	ACA CCG AAC TTC ACA ACC TG	68	This study
P4975	ACC GCG AAG ACT ATC CGT CA	73	This study
P5006	CCT ATG GTT CCT TGC TCA AT	67	This study
P5007	GCC AAT AGC TCA CTG ACG GT	70	This study
P5023	TCC TCA ACA CGC TCT GAT TC	69	This study
P5124	TGG AGT CGT CAA CCG CTT GT	74	This study
P5249	GAA TTG ACA GCG GAA CGC TT	73	This study
P5289	TCA TGT GGC ATT AAT AGT GG	65	This study
P5290	TTC GTC ACT TGG CAA TCA AT	69	This study
P5291	GGA TCA CAT AAG CCA CCA GA	68	This study
P5292	ACC AGC CAT GAA TAT GAA GC	68	This study
P5293	CTA CAG CTA CAG TCA AGA AT	57	This study
P5433	CGT GTC GAG AAT ATA GAT CC	62	This study
P5434	AGG TGA CCT TGC AGG TTC AG	70	This study

Table 2.4.4 continued

P5435	AAT GTG CTC TTC AAG TTG AC	62	This study
P5436	GCT GAT GAA GAT AAC TGA CT	59	This study
P5439	GCT GAC CAC TTA ACC GTG AC	68	This study
P5483	TAC AGG TTG TGA AGT TCG CT	66	This study
P5562	TTC AGC TCG GAG TAA CTC AG	66	This study
P5563	ATC CAG TAT CAC GAA TGC AC	66	This study
P5564	GAA TTC ACT GAC CTG ACA CT	62	This study
P5565	GAC GGA ACG TAA TTG CTC AG	69	This study
P5618	GAT TCT GTT ACA TAG GAA GC	59	This study
P5619	CCG CTG AGG ATC TGA ATA CC	70	This study
P5620	AGA TCC TGA TGT GCA TAA GC	68	This study
P5723	GCA TTG ATA CCA ACT GGC AT	69	This study
P5725	CAT AAC GTT GGC AGC TCA CT	69	This study
P5837	GAT CAG ATT GTG GCA CGT CA	70	This study
P5838	CGC CTT GAC ACT CCA GTA TG	69	This study
P5839	TAG CGT TAC GGA TCC AAC TG	69	This study
P5840	TCA CAA CGC ACT CAG TTA TT	64	This study
P5842	CTG GCC TCC TGA GCA ATT AC	70	This study
P5844	AAC AGA TCC TGC AAC GTT AT	40	This study
P5845	CGG TTG TCA GTC CAT TAC AC	66	This study
P5846	ACA CGT GGT TCA TCG TCA AG	69	This study
P5847	ATA GCA GAA GCC AAC TTC AC	65	This study
P5848	TGG ATG TGG ATG ACT TCG AT	68	This study
P5849	CAT GGT GAT TAG TAT GCT GG	64	This study
P5850	TCA AGT ACC GGA TAC CAC CT	67	This study

Table 2.4.4 continued

P5851	GGA TCT ATA TTC TCG ACA CG	62	This study
P5852	CGC ACC TGA CGG AAT ATA TG	69	This study
P6012	GCG TAC CTC GTA CCG AAG TC	70	This study
P6034	TTG TGT CTG CTG ACG AGT TA	65	This study
P6035	TCT GCC TGA TTA CAT GAT CC	66	This study
P6054	CGT CCA TCA CTA TAC GAC TG	64	This study
P6109	TCT ATA CAG AGC TTC TGC CA	64	This study
P6246	CTG <u>AAT</u> <u>TCT</u> GAC GCT GAA TCC T	51	This study
P6247	<u>GAG</u> <u>AAT</u> <u>TCA</u> ACC AAC GGC TGC T	58	This study
P6248	<u>CAG</u> <u>AAT</u> <u>TCG</u> GTT GTG CAT GGA T	51	This study
P6256	GCT CAG TAT CAT TCA GTG	55	This study
P6257	AGT CTA TCG ACA GCT TAC	53	This study
P92388	GGT TGT GCA TGG ATT TCT GT	68	This study

PCR product expected at 72°C; followed by a final extension at 72°C. If the PCR product size was unknown, an extension time of 4 min was used.

2.15.2 Rapid Screening of chromosomal mutations and plasmid libraries

Rapid PCR based screening of plasmid libraries and chromosomal mutants was carried out using pools of cultures and a cross plate technique. Cells were prepared for PCR analysis by a modification of previously described methods (Gussow & Clackson, 1989; Holmes & Quigley, 1981). Briefly, a portion of a fresh bacterial colony was scraped from a NA plate and resuspended in an Eppendorf tube containing 100 µl of sterile Milli-Q H₂O. The tube was boiled vigorously for 5 min and then allowed to cool to RT before centrifugation (20 000×g, 5 min, Eppendorf) to pellet cellular debris. The supernatant was added to a fresh tube and used immediately.

Bacterial cell lysates were screened using the general PCR conditions outlined in Section 2.15.1. If large numbers of colonies were to be screened, lysates were pooled in the following manner (see Figure 2.1). Bacterial colonies to be screened were patched in batches of 50 onto an appropriately supplemented NA plates. Cells from each row and each column of each NA plate were removed and pooled in an Eppendorf tube subsequent to preparation of cell lysates, see above. Each of the 16 pooled cell lysates was subjected to PCR analysis and the amplicons analysed on a 1% TAE agarose gel. After PCR, the intersecting positive row and column pools were used to identify the positive single colony(s) on each NA patch plate. PCR of each individual lysate was carried out to confirm the positive clones.

2.15.3 Plasmid Assisted PCR Rescue (PAPCR)

2.15.3.1 PCR amplification of 5' *X. bovienii* *recA* DNA

X. bovienii T228 chromosomal DNA was doubly digested with *Eco*RI and *Bam*HI, prior to ligation to similarly digested pBR322. After ligation O/N at RT, 100 ng of the ligation mix was added to the standard PCR mixture containing oligonucleotides P1 and P2177. Thermocycling consisted of an initial 2 min at 94°C, then 30 cycles of 1 min at 94°C, 30 sec at 55°C, 3.5 min at 72°C, followed by a final 3.5 min extension at 72°C.

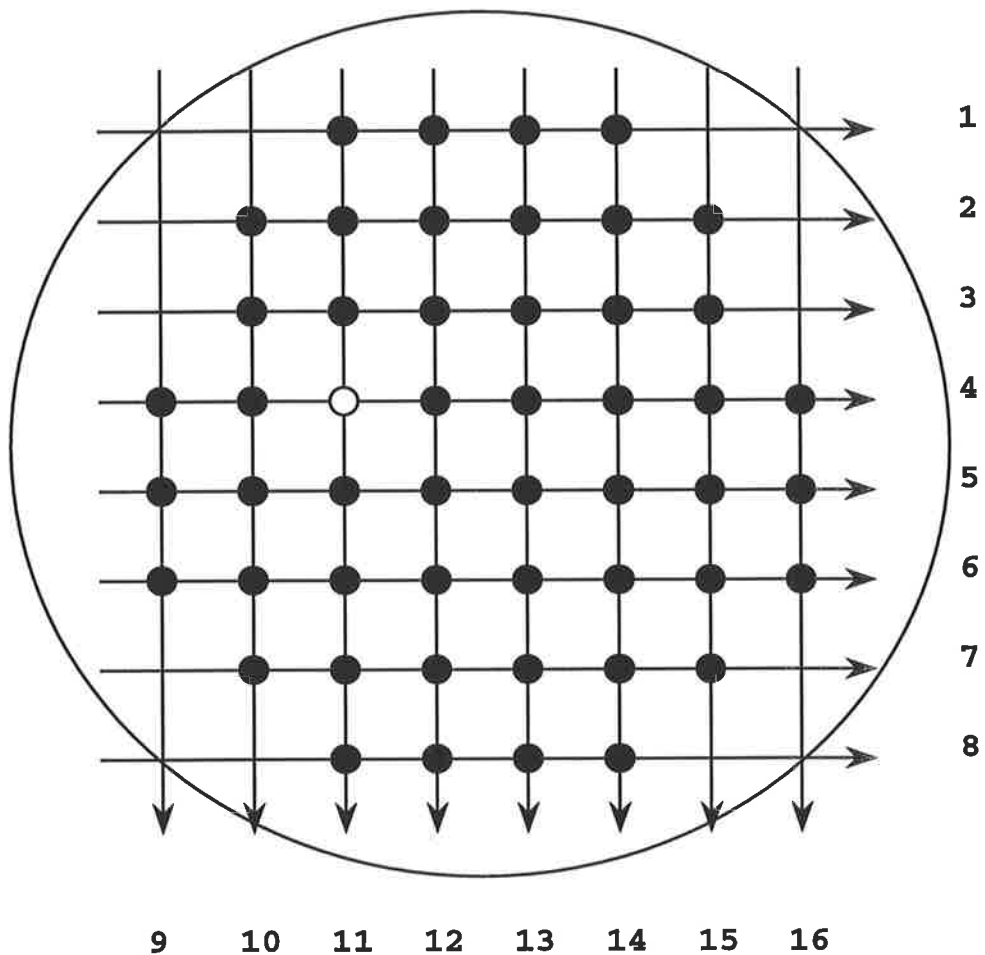


Figure 2.1 Individual bacterial colonies (represented by black dots) were scraped from the NA plate (represented by the circle) using sterile toothpicks and pooled into eppendorf tubes. The 16 eppendorf tubes were subjected to PCR analysis (see Section 2.15.2), and the products visualised on a 1% agarose gel. The intersecting positive row and column (row 4 and column 11 in the above example) were used to identify the correct (white) colony.

2.15.3.2 PCR amplification of 3' *X. bovienii* *xpsC* DNA

X. bovienii chromosomal DNA was digested with *EcoRI* and ligated to similarly digested pBR322. After ligation O/N at RT, 100 ng of the ligation mix was added to the general PCR mixture (see Section 2.15.1) including oligonucleotides P2177 and P5292. Thermocycling consisted of an initial 2 min at 94°C, then 30 cycles of 1 min at 94°C, 30 sec at 66°C, 3.5 min at 72°C, followed by a final 3.5 min extension at 72°C.

2.16 Sequence analysis

2.16.1 Dye-primer sequencing

Dye-primer sequencing reactions were carried out using the PRISM™ Ready reaction Dye primer cycle sequencing kit (Applied Biosystems) according to the manufacturers instructions. Purified plasmid template DNA (see Section 2.7.1) was used at approximately 100 ng/μl. The ddNTP termination solutions were added to template DNA in separate Gene Amp™ 0.5 ml reaction tubes (Perkin-Elmer) as follows;

Reagent	A	C	G	T
ddNTP mix	4 μl	4 μl	8 μl	8 μl
DNA template	1 μl	1 μl	2 μl	2 μl

Each reaction mixture was overlaid with 40 μl Nujol mineral oil (Perkin-Elmer). Reactions were performed in a thermal cycler (Perkin-Elmer). The thermocycling profile consisted of pre-heated to 95°C, with an initial 15 cycles of 95°C for 30 sec, 55°C for 30 sec and 70°C for 1 min, followed by 15 cycles at 95°C for 30 sec and 70°C for 1 min. DNA from the aqueous phase of each tube was then precipitated with 80 μl of 95% (v/v) ethanol and 3 μl of 3 M sodium acetate (pH 5.5) on ice for 15 min. Samples were centrifuged (20 000×g, 20 min, Eppendorf), the pellet washed once in 250 μl 70% (v/v) ethanol, dried *in vacuo* and resuspended in 5 μl of loading buffer [83% (v/v) formamide, 8.3 mM EDTA, pH 8.0] prior to loading onto a 6% polyacrylamide, 8 M urea gel. The gel was electrophoresed on an Applied Biosystems 373A automated sequencer.

2.16.2 Dye-terminator sequencing

Sequencing reactions were carried out on purified double-stranded plasmid DNA according to the manufacturer (Applied Biosystems). To 1 µg DNA template, 9.5 µl terminator premix, 3.2 pmol primer and Milli-Q H₂O were added for a final volume of 20 µl. Reactions were overlaid with 40 µl Nujol mineral oil, and placed in a DNA thermal cycler (Perkin Elmer) and pre-heated to 95°C. Thermal cycling began with an initial denaturation at 96°C for 30 sec, followed by annealing at 50°C for 15 sec and extension at 60°C for 4 min, for 25 cycles. After cycling, the extension product was diluted to a final volume of 100 µl with distilled H₂O, recovered from the mineral oil, and added to an equal volume of a solution of phenol:chloroform:water (7:2:1). Following two extractions, the aqueous layer was recovered by precipitating DNA with 10 µl 5.2 M sodium acetate and 300 µl absolute ethanol and incubated O/N at -20°C. The DNA was pelleted (20 000×g, 20 min, Eppendorf) and dried *in vacuo*. Prior to loading the sample onto a pre-electrophoresed 6% polyacrylamide, 8 M urea gel, the DNA was resuspended in 5 µl of loading buffer and denatured at 95°C for 2 min. The gel was electrophoresed on an Applied Biosystems 373A automated sequencer.

2.17 Analysis of sequence data

Raw sequencing data from the 373A Applied Biosystems automated sequencer were analysed using the Applied Biosystems Seq Ed program version 6.0. Searches for similarity to known DNA and protein sequences in databases were performed using the BLAST2 search service at EMBL (Altschul *et al.*, 1990). Similar DNA and amino acid sequences were aligned using CLUSTALX (Thompson *et al.*, 1994). PHYLIP (J. Felsenstein, University of Washington, USA) was used to determine the phylogenetic relationships of DNA and amino acid sequences. Oligonucleotides were designed using the Primer Designer Version 2 software package (Copyright 1990, 91; Scientific and Educational Software). Open reading frames (ORFs) were identified using ORF Finder (NIH), and mol% G+C analysis carried out using Artemis (Release 4) software package. Transcription start sites were predicted using the Berkeley Drosophila Genome Project Neural Network Promoter Prediction computer package. Hydrophobicity plots were calculated using PROSIS (Kyte & Doolittle, 1982). The amino acid activated by each module in *xpsA* and *xpsB* was predicted using programs found at <http://raynam.chm.jhu.edu/~nrps/> (Challis *et al.*, 2000) and MEGA version 2.1.

2.18 RNA analysis

2.18.1 RNA extraction

RNA extractions from *X. bovienii* T228 O/N cultures were performed using the High Pure RNA Isolation Kit (Roche) in accordance to the manufacturers instructions. All Milli-Q H₂O and solutions were pre-treated with dimethyl pyrocarbonate (DMPC) (Sigma) prior to use in RNA extraction and manipulation procedures.

2.18.2 RNA quantitation

The concentration of RNA in solution was determined by measurement of absorption at 260 nm, assuming an A₂₆₀ of 1.0 is equal to 40 mg RNA/ml (Miller, 1972).

2.18.3 Primer extension analysis

A labelled oligonucleotide, P1208, specific for the mRNA of interest was used to map the 5' terminus. Labelled P1208 was hybridised to the mRNA and extended by reverse transcriptase towards the start of the mRNA, using unlabelled deoxynucleotides to form a single-stranded DNA complementary to the template mRNA. The DNA product was analysed on a standard sequencing gel, where the length of this product defines the start site of transcription.

2.18.3.1 Oligonucleotide labelling

Oligonucleotide P1208, specific to *xpsA* mRNA, was labelled at the 5' end using polynucleotide kinase and γ -[³²P]-dATP. The reaction mix consisted of 1 μ l of primer (150 ng), 1 μ l 100 mM DTT, 1 μ l 10x kinase buffer [500 mM Tris-HCl (pH 7.4), 100 mM MgCl₂], 1 μ l T4 polynucleotide kinase (2 units/ μ l) and 5 μ l γ -[³²P]-dATP (4000 Ci/mmol). After incubating for 45 min at 37°C, the labelled T4 polynucleotide kinase was heat inactivated at 65°C for 10 min. The oligonucleotide was precipitated by addition of 10 μ l 3M NaAc pH 5.2 and 300 μ l absolute ethanol and centrifugation (20 000 \times g, 20 min, Eppendorf) at 4°C.

2.18.3.2 Primer extension reaction

Labelled oligonucleotide P1208 was annealed to 10 µg of total cellular RNA in 10 µl hybridisation solution [10 mM Tris hydrochloride (pH 8.3), 200 mM KCl] at 75°C for 5 min, followed by 42°C for 10 min. 10 µl of this extension mixture was added to 200 units MLV reverse transcriptase (Gibco), 10 mM Tris-HCl (pH 8.3), 60 mM KCl, 4 mM MgCl₂, 4 mM DTT, and 1.0 mM concentrations of each of the four dNTP's. The samples were incubated at 42°C for 60 min. The single stranded DNA was recovered by precipitation with 3M NaAc pH5.2 and absolute ethanol, and dried *in vacuo*. The dried extension products were dissolved in 50% (v/v) formamide by vortexing and heated at 95-100°C for 5 min before being separated on a conventional sequencing gel (6% acrylamide, 7M urea, 1x TBE) at a constant voltage setting of 1400V. The gel dimensions were 20 x 40 cm, with a thickness of 0.4 - 0.5 mm. The gel was exposed for various time periods to a phosphoimage screen. Size comparison markers used on the sequencing gel were γ -[³²P]-dATP labelled *Sau3A1* digested pBluescript (1000, 734, 341, 258, 219, 105, 78, 75, 46, 36, 18 and 17 bp).

2.18.4 Northern analysis

2.18.4.1 DNA probe preparation for use in Northern hybridisation analysis

A PCR generated DNA fragment was used as the probe for Northern analysis. The probe, specific to *xpsA*, was prepared using *X. bovienii* chromosomal DNA as the template, oligonucleotides P6034/P6035 and the PCR based probe labelling method outlined in section 2.12.3.

2.18.4.2 Separation of RNA on denaturing agarose gels

Separation of RNA was performed on 1% denaturing agarose (Agarose LE, Roche) gels (18% (v/v) formaldehyde, 1x MOPS). Components were added to an eppendorf tube in the following order; 10 µl deionised formamide, 2 µl 10x MOPS, 1.2 µl formaldehyde and 10µl RNA (made up to this volume with Milli-Q H₂O if necessary). The RNA solution was heated at 65°C for 15 min to remove RNA secondary structures and placed on ice. The denaturing agarose gel was pre-electrophoresed at 70 V for 10 min in 1x MOPS prior to loading RNA supplemented with 2µl EtBr (1 mg/ml) and 1µl 5x RNA loading dye [25% (v/v) glycerol, 0.5% (w/v) bromophenol blue]. The agarose gel was run in 1x MOPS at 100 V constant

voltage and visualised. The marker used was RNA Molecular Weight marker 1, DIG-labelled (Roche). Marker sizes were; 6948, 4742, 2661, 1821 and 1517 bp.

2.18.4.3 Northern Transfer

The agarose gel was soaked for 10 min in 20x SSC (DMPC treated), and transferred O/N to nylon membrane (Nylon membrane, positively charged, Roche). RNA was fixed to the nylon membrane by baking for 30 min at 120°C.

2.18.4.4 Hybridisation

The nylon membrane was placed in a hybridisation bag (Hybridisation Bags [with spout], Roche) and hybridisation solution (DIG Easy Hyb Granules, Roche) added. The membrane was prehybridised at 42°C for 4 - 6 hr. The DNA probe was boiled for 10 min, added to the membrane and hybridised at 42°C O/N in an Extron HI 2001 hybridisation oven (Bartelt Instruments).

2.18.4.5 Detection

Washing, blocking and detection procedures were performed using the DIG Wash and Block Set (Roche) and DIG Luminescent Detection Kit for Nucleic Acids (Roche) according to the manufacturers instructions. Where required, kit components were diluted with DMPC treated Milli Q water.

2.18.5 Reverse transcription polymerase chain reaction (RT-PCR)

RNA was extracted and quantitated as in sections 2.18.1 and 2.18.2 respectively. The RT-PCR procedure was carried out according to the information provided by SuperScript™ II (Life Technologies). Total RNA (50 ng) was used as a template in which RNA is reverse transcribed to produce complementary DNA (cDNA) templates (the first strand DNA synthesis). Ten percent of the first strand cDNA was used in a standard PCR reaction as outlined in section 2.15.1.

2.19 Isolation of XpsA expressed in *E. coli*

Over-expression of *xpsA* was performed under the control of the T7 RNA polymerase promoter using the pET plasmid expression system (Novagen). Target genes are cloned into pET plasmids under the control of strong bacteriophage T7 transcription signals, and expression is induced by providing a source of T7 RNA polymerase to the host cell. For protein production a recombinant pET based plasmid (carrying a copy of the gene for T7 RNA polymerase under the control of the *lacUV5* promoter which is inducible by IPTG) was used to transform *E. coli* by electroporation. Addition of IPTG to a growing culture induces T7 RNA polymerase, which in turn transcribes the target DNA in the plasmid.

2.19.1 Construction of plasmids for over-expression of XpsA

A 3.1 kb PCR fragment generated by the amplification of *X. bovienii* chromosomal DNA with oligonucleotide P3411/P5435 was cloned into pGEM-T, generating pCT445 (see section 6.2.4.1). Plasmid pCT445 was digested with *NdeI/NotI* and the 3.1 kb PCR fragment subcloned into similarly digested pET29a(+), generating pCT446 (see section 6.2.4.1). Plasmid pCT446 was used to transform *E. coli* BL21(DE3) by electroporation for expression purposes.

2.19.2 Over-expression of XpsA

The over-expression of XpsA, under the control of the IPTG inducible T7 RNA polymerase promoter of pET29a(+), was performed in accordance with the pET System Manual (Novagen, TB055 9th Edition 05/00).

2.20 Preparation of whole cell lysates

Whole cell samples were prepared by pelleting 1 ml of mid-exponential phase culture (20 000×g, 5 min, Eppendorf). The pellets were subsequently resuspended in 100 µl of normal saline and mixed with 100 µl of 2x LUG buffer [62.5 mM Tris-HCl (pH6.8), 2% (w/v) SDS, 10% (v/v) glycerol, 5% (v/v) β-mercaptoethanol and 0.05% (w/v) bromophenol blue] (Lugtenberg *et al.*, 1975). Samples were stored at -20°C.

2.21 Sodium dodecyl sulphate-polyacrylamide gel electrophoresis (SDS-PAGE)

SDS polyacrylamide gel electrophoresis was a modification of the procedure of Lugtenberg (Lugtenberg, *et al.*, 1975). Samples were suspended in LUG buffer and heated to 100°C for 3 min subsequent to loading on 6% gels mounted on a Vertical Slab Gel Unit (model SE400, Hoefer Scientific Instruments). Gels were electrophoresed at 60 V through the stacking gel and 150 V through the running gel. Protein staining was by a 15 min incubation at room temperature in 0.0275 (w/v) Coomassie Brilliant Blue in 7.5% (v/v) acetic acid, 10% (v/v) ethanol and 10% (v/v) methanol. Destaining was by incubation in 7.5% (v/v) acetic acid, 10% (v/v) ethanol and 10% (v/v) methanol for 2 hr. Two types of protein markers used to determine unknown sizes;

1. Prestained Protein Marker, Broad Range (Premixed Format) (New England Biolabs) - MBP- β -galactosidase, 175 kDa; MBP-paramyosin, 83 kDa; glutamic dehydrogenase, 62 kDa; aldolase, 47.5 kDa; triosephosphate isomerase, 32.5 kDa; β -lactoglobulin A, 25 kDa; lysozyme, 16.5 kDa; aprotinin, 6.5 kDa.
2. Prestained SDS-PAGE Standards, Broad Range (BioRad) - myosin, 205 kDa; β -galactosidase, 120 kDa; bovine serum albumin, 84 kDa; ovalbumin, 52.2 kDa; carbonic anhydrase, 36.3 kDa; soybean trypsin inhibitor, 30.2 kDa; lysozyme, 21.9 kDa; aprotinin, 7.4 kDa. Each lot of BioRad markers are specifically calibrated for the correct molecular weight.

2.22 Purification of truncated XpsA

Whole cell samples of IPTG induced *E. coli* BL21[pCT446] were electrophoresed on a 6% SDS-polyacrylamide gel and transferred to nitrocellulose (Schleicher and Schull) at 25 mA for 40 min in 25 mM Tris-HCl (pH 8.3), 192 mM glycine and 5% (v/v) methanol, using a Trans blot SD semi dry transfer cell (Biorad). The nitrocellulose membrane was washed 2x 1 min in normal saline, subsequent to staining with 0.5% (w/v) Amido Black. The membrane was destained with a solution of 7.5% (v/v) acetic acid, 10% (v/v) ethanol and 10% (v/v) methanol for 10 min at RT. The correct band representing XpsA was excised and dissolved in 2 ml of 100% DMSO. An equal volume of sterile CO₃/HCO₃ pH 8.6 was then added drop wise to the DMSO solution whilst continually vortexing. The colloidal powder that precipitates upon

addition of CO_3/HCO_3 pH 8.6 was collected by centrifugation ($20\,000\times g$, 1 min, Eppendorf) and washed 3x in 1.5 ml normal saline. The colloidal powder was finally resuspended in 1.2 ml of normal saline and stored at -20°C in 300 μl aliquots.

2.23 Production of antisera against unprocessed *X. bovienii* T228 XpsA

Antiserum to the truncated XpsA protein from *X. bovienii* T228 was raised by intra-peritoneal (IP) injection of three 7 week old female BALB/C mice with purified XpsA protein prepared from the over-expressed XpsA (see sections 2.19.1 and 2.19.2). Mice were pre-bled and this serum shown not to contain antibodies that cross-reacted with *E. coli* BL21[pET29a(+)]. Mice were immunised IP and either side of the tail with 150 μl and 25 μl respectively of Freund's complete adjuvant (Commonwealth Serum Laboratories) combined with XpsA. Mice were then re-immunised IP at 3, 5 and 7 weeks with 200 μl of Freund's incomplete adjuvant combined with XpsA. At 9 weeks mice were bled from the retro-orbital sinus and sacrificed, the serum was stored at -20°C . A working stock of the antiserum was kept at 4°C with 0.05% (w/v) azide. The antiserum was absorbed against *E. coli* BL21[pET29a(+)] by alternating absorptions at 37°C for 4 hr or O/N at 4°C . Following each absorption the serum was clarified by centrifugation ($20\,000\times g$, 5 min, Eppendorf). This serum is hereafter referred to as anti-XpsA anti serum (α -XpsA).

2.24 Western Immunoblotting

The method used was a modification of Towbin (Towbin *et al.*, 1979). Samples were electrophoresed on 6% polyacrylamide gels and transferred to nitrocellulose (Schleicher and Schull) at 25 mA for 40 min in 25 mM Tris-HCl pH 8.3, 192 mM glycine and 5% (v/v) methanol, using Trans blot SD semi dry transfer cell (Biorad). The nitrocellulose sheet was incubated for 30 min in 5% (w/v) skim milk powder in TTBS [0.05% (v/v) Tween 20, 20 mM Tris-HCl, 0.9% (w/v) NaCl] to block non-specific protein binding sites. Mouse antiserum was diluted 1:100 in TTBS and 0.02% (w/v) skim milk powder, and was incubated with the membrane for 16 hr with gentle agitation. The antiserum was removed and the nitrocellulose membrane washed twice for 10 min in TTBS with gentle agitation. Horseradish peroxidase conjugated to sheep anti-mouse antiserum was added at a dilution of 1:5000 in TTBS and

0.02% (w/v) skim milk powder, and was incubated with the membrane for 2 hr with gentle agitation. The nitrocellulose membrane was then washed twice (10 min) with TTBS followed by 2x 10 min washes in TBS [20 mM Tris-HCl, 0.9% (w/v) NaCl]. The antigen-antibody complex was detected with 9.9 mg 4-chloro-1-naphthol dissolved in 3.3 ml methanol pre-chilled to -20°C and added to 16.5 ml TBS containing 15 µl hydrogen peroxide, until a suitable colour intensity developed.

2.25 Rearing of *Galleria mellonella* larvae cultures

The initial supply of *Galleria mellonella* eggs were obtained from Professor Otto Schmidt (Waite Campus, Adelaide University). Growth medium consisted of 100 gm wheat germ, 1 packet Heinz® high protein baby food, 100 ml honey, 100 ml glycerol, 1 gm torula yeast, 0.15 gm nipagen (Sigma) and the contents of 5 multivitamin capsules (Pluravit). Dry run autoclaved cardboard cut to approximately 10 x 10 cm were added to the growth medium as the larvae deposit themselves between the sheets making collection easier. Larvae were incubated at 28°C, taking between 4 and 5 weeks to go through one full life cycle. All *Galleria mellonella* used were at the sixth instar stage of development.

2.26 LD₅₀ analysis of *X. bovienii* *recA* mutants for *G. mellonella*

P1 and P2 cultures of *X. bovienii* T228/1 and *recA* mutant XB001 were incubated for 12 hr at 28°C with shaking. Bacterial cells were harvested by centrifugation (4 000×g, 5 min, Eppendorf), resuspended in PBS and kept on ice. Serial dilutions of these suspensions were used to infect larvae. Viable counts of bacteria per dose were estimated by triplicate plating of 100 µl volumes of appropriate dilutions on NA.

Sixth-instar larvae were infected with bacteria as follows. Larvae weighing 120-160 mg were selected and surface sterilised with 70% (v/v) ethanol prior to infection. Using a Hamilton syringe, each larva in a group of 10 was then injected with a 10 µl volume of either a bacterial suspension or PBS. Treated larvae were incubated at 28 C for up to 72 hr. At regular intervals, each treatment group was examined and the number of dead or moribund larvae recorded. Estimates of the LD₅₀ of *X. bovienii* strains for *G. mellonella* larvae were then determined (Reed & Muench, 1938).

2.27 UV sensitivity studies

Bacteria to be tested were grown O/N at the correct temperature, with appropriate antibiotic selection. Cultures were pelleted (6 000×g, 10 min, MSE Minor S centrifuge) and washed in normal saline, before being resuspended in normal saline to an OD₆₀₀ of 1.0 (LKB Ultraspec Plus Spectrophotometer, Pharmacia). A 4 mm diameter wire loop was used to streak a standard inoculum of each culture over a distance of 5 cm on NA plates containing appropriate antibiotics. Inoculated plates were allowed to dry for 15 min, before exposure to a UV light source for 0 - 50 sec. UV treated plates were immediately incubated in the dark. The extent of bacterial growth on each plate was compared to control plates that had not been exposed to UV light.

2.28 Recombination proficiency assay to demonstrate RecA function

A recombination proficiency assay was used to demonstrate the ability of the cloned *recA* gene to facilitate recombination. *E.coli* strain JC14604 (Clark, 1973), is a *recA* mutant containing a tandem duplication of the *lacZ* gene, with each copy of the gene containing a different missense mutation. In the presence of functional RecA a recombination event can produce a functional copy of *lacZ*. Cells in which this event occurs can give rise to colonies capable of producing Lac papillae on MacConkey agar (Oxoid CM115).

Plasmids pCT302, pCT302.1, and pCT302.2 were used to transform *E. coli* strain JC14604. Control transformations with pGEM-T and pWKS130 were also performed. All transformants were plated on MacConkey agar, incubated at 37°C for 48 hr and examined for presence of Lac papillae.

2.29 Antimicrobial bioassays

The antimicrobial activity of *X. bovienii* wild type and mutant strains was assessed using an agar overlay technique. *X. bovienii* strains to be tested were streaked onto NA (without antibiotic selection) and incubated for 36 hr at 28°C. *Xenorhabdus* cells were killed by overlaying the agar plate for 15 min with filter paper soaked in 100% chloroform. Plates were allowed to dry upside down for 30 min before the agar surface was overlaid with soft agar

containing 1 ml of an O/N *M. luteus* culture. Overlaid plates were incubated O/N at 37°C and the cleared zones representing inhibition of *M. luteus* growth measured.

The antimicrobial activity of *X. bovienii* T228, XB6246, XB3444 and XB92388 supernatants was compared to a known peptide antibiotic, bacitracin, using the indicator organism *Micrococcus luteus*. *X. bovienii* T228, XB6246, XB3444 and XB92388 were grown in 50 ml of LB for 96 hr at 28°C with agitation. The A_{600} of cultures was measured (Pharmacia LKB-Ultraspec Plus Spectrophotometer) and the fresh media added to adjust the bacteria to approximately 5×10^9 cells/ml. Bacterial cells were then pelleted (6 000×g, 10 min, MSE Minor S centrifuge) and the supernatant passed through a 0.2 µm filter (Millipore, USA). Log phase *M. luteus* was used at 2.5×10^6 cells/ml. 100 µl of *M. luteus* was aliquoted into the wells of a 96 well flat bottom tray (Falcon). 100 µl of filter sterile bacterial cell supernatant was added to the first well of each row and diluted across the row 1:2 to a final dilution of 1:64.

The antibiotic activity of *X. bovienii* strains supernatant was compared with the peptide antibiotic bacitracin. Bacitracin was supplemented with 40 mg/ml ZnSO₄, as the zinc salt form of this antibiotic is required for activity. Bacitracin (400 units/ml) was diluted across the microtitre tray rows 1:2 to a final dilution of 1:64. The positive control consisted of *M. luteus* diluted with sterile LB. Microtitre trays were incubated at 37°C with gentle agitation, and the A_{600} of each well measured every 3 hr for 9 hr (DYNATECH MR 7000 version 3.2 plate reader). The end point reading was taken between 21 – 24 hr. During incubation, microtitre trays were placed in plastic boxes containing wet absorbent material and sealed to prevent evaporation of culture medium onto the microtitre tray lids.

2.30 Transmission Electron Microscopy studies of haemocytes from *G. mellonella* infected with *X. bovienii* XB3444, XB6246 and XB92388

X. bovienii T228, XB6246, XB3444 and XB92388 were grown in LB O/N at 28°C with agitation. Cultures were pelleted (4 000×g, 5 min, Eppendorf) and washed 2x in PBS. The A_{600} of cultures was measured (Pharmacia LKB-Ultraspec Plus Spectrophotometer) and cells adjusted to 1×10^4 cells/ml. Sixth instar *G. mellonella* larvae were injected with 10 µl of

bacterial cells (approximately 100 bacterial cells) or sterile PBS. *G. mellonella* larvae were observed over the next 36 hr and moribund larvae were bled by proleg puncture into fixative solution [4%(v/v) paraformaldehyde, 1.25%(v/v) glutaraldehyde, 4%(w/v) sucrose in PBS, (pH 7.2)]. After fixing O/N at 4°C the bacterial cells were passed through the following solution changes with a 7 000×g, 5min centrifugation (BHG HERMLE model Z 231M) between steps;

1. Washed in PBS + 4% (w/v) sucrose (2x with a 10 min incubation each).
2. Post-fixed in PBS + 2% O₂O₄ for 1hr with agitation
3. Dehydrate
 - 70% (v/v) ethanol (2x with a 30 min incubation each)
 - 90% (v/v) ethanol (2x with a 30 min incubation each)
 - 95% (v/v) ethanol (2x with a 30 min incubation each)
 - 100% ethanol (2x with a 30 min incubation each), + 1 change of 1hr
4. ethanol:resin (O/N)
5. 100% resin (3x of 8 hr each)
6. Embed in resin (Procure Araldite Embedding Kit Epoxy Resin, Probing and Structure Electron Microscopy and Probing Supplies, Thuringowa Central QLD).
7. Polymerise in an oven O/N at 60°C.

Thin sections were cut with a Diatome diamond knife on an LKB Ultracut Ultramicrotome and floated onto 200 mesh copper grids (Graticules Ltd., Tonbridge, U.K.). Sections were stained with 5% (w/v) uranyl acetate in 70% (v/v) ethanol and Reynolds lead citrate [16.25%(w/v) Pb(NO₃)₂, 22.5% (w/v) C₆H₅Na₃O₇ in 1M NaOH] and visualised on a Philips CM 200 Transmission Electron Microscope or Philips CM 100 Scanning Transmission Electron Microscope.

2.31 Schneider's cell cytotoxicity assays

The cytotoxic nature of *X. bovienii* T228, XB6246, XB3444 and XB92388 supernatants was examined using cultured Schneider's cells. Schneider's cells were obtained from the laboratory of Professor Rob Saint (Department of Molecular Biosciences, Adelaide University) and grown in Schneider's Drosophila Media (Gibco BRL) supplemented with sterile 10% (v/v) foetal calf serum (FCS) (Multi Ser™, Trace Bioscience Pty Ltd, Australia).

Schneider's cells were incubated at RT in 100 ml flasks (Blue Plug Seal Cap Flasks, Becton Dickinson) and covered with aluminium foil to exclude light. Schneider cells were split every 3 - 4 days by diluting 10% (v/v) in fresh Schneider's cell media + 10% (v/v) FCS.

X. bovienii T228, XB6246, XB3444 and XB92388 were grown for 96 hr at 28°C with agitation in 10 ml Schneider's Drosophila Media + sterile 10% (v/v) FCS. The A_{600} of cultures was measured (Pharmacia LKB-Ultraspec Plus Spectrophotometer) and fresh media added to adjust the bacteria to approximately 5×10^9 cells/ml. Bacterial cells were pelleted (6 000×g, 10 min, Eppendorf) and the supernatant passed through a 0.2 µm filter (Millipore, USA).

A Neubaur haemocytometer and trypan blue staining were used to enumerate viable Schneider's cells, which were then adjusted to approximately 2.5×10^6 cells/ml. 100 µl of Schneider's cells were aliquoted into rows of a 96 well flat bottom tray (Falcon). 100 µl of filtered bacterial supernatant was then added to the first well in a row. This was repeated for each bacterial strain supernatant. Schneider's cells diluted in fresh Schneider's cell media + 10% (v/v) FCS was used as a positive control. Schneider's cells were incubated at RT, and a 20 µl aliquot from each well observed every hr for up to 6 hr in a Neubaur haemocytometer after trypan blue staining to enumerate live and dead cells.

2.32 β -galactosidase assays

β -galactosidase activity was measured by using a technique designed from work by Miller (Miller, 1972) and Bignon (Bignon *et al.*, 1993). *Xenorhabdus* cultures were grown on mXMM plates or LB plates at 28°C or, in mXMM broth or LB broth at 28°C with aeration. Time of growth and media was depended on the experiment being conducted. *Xenorhabdus* cultures obtained from agar surfaces were scraped off with a wire loop and resuspended in the liquid version of the same media. The A_{600} of cultures was measured (Pharmacia LKB-Ultraspec Plus Spectrophotometer), and dilutions made such that the final culture A_{600} was 0.550 - 0.850. If necessary, cultures were pelleted (6 000×g, 10 min, MSE Minor S centrifuge) and resuspended in a smaller volume of liquid media. 300 µl of diluted (or concentrated) cultures were aliquoted into duplicate wells of a 96 well flat bottom tray (Falcon) and the A_{600} read immediately (DYNATECH MR 7000 version 3.2 plate reader).

500 µl of diluted culture was added to 500 µl of Z buffer [60 mM Na₂HPO₄·7H₂O, 40 mM NaH₂PO₄·H₂O, 10 mM KCl, 1 mM MgSO₄·7H₂O, 50 mM β-mercaptoethanol, adjusted to pH 7.0 and stored at 4°C] containing 1 mg/ml lysozyme and incubated at 37°C for 30 min. Cells were lysed by addition of 2 drops of chloroform, 1 drop of 0.1% (w/v) SDS, vortex/10 sec. Bacterial cell lysates were pelleted (20 000×g, 5 min, Eppendorf), and 100 µl aliquots of supernatant placed in duplicate wells of a 96 well microtitre tray. The negative control was Z buffer containing 0.7 mg/ml ONPG (Roche). The positive control was supernatants of *E. coli* SY327λ*pir*[pCT414]. The microtitre tray and Z buffer plus ONPG solution were incubated at 28°C for 15 min, prior to starting the reaction by the addition of 200 µl of the Z buffer ONPG solution to each well. Optical densities were recorded after 95 min at A₄₁₀ (DYNATECH MR 7000 version 3.2 plate reader). β-galactosidase units were calculated using the following equation;

$$\beta\text{-galactosidase units} = \frac{1000 \times A_{410}}{\text{Time} \times \text{Volume} \times A_{600}}$$

(Time = time of assay in min, eg. 95 min; volume = volume of culture used [before dilution in Z buffer/lysozyme] in ml, eg. 0.5 ml).

2.32.1 β-galactosidase activity using conditioned growth media

Measurement of β-galactosidase activity by bacteria grown in conditioned growth media was essentially conducted as in Section 2.32, except for the following modifications. Conditioned growth media was obtained by culturing *X. bovienii* in LB for 96 hr at 28°C with aeration. Cultures were pelleted (6 000×g, 10 min, MSE Minor S centrifuge) and the supernatant passed through a 0.2 µm filter (Millipore, USA). The conditioned media was diluted 20% (v/v) in fresh LB and used as growth media for further experiments. All bacterial culture dilutions were performed using filter sterile conditioned media.

Chapter 3

Analysis of the role of RecA in *X. bovienii* phase variation

3.1 Introduction

Colony pleiomorphism, or phase variation, is an important factor that apparently determines the association of the *Xenorhabdus* spp. with their nematode symbionts, and the outcome of infection of susceptible insect larvae by the bacterium:nematode parasitic complex.

Xenorhabdus P1 variants produce a range of extracellular products including; protease, lipase, phospholipase C, haemolysin, antibiotic substances and Congo Red binding proteins (Akhurst, 1982a; Boemare & Akhurst, 1988; Akhurst & Boemare, 1990; Nealson *et al.*, 1990). Cytoplasmic inclusion bodies are produced during stationary phase, and are composed of highly crystalline proteins (Couche & Gregson, 1987; Couche *et al.*, 1987). P2 forms are unable to (or only weakly) express many of these putative virulence determinants (Akhurst & Boemare, 1990). However, the role of these determinants in the process of infection is unclear since susceptible *Galleria mellonella* insect larvae are killed equally well by P1 and P2 forms of these bacteria. Nevertheless, production of antibiotic substances by P1 forms prevents putrefaction of the cadaver by other microorganisms, and this helps support an environment conducive for nematode growth and reproduction.

The mechanism responsible for this pleomorphism is not yet understood. In some other bacteria, differential expression of virulence determinants and the process of phase variation, are dependent on expression of functional RecA protein (Kooimey *et al.*, 1987; Ball *et al.*, 1990; Zagaglia *et al.*, 1991). To determine the role of RecA in *X. bovienii* phase variation the *recA* gene was firstly cloned and characterised. UV sensitivity studies and complementation analysis were then used to demonstrate RecA function. A *X. bovienii* *recA* insertion mutant was constructed by allelic-exchange mutagenesis, and phenotypic analysis used to determine if the mutation had any effect on a selection of phase variant characteristics. Finally, LD₅₀ analysis using *Galleria mellonella* insect larvae infected with either *X. bovienii* T228 or the *recA* mutant was used to determine if *recA* has any role in the virulence of these bacteria.

3.2 Results

3.2.1 Cloning and sequence analysis of *X. bovienii* *recA*

The gene encoding RecA shows highly conserved regions of nucleotide sequence. Degenerate oligonucleotides were designed to amplify a 363 bp internal gene fragment and inverse PCR was used to identify nucleotide sequence 5' and 3' of the 363 bp *recA* internal fragment. Additionally plasmid-assisted PCR rescue (PAPCR) was used to identify nucleotide sequence further 5' of the *recA* start codon. This facilitated PCR amplification of the entire *recA* gene and regulatory sequences from *X. bovienii*.

3.2.1.1 Generation of degenerate oligonucleotides for the amplification of an internal *recA* sequence

Degenerate oligonucleotides were synthesised to facilitate PCR amplification of an internal region of the *X. bovienii* *recA* gene. Highly conserved regions of the *recA* gene were identified by alignment of the amino acids from 27 previously characterised *recA* genes (data not shown). Apart from a high degree of invariance, other factors taken into consideration included low degeneracy and complete homology at the 3' end necessary for efficient extension. Oligonucleotide P1067 (coding strand oligonucleotide with 192-fold degeneracy) and P1068 (complementary strand oligonucleotide with 384-fold degeneracy) (see Table 2.4.2 and Figure 3.1) were selected for their low degeneracy and low G+C content, which is characteristic of *Xenorhabdus* DNA (43-44% G+C (Thomas & Poinar, 1979)). Based on the *E. coli* *recA* gene, a PCR product of 360 bp was predicted. A 363 bp internal fragment of the *recA* gene from *X. bovienii* chromosomal DNA was amplified using the degenerate oligonucleotide primers P1067/P1068 and PCR conditions outlined in section 2.15.1 (data not shown). The 363 bp PCR product was cloned into pGEM-T Easy. The ligation mix was used to transform *E. coli* DH5 α by electroporation. Transformants were selected on NA supplemented with Amp, IPTG and X-gal. The correct construct was identified by an *EcoRI* digestion (data not shown) and designated pCT300. BLASTX 2.1.1 analysis of DNA sequence (data not shown) was used to confirm that pCT300 contained a *X. bovienii* based insert with 97% homology and 94% identity over 359 bp to *Yersinia pestis*, *Serratia marcescens*, *Proteus mirabillis* and *Escherichia coli* *recA* nucleotide sequence.

**Forward oligonucleotide P1067
(192-fold degeneracy)**

92 phe ile asp ala glu his ala 98
5' TTT ATT GAT GCT GAA CAT GC 3'
C T C C G C
A A
G

**Reverse oligonucleotide P1068
(384-fold degeneracy)**

211 gly gly thr thr thr glu pro 206
5' CC ACC AGG AGT AGT CTC AGG 3'
T T T T T T T
C C
G

Figure 3.1

Degenerate oligonucleotides used to prime amplification of a 363 bp internal region of *X. bovienii recA*.

Amino acid sequences shown are the consensus sequences for homologous regions of 27 bacterial RecA proteins. Numbers show approximate positions of these amino acids in RecA sequences.

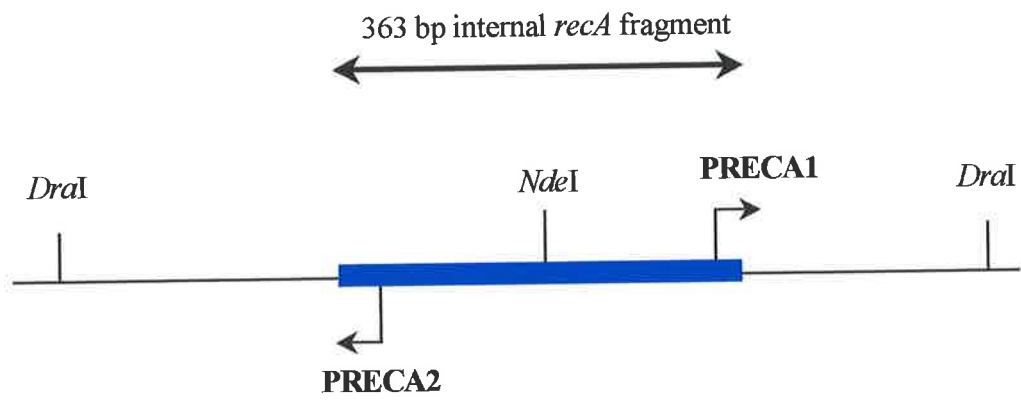
3.2.1.2 Identification of *recA* DNA sequence located 5' and 3' of the 363 bp *recA* internal fragment

Inverse PCR (diagrammatically represented in Figure 3.2) was used to extend the *recA* DNA sequence. Oligonucleotides PRECA1 and PRECA2 were designed from the known *X. bovienii recA* 363 bp nucleotide sequence (section 3.2.1.1), and oriented to read out of the *recA* region to enable amplification of 5' and 3' flanking DNA. *X. bovienii* chromosomal DNA was digested to completion with either *Dra*I, *Eco*RI, or *Hind*III. These fragments were then circularised by T4 DNA ligase followed by digestion with *Nde*I, a restriction enzyme known to cut the cloned 363 bp region of *recA* at a single location between the 5' ends of each oligonucleotide. Linearisation of the circularised fragment resulted in oligonucleotide binding sites being located at either end of the DNA fragment. Using this DNA as a template, oligonucleotide pair PRECA1/PRECA2 were used to amplify a 1.4 kb fragment from the *Dra*I digested chromosomal DNA sample (see section 2.15.1) (data not shown). Direct DNA sequence analysis of the 1.4 kb fragment using PRECA1 and PRECA2 established the 5' and 3' ends of *recA*. Overlapping sequence was then used to merge these data with that of the internal *recA* fragment to finalise the entire *X. bovienii recA* gene sequence (Figure 3.3).

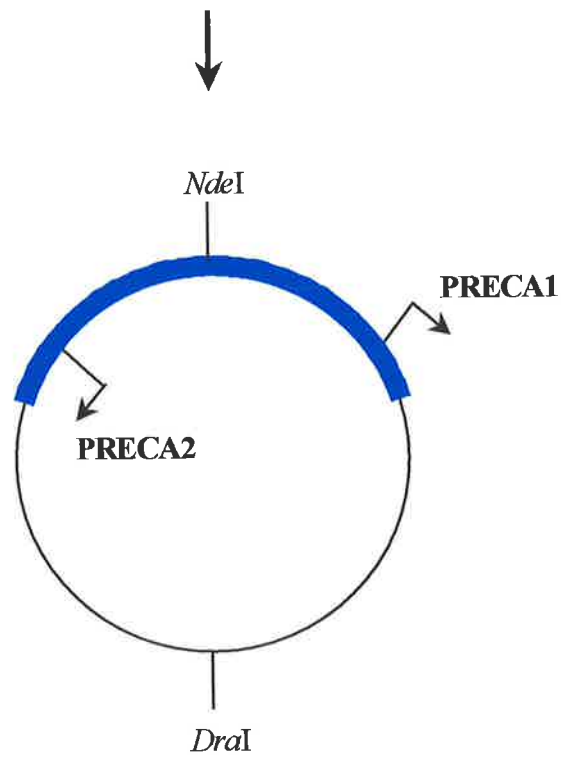
3.2.1.3 Plasmid Assisted PCR Rescue (PAPCR) to identify DNA sequence 5' of *recA*

To assess the function of *X. bovienii recA* in an *E. coli* background (see section 3.2.2.2), a full-length clone of *recA* (including regulatory sequences) was required. 38 bp of DNA sequence 5' to the putative *X. bovienii recA* promoter site was known, however this region was not suitable for oligonucleotide construction due to the presence of substantial nucleotide repeat sequences. Additional DNA sequence data 5' to the known *recA* sequence was obtained by plasmid-assisted PCR rescue (PAPCR) (see section 2.15.3.1) based on a method described by Luo (Luo & Cella, 1994). *X. bovienii* chromosomal DNA was digested with *Eco*RI and ligated to *Eco*RI digested pBR322. The ligation mix was used in a PCR with oligonucleotides P2177 (specific for the tetracycline resistance gene of pBR322) and P4958 (binds to the complementary strand of the *X. bovienii recA* gene sequence at nucleotide positions 91-74) to amplify a 2 kb DNA fragment (data not shown). The PCR product was subjected to direct DNA sequence analysis with P4958, and the subsequent data added to existing *recA* DNA sequence. Oligonucleotides P227 and P2293 were designed from the completed DNA sequence and used to amplify a 2064 bp fragment from *X. bovienii* chromosomal DNA (data

Figure 3.2 Schematic representation of Inverse PCR. Oligonucleotides PRECA1 and PRECA2 were designed to read out of the 5' and 3' ends of the 363 bp *X. bovienii recA* fragment. *X. bovienii* chromosomal DNA was digested with *DraI*, re-ligated, and further digested with *NdeI*. Using the digested DNA as a template, oligonucleotides PRECA1 and PRECA2 were used to PCR amplify a 1.4 kb fragment encoding DNA flanking the 363 bp *recA* internal fragment.



DraI digestion and re-ligation



NdeI digestion and PCR amplification

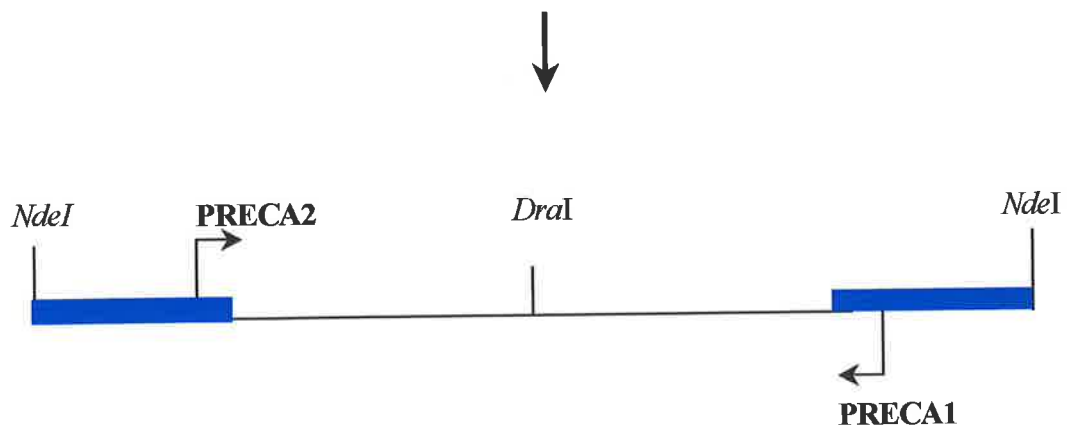


Figure 3.3 Nucleotide sequence of *X. bovienii* T228 *recA*, including regulatory sequences. The nucleotides are numbered to the right hand side in the 5' to 3' direction. The deduced protein sequence of the open reading frame, *recA*, is given below the DNA sequence as single letter amino acid code and is numbered on the right hand side. Putative regulatory elements of *recA*, start codon, ribosome binding site (rbs), -10 region and -35 region are indicated. The translational stop codon and putative termination loop sequences are indicated. Amino acids 60-78 (inclusive) and amino acids 257-281 (inclusive) are highlighted, and represent ATP binding domains I and II respectively. Critical amino acids required for homologous recombination are underlined; 61-R (arginine); 265-Y (tyrosine) and 300-G (glycine). Oligonucleotides P277 and P2293 used to PCR amplify the entire *recA* gene are underlined (see section 3.2.2.1). The position of a unique *EcoRI* restriction site used for subsequent modification of *recA* is also shown. The partial 3' gene sequence of *ygaD*, a protein of unknown function found upstream of several *recA* genes, is indicated.

The entire 2122 nucleotide sequence encoding *recA* and part of *ygaD* has been submitted to Genbank, accession number U87924.

P227

CAGCTTAGTATTGAACTTGGAAAGAACTCCAACGGAAAAAATTATCCTTAACCTGTGCA - 60

GAATCCTGCACAGGGGGCTGGATTGCTAAAGTGATCACAGATATTGCGGGAAGTTCGGCC - 120
TATTTTAACCGCAGTTTCGTGACCTATAGCAATGATTCTAAAAATGAAATGCTGGGTGTA - 180
TCACAGGCATCACTGGTGCAGTTTGGTGCAGTGAACAGGTCGTAAAGAAAATGGCA - 240
GTAGGGGCATTAAAGGCGGCCAGAGCAGATTTTGTCTGTTTCTGTCAGTGGCATCGCAGGT - 300
CCGGATGGTGGCAGTGAAGAAAAACCGACGGGAACGGTCTACTTTGGGTTTACCTACCGT - 360
AATGGTGAGGATGTACATACCGTGACATATCGCCAGCATTTTACGGGTGATCGCAATGCA - 420

DraI

GTACGGCTCCAGGCTGTCATTTTTTCTTTTAAAACACTGCTGGAAGAAATCATAAAAAAT - 480

-35 region

-10 region

TAGCTTGGATGCTGTATGATTATACAGTATAATTAATTCAGCACTTTGGTATCAGAAACG - 540

rbs

recA start

GTTTATCAGCAGTGGGGCAGCCCCTTCATTGCTTACGAAGGAGTAAACATGGCTAACGAT - 600

M A N D - 4

GAAAACAAACAAAAAGCACTAGCAGCGGCGCTGGGTCAAATTGAAAAACAATTTGGTAAA - 660

E N K Q K A L A A A L G Q I E K Q F G K - 24

GGTTCTATCATGCGTCTGGGCGAAAACCGCTCAATGGATGTTGAACTATCTCTACTGGC - 720

G S I M R L G E N R S M D V E T I S T G - 44

TCACTGTCAGTGGATATAGCATTAGGTGCGGGTGGTTTGCCAATGGGCCGTATTGTTGAA - 780

S L S L D I A L G A G G L P M G R I V E - 64

ATATACGGGCCTGAATCTTCGGGTAAGACAACATTGACACTGCAAGTTATTGCTTCTGCC - 840

I Y G P E S S G K T T L T L Q V I A S A - 84

ATP binding domain I

CAGCGTGAAGGCAAAACCTGTGCTTTTTATTGATGCCGAACATGCCCTTGATCCGGTTTAT - 900

Q R E G K T C A F I D A E H A L D P V Y - 104

GCCAAAAAGTTGGGCGTAGATATTGATAACCTGCTGTGCTCCCAGCCTGATACAGGTGAA - 960

A K K L G V D I D N L L C S Q P D T G E - 124

CAGGCACTGGAAATCTGTGATGCCTTGTACGCTCTGGGGCGGTTGACGTCATCGTTGTT - 1020

Q A L E I C D A L S R S G A V D V I V V - 144

GACTCCGTTGCTGCATTGACCCCGAAAGCGGAAATCGAAGGTGAGATCGGCGATTCCCAT - 1080

D S V A A L T P K A E I E G E I G D S H - 164

ATGGGCTTGGCAGCTCGTATGATGAGTCAGGCCATGCGTAAGTTGGCAGGTAACCTGAAA - 1140

M G L A A R M M S Q A M R K L A G N L K - 184

AACTCGAATACTCTGCTAATCTTTATCAACCAGATCCGTATGAAAATTGGTGTGATGTTT - 1200

N S N T L L I F I N Q I R M K I G V M F - 204

GGTAACCCAGAAACCACAACAGGTGGTAATGCACTGAAATTTTATGCATCTGTCCGTTTG - 1260

G N P E T T T G G N A L K F Y A S V R L - 224

GACATCCGCCGCACTGGTTCGTAATAAATGGCGATGAAGTTGTTGGCAGCGAGACTCGT - 1320

D I R R T G S V K N G D E V V G S E T R - 244

EcoRI

GTGAAAGTAGTCAAGAACAAAATTGCGGCACCGTTCAAACAAGCTGAATTCAGATCTTG - 1380

V K V V K N K I A A P F K Q A E F Q I L - 264

TATGGTGAAGGTATTAACACCTTTGGCGAATTGGTCGACTTGGGCGTTAAGCACAAAATG - 1440

Y G E G I N T F G E L V D L G V K H K M - 284

ATP binding domain II

GTCGAAAAAGCAGGTGCATGGTACAGCTATAACGGAGATAAAAATTGGGCAGGGTAAAGCT - 1500

V E K A G A W Y S Y N G D K I G Q G K A - 304

AATGCCACGATTTACCTGAAAGAGCACCCAGAAGTCTCTGCTGAGCTGGATAAAAAACTG - 1560

N A T I Y L K E H P E V S A E L D K K L - 324

CGTGAATTGCTGTTGAATAATACAGGTGGATTACAGTAGTGCAGTCTCTGATTATGTAGCC - 1620

R E L L L N N T G G F S S A V S D Y V A - 344

recA stop

GATTATGAAGATAACGGTGAAGAAGTGAAAAACGAAGAGTTCTAATTACTCGTTCACTCT - 1680

D Y E D N G E E V K N E E F * - 358

termination loop

GTTGTGACAACTGTTTTCTGAAGAACCACATCCTGTGGGATGTGGTTTTTGTTTTTTAT - 1740

AGGAGTAATCAACATCATTGATACAGGGATACTGAAACTGGCTTGACAAACAGACTTTCA - 1800

GAAAATGTCCAGACGAATTACAATGCTGAAAAGCGGATGAATTTATATGGGATTTTACTT - 1860
CTTATGGAAGACATTCTATCTTAACCCTATTTTAATTTATTCGTGAGTTGAAATGGTGAT - 1920
GCGCTATACCACCTCAACCATACATGAATCTGTTTTTTCAGCTTGATTTTCGGGACAATTA - 1980
TGAGCAAAGCACCCTGAGATCCGTCAGGCGTTTCTTGACTTTTTTCACACTAAAGGGC - 2040

P2293

ACCAG**ATAGTACCAAGCAGTTCACT**GGTGCCAAATAATGATCCAACCTGTTGTTCACTAA - 2100



DraI

TGCAGGGATGAACCAG**TTTAAA** - 2122

not shown). The PCR product was cloned into pGEM-T Easy and the ligation mix was used to transform *E. coli* DH5 α by electroporation. Transformants were selected on NA supplemented with Amp, IPTG and X-gal. The correct construct was confirmed by an *Eco*RI digest (data not shown) and designated pCT302. Plasmid pCT302 was sequenced to confirm the presence of *X. bovienii recA* and upstream regulatory sequences (data not shown).

3.2.1.4 Analysis of the *X. bovienii recA* gene sequence

The *X. bovienii recA* gene (Genbank Accession U87924, corresponding to Figure 3.3) was compared with the *recA* sequence of *X. nematophilus* AN6 (Hing Hew, 1997). Nucleotide positions of relevant *X. nematophilus recA* features correspond to their position in the Genebank entry (Genbank Accession AF127333). The entire *X. bovienii recA* gene, including regulatory sequences, is contained in a 1676 bp *Dra*I fragment. The *recA* genes of both *X. bovienii* and *X. nematophilus* consist of an ORF of 1077 bp (including the stop codon) that is preceded by a putative ribosome binding site (-AAGGAG-) [*X. bovienii*, nucleotides 579 – 582; *X. nematophilus*, nucleotides 131 – 136]. Putative promoter sequences were found 76 bp and 47 bp upstream from the initiation codons of the *recA* gene from *X. bovienii* (TTGATG--16bp--TATAAT) [nucleotides 485 – 512] and *X. nematophilus* (TTTATC--17bp--TTCATT) [nucleotides 39 – 66] respectively. Putative stem-loop structures were found 35 and 21 bp downstream from the stop codons of the *X. bovienii* [nucleotides 1705 – 1729] and *X. nematophilus* [nucleotides 1223 – 1249] *recA* genes respectively. Both *recA* genes encode two putative ATP-binding domains located within the coding region at nucleotides 178-234 and 769-843. Codons for the critical arginine and glycine residues for *recA* mediated homologous recombination (Müller & Kokjohn, 1990) are located in both genes at nucleotides 181-183 and 898-900 respectively. Furthermore, the LexA binding site region in both *Xenorhabdus* spp. is almost identical to that of the *E. coli recA* gene (Figure. 3.4).

The *recA* gene sequences from *X. bovienii* and *X. nematophilus* were 85% similar at the nucleotide level and 95% similar at the amino acid level. Furthermore, analysis of the *X. bovienii recA* gene revealed extensive identity at the amino acid level to the *recA* genes of *Erwinia carotovora* (92% identity), *Proteus mirabilis* (87% identity), *Serratia marcescens* (88% identity) and *Yersinia pestis* (91% identity). The *X. nematophilus recA* gene is also homologous at the amino acid level to the *recA* genes of *Erwinia carotovora* (85% identity),

Proteus mirabilis (86% identity), *Serratia marcescens* (87% identity) and *Yersinia pestis* (85% identity).

A partial open reading frame upstream of *recA* was identified showing homology to a group of hypothetical proteins known as YgaD. These open reading frames have been found upstream of a number *recA* sequences, however their function is unknown. The YgaD like sequence upstream of *X. bovienii recA* shows homology to hypothetical proteins upstream of the *recA* genes from *Enterobacter agglomerans* (66% identity), *E. coli* O157:H7 (61% identity) and *Pseudomonas putida* (49% identity).

3.2.1.5 Phylogenetic analysis of *recA* from *Xenorhabdus* spp.

Using the full-length RecA amino acid sequence of *X. bovienii* and *X. nematophilus* and those of 44 other bacteria, distance measures were obtained using the PROTDIST (Dayhoff PAM matrix) program of PHYLIP. A Fitch-Margoliash and Least Squares Method with Evolutionary Clock estimated phylogenetic relatedness of the RecA sequences with the aide of the PHYLIP program KITSCH (Figure 3.5). The unrooted phylogenetic tree was constructed using DRAWTREE. This phenogram showed that the two complete *Xenorhabdus* spp. RecA sequences were most closely related to one another, and furthermore, grouped together with other members of the Enterobacteriaceae family. The tree also clearly shows the separation of representative α proteobacteria, β proteobacteria, γ_1 proteobacteria, γ_2 proteobacteria, Gram-positive bacteria with high GC content, Gram-positive bacteria with low GC content and cyanobacteria into distinct clades.

3.2.2 Assessment of *X. bovienii recA* function in *E. coli*

3.2.2.1 Recombination proficiency assay to demonstrate RecA function

A recombination proficiency assay (see section 2.28) was used to determine whether *E. coli* JC14604 carrying the *X. bovienii recA* gene on plasmid pCT302 could facilitate recombination. *E. coli* JC14604 (Clark, 1973), is a *recA* mutant containing a tandem duplication of the *lacZ* gene, with each copy of the gene containing a different missense mutation. In the presence of functional RecA, a recombination event can produce a functional copy of *lacZ*. Cells in which this event occurs give rise to colonies capable of producing Lac papillae on MacConkey agar.

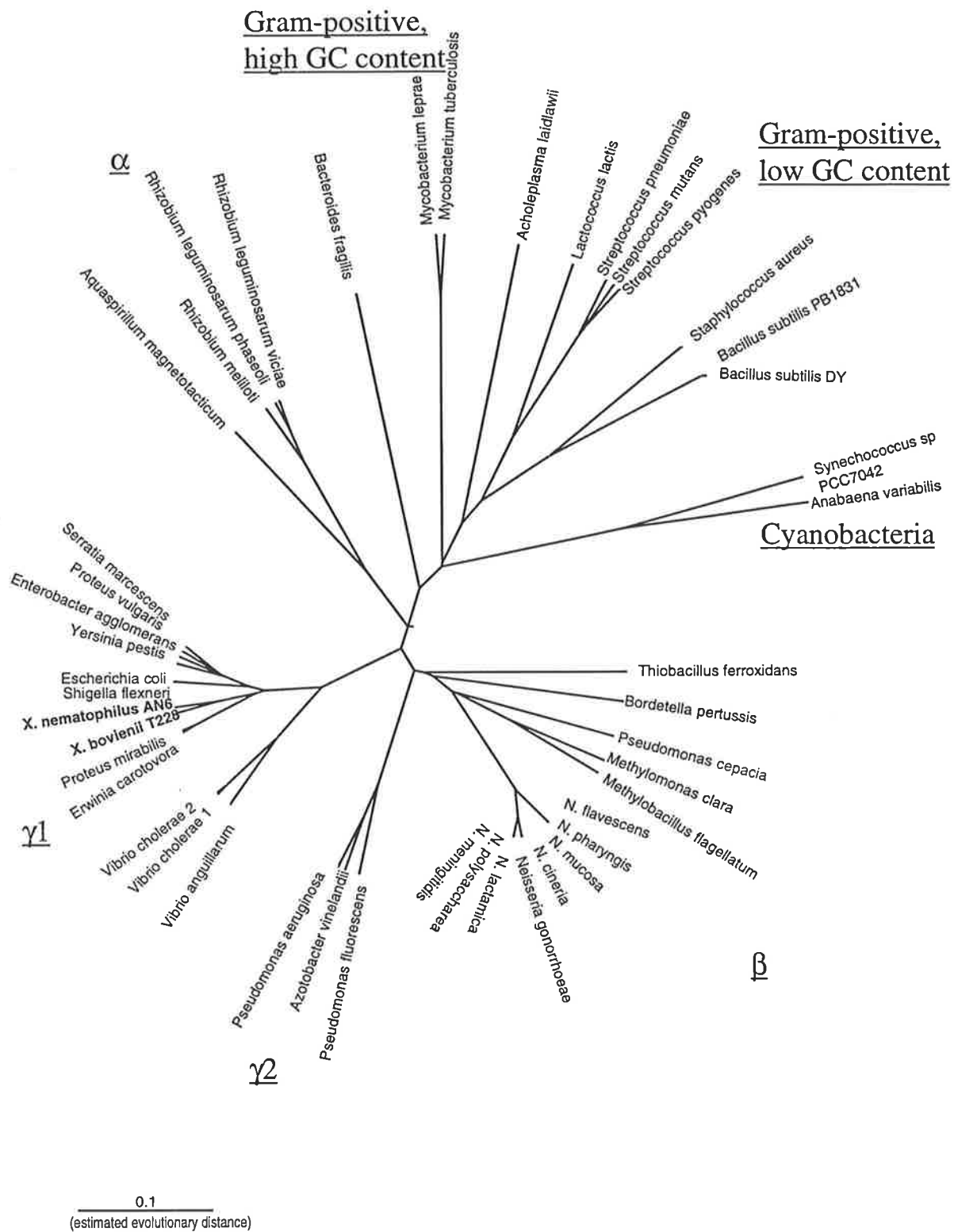


Figure 3.5 Unrooted radial tree produced using distance methods to compare the RecA amino acid sequence of *X. bovienii* T228/1 and *X. nematophilus* AN6/1 to the RecA sequences of 44 Gram positive and Gram negative bacteria. No outgroup was selected.

When grown on MacConkey agar, *E. coli* JC14604[pCT302] did not express lac papillae indicative of recombination events that lead to formation of a functional LacZ protein (data not shown). Two possible explanations for this observation are that the *X. bovienii* gene was not efficiently expressed in an *E. coli* host, or that the copy number of the expression plasmid was too high, which in turn resulted in gene dosage effects. The former was unlikely since other *Xenorhabdus* genes (eg *fliC* and *fliD* for *X. nematophilus* flagella synthesis (Givaudan *et al.*, 1996)), have been successfully expressed in *E. coli*.

To investigate the effect of copy number on *recA* expression, the *recA* gene from pCT302 was subcloned as a 2.1 kb *NotI* fragment into the low copy number vector pWKS130. Plasmid pCT302.1 contained the *recA* gene (and 5' regulatory sequences) cloned into pWKS130 as a *NotI* fragment in the same orientation as the pWKS130 based *lacZ* promoter. Plasmid pCT302.2 was identical to pCT302.1, except the *recA* gene was in the opposite orientation to the *lacZ* promoter. (Figure 3.6) Control transformations with pGEM-T and pWKS130 were also performed.

Clones pCT302.1 and pCT302.2, with *recA* in the same or opposite orientation as the *lacZ* promoter of pWKS130 respectively, were then used to transform *E. coli* JC14604. When plated on MacConkey agar, both clones produced colonies with lac papillae and hence expressed functional RecA (data not shown). These data implicated plasmid copy number as a reason for the failure of pCT302 to promote recombination in *E. coli* strain JC14604. Control transformations of *E. coli* JC14604 with either pGEM-T Easy or pWKS130 did not produce lac papillae on MacConkey agar.

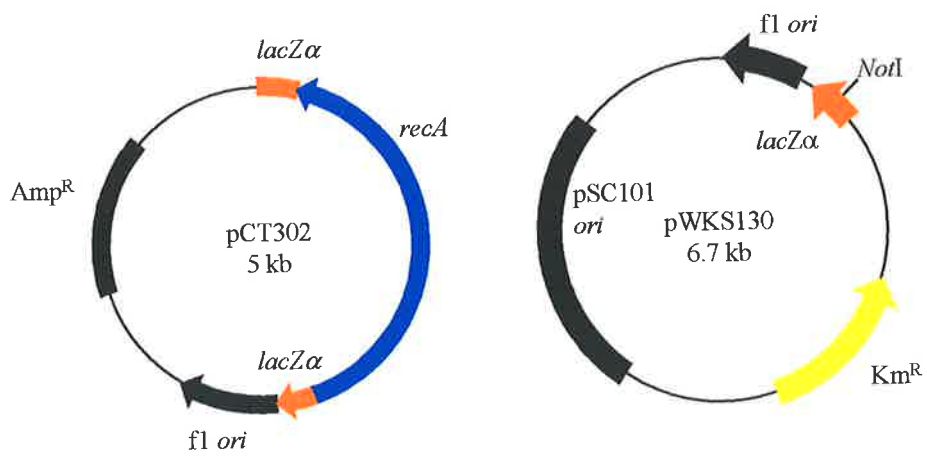
3.2.3 Construction of a *X. bovienii* *recA* insertion mutant

Construction of a *X. bovienii* *recA* insertion mutant was achieved by allelic-exchange mutagenesis. The Km^R cartridge from pBLS15 was inserted into a PCR amplified 850 bp fragment of *recA*, and this construct cloned into the suicide vector pCVD442. By virtue of homologous recombination the *recA*::Km^R construct was recombined into the chromosome of *X. bovienii*, creating a *recA* mutant. Southern hybridisation and PCR analysis were used to confirm the presence of the Km^R cartridge within *recA*.

Figure 3.6 Construction of plasmids, pCT302.1 and pCT302.2.

A 2.1 kb *NotI* DNA fragment from pCT302 which harbours the *recA* gene from *X. bovienii* T228, was subcloned into the *NotI* site of plasmid pWKS130. Clones were selected such that pCT302.1 contained *recA* in the same orientation as the *lacZ* promoter of pWKS130, whilst pCT302.2 contained *recA* in the opposite orientation.

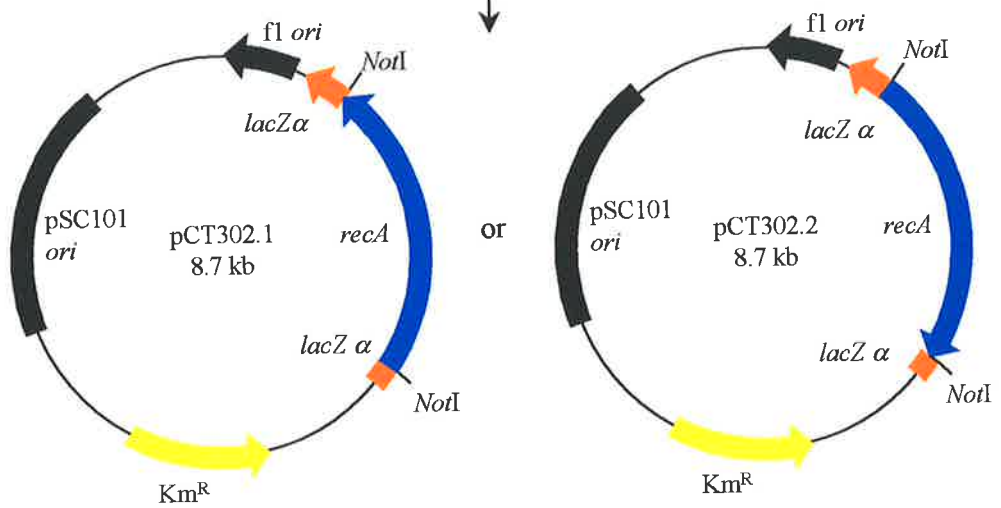
Abbreviations: Amp^R, ampicillin resistance gene; f1 *ori*, f1 origin of replication; pSC101 *ori*, pSC101 origin of replication; Km^R, kanamycin resistance gene; *lacZ* α , *lacZ* promoter region; *recA*, *recA* gene from *X. bovienii* T228.



NotI digestion

NotI digestion

Ligation



3.2.3.1 Construction of a suicide delivery vector for allelic-exchange mutagenesis

A *recA* mutant of *X. bovienii* was constructed using allelic-exchange mutagenesis. Construction of the suicide delivery vector is shown in Figure 3.7. An 850 bp DNA fragment internal to *recA* was amplified using the oligonucleotides PRECAF and PRECAR (see section 2.15.1). The 850 bp DNA fragment was cloned into pGEM-T, and the ligated DNA used to transform *E. coli* DH5 α by electroporation. The transformants were selected on NA supplemented with Amp, IPTG and X-gal. One clone was confirmed by a *SalI/SphI* digest and the correct plasmid designated pCT301. An *EcoRI* fragment encoding a 1.2 kb Km^R gene cartridge from pBSL15 was cloned into *EcoRI* digested pCT301. The ligation mix was used to transform *E. coli* DH5 α by electroporation, and transformants selected on NA supplemented with Amp and Km. This insertion resulted in formation of a *recA::Km^R* construct that comprised of 706 and 144 bp of *Xenorhabdus recA* DNA flanking the 5' and 3' ends of the kanamycin gene cartridge respectively. The resulting plasmid (pCT301.1) was then digested with *SalI* and *SphI* to isolate the *recA::Km^R* construct, and this was ligated to *SalI/SphI* digested pCVD442. The ligation mix was used to transform *E. coli* SY327 λ pir by electroporation, and transformants selected on NA supplemented with Amp and Km. One clone was confirmed by a *SalI/SphI* digest and designated pCT301.2. Plasmid pCT301.2 was used to transform *E. coli* SM10 λ pir by electroporation, and then transferred from *E. coli* SM10 λ pir to P1 *X. bovienii* by conjugal transfer. Co-integrates were selected by their resistance to Amp, Km and Sm, and resolved by plating on NaCl free NA containing 6% (w/v) sucrose (Blomfield *et al.*, 1991). A single sucrose resistant, putative *recA::Km^R* mutant was selected and designated *X. bovienii* XB001.

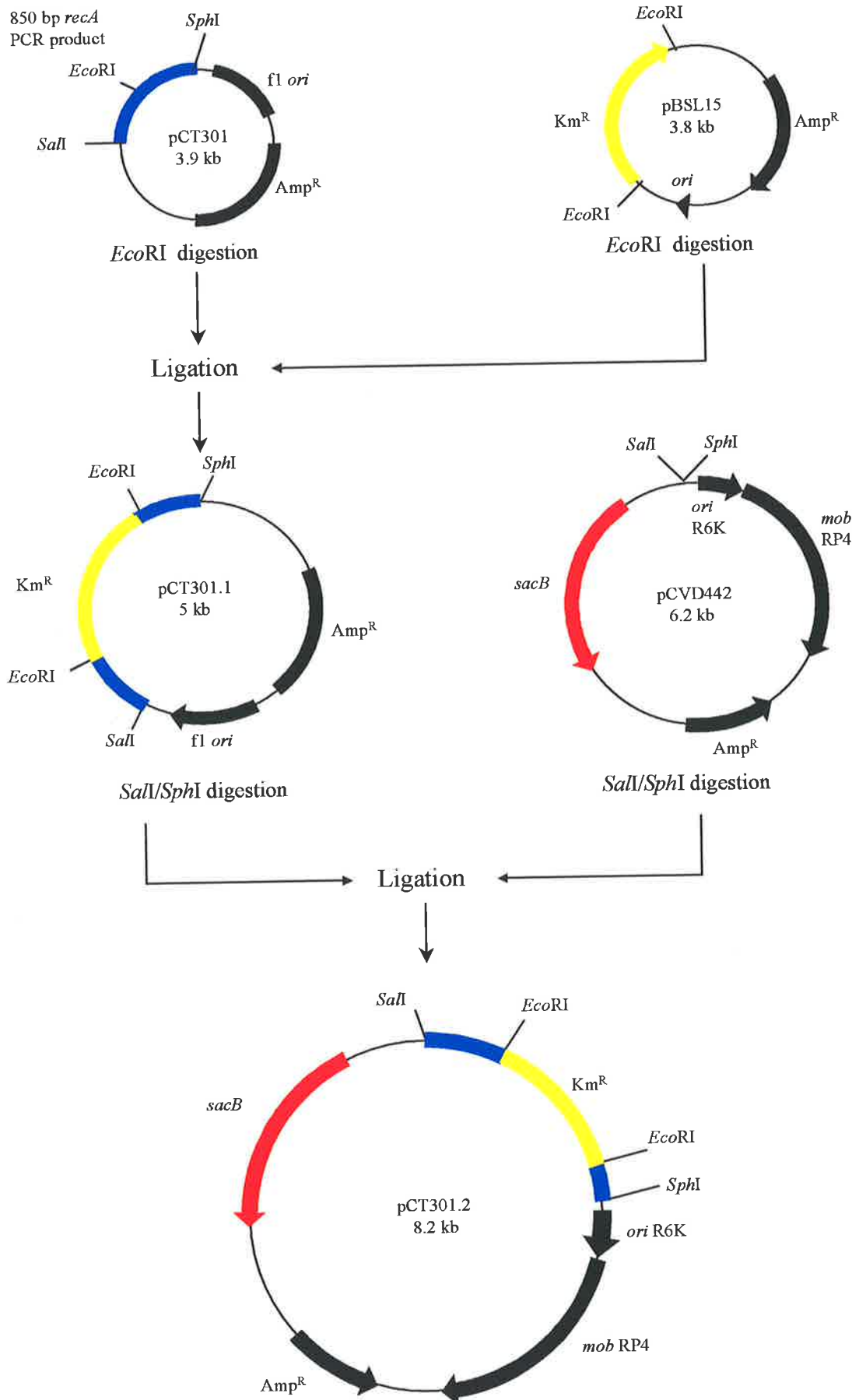
3.2.3.2 Confirmation of a kanamycin-resistance gene cartridge insertion into *X. bovienii recA*

PCR analysis using oligonucleotides PRECAF and PRECAR confirmed an insertion within the *recA* gene of XB001. An 850 bp fragment was amplified from chromosomal DNA isolated from the wild type parent, whilst a 2.05 kb fragment was amplified from XB001 DNA. This corresponded to the insertion of a 1.2 kb Km^R cassette into the chromosomally located *recA* (Figure 3.8). No PCR product was observed for negative control plasmids pGEM-T and pCVD442 as expected. An 850 bp and 2.05 kb PCR product was observed for

Figure 3.7 Construction of plasmids, pCT301.1 and pCT301.2.

A 1.2 kb kanamycin resistance gene (Km^R) from pBSL15 was subcloned into the *EcoRI* restriction site of an 850 bp internal fragment of the *X. bovienii recA* gene, harboured by plasmid pCT301. The subsequent plasmid pCT301.1 was digested with *SalI/SphI* to remove a 2 kb fragment containing *recA* and Km^R , which was subcloned into the similarly digested suicide plasmid pCVD442 to create pCT301.2.

Abbreviations: Amp^R , ampicillin resistance gene; Km^R , kanamycin resistance gene; *mob* RP4, mobilisation region; *sacB*, levansucrase; *ori* R6K, *pir* protein dependent R6K origin of replication; *ori*, origin of replication; *f1 ori*, *f1* origin of replication.



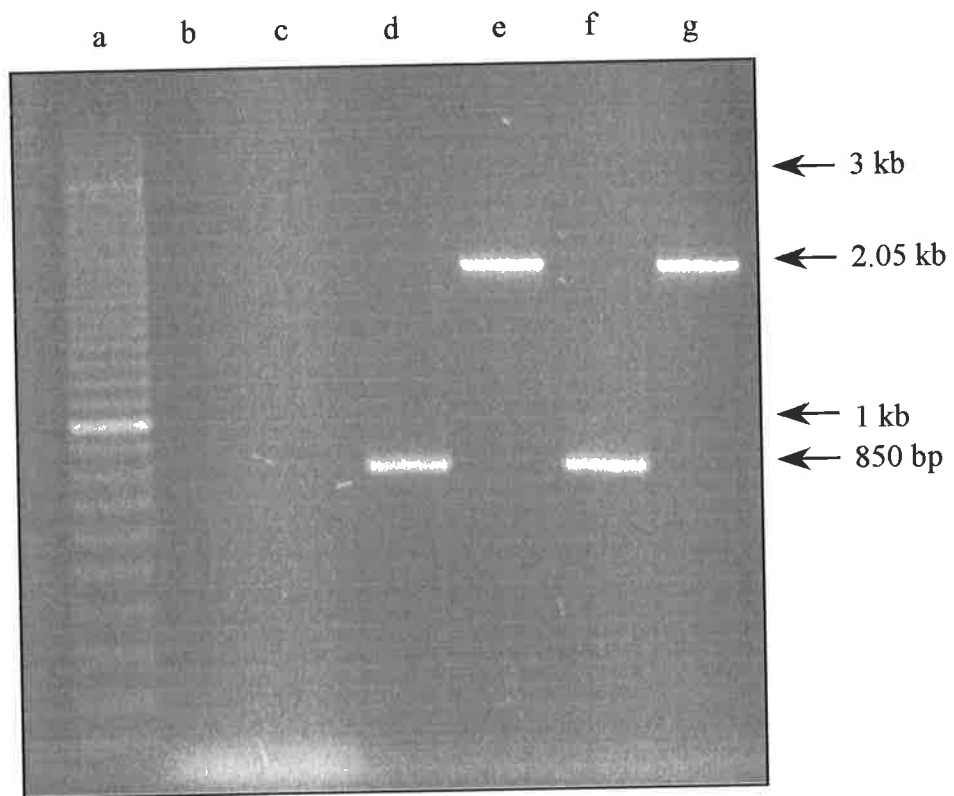


Figure 3.8 PCR analysis of plasmid and chromosomal DNA prepared from *X. bovienii* strains T228, *recA* insertion mutant XB001 and intermediate plasmids used for the construction of XB001 by allelic exchange mutagenesis. The size of PCR products are shown. 100 bp markers (DMW-100M) were used, the 1 and 3 kb bands are indicated.

Lanes:

[a], 100 bp marker;

[b], pGEM-T;

[c], pCVD442;

[d], pCT301;

[e], pCT301.2;

[f], T228 P1;

[g], XB001 P1.

positive control plasmids pCT301 and pCT301.2. These plasmids represent intermediate stages in the construction of *recA* mutant XB001.

Southern hybridisation analysis of *Dra*I digested chromosomal DNA showed that an 850 bp *recA* specific DNA probe (derived from pCT301, see section 3.2.3.1) hybridised with 1.6 kb and 2.8 kb fragments for the wild type and *recA* mutant strains respectively (Figure 3.9). The *recA* specific DNA probe hybridised with an 850 bp fragment for pCT301, and a 2.05 kb fragment for both pCT301.1 and pCT301.2 as expected. These data indicated XB001 contained a single *recA*::Km^R insertion mutation.

3.2.3.3 Theoretical expression of a truncated RecA by *X. bovienii* XB001

DNA sequence analysis of the *recA*::Km junction indicated this construct could theoretically express a truncated RecA protein. The C terminal end of this putative truncated 265 amino acid protein encoded four amino acids (proline, glycine, isoleucine and arginine) derived from the kanamycin resistance cassette. The truncated RecA comprises 72% of the wild type protein (Figure 3.10).

3.2.4 Complementation analysis of *X. bovienii* *recA* insertion mutant XB001

In order to demonstrate complementation of the *recA* mutant XB001, *recA* was cloned into conjugative vector pSUP203 and transferred to this strain by conjugation.

The *recA* gene from pCT302 was isolated as a 2.1 kb *Nco*I/*Pst*I fragment and subcloned into the *Nco*I/*Pst*I digested conjugative vector pSUP203. The ligation mix was used to transform *E. coli* DH5 α by electroporation, and transformants selected on NA supplemented with Tc (Figure 3.11). The correct construct was confirmed by an *Nco*I/*Pst*I digestion and designated pCT303. Plasmid pCT303, was tested in an *E. coli* JC14604 background to confirm that a functional copy of *recA* was present by production of lac papillae on MacConkey agar (see section 2.28) (data not shown). Plasmid pCT303 was used to transform *E. coli* SM10 λ pir by electroporation, and subsequently transferred into *X. bovienii* XB001 by conjugal transfer. Exconjugates were selected on NA supplemented with Sm and Tc. A single isolate, designated *X. bovienii* XB002, was selected for use in complementation analysis. P2 variants of XB002 were obtained by serial broth culture and selection on BTB agar.

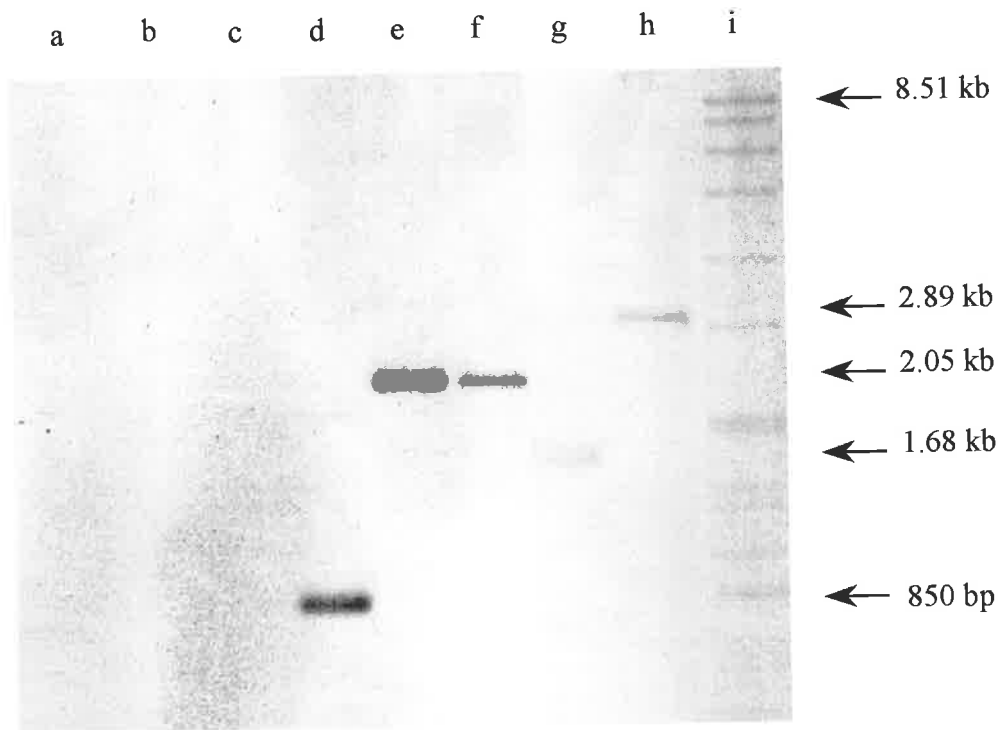


Figure 3.9 Southern hybridisation analysis of plasmid and chromosomal DNA prepared from *X. bovienii* strain T228 and the *recA* insertion mutant XB001. Plasmids pCVD442, pGEM-T and pSUP203 were digested with *Dra*I; plasmid pCT301, pCT301.1 and pCT301.2 were digested with *Sph*I and *Sal*I; chromosomal DNA from T228 and XB001 were digested with *Dra*I. The filter was probed with a digoxigenin labelled 850 bp internal *recA* fragment PCR amplified from pCT301. The size of DNA fragments hybridising with the probe DNA are shown. SPP1 markers are *Bacillus subtilis* phage SPP1 DNA digested with *Eco*RI.

Lanes:

[a], pCVD442;

[b], pGEM-T;

[c], pSUP203;

[d], pCT301;

[e], pCT301.1;

[f], pCT301.2;

[g], *X. bovienii* T228;

[h], *X. bovienii* XB001;

[i], SPP1 marker

Figure 3.10 The deduced nucleotide sequence of *X. bovienii* T228 *recA*::Km, including regulatory sequences. The nucleotides are numbered to the right hand side in the 5' to 3' direction. The deduced protein sequence of the open reading frame, *recA*, is given below the DNA sequence in the single letter amino acid code and is numbered to the right hand side. The putative regulatory elements of the *recA*, start codon, ribosome binding site (rbs), -10 region, -35 region and translational stop codon are indicated. Amino acids 60-78 (inclusive) are highlighted and represent ATP binding domain I. Amino acid 61-R (arginine), required for homologous recombination is underlined. Nucleotide position 886 shows the fusion of the cartridge from mini-Tn5 Km to *recA* by ligation at an *EcoRI* site. Amino acids 262-265 (inclusive) represent the additional amino acids added to the truncated RecA polypeptide.

CAGCTTAGTATTGAACTTGAAAGAACTCCAACGGAAAAATTATCCTTAACCTGTGCA - 60
 GAATCCTGCACAGGGGGCTGGATTGCTAAAAGTGATCACAGATATTGCGGGAAAGTTCGGCC - 120
 TATTTTAACCGCAGTTTCGTGACCTATAGCAATGATTCTAAAAATGAAATGCTGGGTGTA - 180
 TCACAGGCATCACTGGTGCAGTTTGGTGCGGTGAGTGAACAGGTCGTTAAAGAAATGGCA - 240
 GTAGGGGCATTAAAGGCGGCCAGAGCAGATTTTGTCTGTTTCTGTCACTGGCAGTCCGAGGT - 300
 CCGGATGGTGGCAGTGAAGAAAAACCGACGGGAACGGTCTACTTTGGGTTTACCTACCGT - 360
 AATGGTGAGGATGTACATACCGTGACATATCGCCAGCATTTTACGGGTGATCGCAATGCA - 420

DraI

GTACGGCTCCAGGCTGTCATTTTTTCTTTAAACACTGCTGGAAGAAATCATAAAAAAT - 480
 -35 region -10 region
 TAGCTTGATGCTGTATGATTATACAGTATAATTAATTCAGCACTTTGGTATCAGAAACG - 540

rbs *recA* start

GTTTATCAGCAGTGGGGCAGCCCCTTCATTGCTTACGAAGGAGTAAACATGGCTAACGAT - 600
 M A N D - 4
 GAAAACAAACAAAAAGCACTAGCAGCGGCGCTGGGTCAAATTGAAAAACAATTTGGTAAA - 660
 E N K Q K A L A A A L G Q I E K Q F G K - 24
 GGTTCATCATGCGTCTGGGCGAAAACCGCTCAATGGATGTTGAAACTATCTCTACTGGC - 720
 G S I M R L G E N R S M D V E T I S T G - 44
 TCACTGTCACTGGATATAGCATTAGGTGCGGGTGGTTTGCCAATGGGCCGTATTGTTGAA - 780
 S L S L D I A L G A G G L P M **G R I V E** - 64
 ATATACGGCCTGAATCTTCGGGTAAGACAACATTGACACTGCAAGTTATTGCTTCTGCC - 840
I Y G P E S S G K T T L T I Q V I A S A - 84

ATP binding domain I

CAGCGTGAAGGCAAAACCTGTGCTTTTTATTGATGCCGAACATGCCCTTGATCCGGTTTAT - 900
 Q R E G K T C A F I D A E H A L D P V Y - 104
 GCCAAAAAGTTGGGCGTAGATATTGATAACCTGCTGTGCTCCCAGCCTGATACAGGTGAA - 960
 A K K L G V D I D N L L C S Q P D T G E - 124
 CAGGCACTGGAAATCTGTGATGCCTTGTACGCTCTGGGGCGGTTGACGTCATCGTTGTT - 1020
 Q A L E I C D A L S R S G A V D V I V V - 144
 GACTCCGTTGCTGCATTGACCCCGAAAGCGGAAATCGAAGGTGAGATCGGCGATTCCCAT - 1080
 D S V A A L T P K A E I E G E I G D S H - 164
 ATGGGCTTGGCAGCTCGTATGATGAGTCAGGCCATGCGTAAGTTGGCAGGTAACCTGAAA - 1140
 M G L A A R M M S Q A M R K L A G N L K - 184
 AACTCGAATACTCTGCTAATCTTTATCAACCAGATCCGTATGAAAATTGGTGTGATGTTT - 1200
 N S N T L L I F I N Q I R M K I G V M F - 204
 GGTAACCCAGAAACCACAACAGGTGGTAATGCACTGAAATTTTATGCATCTGTCCGTTTG - 1260
 G N P E T T T G G N A L K F Y A S V R L - 224
 GACATCCGCCGCACTGGTTCGGTAAAAAATGGCGATGAAGTTGTTGGCAGCGAGACTCGT - 1320
 D I R R R T G S V K N G D E V V G S E T R - 244

EcoRI

GTGAAAGTAGTCAAGAACAAAATTGCGGCACCGTTCAAACAAGCT**GAATTC**CCGGGGATC - 1380
 V K V V K N K I A A P F K Q A E F P G I - 264

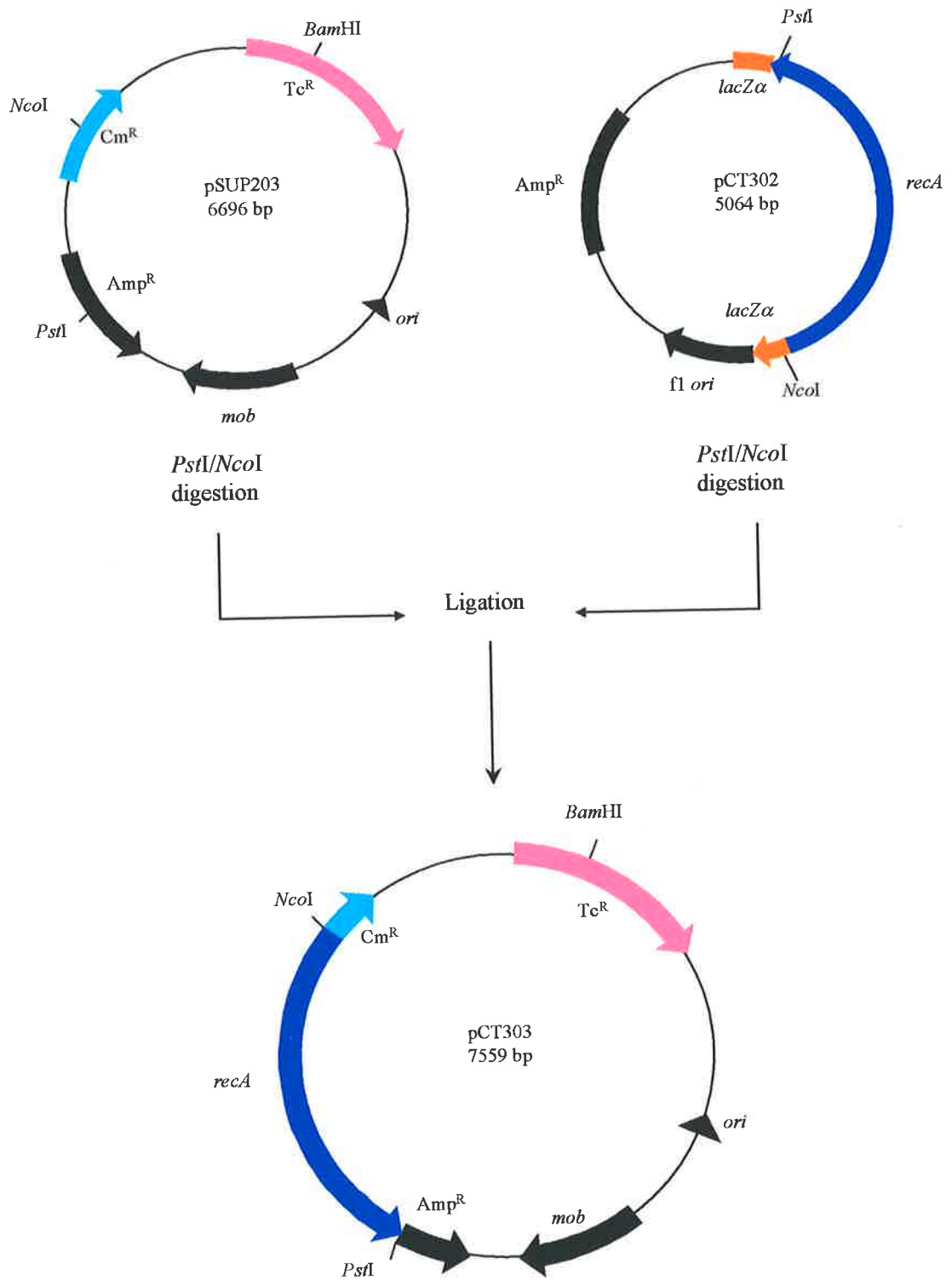
mini-Tn5 Km

CGGTGA - 1386
 R * - 265
stop

Figure 3.11 Construction of plasmid pCT303.

A 2.1 kb *NcoI/PstI* fragment containing the *X. bovienii recA* gene was excised from pCT302. The 2.1 kb fragment was subcloned into the *NcoI/PstI* digested plasmid pSUP203 to create pCT303.

Abbreviations: Amp^R, ampicillin resistance gene; Cm^R, chloramphenicol resistance gene; *lacZα*, *lacZ* promoter region; *mob*, mobilisation region; *ori*, origin of replication; f1 *ori*, f1 origin of replication; *recA*, *X. bovienii recA* gene; Tc^R, tetracycline resistance gene.



3.2.5 Phenotypic comparison of *X. bovienii* T228, XB001 and XB002 with respect to *recA* function

3.2.5.1 Expression of phase dependent phenotypic characteristics by the *recA* insertion mutant (XB001) and the *recA* complemented strain (XB002)

Expression of phospholipase C, haemolysin and protease activity was identical for wild type *X. bovienii* T228, *recA* insertion mutant XB001 and *recA* complemented strain XB002. P1 variants were positive and P2 variants negative for each of these characteristics (Table 3.1).

Table 3.1 Expression of phase dependent characteristics by *X. bovienii* strain T228, the *recA::kan* insertion mutant XB001 and the *recA* complemented mutant XB002. A + denotes a positive phenotype; a - indicates a negative phenotype.

	T228		XB001		XB002	
	P1	P2	P1	P2	P1	P2
Phospholipase C	+	-	+	-	+	-
Haemolysin	+	-	+	-	+	-
Protease	+	-	+	-	+	-
Antimicrobial activity	+	-	+	-	+	-
Congo Red binding	+	-	+	-	+	-

Similarly, antibiotic production and Congo Red binding ability were unaffected by mutations in *recA* (Table 3.1). When P1 forms of XB001 were subcultured onto BTB agar, P2 forms were readily isolated.

Confirmation that pCT303 encoded a functional RecA was obtained by examining the UV light sensitivity (see section 2.27) of the *E. coli recA*⁻ strain, DK1, which carried plasmid

pCT303. *E. coli* DK1[pCT303] (Figure 3.12, lane k) demonstrated increased ability to resist UV-mediated killing when compared to *E. coli* DK1 alone (Figure 3.12, lane i), or *E. coli* DK1 carrying the vector pSUP203 (Figure 3.12, lane j). After 8 seconds exposure to UV no surviving colonies of either *E. coli* DK1 or *E. coli* DK1[pSUP203] were detected, whereas *E. coli* DK1[pCT303] was able to survive up to 44 seconds exposure.

No difference in the UV sensitivity of P1 and P2 strains of *X. bovienii* was detected (Figure 3.12, lanes a and b respectively), although these strains were clearly more sensitive to UV exposure than the complemented *E. coli* strain DK1[pCT303]. P1 and P2 variants of the *X. bovienii recA* insertion mutant XB001 (Figure 3.13, lanes c and d respectively) were extremely sensitive to UV and were unable to survive even brief (< 3 seconds) UV exposure. However, complemented P1 and P2 variants of XB002 (Figure 3.12, lanes e and f respectively) harbouring pCT303 demonstrated partial restoration of resistance to UV-mediated killing (5 seconds) P1 and P2 variants of XB002 carrying only the vector pSUP203 remained UV sensitive (Figure 3.12, lanes g and h respectively).

3.2.6 Analysis of virulence of *recA* mutants for *Galleria mellonella*.

In order to determine whether *recA* played a role in the pathogenicity of *X. bovienii* for susceptible insect larvae, LD₅₀ analysis was used to compare wild type P1 and P2 bacteria and the *recA* mutant *X. bovienii* XB001 (see section 2.26). Sixth instar larvae were infected with known doses of *X. bovienii* T228 or XB001. Control larvae groups were injected with PBS. The viability of the bacterial suspensions used did not change significantly over the time required to infect groups of larvae. Treated larvae were incubated at 28°C for up to 72 h and the number of dead or moribund larvae recorded at regular time intervals.

All strains killed larvae irrespective of the dose applied. Doses greater than five bacteria per larvae consistently killed all larvae within 24 - 36 h, whereas lower doses killed only a proportion of infected larvae. No deaths were recorded for control group of larvae injected with saline. LD₅₀ values were determined directly from plots of percentage dosage mortality vs. mean dose of bacteria (Reed & Muench, 1938). The mean LD₅₀ values obtained from three independent experiments using P1 and P2 wild type strains and *recA* mutant XB001 were 3.1 ± 0.05 , 3.4 ± 1.5 and 2.7 ± 0.9 respectively. One-way analysis of variance indicated these values were not significantly different ($P > 0.05$). These estimates of the LD₅₀ are

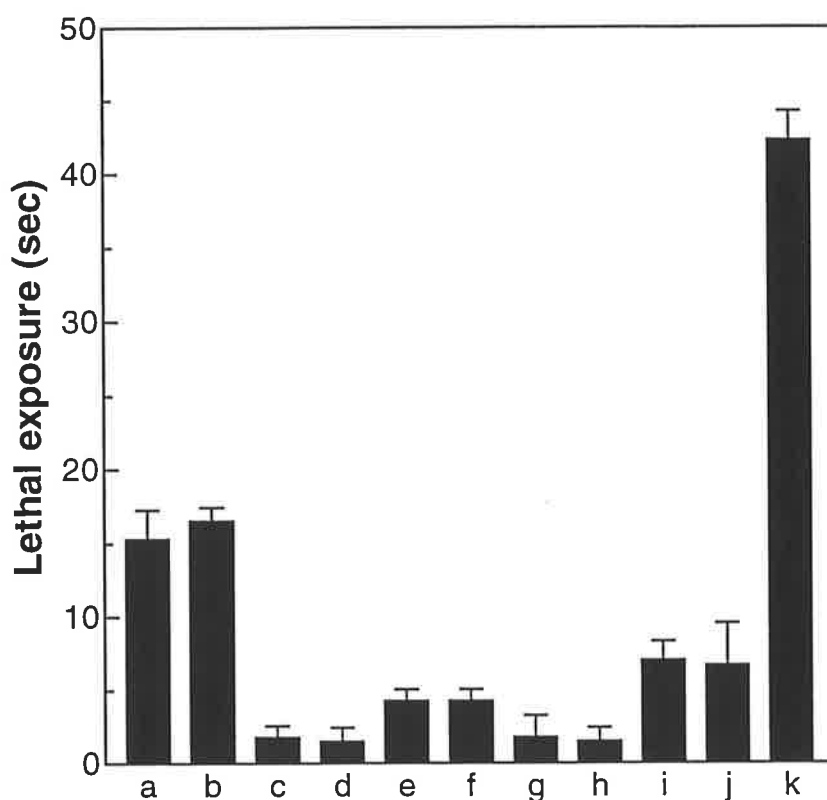


Figure 3.12 Comparison of resistance to UV killing by strains of *X. bovienii* and *E. coli*. Resistance to UV is measured as exposure time required to completely inhibit growth of an inoculum of bacteria on a nutrient agar plate. Results shown are the mean of four independent observations per experimental group. Error bars represent 95% confidence intervals about the mean.

Lanes:

[a], *X. bovienii* T228 P1;

[b], *X. bovienii* T228 P2;

[c], XB001 P1;

[d], XB001 P2;

[e], XB002 P1;

[f], XB002 P2;

[g], XB001[pSUP203] P1;

[h], XB001 [pSUP203] P2;

[i], *E. coli* DK1;

[j], *E. coli* DK1[pSUP203];

[k], *E. coli* DK1 [pCT303]

similar to those reported elsewhere (Pinyon *et al.*, 1996). Typical plots of percentage mortality ratio vs. dose of bacteria were also very similar (Figure 3.13). Furthermore, when doses of bacteria approximating the calculated LD₅₀ (approximately 4 cells per larva) were used, the proportion of larvae dying over a 60 h period was not significantly different for the wild type strain and the *recA* mutant ($P>0.05$, analysis of variance; Figure 3.14).

3.3 Discussion

PCR based techniques were used to clone and sequence the *recA* gene from *X. bovienii* T228. The translated sequence was 95% similar to that of the related species, *X. nematophilus* AN6, and showed considerable similarity to RecA proteins from Gram negative bacteria, in particular *Erwinia carotovora*, *Proteus mirabilis*, *Serratia marcescens* and *Yersinia pestis*.

An evolutionary tree relating *Xenorhabdus* RecA peptide sequences to those of 44 other RecA proteins was constructed. This tree was similar to those constructed previously (Eisen, 1995) and supported the position of *Xenorhabdus* spp. within the family Enterobacteriaceae of the γ proteobacteria.

UV sensitivity, complementation analysis and recombination proficiency assays were used to demonstrate expression of a functional *X. bovienii* RecA protein from plasmids in RecA deficient *E. coli* backgrounds. However, expression was dependent on plasmid vector copy number. This phenomenon has been observed previously, as has RecA protein instability due to expression from high copy number plasmid vectors (Fyfe & Davies, 1990; Stroehler *et al.*, 1994).

Construction of a chromosomal *recA* mutation in *X. bovienii* was achieved by allelic exchange of a *recA::kan* insertion mutation from a pCVD442 based suicide plasmid. Loss of *recA* function by *X. bovienii* XB001 was established using simple UV sensitivity studies. Since a functional relationship exists between homologous recombination and the repair of DNA damage, mutations within *recA* sensitise cells to killing by UV light. Although no difference in the UV sensitivity of P1 and P2 wild type *X. bovienii* strains was noted, the *recA* mutant had significantly reduced ability to repair DNA lesions caused by exposure to UV radiation. Furthermore, resistance to UV induced damage of this mutant could not be restored to wild type levels by complementation with a functional copy of *recA* from plasmid pCT303, even

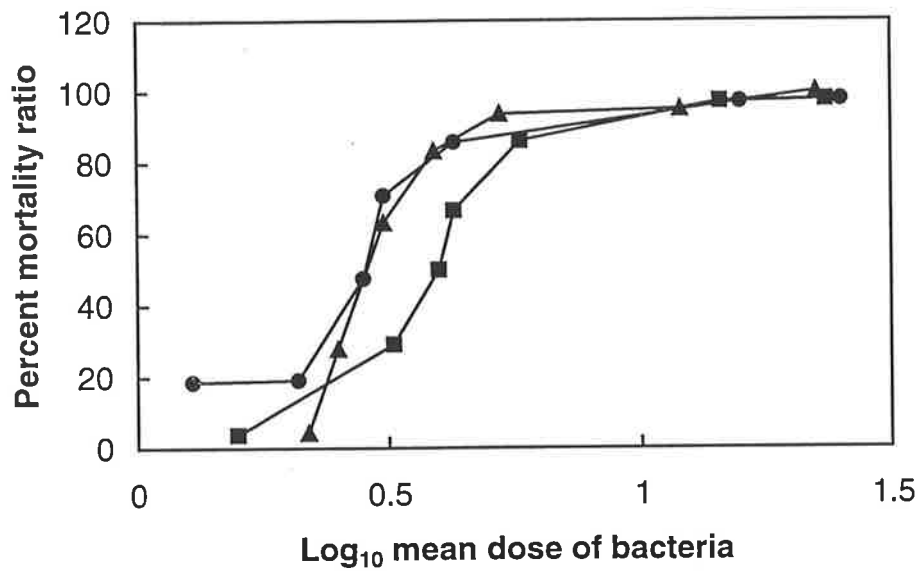


Figure 3.13 Typical dose response curve for *G. mellonella* larvae infected with P1 and P2 *X. bovienii* wild type bacteria or the *recA* insertion mutant (XB001). Symbols: ▲, *X. bovienii* T228/1 P1; ●, *X. bovienii* T228/1 P2; ■, *X. bovienii* XB001 P1

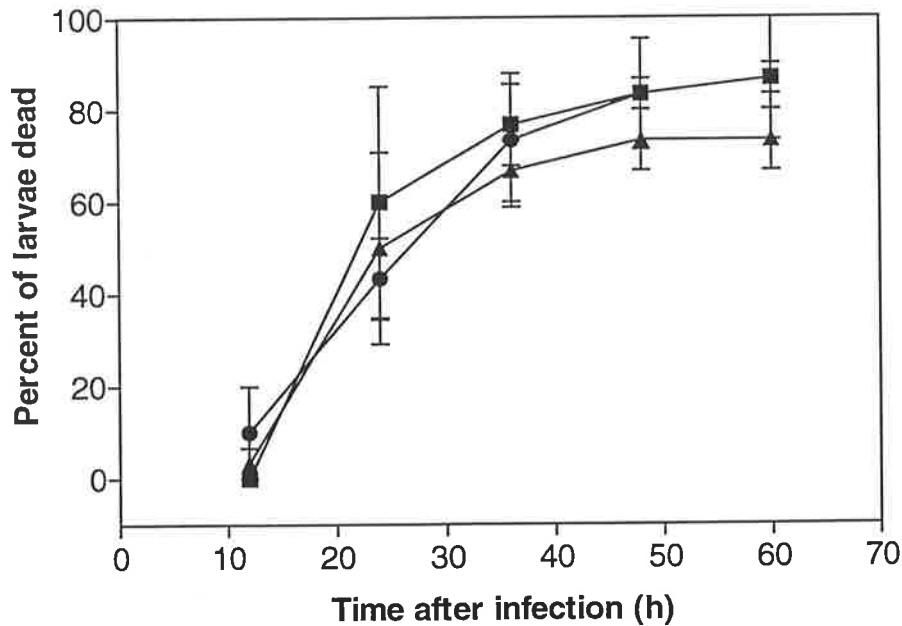


Figure 3.14 Proportion of larvae dying over a 60 hour period following infection with doses of bacteria approximating that of the calculated LD₅₀ for P1 *X. bovienii* T228 (ca 4 cells per larva). Larvae were infected with P1 and P2 *X. bovienii* wild type bacteria or the *recA* insertion mutant (XB001). Symbols: ▲, *X. bovienii* T228/1 P1; ●, *X. bovienii* T228/1 P2; ■, *X. bovienii* XB001 P1

though introduction of pCT303 into *E. coli* DK1 (which has a deletion of the *recA* gene), completely restored resistance to UV radiation for this organism.

Previous *in vitro* work has shown that the single-stranded DNA dependent ATPase activity of RecA is a property of the tetrameric form of the protein (Ogawa *et al.*, 1978). Thus ATPase activity is required for the *in vitro* recombination functions of purified RecA (Radding, 1982; Weinstock *et al.*, 1979), although this is not the case for the proteolytic activity of RecA involved in SOS induction (Phizicky & Roberts, 1981). ATP binding is also required for formation of RecA tetramers and filamentous aggregates of the RecA protein (Ogawa *et al.*, 1978). When *recA1* missense protein and wild type RecA protein of *E. coli* form mixed tetramers in the presence of ATP, a dramatic reduction in ATPase activity is observed (Ogawa *et al.*, 1978). Phenotypically, the *recA1* mutation, Gly-160 to Asp-160, is indistinguishable from a *recA* deletion (Kowalczykowski *et al.*, 1994). Therefore the extent of the reduction of ATPase activity is dependent on the ratio of the two polypeptides. *In vivo*, the recombination activity of wild-type *recA* protein is also significantly reduced in the presence of a non-functional RecA1 polypeptide. This phenomenon is known as negative complementation and has been well documented for cases such as the *lacZ* gene (Muller-Hill *et al.*, 1968), and the *capR* gene (Charette *et al.*, 1982), where the active form of the protein is a tetramer.

Formation of mixed tetramers of RecA may explain the reduced ability of pCT303 to complement the *recA::kan* insertion mutation present in XB001. Mixtures containing truncated proteins comprising up to 79% of the wild type protein, have been shown to promote strong negative complementation (Yarranton & Sedgwick, 1982). Since, the *recA::kan* mutation in XB002 has the potential to express 72% of the wild type protein (starting at the N-terminus), this peptide has the potential to facilitate negative complementation in the presence of wild type RecA. This hypothesis is supported by fact that the truncated RecA protein encoded by the *recA::kan* mutation, did not include the ATP-binding site containing a tyrosine residue which is necessary for co-protease activity and recombination (Cotteril *et al.*, 1982; Knight & McEntee, 1986). Thus co-protease activity and recombination potential should either be reduced or abolished in strain XB002.

The formation of a RecA filament on ssDNA is also essential for recombination and inactivation of repressors such as LexA. Interference with these functions by defective RecA protein could occur by formation of a complete but defective filament in a mixed multimer,

formation of an incomplete and defective filament in a mixed multimer, or loss of filament formation (Kowalczykowski *et al.*, 1994). Residues 41 to 59 (of the *E. coli* RecA) are thought to contain one of the regions responsible for interaction between wild type protein monomers (Freitag & McEntee, 1988). Analysis of the protein-protein interaction sites on the RecA protein using a RecA affinity column has shown that a 90 amino acid fragment from the N-terminal end of RecA hydrophobically interacts with wild-type RecA protein (Freitag & McEntee, 1988). From the distributions of the hydrophobic amino acid residues in these 90 residues, regions 37 to 59 and 73 to 83 were suggested as candidates for the hydrophobic interaction site (Freitag & McEntee, 1988). Thus a truncated RecA protein that has intact interaction sites, but lacks an important region for RecA function, could form a complete but defective filament of mixed multimer. This is a likely scenario for the *recA::Km* mutation constructed (Figure 3.11). The first 90 residues are present, and furthermore, amino acids 37 through to 83 are identical in *E. coli* and *Xenorhabdus* with the exception of residue 83 that were alanine and serine respectively.

Interestingly, wild type, *recA* mutant and complemented mutant strains of *X. bovienii* were identical in terms of expression of known phase dependent characteristics. Furthermore, P1 *X. bovienii recA* mutants were able to convert to P2 forms on extended serial subculture. When taken together with Southern hybridisation analyses that showed no obvious large rearrangements in DNA isolated from P1 and P2 forms (Akhurst & Boemare, 1990), it is very unlikely that *recA* plays a role in phase variation or regulation of phase dependent characteristics of *Xenorhabdus* spp. This conclusion is further supported by larval infection studies that show a *recA* mutant XB001 is able to kill larvae as well as either P1 or P2 forms of the wild-type derivative.

A commonly used approach, which aids genetic analysis of virulence factors and other aspects of bacterial physiology, is the construction of recombination deficient mutants. Results from this study will allow progress in molecular analysis of the basis for pathogenesis of *Xenorhabdus* spp. for susceptible insect larvae as well as other phenotypic characteristics. RecA deficient mutants not only facilitate genetic complementation analyses, but also increase the stability of recombinant plasmids and retention of foreign DNA.

Further work in this area may focus on whether the RecA mutant XB001 is able to support nematode growth and reproduction. Nematodes require *Xenorhabdus* strains for a source of

nutrition and to facilitate breakdown of the insect tissue for nematode digestion. Initially, the ability of nematodes to retain XB001 within their intestine needs to be established. Moreover, studies could examine whether XB001 has a growth defect with respect to the growth and development of the nematode within the insect cadaver.

Chapter 4

Transposon mutagenesis of *X. bovienii* T228, and identification of non-ribosomal peptide synthetase (NRPS) homologous DNA

4.1 Introduction

Bacterial virulence determinants include a wide array of factors that permit colonisation of a specific niche in the host, evasion of host immune responses, direct host toxicity, or invasion of cells and/or tissues. Virulence determinants are often coregulated to best suit the interaction of the organism with the host (Neidhardt, 1996). The ability to vary cell-surface composition often plays a role in evasion of antigen-specific host immune defences. By promoting expression of most the appropriate cell surface or secreted components for a given microenvironment or infection stage, a bacterial pathogen can optimise its virulence potential during infection.

As outlined in Chapters 1 and 3, *Xenorhabdus* species produce a number of cell surface associated and secreted components which are thought to play a role in the pathogenesis of *Xenorhabdus* for a variety of target insect species (Klein, 1990; Forst *et al.*, 1997). Examples of these cellular compounds include protease, lipase, phospholipase C, haemolysin, antibiotic substances and Congo Red binding protein (Akhurst, 1982; Boemare & Akhurst, 1988; Akhurst & Boemare, 1990; Boemare *et al.*, 1997a). P2 forms are unable to (or only weakly) express these putative virulence determinants (Akhurst & Boemare, 1990). When colonies of cells coordinately express these genes, they are termed phase 1 (P1) bacteria. *Xenorhabdus* cells not expressing these genes are termed phase 2 (P2) bacteria. The reason for this colony pleomorphism is the subject of extensive research. One hypothesis to explain this phenomenon is that when P1 *Xenorhabdus* are released into the insect haemolymph by their nematode symbiont, the bacterial cell surface and secreted components are required to breakdown insect tissue providing a nutrient source for the developing dauer nematodes. This is supported by the observation that whilst both P1 and P2 *Xenorhabdus* seem to be equally pathogenic towards insect hosts, the numbers of infective juvenile nematodes recovered from P2 infected insect cadavers are significantly reduced (Akhurst, 1980). Therefore, phase variation in *Xenorhabdus* spp. is likely to play a role in the pathogenesis of *Xenorhabdus* for a variety of insect species via the production of large numbers of infective juvenile nematodes.

As phase variation coordinately affects a large number of specific characteristics, it is possible that these genes are regulated by a common control mechanism that is yet to be characterised (Dunphy *et al.*, 1997; Forst *et al.*, 1997). However this is only speculation and is complicated by the fact that intermediate phases have been noted (Akhurst, 1980). Therefore the control system may be more complex than a master switch that controls a common mechanism.

In this chapter transposon mutagenesis was used as a tool for genetic analysis of phase variant characteristics, with the aim of identifying important regions of DNA required for the expression of a phase variant phenotype. Using the transposon mini-Tn5 Km (De Lorenzo *et al.*, 1990) a bank of independent *X. bovienii* T228 insertion mutants was created and screened for loss or change of a number of phenotypes. The delivery system for the mini-Tn5 transposon is the pUT plasmid (Herrero *et al.*, 1990) that has the π (*pir*) protein-dependent origin of plasmid R6K (Kolter *et al.*, 1978). The plasmid is only maintained in π protein-producing bacteria, and carries the origin of transfer *oriT* of plasmid RP4 that results in conjugal transfer to recipient strains from donor strains expressing RP4-conjugative functions. Plasmid pUTKm carries *tnp**, a mutant *tnp* gene of IS50R that encodes the transposase needed for transposition of the mini-Tn5 elements. Transposon Tn5 has the broadest host range known (Berg, 1989; Berg *et al.*, 1989) and has been effective at generating insertion mutants in a wide variety of Gram negative bacteria (Berg *et al.*, 1989). Importantly, Tn5 has been shown to result in independent insertions in within the *Xenorhabdus* chromosome (Xu *et al.*, 1991). Plasmid pUTKm is particularly useful for mutagenesis of *Xenorhabdus* spp. due to the ability of the plasmid to be transferred from donor to host strains via conjugation (De Lorenzo *et al.*, 1990) as *Xenorhabdus* spp. are known to be extremely difficult to transform (Xu *et al.*, 1991; Forst & Nealson, 1996).

This chapter describes how transposon mutagenesis of *X. bovienii* T288 gave rise to five independent insertions that showed a disruption in lecithinase, haemolysin and antibiotic expression. Also the pattern of Congo Red binding was found to be significantly altered in each mutant. The approach used to clone and sequence *X. bovienii* DNA flanking each transposon mutant is described. Overall, three of the transposon insertion mutants were mapped to a 15 kb gene region that shows significant homology to a family of enzymes known as peptide synthetases.

4.2 Results

4.2.1 Construction of a *X. bovienii* mini-Tn5 Km based transposon mutant bank

4.2.1.1 Conjugal transfer of pUTKm into *X. bovienii* T228

In this study, the Amp^R, Km^R suicide vector pUTKm (De Lorenzo *et al.*, 1990) (Figure 4.1.) was used to demonstrate conjugal transfer from *E. coli* SM10 λ pir (Km^R) to *X. bovienii* T228/1 (Amp^R, Sm^R). Km^R/Sm^R *Xenorhabdus* were isolated at a frequency of 2.1×10^{-5} transconjugates/donor cfu.

4.2.1.2 Southern hybridisation analysis of *X. bovienii* mini-Tn5 Km insertion mutants

To determine whether mini-Tn5 Km had randomly inserted into the chromosome of *X. bovienii*, *Pvu*II digested chromosomal DNA from four randomly selected transconjugates were probed with the DIG labelled Km cartridge by Southern hybridisation. The Km cartridge was excised from pUTKm as a 2298 bp *Sfi*I fragment (see Figure 4.2). In all chromosomal samples the conserved 0.76 kb and 0.36 kb fragments that represent the internal *Pvu*II fragments within mini-Tn5 Km hybridised with the Km probe (see Figure 4.2 and 4.3). The two variable fragments that hybridised to probe DNA represent chromosomal DNA flanking the transposon insertion. Undigested pUTKm DNA was included as a positive control. Chromosomal DNA extracted from wild type *X. bovienii*, and subsequently digested with *Pvu*II did not hybridise with probe DNA under the stringency conditions used. These results suggest this transposon can be used to generate independent insertion mutants in *X. bovienii*.

Figure 4.1 Schematic representation of plasmid pUTKm, used for the transposon mutagenesis of *X. bovienii* chromosomal DNA.

Abbreviations: Amp^R, ampicillin resistance gene; *mob* RP4, mobilisation region; *tnp**, a mutant *tnp* gene of IS50R that encodes the transposase need for transposition of the mini-Tn5 Km element; *ori* R6K, π protein dependent R6K origin of replication; mini-Tn5 Km, Tn5 transposon encoding Km^R as a selectable marker.

Figure 4.2 Schematic representation of 2356 bp transposon mini-Tn5 Km depicted in Figure 4.1. Restriction enzyme sites are indicated, and the numbers in brackets represent the enzyme site nucleotide position. The shaded arrow represents the Km^R gene, neomycin phosphotransferase. The I end and O end sequences represent the 19 bp Tn5 based inverted repeats.

Figure 4.1

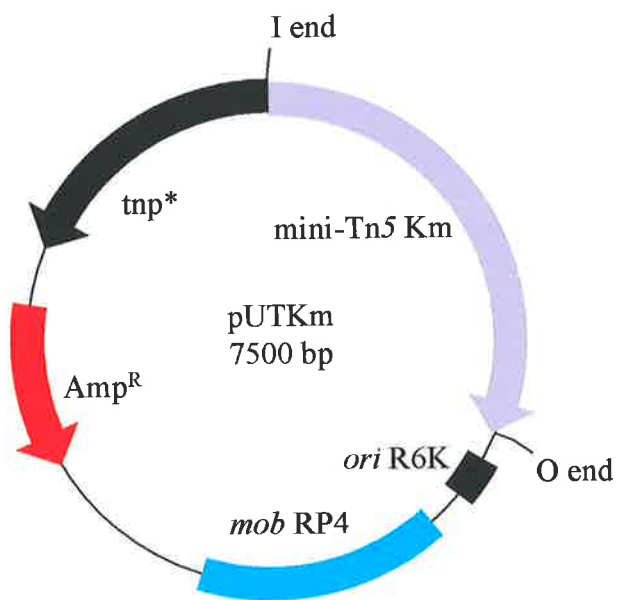
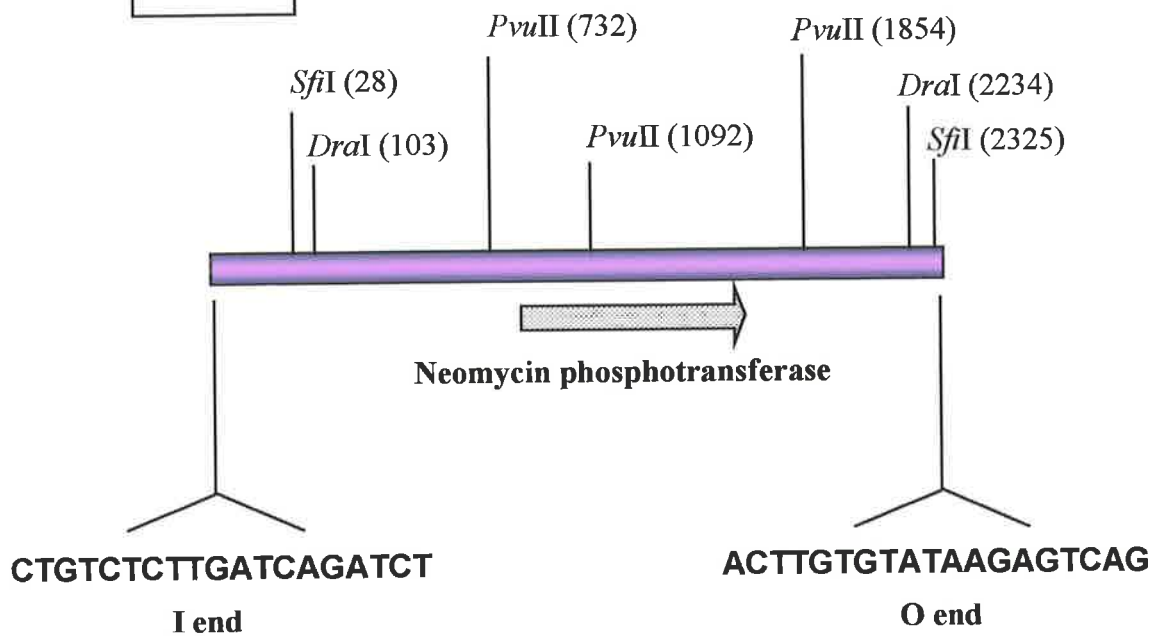


Figure 4.2



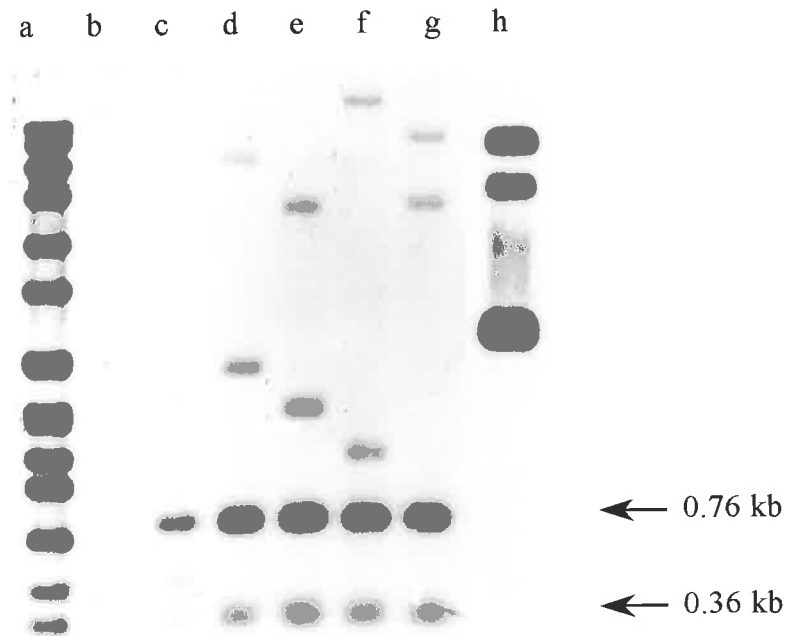


Figure 4.3 Southern hybridisation analysis of plasmid DNA from pUTKm, chromosomal DNA from *X. bovienii* T228 and five randomly selected *X. bovienii* Km^R transconjugates. All chromosomal DNA was digested with *PvuII*. Plasmid DNA from pUTKm remained undigested. The filter was probed with a digoxigenin labelled 2298 bp *SfiI* internal fragment from pUTKm. The size of DNA fragments hybridising with the probe DNA are shown.

Lanes:

[a], SPP1 markers are *Bacillus subtilis* phage SPP1 DNA digested with *EcoRI*;

[b], *X. bovienii* T228 chromosomal DNA digested with *PvuII*;

[c - g], randomly selected *X. bovienii* transconjugate chromosomal DNA digested with *PvuII*;

[h], undigested pUTKm.

4.2.2 Characterisation of mini-Tn5 Km induced transposon insertion mutants of *X. bovienii* T228

4.2.2.1 Phenotypic characterisation of *X. bovienii* transposon insertion mutants

Mini-Tn5 Km induced insertion mutants of *X. bovienii* T228 were screened for the loss of antimicrobial, haemolytic and phospholipase C activity in both P1 and P2 bacteria. Antimicrobial production is common for P1 *Xenorhabdus* spp. (Akhurst, 1982), whilst P2 bacteria have significantly reduced, or no activity (Boemare & Akhurst, 1988). It is hypothesised the role of antimicrobials is maintenance of *Xenorhabdus* during the growth of nematodes in the infected host, therefore avoiding putrefaction of the insect and poor nematode yield (Dutky, 1959; Akhurst, 1982; Chen *et al.*, 1994; Forst & Neelson, 1996). Haemolysin and phospholipase C are expressed by P1, but not P2 bacteria (Boemare & Akhurst, 1988; Akhurst & Boemare, 1990; Neelson *et al.*, 1990). It is speculated that *Xenorhabdus* haemolysin and phospholipase C may be involved in the breakdown of insect tissue by colonising P1 bacteria, providing an enriched nutrient source for nematode growth and reproduction (Akhurst & Boemare, 1990; Forst & Neelson, 1996). Transposon mutants were also screened for loss of Congo Red binding capability which is related to virulence in some Gram negative bacteria (Payne & Finkelstein, 1977).

Of the 5,000 colonies screened, five transposon mutants (designated XB26(20), XB29(45), XB33(21), XB34(45) and XB41(23)) showed a significant disruption of antibiotic activity. When overlaid with *M. lutea* (see section 2.2) the zone of *M. lutea* inhibition was reduced for each mutant when compared to *X. bovienii* (Table 4.1). Both haemolytic and lecithinase activity were also reduced (see section 2.2) when compared to *X. bovienii* (Table 4.1). Each of the five transposon mutants also showed an unusual disruption of Congo Red binding activity. *X. bovienii*, when grown on NA supplemented with 5% (v/v) Congo Red demonstrated a 5-10 mm zone of concentrated Congo Red immediately around the colony. This zone is further surrounded by a very thin (1-2 mm) clear zone, followed by normal Congo Red NA. Each of the five transposon mutants showed a larger zone of clearing (5-7 mm) around colonies, but no concentrated zone of Congo Red. Similar observations, suggesting Congo Red adsorption is genetically variable, have been made for *X. nematophilus* -19061 Tn5 insertion mutants (Xu *et al.*, 1991). Overall these preliminary results suggested

	<i>X. bovienii</i> T228	XB26(20)	XB29(45)	XB33(21)	XB34(45)	XB41(23)
Antimicrobial activity	+++	+ ^a	+ ^a	+ ^a	+ ^a	+ ^a
Congo Red binding	+++	+ ^b	+ ^b	+ ^b	+ ^b	+ ^b
Haemolysis	+++	+	+	+	+	++
Phospholipase C	+++	-	-	+	-	+

Table 4.1 Expression of phase dependent characteristics by *X. bovienii* strain T228 and *X. bovienii* transconjugates XB26(20), XB29(45), XB33(21), XB34(45) and XB41(23). A + denotes the degree of a positive phenotype when compared to wild type bacteria ; a - denotes a negative phenotype.

^a Antibiotic activity is reduced when compared to the wild type, however the degree of reduced activity is variable on numerous repetitions

^b All mutant strains tested showed some degree of Congo Red binding, however the phenotype was still different to wild type bacteria (see section 4.2.2.1).

transposon induced mutations in XB26(20), XB29(45), XB33(21), XB34(45) and XB41(23) may be representative of a region of DNA involved in the expression of a number of phase variant characteristics. Introduction of mini-Tn5 Km into the chromosome of each mutant may have resulted in a polar mutation, therefore affecting downstream genes in the region. Based on the phenotypic observations the regions of *X. bovienii* DNA flanking each transposon insertion was further investigated.

4.2.2.2 Southern hybridisation analysis of *X. bovienii* mini-Tn5 Km insertion mutants XB26(20), XB29(45), XB33(21), XB34(45) and XB41(23)

Southern hybridisation analysis of *Cla*I digested chromosomal DNA from transposon mutants XB26(20), XB29(45), XB33(21), XB34(45) and XB41(23) were probed with the DIG labelled Km cartridge (see section 4.2.1.2). The Km probe hybridised to 4.19 kb and 3.27 kb *Cla*I fragments from XB26(20) and XB29(45) respectively. Furthermore the Km probe hybridised to a fragment greater than 8.51 kb from XB33(21), whilst XB34(45) and XB41(23) both showed fragment sizes of 5.31 kb (Figure 4.4). Southern hybridisation analysis was also used to determine whether mini-Tn5 Km had inserted within the same *Cla*I fragment of XB34(45) and XB41(23). Chromosomal DNA from XB34(45) and XB41(23) were digested with *Eco*RV and probed as above. Probe DNA hybridised to a 3.7 kb fragment from XB34(45), and a 7.1 kb fragment from XB41(23) (Figure 4.5). Since the DNA fragments hybridising with probe DNA are of different sizes, this data indicates the five mutants represent independent transposon insertions.

4.2.3 Identification of *X. bovienii* DNA flanking transposon insertion mutants XB26(20), XB29(45), XB33(21), XB34(45) and XB41(23)

As a first step toward characterising DNA sequence interrupted by transposon mutagenesis, flanking DNA was cloned sequenced and characterised.

4.2.3.1 Cloning of *X. bovienii* chromosomal DNA flanking transposon insertion mutants XB26(20), XB29(45), XB33(21), XB34(45) and XB41(23)

To facilitate nucleotide sequence analysis of chromosomal DNA flanking the I and O ends of each mini-Tn5 Km insertion, the chromosomal DNA from each mutant was digested with

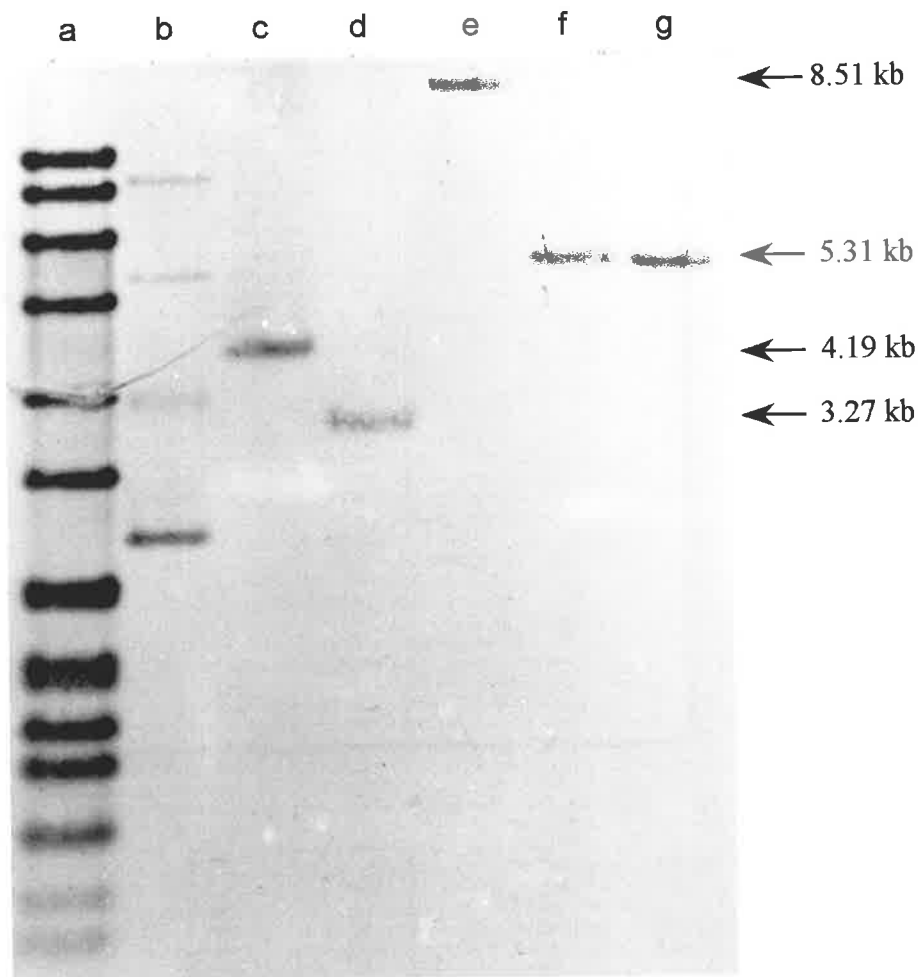


Figure 4.4 Southern hybridisation analysis of plasmid DNA from pUTKm, chromosomal DNA from *X. bovienii* T228, XB26(20), XB29(45), XB33(21), XB34(45) and XB41(23). All chromosomal DNA was digested with *Cla*I. Plasmid DNA from pUTKm remained undigested. The filter was probed with the same digoxigenin labelled 2298 bp *Sfi*I internal fragment from pUTKm used in Figure 4.3. The size of DNA fragments hybridising with the probe DNA are shown.

Lanes:

[a], SPP1 markers are *Bacillus subtilis* phage SPP1 DNA digested with *Eco*RI;

[b], pUTKm;

[c], XB26(20);

[d], XB29(45);

[e], XB33(21);

[f], XB34(45);

[g], XB41(23).

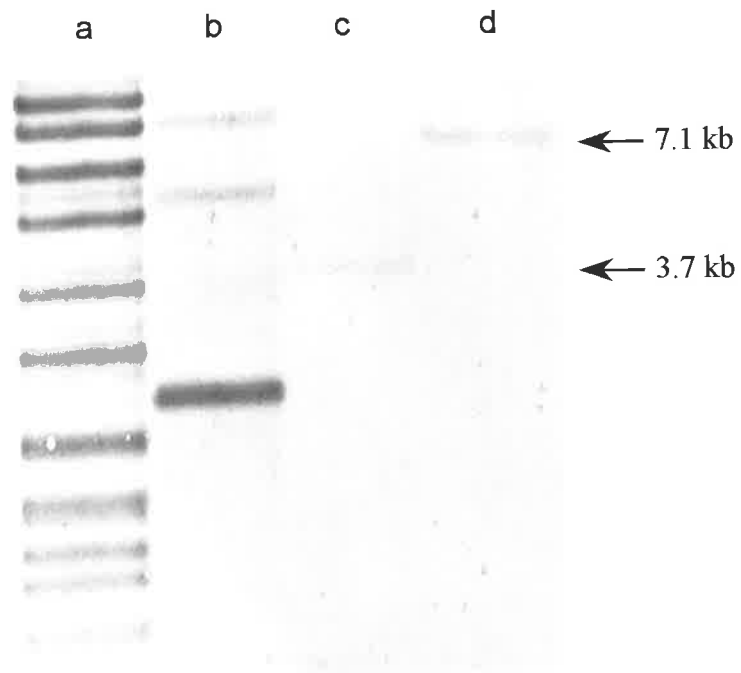


Figure 4.5 Southern hybridisation analysis of plasmid DNA from pUTKm, and chromosomal DNA from XB34(45) and XB41(23). All chromosomal DNA was digested with *EcoRV*. Plasmid DNA from pUTKm remained undigested. The filter was probed with the same digoxigenin labelled 2298 bp *Sfi*I internal fragment from pUTKm used in Figures 4.3 and 4.4. The size of DNA fragments hybridising with the probe DNA are shown.

Lanes:

[a], SPP1 markers are *Bacillus subtilis* phage SPP1 DNA digested with *EcoRI*;

[b], pUTKm;

[c], XB34(45);

[d], XB41(23).

*Cla*I, *Eco*RI or *Hind*III and subsequently cloned into the similarly digested high copy number plasmid pGEM7zf(+). The digested DNA should contain fragments with intact copies of the Km^R gene from Tn5, plus flanking regions of chromosomal DNA. This ligation mix (and all other ligation mixes subsequently discussed in 4.2.3.1) was used to transform *E. coli* DH5 α by electroporation. Transformants were selected by plating on NA supplemented with Amp and Km. Partial digests of chromosomal DNA (*Eco*RI and *Hind*III) were used because mini-Tn5 Km contains most of the common restriction enzyme sites present in the vector. This process was complicated by failure of many unique enzymes to digest *Xenorhabdus* DNA. Often excessive amounts of enzyme (up to 60 units per reaction) were required in order to digest the DNA. Success was initially achieved using *Eco*RI partially digested chromosomal DNA from XB34(45). A 13 kb *Eco*RI fragment was cloned into similarly digested pGEM7zf(+) and designated pCT400.

In an attempt to improve transformation efficiencies, subsequent cloning exercises continued with the low copy number plasmid pBR322. Plasmid pBR322 may improve transformation efficiency by reducing lethal effects on the host cell that can be associated with high copy number vectors such as pGEM7zf(+). Chromosomal DNA up and downstream of the transposon insertion region of mutants XB26(20), XB29(45) and XB34(45) were cloned as *Cla*I fragments to produce pCT401, pCT402 and pCT403 respectively. Chromosomal DNA flanking the transposon insertion region from XB33(21) was cloned as an 8.5 kb *Eco*RV fragment into *Eco*RV digested pBR322 and designated pCT404. Similarly, chromosomal DNA flanking the transposon insertion region from XB41(23) was cloned as a 7.1 kb *Eco*RV fragment into pBR322 and designated pCT405. (See Figure 4.6 for diagrammatical representation of pCT400-405). The ease at which clones were obtained using the low copy number vector pBR322 suggested copy number had considerable impact on the cloning efficiency.

4.2.3.2 Sequence analysis of mini-Tn5 Km

To facilitate nucleotide sequence analysis of pCT400-pCT405 DNA immediately flanking the transposon insertion oligonucleotides were constructed which allowed sequencing out of the transposable element. Detailed sequence information regarding the transposon was not available to facilitate oligonucleotide design. Only the sequence data for the 1.3 kb Km cartridge, removed as an *Eco*RI fragment from pHP45 Ω -Km (Fellay *et al.*, 1987) was

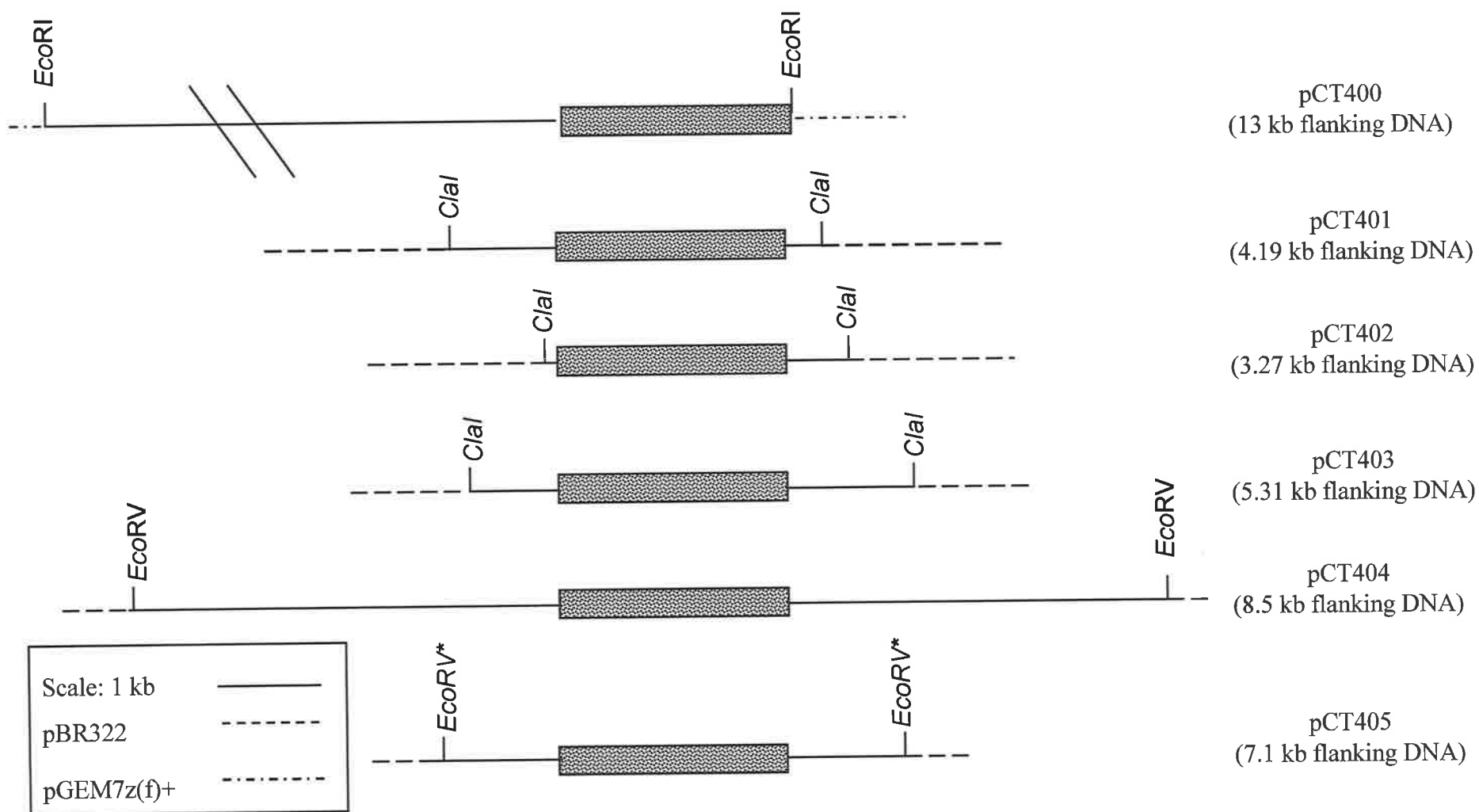


Figure 4.6. Schematic representation of subclones pCT400, pCT401, pCT402, pCT403, pCT404 and pCT405. Restriction enzyme sites used to subclone chromosomal DNA fragments into either pBR322 or pGEM7z(f) are indicated.

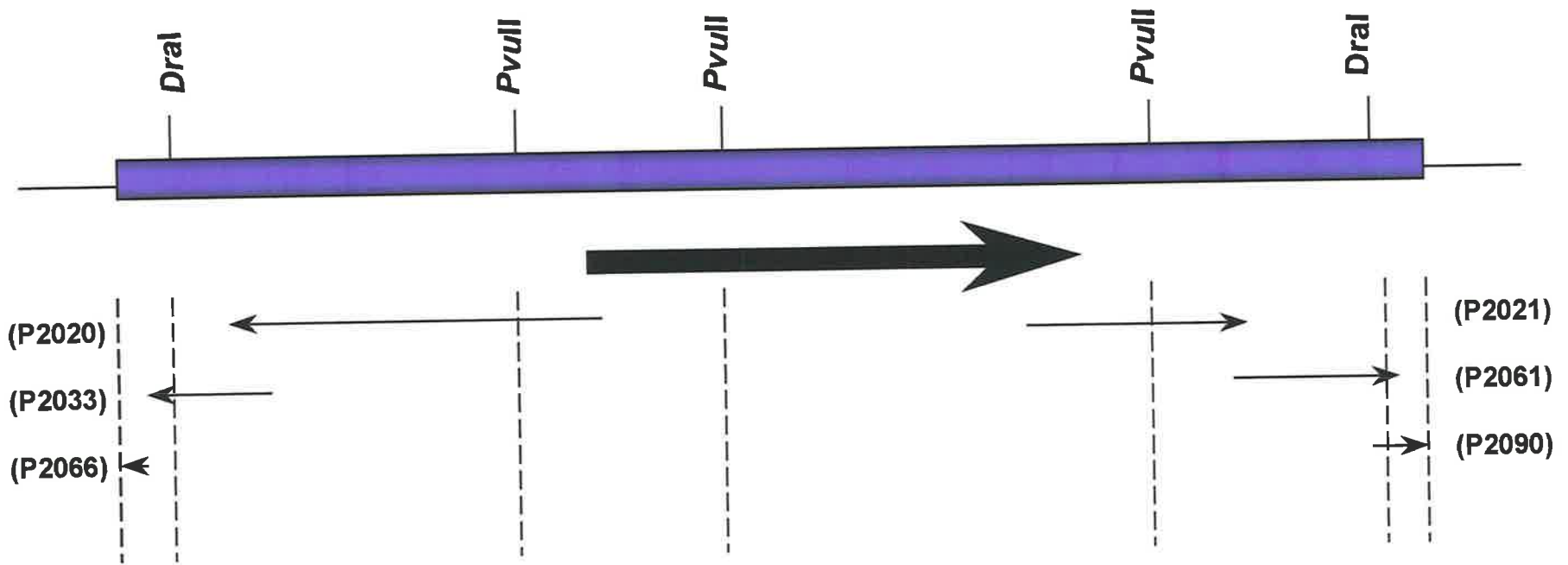
available. As 560 bp and 430 bp of nucleotide sequence were unknown at the 5' and 3' ends of the Km cartridge respectively, oligonucleotides (P2020, P2021, P2033, P2061 and P2066) were constructed to facilitate nucleotide sequence analysis of these regions (Figure 4.7). Nucleotide sequence analysis established mini-Tn5 Km to be 2356 bp (Figure 4.8).

4.2.3.3 Identification and cloning of *X. bovienii* DNA flanking mini-Tn5 Km

Oligonucleotides for sequence analysis out of mini-Tn5 into flanking *Xenorhabdus* DNA could not be designed for several reasons. The inverted repeat regions located at 33-188 bp and 2148-2303 bp of mini-Tn5 are 100% homologous (see Figure 4.9), and consequently cannot be used as priming sites. Furthermore, significant repeated nucleotide sequences within the rest of the mini-Tn5 sequence prevented the design of suitable oligonucleotides within a reasonable distance of the flanking *Xenorhabdus* DNA. Therefore, a Southern hybridisation analysis method was used to facilitate identification and subsequent cloning of *X. bovienii* DNA flanking mini-Tn5 Km.

The mini-Tn5 Km element contains *DraI* restriction sites at positions 103 and 2234, and oligonucleotide P2066 binds to complementary strands located at positions 49 – 68 and 2268 – 2287. Thus digestion of plasmids pCT401 – pCT405 should yield a *DraI* fragment of 2131 bp comprising the majority of the transposable element. The remaining *DraI* DNA fragments flanking the element can be identified by hybridisation with DIG-labelled oligonucleotide P2066. This strategy was employed to clone flanking DNA into *SmaI* digested pGEM7zf(+). Ligated vector and insert preparations were used to transform *E. coli* DH5 α by electroporation. Transformants were selected on NA supplemented with Amp, IPTG and X-gal. Table 4.2 outlines the size of each *DraI* fragment identified by Southern hybridisation analysis and names of the subsequent subclone.

Figure 4.7 A schematic representation of the sequence reactions used to generate the complete nucleotide sequence of transposon mini-Tn5 Km contained on plasmid pUTKm. Synthetic oligonucleotides specifically designed to generate nucleotide sequence overlap are indicated in parentheses. The nucleotide sequence of each oligonucleotide is listed in Table 2.4.3.



Scale: 150 bp



Plasmid pUT



Neomycin
phosphotransferase



Figure 4.8 Nucleotide sequence of mini-Tn5 Km derived from plasmid pUTKm. The nucleotides are numbered to the right hand side in the 5' to 3' direction. The deduced protein sequence of neomycin phosphotransferase is given below the DNA sequence in the single letter amino acid code and is numbered to the right hand side. The 19 bp Tn5 inverted repeat sequences labelled I end and O end are highlighted. The binding positions of oligonucleotide P2066 (nucleotides 49-68 and 2268-2287) and *DraI* restriction sites used for subsequent subcloning procedures are underlined.

The mini-Tn5 Km Genbank accession number is U32991.

CTGTCTCTTGATCAGATCTGGCCACCTAGGCCGAATTCCCAGGGATCCGGTGATTGATTG - 60

I end

DraI

AGCAAGCTTTATGCTTGTAAACCGTTTTGTGAAAAAATTT**TTTAAA**ATAAAAAAGGGGACC - 120

P2066 binding (complementary strand)

TCTAGGGTCCCCAATTAATTAGTAATATAATCTATTAAAGGTCATTCAAAGGTCATCCA - 180
CCGGATCACCTTACCAAGCCCTCGCTAGATTGTTAATGCGGATGTTGCGATTACTTCGCC - 240
CAACTATTGCGATAACAAGAAAAGCGCCTTTCATGATATATCTCCCAATTTTGTGTAGGG - 300
CTTATTATGCACGCTTAAAAATAATAAAAGCGACTTGACCTGATAGTTTGGCTGTGAGCA - 360
ATTATGTGCTTAGTGCATCTAACGCTTGAGTTAACCGCGCCGCGAAGCGGCGTCGGCTTG - 420
AACGAATTGTTAGACATTATTTGCCGACTACCTTGGTGATTCGCCTTTCACGTAGTGGAC - 480
AAAATCAACCAACTGATCTGCGCGAGCTTCACGCTGCCGCAAGCATCAGGGCGCAAGGGC - 540
TGCTAAAGGAAGCGGAACACGTAGAAAAGCCAGTCCGCAGAAACGGTGCTACCCCGGATGA - 600
ATGTCAGCTACTGGGCTATCTGGACAAGGGAAAACGCAAGCGCAAAGAGAAAGAGGTAGC - 660
TTGCAGTGGGCTTACATGACGATAGCTAGACTGGGCGGTTTTATGGACAGCAAGCGAACC - 720
GGAATTGCCAGCTGGGGCGCCCTCTGGTAAGGTTGGGAAGCCCTGCAAAGTAAACTGGAT - 780
GGCTTTCTTGCCGCCAAGGATCTGATGGCGCAGGGGATCAAGATCTGATCAAGAGACAGG - 840
ATGAGGATCGTTTCGCATGATTGAACAAGATGGATTGCACGCAGGTTCTCCGGCCGCTTG - 900

M I E Q D G L H A G S P A A W - 15

start

GGTGGAGAGGCTATTCGGCTATGACTGGGCACAACAGACAATCGGCTGCTCTGATGCCGC - 960
V E R L F G Y D W A Q Q T I G C S D A A - 35

CGTGTTCCGGCTGTCAGCGCAGGGGCGCCCGGTTCTTTTTGTCAAGACCGACCTGTCCGG - 1020
V F R L S A Q G R P V L F V K T D L S G - 55

TGCCCTGAATGAAGTGCAGGACGAGGCAGCGCGGCTATCGTGGCTGGCCACGACGGGCGT - 1080
A L N E L Q D E A A R L S W L A T T G V - 75

TCCTTGCGCAGCTGTGCTCGACGTTGTCACTGAAGCGGGAAGGGACTGGCTGCTATTGGG - 1140
P C A A V L D V V T E A G R D W L L L G - 95

CGAAGTGCCGGGGCAGGATCTCCTGTCTACCTTGCTCCTGCCGAGAAAGTATCCAT - 1200
E V P G Q D L L S S H L A P A E K V S I - 115

CATGGCTGATGCAATGCGGCGGCTGCATACGCTTGATCCGGCTACCTGCCCATTCGACCA - 1260
M A D A M R R L H T L D P A T C P F D H - 135

CCAAGCGAAACATCGCATCGAGCGAGCACGTAAGGATGGAAGCCGGTCTTGTGATCA - 1320
Q A K H R I E R A R T R M E A G L V D Q - 155

GGATGATCTGGACGAAGAGCATCAGGGGCTCGCGCCAGCCGAACTGTTCCGCCAGGCTCAA - 1380
D D L D E E H Q G L A P A E L F A R L K - 175

GGCGCGCATGCCCGACGGCGAGGATCTCGTCTGACCCATGGCGATGCCTGCTTGCCGAA - 1440
A R M P D G E D L V V T H G D A C L P N - 195

TATCATGGTGGAAAATGGCCGCTTTTTCTGGATTTCATCGACTGTGGCCGGCTGGGTGTGGC - 1500
I M V E N G R F S G F I D C G R L G V A - 215

GGACCGCTATCAGGACATAGCGTTGGCTACCCGTGATATTGCTGAAGAGCTTGGCGGCGA - 1560
D R Y Q D I A L A T R D I A E E L G G E - 235

ATGGGCTGACCGCTTCTCGTGCTTTACGGTATCGCCGCTCCCATTTCGAGCGCATCGC - 1620
W A D R F L V L Y G I A A P D S Q R I A - 255

CTTCTATCGCTTCTTGACGAGTTCTTCTGAGCGGGACTCTGGGGTTCGAAATGACCGAC - 1680
F Y R L L D E F F * - 264

stop

CAAGCGACGCCAACCTGCCATCACGAGATTTTCGATTCCACCGCCGCTTCTATGAAAGG - 1740
TTGGGCTTCGGAATCGTTTTCCGGGACGCCGGCTGGATGATCCTCCAGCGCGGGGATCTC - 1800
ATGCTGGAGTTCTTCGCCACCCCGGGCTCGATCCCCTCGCGAGTTGGTTTCAGCTGCTGC - 1860
CTGAGGCTGGACGACCTCGCGGAGTTCTACCGGCAGTGCAAATCCGTCCGCATCCAGGAA - 1920
ACCAGCAGCGGCTATCCGCGCATCCATGCCCCGAACTGCAGGAGTGGGGAGGCACGATG - 1980
GCCGCTTGGTCGACCCGGACGGGACGGATCAGTGAGGGTTTGCAACTGTGGGTCAAGGA - 2040
TCTGGATTTTCGATCACGGCACGATCATCGTGGGAGGGCAAGGGCTCCAAGGATCGGGCC - 2100

TTGATGTTACCGAGAGCTTGGTACCCAGTCTGTGTGAGCAGGGGAATTGATCCGGTGGAT - 2160
GACCTTTTGAATGACCTTTAATAGATTATATTACTAATTAATTGGGGACCCTAGAGGTCC - 2220
DraI **P2066 binding**
CCTTTTTTAT**TTTAAA**ATTTTTTACAAAAACGGTTTACAAGCATAAA**AGCTTGCTCAATC** - 2280
AATCACCGGATCCCCGGGAATTCGTCGACAAGCTGCGGCCGCCTAGGCCGTGGCCGA**ACT** - 2340
FGTGTATAAGAGTCAG - 2356
O end

```

188   TGATCCGGTGGATGACCTTTTGAATGACCTTTAATAGATTATATTACTAATTA
X:.....
2148  TGATCCGGTGGATGACCTTTTGAATGACCTTTAATAGATTATATTACTAATTA

ATTGGGGACCCTAGAGGTCCCCTTTTTTATTTTAAAAATTTTTTCACAAAACG
:.....
ATTGGGGACCCTAGAGGTCCCCTTTTTTATTTTAAAAATTTTTTCACAAAACG

GTTTACAAGCATAAAGCTTGCTCAATCAATCACCGGATCCCCGGAATTCG   32
:.....:X
GTTTACAAGCATAAAGCTTGCTCAATCAATCACCGGATCCCCGGAATTCG   2303

```

Figure 4.9 Alignment of the 156 bp inverted repeat sequences located at nucleotides 32 - 188 and 2148-2303 of mini-Tn5 Km. Note nucleotides 32 – 188 are represented in the reverse complement form. 100% homology is observed over the 156 bp region.

Clone	<i>Dra</i> I fragment 1	<i>Dra</i> I fragment 1 subclone	<i>Dra</i> I fragment 2	<i>Dra</i> I fragment 2 subclone
pCT401	2500 bp	pCT401a	1600 bp	pCT401b
pCT402	3700 bp	pCT402a	1100 bp	pCT402b
pCT403	1160 bp	pCT403a	500 bp	pCT403b
pCT404	700 bp	pCT404a	350 bp	pCT404b
pCT405	2300 bp	pCT405a	480 bp	pCT405b

Table 4.2 Plasmids pCT401, pCT402, pCT403, pCT404 and pCT405 were digested with *Dra*I, and subsequently probed with the digoxigenin labelled oligonucleotide P2066. For each plasmid two fragments were detected which represent the I end or O end of mini-Tn5 Km, and flanking *X. bovienii* based plasmid DNA (data not shown). Sizes of the two fragments detected for each clone are listed. Each fragment was subcloned into *Sma*I digested pGEM7z(f)+ and the ligation mix used to transform *E. coli* DH5 α by electroporation. Transformants were selected on NA supplemented with Amp, IPTG and X-gal. The subclones were selected by *Eco*RI digestion (data not shown), and their designated names are listed. All *Dra*I and *Sma*I sites were destroyed in the cloning process.

4.2.4 Analysis of *X. bovienii* DNA flanking clones pCT401, pCT402, pCT403, pCT404 and pCT405

4.2.4.1 BLASTX 2.1.1 analysis of *X. bovienii* DNA sequence flanking clones pCT401, pCT402, pCT403, pCT404 and pCT405

Nucleotide sequence data from each subclone (described in section 4.2.3.3 and Table 4.2) was generated using the M13 forward and reverse primers. Nucleotide sequence analysis identified either the I end or O end sequence of mini-Tn5 Km for each subcloned *Dra*I fragment along with contiguous *X. bovienii* DNA. The *X. bovienii* nucleotide sequences from each clone (pCT401-pCT405) were compiled (Appendix 1) and submitted for BLASTX 2.1.1 analysis. BLASTX 2.1.1 analysis of XB26(20) translated flanking nucleotide sequence (545 bp) showed homology to non-ribosomal peptide synthetase proteins from *Anabaena* sp (62% homology) (Genbank accession AJ269505); *Pseudomonas syringae* pv. *syringae* (68% homology) (Genbank accession AF047828) and *Streptomyces viridochromogenes* (60% homology) (Genbank accession Y17268). BLASTX 2.1.1 analysis of XB29(45) translated flanking nucleotide sequence (385 bp) showed homology to non-ribosomal peptide synthetase proteins from *Microcystis aeruginosa* (69% homology) (Genbank accession AB019578); *Pseudomonas aeruginosa* (48% homology) (Genbank accession AE004667) and *Pseudomonas syringae* pv. *syringae* (42% homology) (Genbank accession AF047828). BLASTX 2.1.1 analysis of XB34(45) translated flanking nucleotide sequence (531 bp) showed homology to non-ribosomal peptide synthetase proteins from *Anabaena* sp (68% homology) (Genbank accession AJ269505); *Bacillus subtilis* (58% homology) (Genbank accession X72672) and *Bacillus licheniformis* (58% homology) (Genbank accession AF007865). BLASTX 2.1.1 analysis of XB33(21) translated flanking nucleotide sequence (489 bp) showed homology to transcriptional activators from *E. coli*, LeuO (85% homology) (Genbank accession M21150); *Salmonella typhimurium*, LeuO (88% homology) (Genbank accession AF117227) and *Vibrio cholerae*, LysR type activator (86% homology) (Genbank accession AE004318). Finally, BLASTX 2.1.1 analysis of XB41(23) translated flanking nucleotide sequence (589 bp) showed homology to fimbrial chaperone proteins from *Proteus mirabilis* (59% homology) (Genbank accession Z78535) and *E. coli* O157:H7 (57% homology) (Genbank accession AE005662).

Overall, BLASTX 2.1.1 results suggest mutants XB26(20), XB29(45) and XB34(45) have independently inserted into a common region of the *Xenorhabdus* genome yet to be characterised. Transposon mutants XB33(21) and XB41(23) appear to have independently inserted into regions encoding transcriptional activator and fimbrial associated chaperone like proteins respectively.

4.2.4.2 Mapping of transposon insertion mutants XB26(20), XB29(45) and XB34(45)

In view of the similarity of XB26(20), XB29(45) and XB34(45) phenotypes (see section 4.2.2.1) and BLASTX 2.1.1 (see section 4.2.4.1), these transposon insertions were mapped with respect to each other. Oligonucleotides were designed with the intention of using PCR to generate DIG-labelled probes from DNA flanking transposon insertions in XB26(20), XB29(45) and XB34(45). Southern hybridisation analysis using the PCR generated probes would facilitate mapping the chromosomal location of the three transposon insertions with respect to each other. This data would also allow selection of appropriate restriction enzymes useful for cloning of this region of chromosomal DNA into a suitable vector.

As part of mapping the transposon insertions, plasmid pCT400 was included for analysis. Plasmid pCT400 harbours *X. bovienii* chromosomal DNA flanking only the O end of mini-Tn5 Km (see Figure 4.6), and was obtained from insertion mutant XB34(45) as a 13 kb *EcoRI* fragment (see section 4.2.3.1). Therefore, PCR amplification of pCT400 using oligonucleotides designed from nucleotide sequence flanking XB26(20) (P4344/P4345) and XB29(45) (P4346/P4347) could identify regions of homology between each of the three transposon insertion mutants.

PCR analysis of pCT400 and pCT401 plasmid DNA using XB26(20) oligonucleotides P4344/P4345 yielded fragments of approximately 640 bp and 3 kb respectively. The 2360 bp difference between PCR product sizes can be accounted for by the mini-Tn5 Km insertion between priming sites of P4344/P4345, cloned from XB26(20) chromosomal DNA, into pCT401 (see section 4.2.3.1). Nucleotide sequence analysis of the 640 bp and 3 kb PCR products using oligonucleotides P4344 and P4345, confirmed 100% identity between the PCR products (excluding the internal mini-Tn5 Km nucleotide sequence located within the 3 kb PCR product), data not shown.

PCR analysis of pCT400 and pCT402 plasmid DNA using XB29(45) oligonucleotides P4346/P4347 yielded fragments of approximately 400 bp and 2.8 kb respectively. Once again the difference between PCR product sizes can be accounted for by the mini-Tn5 Km insertion between priming sites of P4346/P4347, cloned from XB29(45) chromosomal DNA, into pCT402 (see section 4.2.3.1). Nucleotide sequence analysis of the 400 bp and 2.8 kb PCR products, using oligonucleotides P4346 and P4347, confirmed 100% identity between the PCR products (excluding the internal mini-Tn5 Km nucleotide sequence located within the 2.8 kb PCR product), data not shown.

X. bovienii wild type chromosomal DNA was amplified by PCR with oligonucleotide pairs P4344/P4345 and P4346/P4347. The 600 bp and 400 bp products were sequenced (as above) to confirm the plasmid DNA from pCT400, pCT401 and pCT402 were originally from *X. bovienii* (data not shown).

Taken together, the above results (summarised in Table 4.8) suggest the transposon insertion sites for XB26(20) and XB29(45) were both located on pCT400. As plasmid pCT400 was cloned from XB34(45) chromosomal DNA (see section 4.2.3.1), PCR results suggest the transposon insertion points for XB26(20), XB29(45) and XB34(45) are all located within the 13 kb region of *X. bovienii* DNA located on pCT400 (Figure 4.6).

4.2.5 Nucleotide sequence analysis of pCT400

To precisely map transposon insertion points for XB26(20) and XB29(45) nucleotide sequence analysis of pCT400 was undertaken. As this was a substantial task, a number of carefully planned steps were taken to reach completion.

1. Plasmid pCT400 was created by cloning a partial *EcoRI* digest of XB34(45) chromosomal DNA into pGEM7zf(+) (see section 4.2.3.1). As *EcoRI* sites flank mini-Tn5, the possibility of mini-Tn5 and flanking DNA being from separate regions of the XB34(45) chromosome was resolved. This was achieved by comparing the nucleotide sequence of DNA flanking the transposon insertion contained on plasmids pCT400 and pCT403. Plasmid pCT403 was constructed by cloning a *ClaI* fragment of XB34(45) chromosomal DNA (see section 4.2.3.1), and should contain contiguous DNA as no *ClaI* restriction enzyme sites exist in mini-Tn5 Km.

Oligonucleotide pair	<i>X. bovienii</i> chromosomal DNA	pCT400 plasmid DNA	pCT401 plasmid DNA	pCT402 plasmid DNA
P4344/P4345	639 bp	639 bp	3 kb	-
P4346/P4347	433 bp	433 bp	-	2.8 kb

Table 4.8 Summary of product sizes observed from PCR amplification of plasmids pCT400, pCT401, pCT402 and *X. bovienii* T228 chromosomal DNA. Oligonucleotide pairs used were P4344/P4345 and P4346/P4347. Oligonucleotide sequences are listed in Table 2.4.4. Oligonucleotide pair P4344/P4345 was designed from *X. bovienii* chromosomal DNA nucleotide sequence derived from pCT401. Oligonucleotide pair P4346/P4347 was designed from *X. bovienii* chromosomal DNA nucleotide sequence derived from pCT402.

2. *X. bovienii* chromosomal DNA cloned into pCT400, distal to transposon insertion, was sequenced to confirm this region showed homology to peptide synthetases. Therefore a strategy to efficiently sequence the entire region of *X. bovienii* flanking DNA, and not only that closest to the transposon insertion, was devised.

3. A restriction enzyme map of pCT400 was established to facilitate subcloning, nested deletion construction and nucleotide sequence analysis

4. Nucleotide sequence at the subclone junctions was confirmed to ensure small fragments of DNA not visible on agarose gels were not lost in the subcloning process.

5. Plasmid pCT400 carries *X. bovienii* chromosomal DNA flanking only the O end of mini-Tn5 Km. Chromosomal DNA flanking the I end of mini-Tn5 Km from XB34(45), cloned as pCT403 and pCT403b (see section 4.2.3.3 and Table 2.1), was sequenced and joined to existing nucleotide sequence from pCT400.

6. As pCT400 shows homology to non-ribosomal peptide synthetases across the entire region of cloned *X. bovienii* chromosomal DNA, PAPCR (plasmid assisted PCR) was used to isolate DNA further downstream. Nucleotide sequence analysis of this new DNA region was performed in an attempt to find the end of peptide synthetase homologous DNA.

4.2.5.1 Confirmation pCT400 and pCT403 are from the same mini-Tn5 Km insertion located in XB34(45)

Confirmation that pCT400 and pCT403 are from the same mini-Tn5 Km insertion located in XB34(45), but cloned using different restriction enzymes, was obtained by using the *Dra*I digest and Southern hybridisation analysis using DIG labelled oligonucleotide P2066 strategy (see section 4.2.3.3). Southern hybridisation analysis of pCT400 showed two fragments, 1000 bp and 1300 bp, hybridised to the oligonucleotide probe P2066. The 1000 bp and 1300 bp *Dra*I fragments were independently cloned into *Sma*I digested pGEM7zf(+) and the ligation mixes used to transform *E. coli* DH5 α by electroporation. Transformants were selected on NA supplemented with Amp, IPTG and X-gal. The cloned 1000 bp *Dra*I fragment was designated pCT400a, whilst the cloned 1300 bp *Dra*I fragment was designated pCT400b.

Nucleotide sequence analysis of pCT400a, using the M13 forward and reverse primers showed pCT400a contained the O end of mini-Tn5 Km and flanking *X. bovienii* DNA (data not shown). Alignment of nucleotide sequence from pCT400a, and *X. bovienii* chromosomal DNA flanking the O end of mini-Tn5 Km cloned into pCT403, revealed 100% identity (data not shown). This confirmed pCT400 and pCT403 were both clones from transposon insertion mutant X34(45) obtained using different restriction enzymes.

Nucleotide sequence analysis of pCT400b using M13 forward and reverse primers showed the presence mini-Tn5 Km DNA and pGEM7z(f)+, no *X. bovienii* DNA was identified (data not shown). Plasmid pGEM7zf(+) was the base vector used in construction of pCT400 (see section 4.2.3.1).

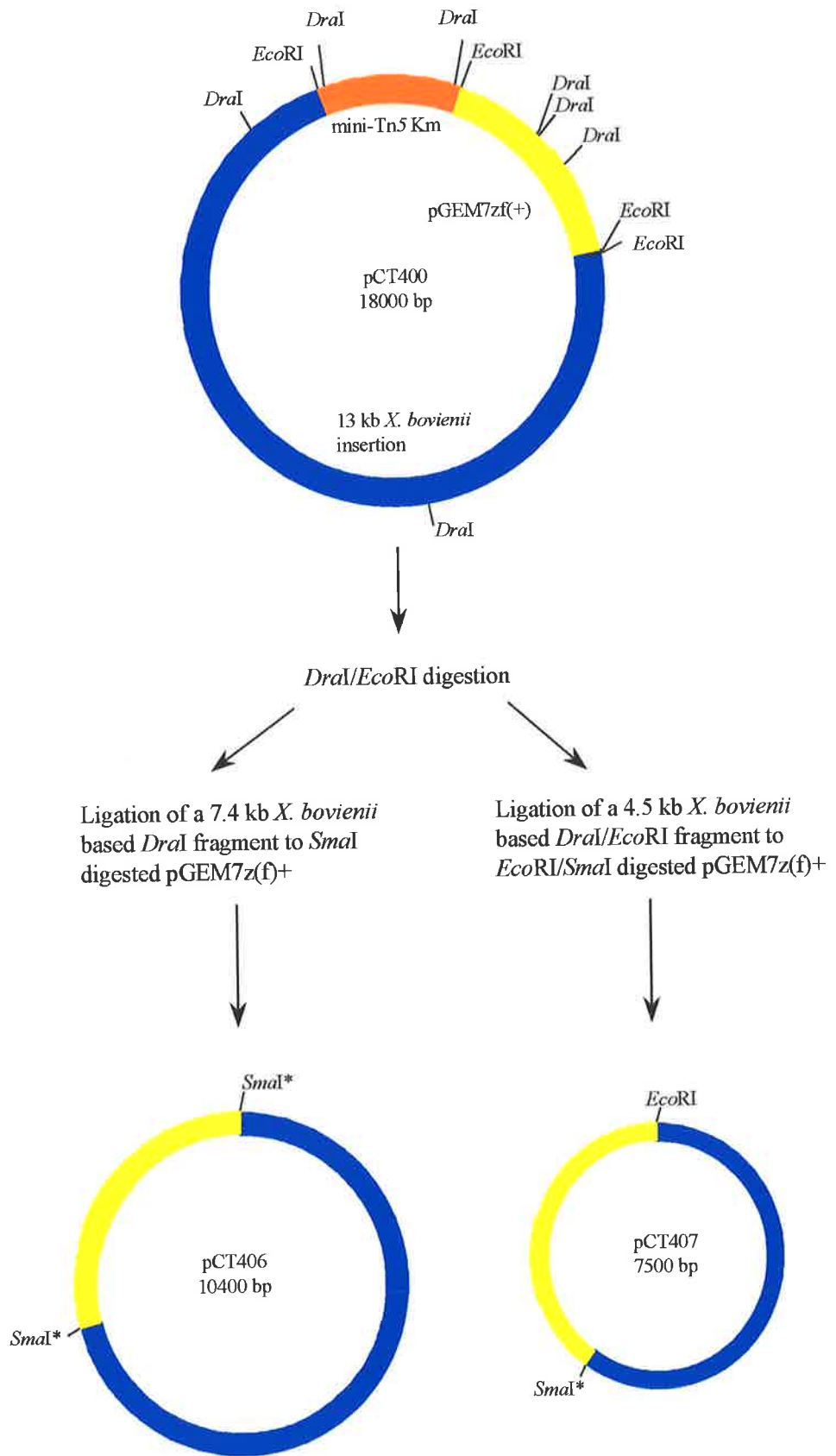
4.2.5.2 BLASTX 2.1.1 analysis of *X. bovienii* DNA distal to the mini-Tn5 Km insertion cloned into pCT400

BLASTX 2.1.1 analysis of *X. bovienii* DNA most distal to the mini-Tn5 Km insertion cloned into pCT400 showed significant homology to the peptide synthetase family of enzymes from *Pseudomonas syringae* pv. *syringae* (78% homology) (Genbank accession AFO478284); *Lysobacter* sp. (70% homology) (Genbank accession X96558) and *Nostoc* sp. (68% homology) (Genbank accession AF204805). Considering the far 5' and 3' DNA regions of pCT400 were found to have significant homology to peptide synthetases, DNA sequence analysis of the entire 13 kb *X. bovienii* region cloned into pCT400 was undertaken.

4.2.5.3 Restriction enzyme and nested deletion analysis of pCT400

Nucleotide sequence information from pCT400a and pCT400b were used to determine the orientation of mini-Tn5 Km and flanking *X. bovienii* DNA within pCT400. *DraI* digestion of pCT400 was used to further establish a restriction map of this plasmid (Figure 4.10). Nucleotide sequence analysis of pCT400 was performed by a combination of subcloning and nested deletion analysis. Plasmid pCT400 was digested with *DraI* and the 7.4 kb fragment representing a portion of *X. bovienii* DNA flanking mini-Tn5 Km was cloned into the *SmaI* site of pGEM7zf(+) to produce pCT406 (Figure 4.10). Similarly a 4.5 kb *EcoRI/DraI* fragment representing a portion of *X. bovienii* DNA flanking mini-Tn5 Km was cloned into *EcoRI/SmaI* digested pGEM7zf(+) to produce pCT407 (Figure 4.10).

Figure 4.10 Restriction map of pCT400 and construction of plasmids pCT406 and pCT407. Plasmid pCT400 was digested with *EcoRI* and *DraI*. A 7.4 kb *X. bovienii* based *DraI* fragment was subcloned into *SmaI* digested pGEM7z(f)+ to create pCT406. A 4.5 kb *X. bovienii* based *EcoRI/DraI* fragment was subcloned into *EcoRI/SmaI* digested pGEM7z(f)+ to create pCT407. Asterisks (*) indicate restriction enzyme sites destroyed in the cloning process.



Plasmids pCT406 (Figure 4.11a and 4.11b) and pCT407 (Figure 4.12.) were subsequently sequenced via nested deletion analysis.

4.2.5.4 Identification of sequence junctions between pCT406, pCT407 and pCT403a

To determine if nucleotide sequence data obtained from pCT406, pCT407 and pCT403a was contiguous, oligonucleotides were designed to sequence across *Dra*I restriction enzyme sites contained within pCT400 DNA. Sequence analysis of pCT400 using oligonucleotide P5725 concluded pCT404a and pCT406 sequences were contiguous (data not shown). Sequence analysis of pCT400 using oligonucleotide P5618 concluded pCT406 and pCT407 sequences were contiguous (data not shown).

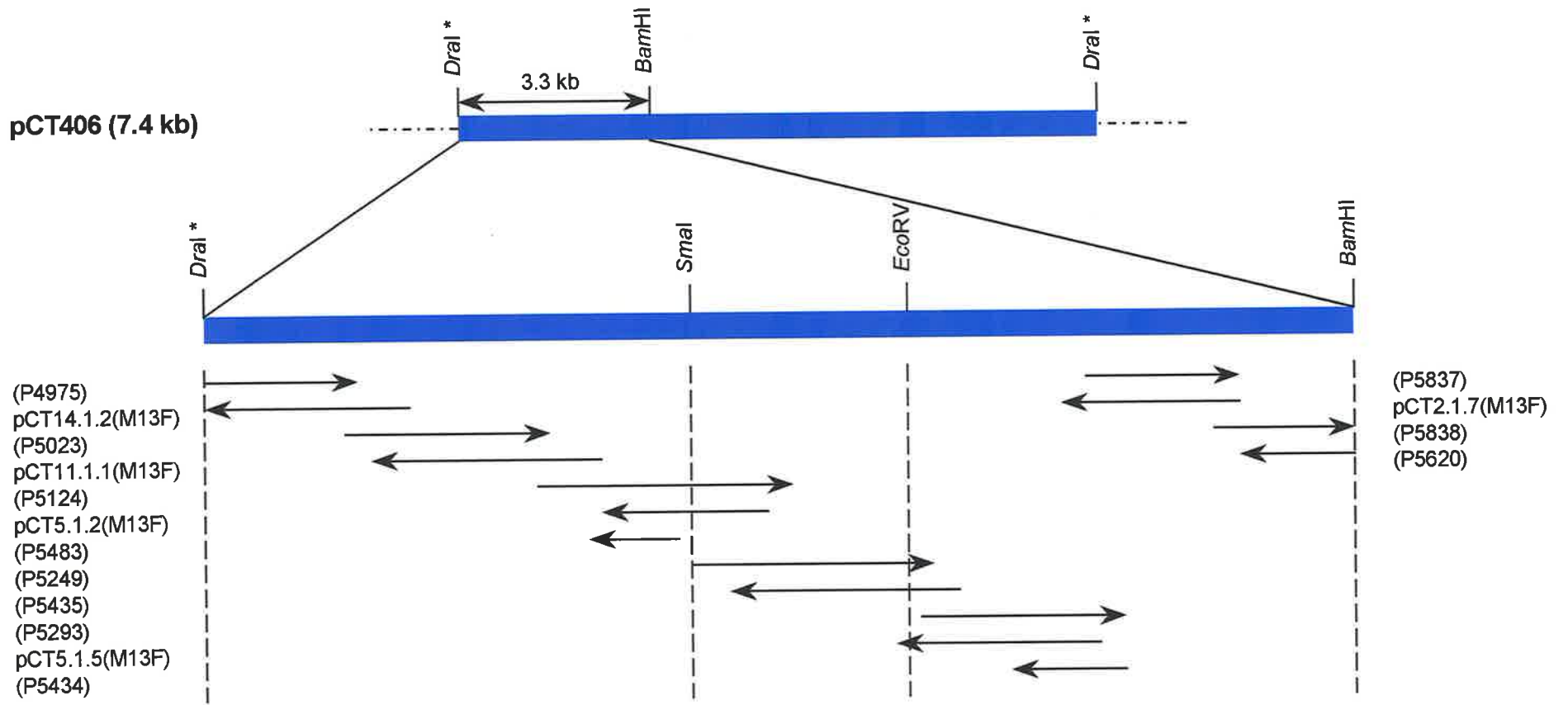
4.2.5.5 Analysis of pCT403 O end sequence.

Nucleotide sequence analysis (using M13 forward and reverse oligonucleotides) of pCT403b assembled a further 285 bp of nucleotide sequence data. A further 934 bp of nucleotide sequence was obtained by sequencing pCT403 plasmid DNA. Figure 4.13 shows the location of pCT403b with respect to pCT403, and the oligonucleotides used to obtain the 285 bp and 934 bp of regions of DNA sequence. This additional sequence data was added to the existing pCT400 nucleotide sequence.

4.2.5.6 Plasmid Assisted PCR (PAPCR) to generate further non-ribosomal peptide synthetase homologous sequence

To establish the full length of non-ribosomal peptide synthetase homologous chromosomal DNA present in *X. bovienii*, Plasmid Assisted PCR (Luo & Cella, 1994) was employed. Partially *Eco*RI digested *X. bovienii* T228 chromosomal DNA was ligated to *Eco*RI digested plasmid pBR322 DNA (see section 2.15.3.2). PCR amplification of the ligation mix using P5292/P2177 (see section 2.15.1) resulted in an approximately 1.5 kb product (data not shown). Oligonucleotide P5292 is homologous to *X. bovienii* DNA most distal to mini-Tn5 Km cloned into pCT400 whilst oligonucleotide P2177 is homologous to pBR322. The 1.5 kb PCR product was gel purified (see section 2.8.5) and cloned into pGEM-T. The ligation mix was used to transform *E. coli* DH5 α by electroporation, and correct clones selected on NA supplemented with Amp, IPTG and X-gal. The resulting clone was designated pCT408.

Figure 4.11a A schematic representation of the sequence reactions used to generate the complete nucleotide sequence of a 3.3 kb portion of pCT406. Oligonucleotides specifically designed to generate nucleotide sequence overlap are indicated in parentheses. Plasmids pCT14.1.2, pCT11.1.1, pCT5.1.2, pCT5.1.5 and pCT2.1.7 were all generated by nested deletion analysis of pCT406 (see section 2.9.1) and sequenced using the M13 forward oligonucleotide (M13F). Asterisks (*) indicate restriction enzyme sites destroyed in the cloning process. The nucleotide sequence of all oligonucleotides used is listed in Table 2.4.4.



Scale: 200 bp



pGEM7zf(+)



Figure 4.11b A schematic representation of the sequence reactions used to generate the complete nucleotide sequence of a 4.1 kb portion of pCT406. Oligonucleotides specifically designed to generate nucleotide sequence overlap are indicated in parentheses. Plasmids pCT8.1.3, pCT6.1R.7, pCT9.1.6, pCT8.1R.9, pCT5.1R.1, pCT2.1.3, pCT4.1R.1, pCT9.1R.2 and pCT6.1R.5 were all generated by nested deletion analysis of pCT406 (see section 2.9.2). Each plasmid was sequenced using either the M13 forward oligonucleotide (M13F) or M13 reverse oligonucleotide (M13R) as indicated in parentheses next to each plasmid name. Asterisks (*) indicate restriction enzyme sites destroyed in the cloning process. The nucleotide sequence of all oligonucleotides used is listed in Table 2.4.4.

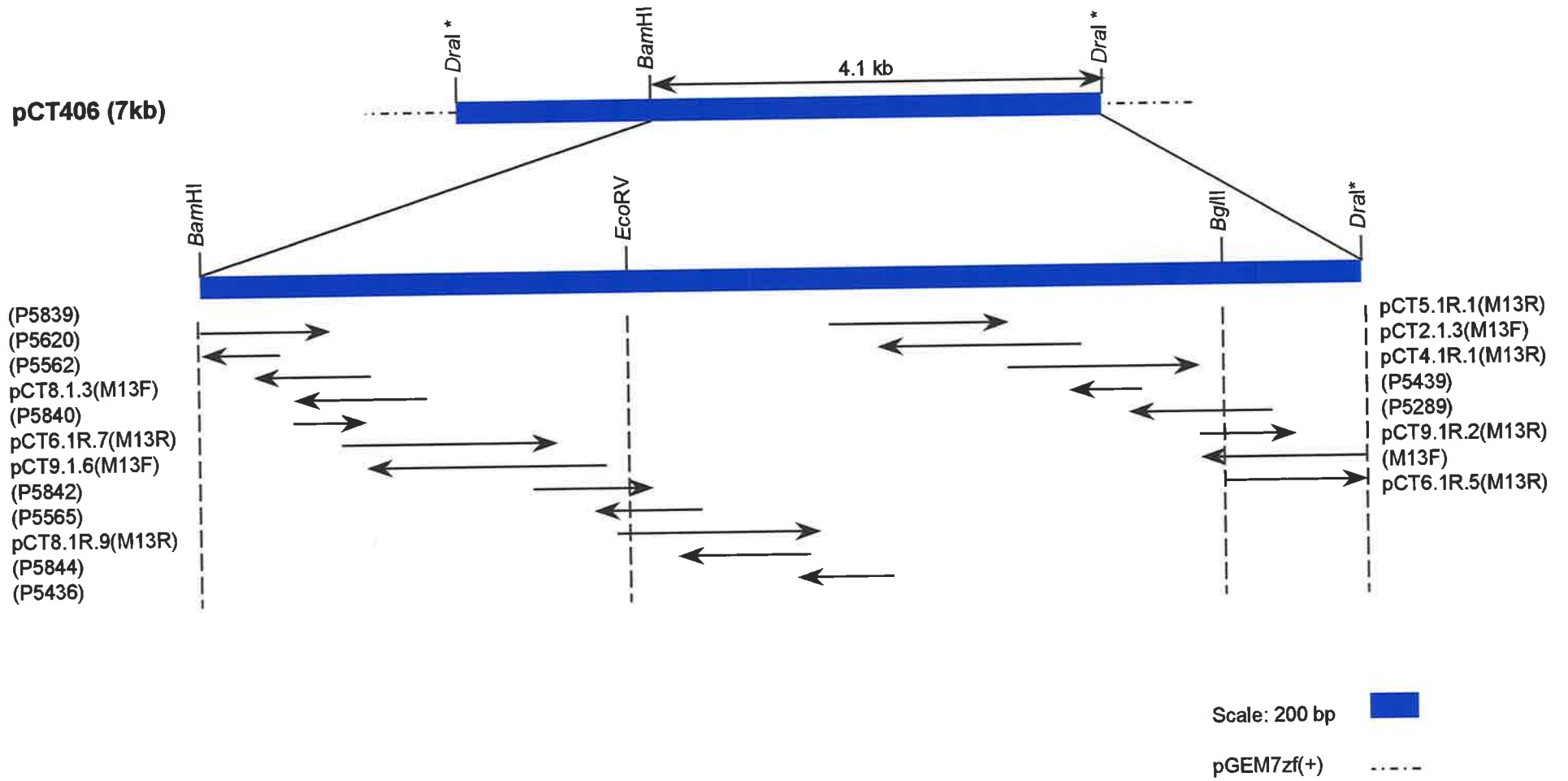


Figure 4.12 A schematic representation of the sequence reactions used to generate the complete nucleotide sequence of the 4.6 kb *DraI/EcoRI* fragment located on pCT407. Oligonucleotides specifically designed to generate nucleotide sequence overlap are indicated in parentheses. Plasmids pCT10.2.1, pCT1.2.1, pCT10.2.2, pCT7.2.4 and pCT5.2.2 were all generated by nested deletion analysis of pCT407 (see section 2.9.1 and 2.9.3). Each plasmid was sequenced using either the M13 forward oligonucleotide (M13F) or M13 reverse oligonucleotide (M13R) as indicated in parentheses next to each plasmid name. Asterisks (*) indicate restriction enzyme sites destroyed in the cloning process. The nucleotide sequence of all oligonucleotides used is listed in Table 2.4.4.

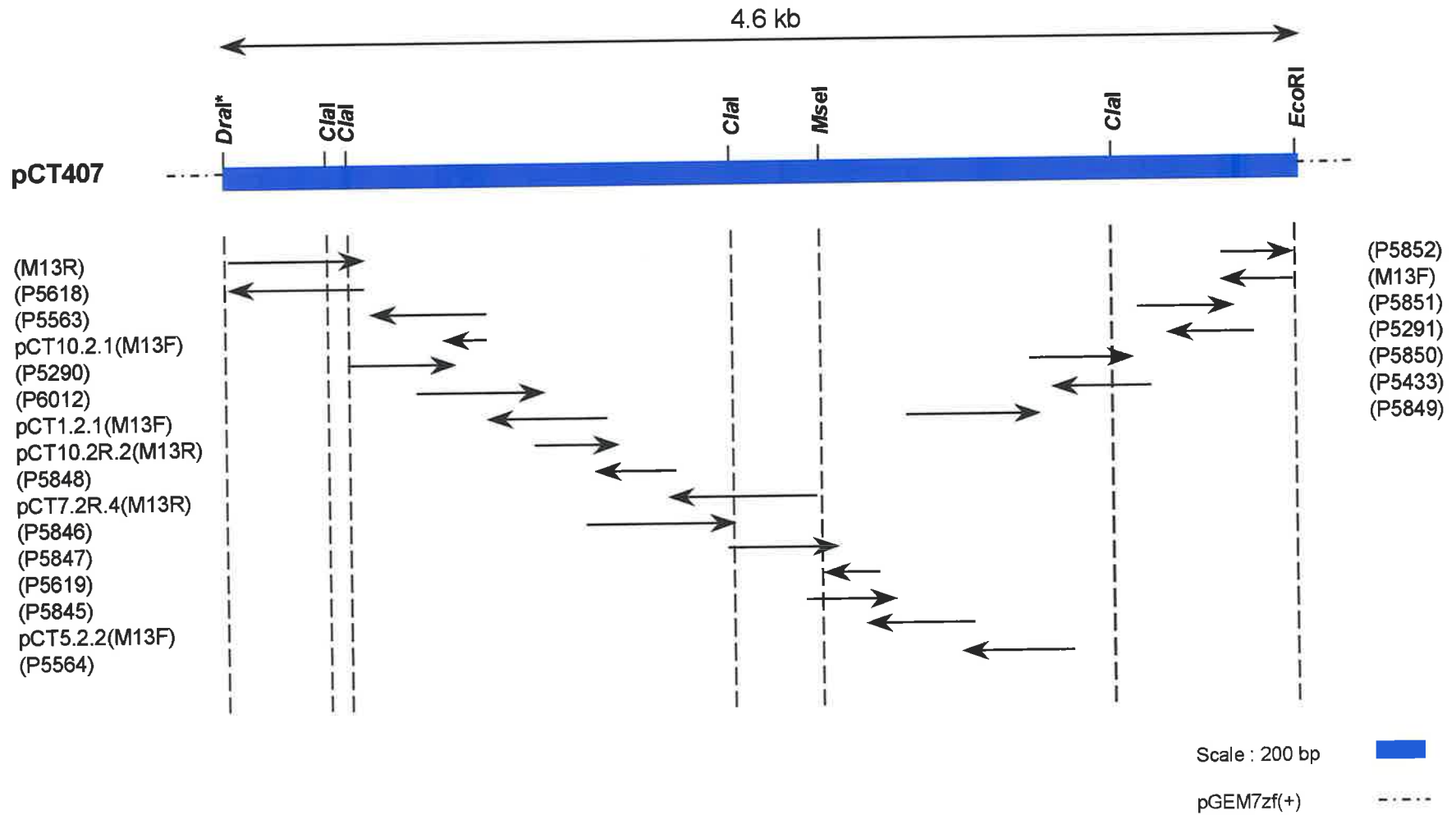
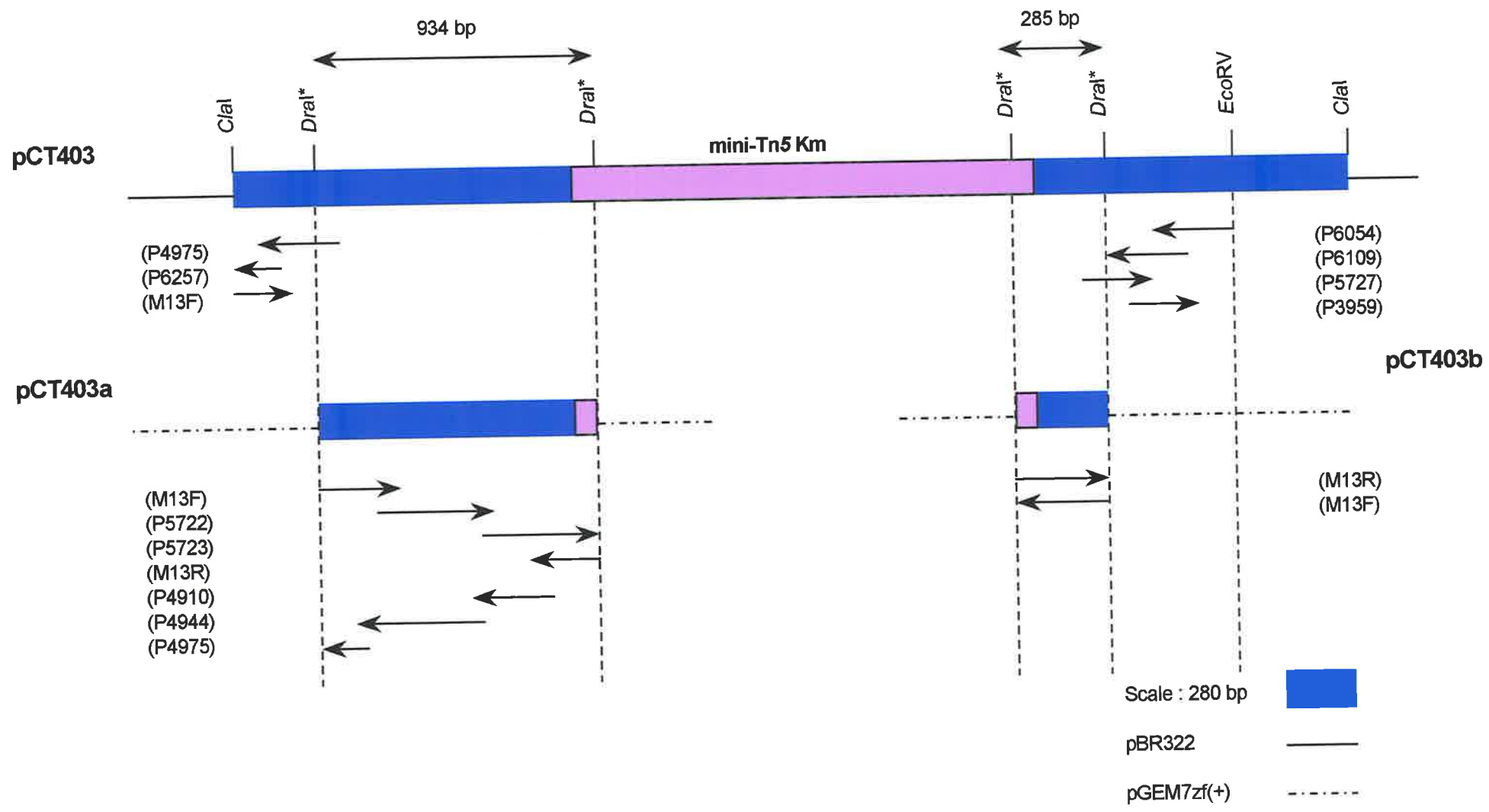


Figure 4.13 A schematic representation of the sequence reactions used to generate nucleotide sequence from pCT403. Oligonucleotides specifically designed to generate nucleotide sequence overlap are indicated in parentheses. The M13 forward (M13F) and M13 reverse (M13R) oligonucleotides were also used for sequence analysis. Plasmids pCT403a and pCT403b were previously generated by *DraI* digestion of pCT403 (see section 4.2.5.1). Asterisks (*) indicate restriction enzyme sites destroyed in the cloning process. The nucleotide sequence of all oligonucleotides used is listed in Table 2.4.4.



Plasmid pCT408 was sequenced using a combination of the M13 forward and reverse oligonucleotides, and nucleotide sequence analysis generated oligonucleotides (Figure 4.14). The pCT408 nucleotide sequence generated was compiled with the pCT400 and pCT403b derived sequence.

4.2.6 Preliminary analysis of compiled nucleotide sequence data from pCT400, pCT403 and pCT408

In total 15,582 bp of *X. bovienii* DNA was sequence (31,164 bp when both strands are considered). Figure 4.15 outlines a summary of the subclones used to generate the nucleotide sequence. Examination of the nucleotide sequence identified two complete and two partial ORFs (Figure 4.16).

4.2.6.1 Partial ORF *xpsD*

The first partial ORF identified was labelled *xpsD*, and consisted of 653 bp of 3' gene sequence (Figure 4.16). BLASTX 2.1.1 analysis of the 653 bp *xpsD* sequence shows homology to ATP-binding cassette (ABC) transporters such as *pvdE* (*P. aeruginosa*) and *syrD* (*P. syringae*) (Table 4.10). Both of these ABC transporters are involved in secretion of the bioactive peptides pyoverdine (siderophore) and syringomycin (plant toxin) respectively. Detailed BLASTX 2.1.1 analysis is presented in Chapter 5.

4.2.6.2 ORFs *xpsA*, *xpsB* (complete) and *xpsC* (partial)

A further 788 bp downstream of *xpsD* is the 3270 bp gene *xpsA*. ORF *xpsA* has the potential to encode a protein of 1089 amino acids with a predicted M_r value of 122,980. 37 bp downstream of *xpsA* is the 9951 bp ORF *xpsB*. ORF *xpsB* has the potential to encode a protein of 3316 amino acids with a predicted M_r value of 368,263. The stop codon of *xpsB* (AATGAAC) overlaps the start codon (AATGAAC) of 1177 bp ORF *xpsC* (Figure 4.16). Individual BLASTX 2.1.1 analysis of *xpsA*, *xpsB* and *xpsC* amino acid sequence shows homology to a number of peptide synthetase amino acid sequences such as NosA (*Nostoc* spp.), syringomycin synthetase (*P. syringae* pv. *syringae*), MycC (*Microcystis aeruginosa*) and lysobactin synthetase (*Lysobacter* spp.).

Figure 4.14 A schematic representation of the sequence reactions used to generate nucleotide sequence from 1.4 kb cloned PCR product located on pCT408. Oligonucleotides specifically designed to generate nucleotide sequence overlap are indicated in parentheses. The M13 forward (M13F) and M13 reverse (M13R) oligonucleotides were also used for sequence analysis. Plasmid pCT407 was previously generated by *DraI* digestion of pCT400 (see section 4.2.5.3). Nucleotide sequence analysis using P5292 confirms pCT407 and pCT408 represent a contiguous segment of *X. bovienii* based DNA. The nucleotide sequence of all oligonucleotides used is listed in Table 2.4.4.

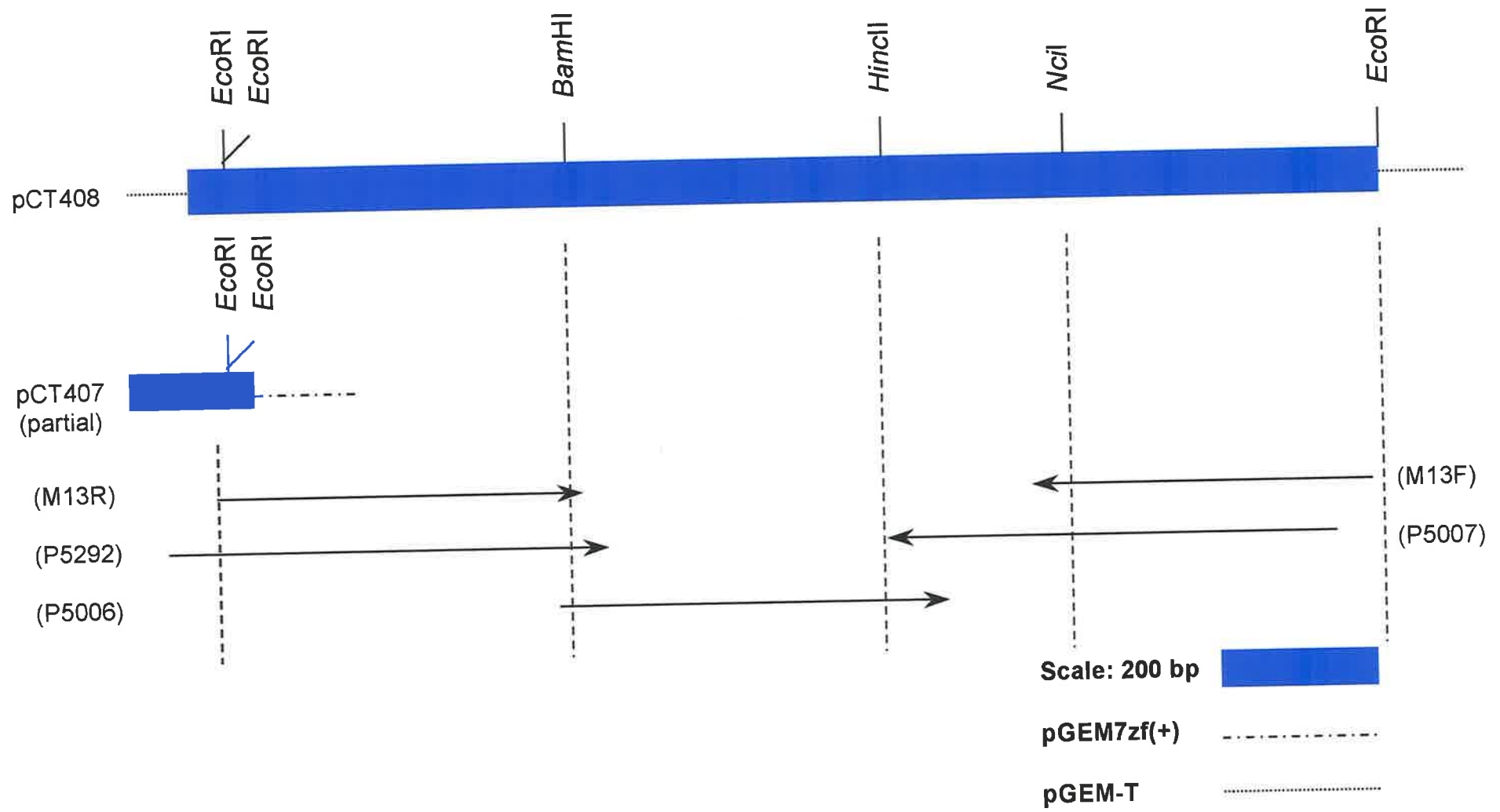
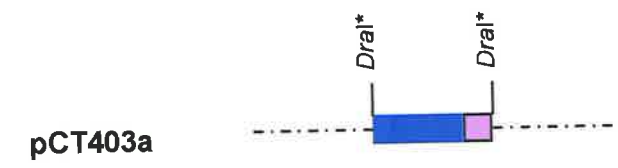
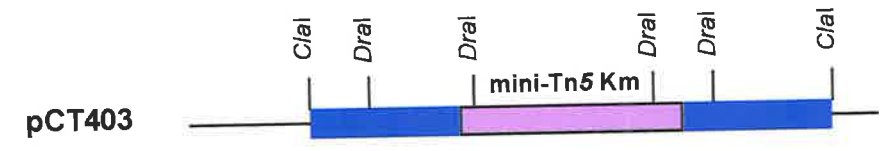
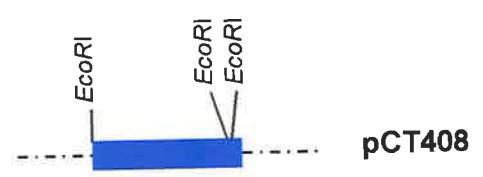
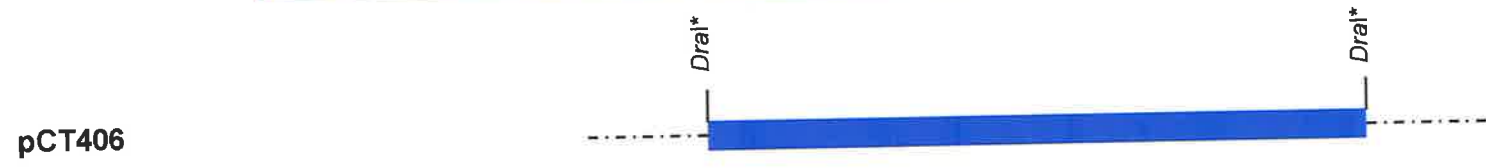
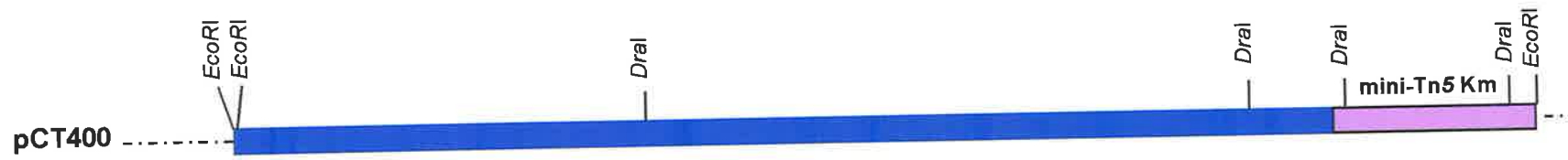


Figure 4.15 A schematic representation of the subclones generated to compile 15,582 bp of *X. bovienii* chromosomal DNA sequence homologous to non-ribosomal peptide synthetases. Astericks (*) indicate restriction sites destroyed in the cloning process.






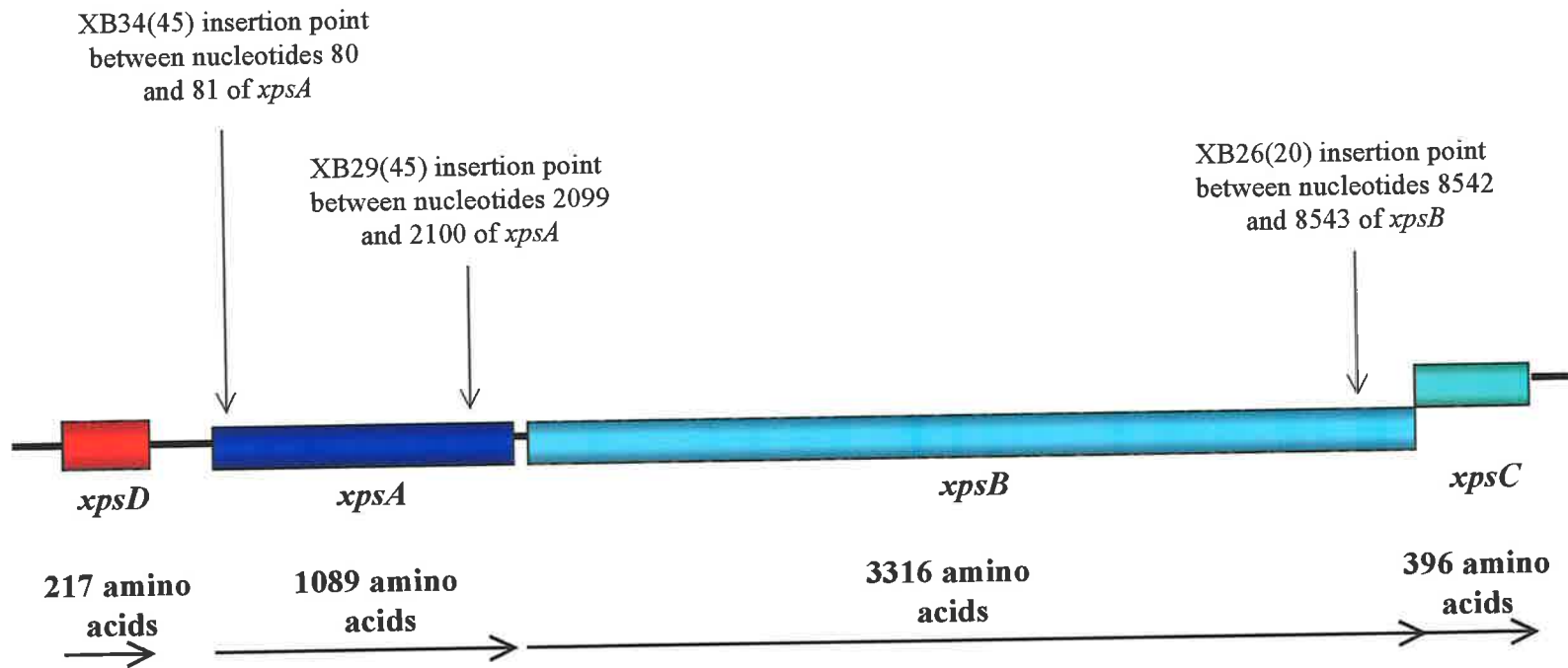
Scale : 800 bp 
 pBR322 
 pGEM7zf(+) 

Figure 4.16 A schematic representation of the organisation of partial ORFs *xpsD* and *xpsC*, and complete ORFs *xpsA* and *xpsB*. The size of each ORF is indicated. The independent insertion points for transposon mutants XB34(45), XB29(45) and XB26(20) are highlighted, and the nucleotide insertion point noted. The stop codon of *xpsB* (CAATTGAC) overlaps the start codon of *xpsC* (CAATGAAC).



Scale: 1000 bp



Detailed analysis of each open reading frame, including BLASTX 2.1.1 analysis, is presented in Chapter 5.

The four genes identified in the region have been labelled *xps* to represent “*Xenorhabdus* peptide synthetase”, and will be hereon referred to by this name.

4.2.6.3 Mapping transposon insertion mutants XB26(20), XB29(45) and XB34(45) to the 15,582 bp *X. bovienii* nucleotide region.

ClustalX alignments of compiled nucleotide sequence from XB26(20), XB29(45) and XB34(45) were independently aligned with the 15,582 bp region (data not shown) to locate the mini-Tn5 Km insertion points. The insertion point for transposon mutant XB34(45) was mapped to between nucleotides 80 and 81 of *xpsA*, XB29(45) mapped to between nucleotides 2099 and 2100 of *xpsA*. The transposon mutant XB26(20) insertion was mapped to between nucleotides 8542 and 8543 of *xpsB*. Figure 4.16 outlines the organisation of *xpsA*, *xpsB*, *xpsC* and *xpsD*; and the location of each transposon insertion within this region.

The compiled nucleotide sequence from either XB33(21) or XB41(23) (see section 4.2.4.1) did not align with the 15, 582 bp region when analysed by ClustalX. These results suggest the transposon insertions from XB33(21) and XB41(23) map outside the 15, 582 bp region.

4.3 Discussion

Phase variation in *Xenorhabdus* sp. was first described by Akhurst (Akhurst, 1980) and has since become an enigma in the field of *Xenorhabdus* sp. genetic analysis. It might be speculated that a master control switch operates to coordinately control all associated phase variation properties, however the presence of some intermediate phase 2 like cultures (Akhurst, 1980; Boemare & Akhurst, 1988) suggests the process may be more complex. One approach to identify regions of DNA involved in the process of phase variation is to isolate genes encoding the relevant phenotypes. Detailed analysis of each genes expression may lead to a better understanding of the control mechanisms involved with regard to phase variation.

In this chapter, transposon mutagenesis was used as a genetic tool to identify regions of chromosomal DNA required for the expression of a number of phase variant phenotypic

characteristics. Transposon mini-Tn5 Km was used to construct a bank of independent transposon insertion mutations within the *X. bovienii* T228 chromosome. Conjugal transfer of mini-Tn5 Km via plasmid pUTKm from *E. coli* SM10 λ pir (Km^R) to *X. bovienii* T228 (Amp^R, Sm^R) was successful, with *X. bovienii* (Amp^R, Km^R, Sm^R) isolated at a frequency of 2.1×10^{-5} transconjugates/donor cfu. This observation was comparable with a previous study that utilised *X. nematophilus* 1906/1 and three different conjugative plasmids, which were shown to be transferred at frequencies ranging 3.0×10^{-3} to 5.0×10^{-7} transconjugates/donor cfu (Xu *et al.*, 1991). Southern analysis of randomly selected transconjugates confirmed the transposon insertions were independent.

Five thousand transposon insertion mutants were screened for the loss or alteration of antimicrobial activity, phospholipase C activity, haemolysin activity and Congo Red binding capabilities. Of these, five transposon mutants showed disruption of all aforementioned phenotypes and were selected for further analysis. Sequence analysis of *X. bovienii* DNA flanking each of the five transposon insertion mutants, and subsequent BLASTX 2.1.1 analysis, revealed three transposon insertion mutants [XB26(20), XB29(45) and XB34(45)] had inserted into a homologous region of the chromosome.

PCR and nested deletion analysis was used to isolate and sequence both strands of a 15.5 kb region of *Xenorhabdus* DNA. Overall, two complete (*xpsA* and *xpsB*) and two partial (*xpsD* and *xpsC*) ORFs were identified. ORF *xpsA* is 3270 nucleotides with the potential to encode for a protein of 1089 amino acids with a predicted M_r value of 122,980. ORF *xpsB* is 9951 nucleotides with the potential to encode for a protein of 3316 amino acids with a predicted M_r value of 368,263. Partial ORFs *xpsD* and *xpsC* are 653 and 1177 nucleotides respectively. The insertion points for transposon mutants XB34(45) and XB29(45) were mapped to between nucleotides 80/81 and 2099/2100 respectively of *xpsA*. The transposon mutant XB26(20) insertion was mapped to between nucleotides 8542/8543 of *xpsB* (Figure 4.16).

Sequence comparison of the peptide sequences of XpsA, XpsB and XpsC with other available protein sequence databases revealed significant homology to a family of enzymes known as non-ribosomal peptide synthetases. Most sequence identity was observed to *Pseudomonas*

syringae pv. *syringae* syringomycin synthetase (Quigley & Gross, 1994) and *Nostoc* sp. NosA (Subbaraju *et al.*, 1997), both peptide antibiotics.

Non-ribosomal peptide synthetases (NRPSs) are multienzyme complexes which range in size between 100 - >1600 kDa (Stachelhaus & Marahiel, 1995), and catalyse the non-ribosomal synthesis of a structurally diverse family of bioactive peptides by mainly soil-borne bacteria and filamentous fungi. Examples of NRPSs include; the immunosuppressive agent cyclosporin (Weber *et al.*, 1994), cell toxin syringomycin (Quigley & Gross, 1994), the biosurfactant called surfactin (Cosmina *et al.*, 1993), and the siderophores mycobactin (Quadri *et al.*, 1988) and yersiniabactin (Gehring *et al.*, 1998). Many antibiotic-like substances are also synthesised by NRPSs such as vancomycin (Chiu *et al.*, 2001) gramicidin (Zuber *et al.*, 1993) to name a few. For a comprehensive list of bacterial and fungal peptide synthetases refer to Konz and Marahiel (Konz & Marahiel, 1999) and Challis *et al.* (Challis *et al.*, 2000).

NRPSs can have a linear, branched linear or cyclic structure and are constructed via an enzymatic system known as the "thiotemplate multienzyme mechanism" (Kleinkauf & von Döhren, 1990). NRPSs can contain non-protein amino acids such as D - amino acids or hydroxy acids, and each amino acid constituent may be modified by *N*-methylation, acylation, glycosylation and covalent linkage to other unusual functional groups (Lipmann, 1980) (Kleinkauf & von Döhren, 1990; Zuber *et al.*, 1993; Mootz & Marahiel, 1997a). The linkage can be as peptide bonds or through the formation of lactones and esters (Stachelhaus & Marahiel, 1995).

The thiotemplate multienzyme mechanism includes the activation of the constituent residues as adenylates on the enzymatic template, the acylation of specific template thiol groups, epimerization or *N*-methylation at this thioester stage, and polymerisation in the sequence directed by the multienzyme structure with the aid of 4'-phosphopantetheine as a cofactor, including possible cyclisation or terminal modification reactions (Kleinkauf & von Döhren, 1990). The thiotemplate mechanism is similar to both fatty acid and polyketide synthesis (Marahiel, 1992; Stachelhaus & Marahiel, 1995).

Bioactive peptides synthesised by non-ribosomal peptide synthetase gene sequences are secreted from the producer cell by ABC (ATP Binding Cassette) transporters. ABC

transporters are found in both prokaryotes and eukaryotes, and are involved in a number of processes such as substrate specific uptake; export of amino acids, sugar, inorganic salts, polysaccharides, peptides and proteins; signal transduction; drug and antibiotic resistance; antigen presentation; bacterial pathogenesis and sporulation (Fath & Kolter, 1993). Sequence comparison of XpsD with available protein databases revealed significant homology to peptide synthetase associated ABC transport genes. Most sequence identity was observed to *Pseudomonas aeruginosa* PvdE and *Pseudomonas syringae* SyrD. SyrD is proposed to function as an ATP driven efflux pump, and is believed to be a member of the highly selective secretion family of ABC transport proteins (Quigley & Gross, 1994). The primary function of SyrD is proposed to be antimicrobial resistance whereby the producer cell secretes away the harmful compound, therefore preventing host cell damage. Evidence for this hypothesis is provided by the fact that *syrD* mutants show a down regulation in peptide synthetase (syringomycin) production (Quigley & Gross, 1994).

Pseudomonas aeruginosa encodes a siderophore pyoverdine that is synthesised by a non-ribosomal mechanism and positively regulated by PtxR, a LysR family activator protein (Stintzi *et al.*, 1999). Interestingly, *X. bovienii* chromosomal DNA flanking transposon mutant XB33(21) was found to have good homology to transcriptional regulators LeuO and *Vibrio cholerae* LysR type transcriptional regulator (LTTR) (see section 4.2.4.1). The LysR transcriptional regulator family is diverse, being composed of more than 50 similar-sized autoregulatory transcriptional regulators. In response to different coinducers LTTRs activate transcription of linked and unlinked genes encoding extremely diverse functions (Schell, 1993). Considering the large size and diverse function of the LTTRs, it was felt prudent to firstly investigate the NRPS region of *X. bovienii*. XB33(21) shows a reduction in haemolysis, phospholipase C activity, Congo Red binding and antimicrobial activity when compared to wild type *X. bovienii* (see section 4.2.2.1). Future work could investigate the possible regulatory effects of a putative LTTR on the expression of a *X. bovienii* NRPS.

A phosphopantetheinyl transferase homolog found in *Photorhabdus luminescens* has been shown to be essential for the growth and reproduction of the entomopathogenic nematode *Heterorhabditis bacteriophora* (Ciche *et al.*, 2001). Phosphopantetheinyl transferases catalyse the transfer of the phosphopantetheinyl moiety from coenzyme A to a holo-acyl, -aryl, or -peptidyl carrier protein(s) required for the biosynthesis of fatty acids, polyketides or nonribosomal peptides (Ciche *et al.*, 2001). A mutant in the phosphopantetheinyl transferase

homolog isolated by Ciche consistently failed to support nematode growth and reproduction. This mutant was also defective in the production of siderophore and antibiotic activities (Ciche, *et al.*, 2001). Results from the Ciche study support the investigation of a putative NRPS in *X. bovienii*, and any possible role for products of this enzyme in virulence.

In conclusion, this chapter has described the transposon mutagenesis of *X. bovienii* with mini-Tn5 Km and the subsequent isolation of a 15.5 kb region of DNA showing homology to a family of bioactive peptide synthetases. Two complete (*xpsA* and *xpsB*) and two partial (*xpsD* and *xpsC*) ORFs were identified. ORF *xpsA* is 3270 nucleotides with the potential to encode for a protein of 1089 amino acids with a predicted M_r value of 122,980. ORF *xpsB* is 9951 nucleotides with the potential to encode for a protein of 3316 amino acids with a predicted M_r value of 368,263. Partial ORFs *xpsD* and *xpsC* are 653 and 1177 nucleotides respectively.

The next chapter in this thesis describes the detailed computer analysis of ORFs *xpsA*, *xpsB*, *xpsC* and *xpsD* at the nucleotide and amino acid level, providing further evidence that this 15.5 kb region encodes a novel peptide synthetase in *X. bovienii* T228.

Chapter 5

Computer analysis of the 15.5 kb region of DNA encoding a putative non-ribosomal peptide synthetase from *X. bovienii* T228

5.1 Introduction

Chapter four described the transposon mutagenesis of *X. bovienii* T228 using mini-Tn5 Km. Five independent insertions which disrupted lecithinase, haemolysin, Congo red and antimicrobial expression were examined at the nucleotide level. Three of the five insertions mapped to a 15.5 kb region of *X. bovienii* chromosomal DNA with significant homology to a family of enzymes known as non-ribosomal peptide synthetases (NRPS).

This chapter describes detailed analysis of the 15.5 kb region at both the nucleotide and amino acid level. Analysis of this region will include: nucleotide sequence composition, gene regulatory features, gene organisation, amino acid composition, BLASTX analysis of amino acid sequence data, hydropathy plots, amino acid motif identification and phylogenetic analysis. Overall, this chapter provides evidence to support the hypothesis that the 15.5 kb region encodes a novel NRPS.

5.2 Results

5.2.1 Gene organisation and general features

As outlined in chapter four, translation of the 15,582 bp of DNA sequence flanking three independent mini-Tn5 Km insertions from *X. bovienii* revealed two partial and two complete ORFs. Figure 5.1 shows the annotated nucleotide sequence of the 15,582 bp region, corresponding translated amino acid sequence and important features at both the nucleotide and amino acid level.

The order of genes identified is *xpsD*, *xpsA*, *xpsB* and *xpsC*. Partial ORFs *xpsD* and *xpsC* are 653 and 1177 bp respectively. Complete ORF *xpsA* is 3270 bp with the potential to encode for a protein of 1089 amino acids with a predicted M_r value of 122,980. Complete ORF *xpsB*

Figure 5.1 Nucleotide sequence of *X. bovienii* T228 non-ribosomal peptide synthetase (NRPS) genes *xpsA*, *xpsB*, *xpsC* and *xpsD*, including regulatory sequences. The nucleotides are numbered to the right hand side in the 5' to 3' direction. The deduced protein sequence of each complete or partial open reading frame is given below the DNA sequence in single letter code format and is numbered on the right hand side. Putative regulatory elements of *xpsA*, *xpsB* and *xpsC*; start codon, stop codon and ribosome binding site (rbs) are indicated. Primer extension analysis was used to estimate the +1 position of the *xpsABC* transcript at nucleotide 1028 (+1E). Computer analysis of the nucleotide sequence upstream of the *xpsA* ATG codon identified other potential +1 sites, these are indicated as +1(P1) and +1(P2). The corresponding -10 and -35 regions for +1(P1) and +1(P2) are labelled as -10(P1), -35(P1) and -10(P2), -35(P2) respectively. The stop codon and putative termination loop sequences of *xpsD* are indicated. Motif sequences typical of ATP binding cassette (ABC) transport proteins located in XpsD are highlighted in red.

Modules and domains typical of NRPS present in *xpsA*, *xpsB* and *xpsC* are indicated by a vertically labelled line running down the right hand side of the corresponding amino acid sequence. Core sequences of each domain are highlighted and numbered. Green - condensation domain (C); blue - adenylation domain (A) and yellow - thiolation domain (T).

Open reading frames *xpsD* and *xpsC* are incomplete. The stop codon of *xpsB* (14393 – CAATGAAC - 14400) overlaps the start codon of *xpsC* (14393 – CAATGAAC - 14400).

The Genbank accession number of this nucleotide sequence is AF455810.

ATCGTCCATCACTATACTGATAAAGAAAAACGTCAGTTTATGCTCGGCCCTTTAAGC - 60
I V H H Y T T D K E K R Q F M L G P L S - 20

WALKER A MOTIF

CTGAAAATATCTCAGGGCGAAATTGTCTTTATTGTCGGGGTAATGGTAGCGGTAAGACC - 120
L K I S Q G E I V F I V **S G N G S G K** T - 40

ACGTTAGCCATGATGCTGGTTCGGTTTATTTCGAACAGGAATCCGGTCTATCTGGCTTAAC - 180
T L A M M L V G L F E Q E S G S I W L N - 60

GGTGTCAAGATGGATGCATCTAACAAATGTCCACTATCGCCAATTCTTTTCCGCTGTATTT - 240
G V K M D A S N N V H Y R Q F F S A V F - 80

TCCAACATCATCTATTTGATCAGCTCTTAAATACCGGTACAGACGTCACAGAGAAAGCG - 300
S N Y H L F D Q L L N T G T D V T E K A - 100

ACTCATTACATTCAGGCATTAACATGGGTCACAAAGTGAAGATTATTGATGGTAAATTC - 360
T H Y I Q A L N M G H K V K I I D G K F - 120

LINKER PEPTIDE

TCTACGACAGAGCTTTCAGCCGGTCAAAGAAAAGCGGCTGGCTTTGGTCGCTGCTTATTTG - 420
S T T E **L S A G Q R K R** L A L V A A Y L - 140

WALKER B MOTIF

GAAGACCGCCCTCTTTATCTTTTTGATGAGTGGGCTGCTGACCAAGATCCGGTGTTTAAA - 480
E D R P **L Y L F D E W** A A D Q D P V F K - 160

CGGCTGTTCTATACAGAGCTTCTGCCAGAGTTAAGGTCTCGTGAAAAACGGTTATTGTG - 540
R L F Y T E L L P E L R S R G K T V I V - 180

INVARIANT HISTIDINE

ATTAGCCATGACAATGCTTATTTTCGATATTGCTGAACGTGTTATTAACCTGGAAGATGGT - 600
I S **I** D N A Y F D I A E R V I K L E D G - 200

xpsD stop

AATATTAAGAAATAAATAATCATAGTCATGAAACCATTACGGAACTAAAATAAATAACC - 660
N I K E I N N H S H E T I T E L K * - 217

xpsD termination loop

ACCCCAAATAAATGACCATGATATATTTTTTATTCATTCC**AAGAGCCTATTTTAATAGGC** - 720

TCTTTTTTTTTATTAACTTACATTATTAATAATTATTATATAATATAAATTATTAACAACGCA - 780

GATACACATTACCTGTAATAAAATTAGATACATAAGTAAAACACGGCTAACCATGCAAAA - 840

TACATTGATTTAATATATAATTCATTCTCTCGAATGTCATGAAAAAATCAAAGTATATTT - 900

TCTGAACAAAATGAAATTTGCTTATCAGTTTTTTTTAAATATTCCATTCTTTTTCTAAGG - 960

ATGGCATATTTTTTATTATTTTATACAT**TTCACA**GCATGATTTTTCTTGCT**GAAAAAT**AGAT - 1020

+1 (P2) -35 (P1) -10 (P1) +1 (P1)
CGTTTTG**ACTTTT****TTTAAC**CCAGTTTTTTTTAGTTG**TAGATT**GGATT**T**CTAGTTTTATTTTT - 1080
+1 (E1)

TGTTTTATCAGTTCTCATACTTTTTTATTTTCATATGCCATAAAAA**AAGGGAG**CTATAAA - 1140

xpsA start
ATGAACCACCCTGAAAAGTTGAAGCCATTTGCTTTATCCGAAGCACAAAAGCAGCCGTTGG - 1200
M N H P E K L K P F A L **S E A Q S S R W** - 20

TTTCAATATCAAATTAACCCAAGCCAACGTGGGCGAAATAATGGTGCGTTTTGTGCCAGA - 1260
I Y Q I N P S Q R G R N N G A F C A R - 40

GTTGAGGGGTTAAACGCTCAAGATTTAGAAGATGCACTCAATCACCTGATCAAGCGTCAC - 1320
V E G L N A Q D L E D A L N H L I K [REDACTED] - 60

CCGATGCTACGAGCCAGTTTTGGGCTATACGATGGCGAATTGGGATATCGCATAGCAGAG - 1380
E M L R A S E G L Y D G E L G Y R I A E - 80

C2
AATAGCGAAATCAAAGTTCAGACACATGATGCCCGGCACCTCAGCGAAGACACTCTTCAG - 1440
N S E I K V Q T H D A R H L S E D T L Q - 100

CAACTTGTATTTGACGATTGCCGGCATGTTCTCGATCTGGAAAATCCGCTGCGCTTTTAT - 1500
Q L V F D D C R H V L D L E N P L R F Y - 120

GCCAGTTGGTATCAATGCAATGCGCAAGAAAGTGTCTTGGTATTGACGTT**CGATCACTTA** - 1560
A S W Y Q C N A Q E S V L V L T **E D B L** - 140

GTTGTCGATGGTGGTCTTACTGGCTGTTGCTGGAAGAACTCGGCATGATTCTGACCTCA - 1620
V V D G W S Y W L L L E E L G M I L T S - 160

C3
CAGGAATTGGAACCGATATCAGAACACAGTTATCAAGATTATGTTTCATGGCAGCAGCAA - 1680
Q E L E P I S E H S **Y Q D Y V S W** Q Q Q - 180

C4
TGGTTAAACAGTAAAAGTGCAAAAAACAACAACAATTCTGGTGCATAATCTGGCTGGT - 1740
W L N S K S A K K Q Q Q F W C D N L A G - 200

AATTTGAGCTCATTATCATGGCCAATAAAAATCGGATCCGTACAAAACGGGGTAGATAAC - 1800
N L S S L S W P I K I G S V Q N G V D N - 220

AACGCCTCCCCTCCAATTACGGATAAGATCACGGCGTTCGGTAGAATCCCTGATGATTTA - 1860
N A S P P I T D K I T A F G R I P D D L - 240

GCCCTTAAGCTGTGTTCTATGGCATCTGAATACGGCAACAGCCTGTTTCGCTATTTTTCTG - 1920
A L K L C S M A S E Y G N S L F A I F L - 260

TCTGCCTATCAAATCCTGCTTAATCGCTATACCGCGCAGGACGATATCGTTATCGGCTCA - 1980
S A Y Q I L L N R Y T A Q D D I V I G S - 280

ATGATGCCGGGTCCGAGTCAAGCTAAATGGGGTAAGTTGGTAGGGGAATTTGTCAATCCG - 2040
M M P G R S Q A K W G K L **V G E F V N E** - 300

C5
GTCGCTTTACGGGGTCAAATCAACGGTAATGTCACGTACAGGAACATATTCTTCAAACC - 2100
V A L R G Q I N G N V T V Q E H I L Q T - 320

GCGAAGACTATCCGTCAGGCGATTGAAAACCAGAGATACCCTTTACCAAGGTTCTGGAA - 2160
A K T I R Q A I E **N Q R Y P F T** K V L E - 340

C6
CAATTTAAATTACAGCGCACTGCGGATACGCATCCGGTTTTCCAGACTCTGATGACCTTT - 2220
Q F K L Q R T A D T H P V F Q T L M T F - 360

CAAAAACCCAGATATGTTAGTGAGCTGCCAACGTTATGGATGGATGACGATTCCAGCAGC - 2280
Q K P R Y V S E L P T L W M D D D S S T - 380

ACAGTGCATTGGGGTGGCGCGGAATTAAGGCCTTTCCACATCCTCTTTATGCCGATACC - 2340
T V H W **S G A E L R P F** P H P L Y A D T - 400

C7
CCCGTCCCCCTGATGGTGAATATGATGGAGGTCAATCAACAGATCCGTTGTCATTTCCAT - 2400
P V P L M V N M M E V N Q Q I R C H F H - 420

TACGATCCCCAAGTGTTCGATGCTGAGTTAATCAATCAACTCATAAAAAATCTCATCACC - 2460
Y D P Q V F D A E L I N Q L I K N L I T - 440

CTGCTCACGGCAATGGCGGATAACCAACAACAGTCTATCGACAGCTTACCGCTGATGGAT - 2520
L L T A M A D N Q Q Q S I D S L P L M D - 460

X
P
S
A

M
O
D
U
L
E

1
C

D
O
M
A
I
N

GAGCAGGAACACCAGCAGGTTCTCTATGATTTTAAACAAGACGGATAAGCCTTTTCCTCAA - 2580
E Q E H Q Q V L Y D F N K T D K P F P Q - 480

CACGCTCTGATTCATCAATTATTTCGAACAGCAAGCCGAACGCACGCCTGACGCCATCGCC - 2640
H A L I H Q L F E Q Q A E R T P D A I A - 500

CTGAGTTGCGGTGATAAGGCGTTAAGCTATAACCGAACTTAACCAACAAGCCAATCGATTG - 2700
L S C G D K A **L S Y T E I** N Q Q A N R L - 520
A1

GCTCATGCCTTAATTAAGCTGGTATTCGTCCGGATAATCGTGTGCGCTATCTGCATGGAG - 2760
A H A L I K A G I R P D N R V A I C M E - 540

CGCAGTCTGGAGATGGTCATTGGCCTGCTGGGAATATTAAAAGCCGGCGCTGCTTACGTT - 2820
R S L E M V I G L L G I **L K A G A A Y V** - 560
A2

CCGCTCGACCCCTGAATATCCGACAGATCGGCTCGGCAATATTCTGTGACAGAGTGACCCT - 2880
P L D P E Y P T D R L G N I L S D S D P - 580

GCACTTCTGCTGATTCATCAGGCCTGCAAGATCATTTACCGATGACAACTATGCCTGTA - 2940
A L L L I H H G L Q D H L P M T T M P V - 600

TGGGTATGGAGAGTGAAGAGTATCGAACAAATATCGCCAGTCAGCCGACGGATAACCCG - 3000
W V L E S E E Y R T N I A S Q P T D N P - 620

GTTGCCACCGATTTAGGTCTGACGTCCCGCCATTTAGCCTATGTGCTTTACACCTCTGGC - 3060
V A T D L G L T S R H **L A Y V L Y T S G** - 640
A3

TCAACAGGCTTACCGAAAGGGGTATGAATGAGCACCGTGGAGTCGTCACCGCTTGTTG - 3120
S T G L P K G V M N E H R G V V N R L L - 660

TGGGCGCAGGATGAATATCAATTAACCTCAGCATGATCGGGTATTGCAAAAAACACCGTTC - 3180
W A Q D E Y Q L T Q H D R V L Q K T P F - 680

AGTTTTGATGTCTCAGTCTGGGAGTTTTTCTGCCTCTGCTTGCCGGCACTCAATTAGTC - 3240
S **F D V S** V W E F F L P L L A G T Q L V - 700
A4

ATGGCGCGTCCCCTGGTGCATAAGGAAGCGCTCTATCTGCTGGAAGAAATCGAAGCGCGG - 3300
M A R P G G H K E A L Y L L E E I E A R - 720

GGCATTACTACCCCTCATTTTGTGCCTTCCATGCTGCAAAGTTTTATTATCTGACACCC - 3360
G I T T L H F V P S M L Q S F I H L T P - 740

GCCGGCCGTTGCCCTTCTTTGCGTCAGATTTTGTGCGAGCGGAGAAGCCTTGTGCTATTCC - 3420
A G R C P S L R Q I L C S G E A L S Y S - 760

TTACAACAGCAGTGTCTGGCTCATTTTGTCTCACAGCGAACTTACAACCTGTATGGCCCG - 3480
L Q Q Q C L A H F A H S E L H **N L Y G F** - 780
A5

ACGGAAGCCGCAATCGATGTCACCTCTTGGCGATGTGTACCCGATCAGCATATCGGTCTG - 3540
T E A A I D V T S W R C V P D Q H I G L - 800

GTTCCCATTTGGTCACCCTATCGACAATACCCAGATCTATATCCTTGATAAACATGATCAG - 3600
V P I G H P I D N T Q I Y I L D K H D Q - 820
CCTGTTCCCATTTGGCGTAATCGGGGAAATTTATATCGCGGGTGCGGGTGTTGCCCGGGT - 3660
P V P I G V I **G E I Y I A G A G V A R G** - 840
A6

TATCTGAATAAACCGGAATTGACAGCGGAACGCTTTATCCGTGATCCGTTTCAAGTCAGCAT - 3720
Y L N K P E L T A E R F I R D P F S Q H - 860

CCTGACATGCGGATGTACAAAACCGGCGACATCGGGCGTTGGCTAGCCGATGGCAGCATC - 3780
P D M R M **Y K T G D I** G R W L A D G S I - 880
A7

GATTATCTGGGACGCAACGACTTTTCAAGGTCAGGATACGGGGAAATCGCATTGAAGTGGG - 3840
D Y L **G R N D F Q V K I R G N R I E L G** - 900

X
P
S
A

M
O
D
U
L
E

1
A

D
O
M
A
I
N

A8
GAAATTGAAGCGCGCCTGGCTCAGTCTGACGGCGTTCAGAATGTGATTGTTATCGCCCCGT - 3900
E I E A R L A Q S D G V Q N V I V I A R - 920

GAATATGATGCCGGAGATACACGGCTAGTCGCTTATCTCATCCCCAAGCCCGCGTCACT - 3960
E Y D A G D T R L V A Y L I P K P G V T - 940
P6035

CTGAGCATTCTGCTCTACGGGAACAAGTGGGCGGCAGTCTGCCTGATTACATGATCCCG - 4020
L S I P A L R E Q V G G S **L P D Y M I E** - 960
A9

AGTGCATTTGTGATGCTGGATGCTTCCCACTCACCCTGAATGGCAAATTGGATCGTAAA - 4080
S A F V M L D A F P L T **L N G K L D R** K - 980
A10

GCTCTGCCTGCGCCCGATCACTCAGCCGTCCTCACACGGGAATATGCGGCGCCACAAGGT - 4140
A L P A P D H S A V L T R E Y A A P Q G - 1000

GAAACCGAAGAACAACCTGGCCGATATCTGGCAAAGTTACTGAAAATCGATCGCGTTGGG - 4200
E T E E Q L A D I W Q K L L K I D R V G - 1020

XPSA MODULE 1 T DOMAIN

CGTAATGACAACCTTTTTCGAACCTGGGGGGTCACTTCGCTGCTGATGCTACAGCTACAGTCA - 4260
R N D N F F E L G G H S L L M L Q L Q S - 1040

AGAATAAGTGAAAACCTTTGATGTCGAACTCTCTATTCAACAATTATTTGCACACCCCACT - 4320
R I S E N F D V E L S I Q Q L F A H P T - 1060

ATTTGTCAACTTGAAGAGCACATTATTGATGCTCAGTTACTGCAATTTGACGCTGAATCC - 4380
I C Q L E E H I I D A Q L L Q F D A E S - 1080

xpsA stop rbs
TTGCAAGATCTCTACAAAACAATGGGT**TA**ATTCTGGTTTT**TA**ACTGGCTT**TGAATGG**TAC - 4440
L Q D L Y K T M G * - 1089

xpsB start
TTAAAA**ATGA**ATGATAATGAATTAATATCTTTACCATTAGCAGAACGTAAAAGACTACT - 4500
M N D N E L I S L P L A E R K R L L - 18
P6034

TGAGTTAGCTAAAGCAGCAAAACTAACTCGTCAGCAGACACAAAAACAGAAATCCATGC - 4560
E L A K A A K L T R Q Q T Q K T E I H A - 38

ACAACCCCGTGATGGGAATGTGCCATTGTCTGCGGCAACAGCGCCTCTGGTTTTTAAAC - 4620
Q P R D G N V P L **S W A Q Q R L W F L** T - 58
C1

GCAATTAGATCCCGCGGCACAAACGGCATAACCACATGTGCGGAGGGCTGAACCTGCAAGG - 4680
Q L D P A A Q T A Y H M S A G L N L Q G - 78

TCACCTGAATCAGAACGCGCTTAAAGCCGCGCTGGATCAGATTGTGGCACGTCATGAAAT - 4740
H L N Q N A L K A A L D Q I V A **R H E T** - 98
C2

TCTGCGTACCACCATCGTGGACGTCGAAGGACAGCCCCAACAAATCATTGGCAGTGCCGA - 4800
L R T T I V D V E G Q P Q Q I I G S A D - 118

TAGTGGTTTTGCGTTATCTGTACAAGATCTCAGCCCGTTACCCAGCACAGAACAGCAGGC - 4860
S G F A L S V Q D L S P L P S T E Q Q A - 138

GGCTGTAGAAGAATGCGCCAGCGTGAAGCCCTCCTTCCCTTCGATTTTACTCAGGGGCC - 4920
A V E E C A Q R E A L L P F D F T Q G P - 158

TTTGATTAGGGGCGACTGCTCCGTCTGGCAGAAGAGGCCATGTTCTGTTATTAACCTCA - 4980
L I R G R L L R L A E E S H V L L L T **■** - 178

X
P
S
B
M
O
D
U
L
E
1
C
D
O
M
A
I
N

GCATCACATCATCTCCGATGGCTGGTCCGTCAATATCTTGATGCAGGAACTTTCCACGCT - 5040
H H I I S D G W S V N I L M Q E L S T L - 198
 C3

TTATCAGGCCTTCTGTCAGGATCAGGCCGAACCATTACCCGCCTTGACACTCCAGTATGC - 5100
 Y Q A F C Q D Q A E P L P A L T L Q - 218
 C4

TGACTATGCGCTCTGGCAGCGGCAATGGTTACAGGGTGACGTGCTGGAAAAACAGTTAGA - 5160
D Y A L W Q R Q W L Q G D V L E K Q L D - 238

CTACTGGCGCAGTGAATTGCAGGGCGCACCCGGTGATTTTATAGTTACCCACCGACAAACC - 5220
 Y W R S E L Q G A P V I L E L P T D K P - 258

CGCTCCAACCCAACAGAGTTATGCCGGAAGCCGGTTCGATATAACACTGCCGCCTGCATT - 5280
 R P T Q Q S Y A G S R V D I T L P P A L - 278

GAGTACCGAGTTAAAGGCATTTCAGTCAGCGTCACGGCATTACCTTATTTATGACCTTATT - 5340
 S T E L K A F S Q R H G I T L F M T L L - 298

GGCCGATGGGCGGTATTACTTTCCCGTATCAGCGGACAACACGATCTGGTGATAGGCTC - 5400
 A G W A V L L S R I S G Q H D L V I G S - 318

TCCCGTCGCGAATCGCCAACGGCATGAGCTGGAGCCGCTAATAGGCTTTTTTTGTCAATAC - 5460
 P V A N R Q R H E L E P L **I G F F V N W** - 338
 C5

GTTAGCGTTACGGATCCAACCTGGGTGACAACCCAGCGTCAGCGAGCTGTTGGCACGGGT - 5520
L A L R I Q L G D N P S V S E L L A R V - 358

GAAAAATCATGCTCTGGGGGCTTATGCACATCAGGATCTGCCATTCGAGCAATTAGTTGA - 5580
 K N H A L G A Y A **H Q D L P F E E** Q L V E - 378
 C6

GGCGTTAAACCGCCGCGTAGCTTGGGCCATAGTCCTATTTTCAAGTGATGCTGGCTCT - 5640
 A L K P P R S L G H S P I F Q V M L A L - 398

GGATAATACGCCGGGACAGCAATATTTTCGAGCTGGATGGGCTGCATCTGCATGAACTGCC - 5700
 D N T P G Q Q Y F E L **D G L H L H E L** P - 418
 C7

ACGAACCCGAGACAGTGCCTATTTTGACCTGACCTTAACACTGAATGATACTGAGCAAAG - 5760
 R T R D S A Y F D L T L T L N D T E Q S - 438

TTTAGTCGGTGATCTGGAATATGCCAGTGATCTTTTTGAACATGCCAGCATTGAGCGGAT - 5820
 L V G D L E Y A S D L F E H A S I E R M - 458

GGTCGGTTACCTGCAAACCATCCTGTCAGCTATGGTGGCCGATGACAGCCTGCGGGTAGA - 5880
 V G Y L Q T I L S A M V A D D S L R V D - 478

CGATCTTCCCCTGCTGACCTCTTCACAACGCACTCAGTTATTGGCGAACTTTAACGATAC - 5940
 D L P L L T S S Q R T Q L L A N F N D T - 498

CGCCATTCCATATCCAAAAATGCTCTGATCCATCAGTTGTTTCGAACAACAGGTGGAGCG - 6000
 A I P Y P K N A L I H Q L F E Q Q V E R - 518

CACTCCTGATAAAATTGCCCTGGTCTGGGGAGAACTCAACTGAGTTACTCCGAGCTGAA - 6060
 T P D K I A L V W G E T Q **L S Y S E I** N - 538
 A1

TCAGCGAGCCAATCAACTGGCACACAGCATAATGGCATCGGGAGTCCATCCGGATGATCG - 6120
 Q R A N Q L A H S I M A S G V H P D D R - 558

CGTCGCAATTTGTGCCGAGCGCAGTCTGGATATGGTCATCGGCTTCGTAGGGATTTTGAA - 6180
 V A I C A E R S L D M V I G F V G I **L K** - 578

GGCGGGCGCCAGTTACATTCCGCTGGACCCCAATCACCCGACTGAACGGCTGGCTTATAT - 6240
A G A S Y I P L D P N H P T E R L A Y M - 598
 A2

X
P
S
B

M
O
D
U
L
E

1

C

D
O
M
A
I
N

GCTGTCTGACAGTCAGCCAGTATTAATGCTCACTCAGCAGCACCTGAAAGCCCGCCTGCC - 6300
L S D S Q P V L M L T Q Q H L K A R L P - 618

TGTCACAAACATAACCGGTATGGGCACTGGATAGTGAAGAACATCAAACCTGTATCGCCAG - 6360
V T N I P V W A L D S E E H Q T C I A S - 638

TCAGCCAAAAGACAATATCGACGCGTCTCAGCTAGGGCTGACCTCACAGAATCTGGCTTA - 6420
Q P K D N I D A S Q L G L T S Q N **L A Y** - 658
A3

TGTGTTATACACCTCCGGTTCGACTGGCCTGCCTAAAGGCGTCATGATCGAACACCAGAA - 6480
V L Y T S G S T G L P K G V M I E H Q N - 678

TGTGGTGCACCTTAATCCATTCTCAGTTCAGATGTCAAATTGACACCGCATGATTGCGT - 6540
V V H L I H S Q F Q M S K L T P H D C V - 698

ACTGCAATTTGCCTCTTTCGGATTTGATAACTCTGTTGCTGAAATTTTCCCGACATTTGC - 6600
L Q F A S F G **F D N S** V A E I F P T F A - 718
A4

TATAGGGGCAACGGTCGTTTTGCGGCCAGACCATATCAAGGTGCCGGATACGGAATTTAT - 6660
I G A T V V L R P D H I K V P D T E F I - 738

TACCTTTCTGCAAAATCAGGGCATCACAGTTGTGATTTGCCACCGCTTTCTGGCACCT - 6720
T F L Q N Q G I T V V D L P T A F W H L - 758

GTGGGCACAAGAAATCAGCGCCGGTTATAGCTGGCCTCCTGAGCAATTACGTTCCGTCGC - 6780
W A Q E I S A G Y S W P P E Q L R S V A - 778

GGCCGGAGGAGAAAAGCCGAGCACCGCCATCTGGTCACGTGGCTATCCAGTCTGGCAC - 6840
A G G E K A E H R H L V T W L S S P G T - 798

ACAAAATGCCGCTGGCTCAATACCTATGGCCCGACAGAAACCACCGTCAATGCAACCTC - 6900
Q K C R W **L N T Y G P T E T** T V N A T S - 818
A5

GATCGTTATCGATAAAGAAAATCTCTGCACCTATGAAGATATCCCGATAGGCCGGCCTAT - 6960
I V I D K E N L C T Y E D I P I G R P I - 838

CGCCAATACCCGGATCTATATTCTGGATCAACGCGGTCAACCCGTCCCGATTGGCGTAAA - 7020
A N T R I Y I L D Q R G Q P V P I G V N - 858

TGGCGAAATTCATATCAGTGGCAGCGGGGTTGCGCGGGGTATCTGAACCGGTCTGAGCT - 7080
G E I H I S G S G V A R G Y I N R S E L - 878
A6

GACAGCAGAACGTTTTATTCAAGATCCCTTCAGTGACATCCCCGGCGCCCGTATGTACAA - 7140
T A E R F I Q D P F S D I P G A R M **Y K** - 898

AACCGGCGATTTAGGACGCTGGCTACCGGATGGCACCATCAGCTATTCGGGTTCGCAATGA - 7200
T G D I G R W L P D G T I S Y S **G R N D** - 918
A7

CTTTCAGGTCAAATTCGCGGCTTCCGCATTGAGTTGGGTGAGATAGAAGCTCAACTGGC - 7260
F Q V K I R G F R I E L G E I E A Q L A - 938
A8

AACCTGCGCGGGCGTCAAAGATGCCGTTGTCATCGTCAGAGAAGATGACAACGGCGATAA - 7320
T C A G V K D A V V I V R E D D N G D K - 958

ACGTCTGGTTGCTTACTTAATCCCACAGTCTGGTGCAATTCTGAACGCGCCAGCCTGCG - 7380
R L V A Y L I P Q S G A I L N A A S L R - 978

TGAACAACCTCAGTGTCAATCTGGCAGATTACATGCTGCCAAGTGCCTTTGTTACTACTGGA - 7440
E Q L S V N **L A D Y M L P** S A F V T L E - 998
A9

AGCCTTCCCGTTAAATCAGAACGGTAAGATAGACCGCCCGCCCTGCCGCTCCGGATCG - 7500
A F P L N Q **N G K I D R** P A L P A P D R - 1018
A10

X
P
S
B

M
O
D
U
L
E

1

A

D
O
M
A
I
N

TTCGGCCAGCGTCAGCCGCGAATATGCTGAACCTCAGGGTGAAATCGAGCAACAACCTGGC - 7560
 S A S V S R E Y A E P Q G E I E Q Q L A - 1038
 XPSB MODULE 1
 CGCTATCTGGCAAATTTATTGGGATTGGAGCGAATCGGCCGCTATGACAGTTTCTTTGA - 7620
 A I W Q N L L G L E R I G R Y **D S F F E** - 1058

 T DOMAIN
 ACTGGGTGGACATTCTTTATTAACCGTCCAGGTCGCATCCCGTTTGCCTCAGTCTCTGAA - 7680
L G G H S L L T V Q V A S R L R Q S L N - 1078
 TATTGAAATAACGTTGCAGGATCTGTTTACTCAACCGGTATTAGCGGACTTAGCGCAATC - 7740
 I E I T L Q D L F T Q P V L A D L A Q S - 1098
 ATTGGTGACAGCGACCCAGTCAACACAACCGATGATCTTACCCGCCAACCGTGAGCAAGC - 7800
 L V T A T Q S T Q P M I L P A N R E Q A - 1118
 ATTACCCCTATCCTGGACACAGCAACGTCTCTGGTTTTTGGCTCAGTTAGATCCCGCCGC - 7860
 L P L **S W T Q Q R L W F L** A Q L D P A A - 1138
 C1
 CCAGACGGCATAACAACATGTCGGGGCGGGCTGCACCTGCAAGGCCACCTGAACCAGAACGC - 7920
 Q T A Y N M S G G L H L Q G H L N Q N A - 1158
 GCTTAAAGCCGCGTTGGATCGCATCGTTGCCCGTCATGAAATTCTACGCACCACCATCGT - 7980
 L K A A L D R I V A **R H E I L R T T I** V - 1178
 C2
 GCAGGCCGAAGGGAAAGCCCGGCAAGTCATTGGTGATGCAGATTGCGGTTTTTCTTTAAC - 8040
 Q A E G K A R Q V I G D A D C G F S L T - 1198
 TGTCGGGATCTTAGTCAGTTATCTTCATCAGCGCAGCAGGCAACCATTGAGGAATGCGC - 8100
 V R D L S Q L S S S A Q Q A T I E E C A - 1218
 CCAATTTGAAGCCAGCCATCCTTTTCGATTTTGCGCAAGGGCCGTTAATCCGCGCTCAACT - 8160
 Q F E A S H P F D F A Q G P L I R A Q L - 1238
 GCTTAAACTCGGCGAGCAGCAACATGTTCTGCTATTGACCCCAACATCACATTATTTCCGA - 8220
 L K L G E Q Q H V L L L T **Q H H I I S L** - 1258
 C3
 TGGCTGGTCGCTTAATGTATTGATGAACGAACTTTCTGCGCTGTACCAAGCCTTCGGTCA - 8280
G W S L N V L M N E L S A L Y Q A F G Q - 1278
 GGGGCAAGCTGATCCATTGCCTGCATTAGCCATTCAATATGCCGACTATGCGGTTTGGCA - 8340
 G Q A D P L P A L A I Q **Y A D Y A V W** Q - 1298
 C4
 ACGGCAATGGCTGCAAGGCGAAAGGCTGGAAAACAGTTGAGTTACTGGCGCAATGAGTT - 8400
 R Q W L Q G E R L E K Q L S Y W R N E L - 1318
 ACAAGATGCCCCACCTTATTAGAACTGCCTACTGATAAAGTCCGCCGTCAGTACAGAG - 8460
 Q D A P T L L E L P T D K V R P S V Q S - 1338
 TTATCATGGTGATCAGGTCACGTTCACTTTATCGCCGGAATTAATTCAGGGTTAAGGGC - 8520
 Y H G D Q V T F T L S P E L N S G L R A - 1358
 ATTGAGCCAGCGCCACGGTGGCAGCTTGTTCATGACATTACTGGCCGGCTGGGGAATTTT - 8580
 L S Q R H G A T L F M T L L A G W G I L - 1378
 GCTGTCACGGTTAAGTGGTCAGCCCCGATTTAGTGATTGGTACTCCCGTCGCCAACCGCCA - 8640
 L S R L S G Q P D L V I G T P V A N R Q - 1398
 GTACAGCGAGTTGGAGCCTTTAATCGGCTTCTTCGCCAATACTGGCCCTGAGAATCAA - 8700
 Y S E L E P L **I G F F A N T L A L R** I K - 1418
 C5
 GTTAGAAGATAACCCGACCGTCAGCGCATTATTGGCAAGAGTGAAGGCTCATGCGCTGGA - 8760
 L E D N P T V S A L L A R V K A H A L E - 1438

X
 P
 S
 B

 M
 O
 D
 U
 L
 E

 2
 C

 D
 O
 M
 A
 I
 N

AGCCTACGCCCATCAGGATCTGCCATTTGAACAATTAGTCGAAGTGCTACAACCGCCACG - 8820
 A Y A **H Q D L P F E** Q L V E V L Q P P R - 1458
 C6
 CAGTTTAAGTCACAGTCCGATTTTCCAAGTCATGTTGGCTTTAGATAATACATCCAGTAA - 8880
 S L S H S P I F Q V M L A L D N T S S K - 1478
 ACAAAGTTTTCGAATTGGCGGAATTGAGCCTCAATCCGCTGGCGCTGACCAGAAATAGTGC - 8940
 Q S F E L **A E L S L N P I** A L T R N S A - 1498
 C7
 CCATTTTGTACTCTCACTCTGGCACTGAGTGACACCGAAAATAGTCTGACATGTGAGTTGGA - 9000
 H F D L T L A L S D T E N S L T C E L E - 1518
 ATATGCCAGCGATCTTTTTGAACGTTCCAGTATCGAGCGCATGGCGGGTTATCTGCAAAA - 9060
 Y A S D L F E R S S I E R M A G Y L Q N - 1538
 CCTGCTGGCGCGATGGTCGCTGATGACAACCTGCGAGTCGCAGATCTGCCACTATTAAT - 9120
 L L A A M V A D D N L R V A D L P L L M - 1558
 GCCACATGAACGCACTCAATTACTGACCGACTTTAACGATACCGCCGTCACCTATCCGCA - 9180
 P H E R T Q L L T D F N D T A V T Y P Q - 1578
 GGACAAACTGCTGTGCGAGTTATTTGAACAACAGGTAGAGCACACACCTGATGCCATTGC - 9240
 D K L L S Q L F E Q Q V E H T P D A I A - 1598
 CCTAATCTGGGAAGACGCTCAACTCAGTTATGCCGAAGTGAACCAGCGCGCAACCAACT - 9300
 L I W E D A Q **L S Y A E I** N Q R A N Q L - 1618
 A1
 GGCTCACGCCCTGATTGCCTTTGGCGTTCCAGCCCGATGACCGCGTGGCAATTTGTATCGA - 9360
 A H A L I A F G V Q P D D R V A I C I E - 1638
 GCCTAATCTCAACATGGTATTGGGATGCTGGGCATACTCAAAGCCGGTGGCGGTTATGT - 9420
 R N L N M V I G M L G I **L K A G A G Y V** - 1658
 A2
 TCCGCTCGACCCGGAATACCCTGCCGAGCGGCTGGCCTATATCCTGTGACAGAGTGGCC - 9480
P L D P F Y P A E R L A Y I L S D S A P - 1678
 AAAATTACTGCTCACCCAACAGCATTTGCAGGCACAATTGCCGGTAGAGAACTCCCGGT - 9540
 K L L L T Q Q H L Q A Q L P V E K L P V - 1698
 CTGGCAACTGGACGATACTGGCCATTTAAATAGCGTGGCACAGCAACCGACCGATAACCC - 9600
 W Q L D D T G H L N S V A Q Q P T D N P - 1718
 TGATCCACGCCAGTTGGGGCTCTTTCCGCATCATCTGGCCTATATCATCTATACCTCCGG - 9660
 D P R Q L G L F P H H **L A Y I I Y T S G** - 1738
 A3
 CTCTACGGGTCTGCCCAAAGGGGTGATGATTGAACATCACAACGTCGTGAATTTACCTA - 9720
S T G L P K G V M I E H H N V V N F T Y - 1758
 CTCCAATGCCAGACCACTGAACTCAAATCCACTGACCGGTTCTGCAATTTGCGTCAGT - 9780
 S Q C Q T S E L K S T D R V L Q F A S V - 1778
 TTCATTTGATACCGCCGTGTCTGAAATTTTCCCGACGTTGTCAGTCGGGGCGACTTTAAT - 9840
 S **F D T A** V S E I F P T L S V G A T L I - 1798
 A4
 CCTGCGTCCGGCGCATATTCGCATCCCGGATGCCACTTTTAGTCATTTCTTGCAGGAGCA - 9900
 L R P A H I R I P D A T F S H F L Q E Q - 1818
 GCGATCAGCGTCATCGATCTGCCACCGCCTTCTGGCACCACTGGGTACAGGAGATGAA - 9960
 A I S V I D L P T A F W H Q W V Q E M K - 1838
 AGCCGGCCGAGTGGTTTTCAGCTCCCATGTACGTTCCGGTCCGGTCCGGCGGTGAGAAAGC - 10020
 A G R S G F S S H V R S V T V G G E K A - 1858

X
 P
 S
 B
 M
 O
 D
 U
 L
 E
 2
 A
 D
 O
 M
 A
 I
 N

CGAACACCGTCATTTTCGTCACCTTGGCAATCAATGCCGGAAACCCGGCACTGCCGCTGGAT - 10080
E H R H F V T W Q S M P E T R H C R W I - 1878

CGATACTTACGGGCAACGGAAACGACGGTCAGTGCCACTGCGCTGACACTGGATGGCCC - 10140
D T Y G P T E T T V S A T A L T L D G P - 1898
A5

TGCTTCCTATGTAACAGAATCCTTGTGCGATTGGCCGTCCCCTGATCAATACCCACGTTTA - 10200
A S Y V T E S L S I G R P L I N T H V Y - 1918

TATTCTTGATACACAGGGGCGAGCCCGTCCCCATCGGTGTCACCGGAGAAATCTACATTGG - 10260
I L D T Q G Q P V P I G V T **G E I Y I G** - 1938
A6

TGGCGCAGGCGTTGCCCGGGTTATCTGAACCGCCCTGAACTCACCGCCGAGCGTTTTGT - 10320
G A G V A R G Y L N R P E L T A E R F V - 1958

GTCCGACCCATTCCGTGAACAACCCCATGCACGGATGTACCGGACGGGCGATCTGGGCTG - 10380
S D P F R E Q P H A R M **Y R T G D L** G C - 1978
A7

CTGGCGACCGGATGGCACAATTGTCTACCTCGGCCGCAATGATTTTCAGGTCAAGATCCG - 10440
W R P D G T I V Y L **G R N D F Q V K I R** - 1998
A8

CGGCTTTCGCATTGAACTGGGCGAAATTGAGTCTCAGTTGGCCGCTGTACAGGGGTCAG - 10500
G F R I E L G E I E S Q L A A C T G V S - 2018

TGATGCCGTGGTGGTGGCAGCTGAAGAGGGCAGCGGCGATAAACGTCTGGTGGCGTACCT - 10560
D A V V V A R E E G S G D K R L V A Y L - 2038

CGTACCGAAGTCCGATGTACACTGGATGCCGCCAGCCTGCGCGAACAAGTGAGCACCCA - 10620
V P K S D V T L D A A S L R E Q V S T H - 2058

CTTGGCTGAATATATGTTGCCGAGTGCATTTCGTGATACTGGATGCCCTTCCCGCTGAACCC - 10680
L A E Y M L F S A F V I L D A F P L N P - 2078
A9

GAACGGCAAACCTGGATCGCAAGGCGCTGCCCGCACCGGACCACGCCGCCACCGTCAGCCG - 10740
N G K L D R K A L P A P D H A A T V S R - 2098
A10

TGAATATCAAGCTCCTCAGGGAGAGATGGAGCAGCAACTGGCCGTTATCTGGCAAACCTT - 10800
E Y Q A P Q G E M E Q Q L A V I W Q T L - 2118

XPSB MODULE 2 T DOMAIN

GCTGGGGCTGGAACAGGTCCGGGCGTCAGGACAATTTCTTTGAATTGGGTGGGCATTCCCT - 10860
L G L E Q V G R Q **D N F F E L G G H S L** - 2138

GCTGGTGGTCAGCCTGATTGAACAACCTGCGCCAAAGCAGTCTGAATCTGGATGTCAGCGC - 10920
L V V S L I E Q L R Q S S L N L D V S A - 2158

CGTCTTTTCTTCGCCAACACTGGCGGCGATGGCGGCGCGTCTGATAGTGAAAACGTCTGA - 10980
V F S S P T L A A M A A R L I V K T S D - 2178

TGGTGCTACTGGCACTAGCGTACAAAACGTGCCGCCGAATCTCATCACCGACGGTTGTCA - 11040
G A T G T S V Q N V P P N L I T D G C Q - 2198

GTCCATTACACCGGAGATGCTGCCACTGGTGGCACTGACACAGGATAACATTGACCAGAT - 11100
S I T P E M L P L V A L T Q D N I D Q I - 2218

CGTCGCCCCAAATTCCCGGAGGTGTCTCCAATATTGAGGATATCTATCCGTTGGGGCCATT - 11160
V A Q I P G G V S N I Q D I Y P L **C P I** - 2238

GCAGGAAGGCATTCTGTTCCACCATTTACTGGAAACAACCGGTGACACCTATCTCGACAA - 11220
Q E G I L F H H L L E T T G D T Y L D N - 2258
C1

CCAGCTGATGACCTTTGACAGCCGCCCGCGTCTGGACACGTTTTTGTGGCACTACAACA - 11280
Q L M T F D S R P R L D T F L L A L Q Q - 2278

X
P
S
B

M
O
D
U
L
E

2

A

D
O
M
A
I
N

GGTTATCAACCGTCACGATATCCTGCGCAGTGCGGTTCACTGGAACGGCCTGCCGGAGCC - 11340
V I N R H D I L R S A V H W N G L P E P - 2298
C2

GGTACACGTGGTTTCATCGTCAAGCCCCTCTTCCCATGCGGAGCTGACTCTGTCCGGGA - 11400
V H V V H R Q A P L P I A E L T L S P E - 2318

ACACGATGCCGAACAGCAGTTGCGCGATGCTACCGATTCTCGCTCGGTACGGATGGATCT - 11460
H D A E Q Q L R D A T D S R S V R M D L - 2338

GACTCAACCCCCGTTATTGTCTATCAAGCTTGCCAAAGATCCGCATAGTGAAACCTGGTT - 11520
T Q P P L L S I K L A K D P H S E T W F - 2358

TCTGGCTTTACTGCACCACCATCTGGTGTGTGATCACCTGTGCTGGAGATGATATTTAA - 11580
L A L L H H H L V C D H L S L E M I F N - 2378
C3

CGAAGTGCAGGCAATGCTACTGGGACAGGATGACTCGTTGGCACCATCGTTGCCTTACCG - 11640
E V Q A M L L G Q D D S L A P S L P - 2398
C4

CAACTTTATCGCCCAGACCCGCACCGTGCCGCTTGAAAAACATCAGGACTACTTCCACCA - 11700
N F I A Q T R T V P L E K H Q D Y F H Q - 2418

GCTCTGGGTGATATCGATGAACCTACCCTGCCCTTTGGTTTACTCGATATACAAGCAA - 11760
L L G D I D E P T L P F G L L D I Q G N - 2438

CTCTGATGAACAGAGTGAAATAGCAGAAGCCAACCTTCACTTTAGATAACGAACTGGCCCG - 11820
S D E Q S E I A E A N F T L D N E L A R - 2458

AAAAATACGTGACTGCGCCCGTCAGCAGGGCGTCAGTGCGGCGGTATTGTTCCACGTCGC - 11880
K I R D C A R Q Q G V S A A V L F H V A - 2478

TTGGGCGCAGGTAGTGGCGCAATGCAGCGGACGGGATGATGTCGTTTTCGGTACGGTATT - 11940
W A Q V V A Q C S G R D D V V F G T V L - 2498

ACTGGGAAGATTACAGGGAGGCTCAGGTGCCGATCAAGTCCCTCGGTATGTTTATCAATAC - 12000
L G R L Q G G S G A D Q V L G M F I N T - 2518
C5

CTTGCCTGTGCGCGTTTTATTGCAGGAACGCACGGTGCGACAAACCGTTCAGGAACTTA - 12060
L P V R V L L Q E R T V R Q T V Q E T Y - 2538

CCAGCAGTTAAGTTTATTGCTGGAACACGAACAGACCCCGCTGGCCATCGCCCAGCGTTG - 12120
Q Q L S L L L E H E Q T P L A I A Q R C - 2558
C6

CAGCCGTGTGCAGGCGCCTCAACCTCTCTTTAACAGCCTGCTTAATTTCCGCCATAGCCA - 12180
S R V Q A P Q P L F N S L L N F R H S Q - 2578

GCGTGACGATAAACAGTCTGCATCACCAGCTTGGGAAGGTATTCAGATCCTCAGCGGTGA - 12240
R D D K Q S A S P A W E G I Q I L S G E - 2598
C7

AGAACGCAGTAATTATCCTCTGTGCTGGATGTGGATGACTTCGATGATGGCTTTGCCCT - 12300
E R S N Y P L S L D V D D F D D G F A L - 2618

GACCGCCAGTGTAACCGACAGGTTGATCCGGCAGCATTAACTTTTATGGATACCGT - 12360
T A Q C N R Q V D P A R I N T F M D T V - 2638

GCTGAGAGAGCTGGTGGCCGCACTGCAAAACGTCTCTGAACAGAGTATTCAATCTCTCGC - 12420
L R E L V A A L Q N V S E Q S I Q S L A - 2658

CGTCCTGCCGCCAGATGAACGCACTCGGTTACTGGTGGACTTTAACAATACGGCGGCTTC - 12480
V L P P D E R T R L L V D F N N T A A S - 2678

CTATCCGAAAATGTCCTGCTCCACCAGCCATTGAAACAGCAAGCGGAACGCACACCGGA - 12540
Y P Q N V L L H Q P F E Q Q A E R T P E - 2698

X
P
S
B

M
O
D
U
L
E

3

C

D
O
M
A
I
N

GGCCATTGCCTTAATCTGGGAAGGCACTCAGCTCACCTATACCGAACTGAACCAGCGCGC - 12600
 A I A L I W E G T Q **L T Y T E I** N Q R A - 2718
 A1

TAACCAACTGGCACATCACCTGATTTTCGTCCGGCGTTCAGCCCGATGATCGGGTGGCGAT - 12660
 N Q L A H H L I S S G V Q P D D R V A I - 2738

CTGTATCGAACGCAATCTTGACATGGTGTATTAGTATGCTGGGCATATTTAAAAGCCGGTGC - 12720
 C I E R N L D M V I S M L G I **L K A G A** - 2758
 A2

AGGTTACGTTCCGCTCGATCCGGCCTACCCTGCCGAACGTCTGGCCTATATCCTGTCAGA - 12780
G Y V P L D P A Y P A E R L A Y I L S D - 2778

CAGTGCGCCGAAATTACTGCTCACTCAGCAGCATTTCAGGGGCGATTAGCCGTAGAGGA - 12840
 S A P K L L L T Q Q H L Q G R L A V E D - 2798

TCTCCCCGTCTGGCGACTGGACGATGCCGACCATTTAAGTACCGTGGCACAGCAACCGAC - 12900
 L P V W R L D D A D H L S T V A Q Q P T - 2818

CGATAACCCTGACTCACGCCGATTGGAGCTACAGCCGCATCATCTGGCCTATATCATCTA - 12960
 D N P D S R R L E L Q P H H **L A Y I I Y** - 2838
 A3

TACCTCCGGCTCCACCGGACTGCCTAAAGGCGTGATGATTGAGCACCGCAACGTGGTGAA - 13020
T S G S T G L P K G V M I E H R N V V N - 2858

TTTACCTATGCCAGTGTCAAGTCAAGTCAAAATCCACTGACCGCGTCTGCAATT - 13080
 F T Y A Q C Q V S E L K S T D R V L Q F - 2878

TGCCTCGGTTTTCGTTTGATACTGCCGTGTCTGAGATTTTCCCCACATTGGCCGTCGGCGC - 13140
 A S V S **F D T A** V S E I F P T L A V G A - 2898
 A4

GACCTTAATCCTGCGACCGGCGCATATTCAAGTACCGGATAACCCTTTAGTGTATTTCCT - 13200
 T L I L R P A H I Q V P D T T F S D F L - 2918

GCGGGAGCAGGCGATCAGTATCGTGGATCTGCCACCCTTCTGGCACCAGTGGGTACA - 13260
 R E Q A I S I V D L P T A F W H Q W V Q - 2938

GGAGATGAAAGCCGGCCGAGTGGTTTCAGTTCCTGCTGCGTTCGGTCACGGTCGGCGG - 13320
 E M K A G R S G F S S L L R S V T V G G - 2958

TGAAAAGCCGAACCTGCGTCATTACCTCACTTGGCAATCGATGCCGAAACCCGGAATTG - 13380
 E K A E L R H Y L T W Q S M P E T R N C - 2978

CCGCTGGATCGACTCCTACGGGCCAACCGAAACGACCGTTATCACCACGGCGCTGGCACT - 13440
 R W I **D S Y G P T E** T T V I T T A L A L - 2998
 A5

GGACAACCCGACCGCCGATGCTTCCCGTGGGATGGAACGTTGTGCGATTGGCCGCCCGAT - 13500
 D N P T A D A S R A M E T L S I G R P I - 3018

TGCTAATACCCGATCTATATTCTCGACACGCGGGGCGAGCCTGTACCCACCGGCGTCAC - 13560
 A N T R I Y I L D T R G Q P V P T G V T - 3038

CGGAGAAATCTACATTGGCGGCGCGGGGTTGCCCGAGGTTACCTGAACCGGCCTGAACT - 13620
G E I Y I G G A G V A R G Y L N R P E L - 3058
 A6

CACCACCGAACGTTTTGTATCCGATCCCTACAGTGAACCAATGCGCGGATGTACCG - 13680
 T T E R F V S D P Y S E Q P N A R M **Y R** - 3078
 A7

GACAGGCGATCTGGGCTGCTGGCAACCGGATGGCACGATAGTCTATCTCGGCCGCAATGA - 13740
T G D I G C W Q P D G T I V Y L **G R N D** - 3098

CTTTCAGGTCAAGCTCCGTGGCTTCCGCATTGAACTGGGTGAAATCGAAACCCAACTGGC - 13800
F Q V K L R G F R I E L G E I E T Q L A - 3118
 A8

X
P
S
B

M
O
D
U
L
E

3
A

D
O
M
A
I
N

CGCCTGCCTGGGTGTCAAGGATGCCGTGGTGGTGGCGCGTGAAGAGGATGCCGGTGATAA - 13860
A C L G V K D A V V V A R E E D A G D K - 3138

GCGTCTGGTGGCTTATGTGATCCCGCAACCCGATGCGTCTTTGGACGCAGCCAGCCGCTGCG - 13920
R L V A Y V I P Q P D A S L D A A S L R - 3158

TGAACAACCTGAGCACGCACCTGACGGAATATATGCTGCCGAGTGCCTTCGTGATACTGGA - 13980
E Q L S T H **L T E Y M L P** S A F V I L D - 3178
A9

TGCCTTCCCCTGACGCCGAGTGGAAAACCTGGATCGCAAAGCCCTGCCGGCACCCGGTTCG - 14040
A F P L T P **S G K L D R** K A L P A P G R - 3198
A10

TTCCGCCAGCACCCAGCCATGAATATGAAGCCCCTCAAGGTGAAATTGAACCGCAACTGGC - 14100
S A S T S H E Y E A P Q G E I E P Q L A - 3218

XPSB MODULE 3

CGCTATCTGGCAGACCCTGCTGGGACTAGAGCAGGTTGGGCGCCATGATAACTTCTTTGA - 14160
A I W Q T L L G L E Q V G R H **D N F F E** - 3238

T DOMAIN

GTTAGCGGGAATTCATTATCCATCATGCGGTTATCCACTCACCTGCGTGAAGAATTCCA - 14220
L G G N S L S I M R L S T H L R E E F H - 3258

CCTTGAAATTCCTATTGCAGACATTTTTTCATCACTCAACACTGTATAAACTTGCTGAACT - 14280
L E I P I A D I F H H S T L Y K L A E L - 3278

TATTCTATCAAGACAAATTGAAACCTTTTTTCGCCAAGATATAGAGTCCGTACAAAAAGA - 14340
I L S R Q I E T F F A Q D I E S V Q K E - 3298

xpsC rbs xpsB stop

GTGGAGAACCTGTCTGAAGAAGAGTTGCTTGCCATGTTAA**ATGGAGATCAACAATGAAC** - 14400
L E N L S E E E L L A M L N G D Q Q * - 3318

xpsC start

ATGAAC - 14400
M N - 2

ATCAATGAACAACTCTGGATAAATTACGGCAGGCAGTGCTCCAGAAAAAAATTAAGAA - 14460
I N E Q T L D K L R Q A V L Q K K I K E - 22

CGCATCCAAAATAGCCTGAGTACTGAAAAATATCAGATCCAGCCCAGAACTGACCCACAA - 14520
R I Q N S L S T E K Y Q I Q P R T D P Q - 42

CAGGCGTTACCGCTATCCTGGGCGCAGCAGCGCCTATGGTTCCTTGCTCAATTGGATCCC - 14580
Q A L P L **S W A Q Q R L W F I** A Q L D P - 62
C1

GCCGCACAGACGGCGTATCACATACCGGCTGGCCTTCATCTGCAAGGCCAGATGAACCAA - 14640
A A Q T A Y H I P A G L H L Q G Q M N Q - 82

AGCGCATTACAGGCCACGCTGGATAGCCTGGTGGCAGCCATGAAATTTTGCGAACCACC - 14700
S A L Q A T L D S L V A **R H E I L R T T** - 102
C2

ATTGCGCTGGTTCGAGGGGAAAGCACAGCAAATCATTGGCGATGCAGACTGCGGCTTTGCT - 14760
■ A L V E G K A Q Q I I G D A D C G F A - 122

TTAACCATTACAGGATCTCAGTCAGTTGCCTGAAGCAGAACAACAACCACTGTGCAAGAA - 14820
L T I Q D L S Q L P E A E Q Q T T V E E - 142

TATACGCAGTCTGAAGCGAGCCATCCCTTTGATTTTGAACATGGCCCGTTGATACGGGGA - 14880
Y T Q S E A S H P F D F E H G P L I R G - 162

CGATTACTCAAGCTCTCGCAGGATAGCCATATCCTGCTGTTAACTCAGCATCACATTATC - 14940
R L L K L S Q D S H I L L L T **Q H H I I** - 182
C3

X
P
S
C

M
O
D
U
L
E
1

C

D
O
M
A
I
N

TCCGATGGCTGGTCAATCAATGTGTTGATGCAGGAAGTCTCGACGCTTTACCACACTTTC	- 15000	
E D G W S I N V L M Q E L S T L Y H T F	- 202	X
GATCAGGGTCTGGCAAACCCATTACCGCCATTGACGCTCCAGTATGCCGACTATGCGCTC	- 15060	P
D Q G L A N P L P P L T L Q Y A D Y A I	- 222	S
	C4	C
TGGCAACGGCAATGGCTGCAAGGCGAAGTGTGGAAAAACAATTGGATTACTGGTGCAAT	- 15120	M
I Q R Q W L Q G E V L E K Q L D Y W C N	- 242	O
GCACTACAGGATGCCCCCTGCGCTCTTAACACTCCCCACAGACAGACCCCGGCCACAG	- 15180	D
A L Q D A P A L L T L P T D R P R P P Q	- 262	U
CAGAGTTATGCTGGTGAAGCGTTGAGATCACGTTCCCTGCGACGCTGAATGCACAATTA	- 15240	L
Q S Y A G G S V E I T F P A T L N A Q L	- 282	E
AAAACACTCGGCCAACGTCATGGGACAACCTTATTTATGACCCTGTTGGCGGGCTGGGCA	- 15300	1
K T L G Q R H G T T L F M T L L A G W A	- 302	C
GTGTTACTCTCCCGCATCAGTGGACAGAAGGATCTGGTAATAGGCACGCCCGTCGCAAAT	- 15360	D
V L L S R I S G Q K D L V I G T P V A N	- 322	O
CGCCAGCATCGTGAAGTGGAGCCTTTGCTCGGTTTCTTTGTCAATACGTTAGCGCTGCGG	- 15420	M
R Q H R E L E P L L G F F V N T L A L R	- 342	A
	C5	I
GTACAGTTGCATGACAACCCAACCGTCAGTGAGCTATTGGCACAGGTGAAAGCCCATACC	- 15480	N
V Q L H D N P T V S E L L A Q V K A H T	- 362	
CTGAATGCTTACGTGCATCAGGATCTGCCATTGAAACAGTTAGTTGAAGCGTTAAAACCC	- 15540	
L N A Y V H Q D L P F E Q L V E A L K P	- 382	
	C6	
CCGCGCAGCCTGAGCCATAGCCCGATCTTTTCAGGTCATGCTG	- 15582	
P R S L S H S P I F Q V M L	- 396	

is 9951 bp with the potential to encode for a protein of 3316 amino acids with a predicted M_r value of 368,263.

The stop codon of *xpsD*, and start codon of *xpsA* are separated by 486 nucleotides. The *xpsA*, *xpsB* and *xpsC* genes are apparently linked as an operon. This is supported by the observation of only 37 bp between *xpsA* and *xpsB*. ORFs *xpsB* and *xpsC* have overlapping reading-frames, where the stop codon of *xpsB* and the start codon of *xpsC* overlap (see Figure 5.1). From here on when referring to the *xpsA*, *xpsB* and *xpsC* operon the term *xpsABC* will be used.

5.2.1.1 Comparison of the mol% (G+C) of *X. bovienii* *xpsABC* and *xpsD* with the *P. syringae* syringomycin synthesis and export region

The mol% G+C of *X. bovienii* and *P. syringae* nucleotide regions were analysed using the Artemis (Release) 4 software package. Most strikingly, patterns in the mol% G+C over the *X. bovienii* 15,582 bp sequence reflected locations of the *xpsABC* and *xpsD* ORFs. Coding regions showed an average mol% G+C of 50.4% whilst the intergenic region values dropped to 19.2 – 34.2% (Figure 5.2). This result is particularly interesting considering the mol% G+C of *Xenorhabdus* spp. is 43 – 44% (Thomas & Poinar, 1979). In comparison, the *P. syringae* non-ribosomal peptide synthetase coding region has a mol% G+C average of 61.3% which is not significantly different to the *P. syringae* average of 59 – 61% (Guenzi *et al.*, 1998). Intergenic regions have a mol% G+C of 44.6 – 45.8, approximately 15% lower than the *P. syringae* average. Whilst *P. syringae* does show fluctuations in mol% G+C the pattern does not reflect the gene organisation, as is the case for the *xps* gene cluster from *X. bovienii* spp. *P. syringae* was used for comparative purposes because of the significant level of homology that exists between the *X. bovienii* and *P. syringae* peptide synthetase regions (see section Chapter 4, section 4.2.4.1 and this chapter, 5.2.2.2).

5.2.1.2 Analysis of nucleotide regulatory sequences flanking, *xpsABC* and *xpsD*

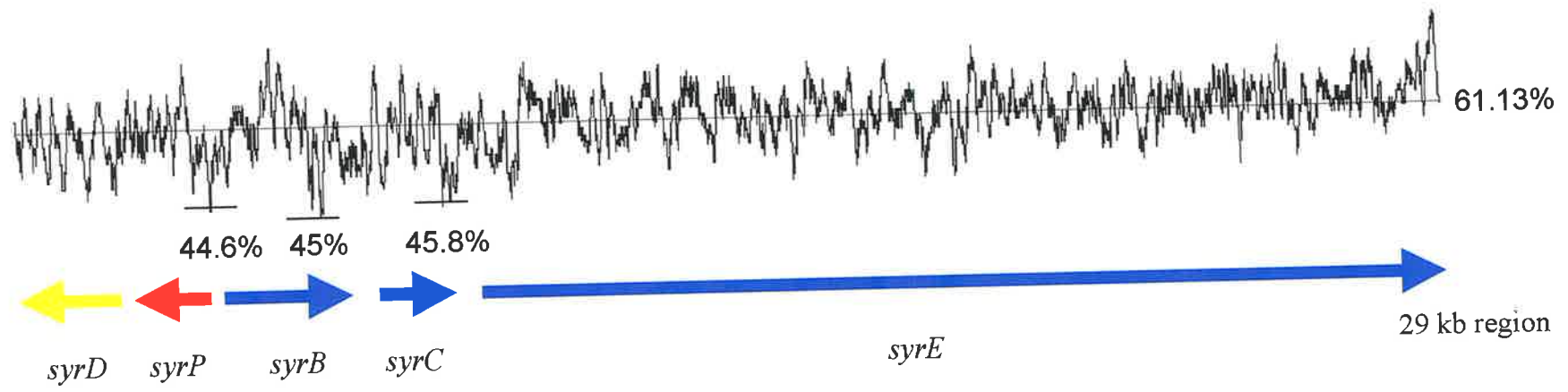
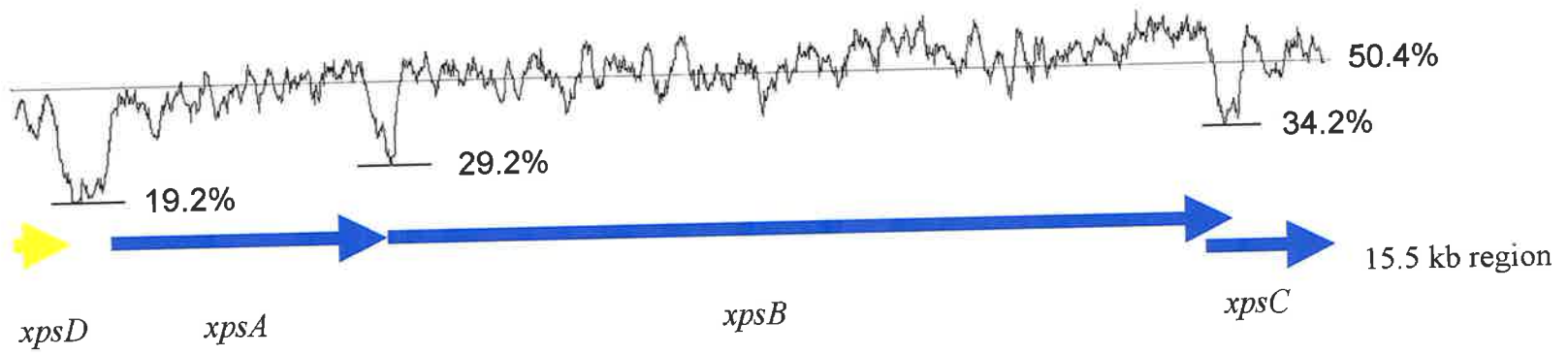
The *xpsABC* promoter region was mapped by primer extension analysis of the 5' end of the *xpsABC* mRNA transcript using oligonucleotide P1208 (highlighted in Figure 5.1). An approximately 181 bp transcript was detected when electrophoresed on a sequencing gel (Figure 5.3). Therefore the +1 site was identified as being 113 bp upstream of the *xpsA* ATG start codon at nucleotide 1028. At spatial regions corresponding to –10 and –35 regions of the

Figure 5.2 Mol% (G+C) plots of non-ribosomal peptide synthetase nucleotide sequences from *X. bovienii* and *P. syringae*.

X. bovienii genes; *xpsABC*, putative peptide synthetase genes; *xpsD*, putative ABC transport gene.

P. syringae genes; *syrB*, syringomycin biosynthetic gene; *syrC*, syringomycin biosynthetic gene; *syrD*, ATP driven efflux pump; *syrE*, syringomycin biosynthetic gene; *syrP*, regulatory protein similar to histidine kinases.

Window size = 100 nucleotides.



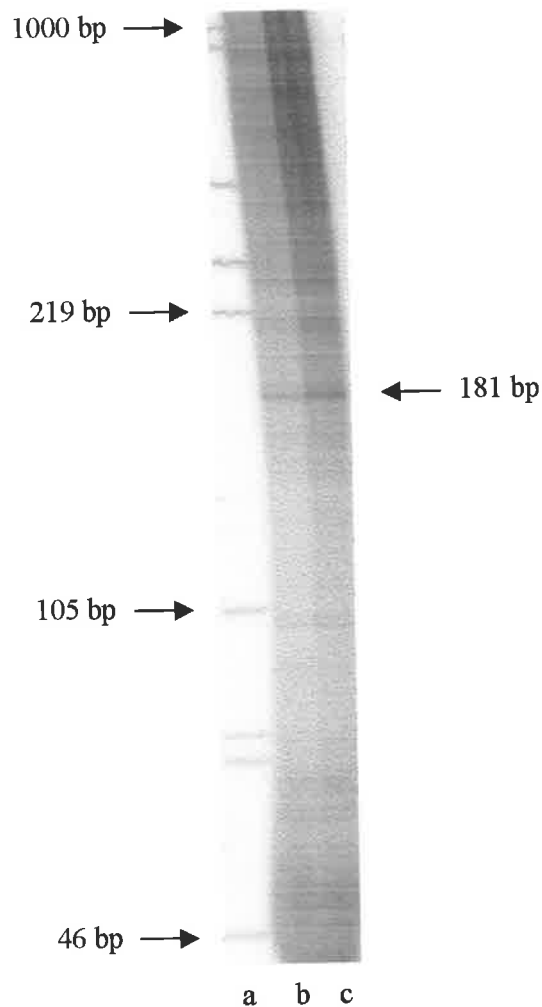


Figure 5.3 Primer extension analysis of *xpsABC* promoter transcripts in *X. bovienii* T228 using oligonucleotide P1208. The marker is *Sau3A*I digested pBluescript (1000, 734, 341, 219, 105, 78, 75, 46, 36, 18 and 17 bp).

Lanes:

[a], pBluescript marker;

[b], 5 ug total cellular RNA;

[c], 10ug total cellular RNA.

The presence of several bands makes a definitive interpretation of these results difficult. The large size of the predicted transcript (>15 kb) indicates that it is unlikely that purification of the entire mRNA can be achieved. Section 5.2.1.3 presents information concerning detection of this transcript by RT-PCR methods.

transcript, fair and poor similarity respectively, when compared with the consensus *E. coli* promoter regions were observed. The primer extension product was not sequenced to determine the precise +1 site.

Computer Analysis of the 5' *xpsA* nucleotide sequence (Berkeley Drosophila Genome Project Neural Network Promoter Prediction computer package) was used to predict a +1 site location. The first predicted +1 site (P1) was located at nucleotide 1066, the second (P2) at nucleotide 1022. At spatial regions corresponding to -10 and -35 regions of each putative transcript, the -10 and -35 regions share good similarity, when compared with the consensus σ^{70} *E. coli* promoter regions. Predicted +1 sites (P1) and (P2), the experimentally determined +1 site (E1) and their associated promoter regions are noted on Figure 5.1 and Table 5.1. Putative ribosome binding sites were located 5' of *xpsA*, *xpsB* and *xpsC* (Figure 5.1 and Table 5.1). All ribosome binding sites show good nucleotide identity to the *E. coli* ribosome binding site consensus sequence.

Table 5.1

Organism	Nucleotide sequence of regulatory elements for gene expression		
	-10	-35	rbs
<i>E. coli</i>	TATAAT	TTGACA	AAGGAGG
<i>X. bovienii xpsA</i>			
E1 (nucleotide 1028)	TAGATC	GCATGA	
P1 (nucleotide 1066)	TAGATT	TTTAAC	
P2 (nucleotide 1022)	GAAAAT	TTCAACA	
<i>xpsA</i>			AAGGGAG
<i>xpsB</i>			TGAATGG
<i>xpsC</i>			ATGGAGA

Additionally, a 10 bp palindromic repeat sequence was identified 46 bp downstream of the *xpsD* stop codon at nucleotide position 701 - 724 (Figure 5.1). This repeat sequence, followed by a poly T tail, potentially represents a transcriptional terminator of *xpsD*.

5.2.1.3 Northern hybridisation analysis to determine the *xpsABC* operon transcript size

Northern hybridisation analysis of RNA extracted from *X. bovienii* O/N cultures was used to determine the size of the *xpsABC* transcript. A DIG-labelled 544 bp DNA probe which spans

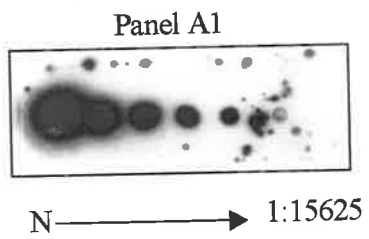
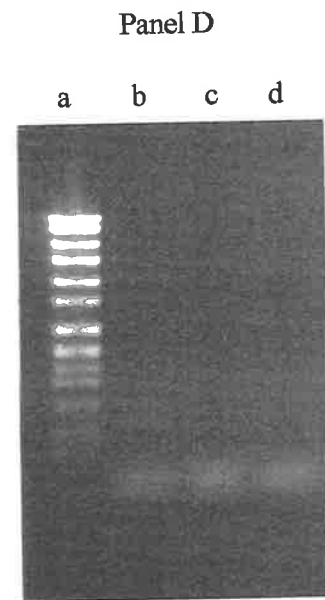
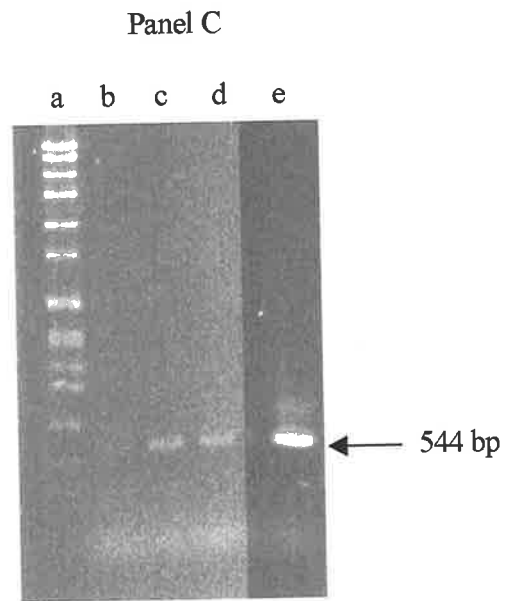
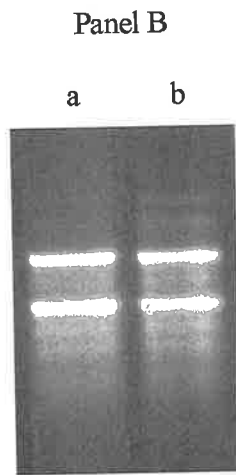
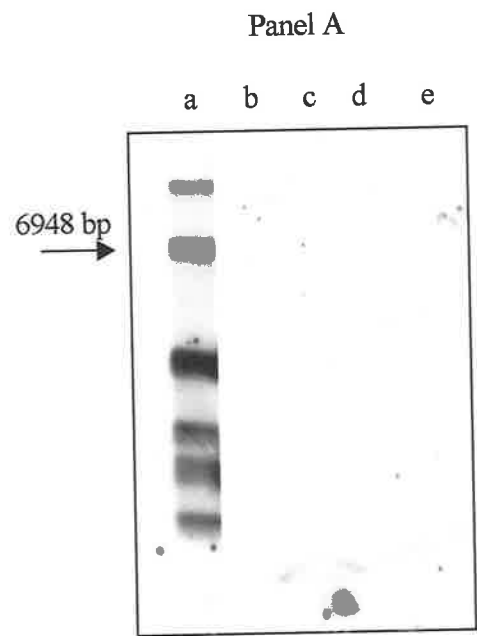
the last 412 bp of *xpsA*, the first 95 bp of *xpsB* and the 37 bp of intervening sequence was constructed by PCR amplification of *X. bovienii* chromosomal DNA with oligonucleotide pair P6034/P6035. Oligonucleotides P6034 and P6035 locations are noted in Figure 5.1. The positive control used was un-labelled PCR product generated by amplification of *X. bovienii* chromosomal DNA with oligonucleotide pair P6034/P6035. The unlabelled 544 bp product was diluted 1:5 out to 1:15625 and spotted onto nitrocellulose. A transcript was not detected after several attempts at Northern hybridisation analysis. Positive controls and the RNA marker were detected (Figure 5.4, panel A), and these results confirmed the technique used. The integrity of RNA samples post bacterial cell extraction was confirmed by electrophoresis in RNase free formamide agarose gels (Figure 5.4 panel B).

Thus, failure to detect may reflect concentration of the transcript. In order to confirm a transcript encoding *xpsABC* is produced by cultures, reverse transcription-PCR (RT-PCR) (see section 2.18.4.6) was used to determine if the *xpsABC* mRNA transcript was present in O/N *X. bovienii* cultures. A 544 bp product was observed when cDNA was amplified using oligonucleotide pair P6034/P6035 (Figure 5.4, panel C), confirming the presence of at least part of the *xpsABC* transcript. RNA samples not incubated with reverse transcriptase did not produce a PCR product, confirming the cDNA based PCR product was not amplified from contaminating chromosomal DNA (Figure 5.4, panel D).

Overall these results suggest that whilst the Northern hybridisation technique and all control experiments are working, there are other factors determining detection of *xpsABC* mRNA transcripts. The DIG-labelled DNA probe did not hybridise to mRNA extracted from *X. bovienii*. Positive control experiments determined RNA integrity, and the presence of the mRNA transcript by RT-PCR. Reasons for not detecting an mRNA transcript could be: (1) the DNA probe was less sensitive than an RNA probe for Northern hybridisation analysis; (2) extremely low levels of *xpsABC* mRNA; (3) the large size of the *xpsABC* mRNA transcript. If *xpsABC* was organized as an operon the mRNA transcript would be at least 16 kb in length. As *xpsC* is incomplete, the minimum nucleotide sequence required to complete the XpsC module is 2 kb. The RNA markers used for this experiment were the largest available, and by extrapolation of the RNA markers and probed mRNA the approximate transcript size may have been determined. If the *xpsABC* operon is extremely large, and this is usually the case for this family of genes, separation of the mRNA transcripts on a formaldehyde agarose gel may not have been efficient.

Figure 5.4 Description of figures.

- Panel A** Lanes:
[a], RNA Molecular Weight marker I (see section 2.18.4.2). Sizes are 6948, 4742, 2661, 1821 and 1517 bp;
[b]-[e] quadruplicate RNA samples extracted from *X. bovienii* and probed with a 544 bp DIG-labelled PCR product generated by amplification of *X. bovienii* chromosomal DNA with oligonucleotides P6034/P6035.
- Panel A1** Positive control. Unlabelled 544 bp PCR product generated by amplification of *X. bovienii* chromosomal DNA with oligonucleotides P6034/P6035 diluted 1:5 out to 1:15625.
- Panel B** Lanes: [a] and [b], duplicate RNA samples extracted from *X. bovienii*.
- Panel C** Lanes:
[a], SPP1 markers are *Bacillus subtilis* phage DNA digested with *EcoRI*;
[b], RT-PCR negative control containing no nucleic acid;
[c, d], duplicate samples of 544 bp PCR product from amplification of cDNA with oligonucleotides P6034/P6035;
[e], 544 bp PCR product from amplification of chromosomal DNA with oligonucleotides P6034/P6035 (positive control).
- Panel D** RT-PCR negative controls.
Lanes: [a], SPP1 markers are *Bacillus subtilis* phage DNA digested with *EcoRI*;
[b], [c] and [d]; triplicate samples of RNA not treated with reverse transcriptase. Absence of the cDNA based PCR product confirms the Panel C PCR product was not amplified from contaminating chromosomal DNA.



5.2.2 Analysis of DNA translation products

5.2.2.1 Comparison of partial ORF *xpsD* to sequences contained within protein databases

The C-terminal 217 amino acid sequence from *xpsD* was compared with peptide sequences present in the Genpept, Swissprot and Pir protein data bases using BLAST® (Basic Local Alignment Search Tool) algorithms (Altschul *et al.*, 1990). The partial C-terminal *xpsD* polypeptide sequence revealed significant similarity to ATP-binding cassette (ABC) transport proteins involved in the secretion of specific bioactive peptides (Table 5.2). Particularly strong similarity was found to PvdE (*P. aeruginosa*) [75% similarity and 53% identity over 158 amino acids] and SyrD (*P. syringae*) [64% similarity and 43% identity over 174 amino acids].

The CLUSTALX multiple alignment program was used to generate protein sequence alignments of XpsD, PvdE and SyrD C-terminal regions (Figure 5.5). Significant structural features of ABC transporters include the Walker A motif, Walker B motif, linker peptide and an invariant histidine residue (Fath & Kolter, 1993). Each of these was located in XpsD, PvdE and SyrD amino acid sequences (Figure 5.5). The Walker A and Walker B motifs are ATP-hydrolysing domains hypothesised to constitute a nucleotide binding fold. The Walker A motif has been suggested to be crucial for the binding of the β - and γ - phosphates of nucleotides by the invariant lysine residue. The conserved aspartate residue in Walker B is thought to play a role in liganding the Mg^{2+} ion that accompanies the nucleotide at Walker A. The linker peptide and invariant histidine residue are essential for the transport function of the protein (Schneider & Sabine, 1998).

The *P. aeruginosa pvdE* ORF is 1647 bp in length, whilst the *P. syringae syrD* ORF is 1701 bp. Therefore, it is likely that approximately 1000 bp 5' to the partial *xpsD* sequence remains to be sequenced. As the gene sequence for *xpsD* is incomplete no further analysis of this region was undertaken.

Table 5.2 Summary BLASTX 2.1.1 analysis of the 654 nucleotide translated *xpsD* sequence. All alignments are gapped.

Subject Organism	Subject Amino Acids Analysed	Similarity (%)	Identity (%)
<i>Pseudomonas aeruginosa</i> , pyoverdine synthetase E (amino acids = 548) Accession Number S54001	357-541	76 (143/185)	55 (103/185)
<i>Pseudomonas syringae</i> , ATP-binding protein SyrD (amino acids = 566) Accession Number M97223	365-553	69 (133/189)	52 (100/189)
<i>Campylobacter jejuni</i> , probable ABC transporter (amino acids = 543) Accession Number A81254	335-534	66 (136/203)	43 (88/203)
<i>E. coli</i> , hypothetical ABC transporter ATP-binding protein YojI (amino acids = 547) Accession Number P33941	341-536	65 (131/199)	43 (86/199)
<i>Thermotoga maritima</i> , ABC transporter, ATP-binding protein (amino acids = 577) Accession Number C72275	356-562	50 (107/210)	29 (61/210)

```

XpsD ----- 120
PvdE VLLSFGGLCLLALVSSIVSDIGTSYVVGQHI IANVRKELGEKVLSAPIEQIERYRTHRLIP
SyrD SLFWFVGLSVVALLFRNGASLFPAYASMRIMTRLRIALCRKILGTPLLEVDRRGAPNVL

XpsD ----- 180
PvdE VLTHDIDTISDFSFSFTPLAIALTITFGCLGYLAYLSVPMFLLTVVAIVIGTAAQYLARS
SyrD LLTSDIPQLNATLLIMPTILVESAVFLEFGIAYLAYLSWVVFAITISLMILGVAMYLLFFM

XpsD ----- 240
PvdE RGFKGFYAARDLEDELQKHHTAIASGAKELRIHRP-SLSHAHGRISSETANNIRDHLISSI
SyrD GGMKFTHKVRDEFTAFNEYTHALVFLGKELKLNIGIRRRWFSRSIQESSVRVAKYNYIER

XpsD ----- 300
PvdE NIFILAKTFGSMLEFFVIGLALTLOAYWPSSNPAAITGFVMVLLYMKGPLEQVVTILPIV
SyrD LWFTAENVGQLTSLVGLLFAAPMFAVIDAKTMSASVLAVLYIMGPLVMLVLSAMPML

XpsD -----IVHHYTTDKEK-----R 360
PvdE SRAQVAFQVAELSERFSSPEPHLLLSEQEAP-----DKTVDSLELRDVRYSPPAVEGSE
SyrD AQGRIACTRLADFGFSINEPHPEPETSADADNVLLLDHKKSWGSIQLKNVHMNYKDPQSSS

Walker A Motif
XpsD QFMLGPLSLKISQGEIVFIVGCNGSGKTTLAMMLVGLFEQESGSIWLNQVMDASNNVHY 420
PvdE PFHLGPINLRIAQGDIVFIVGENGCCGTTLIKLLLGLYRQPSGEILLNGEPVSAETRDDY
SyrD GFALGPIDLTIHSGELVYIVGCNGCGKSTLAKVFCGLYIPQEGQLLLDGAAVTDDSRGDY
* ***:.* * .*:::*** **.*:* * : :*: :.*: *:* : ... .*

Linker
XpsD RQFFSAVFSNYHLFDQLLN---TGTDVTEKATHYIQALNMGHKVKI IDGKFS--TTELSAG 480
PvdE RQLFSTIFADYYLFDLLVQ---GKQASLQATQYLQRL EIAHKVSVMDGNFS--TTDLSTG
SyrD RDLFSAVFSDFHLFNRLIGPDEKEHPSTDQAQTYLSTLGLEDKVKIEGLGYSTTTLSYG
*:***:***:***: * : :* *:. * : .***: . :* ** ** *

Peptide Walker B Motif Invariant Histidine
XpsD QRKRLALVAAYLEDRELYLDEWAADQDPVFKRLFYTELLPELRSRGKTVIVISHDNAYF 540
PvdE QRKRLALINAWLEERPVLVDEWAADQDPAFRRVYFTELLPDLKRQGTIIIVISHDDRYF
SyrD QQRLALVCAAYLEDREIYLLDEWAADQDPPFKRFFYEELLPDLKRRGKTIILITHDDQYF
*:*****: *:*:*: : :***** *:*.* ** ***:*: :***:***: **

XpsD DIAERVIKLEDGNIKEINNHSSETITELK 569
PvdE EMADQLIRLSAGKVVKETETA-----
SyrD QLADRIIKLADGCIVSDVKCAVEGKRA--
*:***:***: * : . : :

```

Figure 5.5 CLUSTALX alignment of the amino acid sequence from *X. bovienii* XpsD with the amino acid sequence of ABC transport proteins PvdE (*P. aeruginosa*, accession number U07359) and SyrD (*P. syringae*, accession number M97223). Amino acid numbers are noted down the right hand side of the page. ATP binding cassette (ABC) transport protein motifs are highlighted and conserved residues are noted in bold type.

5.2.2.2 Comparison of ORF XpsA, XpsB and XpsC polypeptides to sequences contained within protein databases

The 1089, 3316 and 396 amino acid sequences from XpsA, XpsB and XpsC respectively were individually compared with peptide sequences in the Genpept, Swissprot and Pir protein data bases using BLAST® (Basic Local Alignment Search Tool) algorithms (Altschul *et al.*, 1990). Each polypeptide showed significant homology to a family of enzymes known as non-ribosomal peptide synthetases (NRPS) (Tables 5.3, 5.4 and 5.5). (See sections 1.5.3.2.2 and 4.3 for a brief revision of these compounds). XpsA and XpsB displayed most sequence identity, over approximately 1000 amino acids, to NRPS isolated from *Nostoc* spp. (NosA) [both XpsA and XpsB ranged between 52-57%] and *P. syringae* (SyrE) [42-63% and 53-64% respectively]. XpsC displayed most sequence identity (over approximately 350 amino acids) to *P. syringae* (SyrE) [40-70%] and the NRPS from *Nostoc* spp. (NosD) [65-67%].

The most notable features of the BLASTX analysis for polypeptides XpsA, XpsB and XpsC were the presence of repeated regions of identity to the subject amino acid sequence. This observation reflects some important features unique to NRPS.

NRSPs are multifunctional with a modular structural organisation thought to link amino acid residues according to the thiotemplate mechanism (Kleinkauf & von Döhren, 1990). The thiotemplate multienzyme mechanism includes the activation of the constituent residues as adenylates on the enzymatic template, the acylation of specific template thiol groups, epimerization or *N*-methylation at this thioester stage, and polymerisation in a sequence directed by the multienzyme structure with the aid of 4'-phosphopantetheine as a cofactor. Cyclisation or terminal modification reactions are also possible (Kleinkauf & von Döhren, 1990). The thiotemplate mechanism is similar to both fatty acid and polyketide synthesis (Marahiel, 1992) (Stachelhaus & Marahiel, 1995) (see Chapter 1, Figure 1.3).

The primary amino acid composition of the peptide products is determined by the amino acid activating modules located on the peptide synthetase complex. Each module selectively binds, activates and condenses amino acids in an ordered manner. Substrate recognition and activation occurs by reaction with ATP within the adenylation domain of each module. Each module may contain a number of different domains involved in a range of processes required by the thiotemplate mechanism. The minimum module consists of a condensation,

Table 5.3 BLASTX 2.1.1 analysis of the 1089 amino acid XpsA sequence. All alignments are gapped.

Subject Organism	Subject Amino Acids Analysed	Similarity (%)	Identity (%)
<i>Nostoc</i> sp. GSV224, NosA, nostopeptolide biosynthetic protein (amino acids = 4379) Accession Number AF204805	1099-2174	57 (635/1109)	41 (455/1109)
	9-1082	55 (620/1110)	37 (420/1110)
	3282-4332	53 (590/1091)	36 (397/1091)
	2187-3260	52 (591/1113)	36 (404/1113)
<i>Pseudomonas syringae</i> pv. <i>syringae</i> , syringomycin synthetase (amino acids = 9376) Accession Number AFO47828	3-977	57 (578/998)	41 (416/998)
	1072-2065	57 (598/1027)	42 (435/1027)
	3252-4252	54 (577/1046)	39 (410/1046)
	5332-6380	52 (583/1092)	35 (390/1092)
	2165-3152	55 (585/1035)	38 (403/1035)
	4266-5314	55 (601/1081)	36 (395/1081)
	6381-7459	50 (564/1109)	34 (381/1109)
	7534-8519	53 (563/1032)	35 (371/1032)
	8548-9005	42 (210/488)	23 (115/488)
8986-9076	63 (58/91)	39 (36/91)	
<i>Pseudomonas aeruginosa</i> , probable non-ribosomal peptide synthetase (amino acids = 5149) Accession Number AE004667	52-1078	54 (591/1064)	39 (421/1064)
	2586-3601	54 (586/1063)	38 (407/1063)
	4118-5113	50 (534/1054)	33 (350/1054)
	1672-2557	49 (471/938)	33 (315/938)
	3632-3817	39 (76/188)	27 (52/188)
	1101-1276	38 (71/183)	26 (48/183)
<i>Microcystis aeruginosa</i> , ^a MycC, (amino acids = 1290) Accession Number AB019578	10-1054	55 (607/1090)	36 (399/1090)
<i>Brevibacillus brevis</i> , tyrocidine synthetase 3 (TycC) (amino acids = 6486) Accession Number AF004835	1098-2069	56 (571/1014)	37 (376/1014)
	2088-3111	53 (583/1080)	34 (372/1080)
	5240-6233	51 (547/1047)	35 (376/1047)
	3161-4155	52 (55/1041)	34 (363/1041)
	4166-5190	53 (570/1069)	33 (354/1069)
	11-1046	52 (575/1080)	32 (349/1080)

^a One of three peptide synthetase genes from an operon encoding microcystin

Table 5.4 BLASTX 2.1.1 analysis of the 3316 amino acid XpsB sequence. All alignments are gapped.

Subject Organism	Subject Amino Acids Analysed	Similarity (%)	Identity (%)
<i>Pseudomonas syringae</i> pv. <i>syringae</i> , syringomycin synthetase (amino acids = 9376) Accession Number AF047828	5314-8526	63 (2077/3278)	48 (1577/3278)
	4260-7437	58 (1941/3275)	42 (1398/3275)
	1056-4244	56 (1899/3294)	41 (1373/3294)
	4-3183	57 (1867/3266)	41 (1340/3266)
	3232-6382	55 (1849/3290)	39 (1302/3290)
	2125-5314	53 (1804/3366)	36 (1220/3366)
	6361-9026	53 (1497/2784)	38 (1060/2784)
	12-2096	58 (1251/2127)	42 (910/2127)
	7462-9027	55 (910/1629)	39 (647/1629)
	8985-9223	45 (111/245)	28 (69/245)
9010-9083	64 (48/74)	43 (32/74)	
8986-9083	55 (55/98)	39 (39/98)	
<i>Nostoc</i> sp. GSV224, NosA, nostopeptolide biosynthetic protein (amino acids = 4379) Accession Number AF04805	1053-4355	57 (1984/3414)	40 (1393/3414)
	8-3267	55 (1888/3380)	38 (1292/3380)
	10-2194	52 (1206/2289)	35 (802/2289)
<i>Nostoc</i> sp. GSV224, NosC, nostopeptolide biosynthetic protein (amino acids = 3317) Accession Number AF204805	70-3296	56 (1920/3338)	40 (1363/3338)
	1102-3293	60 (1359/2229)	44 (991/2229)
	66-2255	55 (1275/2288)	38 (882/2288)
	2203-3316	60 (689/1135)	43 (496/1135)
<i>Anabaena</i> sp. 90, non-ribosomal peptide synthetase (amino acids = 5060) Accession Number AJ269505	2-3097	56 (1831/3186)	40 (1294/3186)
	1040-3097	61 (1287/2079)	45 (945/2079)
	3-2141	56 (1271/2228)	39 (883/2228)
	3444-4504	60 (664/1095)	45 (497/1095)
	3589-4585	59 (620/1037)	44 (458/1037)
	50-1069	52 (566/1066)	35 (375/1066)
	3444-4596	48 (621/1250)	31 (399/1250)
	4906-5038	62 (89/142)	47 (67/142)
	3444-3575	65 (88/133)	45 (61/133)
	4906-5052	58 (94/159)	40 (64/159)
4906-5038	63 (90/142)	40 (57/142)	

Table 5.5 BLASTX 2.1.1 analysis of the 396 amino acid XpsC sequence. All alignments are gapped.

Subject Organism	Subject Amino Acids Analysed	Similarity (%)	Identity (%)
<i>Pseudomonas syringae</i> pv. <i>syringae</i> , syringomycin synthetase (amino acids = 9376) Accession Number AF047828	5300-5679	69 (267/384)	54 (209/384)
	4262-4613	70 (252/355)	56 (202/355)
	8527-8897	67 (253/371)	52 (196/371)
	6386-6737	69 (245/352)	54 (192/352)
	1056-1372	40 (141/349)	24 (84/349)
	2121-2413	41 (129/308)	23 (71/308)
	3208-3500	41 (130/310)	22 (70/310)
	12-284	36 (106/284)	19 (56/284)
	7535-7828	38 (126/322)	20 (67/322)
<i>Nostoc</i> sp. GSV224, NosD (amino acids = 2450) Accession Number AF204805	4-354	67 (242/353)	50 (180/353)
	1048-1426	65 (249/382)	47 (180/382)
<i>Lysobacter</i> sp., lysobactin synthetase (amino acids = 1575) Accession Number X96558	1028-1379	67 (242/357)	53 (191/357)
	1-312	66 (210/315)	53 (167/315)
<i>Nostoc</i> sp. GSV224, NosC (amino acids = 3317) Accession Number AF204805	2219-2595	64 (249/380)	48 (185/380)
	1118-1508	61 (244/394)	46 (184/394)
	67-422	66 (239/358)	48 (174/358)
<i>Anabaena</i> sp. 90, peptide synthetase (amino acids = 5060) Accession Number AJ269505	2156-2512	66 (241/360)	50 (181/360)
	1054-1431	62 (242/381)	47 (182/381)
	6-364	64 (235/361)	46 (168/361)
	3588-3939	64 (234/356)	48 (174/356)

adenylation and thiolation domain (Konz & Marahiel, 1999) (Challis *et al.*, 2000). Each domain present within a module contains a number of motifs with a specific function that are referred to as core sequences. Table 5.6 outlines the types of domains a module may encode and the core consensus sequence contained within the domain.

5.2.3 Organisation of the XpsA, XpsB and XpsC polypeptide modules and domains

XpsA encodes one module (XpsA M1) containing a condensation, adenylation and thiolation domain. XpsB encodes three modules; XpsB M1, XpsB M2 and XpsB M3. Each of the XpsB modules contains a condensation, adenylation and thiolation domain. XpsC module XpsC M1 is incomplete and only the 5' condensation domain can be identified (refer to Figure 5.1). Figure 5.6 outlines the location of each module and domain for *xpsABC*. Importantly, a thioesterase motif (GxSxG) was not identified confirming more 3' nucleotide sequence is required as this motif is generally found at the C terminal end of the last module in a gene sequence.

5.2.3.1 Alignment of XpsA, XpsB and XpsC domain core sequences with the published core consensus sequence

The core sequence from each domain was aligned with core consensus sequences (Konz & Marahiel, 1999) to determine the level of identity. The adenylation domain core sequences (A1 – A10), show a high level of identity to the published consensus sequence. Notable exceptions are;

1. The *X. bovienii* adenylation domain A2 sequence has a gap when compared to a leucine at the eighth amino acid of the A2 consensus sequence.
2. The adenylation domain A6 consensus sequence encodes a leucine at the third amino acid position, whilst all observed *X. bovienii* sequences encode an isoleucine.

X. bovienii condensation domain core sequences showed an acceptable level of identity when compared to the published consensus sequences. The most critical motif is likely to be C3 (MHHxISDG[WV]S) as this contains the histidine residues involved in the catalytic reaction (Marahiel *et al.*, 1997). XpsA M1 C3 is missing the first histidine, but has the second vital

Table 5.6 A summary of the core motifs from catalytic non-ribosomal peptide synthetase (NRPS) domains. The single letter amino acid code is used for core sequences; alternative amino acids for a particular position are shown in parentheses; x, any amino acid; numbers indicate the spacing between conserved residues.

This table is reproduced from (Konz & Marahiel, 1999).

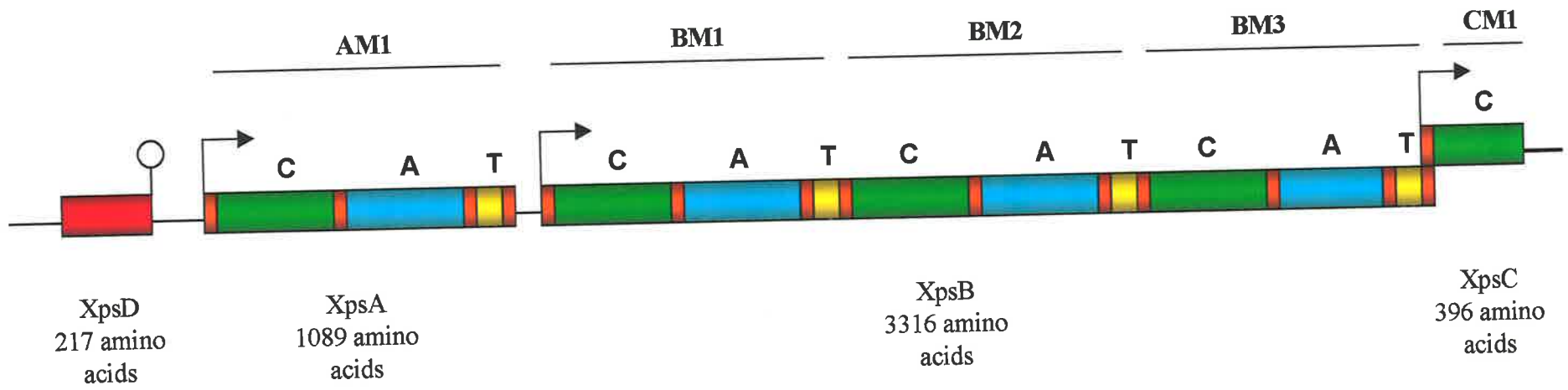
Domain	Core	Consensus sequence*
Adenylation	A1	L(TS)Y _x EL
	A2	LKAG _x AYL(VL)P(LI)D
	A3	LAY _{xx} YTSG(ST)TG _x PKG
	A4	FD _x S
	A5	N _x YGPTE
	A6	GEL _x I _x G _x G(VL)ARGYL
	A7	Y(RK)TGDL
	A8	GR _x D _x QVKIRG _x RIELGEIE
	A9	LP _x YM(IV)P
	A10	NGK(VL)DR
Thiolation	T	D _x FF _{xx} LGG(HD)S(LI)
Condensation	C1	S _x AQ _x R(LM)(WY)X _I
	C2	RHE _x LRT _x F
	C3	MHH _x ISDG(WV)S
	C4	Y _x D(FY)AVW
	C5	(IV)G _x FVNT(QL)X _r
	C6	(HN)QD(YV)PFE
	C7	RD _x SRNPL
Heterocyclisation	Z1	FPL(TS) _{xx} Q _x AY _{xx} GR
	Z2	RH _x (IM)L(PAL) _x (ND)G _x Q
	C3	(DNR) _{4x} D _{xx} S
	Z3	(LI)P _{xx} (PAL) _x (LPF)P
	Z4	(TS)(PA) _{3x} (LAF) _{6x} (IVT)L _{xx} W
	Z5	(GA)(DQN)FT
	Z6	P(IV)VF(TA)S _x L
Z7	QV _x (LI)D _x (QH) ₁₁ X _w (DYF)	
N-methylation	M1	VL(DE)G _x G _x G
	M2	NELS _x YRY _x AV
	M3	VE _x S _x ARQ _x G _x LD

Table 5.6. continued

Epimerization	E1	PIQ _x WF
	E2	HH _x ISDG(WV)S
	E3	D _x LL _x A _x G
	E4	EGHGRE
	E5	RTV _x GWFT _{xx} YP(YV)PFE
	E6	P _{xx} G _x GYG
	E7	FNYLG(QR)
Thioesterase	Te	G(HY)S _x G
Reductase	R1	V(LF)(LV)TG(AV)(TN)G(YF)LG
	R2	V3 _x VRA
	R3	GDL
	R4	VYPY _{xx} LR _x (PL)NV _{xx} T
	R5	GY _{xx} SKW _{xx} E
	R6	RPG
	R7	LE _{xx} (VI)GFL _{xx} P

Figure 5.6 A schematic representation of the *X. bovienii* putative peptide synthetase region. Right facing filled arrows represent the ATG position of *xpsA*, *xpsB* and *xpsC*. The condensation (C), adenylation (A) and thiolation (T) domains of putative peptide synthetases *xpsA*, *xpsB* and *xpsC* are highlighted in green, blue and yellow respectively. Each module consists of a C, A and T domain and module names noted at the top of the diagram. The naming convention for each module is as follows; [AM1], XpsA module 1; [BM1], XpsB module 1; [BM2], XpsB module 2; [BM3] XpsB module 3 and [CM1], XpsC module 1. Refer to Table 5.6 for the core consensus sequences found in each domain. The putative ABC transport gene *xpsD* is highlighted in red and the potential termination loop noted.

Refer to Figure 5.1 for the *xpsD*, *xpsA*, *xpsB* and *xpsC* nucleotide sequence.



histidine residue (Marahiel *et al.*, 1997) and therefore should still be active. The condensation domain C7 motif consensus sequence (RDxSRNPL) is significantly different to those found within *X. bovienii* sequence where only the 3' leucine is conserved in all modules except XpsA M1.

All thiolation domains identified in *X. bovienii* sequence have a gap at the third and sixth amino acid when compared to the published consensus sequence. Table 5.7 shows alignments of the condensation and thiolation core sequences, whilst Table 5.8 shows alignments of the adenylation core consensus sequence with that found within the *X. bovienii* XpsABC sequence. Differences between the consensus and observed the sequences are highlighted.

No further analysis of *xpsC* was undertaken as this gene sequence is incomplete.

5.2.4. Predictive, structure-based modelling of amino acid recognition by the XpsA and XpsB NRPS A domains

Over the past decade substantial progress has been made in the discovery and sequence analysis of NRPS genes from bacteria and fungi, see (Konz & Marahiel, 1999) for a comprehensive list. Many of the NRPSs have an unknown structure and function, however they share characteristic signature sequences (see section 5.2.3.2).

Specificity of the amino acids incorporated into the growing peptide chain is mostly controlled at the adenylation/pantetheinylation step (von Döhren *et al.*, 1997; Belshaw *et al.*, 1999). Recently, crystal structure analysis has been used to identify the substrate-binding pocket of the phenylalanine adenylation domain of the gramicidin S synthetase (GrsA) from *Bacillus brevis* (Conti *et al.*, 1997). The eight amino acids lining the substrate-binding pocket mediate amino acid specificity. The authors concluded that because NRPS adenylation domains share a high degree of sequence identity of between 30 – 60% (Conti *et al.*, 1997), the GrsA structure represents a structural model that all NRPS A domains could fit.

Based on the sequence information derived from crystal structure analysis of GrsA, Challis (Challis *et al.*, 2000) developed a method to predict the amino acids activated by individual adenylation domains directly from sequence data. The protein sequence of over 150 NRPS adenylation domains was aligned with the adenylation domain of GrsA to isolate the eight critical amino acid residues involved in substrate specificity and binding. Phylogenetic

Table 5.7 Alignment of the consensus condensation and thiolation domain core sequences (Konz & Marahiel, 1999) with those obtained from *X. bovienii* XpsABC modules. *X. bovienii* residues identical to the consensus sequence are highlighted in blue, residues which differ are highlighted in red. Residues represented by any amino acid are highlighted in black. The naming of each module is as that set out in Figure 5.6; [AM1], XpsA module 1; [BM1], XpsB module 1; [BM2], XpsB module 2; [BM3] XpsB module 3 and [CM1], XpsC module 1.

N/A = sequence data not available.

Condensation Domain C1				Condensation Domain C2					
		SxAQxR (LM) (WY) xL				RHExLRTxF			
AM1	SEAQSS	R	W	FQ	AM1	RHPMLRAS	F		
BM1	SWAQQR	L	W	FL	BM1	RHEILRTTI			
BM2	SWTQQR	L	W	FL	BM2	RHEILRTTI			
BM3	GPLQEG	I	L	FH	BM3	RHDILRS	AV		
CM1	SWAQQR	L	W	FL	CM1	RHEILRTTI			
Condensation Domain C3				Condensation Domain C4					
		MHHxISDG (WV) S				YxD (FY) AVW			
AM1	FDHLVVDG	W	S	AM1	YQD	Y	VSW		
BM1	QHIIISDG	W	S	BM1	YAD	Y	ALW		
BM2	QHIIISDG	W	S	BM2	YAD	Y	AVW		
BM3	HHHLVCDH	L	S	BM3	YRN	F	IAQ		
CM1	QHIIISDG	W	S	CM1	YAD	Y	ALW		
Condensation Domain C5				Condensation Domain C6					
		(IV) GxFVNT (QL) xxR				(HN)QD (YV) PFE			
AM1	V	GEFVNP	V	ALR	AM1	N	QR	Y	PFT
BM1	I	GFFVNT	L	LAR	BM1	H	QD	L	PFE
BM2	I	GFFANT	L	ALR	BM2	H	QD	L	PFE
BM3	L	GMFINT	L	PVR	BM3	H	EQ	T	PLA
CM1	L	GFFVNT	L	ALR	CM1	H	QD	L	PFE
Condensation Domain C7				Thiolation Domain					
		RDxSRNPL				DxxFFxxLGG (HD) S (LI)			
AM1	GAELRPF			AM1	DN-FF-ELGG	H	S	L	
BM1	DGLHHELF			BM1	DS-FF-ELGG	H	S	L	
BM2	AELSLNPL			BM2	DN-FF-ELGG	H	S	L	
BM3	AWEGIQIL			BM3	DN-FF-ELGG	N	S	L	
CM1	N/A			CM1	N/A				

N/A = sequence data not available

N/P = motif not present

Table 5.8 Alignment of the adenylation domain core sequences (Konz & Marahiel, 1999) with those obtained from *X. bovienii* XpsABC modules. *X. bovienii* residues identical to the consensus sequence are highlighted in blue, residues which differ are highlighted in red. Residues represented by any amino acid are highlighted in black. The naming of each module is as that set out in Figure 5.6; [AM1], XpsA module 1; [BM1], XpsB module 1; [BM2], XpsB module 2; [BM3] XpsB module 3 and [CM1], XpsC module 1.

N/A = sequence data not available.

<p style="text-align: center;">Adenylation Domain A1</p> <p style="text-align: center;">L (TS) YxEL</p> <p>AM1 L S YTEL</p> <p>BM1 L S YSEL</p> <p>BM2 L S YAEL</p> <p>BM3 L T YTEL</p> <p>CM1 N/A</p>	<p style="text-align: center;">Adenylation Domain A2</p> <p style="text-align: center;">LKAGxAYL (VL) P (LI) D</p> <p>AM1 LKAGAAY - V P L D</p> <p>BM1 LKAGASY - I P L D</p> <p>BM2 LKAGAGY - V P L D</p> <p>BM3 LKAGAGY - V P L D</p> <p>CM1 N/A</p>
<p style="text-align: center;">Adenylation Domain A3</p> <p style="text-align: center;">LAYxxYTSG (ST) TGXPKG</p> <p>AM1 LAYVLYTSG S TGLPKG</p> <p>BM1 LAYVLYTSG S TGLPKG</p> <p>BM2 LAYIIYTSG S TGLPKG</p> <p>BM3 LAYIIYTSG S TGLPKG</p> <p>CM1 N/A</p>	<p style="text-align: center;">Adenylation Domain A4</p> <p style="text-align: center;">FDxS</p> <p>AM1 FDVS</p> <p>BM1 FDNS</p> <p>BM2 FDTA</p> <p>BM3 FDTA</p> <p>CM1 N/A</p>
<p style="text-align: center;">Adenylation Domain A5</p> <p style="text-align: center;">NxYGPTE</p> <p>AM1 NLYGPTE</p> <p>BM1 NTYGPTE</p> <p>BM2 DTYGPTE</p> <p>BM3 DSYGPTE</p> <p>CM1 N/A</p>	<p style="text-align: center;">Adenylation Domain A6</p> <p style="text-align: center;">GELxIxGxG (VL) ARGYL</p> <p>AM1 GEIYIAGAG V ARGYL</p> <p>BM1 GEIHISGSG V ARGYL</p> <p>BM2 GEIYIGGAG V ARGYL</p> <p>BM3 GEIYIGGAG V ARGYL</p> <p>CM1 N/A</p>
<p style="text-align: center;">Adenylation Domain A7</p> <p style="text-align: center;">Y (RK) TGDL</p> <p>AM1 Y K TGDI</p> <p>BM1 Y K TGDL</p> <p>BM2 Y R TGDL</p> <p>BM3 Y R TGDL</p> <p>CM1 N/A</p>	<p style="text-align: center;">Adenylation Domain A8</p> <p style="text-align: center;">GRXDXQVKIRGXRIELGEIE</p> <p>AM1 GRNDFQVKIRGNRIELGEIE</p> <p>BM1 GRNDFQVKIRGFRIELGEIE</p> <p>BM2 GRNDFQVKIRGFRIELGEIE</p> <p>BM3 GRNDFQVKLRGFRIELGEIE</p> <p>CM1 N/A</p>
<p style="text-align: center;">Adenylation Domain A9</p> <p style="text-align: center;">LPxYM (IV) P</p> <p>AM1 LPDYM I P</p> <p>BM1 LADYM L P</p> <p>BM2 LAEYM L P</p> <p>BM3 LTEYM L P</p> <p>CM1 N/A</p>	<p style="text-align: center;">Adenylation Domain A10</p> <p style="text-align: center;">NGK (VL) DR</p> <p>AM1 NGK L DR</p> <p>BM1 NGK I DR</p> <p>BM2 NGK L DR</p> <p>BM3 SGK L DR</p> <p>CM1 N/A</p>

N/A = sequence data not available

relationships among these sets and the likely specificity determinants for polar and nonpolar amino acids were determined, with referral to the published biochemical data for NRPS. The binding specificity of more than 80% of known NRPS adenylation domains were correlated with more than 30 amino acid substrates. Similar analyses were performed by Stachelhaus (Stachelhaus *et al.*, 1999), however the method of Challis (Challis *et al.*, 2000) will be used for the purpose of this thesis. Reasons for this choice are;

1. Challis extended the analysis of Stachelhaus by including 33 amino acid substrates for which function of the adenylation domains had been assigned by either direct enzymatic assay or persuasive deduction. For each adenylation domain multiple protein sequences recognizing the same amino acid were required.
2. Challis constructed an extremely useful WWW site to assist with the assignment of a specific amino acid to the adenylation domains of new protein sequences (<http://raynam.chm.jhu.edu/~nrps/>).

5.2.4.1 Alignment of XpsA and XpsB module adenylation domains with the adenylation domain of GrsA

In conjunction with the Challis (Challis *et al.*, 2000) internet site (see section 5.2.4), the XpsA and XpsB adenylation domain amino acid sequences encompassing core sequences A3-A6 (see Figure 5.1) were aligned with that of GrsA using CLUSTALX. The eight critical amino acid residues in GrsA were identified and used as a template to determine the corresponding XpsA and XpsB module amino acid signature sequences. Figure 5.7 shows the CLUSTALX alignment of relevant regions of GrsA with each module from XpsA and XpsB, and highlights the critical amino acid residues.

5.2.4.2 BLAST analysis of the XpsA and XpsB adenylation domain signature sequences

Each of the adenylation domain signature sequences from XpsA and XpsB were analysed by BLAST analysis and compared to an assigned and unassigned database of adenylation domain signature sequences (Challis *et al.*, 2000). The assigned database allows comparison of unknown adenylation domain signature sequences to other signature sequences from NRPS for which the amino acid activated has been experimentally determined. The unassigned database compares the unknown adenylation domain signature sequence to other signature

Figure 5.7 CLUSTALX alignment of the adenylation domain core sequences A3 – A6 (see Figure 5.1 and Table 5.6) from the *Bacillus brevis* GrsA adenylation domain with the *X. bovienii* adenylation domain core sequences A3 – A6 from XpsA M1, XpsB M1, XpsB M2 and XpsB M3. The eight critical amino acid activation residues in GrsA were identified (Challis *et al.*, 2000) and used as a template to determine the corresponding amino acids for each *X. bovienii* module. Each of the eight amino acid residues are highlighted in blue, and the conserved glycine residue in red. The adenylation domain signature sequence for each module is indicated above each set of amino acid residue alignments. Each alignment has been edited to present the relevant features.

XpsA M1 adenylation domain signature sequence = DVWHLSLI

XpsA-M1 FDVSVWEFFLPLLAGTQLVMARPGGHKEALYLLEEIEARGITTLHFVPSMLQSFHILTPAGRCPSL
GrsA-M1 FDASVWEMFMALLTGASLYIILKDTINDFVKFEQYINQKEITVITLPP---TYVVHLDPE-RILSI
** * *
RQILCSGEALSYSLQQQCLAHFAHSELHNLYGPTAAIDVT
QTLITAGSATSPSLVNKWKVKVY---INAYGPTETTICAT
* ** *

XpsB M1 adenylation domain signature sequence = DNADAGTV

XpsB-M1 FDNSVAEIEFPTFAIGATVVLRPDHIKVPDTEFIFLQNGITVVDLP-TAFWHLWAQEISAGYSWP
GrsA-M1 FDASVWEMFMALLTGASLYIILKDTINDFVKFEQYINQKEITVITLPPITYVVHLDPERILS-----
** * *
PEQLRSVAAGGEKAEHRHLVTWLSSPGTQKCRWLNTYGPTETTIVNAT
---IQTLITAGSATSPSLVNKWK-----EKVYINAYGPTETTICAT
* ** * *

XpsB M2 adenylation domain signature sequence = DTSDTGTV

XpsB-M2 FDTAVSEIEFPTLSVGATLILRPAHIRIPDATFSHFLEQQAISVIDLPTAFWHQWVQEMKAGRSGFS
GrsA-M1 FDASVWEMFMALLTGASLYIILKDTINDFVKFEQYINQKEITVITLPPITYVVHLDPERILS-----
** * *
SHVRSVTVGGEKAEHRHFVTWQSMPEHRHCRWIDTYGPTETTIVSAT
--IQTLITAGSATSPSLVNKWK-----EKVYINAYGPTETTICAT
* ** * *

XpsB M3 adenylation domain signature sequence = DTSDTGSV

XpsB-M3 FDTAVSEIEFPTLAVGATLILRPAHIQVPDTEFDFLREQAISIIDLPTAFWHQWVQEMKAGRSGFS
GrsA-M1 FDASVWEMFMALLTGASLYIILKDTINDFVKFEQYINQKEITVITLPPITYVVHLDPERILS-----
** * *
SLLRSVTVGGEKAELRHLYLTWQSMPEHRNCRWIDSYGPTETTIVIT
---IQLITAGSATSPSLVNKWK-----EKVYINAYGPTETTICAT
* ** * *

sequences from NRPS where the amino acid activated, has been predicted, but not experimentally determined.

According to the assigned database, the amino acids most likely to be activated by XpsA M1, XpsB M1, XpsB M2 and XpsB M3 are serine, 6-*N*-hydroxylysine, glutamine and 6-*N*-hydroxylysine respectively. The unassigned database suggests the most likely amino acids activated by XpsA M1, XpsB M1, XpsB M2 and XpsB M3 are cysteine, lysine, glutamic acid and glutamic acid respectively. Table 5.9 summarises the amino acids that are potentially activated by each XpsA and XpsB module when compared to the assigned and unassigned database. Considering the assigned database is supported by experimental evidence, these results will form the basis of further analysis and discussion.

5.2.5 Hydrophobicity analysis and amino acid composition of *X. bovienii* XpsA M1, XpsB M1, XpsB M2, XpsB M3 and other serine activating domains

The assigned database predicts with the most certainty that *X. bovienii* XpsA M1 activates serine (see section 5.2.4.2). This module will be used as the basis for comparative studies between other modules within the *X. bovienii* peptide synthetase gene sequence and serine activating modules from other microorganisms.

5.2.5.1 Module hydrophobicity analysis

Analysis of the hydrophobicity of proteins has been routinely used to demonstrate structural relatedness. The amino acid sequence between the A1 adenylation domain core sequence and the thiolation domain motif was used in this analysis. Hydrophobicity indices were calculated using the program PROSIS and algorithms developed by Kyte and Doolittle (Kyte & Doolittle, 1982).

Hydropathy profiles of serine activating modules from *X. bovienii* XpsA M1, *P. syringae* SyrE M1 (AF047828), *P. aeruginosa* M1 (PAGP_287, unfinished genome database), *E. coli* EntF M1 (M60177) and *S. coelicolor* Cda M1 (AL035640) were aligned (Figure 5.8). Consistently high structural similarity was observed between each of the amino acid segments. Of all sequences analysed, Gram positive *S. coelicolor* showed the most significant differences. Furthermore the *S. coelicolor* amino acid sequence is 56 – 116 amino acids

Table 5.9 A summary of the amino acids potentially activated by each XpsA and XpsB module when the adenylation domain core signature sequence is compared to the assigned and unassigned database (Challis *et al.*, 2000). Under each *X. bovienii* module is a list of the three most related modules that have predicted the amino acid activated by the adenylation domain core signature sequence. A comparison of the assigned and unassigned database predictions is shown.

Abbreviations: [Motif], adenylation domain core signature sequence; [AA], amino acid predicted to be activated by the adenylation domain core signature sequence; [Ser], serine; [6haLys], 6-*N*-hydroxylysine; [Gln], glutamine; [Glu], glutamic acid; [Arg], arginine; [Asp], asparagine; [Cys], cystine; [Lys], lysine; [3hTyr], 3-hydroxytyrosine.

Assigned Database			Unassigned Database		
Module (Accession Number)	Motif	AA	Module (Accession Number)	Motif	AA
XpsA-M1	DVWHL SLI		XpsA-M1	DVWHL SLI	
SyrE-M2 (AAA85160.1)	DVWHL SLI	Ser	PchE-M? (AAC83656.1)	DLFN LSLI	Cys
NosA-M2 (AAF15891.2)	DVWHI SLI	Ser	PvsB-M2 (AAF40220.1)	DAWQ FGLI	Ser?
SyrE-M1 (AAA85160.1)	DLWHL SLI	Ser	Sc-M1 (3127852)	DLFN LSLI	Cys?
XpsB-M1	DNADAG TV		XpsB-M1	DNADAG TV	
MbtF-M1 (CAB08474.1)	DAQDAG CV	6haLys	Hyp1-M? (7476034)	DIEDV GTV	Lys
LchAA-M1 (CAA06323.1)	DAQDLG VV	Gln	Nrp1-M1 (CAA98937.1)	DIEDV GSV	Lys?
LicA-M1 (AAD04757.1)	DAQDLG VV	Gln	FxbC-M4 (AAC82550.1)	DTWDT GLV	Glu?
XpsB-M2	DTSDT GTV		XpsB-M2	DTSDT GTV	
LchAA-M1 (CAA06323.1)	DAQDLG VV	Gln	FxbC-M4 (AAC82550.1)	DTWDT GLV	Glu
LicA-M1 (AAD04757.1)	DAQDLG VV	Gln	Hyp1-M? (7476034)	DIEDV GTV	Lys
BacA-M4 (AAC06346.1)	DAKD IGVV	Glu	Nrp1-M1 (CAA98937.1)	DIEDV GSV	Lys
XpsB-M3	DTSDT GTV		XpsB-M3	DTSDT GTV	
MbtF-M1 (CAB08474.1)	DAQDAG CV	6haLys	FxbC-M4 (AAC82550.1)	DTWDT GLV	Glu
PvdD-M2 (unfinished genome)	DAEDI GAI	Arg	Nrp1-M1 (CAA98937.1)	DIEDV GSV	Lys?
SyrE-M8 (AAA85160.1)	DMKDL GMV	Asp	Van-M2 (CAB45052.1)	DTSK VAAI	3hTyr?

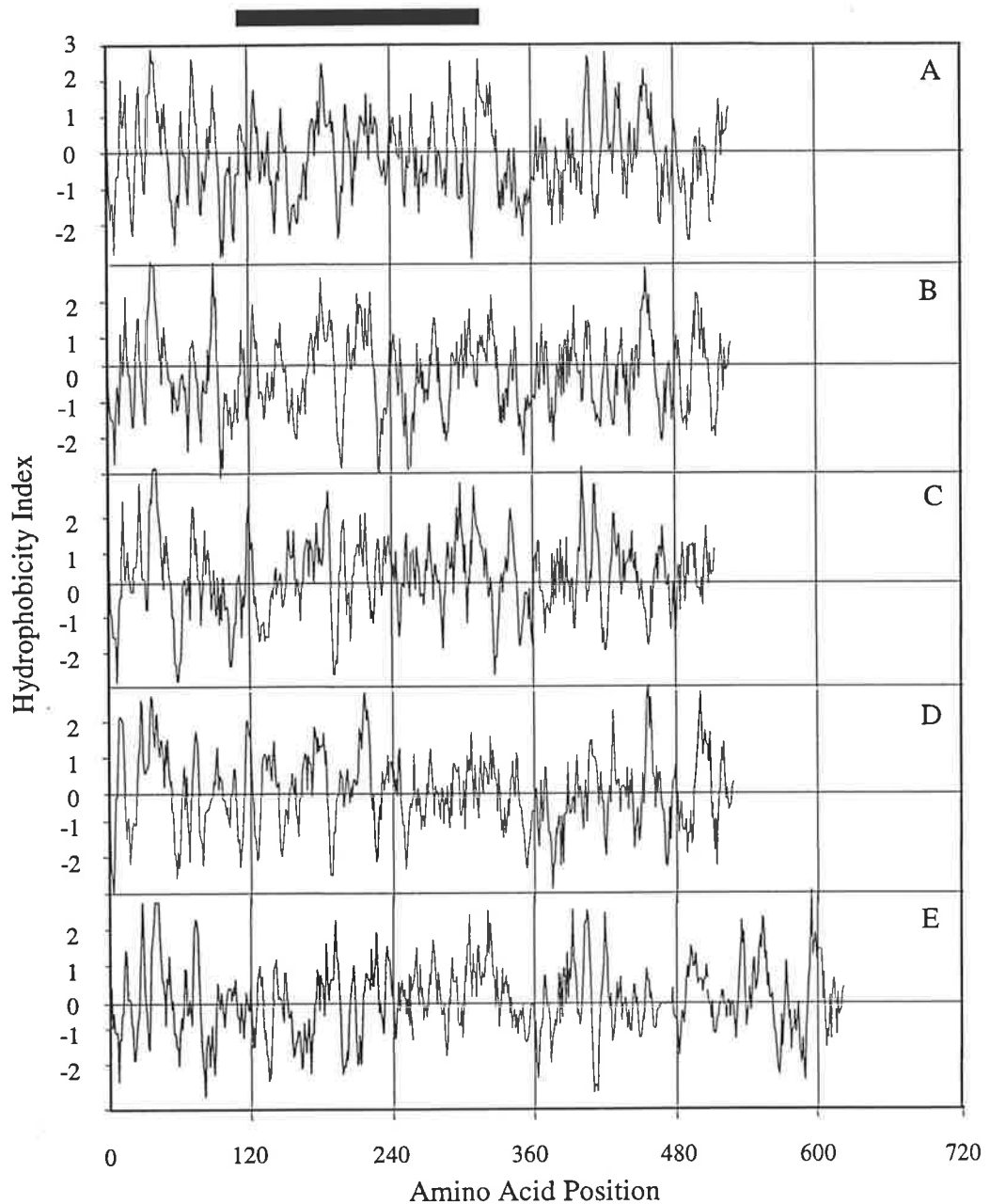


Figure 5.8

Aligned hydropathy profiles of XpsA and other selected serine activating modules from peptide synthetase genes. Hydrophobicity was calculated by the method of Kyte and Doolittle (1982) using a window span of 6 amino acid residues.

Hydrophobic domains are indicated by regions of the graph above the horizontal axis. Also shown is the region of critical residues which determine the amino acid activated by each module. The Genbank accession number and source organism are shown for each plot.

- A. *X. bovienii*, XpsA M1 (526 amino acids)
- B. *P. syringae*, SyrE M1 (AF047828) (572 amino acids)
- C. *P. aeruginosa* M1 (PAGP_287, unfinished genome database Genbank) (512 amino acids)
- D. *E. coli*, EntF M1 (M60177) (528 amino acids)
- E. *S. coelicolor*, Cda M1 (AL035640) (628 amino acids)

longer than the Gram negative sequences. Gram negative serine activation domain amino acid sequences typically show a 14 – 60 amino acid difference in length from Gram positive homologues.

When comparing the hydrophobicity indices of each module from the XpsAB region a remarkable level of structural similarity was consistently observed, even though each module is predicted to activate a different amino acid (except XpsB M1 and XpsB M3) (see section 5.2.4.2). Furthermore module segments selected for analysis were not significantly different in length at 7 – 10 amino acids (Figure 5.9).

5.2.5.2 Module amino acid composition analysis

An analysis of the amino acid composition of XpsA M1, XpsB M1, XpsB M2, XpsB M3 and other selected serine activating modules used for hydrophobicity analysis (see section 5.2.5.1) is shown in Table 5.9. The utilization of amino acids amongst modules isolated from the Gram negative bacterial origins was relatively conserved. For example leucine is the most common amino acid present in the Gram negative protein sequences analysed, comprising 9.94 – 13.47% of each sequence. Alanine was the next most commonly utilized amino acid at between 7.98 – 11.74%. In comparison, the Gram positive *S. coelicolor* module was rich in alanine (16.4%), glycine (13.05%), leucine and proline (9.55%). Whilst the Gram positive protein sequence is approximately 100 amino acids greater than the Gram negative sequences, there are no significant differences in amino acid usage. For all of the protein sequences examined the overall usage of residues with common chemical characteristics was conserved where; neutral polar>neutral nonpolar>acidic=basic.

5.2.6 Phylogenetic analysis of the *X. bovienii* NRPS operon

Based on crystal structure analysis of the GrsA adenylation domain, required for production of the NRPS gramicidin, eight critical amino acids required for adenylation domain substrate recognition have been identified [Conti, 1997 #330]. The eight critical amino acids are located between the adenylation domain A3 – A6 motifs. Challis (Challis *et al.*, 2000) used this region from the GrsA amino acid sequence as a recognition template to facilitate prediction of amino acids activated by other NRPS adenylation domains.

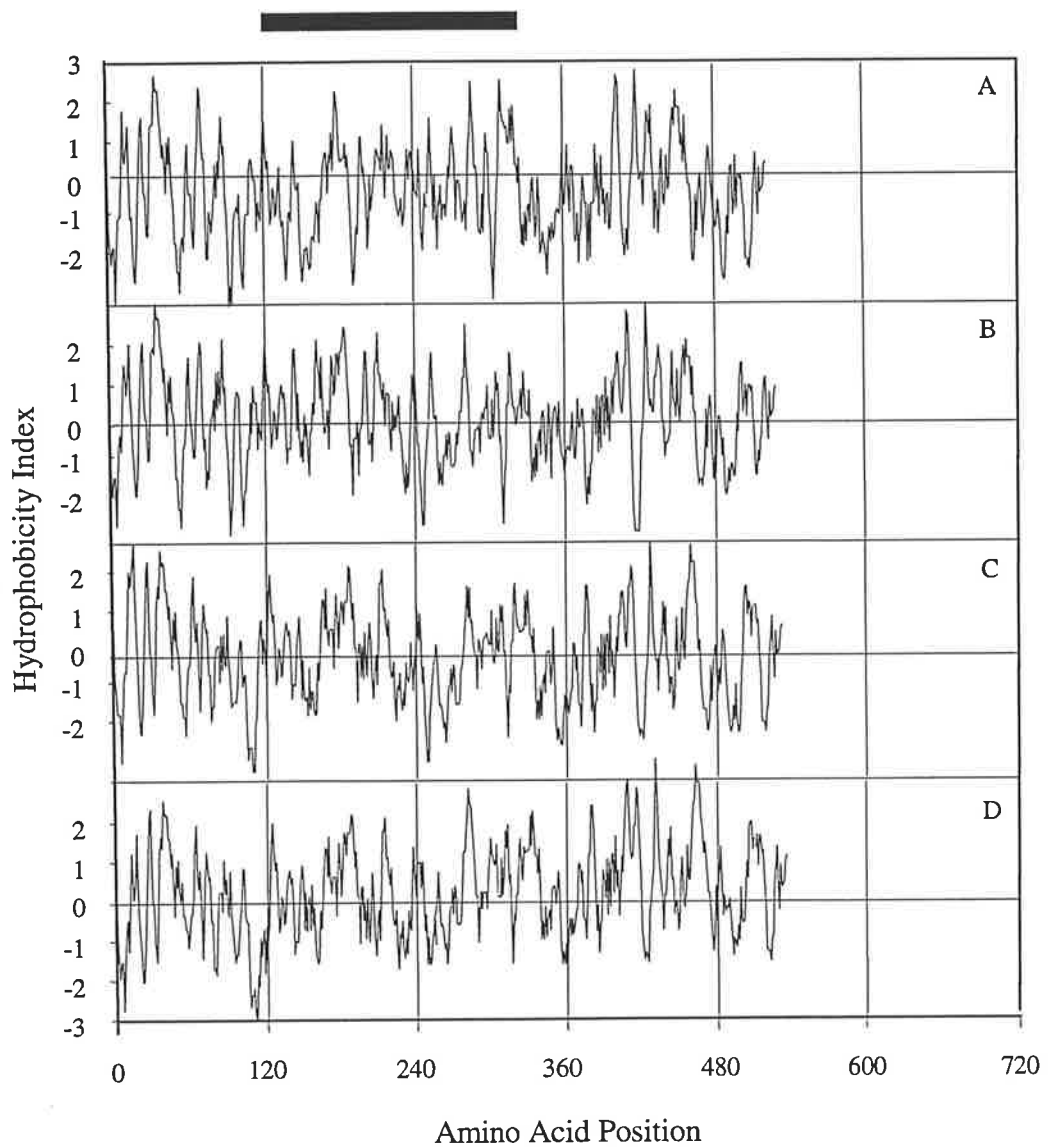


Figure 5.9

Aligned hydropathy profiles of XpsA and XpsB modules 1, 2 and 3. Hydrophobicity was calculated by the method of Kyte and Doolittle (1982) using a window span of 6 amino acid residues.

Hydrophobic domains are indicated by regions of the graph above the horizontal axis. Also shown is the region of critical residues which determine the amino acid activated by each module.

- | | |
|----|--|
| A. | <i>X. bovienii</i> , XpsA M1 (526 amino acids) |
| B. | <i>X. bovienii</i> , XpsB M1 (533 amino acids) |
| C. | <i>X. bovienii</i> , XpsB M2 (533 amino acids) |
| D. | <i>X. bovienii</i> , XpsB M3 (536 amino acids) |

Table 5.9 Comparison of the amino acid composition of *X. bovienii* XpsA and XpsB adenylation and thiolation module regions with other non-ribosomal peptide synthetase adenylation and thiolation module regions.

Amino Acid AA	XpsA M1		XpsB M1		XpsB M2		XpsB M3		AF047828		PAGP_287		M60177		AL035640	
	N	%	N	%	N	%	N	%	N	%	N	%	N	%	N	%
Ala (A)	42	7.98	45	8.44	46	8.63	49	9.14	55	10.43	60	11.71	62	11.74	103	16.4
Cys (C)	5	0.95	6	1.12	5	0.93	5	0.93	3	0.56	5	0.97	7	1.32	3	0.47
Asp (D)	32	6.08	29	5.44	27	5.06	32	5.97	34	6.45	28	5.46	30	5.68	37	5.89
Glu (E)	30	5.7	30	5.62	31	5.81	32	5.97	31	5.88	39	7.61	23	4.35	31	4.93
Phe (F)	14	2.66	18	3.37	19	3.56	15	2.79	12	2.27	11	2.14	19	3.59	14	2.22
Gly (G)	41	7.79	39	7.31	40	7.5	37	6.9	42	7.96	47	9.17	40	7.57	82	13.05
His (H)	19	3.61	15	2.81	19	3.56	13	2.42	17	3.22	11	2.14	11	2.08	13	2.07
Ile (I)	35	6.65	39	7.31	28	5.25	29	5.41	19	3.6	17	3.32	16	3.03	10	1.59
Lys (K)	14	2.66	14	2.62	12	2.25	11	2.05	12	2.27	13	2.53	11	2.08	5	0.79
Leu (L)	67	12.73	53	9.94	56	10.5	61	11.38	71	13.47	64	12.5	66	12.5	60	9.55
Met (M)	11	2.09	8	1.5	8	1.5	8	1.49	10	1.89	10	1.95	13	2.46	6	0.95
Asn (N)	17	3.23	22	4.12	14	2.62	14	2.61	16	3.03	16	3.12	10	1.89	5	0.79
Pro (P)	34	6.46	32	6	33	6.19	33	6.15	35	6.64	28	5.46	42	7.95	60	9.55
Gln (Q)	25	4.75	30	5.62	32	6	28	5.22	30	5.69	22	4.29	31	5.87	8	1.27
Arg (R)	31	5.89	28	5.25	30	5.62	35	6.52	33	6.26	33	6.44	28	5.3	51	8.12
Ser (S)	27	5.13	39	7.31	34	6.37	35	6.52	24	4.55	23	4.49	29	5.49	22	3.5
Thr (T)	26	4.94	28	5.25	34	6.37	39	7.27	20	3.79	13	2.53	29	5.49	46	7.32
Val (V)	31	5.89	34	6.37	41	7.69	35	6.52	42	7.96	45	8.78	39	7.38	50	7.96
Trp (W)	6	1.14	8	1.5	7	1.31	7	1.3	5	0.94	9	1.75	8	1.51	6	0.95
Tyr (Y)	19	3.61	16	3	17	3.18	18	3.35	16	3.03	18	3.51	14	2.65	16	2.54
															0	
Acidic	62	11.78	59	11.06	58	10.87	64	11.94	65	12.33	67	13.07	53	10.03	68	10.82
Basic	64	12.16	57	10.68	61	11.43	59	10.99	62	11.75	57	11.11	50	9.46	69	10.98
Neutral Polar	275	52.31	268	50.34	271	50.92	267	49.87	286	54.33	282	55.16	297	56.29	385	61.36
Neutral Nonpolar	125	23.75	149	27.92	143	26.78	146	27.2	114	21.59	106	20.66	128	24.22	106	16.84
Total	526	100	533	100	533	100	536	100	527	100	512	100	528	100	628	100

All data are derived from the sequences shown in Figures 5.9, 5.10 and from the Genbank database (Accession numbers are shown). Compositional analysis of an amino acid is determined as a percentage of the total number of amino acids per sequence. Acidic (D, E); Basic (H, K, R); Neutral Polar (A, F, G, I, L, M, P, V); Neutral Nonpolar (C, N, Q, S, T, W, Y).

Challis used phylogenetic studies to determine if there were correlations between the A3 – A6 domains of NRPS and the substrate they activated; where the substrate activated had been experimentally determined. This phylogenetic analysis was also repeated using only the eight critical binding pocket amino acids from 154 adenylation domains (Challis *et al.*, 2000). These phylogenetic results were used in designing a software program that predicts amino acid substrates activated by a given adenylation domain (see section 5.2.4).

The A3-A6 motif amino acid sequences, and the eight critical binding pocket amino acids, from the *X. bovienii* NRPS adenylation domains were used to construct phylogenetic trees, similar to Challis, to see how well these modules fit previous amino acid activation predictions (see section 5.2.4.1). The relevant *X. bovienii* NRPS sequences were added to the amino acid data files for the eight amino acid and A3 – A6 (180 - 200 amino acid) analyses and two phylogenetic trees constructed. The amino acid data files characterising other adenylation domains included in this analysis were kindly provided by the Challis research group. Distance matrices were calculated and trees constructed using the unweighted pair group method (UWPGMA).

The 180 – 200 amino acid A3-A6 motifs clustered predominately along genus lines (Figure 5.10). XpsA M1 clustered with three other serine activating domains, whilst XpsB M1, XpsB M2 and XpsB M3 clustered together. XpsB M2 and XpsB M3 were predicted to be the most closely related, and this contrasts strongly with amino acid activation predictions (see section 5.2.4.1) that suggest XpsB M1 and XpsB M3 are involved in the activation of 6-*N*-hydroxylysine

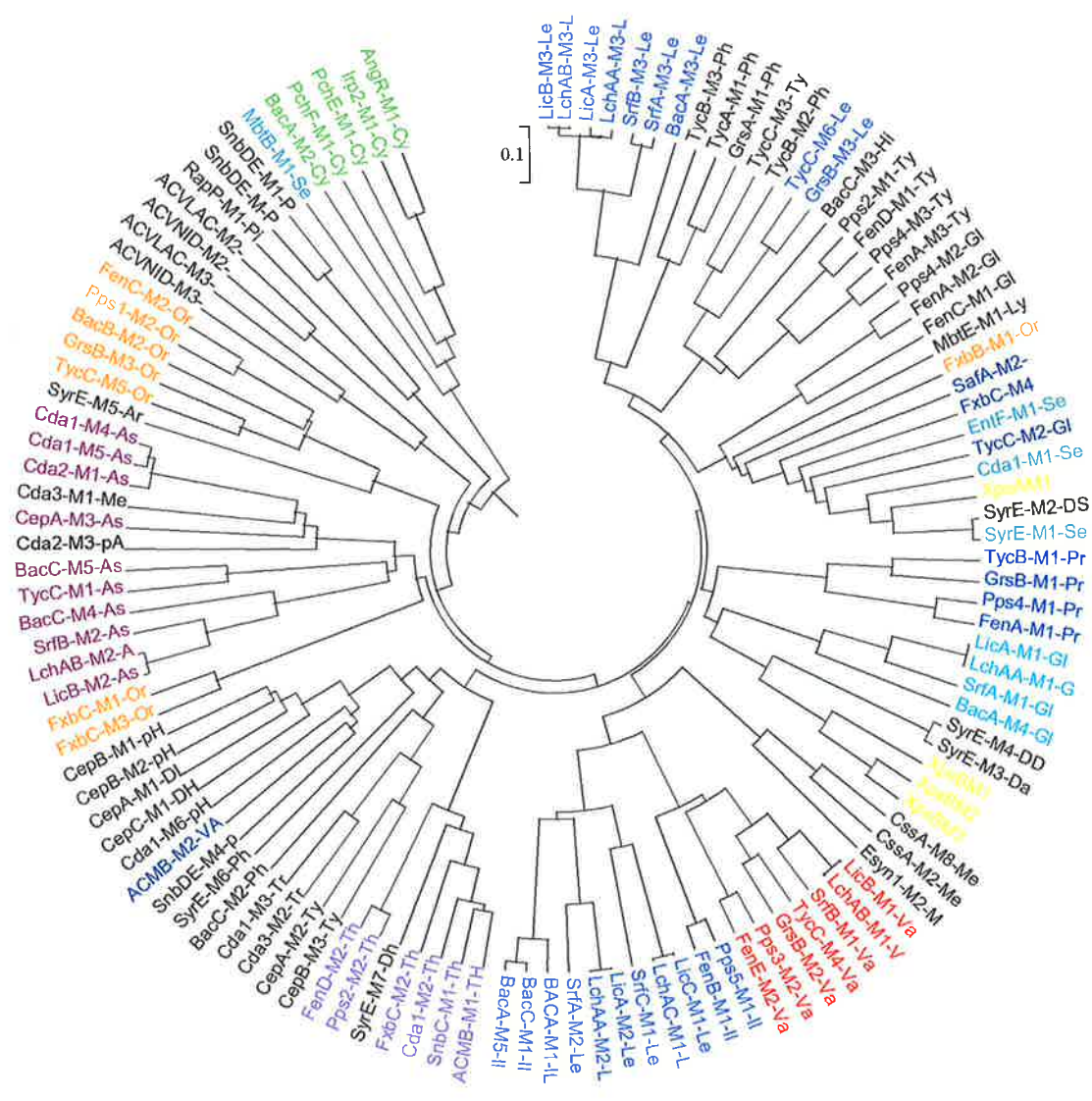
Phylogenetic analysis of the eight amino acids lining the binding pocket of 158 A domains (including the eight amino acid motifs from four *X. bovienii* NRPS derived domains) shows greater clustering on the basis of substrate specificity, rather than genus relatedness (Figure 5.11). XpsA M1 clustered with ten other serine activating domains, in comparison to the A3 – A6 based tree where XpsA M1 only clustered with three serine domains. Once again XpsB M1, XpsB M2 and XpsB M3 cluster together, where XpsB M2 and XpsB M3 are predicted to be the most closely related. XpsB M1, XpsB M2 and XpsB M3 have clustered in a heterogenous area of the eight amino acid based tree (highlighted by the red branches), where a number of adenylation domains have clustered in this region of the tree away from their functional group.

Figure 5.10 Phylogenetic analysis of the 180 – 200 amino acid A3 – A6 motifs from the adenylation domains of a range of NRPS, including the *X. bovienii* NRPS. The amino acid files characterising other adenylation domains included in this analysis were kindly provided by the Challis research group.

Distance matrices were calculated and the tree constructed using MEGA (see Chapter 2, section 2.17).

A3- A6 regions from *X. bovienii* Xps AM1, XpsB M1, XpsB M2 and XpsB M3 are highlighted in yellow. Other major clusters of amino acids are colour coded. Heterogenous regions of the tree are black.

See Appendix B for a full listing of each module used in this analysis.



0.1

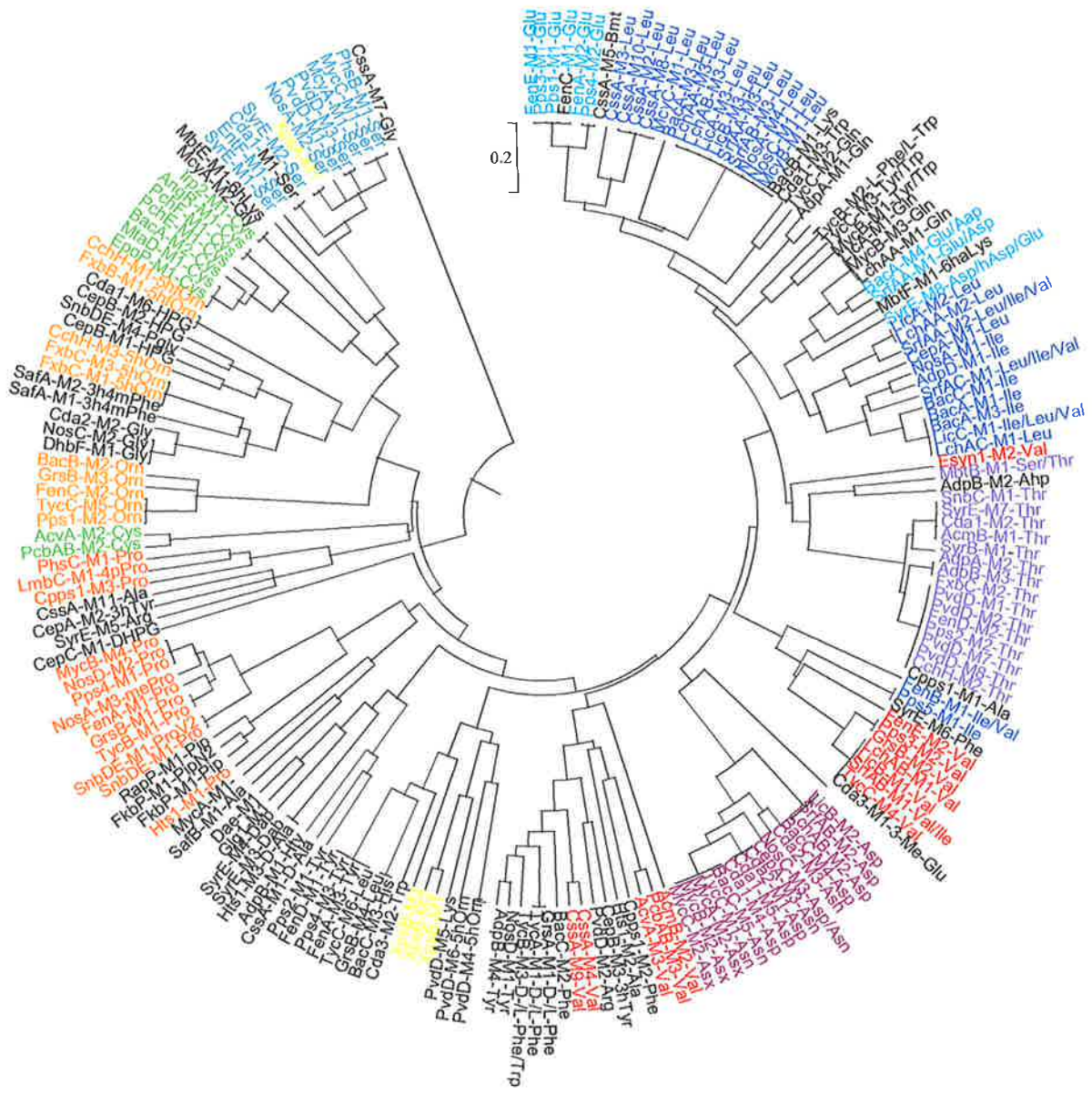
LicB-M3-Le
 LchAB-M3-L
 LicA-M3-Le
 LchAA-M3-L
 SrfB-M3-Le
 SrfA-M3-Le
 BacA-M3-Le
 TycB-M3-Le
 TycA-M3-Ph
 GrsA-M1-Ph
 TycC-M3-Ty
 TycB-M2-Ph
 TycC-M6-Le
 GrsB-M3-Le
 BacC-M3-Hil
 Pps2-M1-Ty
 FenD-M1-Ty
 Fena-M3-Ty
 Pps4-M3-Ty
 FenA-M3-Gl
 Pps4-M2-Gl
 FenA-M2-Gl
 FenC-M1-Gl
 FenC-M1-Ly
 MbtE-M1-Ly
 FxbB-M1-Or
 SafA-M2-
 FxbC-M4
 EniF-M1-Se
 TycC-M2-Gl
 Cda1-M1-Se
 ApsA11
 SyrE-M2-DS
 SyrE-M1-Se
 TycB-M1-Pr
 GrsB-M1-Pr
 Pps4-M1-Pr
 FenA-M1-Pr
 LicA-M1-Gl
 LchAA-M1-G
 SrfA-M1-Gl
 BacA-M4-Gl
 SyrE-M4-Gl
 SyrE-M3-Da
 XpsA2
 XpsA1
 CsaA-M8-Me
 CsaA-M2-Me
 Esyn1-M2-M
 LicB-M1-Va
 TycB-M1-Va
 LchAB-M1-Va
 SrfB-M1-Va
 TycC-M4-Va
 GrsB-M2-Va
 Pps3-M2-Va
 FenE-M2-Va
 FerB-M1-II
 Pps5-M1-II
 LchAC-M1-L
 LchAC-M1-Le
 SrfC-M1-Le
 LicA-M2-Le
 LicA-M1-L
 SrfA-M2-Le
 BACA-M1-IL
 BacC-M1-II
 BacA-M5-II

Figure 5.11 Phylogenetic analysis of the eight amino acids lining the binding pocket of the adenylation domains from a range of NRPS, including the *X. bovienii* NRPS. The amino acid files characterising other adenylation domains included in this analysis were kindly provided by the Challis research group.

Distance matrices were calculated and the tree constructed using MEGA (see Chapter 2, section 2.17).

The eight amino acid regions from *X. bovienii* Xps AM1, XpsB M1, XpsB M2 and XpsB M3 are highlighted in yellow. Other major clusters of amino acids are colour coded. Heterogenous regions of the tree are black.

See Appendix B for a full listing of each module used in this analysis.



5.3 Discussion

In this chapter detailed computer aided analysis of the 15.5 kb *X. bovienii* putative NRPS region at both the nucleotide and amino acid level were described. Two complete and two incomplete ORFs were identified. The deduced gene order was *xpsD*, *xpsA*, *xpsB* and *xpsC*. Partial ORFs *xpsD* and *xpsC* are 653 and 1177 bp respectively. ORF *xpsA* is 3270 bp with the potential to encode for a protein of 1089 amino acids with a predicted M_r value of 122,980. ORF *xpsB* comprises 9951 bp with the potential to encode for a protein of 3316 amino acids with a predicted M_r value of 368,263.

The mol% (G+C) of the 15.5 kb *X. bovienii* putative peptide synthetase region was determined. A striking feature of this analysis was the variance of mol% (G+C), reflecting the location of open reading frames *xpsA*, *xpsB*, *xpsC* and *xpsD*. Marked shifts from the *X. bovienii* mol% (G+C) of 43-44% (Thomas & Poinar, 1979) were observed. Coding regions averaged a mol% (G+C) of 50.4%, whilst intergenic regions recorded between 19.2 – 34.2%. The mol% (G+C) of the *xps* gene region suggests interspecific transfer. The variation in mol% (G+C) indicates the gene cluster may have been assembled from several different sources with a higher mol% (G+C), and subsequently transferred to *X. bovienii*. This phenomenon has been observed in other bacterial species. The *rfb* gene cluster encoding the O antigen repeat units of Gram negative LPS from *E. coli* and *Salmonella enterica* have a mol% (G+C) ranging from 32 – 46% (Reeves, 1993). This contrasts the normal situation where all coding DNA of a given bacterial species has the same mol% (G+C), which in the case of *E. coli* and *S. enterica* is approximately 51%. The extremely low mol% (G+C) found within intergenic regions of the *xps* gene cluster may suggest these regions provide locations for recombination, such that new genes are inserted or deleted.

Alternatively, DNA regions of *xpsABC* rich in A and T nucleotides can provide a regulatory mechanism for transcription attenuation. Transcription attenuation facilitates regulation of gene expression by exploiting RNA sequences and structures. Transcriptional pausing can occur in the initial segment of the leader region, within the gene coding region and/or at the 3' end of the gene. Transcriptional pausing is caused, in part, by formation of an RNA secondary structure in the nascent RNA chain, termed the pause RNA hairpin. The temporary halt to transcription induced by the pause signal allows time for a ribosome to begin synthesis of the polypeptide chain before the Rho-independent termination site is transcribed. Resumption of transcription when the ribosome encounters the paused RNA polymerase is

largely responsible for the synchronisation of transcription and translation that is essential to this class of attenuation mechanisms. The *E. coli* tryptophane (*trp*) biosynthetic operon is an example of transcription attenuation (Landick *et al.*, 1996).

Clues to the size of the DNA region encoding *X. bovienii* NRPS can be derived from results of a *Photorhabdus* genomic sequencing project (Ffrench-Constant *et al.*, 2000). Whilst only 2000 reads of *P. luminescens* nucleotide sequence were performed, the limited information provided a wealth of knowledge regarding the gene sequences carried by this organism. As a comparison of the amount of nucleotide sequence required, 12,000 reads of 400 bases is considered necessary to ensure every cistron is presented in a sample sequence of *Salmonella typhi* equivalent to 1x the genome (4.78-Mbp) (McClelland & Wilson, 1998). The *P. luminescens* sample sequence revealed a significant proportion of sequences showed homology to the NRPS family. Even when taking into account the effects of the large NRPS gene size, these classes of hits were predominant and accounted for 3.7% (80 hits) of the total sequences (Ffrench-Constant *et al.*, 2000). If the genome sample sequence was random, this suggests a significant proportion of the *P. luminescens* genome is homologous to NRPSs. Whether a number of different NRPS like genes, or one very large region is present cannot be determined on the basis of this information. However, as it is common for NRPS genes to be very large, compared with the more usual bacterial ORFs, it would be reasonable to expect the *X. bovienii* NRPS region to be of a similar size.

Whether *Xenorhabdus* and *Photorhabdus* are separate genera can be debated (see Chapter 1, section 1.3), regardless of this *Xenorhabdus* and *Photorhabdus* are very closely related organisms. Based on the literature and experimental evidence it is reasonable to predict the *xpsABC* gene region to be large. Additional nucleotide sequence from this region is required to complete the NRPS gene sequence, and should be considered as the basis for a new project within the laboratory.

ABC transport proteins belong to a family of ubiquitous ATP-driven membrane transporters that share extensive sequence similarity and highly conserved domain organisation. Evidence from the literature suggests ABC transport proteins are usually linked to peptide synthetase gene clusters and play a role in the transport of peptide synthetase products out of the cell. XpsD has remarkable similarities to ATP-Binding Cassette (ABC) transport proteins. Although this sequence is incomplete, several motifs essential for ABC transporter function were identified.

The SyrD ABC transport protein from *P. syringae* pv *syringae* is found upstream of the syringomycin biosynthetic gene cluster and is proposed to be involved in the transport of syringomycin across the cytoplasmic membrane (Quigley & Gross, 1994). Furthermore *syrD* mutants are significantly less virulent than mutants in syringomycin biosynthetic genes. Another example of an ABC transport protein coupled to a NRPS gene is the siderophore exochelin from *Mycobacterium smegmatis*. Upstream of the exochelin biosynthetic cluster is *ExiT*, which is independently transcribed and shows considerable homology to ABC transport proteins. Interestingly *exit* mutants fail to produce exochelin, and furthermore mutants defective in the export of exochelin do not accumulate this siderophore intracellularly (Wenming *et al.*, 1998). It is possible that synthesis and export are tightly coupled. Based on this work it would be interesting to determine if *xpsD* plays a role in secretion of bioactive peptides synthesized by the *xpsABC* gene products.

The *xpsABC* region revealed significant homology at the amino acid level to NRPS. NRPSs are known to be modular genes carrying numerous repeat regions within each module. XpsA was found to contain one module carrying a condensation, adenylation and thiolation domain. XpsB has three modules, each of these also carry condensation, adenylation and thiolation domains. The amino acid sequence for XpsC was incomplete, consequently only the 5' end of one module carrying a condensation domain was identified. The condensation, adenylation and thiolation domain sequences from each module were aligned with the available consensus sequence (Konz & Marahiel, 1999). Significant departures from consensus were noted. This may reflect the only recent large numbers of new NRPS gene sequences reported. Furthermore, deviations from the consensus sequence have been observed for NRPS genes such as coelichelin from *Streptomyces coelicolor* (Challis & Ravel, 2000). Considerable variation from the condensation domain consensus sequence is found in XpsA module 1. The condensation domain C3 motif is considered to be the most critical. The second histidine residue of the C3 motif serves as the base for deprotonation of the NH_3^+ moiety of the thioester-bound nucleophiles prior to amide bond formation (Mootz & Marahiel, 1997). Mutation of the second histidine to a valine abolishes dipeptide formation (Stachelhaus *et al.*, 1998). As the XpsA M1 condensation domain C3 motif encodes the second histidine, the condensation domain is likely to be functional.

Generally, the number of condensation domains coincides in frequency with the number of peptide bonds in the final linear peptide. Condensation domains are conventionally fused to the amino terminal end of modules accepting acyl groups from the preceding module, and

absent in modules activating the first acyl constituent to be incorporated (Mootz & Marahiel, 1997). The *X. bovienii* peptide synthetase region is unusual as XpsA M1, the first module of the *xpsABC* sequence, contains a condensation domain. Unusual positioning of the condensation domain has been observed in other peptide synthetase gene sequences. An extra condensation domain is found at the N-terminus of cyclosporin synthetase (*Tolypocladium niveum*), or at the carboxyl termini of enniatin (*Fusarium scirpi*), HC-toxin (*Cochliobolus carbonum*), and FK506 systems (*Streptomyces* spp. MA6548) (Konz & Marahiel, 1999). According to the organisation and structure of the formed products, it is likely the unusually placed condensation domains are involved in peptide-chain termination and cyclisation. Some of the synthesised molecules are cyclized by the formation of an amide bond (e.g. cyclosporin and HC-toxin) and others by formation of an ester bond (e.g. enniatin and FK506). Condensation domains therefore must be able to catalyse two types of nucleophilic attack on the thioester carboxyl group; one by an amine leading to the formation of an amide bond and the other by a hydroxyl group leading to ester bonds or eventually hydrolysis (Konz & Marahiel, 1999). Based on the unusual positioning of the XpsA M1 condensation domain, the first *X. bovienii* peptide synthetase amino acid may be acylated. In similar systems like surfactin (Cosmina *et al.*, 1993) or fengycin (Tognoni *et al.*, 1995) the first amino acid in the peptide is acylated with a fatty acid.

A domain of significance not identified in the *X. bovienii* peptide synthetase gene sequence was the thioesterase domain. This domain shares sequence homology with thioesterases and carries the signature sequence (Gly-X-Ser-X-Gly) similar to the active-site motif of acyltransferases and thioesterases (Marahiel *et al.*, 1997; von Döhren *et al.*, 1997). Thioesterase domains are often found in modules incorporating the last amino acid into a peptide chain. The full length peptide bound to the last thiolation domain may be transferred to the hydroxyl group of the conserved serine residue within the thioesterase domain to generate a transient acyl-O-enzyme intermediate. This can then be cleaved by an acyl transfer to water and the peptide completed (Cane *et al.*, 1998). The absence of a thioesterase domain supports the conclusion that more nucleotide sequence is required to complete the *X. bovienii* NRPS region.

Based on the crystal structure of the adenylation domain of gramicidin synthetase, the critical amino acid residues lining the substrate binding pocket of GrsA have been identified (Conti *et al.*, 1997). Given the high degree of sequence identity (30 - 60%) of NRPS adenylation domains, it can be concluded that the GrsA structure represents a prototype for all NRPS

adenylation domains (Conti *et al.*, 1997). Critical residues in all known NRPS adenylation domains have been identified that align with eight pocket binding residues in the GrsA adenylation domain and define well conserved recognition templates (Challis *et al.*, 2000). Using this information Challis performed phylogenetic analysis to predict the amino acid substrate activated by an adenylation domain (Challis *et al.*, 2000).

These predictions were made when the eight amino acid motif from each adenylation module was compared to a database of adenylation modules where the amino acid activated had been determined experimentally. A downside to the computer modelling approach for adenylation domain amino acid activation prediction is that most of the biochemical data available has come from only a few microorganisms (eg. *E. coli*, *Bacillus* sp. and *Pseudomonas* sp) even though a vast array of peptide synthetases have been isolated from *Streptomyces* spp. Furthermore, the literature tends to suggest high substrate specificity for each adenylation domain, which may not be correct. This is particularly relevant for recognition of hydrophobic amino acids where relaxed specificity is often observed (Challis *et al.*, 2000).

Phylogenetic analysis of the 180 - 200 amino acids present in A3 – A6 motif from each *X. bovienii* module supports the observations of Challis (Challis *et al.*, 2000). Amino acids from motif A3 – A6 predominantly shows clustering along genus lines, limiting the functional clustering of each domain. Phylogenetic analysis using the 180 amino acids of A3 – A6 is likely to emphasize genus specific mutational evolution rather than functional evolution of the protein. Challis (Challis *et al.*, 2000) suggests prokaryotic activation domains are the result of an evolutionary mechanism involving horizontal transfer. The mol% (G+C) analysis of *X. bovienii* *xpsABC* supports this reasoning. Mol% (G+C) analysis showed the G+C content of *xpsABC* is substantially higher than that of surrounding DNA. This observation suggests *X. bovienii* could have acquired *xpsABC* by horizontal transfer.

Phylogenetic analysis using the eight critical amino acids lining the A3 – A6 binding pocket provides a greater level of functional clustering in agreement with Challis (Challis *et al.*, 2000). However, whilst the XpsA M1 eight amino acid sequence clustered well with ten other serine activating domains, XpsB M1, XpsB M2 and XpsB M3 clustered in a heterogenous area of the tree. Using the computer based modelling program XpsB M1 and XpsB M3 were predicted to activate 6-*N*-hydroxylysine, and XpsB M2 glutamine. Very few examples of lysine based derivatives were present within the database analysed, and may explain this clustering effect. This observation highlights the need to include more

adenylation domain motifs activating a range of substrates from a broader range of microorganisms. Furthermore, whilst this information can serve as a tool for predicting substrate specificity of activation domains from uncharacterised NRPS, a more detailed analysis is required to identify residues critical for substrate recognition and specificity (Challis *et al.*, 2000). Care should be taken when using a computer modelling approach to predict substrate recognition, and as a consequence the amino acid predictions of XpsB M1, XpsB M2 and XpsB M3 in particular need to be approached with caution.

To ultimately elucidate the amino acid each module is predicted to activate, ATP-PPi exchange assays are necessary. ATP-PPi exchange assays require the over-expression of an adenylation domain. This facilitates analysis of ATP-PPi exchange activities of the domain in the presence of a variety of amino acid substrates (Hori *et al.*, 1991). Whilst phylogenetic analysis of the eight amino acids present in the binding pocket can predict the most likely amino acid activated by each adenylation domain, biochemical data will provide the final result.

The *X. bovienii* NRPS amino acid chain order cannot be easily predicted. In most cases the order of amino acids in a final peptide mirrors the module order predicted by the gene sequence. This phenomenon is known as the co-linearity rule. However, NRPSs such as yersiniabactin (Gehring *et al.*, 1998) syringomycin (Guenzi *et al.*, 1998a) and microcystin (Tillett *et al.*, 2000) are being identified which do not observe "co-linearity". Furthermore, the gene sequence of exochelin (*Mycobacterium smegmatis*) reveals six modules whilst the final secreted exochelin is a pentapeptide (Yu *et al.*, 1998). It is unclear if an intermediate hexapeptide is formed and later cleaved into the secreted exochelin, or if the last module in the gene sequence is inactive and not used during peptide synthesis. Considering the first module of *xpsABC* (XpsA M1) has a condensation domain, which as previously discussed is not unknown but certainly unusual, it may be likely that *X. bovienii* peptide synthetase does not follow the co-linearity rule. XpsA M1 may be used to condense the peptide part with another unit involved in the production of a NRPS or related polyketide or fatty acid. To resolve this issue complete nucleotide sequence up and downstream of the *X. bovienii* peptide synthetase region is required. However deduction of the true chain order, and types of amino acids activated, can only be obtained by purification of the peptide compound, followed by structural analysis using a number of approaches, eg. NMR and column chromatography.

NRPS have a broad range of properties including; biosurfactant, antibiotic, antiviral, cytostatic, anticancer and immunosuppressive activities (Konz & Marahiel, 1999; Marahiel, 1997). The *X. bovienii* peptide synthetase function is at present unknown. Jacques Ravel (pers. comm.) suggests a siderophore antibiotic is likely due to the presence of serine and lysine residues which are common to these compounds. Siderophore antibiotics share structural features with naturally occurring siderophores, and use the active transport systems of these compounds to gain access to Gram negative bacteria (Braun, 1999). Whilst Gram negative bacteria have an outer membrane which forms a permeability barrier reducing the access of antibiotics, they are highly susceptible to antibiotics which are actively transported across the outer membrane. Sequence analysis of the *X. bovienii* NRPS gene region, mutant analysis and, most importantly, purification of the final peptide is required to elucidate a function.

Chapter 6

Regulation of expression of the non-ribosomal peptide synthetase gene *xpsA*

6.1 Introduction

Chapter 5 described the analysis of 15.5 kb of *X. bovienii* T228 chromosomal DNA encoding novel NRPSs. The *X. bovienii* NRSP gene cluster is organised as an operon consisting of the structural genes *xpsABC*, and a putative ABC-transport gene *xpsD*.

Environmental factors affecting the expression of NRPSs in other bacterial and fungal species have been well documented. For example ACV (δ -(L- α -aminoadipyl)-L-cysteinyl-D-valine) synthetase is one of several enzymes involved in the biosynthesis of cephalosporins in *Streptomyces*. The production of ACV synthetase by *Streptomyces clavuligerus* grown in chemically defined media supplemented with 120 mM NH₄Cl is sharply reduced (Zhang *et al.*, 1989). This inhibition can be reversed by the addition of Fe²⁺ to cell-free reactions as inorganic phosphate forms insoluble salts with Mg²⁺, Ca²⁺ and Fe²⁺ (Jhang *et al.*, 1989). Glucose (28-140 mM) also produces a concentration-dependent repression on the biosynthesis of ACV (first intermediate of penicillin biosynthetic pathway) in *Penicillium chrysogenum*. Derepression of penicillin biosynthesis occurs after depletion of glucose suggesting a carbon-catabolite repression type of mechanism. Similar results are not observed when bacteria are grown in the presence of lactose (Revilla *et al.*, 1986). As with cephalosporins, production of the phytotoxin syringomycin by *Pseudomonas syringae* pv. *syringae* is repressed by phosphate and increased by Fe²⁺ (Gross, 1985). Production of syringomycin by *Pseudomonas syringae* pv. *syringae* is also influenced by temperature and pH (Gross, 1985).

In *Bacillus* sp. starvation activates antibiotic production, whereby the tyrocidine biosynthetic operon is induced under nutrient limitation through a sporulation dependent mechanism that relieves repression. Genes activated during transition from exponential to stationary phase are controlled primarily at the level of transcription initiation (Marahiel *et al.*, 1993).

Environmental factors affecting the transcription and translation of *X. bovienii* NRPSs are unknown. Transcriptional promoter::reporter gene fusions can be used to facilitate studying gene expression. Transcription from the native promoter is determined by the activity of the

product of the fused reporter gene. Furthermore, generation of antisera against the native protein of interest can be used to examine regulation of translation using Western analysis of wild type culture lysates grown under different environmental conditions.

This chapter describes the construction of an *xpsA-lacZ* transcriptional fusion, mobilisation of DNA encoding the fusion into the *X. bovienii* chromosome by transposon mutagenesis and analysis of *xpsA* transcription by β -galactosidase expression under different conditions. Furthermore the analysis of XpsA translation by the over-expression of XpsA, generation of an XpsA specific antibody and its use in Western analysis of *X. bovienii* T228 whole cell lysates is described.

6.2 Results

To construct an *xpsA-lacZ* transcriptional fusion, DNA encoding the promoter region of *xpsA* was cloned into the multiple cloning site (MCS) of transcriptional fusion vector pMU575 (Figure 6.1). To transfer *xpsA-lacZ* fusion DNA into *X. bovienii* two strategies were considered:

1. Cloning the RP4 *mob* region into the transcriptional fusion vector pMU575 to facilitate conjugal transfer of an *xpsA-lacZ* transcriptional fusion from *E. coli* to *X. bovienii*.
2. Insertion of an *xpsA-lacZ* transcriptional fusion between the direct repeat sequences of a mini-Tn5 Km derivative located on a conjugative suicide vector to facilitate insertion of the *xpsA-lacZ* fusion into the *X. bovienii* chromosome.

6.2.1 PCR amplification of RP4 *mob* and subsequent cloning into transcriptional fusion vector pMU575

PCR amplification of pSUP201.1 DNA using oligonucleotides P3537 and P3538-5 (Table 2.4.1) resulted in an approximately 1.9 kb product (data not shown), which was subsequently cloned into pGEM-T. Oligonucleotide primers P3537 and P3538-5 have *XhoI* restriction sites incorporated into their 5' ends. The ligation mix was used to transform *E. coli* DH5 α by electroporation. Transformants were selected on NA supplemented with Amp, IPTG and X-gal. Plasmid DNA isolated from selected transformants was screened by *XhoI* restriction enzyme digestion (data not shown) and the correct construct designated pCT410 (Figure 6.2).

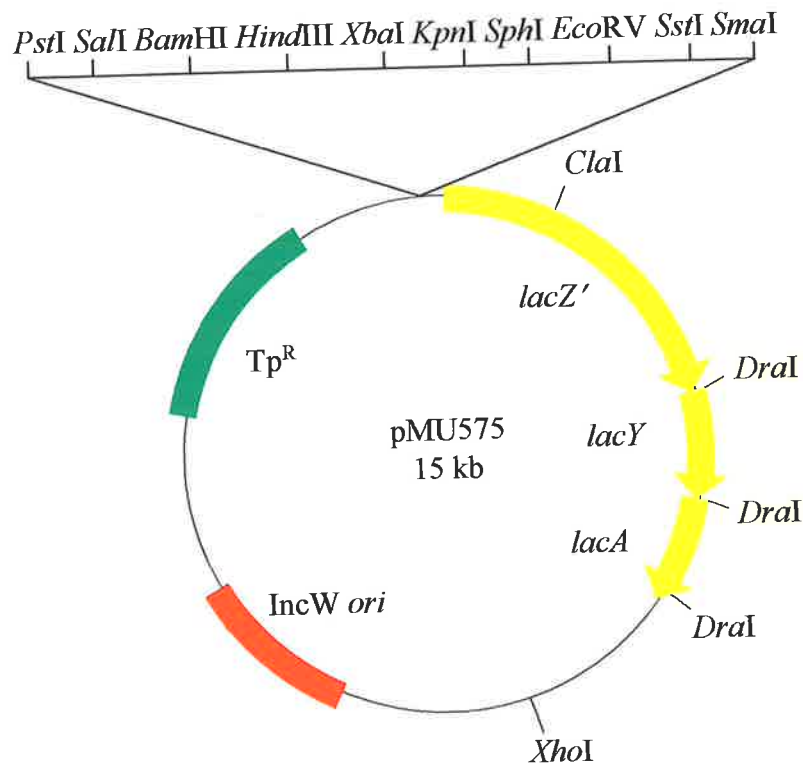


Figure 6.1 Transcriptional fusion vector pMU575 (Praszkier *et al.*, 1989).

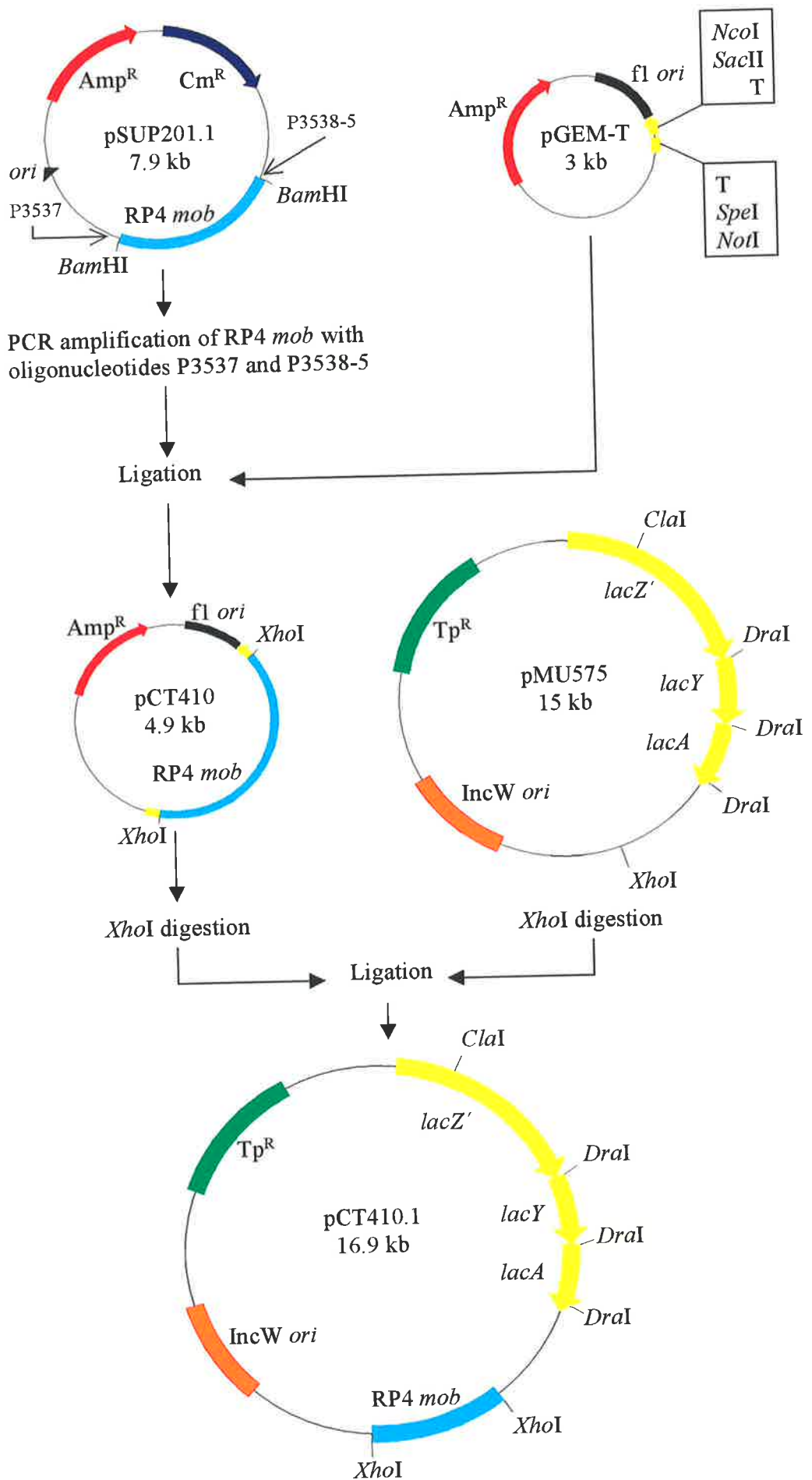
Plasmid pMU575 is a 15 kb trimethoprim resistant vector dependent on an IncW origin of replication. It encodes the β -galactosidase operon (*lacZ'YA*), where DNA encoding the first 55 amino acids of *galk* are fused to the eighth codon of *lacZ*. Upstream of *lacZ'YA* a multiple cloning site (MCS) facilitates cloning of a DNA region with predicted promoter activity. A transcriptional terminator 5' of the MCS prevents read-through into the DNA region under investigation.

Abbreviations: IncW *ori*, IncW based origin of replication; *lacA*, thiogalactoside transacetylase; *lacY*, permease; *lacZ'*, truncated β -galactosidase; Tp^R, trimethoprim resistance gene. Restriction enzyme sites encoded by the MCS are noted.

Figure 6.2 Construction of plasmids pCT410 and pCT410.1

The RP4 *mob* region from plasmid pSUP201.1 was amplified using oligonucleotide pair P3537/P3538-5 resulting in a 1.9 kb fragment. The 1.9 kb fragment was cloned into pGEM-T and designated pCT410. Oligonucleotides P3537 and P3538-5 have *XhoI* sites incorporated into their 5' ends, facilitating the digestion of pCT410 and removal of RP4 *mob* as a 1.9 kb *XhoI* fragment. The 1.9 kb RP4 *mob XhoI* fragment was cloned into *XhoI* digested pMU575 and designated pCT410.1.

Abbreviations: Amp^R, ampicillin resistance; Cm^R, chloramphenicol resistance; f1 *ori*, f1 origin of replication; IncW *ori*, IncW origin of replication; *ori*, origin of replication; *lacA*, thiogalactoside transacetylase; *lacY*, permease; *lacZ'*, truncated β -galactosidase; RP4 *mob*, mobilisation region; Tp^R, trimethoprim resistance gene.



The 1.9 kb RP4 *mob* *Xho*I fragment from pCT410 was cloned into *Xho*I digested pMU575 and the ligation mix used to transform *E. coli* DH5 α by electroporation, followed by selection on NA supplemented with 100 μ g/ml Tp (Figure 6.2). Although previous studies (Praszkier *et al.*, 1989) suggested Tp at a final concentration of 10 μ g/ml when selecting bacteria successfully transformed with pMU575, *E. coli* strains DH5 α , SM10 λ *pir* and DK1 are resistant at this concentration. At a Tp concentration of 100 μ g/ml faint growth of each *E. coli* strain is observed. However *E. coli* DH5 α containing pMU575 derivatives significantly outgrow *E. coli* DH5 α . Strongly Tp resistant colonies were selected and patched onto NA supplemented with 100 μ g/ml Tp. Colonies were then screened by PCR pooling (see section 2.15.2) using oligonucleotides P3537/P3538-5 to amplify the cloned 1.9 kb RP4 *mob* (data not shown). The correct plasmid clone was designated pCT410.1.

6.2.1.1 Conjugal transfer of pCT410.1 from *E. coli* SM10 λ *pir* to *X. bovienii*

Plasmid pCT410.1 was used to transform *E. coli* SM10 λ *pir* (which carries the RP4 *tra*, or transfer, region) by electroporation to facilitate conjugal transfer of the plasmid into *X. bovienii* T228. Conjugations were performed as previously described (see section 2.11).

Plasmid pCT410.1 could not be mobilised from *E. coli* SM10 λ *pir* to *X. bovienii* by conjugal transfer. No colonies were recovered when the conjugation mix was plated onto NA supplemented with Amp/Tp. Positive control plasmid pSUP201.1 was successfully transferred from *E. coli* SM10 λ *pir* to a Rif resistant *X. bovienii* at a frequency of 4.38×10^{-4} (with selection on NA supplemented with Rif/Tp). This indicated that the RP4 *mob* region of pSUP201.1 is capable of mobilising this plasmid from an *E. coli* strain to *X. bovienii* T228. Furthermore, plasmids pSUP201.1 and pCT410.1 were successfully mobilised from *E. coli* SM10 λ *pir* to a rifampicin resistant strain of *E. coli* DH5 α at frequencies of 6.34×10^{-6} (with selection on NA supplemented with Cm/Rif) and 5.78×10^{-6} (with selection on NA supplemented with Rif/Tp) respectively. However, plasmid pMU575, without the cloned RP4 *mob*, could not be conjugatively transferred from *E. coli* SM10 λ *pir* to *E. coli* DH5 α or *X. bovienii*.

These results clearly showed the RP4 *mob* region introduced into pMU575 can initiate conjugal transfer of pCT410.1 from *E. coli* SM10 λ *pir* to *E. coli* DH5 α . Furthermore the fact

that pSUP201.1 can be transferred from *E. coli* SM10 λ pir to *X. bovienii* confirm that conjugative transfer of plasmids to the recipient strain can occur at frequencies similar to that obtained for transfer between *E. coli* strains. Since the pCT410.1 cannot be transferred to *X. bovienii*, this indicates that the IncW based pMU575 cannot be replicated in this recipient host. In the absence of a suitable transcriptional fusion vector for use in *X. bovienii*, the use of Tn5 transposable elements for transfer of an *xpsA-lacZ* fusion to *X. bovienii* was investigated.

6.2.2 Transfer of an *xpsA-lacZ* transcriptional fusion into *X. bovienii* T228 facilitated by mini-Tn5 Km *xylE*

The mini-Tn5 Km transposable element system has been shown to stably insert into the *X. bovienii* genome as a single independent event (see section 4.2.1.2). In this study, the promoter region of *xpsA* was cloned into pMU575 to create a transcriptional fusion with *lacZ*. The fusion was then cloned between the direct repeats of mini-Tn5 *xylE* to facilitate mobilisation of *xpsA-lacZ* into *X. bovienii* by conjugal transfer. Three independent transposon insertions carrying the *xpsA-lacZ* fusion were selected for analysis of β -galactosidase activity when expressed from the *xpsA* promoter.

6.2.2.1 PCR amplification and cloning of the *xpsA* promoter region

Primer extension analysis and computer analysis of *xpsA* nucleotide sequence was used to estimate the *xps* operon promoter region (see section 5.2.1.2). Using this information, oligonucleotide P3679 (annealing 368 nucleotides 5' of the *xpsA* ATG codon) was designed to facilitate PCR amplification of this 438 bp region of DNA with oligonucleotide P6247 (see Table 2.4.4).

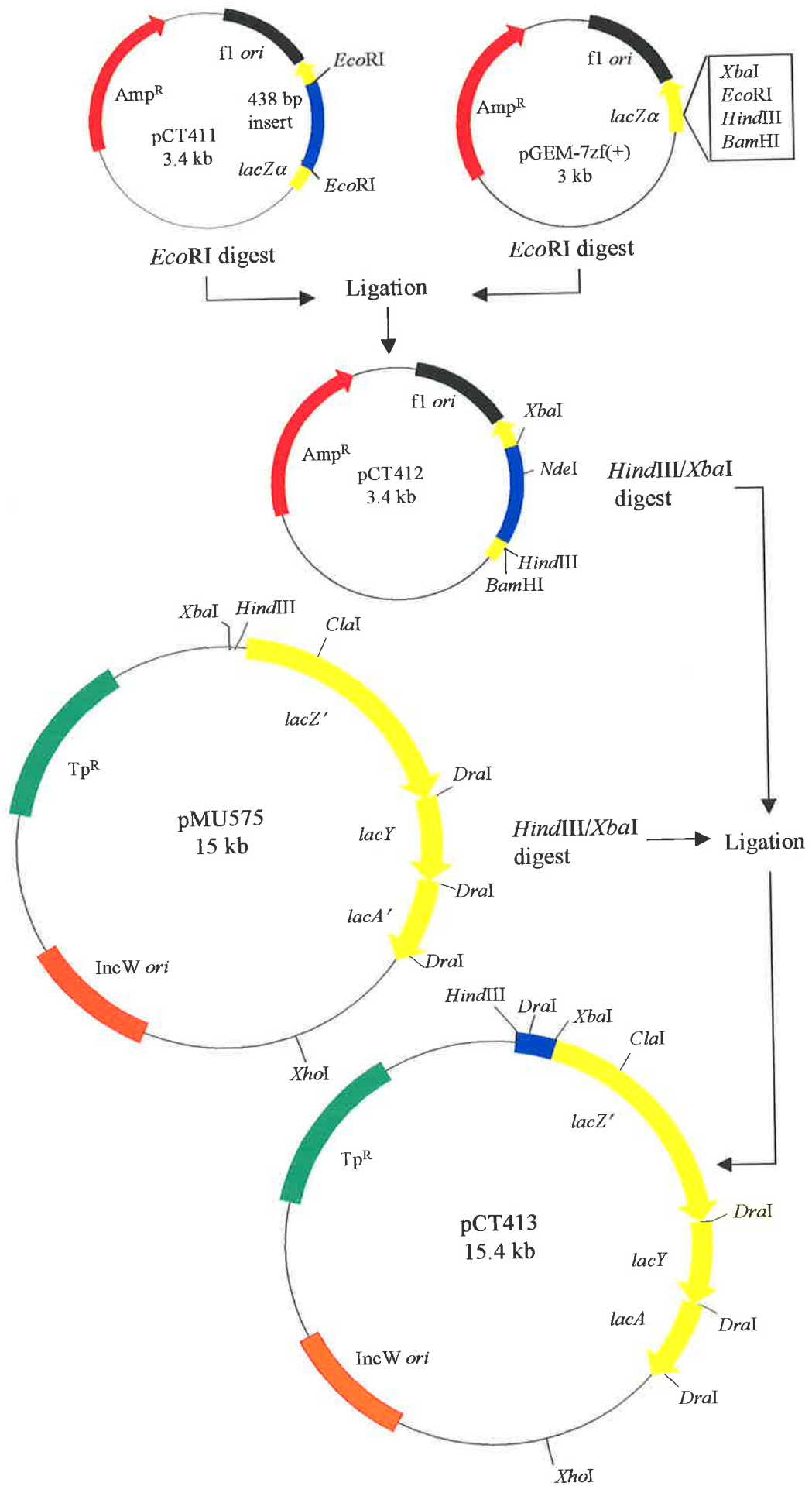
PCR amplification of *X. bovienii* chromosomal DNA with oligonucleotides P3679/P6247 resulted in a 438 bp product (data not shown). The 438 bp PCR product was ligated with pGEM-T Easy, and used to transform *E. coli* DH5 α by electroporation (Figure 6.3). Colonies were selected on NA supplemented with Amp, IPTG and X-gal. Plasmid DNA isolated from clones was confirmed by *EcoRI* digestion (data not shown) and designated pCT411.

The PCR amplified promoter region was removed from pCT411 as a 448 bp *EcoRI* fragment and subcloned into *EcoRI* digested pGEM7zf(+). The ligation mix was used to transform

Figure 6.3 Construction plasmids pCT411, pCT412 and pCT413.

A 438 bp PCR product encoding the *xpsA* promoter region was created by amplification of *X. bovienii* T228 chromosomal DNA by oligonucleotide pair P3679/P6247. The 438 bp PCR product was cloned into pGEM-T Easy and designated pCT411. Plasmid pCT411 was digested with *EcoRI* to excise the PCR product as a 448 bp fragment which was subsequently cloned into *EcoRI* digested pGEM7zf(+) and designated pCT412. *HindIII/XbaI* digestion of pCT412 removed the *xpsA* promoter region as a 0.45 kb fragment which was subsequently cloned into *HindIII/XbaI* digested pMU575 and designated pCT413.

Abbreviations: Amp^R, ampicillin resistance gene; f1 *ori*, f1 origin of replication; IncW *ori*, IncW origin of replication; *lacA*, thiogalactoside transacetylase; *lacY*, permease; *lacZ'*, truncated β -galactosidase; Tp^R, trimethoprim resistance gene.



E. coli DH5 α by electroporation and colonies selected on NA supplemented with Amp, IPTG and X-gal. The orientation of the insert in pGEM7zf(+) was determined using *Bam*HI/*Nde*I digests of plasmid DNA. The correct clone demonstrated a 3.1 kb and 0.3 kb fragment (data not shown), and was designated pCT412 (Figure 6.3). *Hind*III/*Xba*I digestion of pCT412 removed the *xpsA* promoter region as a 0.45 kb fragment (data not shown) that was subcloned into *Hind*III/*Xba*I digested pMU575. The ligation mix was used to transform *E. coli* DH5 α by electroporation, and transformants selected on NA supplemented with 100 μ g/ml Tp and X-gal. Plasmid DNA from *lacZ* positive blue colonies was digested with *Hind*III/*Xba*I to confirm the *xpsA* promoter insertion (data not shown). The correct construct was designated pCT413 (Figure 6.3).

When *E. coli* DH5 α [pMU575] was grown on NA supplemented with 100 μ g/ml Tp and X-gal only white colonies were observed. However when *E. coli* DH5 α [pCT413] was grown on the same media, blue colonies were observed. These results show the 438 bp *xpsA* promoter region cloned into pMU575, and maintained by an *E. coli* DH5 α host, facilitates expression of the promoterless *lacZ* gene.

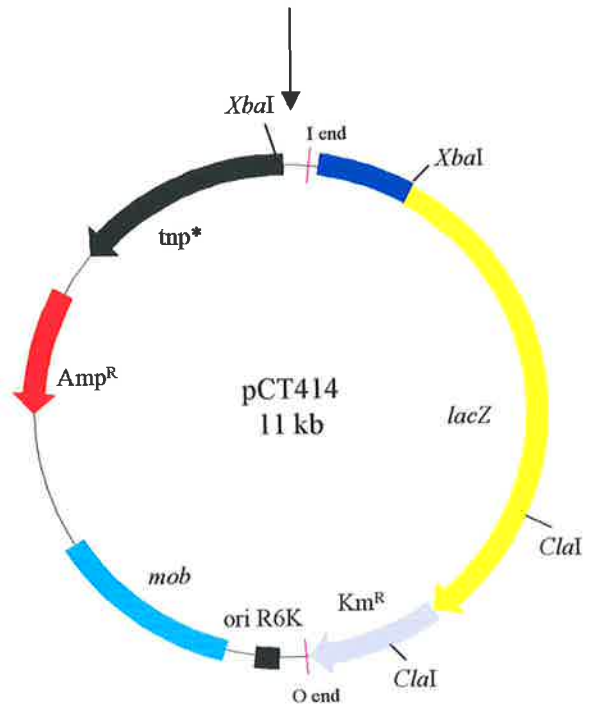
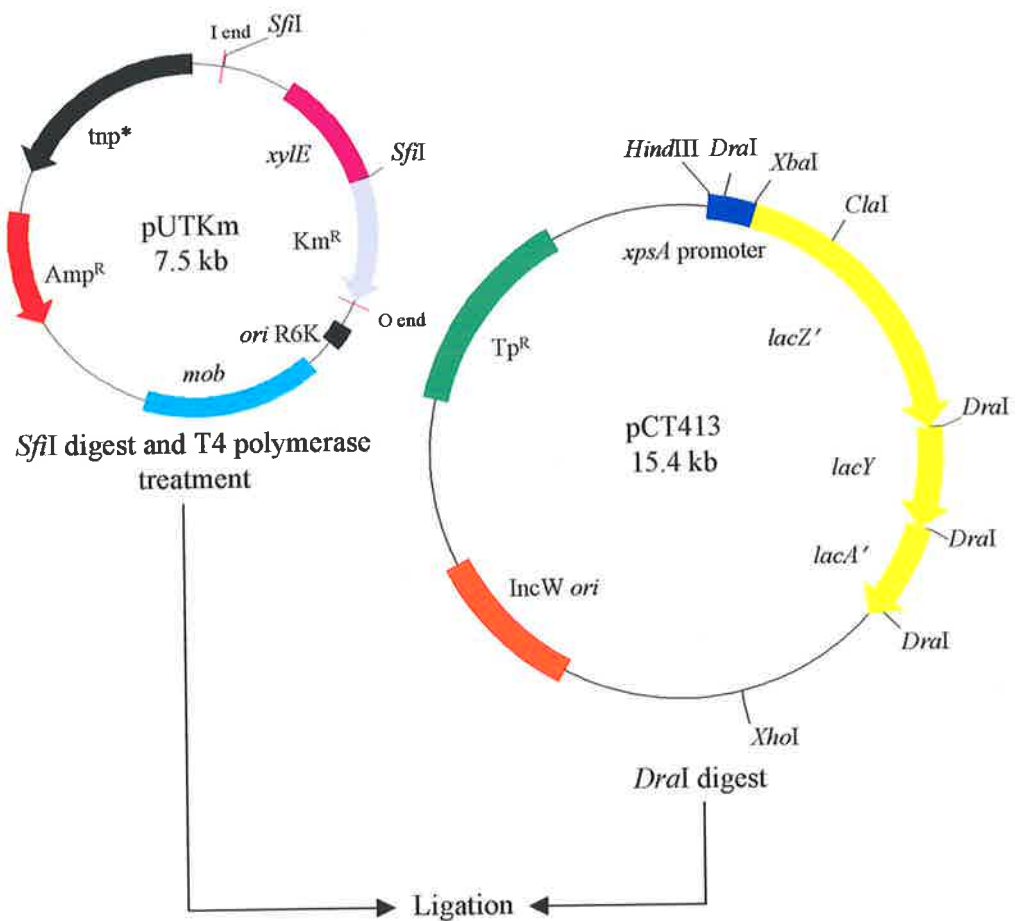
6.2.2.2 Cloning the *xpsA-lacZ* transcriptional fusion into mini-Tn5 *xylE*

To facilitate transposition of the *xpsA-lacZ* transcriptional fusion into the *X. bovienii* chromosome, mini-Tn5 *xylE* (De Lorenzo *et al.*, 1990), a derivative of mini-Tn5 Km, was utilised as the vector. Mini-Tn5 *xylE* is Km^R and able to facilitate transposition of DNA cloned within the direct repeat units (I and O ends) of the transposable element. Mini-Tn5 *xylE* has two convenient *Sfi*I sites located within the transposable element to facilitate cloning of the *xpsA-lacZ* transcriptional fusion, whilst maintaining Km^R to enable selection of exconjugates.

Plasmid pUTKm (which carries mini-Tn5 *xylE*) was digested with *Sfi*I, and the promoterless *xylE* gene removed as a 1.7 kb fragment (data not shown). The remaining plasmid DNA was treated with T4 polymerase to fill the *Sfi*I sites, resulting in blunt ends. The *xpsA-lacZ* fusion was removed from pCT413 as a 3.8 kb *Dra*I fragment (data not shown), and cloned into the linearised pUTKm vector (Figure 6.4). The ligation mix was used to transform *E. coli* SY327 λ *pir* by electroporation and colonies were selected on NA supplemented with Amp, Km and X-gal. *LacZ* positive colonies were selected; *Cla*I and *Xba*I digests used to confirm

Figure 6.4 Construction of plasmid pCT414.

The *xpsA* promoter region, transcriptionally fused to *lacZ*, was removed from pCT413 as a 3.8 kb *DraI* fragment and cloned into pUTKm(*xylE*). The resulting plasmid was designated pCT414. Plasmid pUT Km (*xylE*) had previously been digested with *SfiI* to removed the promoterless *xylE* gene, and subsequently treated with T4 polymerase to create blunt ends. Abbreviations: Amp^R, ampicillin resistance gene; I and O ends, 19 bp terminal repeat sequences of Tn5; IncW *ori*, IncW origin of replication; Km^R, kanamycin resistance gene; *lacA*, thiogalactoside transacetylase; *lacY*, permease; *lacZ'*, truncated β -galactosidase; *mob*, RP4 mobilisation region; *ori* R6K, λ *pir* protein dependent origin of replication; *tnp**, transposase; Tp^R, trimethoprim resistance gene, *xylE*, promoterless catechol 2,3-dioxygenase gene.



the presence and orientation of the *xpsA-lacZ* fusion (Figure 6.5). The correct colony was designated pCT414 (Figure 6.4). This result shows the 438 bp *xpsA-lacZ* translational fusion, excised from pCT413 and cloned between the direct repeats of a mini-Tn5 Km, is able to facilitate expression of the promoterless *lacZ* gene in an *E. coli* SY327 λ *pir* host. Re-ligated pUTKm was used to transform *E. coli* SY327 λ *pir* by electroporation and colonies were selected on NA supplemented with Amp, Km and X-gal. No *lacZ* positive colonies were observed confirming *lacZ* activity of pCT414 was due to the *xpsA-lacZ* transcriptional fusion and not plasmid pUTKm. *Cla*I and *Xba*I digests of religated pUTKm (minus *xyIE*) were compared with pCT414 (Figure 6.5).

Plasmid pCT414 was then used to transform *E. coli* SM10 λ *pir* by electroporation. Transformants were selected on NA supplemented with Amp. This *E. coli* host was used as the donor strain for conjugal transfer of pCT414 to *X. bovienii*, and is innately Km^R and *lacZ* positive.

6.2.2.3 Mobilisation of pCT414 from *E. coli* SM10 λ *pir* to *X. bovienii* T228 by conjugal transfer

Plasmid pCT414 was mobilised from *E. coli* SM10 λ *pir* to *X. bovienii* T228 by conjugal transfer (see section 2.11) and exconjugates selected on NA supplemented with Km and Sm. The conjugation frequency was 5.98×10^{-5} . As it was unknown whether the *xpsA-lacZ* transcriptional fusion would be expressed in a *Xenorhabdus* host grown on NA, exconjugates were primarily selected for Km^R derived from the transposon insertion. Exconjugates were further patched onto NA supplemented with Km, Sm and X-gal. All exconjugates were *lacZ* positive (blue) whilst the wild type *X. bovienii* negative control remained a cream colour. This result shows the *xpsA-lacZ* transcriptional fusion, inserted into the *X. bovienii* chromosome by mini-Tn5 Km, is able to facilitate expression of the promoterless *lacZ* gene when grown on NA.

Exconjugates carrying mini-Tn5 Km containing the *xpsA-lacZ* transcriptional fusion were inoculated onto BTB agar to ensure the presence of both P1 and P2 bacteria. As the *xpsA-lacZ* transcriptional fusion had been introduced into the *X. bovienii* chromosome by random transposon insertion, screening of exconjugates to ensure they were as phenotypically similar to wild type *X. bovienii* as possible was necessary. Therefore exconjugates were tested for the

Figure 6.5 Digestion of pCT414 and pUTKm (after removal of *xylE* and re-ligation of the vector) with *Cla*I and *Xba*I. These digests were used to confirm the presence and orientation of the cloned *xpsA-lacZ* transcriptional fusion.

Lanes:

[a], SPP1 markers, *Bacillus subtilis* phage SPP1 DNA digested with *Eco*RI;

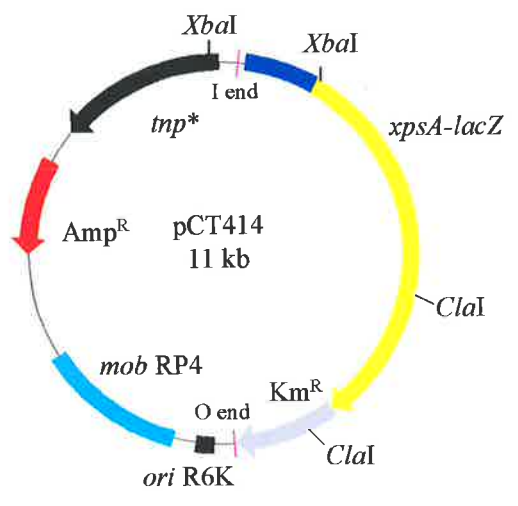
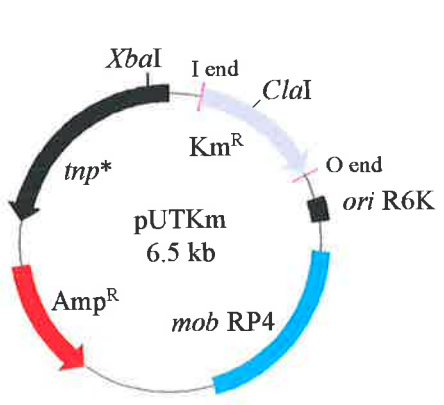
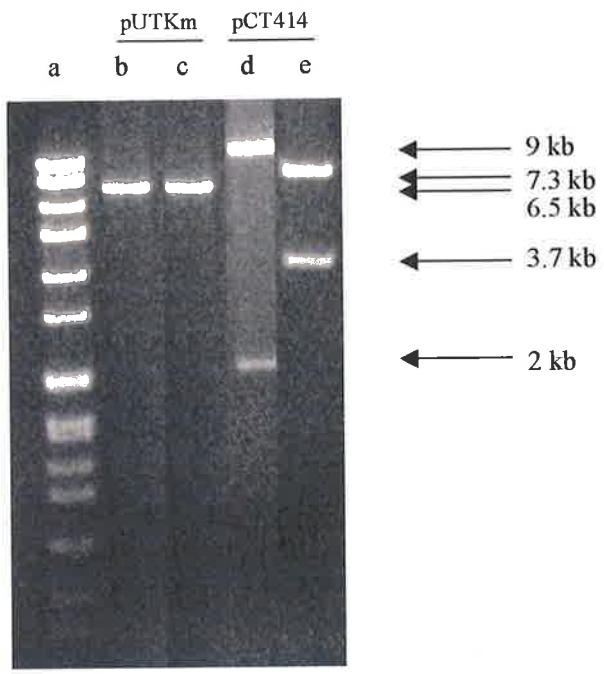
[b], re-ligated pUTKm, *Xba*I;

[c], re-ligated pUTKm, *Cla*I;

[d], pCT414, *Xba*I;

[e], pCT414, *Cla*I.

Plasmid pCT414 and re-ligated pUTKm (minus *xylE*) are diagrammatically represented with the relevant restriction sites.



expression of a number of phase variant characteristics. Exconjugates were confirmed phenotypically by patching onto NA supplemented with Km, Sm and either SRBC, egg yolk, gelatin or Congo red (see section 2.2) to detect haemolytic activity, phospholipase C activity, protease activity and Congo red binding respectively. All exconjugates produced antimicrobial substances capable of inhibiting *M. luteus* (see section 2.2). Three exconjugates carrying the *xpsA-lacZ* transcriptional fusion, which displayed the same phenotype as wild type *X. bovienii* (Table 6.1), were selected for further analysis. The *X. bovienii xpsA-lacZ* transcriptional fusion transposon insertions will be referred to as XB414.1, XB414.2 and XB414.3

6.2.2.4 Confirmation of an *xpsA-lacZ* insertion in XB414.1, XB414.2 and XB414.3

PCR analysis of chromosomal DNA isolated from XB414.1, XB414.2 and XB414.3, using oligonucleotide pair P364/P735, was used to confirm the insertion of *lacZ*. A 371 bp fragment of *lacZ* was amplified from chromosomal DNA isolated from each of the three insertions strains (Figure 6.6, Panel A). No PCR product was observed for the negative control wild type *X. bovienii* chromosomal DNA, whilst a 371 bp product was observed for positive control plasmid DNA purified from pMU575 (Figure 6.6, Panel A).

The presence of *lacZ* DNA was also confirmed by Southern hybridisation analysis of *EcoRI* digested chromosomal DNA from XB414.1, XB414.2 and XB414.3 using a DIG-labelled *lacZ* DNA probe. The DIG-labelled *lacZ* probe was prepared from a 3.2 kb *lacZ* fragment isolated from pMU575 (data not shown). The DIG-labelled *lacZ* probe hybridised to 18.8 kb, 7.7 kb and 21.7 kb DNA fragments from XB414.1, XB414.2 and XB414.3 respectively, as well as positive control pCT414 DNA (Figure 6.6, Panel B). The DNA probe did not hybridise to negative control *X. bovienii* T228 chromosomal DNA.

The PCR and Southern hybridisation data suggest XB414.1, XB414.2 and XB414.3 are the result of independent transposon insertions, and that each carry the *xpsA-lacZ* transcriptional fusion.

Table 6.1

Phenotypic comparison of P1 and P2 *X. bovienii* T228 with *Xenorhabdus xpsA-lacZ* transcriptional fusion mutants XB414.1, XB414.2 and XB414.3. A + denotes activity, a – denotes no activity.

	Antimicrobial Activity	Congo Red Binding	Protease Activity	Haemolysin Activity	Phospholipase C Activity
Wild type					
<i>X. bovienii</i> T228 P1	+	+	+	+	+
<i>X. bovienii</i> T228 P2	-	-	-	-	-
Transcriptional fusion mutants					
XB414.1 P1	+	+	+	+	+
XB414.1 P2	-	-	-	-	-
XB414.2 P1	+	+	+	+	+
XB414.2 P2	-	-	-	-	-
XB414.3 P1	+	+	+	+	+
XB414.3 P2	-	-	-	-	-

Figure 6.6

Panel A

PCR analysis of transposon insertions carrying the *xpsA-lacZ* transcriptional fusion. PCR was used to test the presence of a *lacZ* fragment in XB414.1, XB414.2 and XB414.3. Oligonucleotide pair P364/P735 generated a 371 bp PCR product when used to amplify pCT414 plasmid DNA and XB414.1, XB414.2 and XB414.3 chromosomal DNA. Negative control samples (lane b, no DNA and lane d, *X. bovienii* T228 chromosomal DNA) did not generate a product. 100 bp markers (DMW-100) were used and the 1 kb band is indicated.

Panel B

Southern hybridisation analysis of *EcoRI* digested chromosomal DNA from *X. bovienii* T228, XB414.1, XB414.2 and XB414.3. Positive control plasmid pCT414 remained undigested. The filter was probed with a digoxigenin labelled 3.2 kb *BamHI/DraI* fragment encoding *lacZ* from pMU575. The sizes of DNA fragments hybridising with probe DNA are shown.

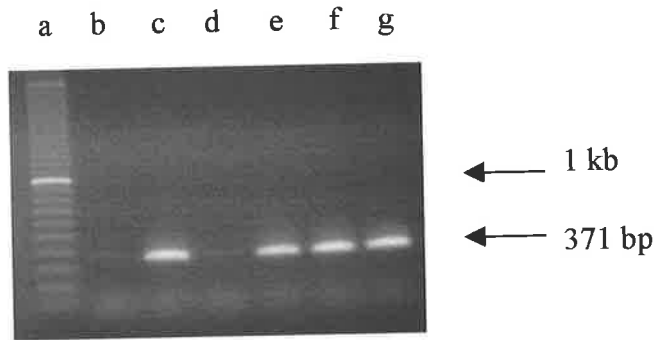


Figure 6.6 Panel A

Lanes:

- [a], 100 bp marker DMW-100M (the 1 kb band is noted);
- [b], no DNA;
- [c], pCT414;
- [d], *X. bovienii* T228 chromosomal DNA;
- [e], XB414.1 chromosomal DNA;
- [f], XB414.2 chromosomal DNA;
- [g], XB414.3 chromosomal DNA

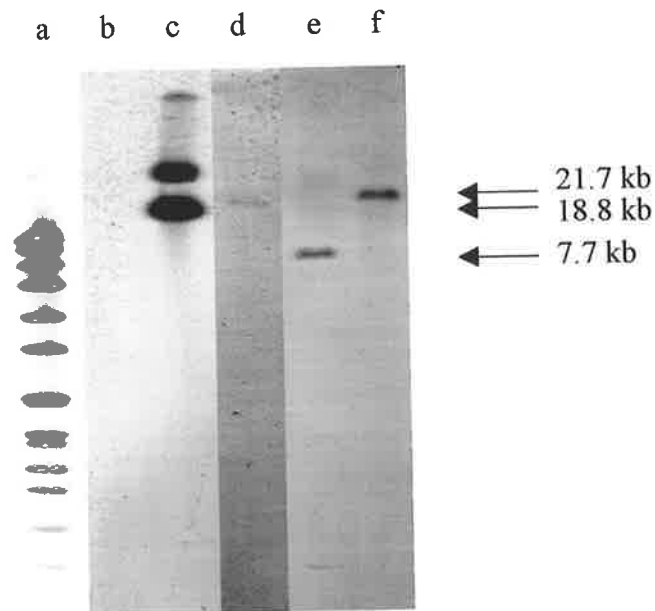


Figure 6.6 Panel B

Lanes:

- [a], SPP1 marker; *Bacillus subtilis* phage SPP1 DNA digested with *Eco*RI;
- [b], *Eco*RI digested *X. bovienii* T228 chromosomal DNA;
- [c], undigested pCT414;
- [d], *Eco*RI digested XB414.1 chromosomal DNA;
- [e], *Eco*RI digested XB414.2 chromosomal DNA;
- [f], *Eco*RI digested XB414.3 chromosomal DNA

6.2.3 Influence of culture conditions on expression of *xpsA-lacZ* fusions by XB414.1, XB414.2 and XB414.3

6.2.3.1 Refinement of β -galactosidase assay conditions

Preliminary studies showed each transposon mutant carrying the *xpsA-lacZ* transcriptional fusion expressed β -galactosidase when grown in nutrient media containing the substrate X-gal. To quantitatively test expression of β -galactosidase by strains carrying the *xpsA-lacZ* fusion, a modified Miller assay was employed.

Wild type *X. bovienii* and the transposon mutants carrying transcriptional fusions were grown O/N at 28°C in LB broth. *E. coli* SY327 λ pir[pCT414] and *E. coli* SY327 λ pir were included as positive and negative controls respectively. *E. coli* SM10 λ pir, used as a donor for conjugal transfer of pCT414 to *X. bovienii*, could not be used as a negative control since this host is β -galactosidase positive.

Preliminary experiments using the standard Miller protocol (Miller, 1972) clearly indicated that ONPG was hydrolysed by cultures of XB414.1, XB414.2 and XB414.3. However, most of the β -galactosidase activity was associated with cells and cellular debris. Thus calculation of the number of β -galactosidase units in experimental samples was usually small or negative in magnitude¹. To address this problem, cultures to be tested were treated with Z buffer as per

¹ According to the standard Miller protocol, β -Gal units are calculated using the following equation.

$$\beta\text{-Galactosidase Units} = \frac{1000(A_{410} - 1.75 \times A_{570})}{t \times V \times A_{600}}$$

Where A_{410} = a combination of absorbance by the *o*-nitrophenol and light scattering by the cell debris, A_{570} = light scattering from cell debris (no contribution from *o*-nitrophenol), A_{600} = absorbance by the culture to be tested prior to the assay, t = time of assay in minutes, V = volume of culture used in ml prior to dilution in Z buffer. The light scattering at 410 nm is proportional to that at 570 nm. For *E. coli*, the A_{410} light scattering = $1.75 \times A_{570}$. If the A_{570} of the sample to be tested is $> A_{410}$ then the β -galactosidase units estimated will be small or negative in magnitude. This situation can occur when cells present in the sample have not been lysed or there is significant material that absorbs at a wavelength of 570 nm. In addition, since the original assay was developed for *E. coli*, *Xenorhabdus* cultures may contain significant material that absorbs at a wavelength of 570 nm that affects the calculation of β -galactosidase units.

the standard protocol, centrifuged to remove cells and cellular debris and the supernatant tested for β -galactosidase activity. Supernatants obtained contained little β -galactosidase activity and this result indicated much of the activity resided with the cell pellets. One possible explanation for this result is that cells to be tested were not efficiently lysed by the Z buffer.

To test this hypothesis, lysozyme (1mg/ml) was added to the Z buffer, in which bacterial cells were diluted, prior to centrifugation and testing of the supernatant for β -galactosidase activity. Units of β -galactosidase activity were calculated using a modified version of the Miller equation that accounts for the absence of cellular debris². The β -galactosidase activity with and without the addition of lysozyme, of wild type *X. bovienii*, XB414.1, XB414.2 and XB414.3 grown in LB broth was then compared. Significant differences were observed between cultures treated with lysozyme and those not treated (Figure 6.7). Supernatants prepared from the positive control culture *E. coli* SY327 λ pir[pCT414], showed a 4 fold increase in β -galactosidase activity when cultures were treated with lysozyme, whilst XB414.1, XB414.2 and XB414.3 showed a 3 – 5 fold increase. As expected supernatants prepared from negative control cultures *X. bovienii* T228 and *E. coli* SY327 λ pir showed no activity (Figure 6.7). This data indicated that addition of lysozyme to Z buffer was required to ensure efficient lysis of *Xenorhabdus* cells and release of cytoplasmic β -galactosidase. Consequently, lysozyme was routinely added to Z buffer for all subsequent experiments.

² Modified Miller equation.

$$\beta\text{-Galactosidase Units} = \frac{1000 \times A_{410}}{t \times V \times A_{600}}$$

(Where A_{410} , A_{600} , t and V are defined as for Footnote 2.)

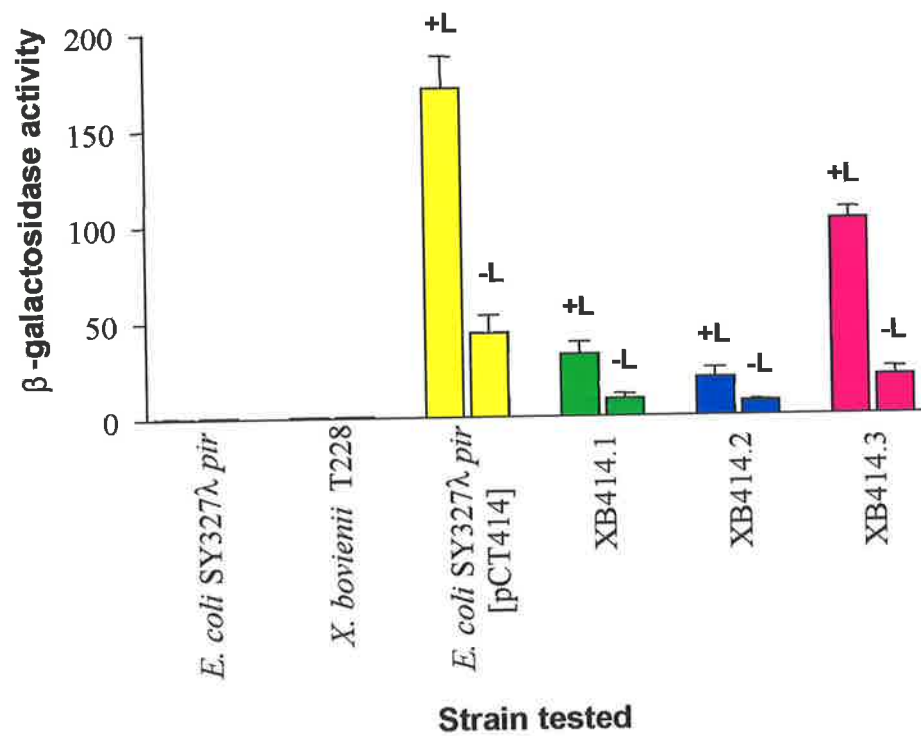


Figure 6.7 Comparison of β -galactosidase activity for cultures treated with Z buffer containing 1 mg/ml (+L) and those treated with Z buffer alone (-L).

β -galactosidase activity for *E. coli* SY327 λ *pir* and *X. bovienii* T228 was less than 1.0. Error bars represent the standard deviation.

6.2.3.2 Growth of wild type *X. bovienii*, XB414.1, XB414.2 and XB414.3 on Luria Bertani medium (LB) and *Xenorhabdus* minimal medium (XMM) and expression of *xpsA-lacZ* fusions

To investigate the nutritional requirements that may affect expression of *X. bovienii* NRSP, this organism was grown in a rich (LB medium) and minimal (XMM) growth media. Interestingly, *X. bovienii*, XB414.1, XB414.2 and XB414.3 grow poorly in XMM broth, but grow well on XMM agar. For this reason, cultures to be tested were grown on solid medium and resuspended in the corresponding liquid medium prior to testing expression of β -galactosidase

XB414.1, XB414.2 and XB414.3 were cultured on LB agar or XMM agar at 28°C O/N, cells harvested from the medium surface and resuspended in corresponding liquid medium at an A_{600} about 1.0. The β -galactosidase activity of these suspensions were then determined. A 3 fold difference in β -galactosidase activity of transcriptional fusion mutants grown on an LB agar surface compared with those grown on XMM medium was observed. As expected *X. bovienii* T228 and *E. coli* SY327 λ *pir* cultures expressed negligible β -galactosidase activity. The positive control *E. coli* SY327 λ *pir*[pCT414] showed no difference in β -galactosidase expression when cultured on either XMM or LB agar media (Figure 6.8).

The β -galactosidase activity of XB414.1, XB414.2 and XB414.3 grown in LB broth and on LB agar was then compared. Unexpectedly, the β -galactosidase activity of XB414.1, XB414.2 and XB414.3 grown O/N on LB agar, and resuspended in fresh LB broth for testing, was found to express 2-3 fold higher levels of β -galactosidase than those grown O/N in LB broth (Figure 6.9). This differential response observed could not be demonstrated for cultures of *E. coli* SY327 λ *pir*[pCT414]. However β -galactosidase levels expressed by this strain were 2-5 fold higher than those observed for cultures of XB414.1, XB414.2 and XB414.3 (Figure 6.9). As expected *X. bovienii* T228 and *E. coli* SY327 λ *pir* expressed negligible amounts of β -galactosidase.

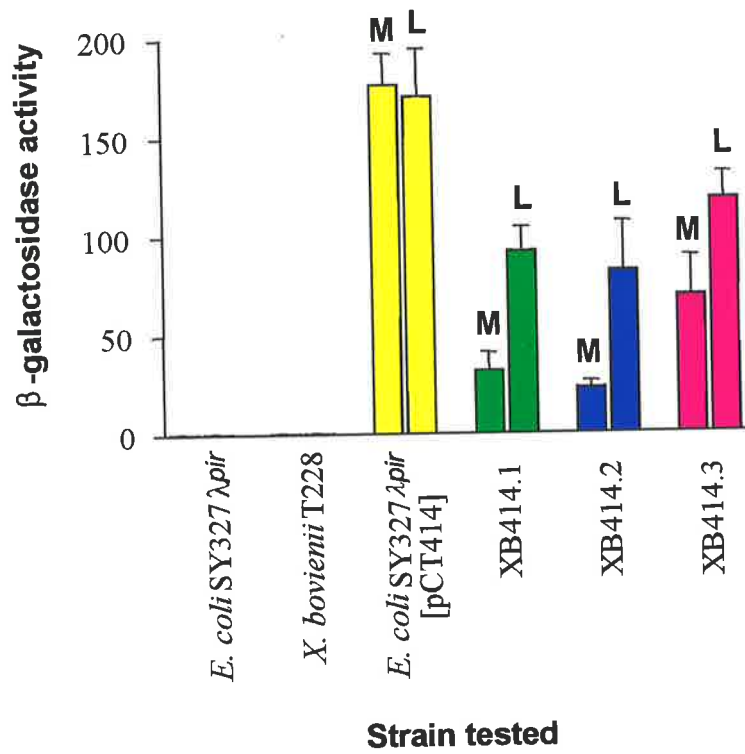


Figure 6.8 Comparison of β -galactosidase activity for cultures grown on LB agar (L) or XMM agar (M).

β -galactosidase activity for *E. coli* SY327 λ pir and *X. bovienii* T228 was less than 1.0. Error bars represent the standard deviation.

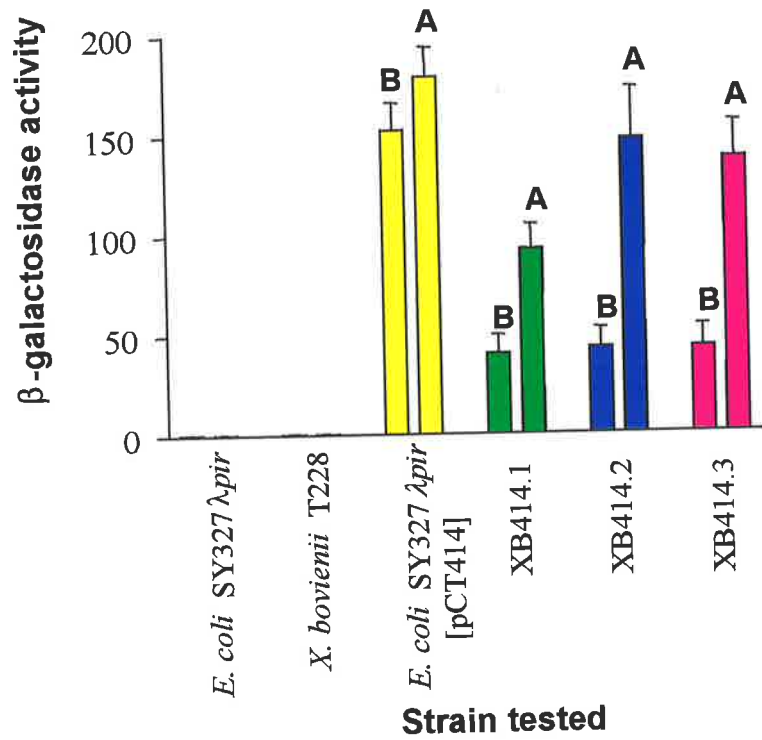


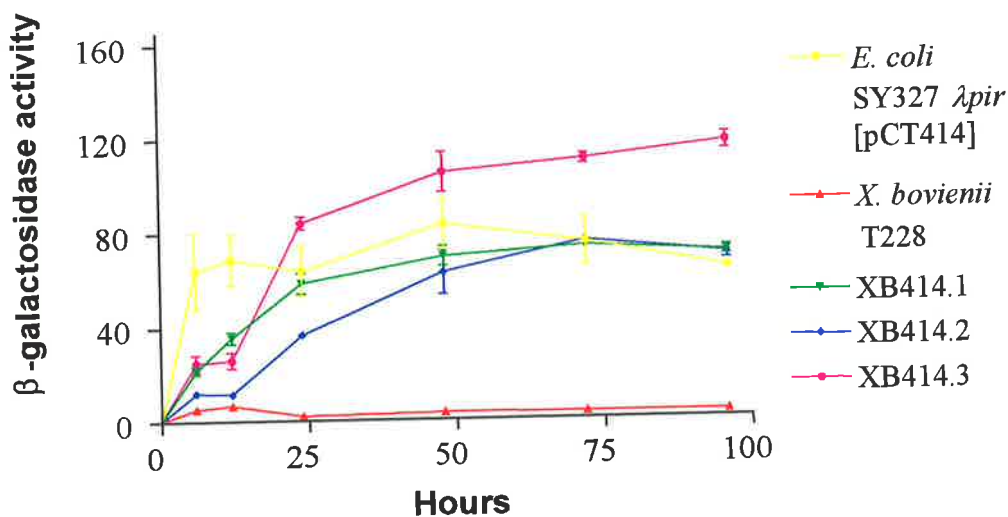
Figure 6.9 Comparison of β -galactosidase activity for cultures grown in LB broth (B) or on LB agar (A).

β -galactosidase activity for *E. coli* SY327 λ pir and *X. bovienii* T228 was less than 1.0. Error bars represent the standard deviation.

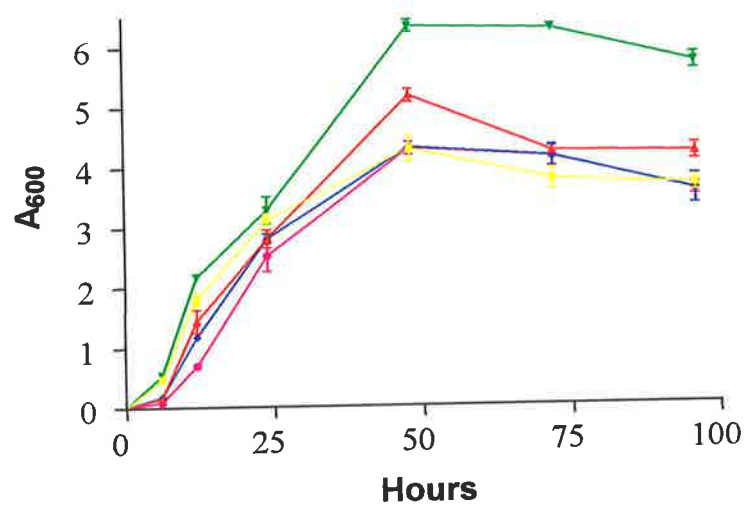
6.2.3.3 β -galactosidase expression by XB414.1, XB414.2 and XB414.3 at different initial cell culture densities over a 96 hr time period

In section 6.2.3.3, β -galactosidase expression by XB414.1, XB414.2 and XB414.3 was shown to increase when cultures were grown on LB agar O/N compared with culture in LB broth. This observation may be explained by a quorum sensing mechanism that acts in *Xenorhabdus* culture. Signalling molecules that represent a component of such a mechanism would be expected to be concentrated in an agar, and accumulate only slowly in broth culture. If this hypothesis were correct, the differential expression of β -galactosidase by solid vs liquid cultures could indicate the importance of signalling and cell density in the expression of NRPS. If a quorum sensing mechanism is involved in expression of XpsA, expression in extended culture should occur as signalling molecules accumulate to critical levels. To test the hypothesis that a signalling molecule may be involved in expression of XpsA, cultures of XB414.1, XB414.2 and XB414.3 were grown in LB broth for up to 96hr at 28°C with shaking. Samples of cultures were tested for β -galactosidase activity after 6, 12, 24, 48, 72 and 96 hr incubation. As expected the β -galactosidase activity of *E. coli* SY327 λ *pir* and *X. bovienii* was negligible. However by 6 hr, samples of *E. coli* SY327 λ *pir*[pCT414] cultures expressed 65 units of β -galactosidase and maintained this level of expression over 96hr (Figure 6.10, Panel A). This level of expression was independent of the increase in culture density (Figure 6.10, Panel B).

By comparison, the β -galactosidase activity of XB414.1, XB414.2 and XB414.3 cultures gradually increased over time. After 96 hrs incubation, an approximately 6 fold increase in β -galactosidase activity was observed compared to the 6 hr time point. Furthermore, the β -galactosidase activity of these cultures equalled or exceeded that of *E. coli* SY327 λ *pir*[pCT414] (Figure 6.10, Panel A). In addition, the change in β -galactosidase activity coincided with an increase in culture cell density (Figure 6.10, Panel B). These results suggest the expression of *X. bovienii* NRSP is dependent on culture density.



Panel A



Panel B

Figure 6.10

Panel A β -galactosidase activity of cells from cultures grown in LB broth for 96 hrs at 28° C.

The negative controls *E. coli* SY327 λ pir and *X. bovienii* T228 showed negligible β -galactosidase activity (less than 1.0). And were not graphed to simplify interpretation. Error bars represent the standard deviation.

Panel B A_{600} of Panel A strains over the same 96 hr time period.

6.2.3.4 β -galactosidase activities of XB414.1, XB414.2 and XB414.3 at different initial cell culture densities over a 96 hr time period in 20% (v/v) conditioned LB broth

Cell density dependent gene expression has been reported previously for *X. bovienii*. This phenomenon is thought to be controlled by a homoserine lactone autoinducer expressed by these bacteria (Dunphy *et al.*, 1997). To test the hypothesis that a signalling molecule is required to reach a critical level for optimum expression of *X. bovienii* NRSP, the 96 hr time course experiment was repeated using conditioned media which presumably contained high levels of the signalling molecule. The culture supernatant from a 96 hr LB culture of *X. bovienii* was collected and filter sterilised using a 0.22 μ m filter. The filtered supernatant was diluted to a final concentration of 20% (v/v) in fresh LB broth and used as a potential source of autoinducer (Dunphy *et al.*, 1997). The results of these experiments are shown in Figure 6.11. Control cultures of *X. bovienii* T228 and *E. coli* SY327 λ pir, expressed negligible levels of β -galactosidase in the presence and absence of conditioned medium (Figure 6.11, Panel A and Panel B). Furthermore, the β -galactosidase activity of XB414.1, XB414.2 and XB414.3 cultures grown in the presence and absence of conditioned media was not significantly different at any time point during extended culture. In particular, expression of β -galactosidase by strains carrying the *xpsA-lacZ* fusion was not significantly different during the first 25 hours of culture. In the presence of an autoinducer signalling molecule, it was expected that expression of β -galactosidase by strains carrying the transcriptional fusion would be significantly increased during the early stages of culture. In the absence of any significant effect of conditioned media on expression from the *xpsA-lacZ* fusion, this data indicates *xpsA* is probably not regulated by an autoinducer signalling molecule.

6.2.4 Translation of XpsA

In the previous section, a promoter-reporter gene fusion was used as a tool to examine aspects of regulation of *xpsA* at the transcriptional level. To obtain information about expression of the *xpsA* gene product in *Xenorhabdus*, the gene was over-expressed in *E. coli* BL21 and preparations of this strain used to raise antibodies that could be used as a tool in Western analysis. PCR was used to amplify *xpsA*. The amplicon was then cloned into pET29a(+) under control of the T7 RNA polymerase promoter (see section 2.19 – 2.23).

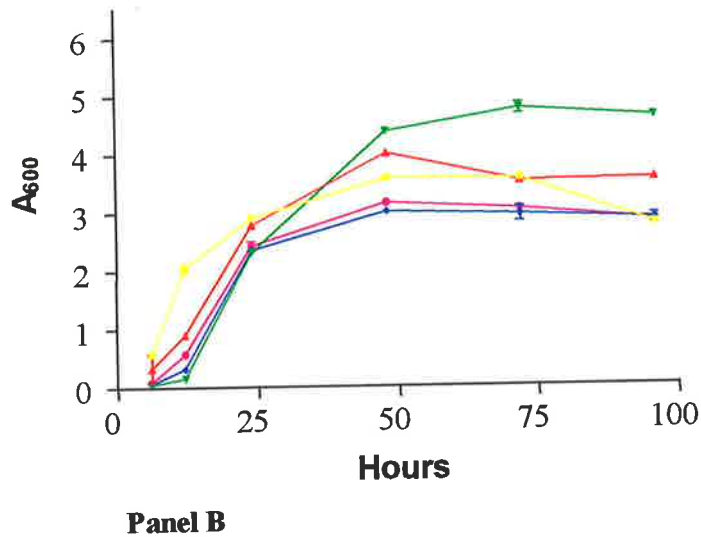
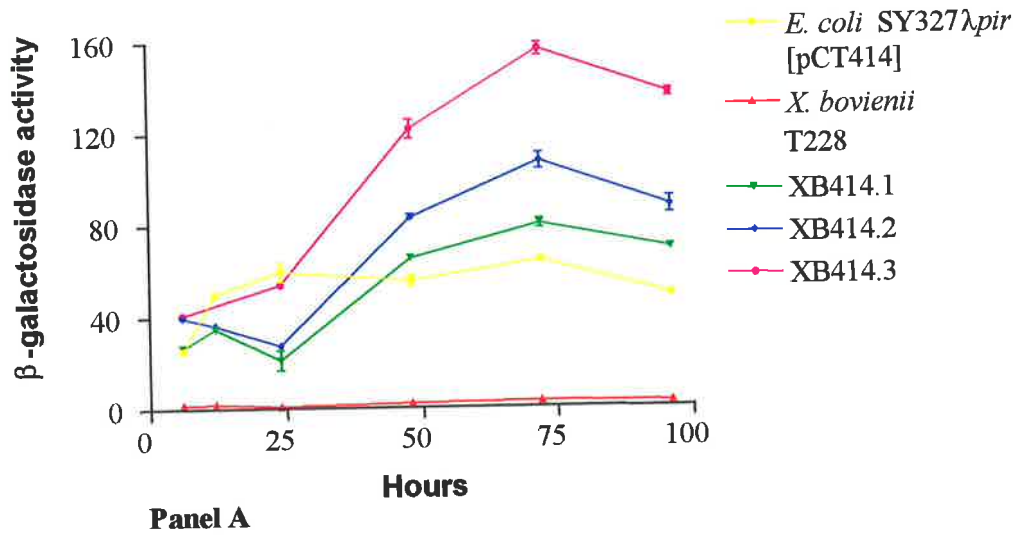


Figure 6.11

Panel A β -galactosidase activity of cells from cultures grown in 20% (v/v) conditioned LB broth for 96 hrs at 28° C.

The negative controls *E. coli* SY327 λ pir and *X. bovienii* T228 showed negligible β -galactosidase (less than 1.0), and results were not graphed to simplify interpretation. Error bars represent the standard deviation.

Panel B A_{600} of Panel A strains over the same 96 hr time period.

The over-expressing strain was used to immunise mice. Pooled sera were then used as a source of anti-XpsA antibodies.

6.2.4.1 Construction of XpsA expression vectors pCT445 and pCT446

PCR was used to amplify a 3209 bp product encoding *xpsA* from *X. bovienii* T228 chromosomal DNA using oligonucleotides P3412/P5435 (data not shown). Forward oligonucleotide primer, P3412, incorporates an *NdeI* restriction enzyme site at the ATG position of *xpsA*. The reverse primer P5435 binds 66 bp from the 3' of *xpsA*. The PCR product was cloned into pGEM-T and the ligation mix used to transform *E. coli* DH5 α by electroporation. Transformants were selected on NA supplemented with Amp, IPTG and X-gal. Plasmid DNA isolated from transformants were confirmed by an *NdeI/NotI* digestion (data not shown) and the plasmid designated pCT445. Digestion of pCT445 DNA with *NdeI/NotI* removed the PCR product as a 3225 bp fragment. This fragment was then cloned into *NdeI/NotI* digested pET29a(+) (Figure 6.12). The ligation mix was used to transform *E. coli* BL21 and transformants selected on NA supplemented with Km. Colony pooling and subsequent PCR analysis using oligonucleotides P3412/P5435 identified a positive clone, designated pCT446, by the presence of a 3209 bp PCR product (data not shown). Plasmid pCT446 was further confirmed by digestion with *NdeI/NotI* (data not shown). Final confirmation of pCT446 was obtained by dye-terminator sequencing of plasmid DNA using the T7 promoter primer. Details of the 5' and 3' ends of the construct are shown in Figure 6.13.

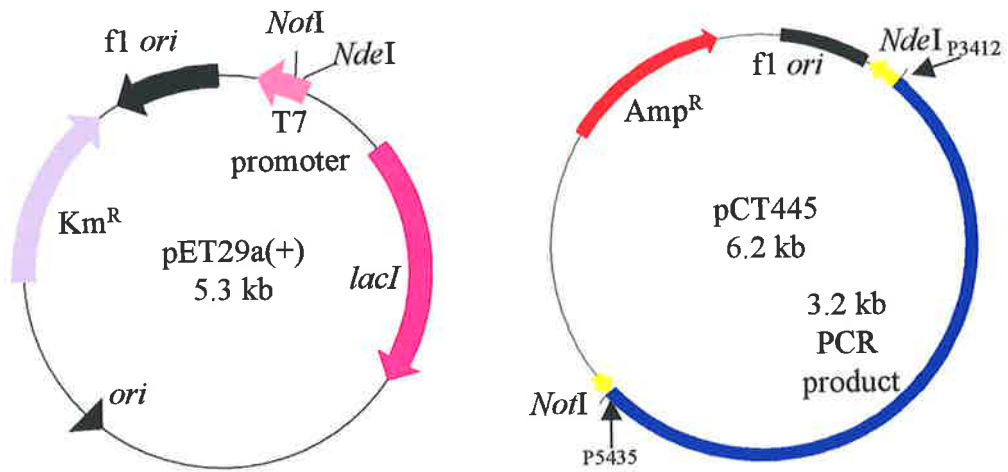
6.2.4.2 Over-expression of XpsA in *E. coli* BL21

E. coli BL21[pCT446] was induced with 0.4 mM IPTG and whole cell lysates analysed by electrophoresis on a 10% SDS-polyacrylamide gel (see section 2.21). A protein of approximately 120 kDa was found to be expressed by *E. coli* BL21[pCT446] whole cell lysates, but not by the negative control strains *E. coli* BL21 and *E. coli* BL21[pET29a(+)] (Figure 6.14). The predicted M_r of XpsA is 122,980 Da (see Chapter 4, section 4.2.6.2). The molecular size of the over-expressed 66 bp (32 amino acid) truncated XpsA is in good agreement with the predicted size.

Figure 6.12 Construction of plasmids pCT445 and pCT446.

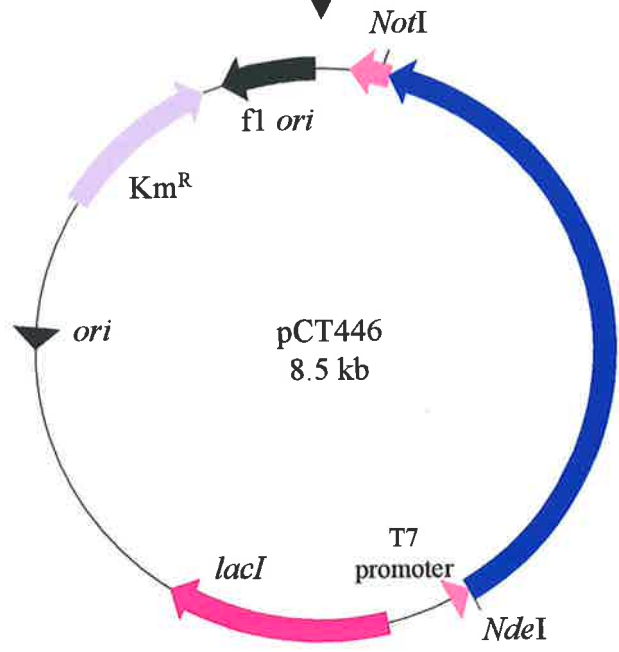
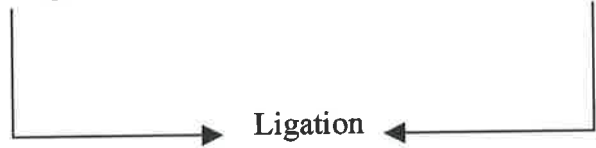
A 3270 bp PCR product, created by amplification of *X. bovienii* T228 chromosomal DNA by oligonucleotide pair P3412/P5435, was cloned into pGEM-T and designated pCT445. Plasmid pCT445 was digested with *NdeI/NotI* to excise the PCR product as a 3225 bp fragment, which was subsequently cloned into *NdeI/NotI* digested pET29a(+) and designated pCT446.


Abbreviations: Amp^R, ampicillin resistance gene; f1 *ori*, f1 origin of replication; Km^R, kanamycin resistance gene; *lacI*, lac repressor gene; *ori*, origin of replication; T7 promoter, T7 promoter region.



NdeI/NotI digestion

NdeI/NotI digestion



T7 promoter


AGATCGATCTCGATCCCGCGAAAT**TAATACGACTCACTAT**AGGGGAATTGTGAGCGGATA - 60
rbs NdeI

ACAATCCCCTCTAGAAATAATTTTGTTTAACTTTAAG**GAAGGAGATATACATATGAACCA** - 120
M N H


CCCTGAAAAGTTGAAGCCATTTGCTTTATCCGAAGCACAAAGCAGCCGTTGGTTTCAATA - 180
 P E K L K P F A L S E A Q S S R W F Q Y

·
 ·
 ·
 ·

AGAACAACGGCCGATATCTGGCAAAAGTTACTGAAAATCGATCGCGTTGGGCGTAATGA - 3180
 E Q L A D I W Q K L L K I D R V G R N D

CAACTTTTTCGAACTGGGGGGTCATTCGCTGCTGATGCTACAGCTACAGTCAAGAATAAG - 3240
 N F F E L G G H S L L M L Q L Q S R I S

P5435

TGAAAACCTTGTATGTCGAACTCTCTATTCAACAATTATTTGCACACCCCACTATTT**GTCA** - 3300
 E N F D V E L S I Q Q L F A H P T I C 

NotI


ACTTGAAGAGCACATTAATCACTAGT**GCGGCCGCACTC**  pET29a(+)
 L E E H I I H *

Figure 6.13 Nucleotide sequence of *xpsA* cloned into the *NdeI/NotI* sites of expression vector pET29a(+). The nucleotides are numbered to the right hand side in the 5' to 3' direction. The deduced protein sequence of the open reading frame is given below the DNA sequence in single letter code format. Only the 5' and 3' ends of *xpsA* are shown. See Chapter 5, Figure 5.1 for the entire nucleotide and amino acid sequence of *xpsA*.

The T7 promoter region and rbs (ribosome binding site) are noted. Oligonucleotide P5435 was used with P3412 to amplify a 3209 bp PCR product from *X. bovienii* chromosomal DNA.

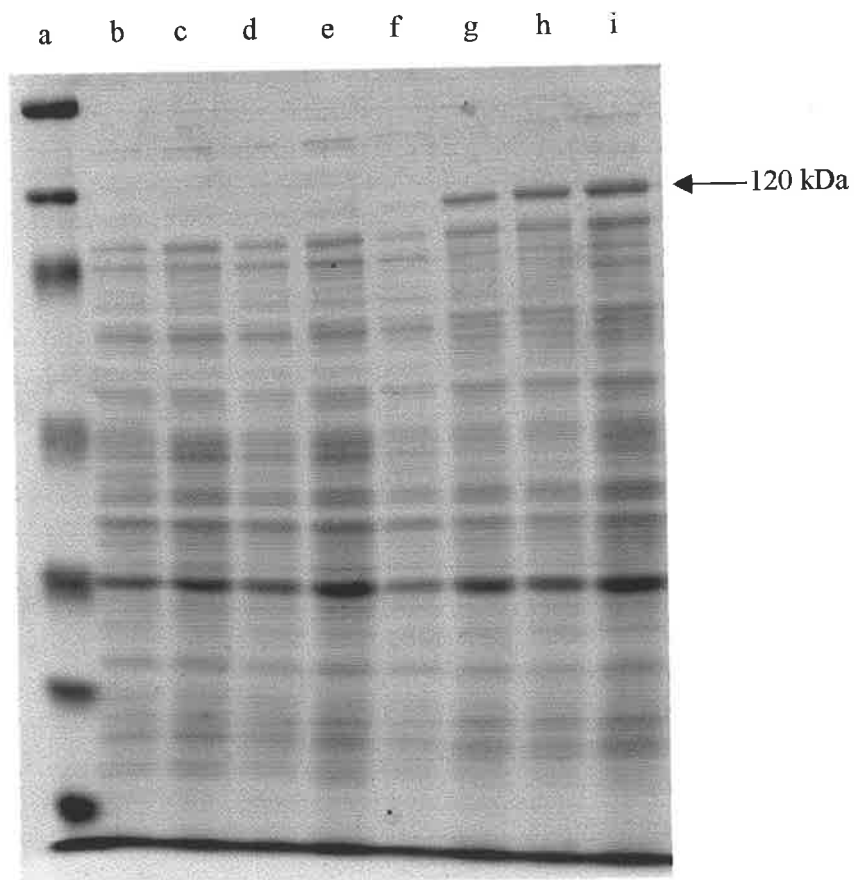


Figure 6.14 Over-expression of XpsA in *E. coli* BL21[pCT446]. Cultures were induced with 0.4 mM IPTG and samples taken 2 hr, 4 hr and O/N post induction.

Lanes:

- [a], BIORAD Prestained SDS-PAGE Standards (205, 120, 84, 52.2, 36.3, 30.2, 21.9 kDa)
- [b], *E. coli* BL21 (non-induced)
- [c], *E. coli* BL21 (O/N after induction)
- [d], *E. coli* BL21 [pET29a(+)] (non-induced)
- [e], *E. coli* BL21 [pET29a(+)] (O/N after induction)
- [f], *E. coli* BL21[pCT446] (non-induced)
- [g], *E. coli* BL21 [pCT446] (2 hr after induction)
- [h], *E. coli* BL21 [pCT446] (4 hr after induction)
- [i], *E. coli* BL21 [pCT446] (O/N after induction)

Whole cell lysates of *E. coli* BL21[pCT446], induced with 0.4 mM IPTG, were separated by SDS PAGE and the proteins transferred to nitrocellulose. The 120 kDa XpsA protein band was excised, dissolved in DMSO, reconstituted as a colloidal suspension in bicarbonate solution and combined with incomplete Freund's adjuvant. The antigen preparation was then used to raise a polyclonal antiserum in mice as described in Sections 2.19 – 2.23. The antiserum was absorbed with whole *E. coli* BL21 [pET29a(+)].

To determine if the absorbed XpsA antiserum could detect XpsA expressed by *X. bovienii*, whole cell lysates were subjected to Western analysis. Based on the results of section 6.2.3, which suggested cell density is important for *xpsA* transcription, *X. bovienii* T228 was grown in LB broth for up to 96 hrs at 28°C. Cell culture samples were taken at 6, 12, 24, 48 72 and 96 hr. The initial culture OD (A_{600}) was recorded (Figure 6.15, Panel A), prior to adjustment to an OD of 1.0. Whole cell lysates of *X. bovienii* (equivalent to 2×10^7 cells) from each time point were electrophoresed on a 10% SDS-polyacrylamide gel, along with the negative control *E. coli* BL21[pET29a(+)] and positive control *E. coli* BL21[pCT446]. The results are shown in Figure 6.15, Panel B. *E. coli* BL21[pCT446] whole cell extracts contained a 120 kDa protein, but not *E. coli* BL21[pET29a(+)]. However the *X. bovienii* T228 whole cell lysates contained other proteins of approximately 39 and 43 kDa that were differentially expressed over the 96 hr culture incubation period (Figure 6.15, Panel B).

Western analysis of the SDS-PAGE separated whole cell lysates are shown in Figure 6.15, Panel C. When used at a 1:100 dilution, the XpsA antiserum reacted strongly with the 120 kDa protein expressed by *E. coli* BL21[pCT446]. This anti-XpsA reacting protein was absent in the negative control *E. coli* BL21[pET29a(+)]. Other smaller XpsA reactive proteins were present in the *E. coli* BL21[pCT446] sample which were not present in the vector control.. These proteins may represent degradation products of the 120 kDa protein that can be detected by the XpsA antisera. Surprisingly, the XpsA antiserum did not react with a 120 kDa protein prepared from the *X. bovienii* T228 cultures. However, other common cross reactive proteins were identified in all cell lysates tested.

Figure 6.15

Panel A

A_{600} of the *X. bovienii* T228 cultured in LB at 28°C for up to 96 hrs. Samples were taken at 6, 12, 24, 48, 72 and 96 hrs. Samples of this culture were used for SDS-PAGE and Western analysis discussed below.

Panel B

Whole cell samples from 0.4 mM induced IPTG *E. coli* BL21[pET29a(+)] and *E. coli* BL21[pCT446], and *X. bovienii* taken after 6, 12, 24, 48, 72 and 96 hrs culture in LB broth were adjusted to an A_{600} of 1.0 and solubilised in 1x LUG buffer.

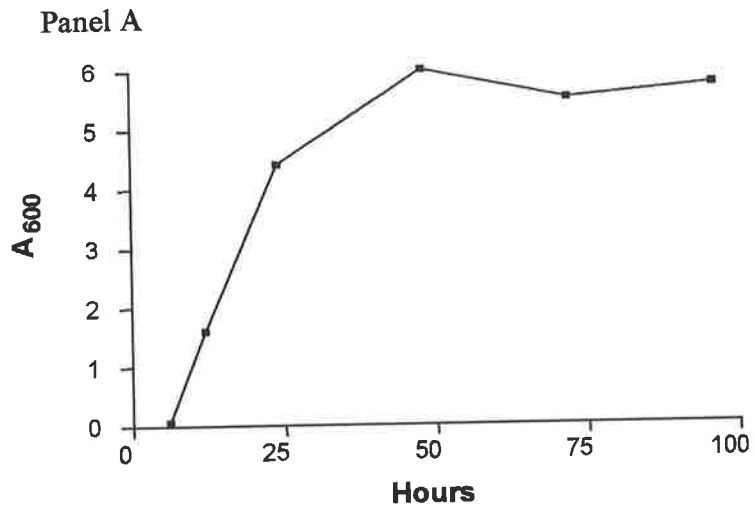
Samples were electrophoresed on a 10% SDS-polyacrylamide gel. The overexpressed 120 kDa XpsA produced by *E. coli* BL21[pCT446] is indicated. Two other proteins, 43 and 39 kDa, showing variable expression are indicated.

Lanes:

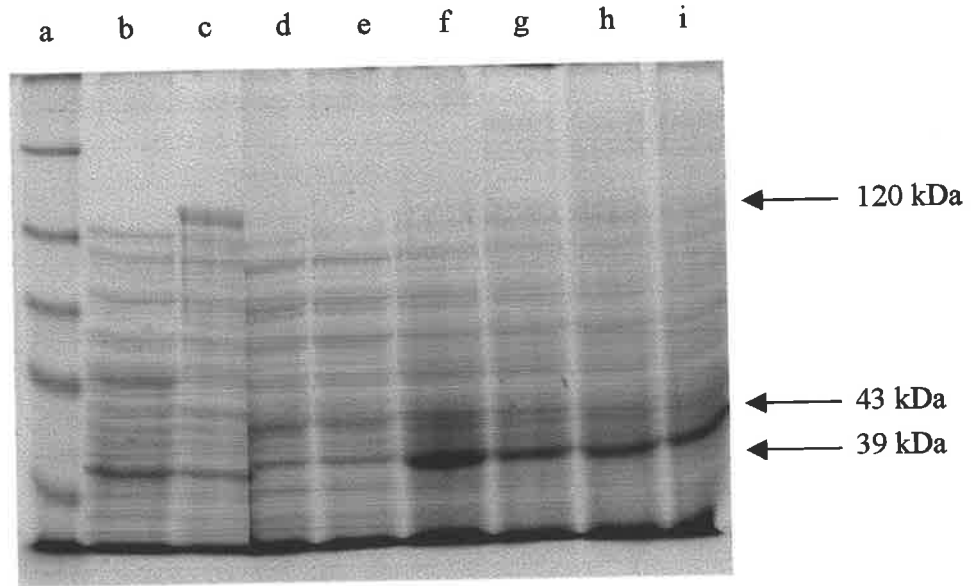
- [a], NEB Prestained protein marker (175, 83, 62, 47.5, 32.5 kDa);
- [b], *E. coli* BL21 [pET29a(+)] (0.4 mM IPTG induced negative control);
- [c], *E. coli* BL21 [pCT446] (0.4 mM IPTG induced positive control);
- [d], *X. bovienii* T228, 6hr;
- [e], *X. bovienii* T228, 12 hr;
- [f], *X. bovienii* T228, 24 hr;
- [g], *X. bovienii* T228, 48 hr;
- [h], *X. bovienii* T228, 72 hr;
- [i], *X. bovienii* T228, 96 hr

Panel C

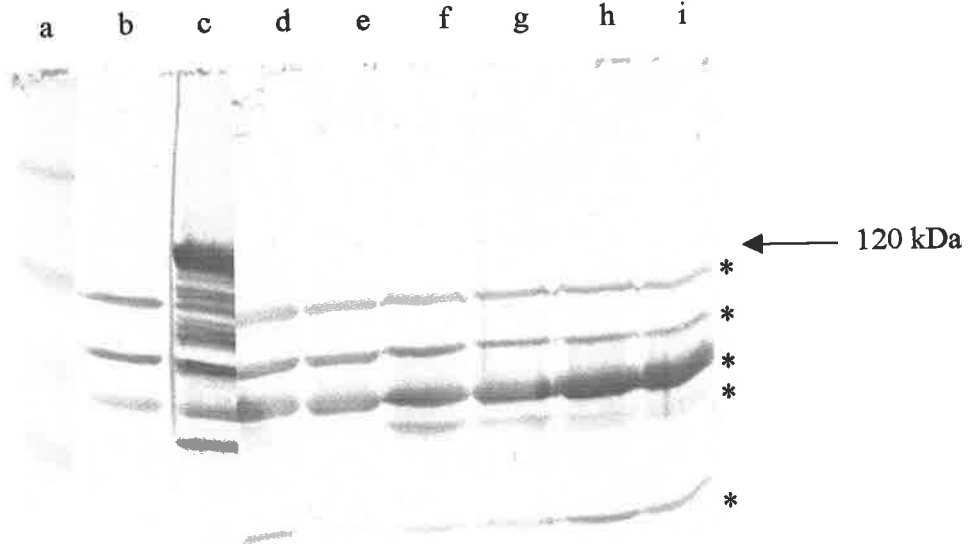
Western analysis of whole cell samples from Panel A using XpsA antiserum. Whole cell lysates were electrophoresed on an 8 % SDS-polyacrylamide gel and transferred to nitrocellulose. At a 1:100 dilution XpsA antiserum reacted with the overexpressed 120 kDa XpsA from *E. coli* BL21[pCT446]. XpsA antisera did not react with any proteins of a similar size in *X. bovienii* T228 samples. The stained bands in lanes [d] – [i] represent cross-reactive antigens. Lane order is the same as Panel B.



Panel B



Panel C



6.3 Discussion

The primary goals of this chapter were to experimentally confirm the *xpsA* promoter region, identify environmental factors controlling transcription and translation of the *X. bovienii* NRPS operon and demonstrate expression of XpsA using an antisera raised against purified XpsA. Identification of transcription was facilitated by measurement of β -galactosidase activity generated by *xpsA-lacZ* transcriptional fusions.

The *xpsA-lacZ* fusion was transferred into *X. bovienii* on a Tn5 based transposable element as a means of incorporating a single copy of the *xpsA-lacZ* transcriptional fusion into the *X. bovienii* chromosome. Mini-Tn5 Km elements constructed by (De Lorenzo *et al.*, 1990) can be used to create stable chromosomal insertions by cloning the *xpsA-lacZ* transcriptional fusion between the 19 bp terminal repeat sequences (I and O end). When transferred to *Xenorhabdus* by conjugative transfer via a suicide vector, independent transposon insertion mutants that carry *xpsA-lacZ* transcriptional fusion can be created. Three such constructs were selected and expression of β -galactosidase used to determine the effects of growth conditions on transcription of *xpsA*.

Chromosomal DNA flanking XB414.1, XB414.2 and XB414.3 was not characterized because each strain was not growth impaired, have essentially identical β -galactosidase activity and within the limitations of this study, were phenotypically identical to the wild type parent. However, the effects of insertion mutation induced polarity on expression of *xpsA* cannot be excluded even though this is unlikely. Ideally, strains carrying the transcriptional fusions should be constructed by introduction from single copy or low copy number vectors into a *recA* host background. This preferred approach was attempted, but rejected because the available IncW based, low copy number *lacZ* fusion vector (Praszkier *et al.*, 1989) was shown to be unable to replicate in *X. bovienii*. The use of low copy number vectors in this context is important to avoid gene dosage effects that might titrate out *xpsA* interacting regulatory proteins.

In this chapter, the specific environmental requirements for expression of *X. bovienii* NRSP were to be investigated. The effects of iron, pH and temperature, for example, on regulation of NRPS from a range of microorganisms such as *Pseudomonas syringae* (Gross, 1985), *Streptomyces* sp. (Zhang *et al.*, 1989) and *Penicillium* sp. (Revilla *et al.*, 1986) have already

been established. However, this approach ideally requires the use of chemically defined *Xenorhabdus* minimal growth medium. In the absence of a suitable minimal growth medium, depletion of specific ions from growth media by addition of sequestering agents could be used as a means to examine the influence of ions on regulation of expression of the NRPS. Both approaches are extensively reported in the literature. In the absence of a chemically defined growth medium for *X. bovienii*, a simple mineral salts solution containing glucose and casamino acids was used as a minimal growth medium for studies of culture cell density on expression of *xpsA*.

Cell culture density was found to affect *xpsA* expression when *X. bovienii* transposon insertions, carrying an *xpsA-lacZ* transcriptional fusion, were grown in LB medium. β -galactosidase activity expressed by cultures encoding the *xpsA-lacZ* fusion, increased with culture cell density. However, the expression of *xpsA-lacZ* from *E. coli* SY327 λ *pir* [pCT414] was not affected by cell culture density. Expression of β -galactosidase from *E. coli* SY327 λ *pir* [pCT414] was initially higher than that of XB414.1, XB414.2 or XB414.3, but remained constant and did not increase in accordance with cell culture density. However, by the 72 hr sampling point β -galactosidase activity from a single copy on the chromosome of XB414.1, XB414.2 and XB414.3 was greater than that for *E. coli* SY327 λ *pir*[pCT414]. The high copy number of the vector used to construct pCT414 probably accounts for the initially high levels of β -galactosidase expressed by *E. coli* SY327 λ *pir* [pCT414]. Furthermore as β -galactosidase expression by *E. coli* SY327 λ *pir* [pCT414] is not cell density dependent, in comparison to *Xenorhabdus* cultures, it is likely that a molecule involved in the control of *xpsA* expression is absent in the *E. coli* SY327 λ *pir* host.

The increase in β -galactosidase activity of XB414.1, XB414.2 and XB414.3, which occurred as the entire cell culture density increased, suggested a quorum sensing control mechanism may be involved in regulation of expression of *xpsA*. This type of regulation is typically mediated by the accumulation of one or more self produced signal molecules in the external environment. The signal will diffuse away from the producing cell and be undetected by cells present in a low density population. Only at a relatively high cell density, or in a confined space, will the signal accumulate to the critical concentration required to initiate gene expression (Gray, 1997).

A diverse array of functions, such as luminescence, virulence, conjugation and antibiotic production, are regulated by quorum sensing mechanisms (Gray, 1997). The quorum sensing signaling molecules for Gram negative bacteria are usually *N*-acylhomoserine lactone metabolites and are generally referred to as autoinducers (De Kievit & Iglewski, 2000). In general, autoinducers are host specific, although some are known to be effective in other unrelated hosts. For example, *N*- β -hydroxybutanoyl homoserine lactone (HBHL), the autoinducer of the luminescent system of *Vibrio harveyi*, has been shown to restore virulence to avirulent mutants of *Xenorhabdus nematophilus* (Dunphy *et al.*, 1997). In this study, HBHL stimulated lipase activity secretion by avirulent *X. nematophilus* and lowered the phenoloxidase activity in the haemolymph of insects infected with *X. nematophilus*. Furthermore, mortality of the insects infected with avirulent *X. nematophilus* was restored upon injection with HBHL. Chloroform extraction of medium conditioned with wild-type *X. nematophilus* facilitated the isolation of a compound with the same chromatographic mobility as HBHL. This compound was shown to stimulate the luminescence of a dim autoinducer-dependent mutant of *V. harveyi*. Transfer of the *V. harveyi lux* operon into avirulent and wild-type *X. nematophilus* generated dim and bright luminescent strains respectively (Dunphy *et al.*, 1997). These results indicated HBHL-dependent regulatory systems exists in *V. harveyi* and *X. nematophilus*.

If a quorum sensing mechanism regulates *X. bovienii* NRPS expression, the β -galactosidase activity of *xpsA-lacZ* transcriptional constructs should increase earlier when cultured in the presence of conditioned media containing the signaling molecule. However addition of conditioned media to cultures of *Xenorhabdus xpsA-lacZ* constructs had no effect on expression of β -galactosidase. Thus it is unlikely that a quorum sensing mechanism is involved in expression of *xpsA*. Alternatively, the concentration of signaling molecule in the conditioned media might not have been sufficient to elicit early induction of *xpsA-lacZ* expression. The long incubation times used may also have resulted in degradation of autoinducer. These issues may only be resolved satisfactorily by addition of purified preparations of homoserine lactone autoinducer to *Xenorhabdus xpsA-lacZ* cultures.

Global control of quorum sensing is likely to be very complex. The influence of many regulators on quorum sensing suggests the accumulation of an autoinducer is only part of what bacteria assess before initiating a group response. Consequently bacteria may have the ability to initiate different sets or subsets of group responses depending on the specific environmental

conditions under which dense bacterial populations arise (Gray, 1997). As functions are often controlled by a number of overlapping systems care should be taken when labeling something as a strictly autoinducible response. The best approach is to activate gene expression at the transcriptional level, however even the apparent activation of a gene in response to autoinducer does not necessarily prove direct regulation (Gray, 1997).

An alternative explanation for the culture cell density dependent transcription of *xpsA* is that expression is linked to cell culture starvation. In *Bacillus* species, starvation is known to lead to the induction of genetic competence, sporulation, the synthesis of degradative enzymes, motility and peptide antibiotic production (Marahiel *et al.*, 1993). The genes that function in these processes are activated during the transition from exponential to stationary phase and are controlled by a mechanism that operates primarily at the level of initiation of transcription.

Signals affecting the translation of *X. bovienii* NRPS are uncharacterized. As an alternative to constructing a translation fusion in a similar manner to the *xpsA-lacZ* transcriptional fusion, an XpsA antiserum was produced. The aim of this approach was to examine the translation of XpsA under different environmental conditions using an XpsA antiserum and Western analysis of *X. bovienii* culture whole cell lysates.

XpsA was successfully overexpressed in *E. coli* BL21 as a 120 kDa protein. However although the XpsA antiserum generated in this study reacted strongly with this protein when expressed in *E. coli*, it did not react with any protein of this size in *X. bovienii* T228 whole cell lysates. The antiserum was prepared by immunization of mice with *E. coli* cells expressing a 32 amino acid C-terminal truncated form of XpsA. Since the antiserum reacted with the truncated form of XpsA expressed by *E. coli*, it would be expected that the antiserum would react with the form of XpsA expressed by *X. bovienii*. The C-terminal 32 amino acids are unlikely to play a role in reactivity unless these amino acids direct important tertiary structure necessary for correct folding of the peptide synthetase gene product. A survey of the literature indicates antibodies have previously been generated against other NRPSs. For example, in *Bacillus brevis*, synthesis of gramicidin is catalysed by gramicidin S synthetase 1 (GS1) and 2 (GS2). GS1 and GS2 have both been overexpressed in an *E. coli* host and used to generate specific antisera. Purified and concentrated GS1 and GS2 from *B. brevis* were found to react with the appropriate antisera (Hori *et al.*, 1991). Assuming the NRPS genes are expressed in

X. bovienii it should be possible to generate XpsA specific antibodies for use as a probe in studies concerning regulation of expression.

An alternative explanation for failure to detect presence of the XpsA NRPS, may be the concentration of anti-XpsA antibodies present in the pooled mouse serum. This could be resolved by using higher concentrations of the antiserum in Western analysis (ie. <1:100). This was not done because of the small volume of serum available (3 ml). However, a preferred approach would be to use C-terminal His tag technology to selectively isolate and purify XpsA expressed in an *E. coli* host. Immunisation of animals with purified XpsA should result in a polyclonal antiserum with high titres of specific antibodies and low levels of unwanted antibodies.

As many NRPS genes are extremely large; some more than 15 kb (Challis *et al.*, 2000; Konz & Marahiel, 1999) and *X. bovienii* NRPS is no exception. The cellular energy investment for transcription and translation of the DNA region is therefore significant. If the NRPS is relatively stable with cells and is able to express a large amount of bioactive peptide product, then only low levels of expression of the NRPS may be required. In this case it would be reasonable to hypothesise that the levels of XpsA may be too low to detect by Western analysis using the XpsA antiserum at a dilution of 1:100. Previous attempts to isolate bioactive peptides from *X. bovienii* cultures by column chromatography have only been partially successful (Granger, 2000). These studies indicated the bioactive peptide product was present in low levels making isolation and purification problematic. This indirect evidence suggests the final peptide product by the non-ribosomal thiotemplate mechanism and hence also the NRPS, is expressed in low levels.

The fact that whole cell lysates of *E. coli* BL21[pCT446] contained several unique proteins which reacted with the XpsA antiserum suggests XpsA may degrade either during culture, or during preparation for Western analysis. To establish whether these extra bands are the result of degradation of the 120 kDa over expressed XpsA, the preparative procedures used for Western analysis should include protease inhibitors.

In conclusion, future work concerning a study of regulation of expression of NRPS in *X. bovienii* should focus on the construction of low copy number plasmid based *xpsA* transcriptional and translational fusions. This approach should completely eliminate potential

for introduction of mutation induced polarity, or the disruption of a genes necessary for the expression of *X. bovienii* NRPS. Furthermore, a chemically defined minimal medium that supports growth of this organism is a necessity for future studies of environmental regulation of expression of NRPS.

Chapter 7

Construction and analysis of *X. bovienii* non-ribosomal peptide synthetase in-frame deletion mutants

7.1 Introduction

Chapter six described the construction of *xpsA::lacZ* transcriptional fusion mutants to facilitate examination of *xpsABC* transcription regulation. Results of the *xpsA::lacZ* transcriptional fusion studies showed the level of *xpsABC* mRNA increases over time in accordance to cell density. These results suggested *xpsABC* transcription is regulated by a quorum sensing mechanism. Quorum sensing has previously been identified in *Xenorhabdus* species, and is controlled by a homoserine lactone autoinducer molecule (Dunphy *et al.*, 1997). It is unknown if *xpsABC* is also controlled by the homoserine lactone autoinducer.

This chapter describes analysis of the effect of a *Xenorhabdus* peptide, produced by NRPS, on bacteria and insect cell viability in order to determine a function for this compound. As the *xpsABC* transcription expression profile was known (see Chapter 6) experiments were designed to incorporate the maximum level of *xpsABC* expression.

To facilitate these experiments in-frame deletions were independently constructed within *xpsA*, *xpsB* and *xpsAB* using homologous recombination and the suicide vector pCVD442. *X. bovienii* T228 and *xpsAB* in-frame deletion mutant bacteria were compared for their ability to inhibit insect cells both *in vivo* and *in vitro*. Furthermore each in-frame deletion mutant was compared against wild type bacteria for the ability to inhibit the indicator organism *M. luteus*. Whilst transposon mutants XB26(20), XB29(45) and XB34(45) represent mutations within *xpsA* or *xpsB*, their polarity does not ensure downstream genes are not affected. For this reason in-frame deletion mutations within these genes were constructed to eliminate this issue.

7.2 Results

PCR and homologous recombination were used in the construction of each in-frame deletion mutant. The far 5' and 3' end of *xpsA*, including flanking DNA, were independently amplified from *X. bovienii* chromosomal DNA. Oligonucleotides were designed to incorporate an *EcoRI* restriction enzyme site at one end of each PCR product. *EcoRI* digestion and ligation of the PCR products resulted in a fragment of DNA encoding an in-frame deletion of *xpsA*, characterised by an *EcoRI* site. This fragment was cloned into the suicide vector pCVD442, transferred to *X. bovienii* by conjugation and the in-frame deletion version of *xpsA* exchanged with wild type *xpsA* by homologous recombination. The partial deletion of *xpsA* was confirmed by PCR and Southern hybridisation analysis. A similar strategy was used to construct in-frame deletions within *xpsB* and *xpsAB*.

7.2.1 Construction of the *xpsA* in frame deletion mutant XB6246

The *X. bovienii xpsA* ORF is 3270 nucleotides. An in-frame deletion of 2601 bp was constructed, and this transferred to *X. bovienii* by allelic exchange to create a non-polar *xpsA* deletion mutant XB6246.

7.2.1.1 Cloning of DNA generated by PCR amplification of *X. bovienii* chromosomal DNA, using oligonucleotide pairs P6054/P6247 and P6246/P6256.

The oligonucleotide pair P6247/P6054 was used to PCR amplify a 1209 bp fragment, encoding the 3' end of *xpsD* and the 5' end of *xpsA*, from *X. bovienii* chromosomal DNA (data not shown). Similarly, the oligonucleotide pair P6246/P6256 was used to PCR amplify a 1397 bp fragment, encoding the 3' end of *xpsA* and the 5' end of *xpsB*, from *X. bovienii* chromosomal DNA (data not shown). Both oligonucleotides P6246 and P6247 bind within *xpsA* and have *EcoRI* restriction enzyme sites incorporated into their 5' ends.

The 1209 and 1397 bp PCR products were digested with *EcoRI* and ligated together to produce a 2604 bp fragment (data not shown). Since the undigested ends of the ligated PCR products had an A nucleotide incorporated by *Taq* polymerase during amplification, the 2064 bp fragment were cloned into pGEM-T. The subsequent ligation mix was used to transform *E. coli* DH5 α by electroporation, and transformants selected by plating on NA supplemented

with Amp, IPTG and X-gal. The correct construct (pCT420), was selected by PCR amplification of a 1381 bp fragment (data not shown) using oligonucleotides P6034/P6054 (Figure 7.1). Had the P6054/P6247 *EcoRI* digested PCR fragment had ligated with itself and then to pGEM-T, a 2396 bp amplicon would have been produced from plasmid DNA using the oligonucleotide pair P6034/P6054. Similarly, had the P6246/P6256 *EcoRI* digested PCR fragment ligated with itself and then to pGEM-T, a 362 bp amplicon would have been produced using the oligonucleotide pair P6034/P6054. Nucleotide sequence analysis of plasmid pCT420 using P6034 confirmed the presence of an *EcoRI* site and maintenance of the correct reading frame (Figure 7.2).

7.2.1.2 Construction of plasmid pCT421 and pCT422

Restriction enzyme digestion of pCT420 plasmid DNA with *SalI/SphI* removed the correctly ligated PCR products as a 2658 bp fragment (data not shown). This fragment was ligated to *SalI/SphI* digested pCVD422, and the ligation mix used to transform *E. coli* SY327 λ *pir* by electroporation. Transformants were selected on NA supplemented with Amp, and screened by *SalI/SphI* restriction enzyme digestion to recover the cloned 2658 bp fragment (data not shown). The correct construct was designated pCT421 (Figure 7.1).

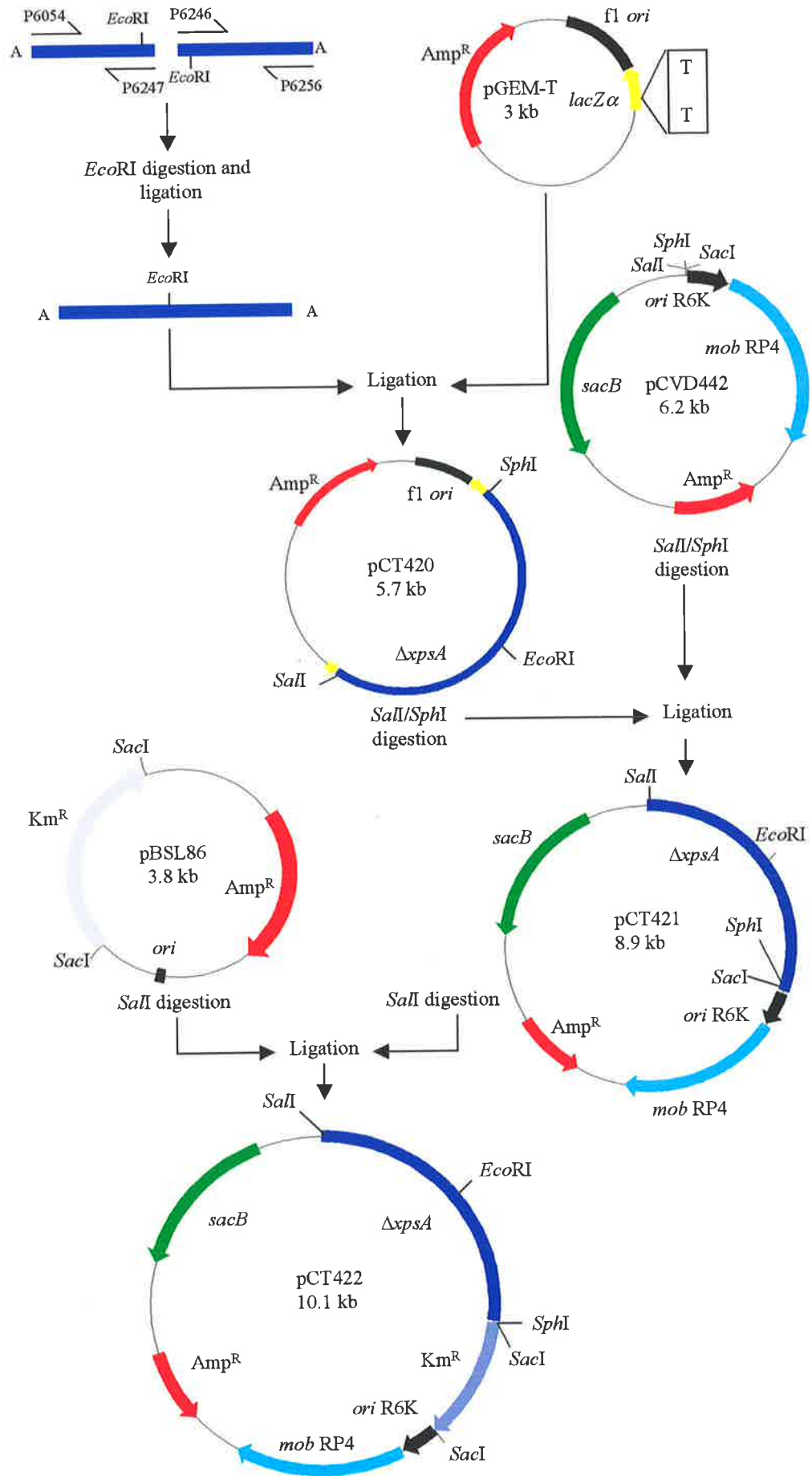
To facilitate selection of pCT421 (Amp^{R}) to *X. bovienii* T228 ($\text{Amp}^{\text{R}}/\text{Sm}^{\text{R}}$) following conjugative transfer from *E. coli* SY327 λ *pir*, an additional antibiotic selection marker (Km^{R}) was inserted into the vector component of this plasmid. The Kan cartridge from plasmid pBSL86 was removed as a 1.2 kb *SacI* fragment (data not shown) and cloned into a unique *SacI* site within the pCVD422 derived DNA of pCT421 (Figure 7.1). The ligation mix was used to transform *E. coli* SY327 λ *pir* by electroporation, and transformants selected on NA supplemented with Amp and Km. Plasmid DNA from selected transformants was screened by digestion with *SacI* to confirm the presence of the 1.2 kb Km cartridge (data not shown). The correct construct was designated pCT422 (Figure 7.1).

Plasmid pCT422 was used to transform *E. coli* SM10 λ *pir* by electroporation. Transformants were selected on NA supplemented with Amp and Km. This construct was then used to transfer pCT422 to *X. bovienii* T228 by conjugation.

Figure 7.1 Construction of plasmids pCT420, pCT421 and pCT422.

A 2604 bp fragment, with overhanging A nucleotides at the 5' and 3' ends, was cloned into pGEM-T and designated pCT420. The 2604 bp fragment was created by *EcoRI* digestion, and ligation, of PCR products from the amplification of *X. bovienii* T228 chromosomal DNA with oligonucleotide pairs P6054/P6247 and P6246/P6256. Restriction enzyme digestion of pCT420 with *SalI/SphI* removed the ligated PCR products as a 2658 bp fragment, which was subsequently subcloned into *SalI/SphI* digested pCVD442 to create pCT421. A 2.1 kb *SacI* fragment, encoding Km^R, from pBSL86 was cloned into the *SacI* site of pCT421 to create pCT422. See section 7.2.1.1 – 7.2.1.2 for full details.

Abbreviations: Amp^R, ampicillin resistance gene; f1 *ori*, f1 origin of replication; Km^R, kanamycin resistance gene; *lacZα*, *lacZ* promoter region; *mob* RP4, mobilisation region; *ori*, origin of replication; *ori* R6K, *pir* protein dependent R6K origin of replication; *sacB*, levansucrase; $\Delta xpsA$, $\Delta xpsA$ with a 2601 bp in-frame deletion.



Panel A

Nucleotide sequence of reading frame *xpsA* after a 2601 bp (867 amino acid) inframe deletion.

```
xpsA start
ATGAACCACCCTGAAAAGTTGAAGCCATTTGCTTTATCCGAAGCACAAAGCAGCCGTTGG - 60
M N H P E K L K P F A L S E A Q S S R W - 20

TTGAATTCTGACGCTGAATCCTTGCAAGATCTCTACAAAACAATGGGTTAA - 111
L N S D A E S L Q D L Y K T M G * - 36
                                     xpsA stop
```

Panel B

Nucleotide sequence of reading frame *xpsB* after a 9648 bp (3216 amino acid) inframe deletion.

```
xpsB start
ATGAATGATAATGAATTAATATCTTTACCATTAGCAGAACGTAAAAGACTACTTGAGTTA - 60
M N D N E L I S L P L A E R K R L L E L - 20

GCTAAAGCAGCAAAACTAACTCGTCAGCAGACACAAAAACAGAAATCCATGCACAACCG - 120
A K A A K L T R Q Q T Q K T E I H A Q R - 40

GAATTCCACCTTGAAATTCCTATTGCAGACATTTTTTCATCACTCAACACTGTATAAACTT - 180
E F H L E I P I A D I F H H S T L Y K L - 60

GCTGAACTTATTCTATCAAGACAAATTGAAACCTTTTTTCGCCCAAGATATAGAGTCCGTA - 240
A E L I L S R Q I E T F F A Q D I E S V - 80

CAAAAAGAGTTGGAGAACCTGTCTGAAGAAGAGTTGCTTGCCATGTTAAATGGAGATCAA - 300
Q K E L E N L S E E E L L A M L N G D Q - 100

CAATGA - 306
Q * - 101
    xpsB stop
```

Figure 7.2

Panel A Nucleotide sequence data from pCT420 using oligonucleotide P6034 to confirm the presence of an *EcoRI* site (underlined) within *xpsA*, and maintenance of the correct reading frame. The same nucleotide sequence was obtained from pCT432 to confirm an *EcoRI* site and the correct ORF in the *xpsA* of XB92388.

Panel B Nucleotide sequence data from pCT425 using oligonucleotide P6257 to confirm the presence of an *EcoRI* site (underlined) within *xpsB*, and maintenance of the correct reading frame.

7.2.1.3 Construction of *xpsA* deletion mutant XB6246

To facilitate allelic exchange mutagenesis of the *xpsA* deletion mutation, the suicide plasmid pCT422 was transferred to P1 *X. bovienii* by conjugation and exconjugates selected on NA supplemented with Km and Sm. To eliminate co-integrates, ten exconjugates were selected and grown O/N in NB without antibiotic selection at 28°C. Broths were diluted 10^{-2} , 10^{-4} and 10^{-6} and plated onto NaCl free NA supplemented with 6% sucrose. Sucrose resistant exconjugates were replica patched onto NA and NA supplemented with Km. Of the 200 exconjugates replica patched, 199 were Km sensitive.

Km sensitive colonies were screened for a 2601 bp deletion in *xpsA* by the PCR amplification pooling method using the oligonucleotide pair P6034/P6109 (see section 2.15.2). These oligonucleotides span the region deleted from *xpsA* and allow amplification of an 895 bp fragment from putative deletion mutants. The PCR conditions were optimised to amplify this product. Exconjugates tested generated the 895 bp product (Figure 7.3, Panel A). No product was amplified from wild type *X. bovienii* T228 chromosomal DNA because the PCR conditions used were insufficient to allow amplification of an approximately 4 kb product.

To confirm the deletion mutation, separate PCR reactions were set up using oligonucleotide pairs P6034/P6035 and P5727/P6109. Oligonucleotides P6035 and P5727 will only hybridise to the DNA section deleted from *xpsA*. Hence PCR products will only be generated from wild type *xpsA*. As expected 540 bp (P6034/P6035) and 818 bp (P5727/P6109) products were amplified from *X. bovienii* T228 DNA (Figure 7.3, Panel A). No PCR products were obtained from any putative *xpsA* deletion mutants.

Samples consisting of no DNA, pCVD442 plasmid DNA and pBSL86 plasmid DNA were used as negative control samples for all PCR reactions. Positive control plasmid DNA from pCT422 generated an 895 bp fragment when PCR amplified with oligonucleotide pair P6109/P6034 (Figure 7.3, Panel A). One *xpsA* in frame deletion mutant was selected and designated *X. bovienii* strain XB6246.

To further confirm a 2601 bp deletion in *xpsA*, *EcoRI* digested chromosomal DNA from *X. bovienii* T228 and *X. bovienii* XB6246 were probed with the DIG labelled 2658 nucleotide fragment from *SalI/SphI* digested pCT420.

Figure 7.3

Panel A

PCR analysis of plasmid and chromosomal DNA prepared from *X. bovienii* T228, XB6246 and plasmids used in the construction of XB6246 by allelic exchange mutagenesis. The size of PCR products is shown. 100 bp markers (DMW-100) were used and the 1 kb band is indicated. Above each lane the oligonucleotide pair used for PCR amplification of plasmid and chromosomal DNA samples is shown. Positive lanes e, g, l and r are italicised.

Panel B

Southern hybridisation analysis of plasmid and chromosomal DNA prepared from *X. bovienii* strains T228 and XB6246. Plasmids pGEM-T, pCVD442 and pCT422 remain undigested. Chromosomal DNA from *X. bovienii* T228 and XB6246 were digested with *EcoRI*. The filter was probed with a digoxigenin labelled 2658 bp fragment derived from the *SalI/SphI* digestion of pCT420. The sizes of DNA fragments hybridising with probe DNA are shown.

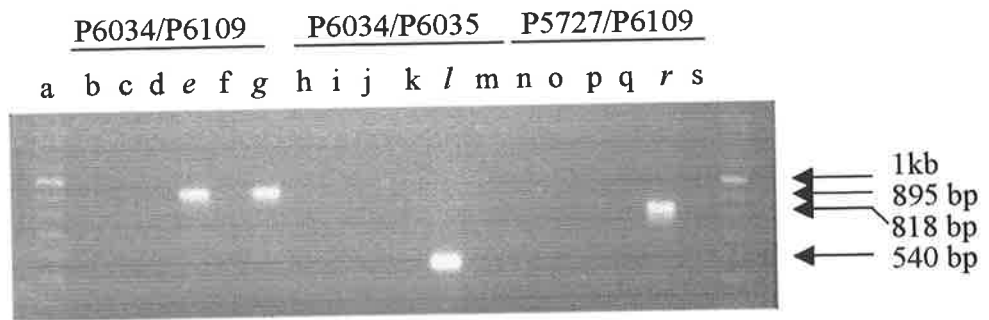


Figure 7.3 Panel A.

Lanes:

- [a], 100 bp marker DMW-100M, [the 1 kb band is noted];
- [b, h and n], no DNA negative control;
- [c, i and o], pCVD442 vector negative control;
- [d, j and p], pBSL86 vector negative control;
- [e, k and q] pCT442;
- [f, l and r] *X. bovienii* T228 chromosomal DNA;
- [g, m and s], XB6246 chromosomal DNA.

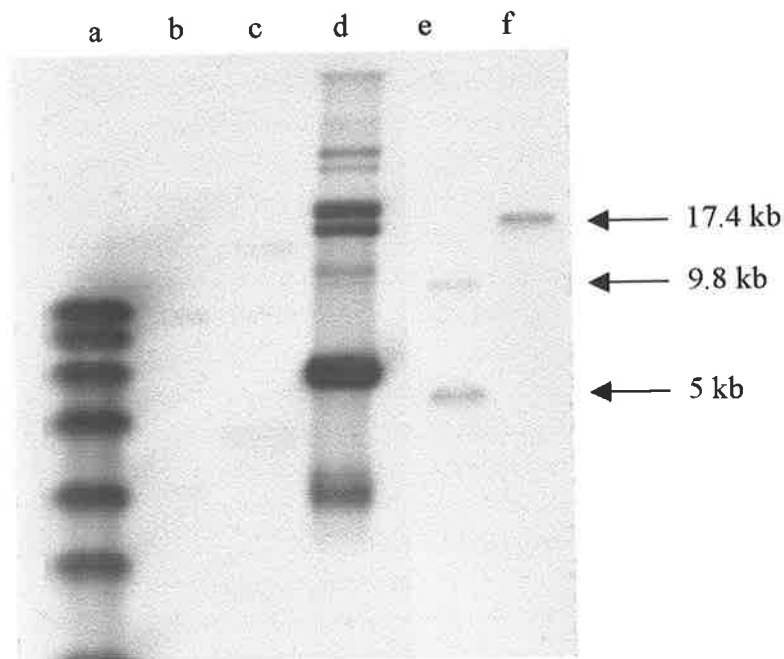


Figure 7.3 Panel B.

Lanes:

- [a], SPP1 marker, *Bacillus subtilis* phage SPP1 DNA digested with *EcoRI*;
- [b], undigested pGEM-T;
- [c], undigested pCVD442; [d], undigested pCT442;
- [e], *EcoRI* digested XB6246 chromosomal DNA;
- [f], *EcoRI* digested *X. bovienii* T228 chromosomal DNA.

An approximately 17.4 kb fragment from *X. bovienii* T228 hybridised with the DIG labelled probe, compared to two fragments of approximately 9.8 kb and 5 kb from XB6246 (Figure 7.3, Panel B). These data confirmed an additional *EcoRI* site has been incorporated into the region of the XB6246 chromosome hybridising with the DIG labelled probe, and that a 2.6 kb region of chromosomal DNA has been deleted. Furthermore, Southern hybridisation analysis mapped an additional and unrelated *EcoRI* site approximately 3.8 kb 5' of the *xpsD* nucleotide sequence. Figure 7.4 outlines a schematic representation of Southern hybridisation and PCR analysis used to confirm the 2601 bp deletion.

7.2.2 Construction of the *xpsB* in-frame deletion mutant XB3444

The *X. bovienii xpsB* ORF is 9951 nucleotides. An in-frame deletion of 9648 bp internal to *xpsB* was created using allelic exchange. The method used was similar to that used to create a deletion in *xpsA*.

7.2.2.1 Cloning of DNA generated by PCR amplification of *X. bovienii* chromosomal DNA, using oligonucleotide pairs P6248/P6257 and P5292/P6249

Oligonucleotide pair P6248/P6257 was used to PCR amplify a 2083 bp fragment, encoding the 3' end of *xpsA* and 5' end of *xpsB*, from *X. bovienii* chromosomal DNA (data not shown). Oligonucleotide P6248, which binds within *xpsB*, has an *EcoRI* restriction enzyme site incorporated into the 5' end. Oligonucleotide pair P5292/P6249 were used to PCR amplify a 1622 bp fragment encoding the 3' end of *xpsB* and 5' end of *xpsC* from pCT408 plasmid DNA (see Chapter 4, section 4.2.5.6) (data not shown).

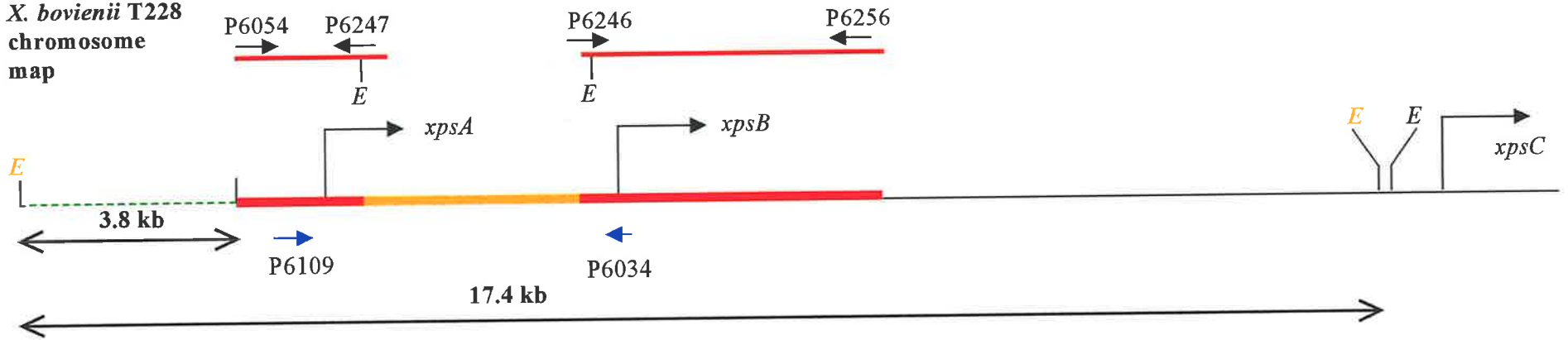
Although oligonucleotide P5292 did not incorporate an *EcoRI* restriction enzyme site, an *EcoRI* site at nucleotide position 14170 of the *xpsABCxpsD* region (see Chapter 5, Figure 5.1) was utilised as an alternative. Thus, the *EcoRI* site incorporated into P6248 was designed such that the *xpsB* deletion would be in frame when ligated to the *EcoRI* digested P5292/P6249 PCR product.

EcoRI digestion of the 2083 bp and 1622 bp PCR products resulted 2081 and 1460 bp fragments respectively (data not shown).

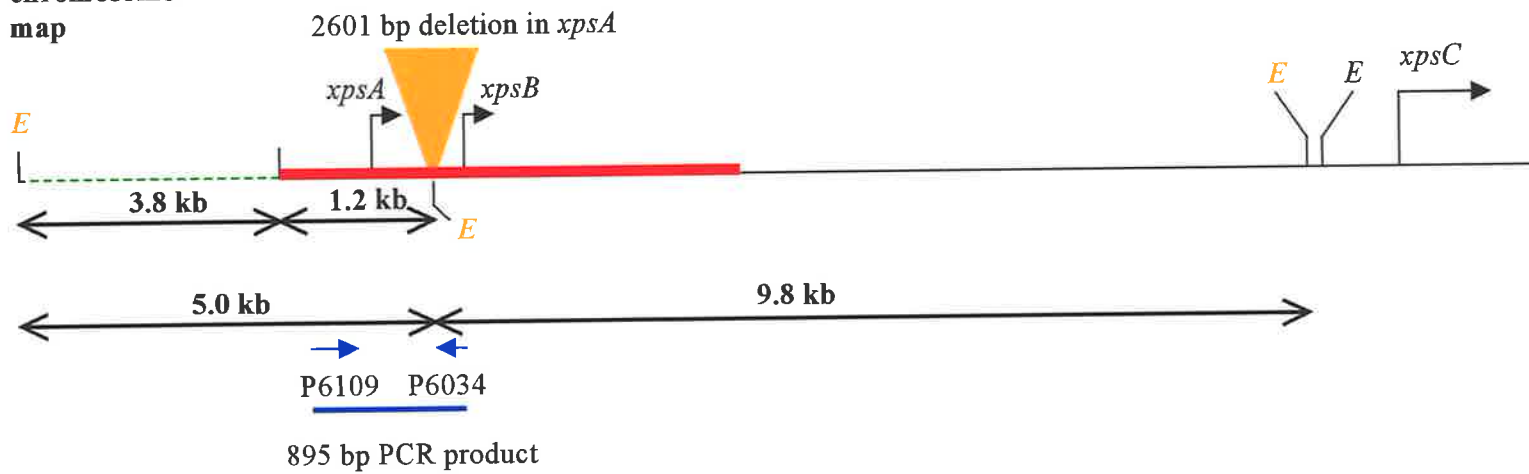
Figure 7.4 A simple schematic diagram further describing the results of Southern hybridisation analysis of XB6246 *EcoRI* digested chromosomal with a 2658 bp DIG labelled probe (see Figure 7.3 Panel A). The location of PCR products generated by amplification of *X. bovienii* T228 chromosomal DNA with oligonucleotide pairs P6054/P6247 and P6246/P6256 are highlighted in red at the top of the figure. The ligated PCR products were subsequently used to generate a 2658 bp DIG labelled probe by *SalI/SphI* digestion of pCT420. The location of binding of the 2658 bp DIG probe to *X. bovienii* T228 and XB6246 chromosomal DNA is highlighted in red on their respective chromosomal maps. The deletion of 2601 bp of DNA from *xpsA*, and incorporation of an *EcoRI* site, is noted by an orange triangle on the XB6246 chromosomal map. The region of *xpsA* deleted is also shown as an orange line on the *X. bovienii* T228 chromosomal map. *EcoRI* sites critical for interpreting the Southern hybridisation results shown in Figure 7.3 are highlighted in orange. An additional *EcoRI* site mapped 3.8 kb upstream of *xpsA* is highlighted by a green dotted line.

Oligonucleotides P6109/P6034 are highlighted in blue, and the PCR product generated by amplification of XB6246 chromosomal DNA with these oligonucleotides is highlighted in blue at the bottom of the figure.

***X. bovienii* T228
chromosome
map**



**XB6246
chromosome
map**



Several attempts to ligate the *EcoRI* digested PCR products together, and then with pGEM-T (the same strategy as used in section 7.2.1.1) were unsuccessful. Therefore an alternative strategy was devised.

7.2.2.2 Construction of plasmids pCT423 and pCT424

The 2083 and 1622 bp PCR products (see section 7.2.2.1) were independently ligated to pGEM-T and each construct used to independently transform *E. coli* DH5 α by electroporation. Transformants were selected on NA supplemented with Amp, IPTG and X-gal. Clones carrying the 1622 bp PCR product were confirmed by digestion with *EcoRI/SalI* (data not shown) and designated pCT423 (Figure 7.5). A clone carrying the 2083 bp PCR product was confirmed by digestion with *EcoRI/SphI* (data not shown) and designated pCT424 (Figure 7.5).

7.2.2.3 Construction of plasmids pCT425, pCT426 and pCT427

Plasmid pCT424 was digested with *EcoRI/SphI* to excise the cloned PCR product as 2106 bp fragment (data not shown). The 2106 bp *EcoRI/SphI* fragment was ligated to *EcoRI/SphI* digested pCT423 and the mix used to transform *E. coli* DH5 α by electroporation. Transformants were selected on NA supplemented with Amp. The correct clone was confirmed by digestion with *SalI/SphI* (data not shown) and designated pCT425 (Figure 7.5). The nucleotide sequence analysis of pCT425 using oligonucleotide P6257 confirmed the presence of an *EcoRI* site and maintenance of the correct ORF (see Figure 7.2).

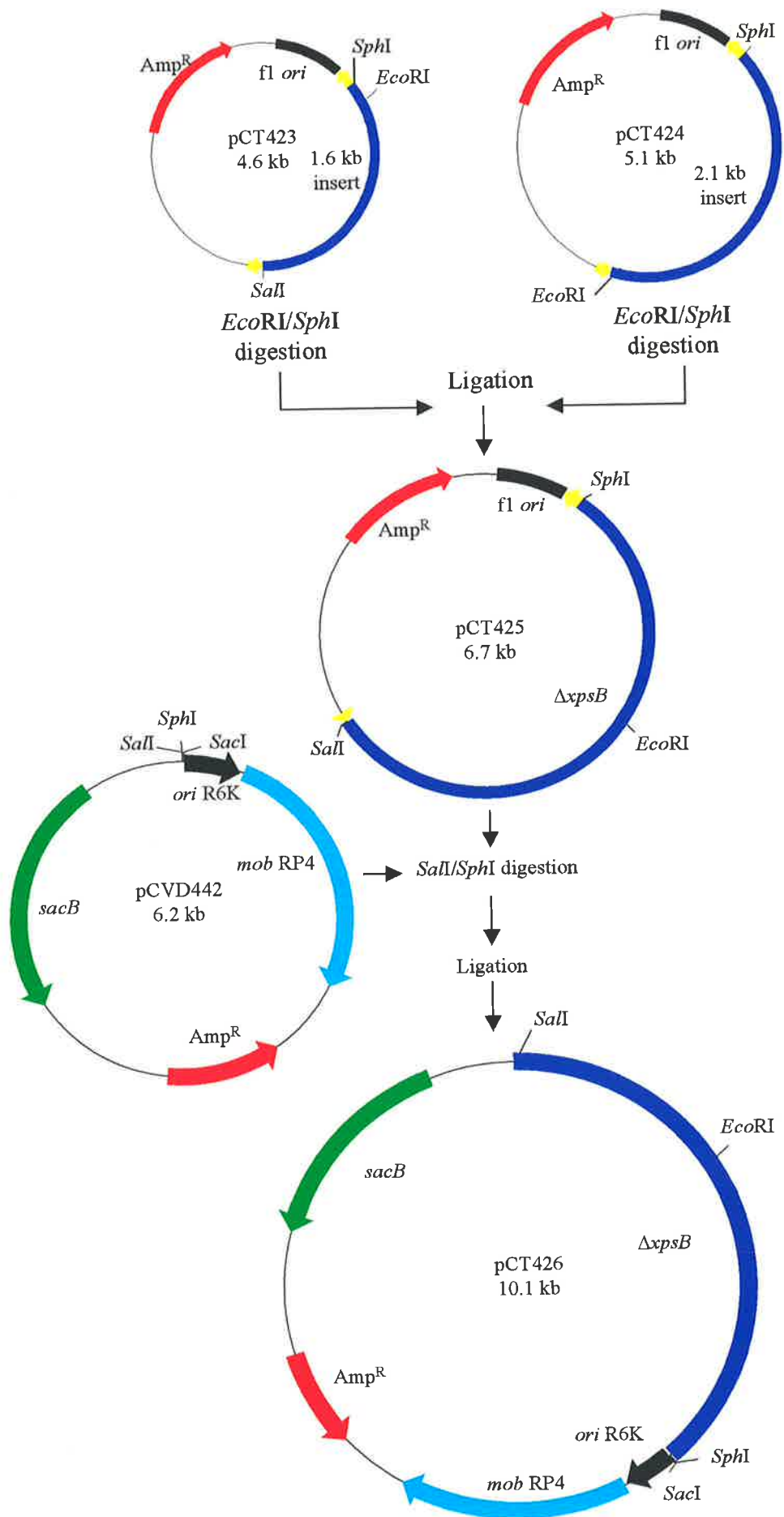
Plasmid pCT425 was digested with *SalI/SphI* to excise the ligated PCR products as a 3588 bp fragment (data not shown), which was subsequently ligated to *SalI/SphI* digested pCVD442. The ligation mix was used to transform *E. coli* SY327 λ *pir* by electroporation and transformants selected on NA supplemented with Amp. The correct clone was confirmed by digestion with *SalI/SphI* (data not shown) and designated pCT426 (Figure 7.5).

The additional marker (see section 7.2.1.2) was provided by restriction enzyme digestion of pBSL86 to remove the Km^R cartridge as a 1.2 kb *SacI* fragment (data not shown). The 1.2 kb *SacI* fragment was cloned into a unique *SacI* site within the pCVD422 derived DNA of pCT426.

Figure 7.5 Construction of plasmids pCT423, pCT424, pCT425 and pCT426.

A 1622 bp PCR product, created by the amplification of *X. bovienii* T228 chromosomal DNA by oligonucleotides P5292/P6249, was cloned into pGEM-T and designated pCT423. A 2083 bp PCR product, created by the amplification of *X. bovienii* T228 chromosomal DNA by oligonucleotides P6248/P6257, was cloned into pGEM-T and designated pCT424. Plasmid pCT424 was digested with *EcoRI/SphI* to excise the PCR product as a 2106 bp fragment, which was subsequently cloned into *EcoRI/SphI* digested pCT423. The resulting plasmid was designated pCT425. Plasmid pCT425 was digested with *SalI/SphI* to excise the ligated PCR products as a 3588 bp fragment, which was subsequently cloned into *SalI/SphI* digested pCVD442 to create pCT426. See section 7.2.2.1 – 7.2.2.3 for details.

Abbreviations: Amp^R, ampicillin resistance gene; *f1 ori*, *f1* origin of replication; *mob* RP4, mobilisation region; *ori* R6K, *pir* protein dependent R6K origin of replication; *sacB*, levansucrase; Δ *xpsB*, *xpsB* with a 9648 bp in-frame deletion.



The ligation mix was used to transform *E. coli* SY327 λ *pir* by electroporation and transformants selected on NA supplemented with Amp and Km. The correct clone was confirmed by digestion with *Sac*I (data not shown) and designated pCT427 (Figure 7.6).

Plasmid pCT427 was used to transform *E. coli* SM10 λ *pir* by electroporation in preparation for transfer to *X. bovienii* T228 by conjugation. Transformants were selected on NA supplemented with Amp and Km.

7.2.2.4 Construction of *xpsB* deletion mutant XB3444

To facilitate allelic exchange of the *xpsB* deletion, the suicide plasmid pCT427 was transferred to P1 *X. bovienii* by conjugation and exconjugates selected on NA supplemented with Km and Sm. Elimination of co-integrates was carried out as described in section 7.2.1.4. Of the 200 exconjugates replica patched onto NA and NA supplemented with Km, 193 were Km sensitive.

Km sensitive colonies were screened for a 9648 bp deletion in *xpsB* by the PCR amplification pooling method. The oligonucleotides used were P3533/P6035. These oligonucleotides span the region deleted from *xpsB* and are predicted to allow amplification of a 934 bp product from putative deletion mutants (Figure 7.7, Panel A). The PCR conditions were optimised to amplify this product. Exconjugates tested amplified this product. No product was amplified from wild type *X. bovienii* T228 DNA because PCR reaction conditions were insufficient to allow amplification of an approximately 9 kb product.

To confirm the deletion mutant, separate PCR reactions were set up using oligonucleotides pairs P5620/P6035 and P3533/P5852. Oligonucleotides P5620 and P5852 will only hybridise to DNA sections deleted from *xpsB*. Hence PCR products will only be generated from wild type *xpsB*. As expected a 1561 bp (P5620/P6035), and 638 bp (P3533/P5852) product were amplified from *X. bovienii* T228 chromosomal DNA (Figure 7.7, Panel A). No products were obtained from DNA derived from any putative *xpsB* deletion mutant.

Samples consisting of no DNA, pCVD442 plasmid DNA and pBSL86 plasmid DNA were used as negative control samples for all PCR reactions. Positive control plasmid DNA from pCT427 generated a 934 bp fragment when amplified with oligonucleotide pair P3533/P6035

Figure 7.6 Construction of plasmid pCT427.

A 2.1 kb *SacI* fragment, encoding Km^R , from pBSL86 was cloned into the *SacI* site of pCT426 to create pCT427. See section 7.2.2.3 for full details.

Abbreviations: Amp^R , ampicillin resistance gene; Km^R , kanamycin resistance gene; *mob* RP4, mobilisation region; *ori*, origin of replication; *ori* R6K, *pir* protein dependent R6K origin of replication; *sacB*, levansucrase; $\Delta xpsB$, $\Delta xpsB$ with a 9648 bp in-frame deletion.

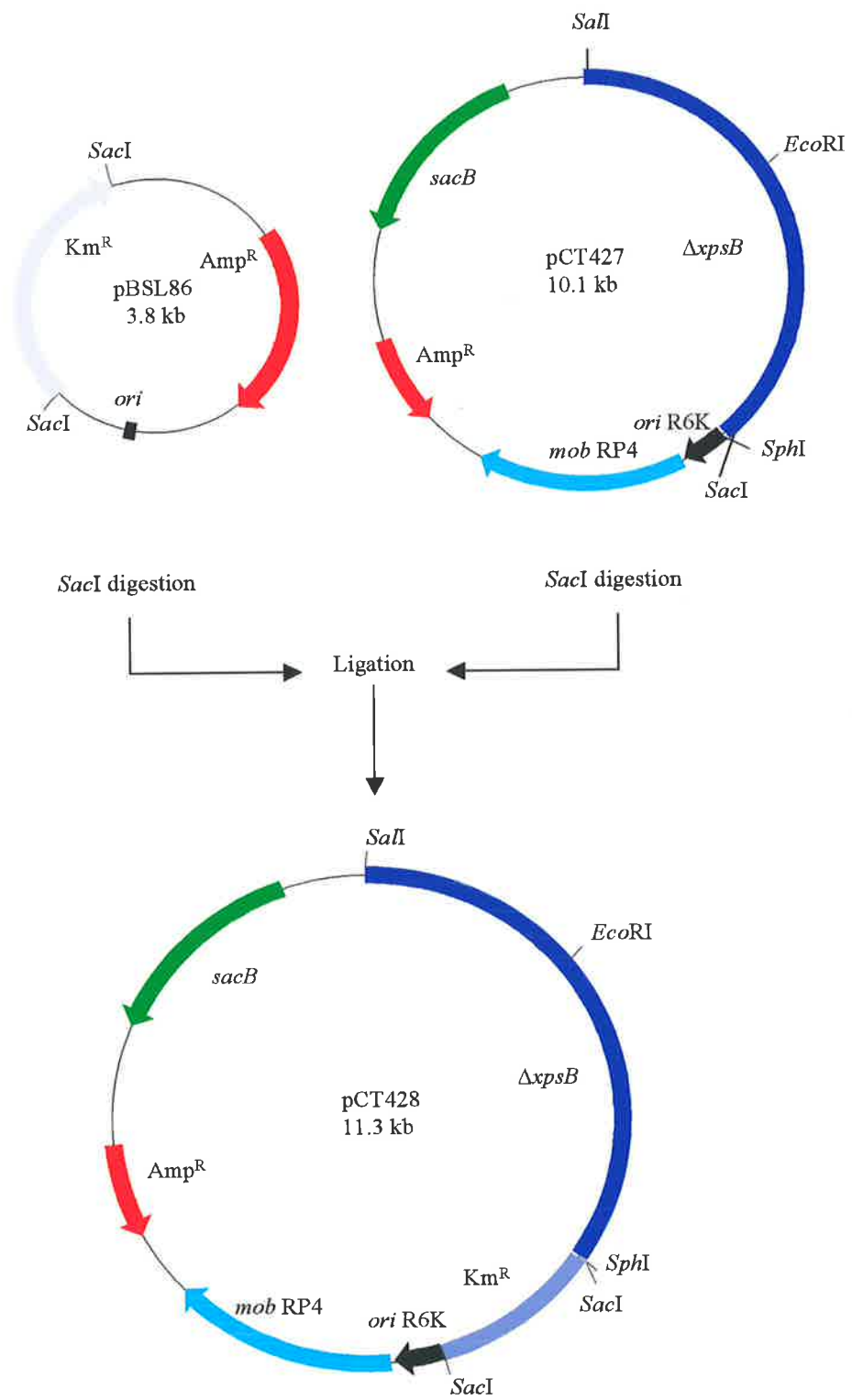


Figure 7.7

Panel A

PCR analysis of plasmid and chromosomal DNA prepared from *X. bovienii* T228, XB3444 and plasmids used in the construction of XB3444 by allelic exchange mutagenesis. The sizes of PCR products are shown. 100 bp markers (DMW-100) were used and the 1 kb band is indicated. Above each lane the oligonucleotide pair used for PCR amplification of plasmid and chromosomal DNA samples is shown. Positive lanes e, g, l and r are italicised.

Panel B

Southern hybridisation analysis of plasmid and chromosomal DNA prepared from *X. bovienii* strains T228 and XB3444. Plasmids pGEM-T, pCVD442 and pCT427 remained undigested. Chromosomal DNA from *X. bovienii* T228 and XB3444 were digested with *Eco*RI. The filter was probed with a digoxigenin labelled 3588 bp fragment derived from the *Sal*I/*Sph*I digestion of pCT426. The size of DNA fragments hybridising with probe DNA are shown.

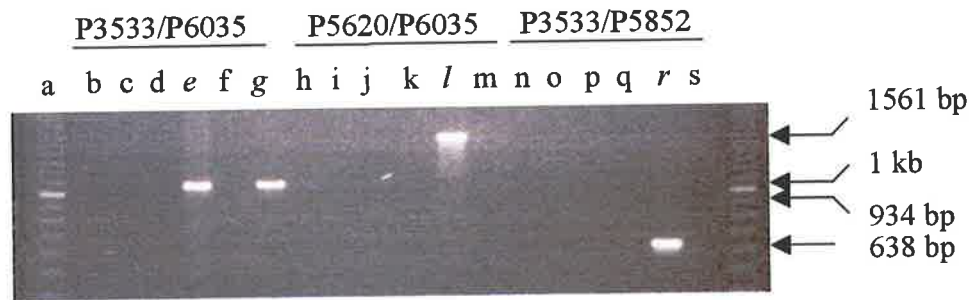


Figure 7.7 Panel A.

Lanes:

- [a], 100 bp marker DMW-100M, [the 1 kb band is noted];
- [b, h and n], no DNA negative control;
- [c, i and o], pCVD442 vector negative control;
- [d, j and p], pBSL86 vector negative control;
- [e, k and q] pCT427;
- [f, l and r] *X. bovienii* T228 chromosomal DNA;
- [g, m and s], XB3444 chromosomal DNA.

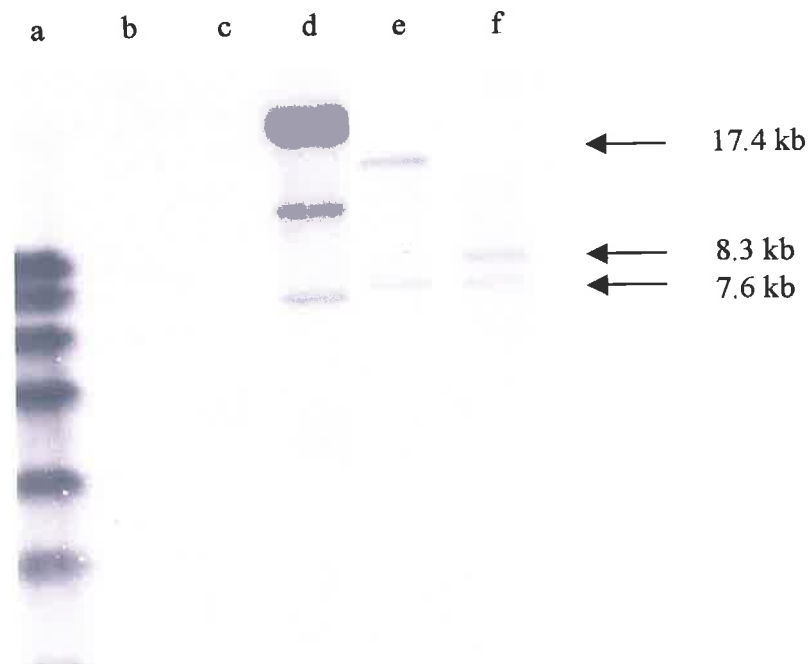


Figure 7.7 Panel B.

Lanes:

- [a], SPP1 marker, *Bacillus subtilis* phage SPP1 DNA digested with *EcoRI*;
- [b], undigested pGEM-T;
- [c], undigested pCVD442; [d], undigested pCT427
- [e], *EcoRI* digested *X. bovienii* T228;
- [f], *EcoRI* digested XB3444 chromosomal DNA

(Figure 7.7, Panel A). One *xpsB* in frame deletion mutant was selected and designated *X. bovienii* strain XB3444.

To confirm a 9648 bp deletion in *xpsB*, *EcoRI* digested chromosomal DNA from *X. bovienii* T228 and XB3444 were probed with the DIG labelled 3588 bp fragment generated by *Sall/SphI* digestion of pCT426. Two fragments of approximately 17.4 kb and 7.6 kb from *X. bovienii* T228 hybridised with the DIG labelled probe (Figure 7.7, Panel B). In comparison, two fragments of approximately 8.3 kb and 7.6 kb from XB3444 hybridised with the DIG labelled probe (Figure 7.7, Panel B). These data indicated an additional *EcoRI* site had been incorporated into the region of XB3444 chromosome hybridising with the DIG labelled probe. Furthermore a deletion of approximately 10 kb of chromosomal DNA from this region in XB3444 was confirmed. The Southern hybridisation results also suggested an *EcoRI* restriction enzyme site is located approximately 6.2 kb 3' of the known *xpsC* nucleotide sequence. Figure 7.8 outlines a schematic representation of Southern hybridisation and PCR analysis used to confirm the 9448 bp deletion.

7.2.3 Construction of the *xpsA/xpsB* double in-frame deletion mutant XB92388

To create a strain with a deletion in both *xpsA* and *xpsB*, XB3444 was used as the base strain as this carried an existing 9.6 kb deletion mutation within *xpsB* (see section 7.2.2.5). The previously constructed *xpsA* deletion mutation encoded on plasmid pCT422 (see section 7.2.1.1 - 7.2.1.4) could not be used to delete a 2601 nucleotide portion of *xpsA*, as a significant portion of homologous DNA required for recombination had been deleted in the construction of XB3444 (see section 7.2.2.1 - 7.2.2.5). Consequently an alternative strategy was required. This section describes the strategy used. The steps are shown diagrammatically in Figure 7.9

7.2.3.1 Construction of plasmids pCT430 and pCT431

The 1209 bp and 207 bp PCR products amplified from *X. bovienii* T228 chromosomal DNA using oligonucleotides P6054/P6247 and P6246/P92388 respectively, were independently ligated to pGEM-T and used to transform *E. coli* DH5 α by electroporation. Transformants were selected on NA supplemented with Amp, IPTG and X-gal. A clone carrying the 207 bp

Figure 7.8 Schematic diagram further describing the results of Southern hybridisation analysis of XB3444 *EcoRI* digested chromosomal with a 3588 bp DIG labelled probe (see Figure 7.X). The location of PCR products generated by amplification of *X. bovienii* T228 chromosomal DNA with oligonucleotide pairs P6257/P6248 and P5292/P5249 are highlighted in red at the top of the figure. The ligated PCR products were subsequently used to generate a 3588 bp DIG labelled probe by *SalI/SphI* digestion of pCT426. The location of binding of the 3588 bp DIG probe to *X. bovienii* T228 and XB3444 chromosomal DNA is highlighted in red on their respective chromosomal maps. The deletion of 9648 bp of DNA from *xpsB*, and incorporation of an *EcoRI* site, is noted by an orange triangle on the XB3444 chromosomal map. The region of *xpsB* deleted is also shown as an orange line on the *X. bovienii* T228 chromosomal map. *EcoRI* sites critical for interpreting the Southern hybridisation results shown in Figure 7.7 are highlighted in orange. The additional *EcoRI* site mapped 6.2 kb downstream of *xpsC* is highlighted by a green dotted line.

Oligonucleotides P6035/P3533 are highlighted in blue, and the PCR product generated by amplification of XB3444 chromosomal DNA with these oligonucleotides is highlighted in blue at the bottom of the figure.

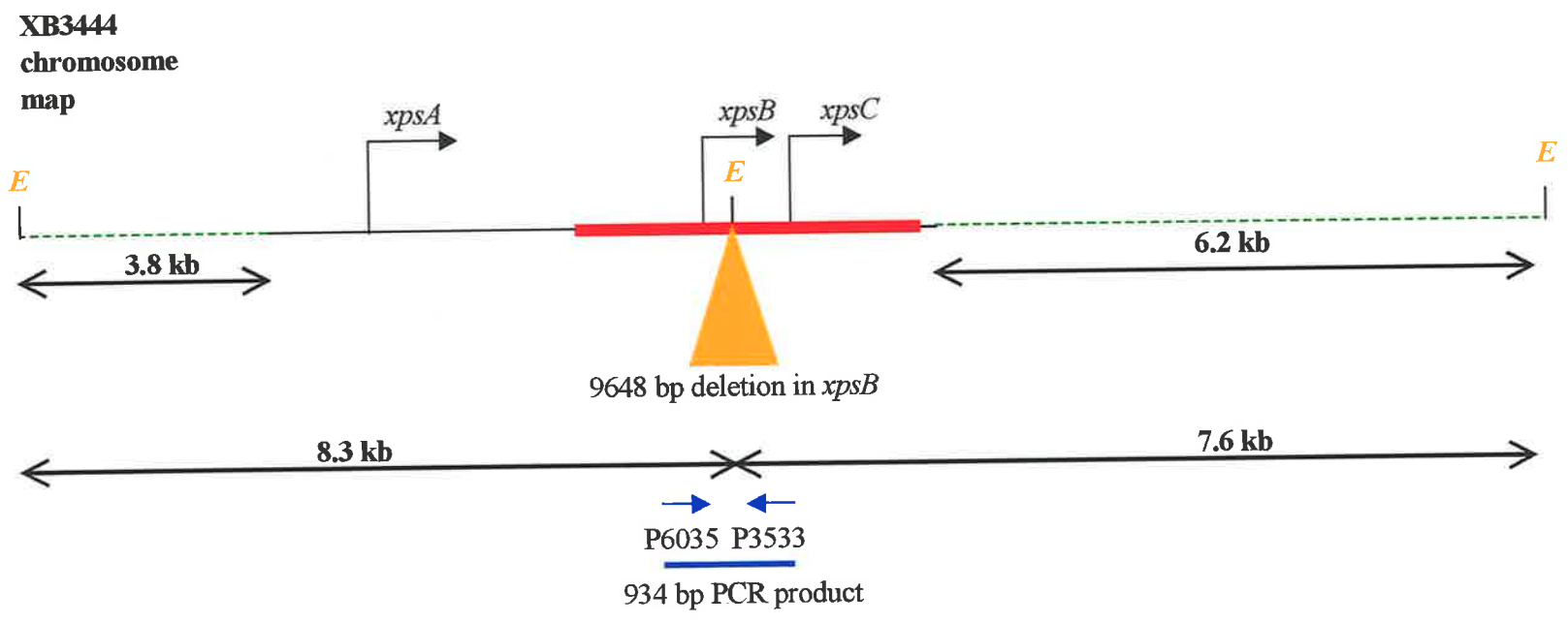
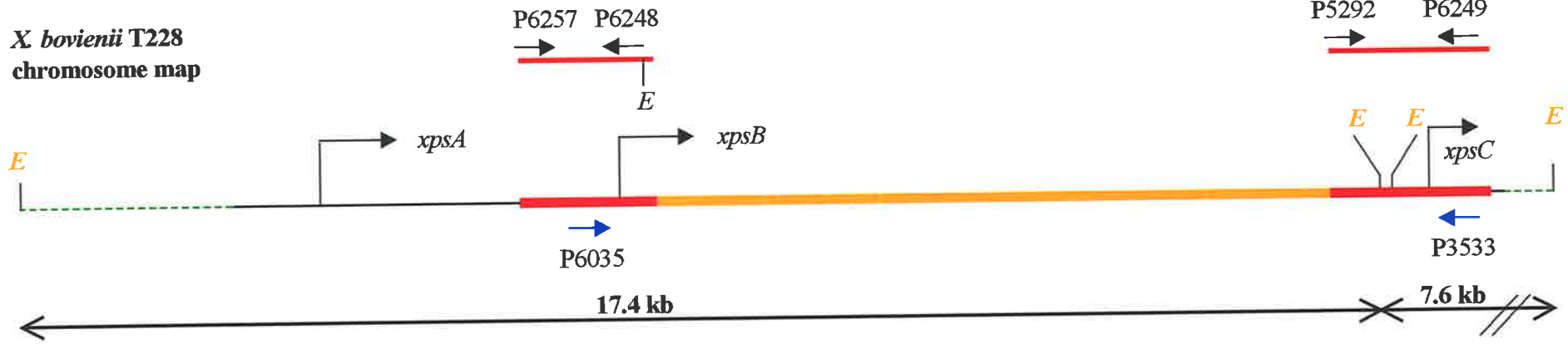
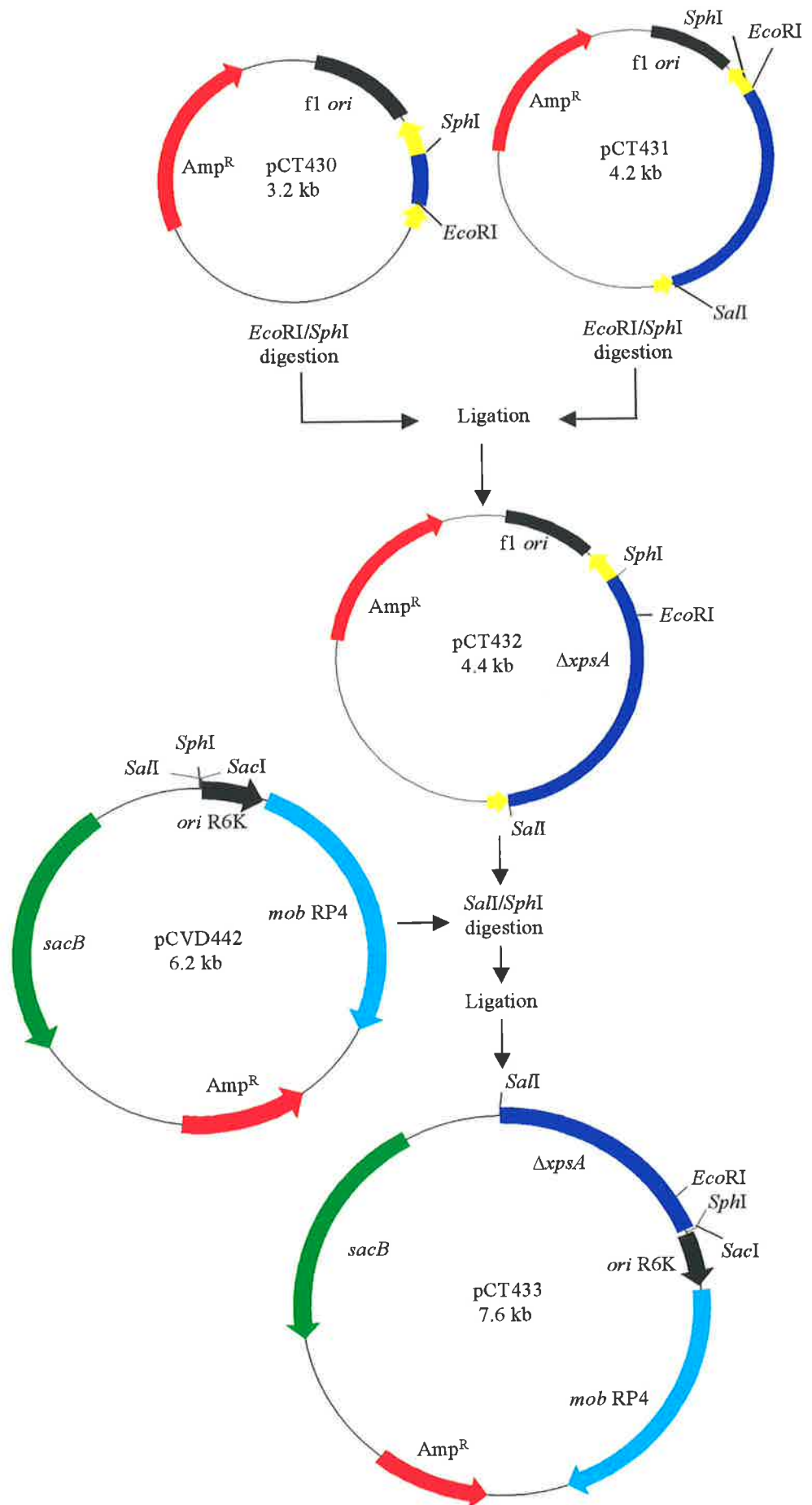


Figure 7.9 Construction of plasmids pCT430, pCT431, pCT432 and pCT433.

A 207 bp PCR product, created by the amplification of *X. bovienii* T228 chromosomal DNA by oligonucleotides P6246/P92388, was cloned into pGEM-T and designated pCT430. A 1209 bp PCR product, created by the amplification of *X. bovienii* T228 chromosomal DNA by oligonucleotides P6054/P6247, was cloned into pGEM-T and designated pCT431. Plasmid pCT430 was digested with *EcoRI/SphI* to excise the PCR product as a 231 bp fragment, which was subsequently cloned into *EcoRI/SphI* digested pCT431. The resulting plasmid was designated pCT432. Plasmid pCT432 was digested with *SalII/SphI* to excise the ligated PCR products as a 1456 bp fragment, which was subsequently cloned into *SalII/SphI* digested pCVD442 to create pCT433. See section 7.2.3.1 – 7.2.3.3 for details.

Abbreviations: Amp^R, ampicillin resistance gene; *f1 ori*, *f1* origin of replication; *mob* RP4, mobilisation region; *ori* R6K, *pir* protein dependent R6K origin of replication; *sacB*, levansucrase.



PCR was confirmed by digestion with *EcoRI/SphI* (data not shown) and designated pCT430 (Figure 7.9). A clone carrying the 1209 bp PCR product was confirmed by digestion with *EcoRI/SalI* (data not shown) and designated pCT431 (Figure 7.9).

7.2.3.2 Construction of plasmids pCT432, pCT433 and pCT434

Plasmid pCT430 was digested with *EcoRI/SphI* to excise the cloned PCR product as a 231 bp fragment (data not shown), which was subsequently ligated to *EcoRI/SphI* digested pCT431, and used to transform *E. coli* DH5 α by electroporation. Transformants were selected on NA supplemented with Amp. The correct clone was selected by digestion with *SalI/SphI* (data not shown) and designated pCT432 (Figure 7.9). Nucleotide sequence analysis of pCT432 using oligonucleotide P3679 confirmed the presence of an *EcoRI* site and maintenance of the correct ORF (see Figure 7.2).

Plasmid pCT432 was digested with *SalI/SphI* to excise the ligated PCR products as a 1456 bp fragment (data not shown), and this was subsequently ligated to *SalI/SphI* digested pCVD442 to form pCT433 (Figure 7.9). This construct was then used to transform into *E. coli* SY327 λ *pir* by electroporation. Transformants were selected on NA supplemented with Amp, and screened by *SalI/SphI* digestion (data not shown) to recover the 1456 bp fragment. .

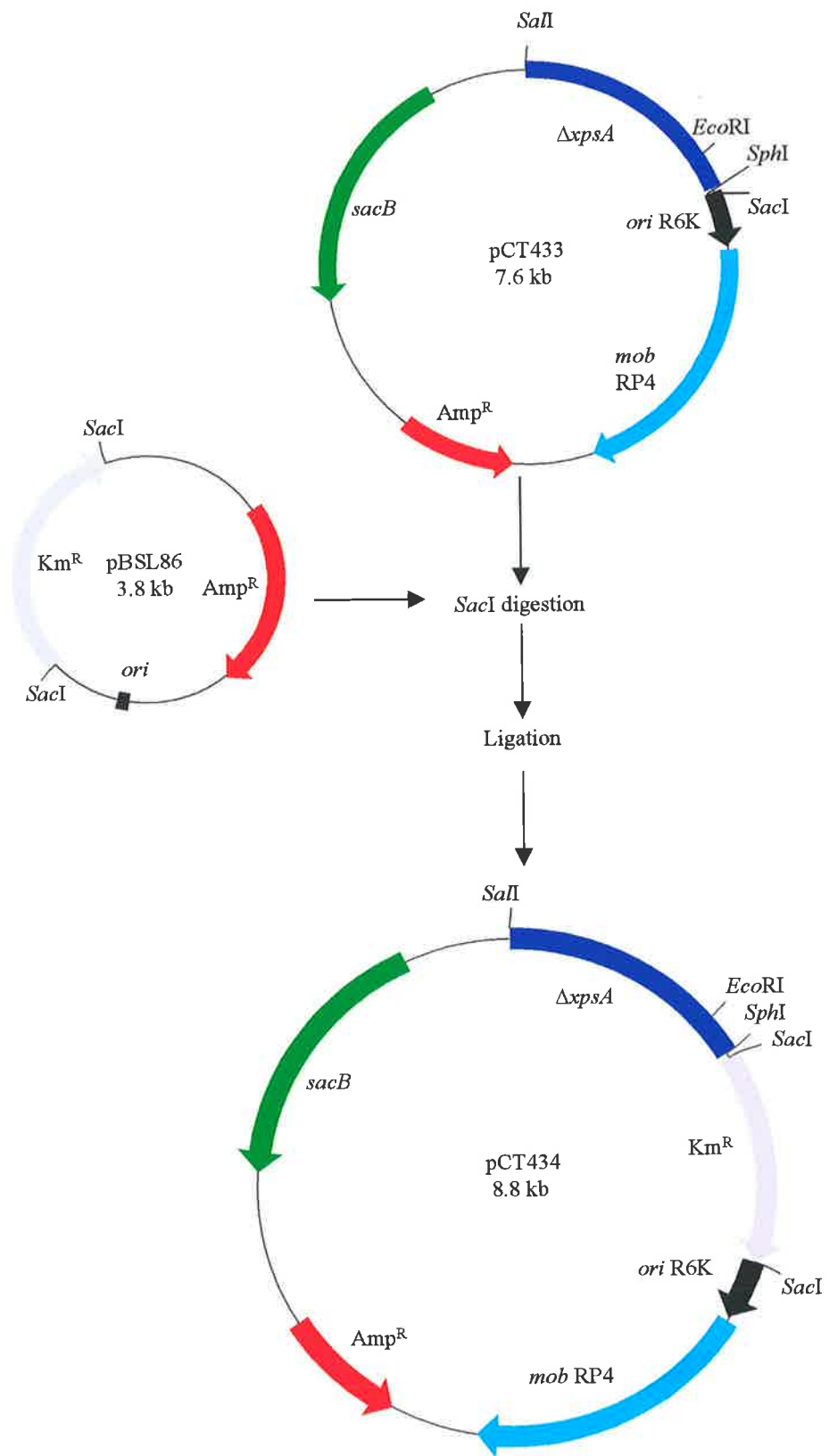
Since pCT433 was to be transferred to XB3444 by conjugation, an additional selectable marker for this construct was required to select for suitable exconjugates (see section 7.2.1.2). The Km cartridge from pBSL86 was removed as a 1.2 kb *SacI* fragment (data not shown) and cloned into a unique *SacI* site within the pCVD422 derived DNA of pCT433. The ligation mix was to transform *E. coli* SY327 λ *pir* by electroporation and transformants selected on NA supplemented with Amp and Km. Transformants were screened by digestion with *SacI* (data not shown) and the correct construct designated pCT434 (Figure 7.10).

Plasmid pCT434 was used to transform *E. coli* SM10 λ *pir* by electroporation in preparation for transfer to XB3444 by conjugation. Transformants were selected on NA supplemented with Amp and Km.

Figure 7.10 Construction of plasmid pCT434.

A 2.1 kb *SacI* fragment, encoding Km^R, from pBSL86 was cloned into the *SacI* site of pCT433 to create pCT434. See section 7.2.3.3 for full details.

Abbreviations: Amp^R, ampicillin resistance gene; Km^R, kanamycin resistance gene; *mob* RP4, mobilisation region; *ori* R6K, *pir* protein dependent R6K origin of replication; *sacB*, levansucrase; $\Delta xpsA$, *xpsA* with a 2601 bp in-frame deletion.



7.2.3.3 Construction of *xpsA/xpsB* double deletion mutant XB92388

Plasmid pCT434 was transferred to P1 *X. bovienii* XB3444 by conjugation and exconjugates selected on NA supplemented with Km and Sm. Cointegrates were eliminated as described in section 7.2.1.4. Of 200 exconjugates replica patched onto NA and NA supplemented with Km, 197 were Km sensitive.

Km sensitive colonies were screened for a 2601 nucleotide deletion in *xpsA* by the PCR amplification pooling method. The oligonucleotides used were P6034/P6109. These primers span the region deleted from *xpsA* and are predicted to allow amplification of an 895 bp product from putative deletion mutants. The PCR was optimised to amplify this product. Exconjugates tested generated the 895 bp product (Figure 7.11, Panel A). No product was amplified from wild type *X. bovienii* T228 chromosomal DNA because the PCR reaction conditions used were insufficient to allow amplification of an approximately 4 kb product.

To confirm the deletion mutant, separate PCR reactions were set up using oligonucleotide pairs P6034/P6035 and P5727/P6109. Oligonucleotides P6035 and P5727 only hybridise to the DNA section deleted from *xpsA*. As expected 540 bp (P6034/P6035) and 818 bp (P5727/P6109) products were amplified from *X. bovienii* T228 chromosomal DNA (Figure 7.11, Panel A). No products were obtained from chromosomal DNA derived from putative *xpsA* deletion mutants.

Samples consisting of no DNA, pCVD442 plasmid DNA and pBSL86 plasmid DNA were used as negative control samples for all PCR reactions. Positive control plasmid DNA from pCT434 and XB6246 chromosomal DNA generated an 895 bp fragment when amplified with oligonucleotide pair P6034/P6109 (Figure 7.11, Panel A). One *xpsAB* in frame deletion mutant was selected and designated *X. bovienii* strain XB92388.

To confirm a 2601 nucleotide deletion in *xpsA*, *EcoRI* digested chromosomal DNA from *X. bovienii* T228 and XB92388 were probed with the DIG labelled 1456 nucleotide fragment generated by *SalI/SphI* digestion of pCT433. One fragment of approximately 17.4 kb from *X. bovienii* T228 hybridised with the DIG labelled probe (Figure 7.11, Panel B). In comparison, two fragments of approximately 5 kb and 200 bp from XB92388 hybridised with the DIG labelled probe (Figure 7.11, Panel B). These data indicated an additional *EcoRI* site had been

Figure 7.11

Panel A

PCR analysis of plasmid and chromosomal DNA prepared from *X. bovienii* T228, XB92388 and plasmids used in the construction of XB92388 by allelic exchange mutagenesis. The sizes of PCR products are shown. 100 bp markers (DMW-100) were used and the 1 kb band is indicated. Above each lane the oligonucleotide pair used for PCR amplification of plasmid and chromosomal DNA samples is shown. Positive lanes e, g, h, m and s are italicised.

Panel B

Southern hybridisation analysis of plasmid and chromosomal DNA prepared from *X. bovienii* strains T228 and XB92388. Plasmids pGEM-T, pCVD442 and pCT434 remained undigested. Chromosomal DNA from *X. bovienii* T228 and XB92388 were digested with *EcoRI*. The filter was probed with a digoxigenin labelled 1456 bp fragment derived from the *SalI/SphI* digestion of pCT433. The size of DNA fragments hybridising with probe DNA are shown.

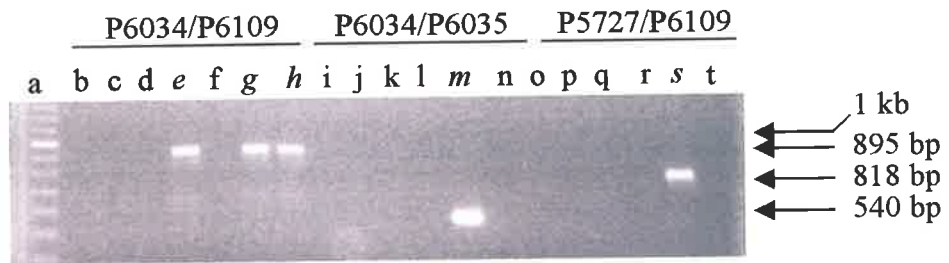


Figure 7.11 Panel A.

Lanes:

- [a], 100 bp marker DMW-100M, [the 1 kb band is noted];
- [b, i and o], no DNA negative control;
- [c, j and p], pCVD442 vector negative control;
- [d, k and q], pBSL86 vector negative control;
- [e, l and r], pCT434;
- [f, m and s], *X. bovienii* T228 chromosomal DNA;
- [g, n and t], XB92388 chromosomal DNA;
- [h], XB6246 chromosomal DNA.

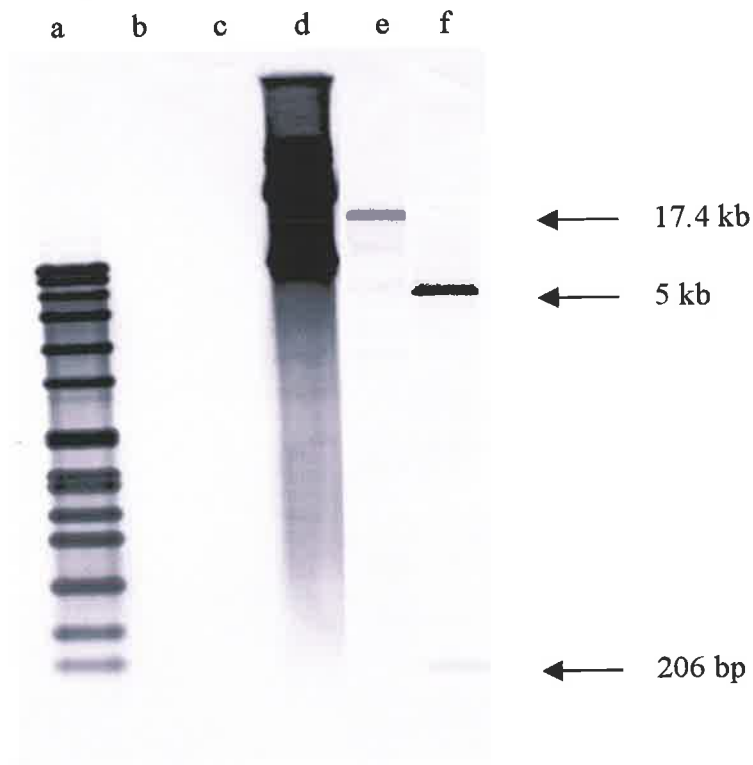


Figure 7.11 Panel B.

Lanes:

- [a], SPP1 marker, *Bacillus subtilis* phage SPP1 DNA digested with *EcoRI*;
- [b], undigested pGEM-T;
- [c], undigested pCVD442; [d], undigested pCT434
- [e], *EcoRI* digested *X. bovienii* T228;
- [f], *EcoRI* digested XB92388 chromosomal DNA.

incorporated into the *xpsA* region of the XB92388 chromosome hybridising with the DIG labelled probe, Furthermore, approximately 2.6 kb of chromosomal DNA had been deleted. Additionally, these results confirmed the presence of an additional *EcoRI* site 3.8 kb 5' of *xpsD*. Figure 7.12 outlines a schematic representation of the Southern hybridisation data and PCR analysis used to confirm the 2601 bp deletion.

7.2.3.4 Summary of modules and domains deleted in XB3444, XB6246 and XB92388

Each of the *X. bovienii* in frame deletion mutants of *xpsA* and *xpsB* had all domains within the appropriate module deleted. In XB6246 the adenylation and thiolation domains, and 95% of the condensation domain from module one (M1) of *xpsA* were deleted. In XB3444 all domains were removed from each of the three modules of *xpsB*. Deletion mutant XB92388 was a combination of these two mutations (Figure 7.13).

7.2.4 Phenotypic characterisation of deletion mutants XB3444, XB6246 and XB92388

Defined mutations, such as in frame deletions, provide a tool to examine gene function. In frame deletions eliminate issues of polarity and facilitate comparison of wild type and mutant bacteria. The peptide products of various peptide synthetases are reported to have antimicrobial, cytotoxic, immunosuppressive, antiviral, anticancer and surfactant properties (Konz & Marahiel, 1999; Challis *et al.*, 2000). As these bioactive peptides are generally transported out of the bacterial cell by ABC transport proteins, broth culture fluids derived from isogenic *xps* strains can be tested for presence or absence of these peptides through the use of suitable assays. Since Xps peptide synthetase expression is cell density dependent (see Chapter 6), these studies can be carried out under culture conditions that ensure expression in the wild type strain.

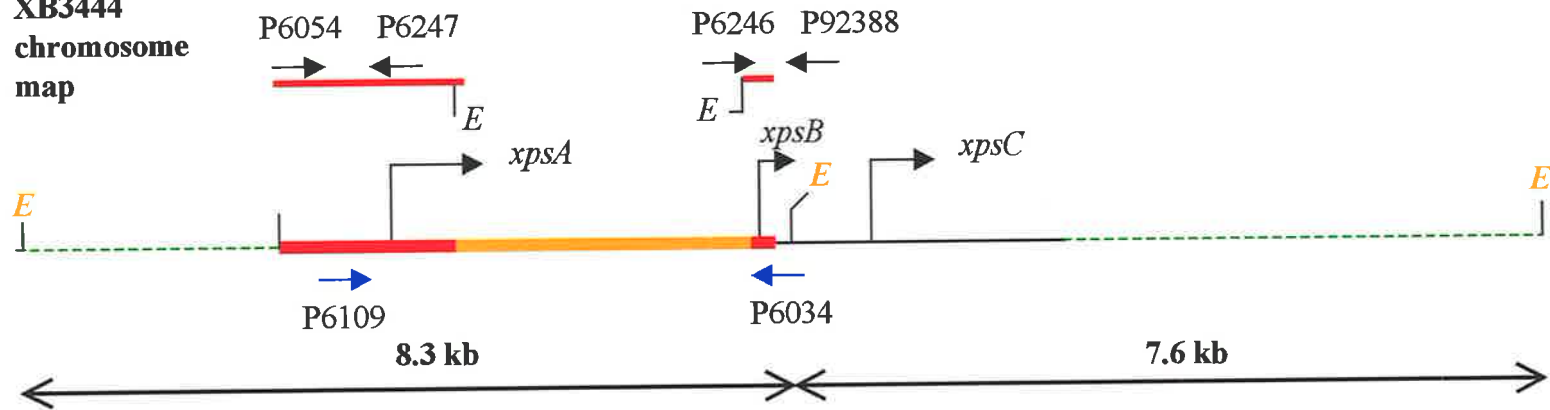
The role of *X. bovienii* peptide synthetases in the synthesis of antimicrobial and/or cytotoxic compound was examined. The ability of wild type and mutant bacteria to inhibit the growth of indicator organism *M. luteus*, on solid and in liquid media, was assessed. The cytotoxic activity of wild type and mutant bacteria was assessed by injecting whole wild type or inframe

Figure 7.12 A simple schematic diagram further describing the results of Southern hybridisation analysis of XB92388 *EcoRI* digested chromosomal with a 1456 bp DIG labelled probe (see Figure 7.X). The location of PCR products generated by amplification of *X. bovienii* T228 chromosomal DNA with oligonucleotide pairs P6054/P6247 and P6246/P92388 are highlighted in red at the top of the figure. The ligated PCR products were subsequently used to generate a 1456 bp DIG labelled probe by *SalI/SphI* digestion of pCT433. The location of binding of the 1456 bp DIG probe to *X. bovienii* T228 and XB92388 chromosomal DNA is highlighted in red on their respective chromosomal maps. The deletion of 2601 bp of DNA from *xpsA*, and incorporation of an *EcoRI* site, is noted by an orange triangle on the XB92388 chromosomal map. The region of *xpsA* deleted is also shown as an orange line on the XB3444 chromosomal map. *EcoRI* sites critical for interpreting the Southern hybridisation results shown in Figure 7.11 are highlighted in orange.

Note: This figure shows the chromosomal map of XB3444, as the construction of XB92388 was based on this strain.

Oligonucleotides P6109/P6034 are highlighted in blue, and the PCR product generated by amplification of XB92388 chromosomal DNA with these oligonucleotides is highlighted in blue at the bottom of the figure.

**XB3444
chromosome
map**



**XB92388
chromosome
map**

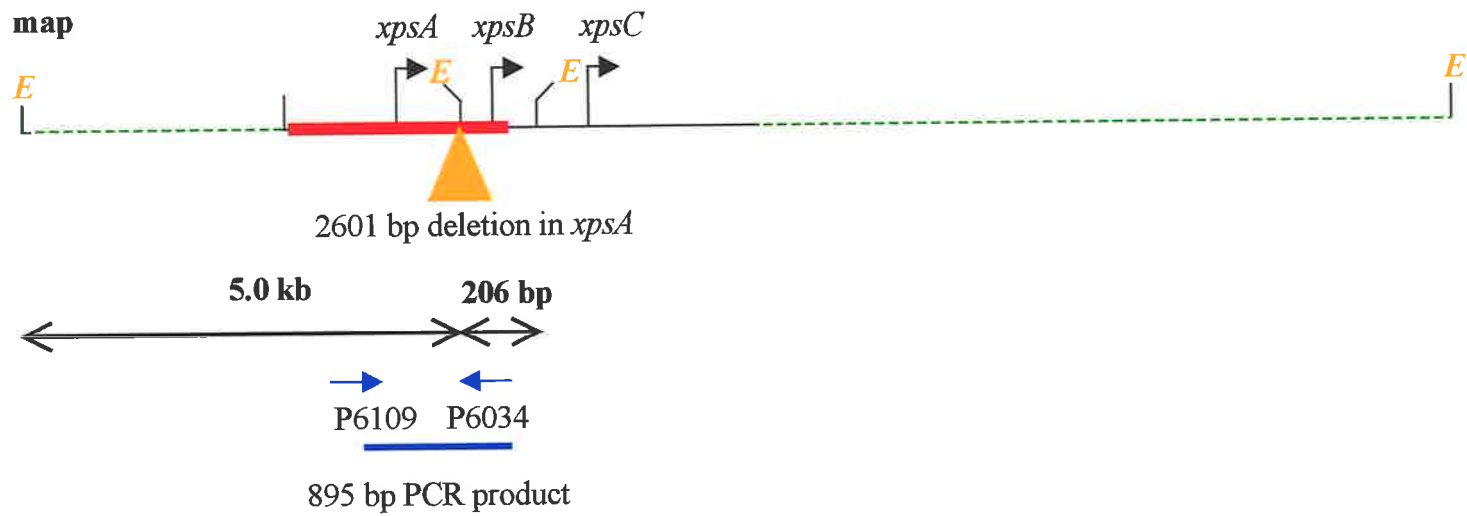
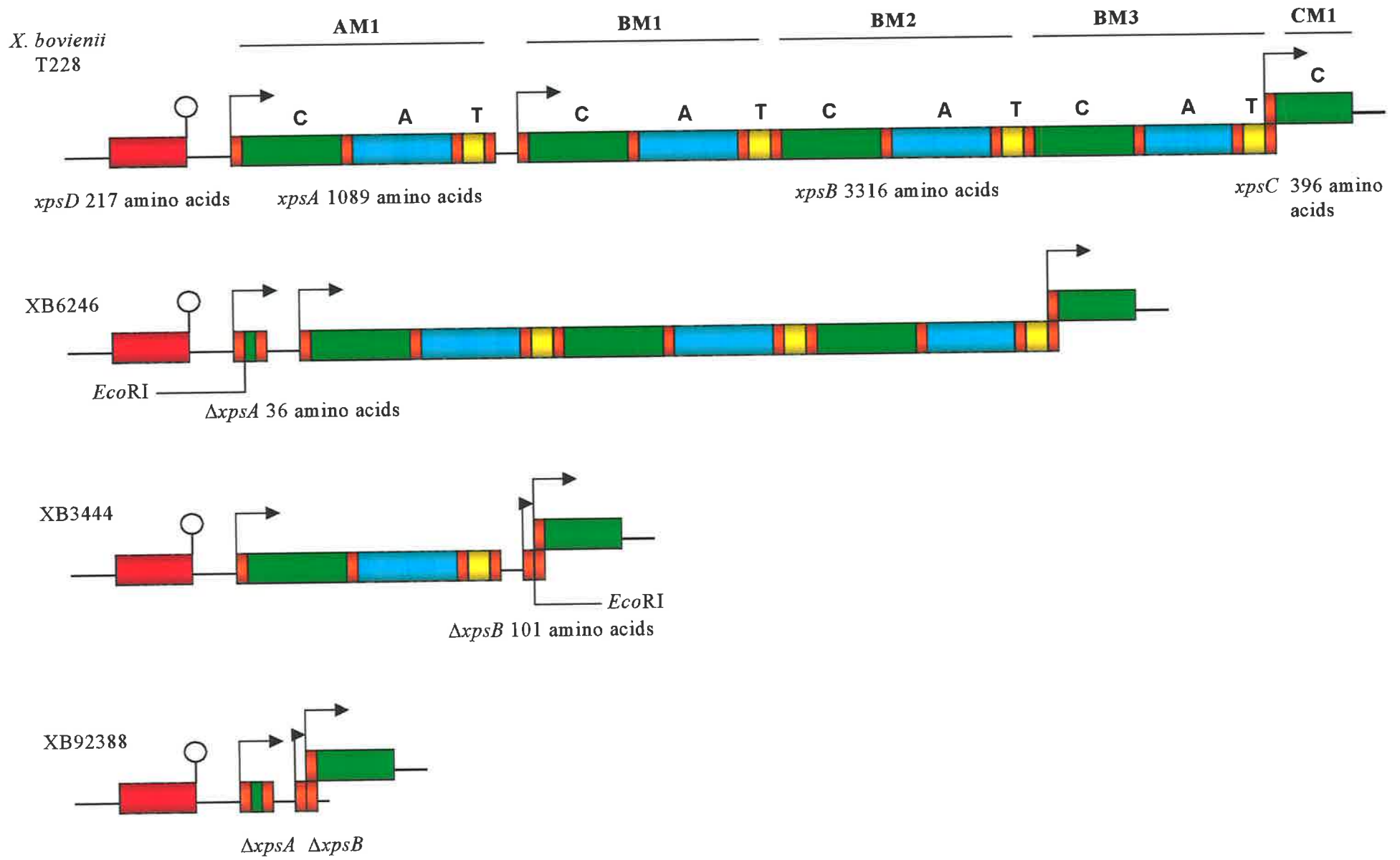


Figure 7.13 Schematic representation of inframe deletions within *xpsA* and *xpsB*. The final size of *xpsA* and *xpsB*, and location of the introduced *EcoRI* sites are noted. The adenylation, thiolation and 95% of the condensation domains from *xpsA* were deleted to create XB6246. All adenylation, condensation and thiolation domains from each module of *xpsB* were deleted to create XB3444. XB92388 is a combination of the *xpsA* and *xpsB* deletions. Abbreviations: A, adenylation domain; C, condensation domain; T, thiolation domain; M1, module 1; M2, module 2 and M3, module 3.



deletion bacterial cells into *G. mellonella* larvae. The affect on *G. mellonella* haemocytes was then examined by transmission electron microscopy (TEM). The viability of *Drosophila* insect cell line, Schneider's cells, in the presence of wild type and mutant bacteria supernatants was also used to assess cytotoxic activity.

7.2.4.1 Expression of phase dependent characteristics by XB3444, XB6246 and XB92388

The expression of phase dependent characteristics by in frame deletion mutants XB3444, XB6246 and XB92388 were compared to wild type *X. bovienii*. Wild type and mutant bacteria demonstrated similar Congo Red binding properties. Colonies showed an accumulation of Congo Red, whilst agar surrounding the colonies became discoloured. Wild type and mutant bacteria both showed significant alpha haemolysis when grown on agar supplemented with SRBC (Table 7.1). However the transposon mutants XB34(45) and XB29(45) (which contain insertions in *xpsA*) and XB26(20) (which contains an insertion in *xpsB*) have altered Congo Red binding and haemolytic phenotypes (see Chapter 4, section 4.2.2.1). These conflicting results suggest the transposon induced polar mutation has disrupted expression of genes downstream of *xpsABC*.

By contrast all in-frame deletion mutants and transposon mutants with insertions corresponding to *xpsA* and *xpsB* shows a variable but reduced level of antimicrobial activity against *M. luteus* when compared to the activity of wild type *X. bovienii*. Figure 7.14, Panel A shows examples of the type of inhibition zones observed when assessing in frame deletion mutants and wild type bacteria for antimicrobial activity. Panel (A1) depicts the growth of *M. luteus* on NA conditioned with wild type *X. bovienii*. Panels (A3) and (A4) depict examples of altered zones of inhibition respectively. Panel (A2) depicts an uneven inhibition zone created by the growth of *M. luteus* on NA conditioned with XB92388. The irregular inhibition zones of *M. luteus* were often seen when *M. luteus* was grown on NA conditioned with one of the deletion mutants. Results obtained were qualitative as the experimental protocol was not standardised. Therefore the comparison of inhibition zone sizes and shapes can only be used as a guide to the extent of antimicrobial activity and/or indicator organism sensitivity.

	<i>X. bovienii</i> T228	XB3444	XB6246	XB92388
Antibiotic activity	+++	+ ^a	+ ^a	+ ^a
Congo Red binding	+++	+++	+++	+++
Haemolysis	+++	+++	+++	+++
Phospholipase C	+++	- ^b	- ^b	- ^b

Table 7.1 Expression of phase dependent characteristics by *X. bovienii* strain T228 and *X. bovienii* deletion mutants XB3444, XB6246 and XB92388. A + denotes the degree of a positive phenotype when compared to wild type bacteria ; a - denotes a negative phenotype.

^a Antimicrobial activity is reduced when compared to the wild type, however the degree of reduced activity and zone shape is variable on numerous repetitions (see Figure 7.14).

^b Wild type *X. bovienii* T228 showed an opaque halo around and under the colony when grown on NA supplemented with 5% egg yolk (see Chapter 2, section 2.2). In comparison, deletion mutants XB3444, XB6246 and XB92388 showed no opacity around or under colonies when grown under the same conditions (see Figure 7.15).

Figure 7.14

Panel A

Inhibition of *M. luteus* by *X. bovienii* strains.

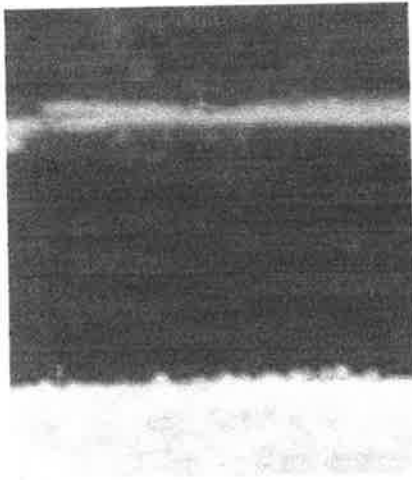
Typical examples of zones of growth inhibition formed when *M. luteus* is grown in overlay on NA conditioned by *X. bovienii*. Panel A1 depicts the growth of *M. luteus* when grown on NA conditioned with *X. bovienii* T228. Panel A2 depicts an uneven inhibition zone created by the growth of *M. luteus* on NA conditioned by XB92388 ($\Delta xpsA\Delta xpsB$). Panels A3 and A4 depict typical examples of reduced and no zones of *M. luteus* growth inhibition on NA conditioned by XB92388 and P2 *X. bovienii* respectively.

Panel B

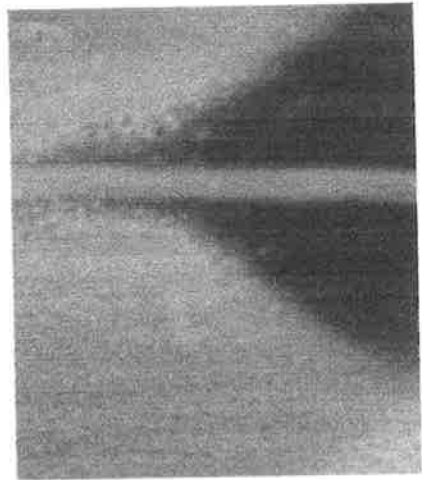
Phospholipase C activity of *X. bovienii* T228 and *xpsAB* in-frame deletion mutant XB92388. Panel B1 shows the typical reaction for wild type strains of *X. bovienii*. Panel B2 shows the typical negative phospholipase C phenotype demonstrated for all in-frame deletion mutants.

Panel A

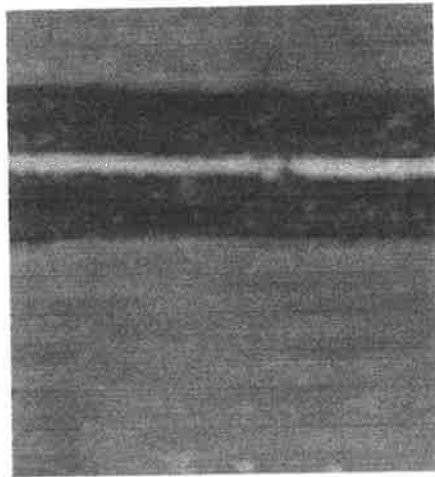
1



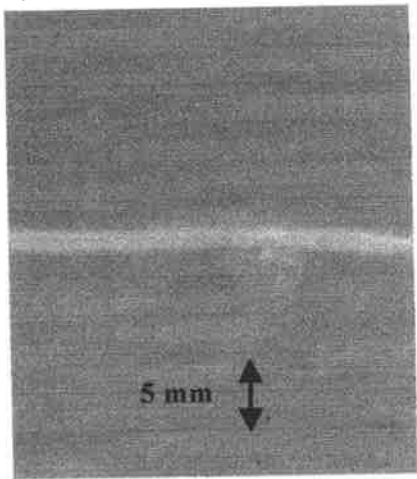
2



3

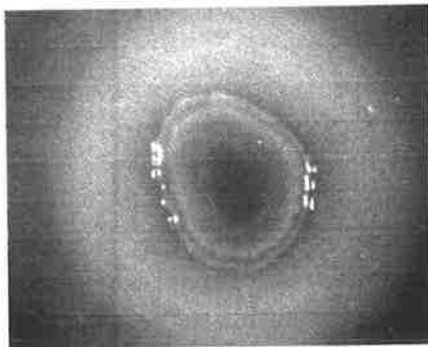


4

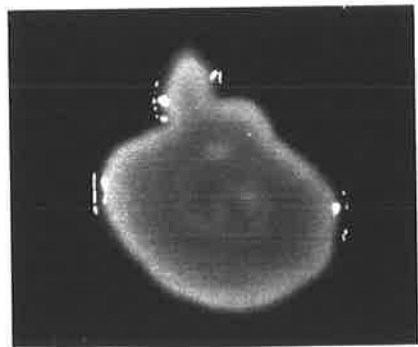


Panel B

1



2



The transposon mutant (XB26(20), XB29(45) and XB34(45)) and in frame deletion mutant (XB3444, XB6246 and XB92388) bacteria all showed similar phenotypes with respect to phospholipase C activity. Wild type *X. bovienii* demonstrated an opaque halo around and under the colony when grown on NA supplemented with 5% egg yolk. By comparison the transposon mutants (see Chapter 4, section 4.2.2.1) and in frame deletion mutants showed no opacity around or under colonies. Figure 7.14, panel (B1) depicts an example of wild type *X. bovienii* grown on NA supplemented with 5% egg yolk, whilst panel (B2) depicts a typical in frame deletion mutant under the same conditions.

7.2.4.2 Quantitation of XB3444, XB6246 and XB92388 antimicrobial activity against *M. luteus*

The antimicrobial activity of *Xenorhabdus* cultures was measured as follows. Filter sterilised culture supernatants derived from *X. bovienii* wild type and in frame *xps* deletion mutants were serially diluted and added to NB suspensions of *M. luteus* to achieve final dilutions ranging from 1:2 to 1:64. Similarly, a stock solution of bacitracin was added to suspensions of *M. luteus* to achieve a range of concentrations from 200 – 6.25 mg/ml. Treated cell suspensions were then incubated at 28C and the culture OD monitored. Changes in A_{600} relative to untreated control suspensions were determined and expressed as the relative growth of *M. luteus*. The results of these inhibition studies are shown in Fig. 7.15.

The highest concentrations of wild type and deletion mutant culture supernatant tested, inhibited growth of *M. luteus* to the same extent as the highest concentration of bacitracin (Fig. 7.15 Panel A). The relative growth of treated suspensions of *M. luteus* decreased by 50% over 9 hours. After 24 hr incubation, the relative growth index decreased to less than 20% of that of the untreated control cultures.

As expected, lower dilutions of supernatants were less able to inhibit the growth of *M. luteus* (Fig. 7.15 Panels B – F). However, at the lowest supernatant dilution tested (1:64), growth of *M. luteus* was equivalent to that of the untreated control suspensions. At intermediate dilutions, supernatants derived from the deletion mutants inhibited *M. luteus* growth to a greater extent than that derived from the wild type parent culture. In particular, supernatant derived from cultures of the *xpsAB* double deletion mutant (XB92388), and to a lesser extent the single *xps* deletion mutants (XB3444 and XB6246), was able to strongly inhibit growth of

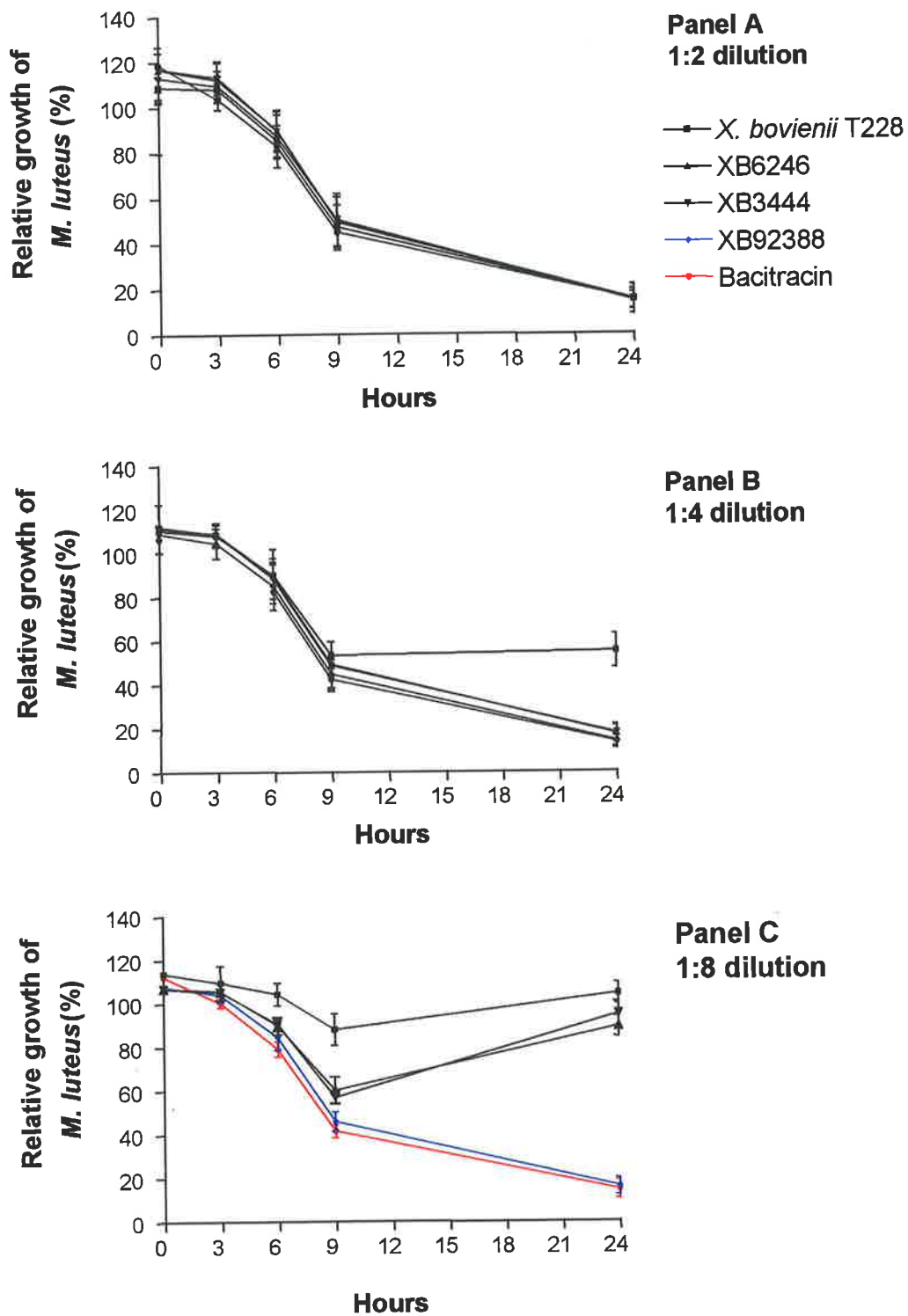


Figure 7.15 Relative growth of *M. luteus* after application of 1:2, 1:4 and 1:8 dilutions of filter sterile culture supernatants from *X. bovienii* T228, XB3444, XB6246, XB92388 and bacitracin (the first dilution is equivalent to 200 mg/ml).

Changes in treated *M. luteus* A_{600} relative to untreated control suspensions were determined and expressed as the relative growth of *M. luteus*.

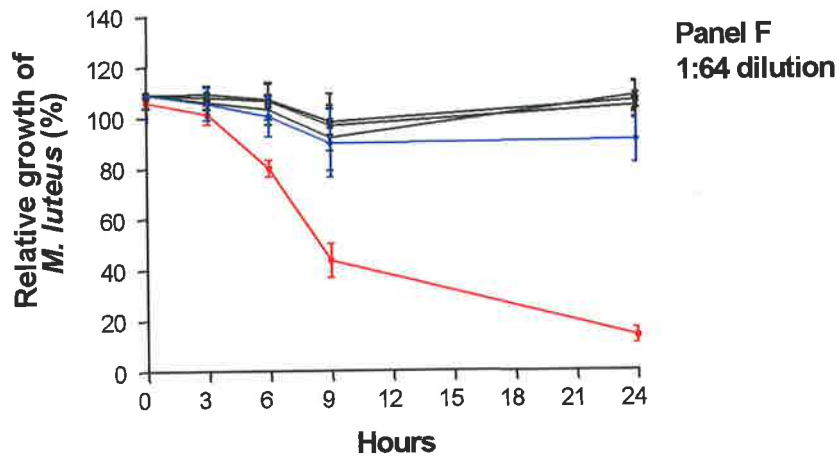
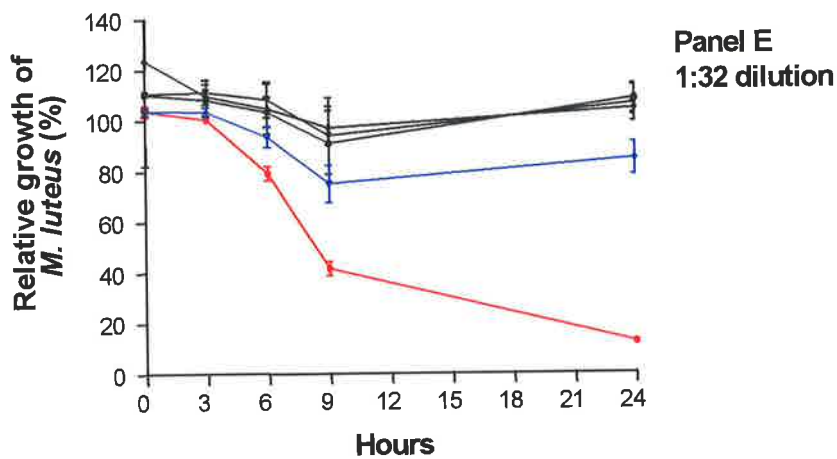
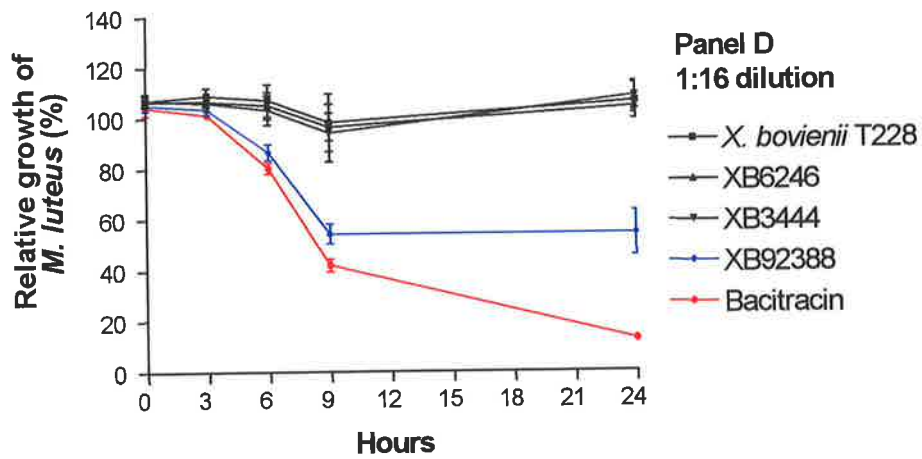


Figure 7.15 Relative growth of *M. luteus* after application of 1:16, 1:32 and 1:64 dilutions of filter sterile culture supernatant from *X. bovienii* T228, XB3444, XB6246, XB92388 and bacitracin.

Changes in treated *M. luteus* A_{600} relative to untreated control suspensions were determined and expressed as the relative growth of *M. luteus*.

M. luteus even when diluted to 1:32. Interestingly, while intermediate concentrations of culture supernatants were able to inhibit growth of *M. luteus* for up to 9 hours, longer incubation allowed significant growth of *M. luteus* to occur (Figure 7.15, Panels C – E). Nevertheless, all concentrations of bacitracin used strongly inhibited growth of *M. luteus*.

7.2.4.3 *In vivo* effects of *X. bovienii* T228, XB3444, XB6246 and XB92388 on *Galleria mellonella* haemocytes

The effect of wild type and in frame deletion mutant bacteria on *G. mellonella* haemocytes was examined under *in vivo* conditions. Log phase bacteria were injected into *G. mellonella*. Moribund larvae were bled and the haemocytes embedded in epoxy resin. Stained thin sections of embedded haemocytes were examined by transmission electron microscopy (see section 2.30). Haemocytes from non-infected and PBS injected *G. mellonella* were used as control samples.

Haemocytes recovered from non-infected and sterile PBS only injected *G. mellonella* showed no evidence of apoptosis or cytoplasmic membrane damage when examined by TEM. The majority of cells examined were morphologically similar to plasmatocytes and granulocytes. These results suggest *G. mellonella* haemocytes can be prepared for examination by TEM without damage. Furthermore, injection of sterile PBS does not affect the integrity of haemocytes derived from *G. mellonella*.

Control haemocytes and haemocytes recovered from *G. mellonella* infected with *X. bovienii* T228 or a deletion mutants (XB3444, XB6246 or XB92388) showed no evidence of cell damage when examined by TEM. No evidence of apoptosis or cytoplasmic membrane damage was observed. Furthermore, invasion of haemocytes by either wild type or mutant *Xenorhabdus* was not observed. Figure 7.16 shows a compilation of typical TEM images.

Under the experimental conditions used, neither *X. bovienii* wild type or *xps* deletion mutants adversely affect plasmatocyte or granulocyte populations of *G. mellonella*.

Figure 7.16 Transmission electron micrographs of *G. mellonella* haemocytes obtained from insects injected with sterile PBS, *X. bovienii* T228 or XB92388. Images present are typical of those also found for XB3444 and XB6246. Granulocytes are labelled (G) and plasmatocytes (P).

Panel A: Granulocyte from control (uninjected) *G. mellonella*.

Panel B: Plasmatocytes and granulocyte from PBS injected *G. mellonella*.

Panel C: Plasmatocyte from *X. bovienii* T228 injected *G. mellonella*.

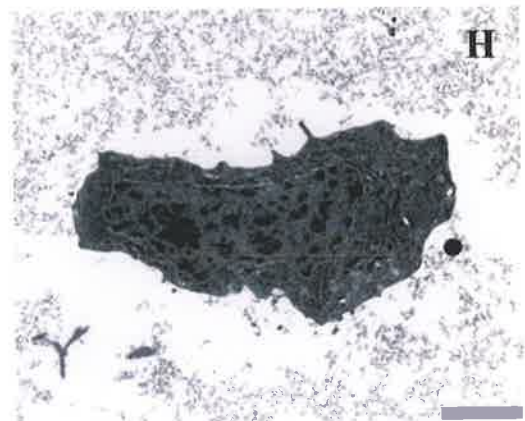
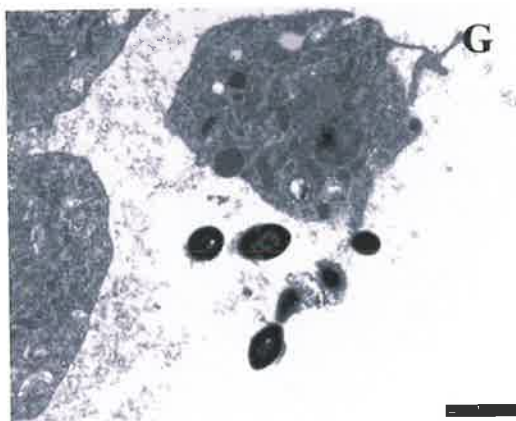
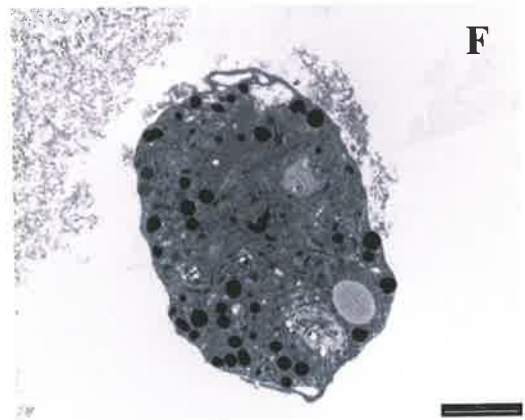
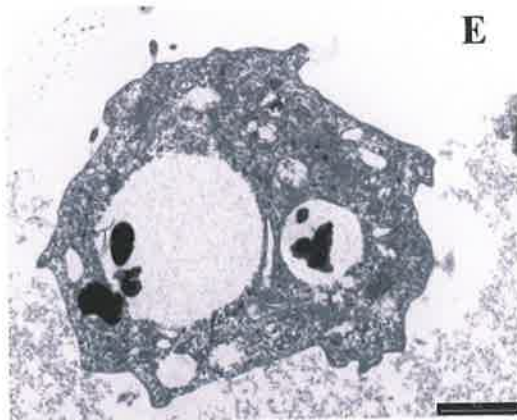
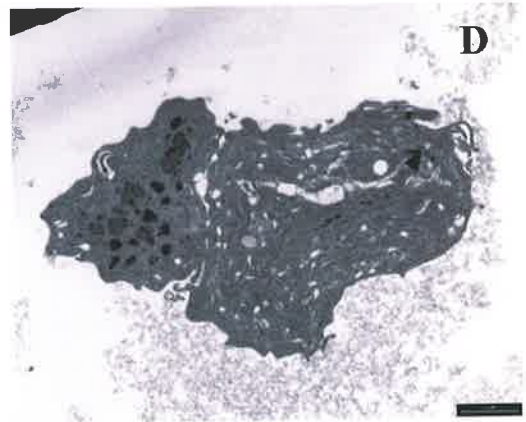
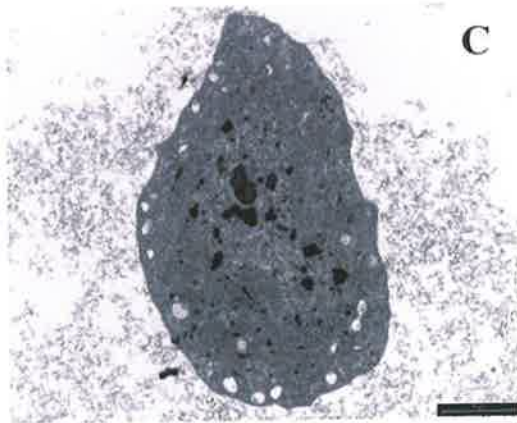
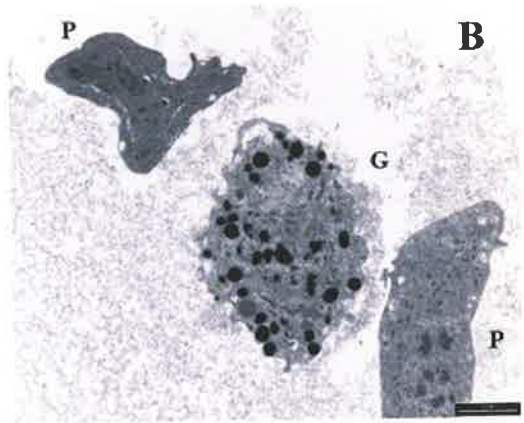
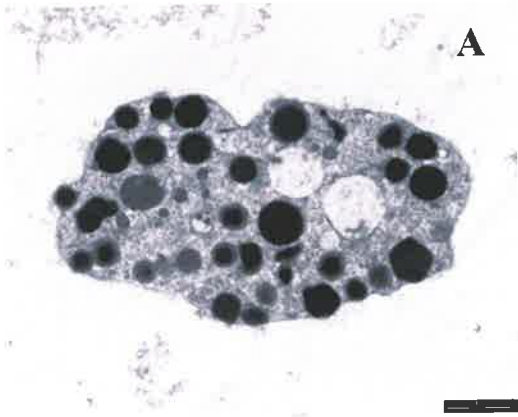
Panel D: Plasmatocyte from *X. bovienii* T228 injected *G. mellonella*.

Panel E: Plasmatocyte from XB92388 injected *G. mellonella*.

Panel F: Granulocyte from XB92388 injected *G. mellonella*.

Panel G: Plasmatocyte from XB92388 injected *G. mellonella*.

Panel H: Plasmatocyte from XB92388 injected *G. mellonella*.



7.2.4.4 Cytotoxicity of *X. bovienii* T228, XB3444, XB6246 and XB92388 culture supernatants for Schneider's cells.

To examine the potential cytotoxic activity of *X. bovienii* culture supernatants for insect cells, Schneider's cells were incubated in the presence of wild type and *xps* mutant culture supernatants. To eliminate the potential effects of standard bacteriological growth medium components on Schneider's cell viability, the test bacteria were cultured in Schneider's cell media. Supernatant fluids derived from these cultures were then used to test the cytotoxicity for Schneider's cells. The percentage of viable Schneider's cells remaining after treatment was determined by a trypan blue exclusion staining method. (see section 2.31).

Positive control cultures of Schneider's cells maintained a consistent level of viability (ca. 100%) over the entire experiment (Figure 7.17).

When bacterial culture supernatants were added to Schneider's cell preparations a steady and significant reduction in cell viability was observed over a 6 hr incubation period. Similar changes in viability were observed for all bacterial culture supernatants tested. Unlike the bioassay experiments in section 7.2.4.2, the effect of bacterial cell supernatants on Schneider's cell viability was only tested at a 1:2 dilution of supernatant. Given the gradual rate of Schneider's cell death observed with the 1:2 diluted supernatant, further dilutions of bacterial cell supernatant would not have yielded any further significant results.

Whilst the viability of Schneider's cells did decline in the presence of each bacterial cell supernatant, no conclusions regarding the effects of in-frame deletions in *xpsA*, *xpsB* or *xpsAB* could be drawn from this experiment.

7.3 Discussion

Chapter 4 described the mapping of transposon insertion mutants XB34(45) and XB29(45) to *xpsA*, and XB26(20) to *xpsB*. Although each of these transposon mutants contain a polar insertion which results in phenotypic defects, the polarity effects on expression of downstream genes is unknown. In order to overcome the problems associated with polar insertions, in-frame deletion mutations in *xpsA* and *xpsB* were constructed and used in attempts to ascribe experimentally determined function to the *xps* genes. In addition, these deletion mutants were

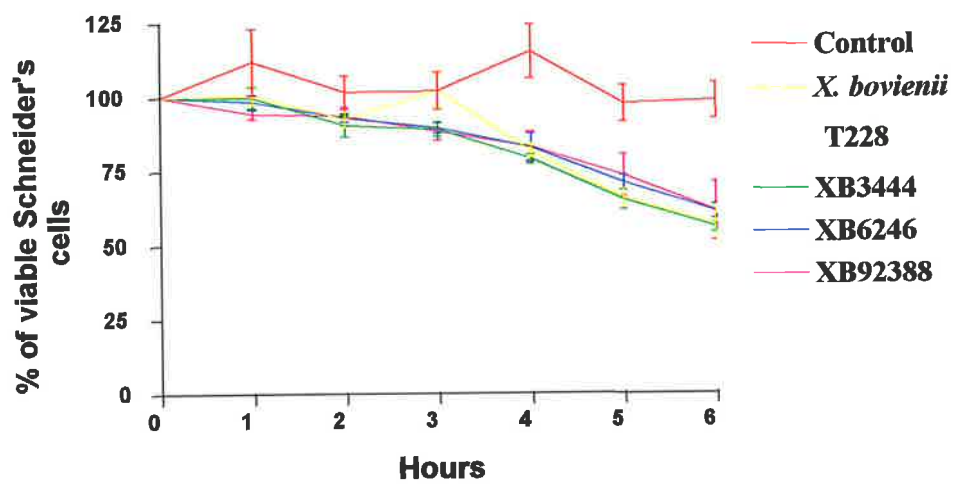


Figure 7.17 Viability of Schneider's cells after incubation with filtered supernatants from *X. bovienii* T228, XB3444, XB6246 and XB92388. Control Schneider's cells were incubated with sterile Schneider's cell media + 10% (v/v) FCS. The percentage of viable Schneider's cells incubated in each supernatant was determined relative to the control.

compared to the existing transposon mutants. Nevertheless, it should be noted that these studies considered *xpsA* and *xpsB* independently of the putative and apparently co-transcribed peptide synthetase gene *xpsC* as well as any other as yet undescribed *xps* related genes.

A combination of PCR and homologous recombination were used in the construction of each in-frame deletion, whilst PCR and Southern hybridisation analysis were used to confirm each construct. In-frame deletion mutant XB6246 was constructed by deletion of 2601 bp from *xpsA*, whilst in-frame deletion mutant XB3444 was constructed by deleting 9648 bp from *xpsB*. The double in-frame deletion mutant XB92388 was constructed by deletion of these portions of *xpsA* and *xpsB* in the same *X. bovienii* strain.

Several phase variant phenotypes of in-frame deletion mutants XB6246, XB3444 and XB92388 were compared with transposon insertion mutants XB26(20), XB29(45) and XB34(45). Transposon insertion mutants XB26(20), XB29(45) and XB34(45) show a disruption in haemolytic activity and Congo Red binding (see Chapter 4, section 4.2.2.1). By comparison, the in frame *xps* deletion mutants XB6246, XB3444 and XB92388 demonstrated normal haemolytic and Congo Red binding activity. These results suggested the transposon insertions created polar effects on genes encoding haemolytic and Congo Red binding functions. However, both the transposon and the in-frame deletion mutants of *xpsA* and *xpsB* display disrupted phospholipase C and antimicrobial activity and these phenotypic changes are therefore likely to represent either direct or cryptic effects on the mutations within the *xps* genes. The fact that the same results were obtained for both types of mutants eliminates the possibility of polar defects.

Transposon mutant induced polarity effects with respect to haemolysis and Congo Red binding activity may occur for a number of reasons. Genes encoding haemolysis and Congo Red binding may be directly affected by a frame-shift due caused by the transposon insertion; this could result in missense and non-sense mutations which disrupt gene integrity. Other genes involved in expression at the transcriptional and/or translational level, transport and secretion may be downstream and affected by an upstream polar transposon insertion. Interestingly, other groups have reported a variety of cryptic effects following mutation of genes in the related organism, *X. nematophilus*. For example, Givaudan and Lanois (Givaudan & Lanois, 2000) reported that expression of haemolysin by the closely related *X. nematophilus* may be dependent on the transcriptional activator of flagellar genes *flhDC*.

X. nematophilus flhDC null mutants show an absence of intracellular haemolytic activity, and an unusual form of haemolysis on NA supplemented with SRBC known as annular haemolysis. Disruption of chemotaxis and lipolysis of Tween 20, 40 and 60 were also observed for *X. nematophilus flhDC* null mutants. Disruption of the *flhDC* gene did not affect phospholipase C or antimicrobial activity, however, a 20-50% reduction of phospholipase C and antimicrobial activity was observed when *flhDC* was placed *in trans* in both the wild type and *flhDC* null mutant strains (Givaudan & Lanois, 2000). The reason for this observation has not been established.

Xenorhabdus spp. express phospholipase C (Thaler *et al.*, 1998), however the gene sequence has not been identified. Thaler (Thaler *et al.*, 1998) isolated five enzymatic isomers responsible for phospholipase C activity from the supernatant of *X. nematophilus* P1 cultures. Substrate specificity of the *X. nematophilus* P1 lecithinase suggested a phospholipase C preferentially active on phosphatidylcholine could be isolated. Assuming that the phospholipase C gene(s) in *X. bovienii* have a similar genetic organisation, then disruptions in the *xpsAB* peptide synthetase gene region should not completely disrupt expression of phospholipase C. However in-frame deletions within the *xpsAB* genes encoding peptide synthetases clearly have an effect on phospholipase C expression. Several explanations may account for this phenomenon. *X. bovienii* peptide synthetase may directly affect transcription, translation, processing, transport and/or secretion of phospholipase C. The peptide synthetase gene region may be higher in gene expression hierarchy, and affect the expression of another phospholipase C dependent gene. Alternatively, the bioactive peptide product of the *xpsAB* genes may interact with the egg yolk components of Egg Yolk agar to produce the characteristically slow formation of precipitate around bacterial colonies. Disruption of the *xpsAB* genes would be expected to eliminate this effect. One way to confirm the latter hypothesis would be to apply purified preparations of the bioactive peptide product of the peptide synthetase(s) to Egg Yolk agar.

Xenorhabdus spp. are known to produce a broad range of potent antimicrobial compounds such as bacteriocins and antibiotics with broad spectrum activity against different bacteria, fungi and yeasts (Akhurst, 1982; Forst & Neilson, 1996; Forst *et al.*, 1997). The wide array of antimicrobials expressed by a single *Xenorhabdus* strain can be particularly problematical for studies designed to identify genes involved in antimicrobial production. Mutations in genes responsible for one anti-microbial substance cannot be selected for example, by

screening for colonies by plating against sensitive indicator strains. Conversely, without specific phenotypic tests, the use of defined mutations to establish gene function may also be problematical. In this study a range of phenotypic tests were employed in combination with defined mutations within the *xpsAB* genes as a means of determining probable gene function. Semi-quantitative assays that examined the inhibitory effect of culture supernatants on growth of *M. luteus* were used in attempts to assess potential peptide synthetase dependent antimicrobial activity. However, the most appropriate way to determine the function of *X. bovienii* peptide synthetase, without interference from other antimicrobial, is to purify the compound.

The construction of in frame deletion mutants represents an important step in the process of achieving that goal. Fractionation of antimicrobial peptides from cultures of wild type and deletion mutant bacteria using HPLC and other chromatographic techniques would allow a identification of the compound of interest by difference. Purification of the bioactive peptide(s) would also facilitate determination of structure by NMR and mass spectrometry.

X. bovienii peptide synthetases are predicted to assemble a siderophore antibiotic (see Chapter 5). Transposon insertions and in-frame deletion mutations within the putative peptide synthetase genes all resulted in a reduction in antimicrobial activity when this was tested using the agar overlay method with *M. luteus* as the indicator strain. Surprisingly, the zones of *M. luteus* inhibition obtained when testing expression of antimicrobial substances by deletion mutants was often unevenly shaped (see Figure 7.14). This behaviour is difficult to explain. The *X. bovienii* culture streak in all cases was uniform and hence the amount of antimicrobial substance produced at any point along the length of the streak was likely to be uniform. Localised changes from the P1 to P2 form also seem unlikely as this phenomenon was never observed for wild type cultures.

Nevertheless, these results are in contrast to data obtained when a semi-quantitative method was used to compare the antimicrobial activity of *Xenorhabdus* broth culture supernatants. Surprisingly, the antimicrobial capacity supernatants obtained from in-frame deletion mutant was greater than of supernatants derived from cultures of the wild type parent. In particular, culture supernatant from the double deletion mutant XB92388 ($\Delta xpsA xpsB$) had the greatest level of anti-microbial activity against the indicator strain, *M. luteus*. Apparently, deletion of *xpsAB* modules from *X. bovienii* peptide synthetase results in an increase in antimicrobial

capacity when culture supernatant is added directly to liquid cultures of *M. luteus*. There are several explanations for these unexpected observations. The most obvious is that deletion of peptide synthetase modules results in the production of a different spectrum of antimicrobial compounds that are more effective against *M. luteus* than that of the wild type *X. bovienii*. This process could be regarded as analogous to peptide synthetase module swapping for creation of new compounds. Another explanation for the observations is that the other antimicrobial compounds known to be expressed by *Xenorhabdus* spp. are produced at higher concentrations in the absence of XpsAB synthetase activity. However, in view of the fact that a reduction in size of *M. luteus* growth inhibition zones noted for the agar overlay assays of the antimicrobial activity of deletion mutants, this seems unlikely. Indeed an increase in the size of growth inhibitory zones would be expected in this case.

How then can the apparently conflicting data obtained for the agar overlay technique and the semi-quantitative liquid culture assays be reconciled? Why should the former technique suggest the deletion mutants display a reduced antimicrobial activity, whereas the latter indicate an apparent increase in anti-microbial activity? Given the heterogeneity of antimicrobial substances potentially expressed by *Xenorhabdus* this is a question that may be difficult to resolve until such time as the *xps* genes are cloned and expressed in a host devoid of biochemical pathways which result in formation of other antimicrobial substances. However, it is clear that the overlay technique relies on diffusion of the bioactive agent(s) from the producer cells into the growth medium, whereas the semi-quantitative method involves exposure of all indicator cells to the bioactive agent(s). Thus if *xpsAB* deletion mutants express a new peptide based bioactive agent (eg. one dependent on *xpsC*) which differs in size, and hence ability to diffuse into agar media, then it is possible to explain these conflicting results. A bioactive peptide which is larger, or structurally more complex, would diffuse more slowly into an agar medium and hence the size of an *M. luteus* growth inhibition zone would be smaller. Conversely, the semi-quantitative assay would be unaffected by the changes and would reflect the anti-microbial activity of the bioactive agent(s) accordingly.

In an age where the incidence of multiply drug resistant microbial pathogens is increasing, there is an urgent need to produce new clinically significant anti-microbial agents and pharmaceutical products. Peptide synthetases that form antimicrobial agents can provide enormous potential for the rational design of new bioactive peptides by recombination of the biosynthetic genes (Mootz *et al.*, 2000). By altering the module order and arrangement of

modification domains of peptide synthetases, a large array of new bioactive peptides could be produced. However an understanding of the complex interactions that exist between domains and what ultimately determine functionality, has yet to be achieved. Deletion of condensation domains results in complete loss of any detectable adenylation domain activity. Additionally, construction of hybrid peptide synthetases by incorporation of condensation domains obtained from other modules can cause the loss of any detectable activity associated with adenylation domains (Symmank *et al.*, 1999). Furthermore, significant reduction (ca. 90%) in tyrocidin synthetase A adenylation activity has been reported when short deletions in the adenylation domain N-terminal region are made (Quadri *et al.*, 1998). These observations may be the result of as yet unknown interactions and recognition processes between condensation and adenylation domains. Non-specific effects caused by the hybrid condensation domains, such as prevention or alteration of folding of the recombinant enzyme, could also account for the inactivity of adenylation domains (Symmank *et al.*, 1999). There are also reports of hybrid condensation domains which demonstrate functional adenylation domains, although this depends on the fusion site (Symmank *et al.*, 1999). Furthermore, recognition processes between specific adenylation and thiolation domains are suspected to exist (Weinreb *et al.*, 1998). For example, the carboxyl-terminal thioesterase region of the *Bacillus subtilis* surfactin synthetase operon has successfully been moved to the end of an internal amino acid binding domain to produce a peptide synthetase capable of producing truncated peptides (de Ferra *et al.*, 1997).

Each of the *X. bovienii* mutants containing in-frame deletions within *xpsA* and/or *xpsB* had all domains within the targeted module deleted. In XB6246 the adenylation and thiolation domains, and 95% of the condensation domain from module one (M1) of *xpsA* were deleted. In XB3444 all domains were removed from each of the three modules of *xpsB*. Deletion mutant XB92388 carried both of these mutations. As almost each domain was completely deleted, the corresponding modules should have no residual activity. Condensation domains are generally found at the 5' end of the peptide synthetase sequence and are important for initiation of construction of a peptide synthetase compound. As each gene identified so far in the peptide synthetase operon (*xpsABC*) has a condensation domain, construction of a truncated version peptide synthetase might occur. However, as each mutant has a residual amount of DNA from each module still present within the operon, the possibility of interference with prevention or alteration of folding steps of the recombinant enzyme does exist. Interactions between domains and modules, and the effects of mutations within these

regions has not been fully deduced and reported in the available literature. Furthermore, the complete nucleotide sequence of *X. bovienii* peptide synthetase has not been identified, and the number of genes and modules contained within this operon is unknown. Therefore the final size of the peptide synthetase, and the impact of deleting several modules is unknown.

Peptides assembled by peptide synthetases are known to have a variety of biological activities. Some are strongly antibacterial, while other types act as surfactants and toxins. Given the array of different biological activities displayed, the potential for XpsAB dependent bioactive peptides to interact with larval haemocytes was examined. In the absence of purified peptides, this was attempted by comparing the effects of the deletion mutants and the wild type parent on haemocytes for loss of effect. Two approaches were used. The first involved the examination of haemocytes extracted from larvae experimentally infected with bacteria, by transmission electron microscopy. The second approach involved an assessment of the effect of bacterial culture supernatants on viability of Schneider's cells.

No differential effect on haemocyte structure and integrity was observed for haemocytes extracted from larvae infected with cultures of either the mutants or the wild type parent. This result indicated that within the limitations of the experimental approach used, peptides formed by XpsAB are unlikely to affect *G. mellonella* haemocyte integrity. While different types of insect haemocyte were identified, a comprehensive classification was not possible since individual cells can have very different appearances depending on the conditions and technique used to study them. Attempts have been made to synonymise haemocytes across the different insect orders and reduce them to six main types prohaemocytes, plasmatocytes, granulocytes (which are probably the same as cystocytes or coagulocytes), spherulocytes, oenocytoids and adipohaemocytes (Rowley & Ratcliffe, 1981; Gupta, 1985; Gupta, 1991). Prohaemocytes make up less than 5% of the total haemocyte population; plasmatocytes and granulocytes each make up more than 30% of the total haemocyte population. Granulocytes are probably intermediates of plasmatocytes (Chain *et al.*, 1992). Combined, spherulocytes, oenocytoids and adipohaemocytes make up a small percentage of the total haemocyte population. Given these statistics it is not surprising that mainly plasmatocyte and granulocyte populations were the likely cell types observed by TEM under the current experimental conditions.

Wounding of *G. mellonella* larvae causes a marked decline in haemocyte counts. If the wound is accompanied by entrance of pathogenic bacteria, such as *Xenorhabdus* spp., the haemocyte count does not recover for a long period of time (Chapman, 1998). The sudden reduction in numbers is mainly due to plasmatocyte removal in association with nodule or capsule formation (see Chapter 1, section 1.6.5.2). Sustained low haemocyte counts are associated with the entrance of pathogenic bacteria and is a reflection of haemocytes adhering to the capsule. Consequently after injection with wild type or deletion mutant *Xenorhabdus moribund* larvae should have developed nodules in response to a *Xenorhabdus* infection. Furthermore, numbers and types of circulating haemocytes collected for examination by TEM should have been reduced. Given the small number (30) images examined, and the few types of haemocytes observed, it is difficult to draw clear conclusions about the effects of *xpsAB* mutations to be drawn from these experiments. Nevertheless, as a side issue, this approach clearly showed that *X. bovienii* does not invade haemocytes and therefore is unlikely to be a facultative intracellular pathogen.

In an attempt to overcome this difficulty the impact of bacterial culture supernatant on viability of Schneider's cells was tested. The advantage of this approach is the use of large numbers of cells in an assay that is easily repeatable. Supernatants derived from cultures of the wild type parent and deletion mutants initiated a gradual decline in Schneider's cell viability. No significant differences in cell viability were observed. These results suggested that although a number of cytotoxic factors are present in the bacterial cell supernatants, this toxicity is not the result of a bioactive peptide synthesised by XpsAB.

Although the Schneider's cell assay provided a quantifiable estimate of the cytotoxicity of bacterial cell supernatants, the experiments should/could be repeated using:

1. a number of other insect cell lines to eliminate cell line specific effects.
2. *G. mellonella* haemocyte monolayers. Whilst haemocytes are difficult to collect and manipulate *in vitro*, haemocyte monolayers have been developed previously (Dunphy & Webster, 1984; Brookman *et al.*, 1988; Dunphy, 1994; Maxwell *et al.*, 1995).

While these alternative approaches may help resolve the involvement of XpsAB synthesised bioactive peptides in pathogenesis of insects, clearly the value of using purified peptides as opposed to culture supernatants as a source of these compounds cannot be overvalued. Purified peptides would allow a direct examination of effects on insect cell lines without

interference from other compounds produced by *Xenorhabdus*. Previous reports have suggested a link between phosphopantetheinyl transferase expression, which can be related to NRPSs, and the viability of nematode cultures (Ciche *et al.*, 2001). Therefore future work on the *X. bovienii xpsABC* region should examine the affect of this putative bioactive peptide on nematode growth and development.

Chapter 8

General discussion

8.1 Introduction

The primary aim of this thesis was to identify and characterise the expression of a phase variant characteristic from *X. bovienii* T228 in an attempt to contribute to the body of knowledge relating to this subset of genes. *X. bovienii* mutants were generated by transposon mutagenesis, and those mutants screened for loss of a phenotype normally associated with phase variation eg. haemolytic and phospholipase C activity. Transposon insertions were mapped with respect to each other; the region of DNA identified sequenced and shown to have homology to non-ribosomal peptide synthetases (NRPSs). Aspects of regulation of the NRPS gene region were determined at the transcriptional level, and in-frame deletion mutants were constructed to facilitate functional analysis. To assist the primary aim it was considered necessary to construct a RecA mutant of *X. bovienii*, to facilitate genetic complementation analysis and increase the stability of recombinant plasmids and foreign DNA. As a side issue the impact of a RecA mutant on *X. bovienii* phase variation and pathogenesis for insect larvae was assessed.

8.2 RecA is not required for *X. bovienii* phase variation

PCR based techniques were used to clone and sequence the *recA* gene from *X. bovienii* T228. The 1077 bp gene sequence was 85% similar at the nucleotide level and 95% similar at the amino acid level to the RecA of *X. nematophilus*. *X. bovienii* RecA also showed considerable similarity to the RecA proteins from other Gram negative bacteria including *Erwinia carotovora*, *Proteus mirabilis*, *Serratia marcescens* and *Yersinia pestis*. ATP binding domains I and II were identified in the *X. bovienii* RecA amino acid sequence, along with critical residues required for a functional RecA protein. UV sensitivity studies, complementation analysis and recombination proficiency assays were used to demonstrate expression of a functional RecA protein from plasmids in RecA deficient backgrounds.

Allelic-exchange mutagenesis was used to construct a chromosomal *recA* mutation in *X. bovienii* (XB001). UV sensitivity studies established the *recA* mutant (XB001) had a

significantly reduced ability to repair DNA lesions caused by exposure to UV radiation. Furthermore, the UV sensitivity of P1 and P2 forms of the *recA* mutant were identical. In addition, resistance to UV induced damage of the *recA* mutant could not be restored to wild type levels by complementation with a functional copy of *recA* encoded by plasmid pCT303 even though a strain of *E. coli* DK1 (which has a deletion of the *recA* gene) carrying this plasmid showed completely restored resistance to UV radiation. This phenomenon may be explained by the fact that the *recA* insertion mutant, XB001, has the potential to express 72% of the wild type RecA protein. Thus in the presence of the plasmid encoded RecA protein, formation of mixed RecA tetramers could potentially occur, resulting in negative complementation, whereas complementation of the *recA* deletion in *E. coli* DK1 would result in only plasmid derived RecA protein.

Interestingly wild type, *recA* mutant and complemented strains of *X. bovienii* were identical in terms of their expression of known phase dependent characteristics. P1 bacteria were able to convert to P2 bacteria on extended serial subculture. When taken together with Southern hybridisation analyses that showed no obvious large rearrangements in DNA isolated from P1 and P2 bacteria (Akhurst & Boemare, 1990), it is very unlikely that *recA* plays a role in phase variation or regulation of phase dependent characteristics of *Xenorhabdus* spp. This conclusion was further supported by *G. mellonella* larval infection studies showing *recA* mutant XB001 was as pathogenic as either P1 or P2 forms of the wild type derivative.

Although RecA seems not to be involved in the virulence of *X. bovienii* strains, or indeed the phenomenon of phase variation, the ability of the RecA mutant XB001 to support nematode growth and reproduction should be investigated. Nematodes apparently require *Xenorhabdus* cells as a source of nutrition and to degrade insect tissue for nematode digestion. Thus future studies could examine whether presence of XB001 affects the growth and development of the nematode within the insect cadaver. Furthermore the ability of nematodes to retain XB001 within their intestine needs to be established.

The *recA* mutant XB001 represents an important development for further genetic analysis of *X. bovienii*. Recombination deficient mutants are useful in the study of virulence factors and bacterial physiology. Thus a *recA* mutant can facilitate genetic complementation analysis and increase the stability of recombinant plasmids and retention of foreign DNA.

8.3 Transposon mutagenesis of *X. bovienii* T228 and identification of non-ribosomal peptide synthetase (NRSP) homologous DNA

Transposon mutagenesis, facilitated by mini-Tn5 Km, was used to identify *X. bovienii* strains with altered phase dependent phenotypes. Southern hybridisation analysis of DNA from randomly selected mutants confirmed the transposon insertions were independent. Five independent insertions [XB26(20), XB29(45), XB33(21), XB34(45) and XB41(23)] that showed a loss of phospholipase C, haemolysin, antimicrobial and Congo Red binding activity were selected for further analysis. Mini-Tn5 Km and flanking chromosomal DNA from each transposon insertion mutant was cloned and sequenced. BLASTX analysis of cloned chromosomal DNA from XB41(23) revealed homology at the amino acid level to a fimbrial assembly chaperone-like protein. Interestingly, BLASTX analysis of chromosomal DNA sequence flanking transposon mutants XB26(20), XB29(45) and XB34(45) showed each had inserted into a region homologous to NRPSs.

BLASTX analysis of cloned chromosomal DNA from XB33(21) revealed homology at the amino acid level to LeuO, the probable activator of the LeuABCD operon. LeuO is also a member of the LysR family of transcriptional activators shown to be involved in the expression of other NRPSs (Stintzi *et al.*, 1999). Whilst three other transposon insertion mutants showing a similar phenotype to XB33(21) had inserted in DNA regions homologous to NRPSs; it was felt prudent to firstly investigate the NRPS region. Future work could focus on transposon mutant XB33(21) and investigation of the putative LysR-type transcriptional activator encoded by this region of DNA. Non-polar mutagenesis of the LysR-type transcriptional activator could be used as a tool to establish a role of this activator in expression of *X. bovienii* NRPSs.

8.4 Sequence analysis of 15,582 bp of cloned *X. bovienii* chromosomal DNA identifies ORFs *xpsA*, *xpsB*, *xpsC* and *xpsD*

Overall 15,582 bp of *X. bovienii* T228 chromosomal DNA was sequenced. Two complete (*xpsA* and *xpsB*) and two partial (*xpsD* and *xpsC*) ORFs were identified. The partial ORF *xpsD* was 653 bp and showed homology at the amino acid level to ATP-binding cassette (ABC) transporters required for secretion of the bioactive peptides pyoverdine (PvdE) and

syringomycin (SyrD). A further 788 bp downstream of *xpsD*, the complete ORF *xpsA*, has the potential to encode a protein of 1089 amino acids with a *Mr* value of 122,980. 37 bp downstream of *xpsA* is *xpsB* that has the potential to encode a 3316 amino acid protein with a predicted *Mr* value of 368,263. The stop codon (ATGA) of *xpsB* overlaps the start codon (ATGA) of the partial 1177 bp ORF *xpsC*. ORFs *xpsA*, *xpsB* and *xpsC* are predicted to have an operon arrangement. The final gene order of this region was 5'-*xpsD xpsABC*-3'. BLASTX analysis of *xpsA*, *xpsB* and *xpsC* individually, showed homology at the amino acid level to a range of NRPS genes such as syringomycin (*P. syringae* pv. *syringae*) (Guenzi *et al.*, 1998), nostopeptolide biosynthetic genes (*Nostoc* sp GSV224) (Subbaraju *et al.*, 1997), tyrocidine synthetase (*Brevibacillus brevis*) (Mootz & Marahiel, 1997) and lysobactin synthetase (*Lysobacter* sp.) (Bernhard *et al.*, 1996).

Primer extension analysis identified the NRPS +1 site as being 113 bp upstream of the *xpsA* NRPS start codon. Whilst predictions were made on the basis of experimental observation and computer aided analysis, the transcript was not sequenced to unequivocally determine the exact location of the +1 site. This is essential if further work regarding the role of a LysR-type transcriptional activator on expression of *X. bovienii* NRPS is investigated.

8.5 *X. bovienii* NRPS is predicted to encode a siderophore antibiotic

Based on sequence information derived from the crystal structure analysis of GrsA (Conti *et al.*, 1997), Challis (Challis *et al.*, 2000) developed a method to predict the amino acids activated by individual adenylation domains directly from their amino acid sequence. Using this information the amino acids most likely to be activated by XpsA M1, XpsB M1, XpsB M2 and XpsB M3 adenylation domains were predicted to be serine, 6-*N*-hydroxylysine, glutamine and 6-*N*-hydroxylysine respectively. The presence of serine and lysine residues indicate the *X. bovienii* NRSP is likely to be a siderophore antibiotic (Jacques Ravel, pers. comm.). Whilst computer analysis of NRPS amino acid sequences can predict the most likely amino acid activated by each module, biochemical data is required to confirm this. Most of the biochemical data used by Challis to construction the database were derived from only a few microorganisms (eg. *E. coli*, *Bacillus* sp. and *Pseudomonas* sp.), even though a large number of NRPS have been isolated from other microorganisms such as *Streptomyces* sp.

In this thesis the *X. bovienii* NRPS A3-A6 domains and eight amino acid binding pocket sequences, from each adenylation domain, were separately compared to other NRPS amino acid sequences using phylogenetic algorithms. The eight amino acid binding pocket sequences from each adenylation domain showed a greater level of functional clustering in agreement with Challis (Challis *et al.*, 2000). However the *X. bovienii* NRPS eight amino acid binding pocket sequences clustered in a heterogenous region of the tree, where only a few examples of the amino acid they were predicted to activate were present. This emphasised the need to compare more adenylation domains that activate a wider variety of substrates. If only a few examples of adenylation domains activating an amino acid species are used in a phylogenetic study, caution must be exercised when making predictions. In the case of *X. bovienii* NRPS, where XpsB M1, XpsB M2 and XpsB M3 clustered with a heterogenous group of adenylation domains biochemical data will be required to unequivocally resolve the amino acid(s) activated. This could be achieved by over-expression of adenylation domains and analysis of ATP-PPi exchange assays in the presence of different amino acids.

To determine all amino acids activated by the *X. bovienii* NRPS gene region the complete nucleotide sequence of all component NRPS will be required. However deduction of the true chain order can only be obtained by purification of the bioactive compound(s) followed by structural analysis using NMR and mass spectrometry. Clearly future work will require purification of the bioactive peptide(s) as a necessary first step.

8.6 XpsD Motifs predict an ABC transport function

Bioactive peptides synthesised by NRPS gene sequences are secreted from the producer cell by ABC (ATP Binding Cassette) transporters. Sequence comparison of XpsD with available protein databases revealed homology to NRPS associated ABC transport genes. Most sequence identity was observed to *Pseudomonas aeruginosa* PvdE (Tsuda *et al.*, 1995) and *Pseudomonas syringae* pv. *syringae* SyrD (Quigley *et al.*, 1993). SyrD is proposed to function as an ATP driven efflux pump, and believed to be a member of the highly selective secretion family of ABC transport proteins (Quigley & Gross, 1994). The primary function of SyrD is proposed to be antimicrobial resistance whereby the producer cell secretes away the harmful compound, therefore preventing host cell damage. Evidence for this hypothesis is provided by the fact that *syrD* mutants show a down regulation in peptide (syringomycin) production (Quigley & Gross, 1994).

If *xpsD* mutants function in a similar way to *P. syringae* pv. *syringae* *syrD* mutants and down regulate expression of peptide products, construction of *xpsD* mutants may facilitate purification of the *X. bovienii* bioactive peptide. A comparison of *X. bovienii* wild type and *xpsD* mutant strains using column chromatography would aid identification of the peptide product in the wild type strain when column elution profiles are compared.

8.7 *X. bovienii* NRPS transcription is cell culture density dependent

The expression of three independent *xpsA-lacZ* transcriptional fusions (XB414.1, XB414.2 and XB414.3) carried on the *X. bovienii* chromosome were dependent on cell culture density. β -galactosidase activity of each *xpsA-lacZ* fusion rose 2 - 3 fold when grown over a 96 hr period. In comparison the β -galactosidase activity expressed from plasmid pCT414 (carrying the *xpsA-lacZ* transcriptional fusion) when maintained by *E. coli* SY327 λ pir was not affected by cell culture density. The high copy number of the vector used to construct pCT414 probably accounts for the initially high levels of β -galactosidase activity in *E. coli*. However, by the 72 hr sampling point β -galactosidase activity from a single copy on the chromosome of XB414.1, XB414.2 and XB414.3 was greater than that for *E. coli* SY327 λ pir [pCT414].

One explanation for this phenomenon is that *X. bovienii* NRPS transcriptional expression is controlled by a quorum sensing mechanism. *N*- β -hydroxybutanoyl homoserine lactone (HBHL), the autoinducer of the luminescent system of *Vibrio harveyi*, has been shown to restore virulence to avirulent mutants of *X. nematophilus*. Furthermore a compound isolated from *X. nematophilus* conditioned media, with the same chromatographic mobility as HBHL, was shown to stimulate the luminescence of a dim autoinducer-dependent mutant of *V. harveyi* (Dunphy *et al.*, 1997). These observations suggest the presence of a HBHL autoinducer like molecule in *X. nematophilus*, and probably *X. bovienii*. To test this hypothesis, the *X. bovienii* *xpsA-lacZ* transcriptional fusion mutants were grown in 20% (v/v) conditioned media, and the β -galactosidase activity measured over a 96 hr time period. An earlier increase in *xpsA-lacZ* transcription, due to the increased level of autoinducer, was expected but not observed. This observation indicated expression of the NRPS is not dependent on an autoinducer.

To eliminate a role for autoinducer involvement in *xpsA* expression, β -galactosidase activity of *xpsA-lacZ* transcriptional fusions should be measured after the additional of an external

source of autoinducer to culture media. This would eliminate the possibility that autoinducer may (a) not have been present in conditioned media at a level sufficient to facilitate early expression of the *xpsA-lacZ* fusion and/or (b) have degraded in the conditioned media, and therefore be unable to induce *xpsA-lacZ* expression.

An alternative mechanism explaining the pattern of *X. bovienii* NRPS transcription is that expression is linked to starvation of the bacterial cell culture. In *Bacillus* sp. starvation leads to the activation of a number of processes that affect the ability to survive during periods of nutritional stress. Activities that are induced include the development of genetic competence, sporulation, the synthesis of degradative enzymes, motility, and antibiotic production (Marahiel *et al.*, 1993). The genes that function in these processes are activated during the transition from exponential to stationary phase and are controlled by mechanisms that operate primarily at the level of transcription initiation. One class of genes functions in the synthesis of special metabolites such as the peptide antibiotics tyrocidine (*tyc* operon) (Mootz & Marahiel, 1997) and gramicidin S (*grs* operon) (Kratzschmar *et al.*, 1989) as well as the cyclic lipopeptide surfactin (*urfA* operon) (Cosmina *et al.*, 1993). *Xenorhabdus* antimicrobials are expressed in the late exponential phase; where the nutrient source from either a culture media or insect cadaver would probably be declining. Therefore it may not be unreasonable to hypothesise that a putative NRPS antimicrobial from *X. bovienii* is affected by culture starvation.

8.8 XpsA levels could not be detected using α -XpsA antisera

XpsA was successfully overexpressed in *E. coli* BL21 as a 120 kDa protein. Although the XpsA antiserum generated in this study reacted strongly with this protein when expressed in *E. coli* BL21, it did not react with a protein of this size in *X. bovienii* whole cell lysates. Antibodies against NRPS have been generated previously (Hori *et al.*, 1991) therefore it should be possible to generate XpsA specific antibodies for detection of this protein. A reason for the failure of this antiserum to detect XpsA in *X. bovienii* might be the lack of an important epitope required for antisera production due to the use of a slightly truncated protein. Alternatively, the levels of XpsA expressed may be so minimal that even low antisera dilutions (0.01) cannot detect the protein.

Peptides from a wide array of organisms have been studied for their antimicrobial properties. Cecropins produced by insects (Hultmark *et al.*, 1980; Hultmark *et al.*, 1982) and pigs (Lee *et al.*, 1989) have potent antimicrobial activity. Syringomycin, produced by *P. syringae* pv. *syringae*, is also a potent antimicrobial (de Lucca *et al.*, 1999). If these compounds are extremely potent only a small amounts are required. Considering the often large size of genes encoding NRPSs, bacterial cell energy expenditure would be reduced if only small amounts of the final peptide are produced. Therefore the inability for antisera to detect the NRPS template by Western analysis may be reasonable.

Potential work should consider over-expressing the entire XpsA protein in *E. coli* BL21, and using His tag technology to selectively isolate and purify the protein. Over-expression of the entire protein would facilitate the inclusion of all epitopes for antiserum production, whilst His tag technology would provide a purer form of the protein and reduce unwanted background antibodies. As an alternative to Western analysis, XpsA expression could be determined using a translational fusion vector in a similar manner to the transcription fusion vector used in previous experiments. Furthermore the construction of transcriptional and translational *lacZ* fusions by homologous recombination with the *X. bovienii* chromosome, rather than transposon insertion, would overcome any possibility of disrupting genes important for NRPS expression. A clear limitation to this approach is that expression of NRPS genes at the translational level does not necessarily ensure production of the bioactive peptide. The NRPS protein is used as a template for production of the bioactive peptide by the thiotemplate synthesis mechanism. Whether the same signals are required for protein expression and subsequent bioactive peptide formation in *X. bovienii* is unknown. Development of an assay to directly detect the presence of the *X. bovienii* bioactive peptide would resolve this issue.

8.9 Antimicrobial activity of *X. bovienii* NRPS

In-frame deletions within *xpsA* (XB6246), *xpsB* (XB3444) and *xpsAB* (XB92388) were constructed to facilitate deduction of *xpsAB* function without polar effects due to transposon insertions. Interestingly XB6246, XB3444 and XB92388 demonstrated normal haemolytic and Congo Red binding activity in contrast to transposon mutants XB26(20), XB29(45) and XB34(45). These results suggested the transposon induced mutations induced polarity with

respect to Congo Red binding and haemolytic activity, and that the genes encoding these phenotypes may be located downstream of the NRSP region.

By contrast, the in-frame deletion mutants XB6246, XB3444 and XB92388 showed a disruption in phospholipase C and antimicrobial activity similar to that of transposon mutants XB26(20), XB29(45) and XB34(45). Thus these phenotypic changes are likely to represent direct or cryptic effects on the mutations within the *xps* genes. The fact that the same results were obtained for both types of mutants eliminated the possibility of polar defects. *X. bovienii* NRPS, or final peptide product, may directly affect transcription, translation, processing, transport and/or secretion of phospholipase C; or affect the expression of another phospholipase C dependent gene. Alternatively the bioactive peptide(s) secreted by *X. bovienii* may interact with the egg yolk components of Egg Yolk agar forming a precipitate. This hypothesis should be tested by adding purified peptide to Egg Yolk agar.

By comparison of *X. bovienii* wild type and the *xps* in-frame deletion mutants, the putative bioactive peptide(s) expressed by *xpsAB* gene product were shown to be not cytotoxic for Schneider's cells or *G. mellonella* larval haemocytes.

By contrast, semi-quantitative assays of the antimicrobial activity of the *X. bovienii* against the indicator organism *M. luteus* suggested a possible role for NRPS dependent peptides. However, this type of analysis is complicated by the fact that *Xenorhabdus* strains are known to express several antimicrobial compounds (xenorhabdins, xenocoumacins, indole derivatives – see Chapter 1). Furthermore, it is unknown what impact, if any, NRPS have on expression of these compounds. These problems can only be resolved by expression of the NRPS genes in a host unable to produce other antimicrobial compounds. Nevertheless, several interesting observations were made. In particular, the double deletion mutant XB92388 exhibited greater antimicrobial activity against *M. luteus* than wild type *X. bovienii*. Deletion of modules from the *X. bovienii* NRPS gene sequence might have resulted in the production of a more potent antimicrobial. The number of NRPS genes and modules contained within the *X. bovienii* NRPS operon is unknown; therefore the impact of deleting one or two modules on the final product is also unknown. The modular nature of NRPS facilitates the potential for the rational design of new peptide compounds by recombination of biosynthetic genes (Mootz *et al.*, 2000). By altering the module order and arrangement of modification domains a potentially limitless number of new bioactive peptides could be

produced. Furthermore, the complex interactions between domains within a given module, and between modules, are poorly understood.

In conclusion, it is absolutely critical that the bioactive peptide produced by *X. bovienii* T228 is purified from conditioned cell media. This will be the only way to unequivocally examine the role of the bioactive peptide in pathogenesis of *X. bovienii* for insect larvae. Work described in this thesis indicates some basic culture conditions required to maximise expression of the NRPS. Whether this translates into increased yields of bioactive peptide is yet to be resolved. Ideally, the NRPSs should be expressed in a foreign host to eliminate the complications of toxins and other antimicrobial compounds normally expressed by *X. bovienii*. Whether this is achievable will depend on identification of any genes involved in resistance to bioactive peptides as well as solving the problem of moving the very large NRPS gene region to an alternative host.

APPENDIX A

X. bovienii DNA sequence^a flanking transposon insertion mutants XB26(20), XB29(45), XB33(21), XB34(45) and XB41(23).

X. bovienii DNA sequence flanking the mini-Tn5 insertion point of XB26(20)

GCATATTAAA AGCCGGTGCA GGTACGTTT CGCTCGATCC GGCCTACCC	50
GCCGAACGTC TGGCCTATAT CCTGTCAGAC AGTGCGCCGA AATTACTGCT	100
CACTCAGCAG CATTTCAGG GCGGATTAGC CGTAGAGGAT CTCCCCGCT	150
GGCGACTGGA CGATGCCGAC CATTTAAGTA CCGTGGCACA GCAACCGACC	200
GATAACCCTG ACTCACGCCG ATTGGAGCTA CAGCCGCATC ATCTGGCCTA	250
TATCATCTAT ACCTCCGGCT CCACCGGACT GCCTAAA↓GG CGTGATGATT	299
GAGCACCGCA ACGTGGTGAA TTTCACCTAT GCCCAGTGTC AGGTCAGTGA	349
ACTCAAATCC ACTGACCGCG TCCTGCAATT TGCCTCGGTT TCGTTTGATA	399
CTGCCGTGTC TGAGATTTTC CCCACATTGG CCGTCGGCGC GACCTTAATC	449
CTGCGACCGG CGCATATTCA AGTACCGGAT ACCACCTTTA GTGATTTCCCT	499
GCGGGAGCAG GCGATCAGTA TCGTGGATCT GCCCACC GCC TTCTGG	545

X. bovienii DNA sequence flanking the mini-Tn5 insertion point of XB29(45)

TTGCCACCGA TTTAGGTCTG ACGTCCCGCC ATTTAGCCTA TGTGCTTTAC	50
ACCTCTGGCT CAACAGGCTT ACCGAAAGGG GTCATGAATG AGCACCGTGG	100
AGTCGTCAAC CGCTTGTTGT GGGCGCAGGA TGAATATCAA TTAACCTCAGC	150
ATGATCGGGT ATTGCAAAAA ACACCGTTCA GTTTTGATGT CTCAGTCTGG	200
GAGTTTTTCC TGCCTCTGCT TGCCGGCACT CAATTAGTC↓ ATGGCGCGTC	249
CCGGTGGTCA TAAGGAAGCG CTCTATCTGC TGGAAGAAAT CGAAGCGCGG	299
GGCATTACTA CCCTTCATTT TGTGCCTTCC ATGCTGCAAA GTTTTATTCA	349
TCTGACACCC GCCGGCCGTT GCCCTTCTTT GCGTCA	385

X. bovienii DNA sequence flanking the mini-Tn5 insertion point of XB33(21)

GTATAAATA GAATGCCATT GGTATATGCAT ATTTATTTTT GTACAAGGAA	50
GGATCTCAAT TTAATTTCTA ACAAATTGGG GTGATTGATC TTATTAATTG	100
GTATGGCGGT TTAGTGTGTC AAAATGTTGC ATTGGGACAC TGCCAATATT	150
CCGTTATTTA ATGAGGTGCG TGCAATAAAT TTAGTGGAGT GAAATAATGA	200
CTGGATATAA TTCAGTAACG ACAAGAAGAA AAGAATCATG TGAAGTGCAA	250
TTGCGCAGTG TGGATCTCAA TTT↓GCTTAC TGTGTTTGAT GCTGTAATGC	299
AAATGCAGAA CATTACACGT GCGGCTCAGG CACTGGGAAT GTCACAACCG	349
GCTGTCAGTA ATGCGGTA CTCCGCTAAAA ACTATGTTTG ATGATGAGTT	399
GTTTGTGCGC TATGGCCGTG GCATTC AACGCAAGA GCAAAACAGC	449
TCTTTGGGCC ACTCAGACAG GCACTTCAA ATTGACCAAT	489

X. bovienii DNA sequence flanking the mini-Tn5 insertion point of XB34(45)

AATATATAAT	TCATTCTCTC	GAATGTCATG	AAAAAATCAA	AGTATATTTT	50
CTGAACAAAA	TGAAATTTGC	TTATCAGTTT	TTTTAAAATA	TTCCATTCTT	100
TTTCTAAGGA	TGGCATATTT	TTTATTATTT	TATACATTCA	CAGCATGATT	150
TTTCTTGCTG	AAAATAGATC	GTTTTGACTT	TTTTAACCCA	GTTTTTTTAG	200
TTGTAGATTT	GGATTCTAGT	TTTATTTTTT	GTTTTTATCAG	TTCTCATACT	250
TTTTTATTTT	CATATGCCCA	TAAAAAAGGG	AGCTATAAAA	TGAACCACCC	300
TGAAAAGTTG	AAGCCATTTG	CTTTATCCGA	AGCACAAAGC	AGCCGTTGGT	350
TTCAATATCA	AATTAACCC↓	AAGCCAACGT	GGGCGAAATA	ATGGTGCGTT	399
TTGTGCCAGA	GTTGAGGGGT	TAAACGCTCA	AGATTTAGAA	GATGCACTCA	449
ATCACCTGAT	CAAGCGTCAC	CCGATGCTAC	GAGCCAGTTT	TGGGCTATAC	499
GATGGCGAAT	TGGGATATCG	CATAGCAGAG	AA		531

X. bovienii DNA sequence flanking the mini-Tn5 insertion point of XB41(23)

GCGCGATCTG	GATCTGATAC	GAATGAAAAA	TCCAGTATCT	TCAATTACGA	50
TGGGTATATA	TTCTGGCTAA	ATGTGACGTC	TATTCCTGAA	ACTGTAAAAT	100
CACGTGCAGA	TGTCAATCAG	TTACAGATTG	TTGTTAACTC	GCGATTAAAA	150
CTATTCTACC	GCCCTACACA	ACTGGAAGAG	AACTCGGGGG	AGGCTTATAA	200
GCAATCAAG	TTCAGGAAAG	AAAATGGTGT	ATTAATTGCA	GAGAATTCCA	250
CACCTTATTT	T↓CCTTATTT	TATTTCTCTT	TCACATCTAA	AAGTGGACGG	299
AAAAGAAATT	GAAGGAGCGG	GTATGATTAA	TCCCTTTAGC	CAATCAAGTT	349
GGCCATTTTC	TGTCAAAAAT	GCGAAAAATG	TCAGTTGGAA	AGGAATCAAT	399
GATTACGGTG	GAGTCACACA	GGAAGAACTC	GCAGATCTTT	AGGTTATTTA	449
TTAATTTTAA	TTAGATTGTC	GGAAGATTGA	ATATGTCAAA	AAATATAAAG	499
CATAATCTTG	CTGAGGAATT	GTGCGAAGGC	AAGTATTATC	GATTATGGCT	549
GCCTATATTT	ATCATGATAG	GGAGTTTTTC	TTATCATTTT		589

↓ denotes the mini Tn5 Km insertion point.

^a nucleotides are labelled on the right hand side.

APPENDIX B

Listing of the adenylation modules used for phylogenetic analysis (see Chapter 5, Figures 5.10 and 5.11).

The information listed for each module includes; database, accession number, protein name, module number of the protein, amino acid activated by the module, full name of the final peptide product. This listing was kindly provided by the Challis research group (Department of Chemistry, The Johns Hopkins University, Baltimore, Maryland).

gb	AAA25234.1	Dae-M1	D-alanyl lipotechoic acid
gb	AAC06284.1	Glg1-M1	D-alanine activating enzyme.
emb	CAB15876.1	DltA-M1-D-Ala	D-alanyl-D-alanine carrier protein ligase (Dcl).
emb	CAA82227.1	CssA-M1-D-Ala	Cyclosporine synthetase
gb	AAA33023.1	Hts1-M3-D-Ala	HC-toxin synthetase
gb	AAC44128.1	SafB-M1-Ala	saframycin Mx1 synthetase B
emb	CAB39315.1	Cpps1-M1-Ala	d-lysergyl-peptide-synthetase
emb	CAA82227.1	CssA-M11-Ala	Cyclosporine synthetase
gb	AAA33023.1	Hts1-M2-Ala	HC-toxin synthetase
gb	AAC82549.1	FxbB-M2-BetaAla	Exochelin synthetase
gb	AAA85160.1	SyrE-M5-Arg	syringomycin biosynthesis enzyme
emb	CAA11794.1	CepA-M3-Asn	Chloroeremomycin
emb	CAB38517.1	Cda2-M3-Asn	CDA peptide synthetase II
gb	AAC06348.1	BacC-M5-Asn	bacitracin synthetase 3
gb	AAC45930.1	TycC-M1-Asn	tyrocidine synthetase 3
emb	CAB38518.1	Cda1-M4-Asp	CDA peptide synthetase I
emb	CAB38517.1	Cda2-M1-Asp	CDA peptide synthetase II
emb	CAB38518.1	Cda1-M5-Asp	CDA peptide synthetase I
gb	AAC06348.1	BacC-M4-Asp	bacitracin synthetase 3
emb	CAA06324.1	LchAB-M2-Asp	lichenysin A synthetase
gb	AAD04758.1	LicB-M2-Asp	lichenysin D synthetase B
dbj	BAA08983.1	SrfAB-M2-Asp	surfactin synthetase B
gb	AAA85160.1	SyrE-M8- Asp/hAsp/Glu	syringomycin synthetase
emb	CAA82227.1	CssA-M5-Bmt	Cyclosporine synthetase
emb	CAA78044.1	AngR-M1-Cys	Anguibactin synthetase
gb	AAA27636.1	Irp2-M1-Cys	Yersiniabactin synthetase
gb	AAC83657.1	PchF-M1-Cys	Pyochelin synthetase
gb	AAC83656.1	PchE-M1-Cys	Pyochelin synthetase
gb	AAC06346.1	BacA-M2-Cys	Bacitracin synthetase 1
sp	P25464	PcbAB-M2-Cys	ACV synthetase

emb	CAA38631.1	AcvA-M2-Cys	ACV synthetase
gb	AAA85160.1	SyrE-M3-Dab	syringomycin synthetase
gb	AAA85160.1	SyrE-M4-Dab	syringomycin synthetase
emb	CAA06323.1	LchAA-M1-Gln	lichenysin A synthetase
gb	AAD04757.1	LicA-M1-Gln	lichenysin D synthetase
gb	AAC45930.1	TycC-M2-Gln	tyrocidine synthetase 3
gb	AAB80955.1	FenA-M2-Glu	fengycin synthetase
emb	CAA84363.1	Pps4-M2-Glu	Fengycin synthetase
gb	AAC36721.1	FenC-M1-Glu	Fengycin synthetase
emb	CAA84360.1	Pps1-M1-Glu	Fengycin synthetase
gb	AAB80956.1	FenE-M1-Glu	Fengycin synthetase
emb	CAA84362.1	Pps3-M1-Glu	Fengycin synthetase
gb	AAC06346.1	BacA-M4-Glu/Aap	Bacitracin synthetase 1
dbj	BAA08982.1	SrfAA-M1- Glu/Asp	surfactin synthetase
emb	CAB38876.1	Cda3-M1-3-Me- Glu	CDA peptide synthetase III
gb	AAC44128.1	SafB-M2-Gly	saframycin Mx1 synthetase B
emb	CAB38517.1	Cda2-M2-Gly	CDA peptide synthetase II
emb	CAB15186.1	DhbF-M1-Gly	siderophore 2,3-dihydroxybenzoate
emb	CAA82227.1	CssA-M7-Gly	cyclosporine synthetase
gb	AAC06348.1	BacC-M3-His	bacitracin synthetase 3
gb	AAC06346.1	BacA-M1-Ile	Bacitracin synthetase 1
gb	AAC06346.1	BacA-M3-Ile	Bacitracin synthetase 1
gb	AAC06348.1	BacC-M1-Ile	bacitracin synthetase 3
gb	AAD04759.1	LicC-M1- Ile/Leu/Val	lichenysin synthetase
gb	AAB00093.1	FenB-M1-Ile/Val	fengycin synthetase
emb	CAA84364.1	Pps5-M1-Ile	fengycin synthetase
emb	CAA11794.1	CepA-M1-Leu	Chloroeremomycin synthetase
gb	AAC06346.1	BacA-M3-Leu	Bacitracin synthetase 1
emb	CAA06323.1	LchAA-M3-Leu	lichenysin synthetase
emb	CAA06324.1	LchAB-M3-Leu	lichenysin synthetase
gb	AAD04757.1	LicA-M3-Leu	lichenysin synthetase A
gb	AAD04758.1	LicB-M3-Leu	lichenysin synthetase B
dbj	BAA08982.1	SrfAA-M3-Leu	surfactin synthetase
dbj	BAA08983.1	SrfAB-M3-Leu	surfactin synthetase
emb	CAA06325.1	LchAC-M1-Leu	lichenysin synthetase
gb	AAD04757.1	LicA-M2-Leu	lichenysin synthetase A
emb	CAA06323.1	LchAA-M2-Leu	lichenysin synthetase
dbj	BAA08982.1	SrfAA-M2- Leu/Ile/Val	surfactin synthetase

dbj	BAA08985.1	SrfAC-M1- Leu/Ile/Val	surfactin synthetase
emb	CAA43838.1	GrsB-M4-Leu	Gramicidin B synthetase B
gb	AAC45930.1	TycC-M6-Leu	tyrocidine synthetase 3
emb	CAA82227.1	CssA-M3-Leu	Cyclosporine synthetase
emb	CAA82227.1	CssA-M10-Leu	Cyclosporine synthetase
emb	CAA82227.1	CssA-M2-Leu	Cyclosporine synthetase
emb	CAA82227.1	CssA-M8-Leu	Cyclosporine synthetase
gb	AAC06347.1	BacB-M1-Lys	bacitracin synthetase 2
gnl	PID e279967	MbtE-M1-6hLys	Exochelin synthetase
emb	CAB08474.1	MbtF-M1-6haLys	Exichelin synthetase
gb	AAC82549.1	FxbB-M1-5hfOrn	Exocheline synthetase
gb	AAC82550.1	FxbC-M1-5hOrn	Exochelin synthetase
gb	AAC82550.1	FxbC-M3-5hOrn	Exochelin synthetase
gb	AAC06347.1	BacB-M2-Orn	bacitracin synthetase 2
gb	AAC36721.1	FenC-M2-Orn	Fengycin synthetase
emb	CAA84360.1	Pps1-M2-Orn	Fengycin synthetase
emb	CAA43838.1	GrsB-M3-Orn	Gramicidin B synthetase B
gb	AAC45930.1	TycC-M5-Orn	tyrocidine synthetase 3
gb	AAA85160.1	SyrE-M6-Phe	syringomycin synthetase
gb	AAC06348.1	BacC-M2-Phe	bacitracin synthetase 3
emb	CAA33603.1	GrsA-M1-D-/L- Phe	Gramicidin synthetase A
gb	AAC45928.1	TycA-M1-D-/L- Phe	tyrocidine synthetase 1
gb	AAC45929.1	TycB-M3-D-/L- Phe/Trp	tyrocidine synthetase 2
gb	AAC45929.1	TycB-M2-L- Phe/L-Trp	tyrocidine synthetase 2
emb	CAB39315.1	Cpps1-M2-Phe	d-lysergyl-peptide-synthetase
gb	AAC68816.1	FkbP-M1-Pip	FK506 peptide synthetase
emb	CAA60461.1	RapP-M1-Pip	Rapamycin synthetase
emb	CAA72312.1	SnbDE-M1-Pro	Pristinamycin I synthetase
emb	CAA72310.1	SnbDE-M1-Pro	Virginiamycin S synthetase
gb	AAB80955.1	FenA-M1-Pro	fengycin synthetase
emb	CAA84363.1	Pps4-M1-Pro	Fengycin synthetase
gb	AAC45929.1	TycB-M1-Pro	tyrocidine synthetase 2
emb	CAA43838.1	GrsB-M1-Pro	Gramicidin B synthetase B
emb	CAB39315.1	Cpps1-M3-Pro	d-lysergyl-peptide-synthetase
gb	AAA33023.1	Hts1-M1-Pro	HC-toxin synthetase
gb	AAA92015.1	EntF-M1-Ser	enterobactin synthetase
emb	CAB38518.1	Cda1-M1-Ser	CDA peptide synthetase I

gb	AAA85160.1	SyrE-M1-Ser	syringomycin synthetase
gb	AAA85160.1	SyrE-M2-Ser	syringomycin synthetase
emb	CAA11795.1	CepB-M1-HPG	Chloroeremomycin synthetase
emb	CAA11795.1	CepB-M2-HPG	Chloroeremomycin synthetase
emb	CAB38518.1	Cda1-M6-HPG	CDA peptide synthetase I
emb	CAA11796.1	CepC-M1-DHPG	Chloroeremomycin synthetase
emb	CAA72312.1	SnbDE-M4-Pgly	Pristinamycin I synthase
emb	CAB03756.1	MbtB-M1-Ser/Thr	Exochelin synthetase
gb	AAC82550.1	FxBc-M2-Thr	Exochelin synthetase
gb	AAC38442.1	AcmB-M1-Thr	actinomycin synthetase II
emb	CAB38518.1	Cda1-M2-Thr	CDA peptide synthetase I
emb	CAA72311.1	SnbC-M1-Thr	Pristinamycin I synthase 2
gb	AAA85160.1	SyrB-M1-Thr	syringomycin synthetase 2
gb	AAB60198.1	PvdD-M1-Thr	pyoverdine synthetase D
gb	AAB60198.1	PvdD-M2-Thr	pyoverdine synthetase D
gb	AAC80285.1	SyrE-M7-Thr	syringomycin synthetase
emb	CAA09819.1	FenD-M2-Thr	fengycin synthetase
emb	CAA84361.1	Pps2-M2-Thr	fengycin synthetase
emb	CAB38518.1	Cda1-M3-Trp	CDA peptide synthetase I
emb	CAB38516.1	Cda3-M2-Trp	CDA peptide synthetase III
emb	CAA11794.1	CepA-M2-3hTyr	Chloroeremomycin synthetase
emb	CAA11795.1	CepB-M3-3hTyr	Chloroeremomycin synthetase
gb	AAC44129.1	SafA-M1-3h4mPhe	saframycin Mx1 synthetase A
gb	AAC44129.1	SafA-M2-3h4mPhe	saframycin Mx1 synthetase A
gb	AAB80955.1	FenA-M3-Tyr	fengycin synthetase
emb	CAA84363.1	Pps4-M3-Tyr	fengycin synthetase
emb	CAA09819.1	FenD-M1-Tyr	fengycin synthetase
emb	CAA84361.1	Pps2-M1-Tyr	fengycin synthetase
gb	AAC45930.1	TycC-M3-Tyr/Trp	tyrocidine synthetase 3
gb	AAC38442.1	AcmB-M2-Val	actinomycin synthetase II
gb	AAB80956.1	FenE-M2-Val	fengycin synthetase
emb	CAA84362.1	Pps3-M2-Val	fengycin synthetase
emb	CAA43838.1	GrsB-M2-Val	Gramicidin synthetase B
emb	CAA06324.1	LchAB-M1-Val	Linchenysin synthetase
gb	AAD04758.1	LicB-M1-Val	lichenysin synthetase B
dbj	BAA08983.1	SrfAB-M1- Val/Ile	surfactin synthetase
gb	AAC45930.1	TycC-M4-Val	tyrocidine synthetase 3
emb	CAA79245.1	Esyn1-M2-Val	enniatin sythetase
emb	CAA82227.1	CssA-M4-Val	cyclosporine synthetase
emb	CAA82227.1	CssA-M9-Val	cyclosporine synthetase
emb	CAA40561.1	PcbAB-M3-Val	ACV synthetase

emb	CAA38631.1	AcvA-M3-Val	ACV synthetase
pir	S69812	LmbC-M1-4pPro	Lincomycin synthetase
gb	AAF26925.1	EpoP-M1-Cys	Epothilone synthetase
gb	AAF15891.2	NosA-M1-Ile	Nostopeptolide synthetase
gb	AAF15891.2	NosA-M2-Ser	Nostopeptolide synthetase
gb	AAF15891.2	NosA-M3-mePro	Nostopeptolide synthetase
gb	AAF15891.2	NosA-M4-Leu	Nostopeptolide synthetase
gb	AAF17280.1	NosC-M1-Leu	Nostopeptolide synthetase
gb	AAF17280.1	NosC-M2-Gly	Nostopeptolide synthetase
gb	AAF17280.1	NosC-M3- Asp/Asn?	Nostopeptolide synthetase
gb	AAF17281.1	NosD-M1-Tyr	Nostopeptolide synthetase
gb	AAF17281.1	NosD-M2-Pro	Nostopeptolide synthetase
genome sequencing		PvdD-M1-Ser	Pyoverdin synthetase
genome sequencing		PvdD-M2-Arg	Pyoverdin synthetase
genome sequencing		PvdD-M3-Ser	Pyoverdin synthetase
genome sequencing		PvdD-M4-5hOrn	Pyoverdin synthetase
genome sequencing		PvdD-M5-Lys	Pyoverdin synthetase
genome sequencing		PvdD-M6-5hOrn	Pyoverdin synthetase
genome sequencing		PvdD-M7-Thr	Pyoverdin synthetase
genome sequencing		PvdD-M8-Thr	Pyoverdin synthetase
dbj	BAA83992.1	McyA-M1-Ser	Microcistin synthetase A
dbj	BAA83992.1	McyA-M2-Gly	Microcistin synthetase A
dbj	BAA83993.1	McyB-M1-Leu	Microcistin synthetase B
dbj	BAA83994.1	McyC-M1-Leu	Microcistin synthetase B
gb	AAF19812.1	MtaD-M1-Cys	Myxothiazol synthetase
gb	AAF08795.1	MycA-M1-?	mycosubtilin synthetase A
gb	AAF08795.1	MycA-M2-Asx	mycosubtilin synthetase A
gb	AAF08796.1	MycB-M1-Tyr/Trp	mycosubtilin synthetase B
gb	AAF08796.1	MycB-M2-Asx	mycosubtilin synthetase B
gb	AAF08796.1	MycB-M3-Gln	mycosubtilin synthetase B
gb	AAF08796.1	MycB-M4-Pro	mycosubtilin synthetase B
gb	AAF08797.1	MycC-M1-Ser	mycosubtilin synthetase C
gb	AAF08797.1	MycC-M2-Asx	mycosubtilin synthetase C

gb	CAC01603.1	AdpA-M1-Gln	Anabaenopeptilide synthetase A
gb	CAC01603.1	AdpA-M2-Thr	Anabaenopeptilide synthetase A
gb	CAC01604.1	AdpB-M1-Hty	Anabaenopeptilide synthetase B
gb	CAC01604.1	AdpB-M2-Ahp	Anabaenopeptilide synthetase B
gb	CAC01604.1	AdpB-M3-Thr	Anabaenopeptilide synthetase B
gb	CAC01604.1	AdpB-M4-Tyr	Anabaenopeptilide synthetase B
gb	CAC01606.1	AdpD-M1-Ile	Anabaenopeptilide synthetase D
gb	CAB53322	CchH-M1-5hfOrn	Coelichelin synthetase
gb	CAB53322	CchH-M2-Thr	Coelichelin synthetase
gb	CAB53322	CchH-M3-5hOrn	Coelichelin synthetase
gb	CAB93684	PhsC-M1-Pro	Phosphitricin synthetase
gb	CAB93683	PhsB-M1-Ser	Phosphitricin synthetase
gb	AAF86395	FkbP-M1-Pip	FK520 Synthetase

Chapter 9

Bibliography

- Ackermann, H. W. & Dubow, M. S. (1987). General Properties of Bacteriophages. In *Viruses of Prokaryotes*. Boca Raton, USA: CRC Press.
- Aguillera, M. M., Hodge, N. C., Stall, R. E. & Smart, G. C. (1993). Bacterial Symbionts of *Steinernema scapterisci*. *J. Invert. Pathol.* **62**, 68-72.
- Akhurst, R. J. (1983). Taxonomic study of *Xenorhabdus*, a genus of bacteria symbiotically associated with insect pathogenic nematodes. *Int. J. Syst. Bacteriol.* **33**, 38-45.
- Akhurst, R. J. (1980). Morphological and functional dimorphism in *Xenorhabdus* spp., bacteria symbiotically associated with the insect pathogenic nematodes *Neoaplectana* and *Heterorhabditis*. *J. Gen. Microbiol.* **121**, 303-309.
- Akhurst, R. J. (1982). Antibiotic activity of *Xenorhabdus* spp., bacteria symbiotically associated with insect pathogenic nematodes of the families Heterorhabditidae and Steinernematidae. *J. Gen. Microbiol.* **128**, 3061-5.
- Akhurst, R. J. (1982a). A *Xenorhabdus* sp. (Eubacteriales: Enterobacteriaceae) symbiotically associated with *Steinernema kraussei*. *Rev. Nematol.* **5**, 277.
- Akhurst, R. J. (1983). *Neoaplectana* species: specificity of association with bacteria of the genus *Xenorhabdus*. *Exp. Parasitol.* **55**, 258-63.
- Akhurst, R. J. (1986). *Xenorhabdus nematophilus* subsp. *beddingii* (Enterobacteriaceae) a new subspecies of bacteria mutualistically associated with entomopathogenic nematodes. *Int. J. Syst. Bacteriol.* **36**, 454.
- Akhurst, R. J. (1986a). *Xenorhabdus nematophilus* subsp. *poinarii*: its interaction with insect pathogenic nematodes. *Syst. Appl. Microbiol.* **36**, 142-147.
- Akhurst, R. J. (1993). Bacterial Symbionts of Entomopathogenic Nematodes - the Power behind the Throne. In *Nematodes and the biological control of insect pests*, pp. 127-135. Edited by R. Bedding, R. J. Akhurst & H. Kaya. Melbourne: CSIRO Publications.
- Akhurst, R. J. & Boemare, N. E. (1986). A non-luminescent strain of *Xenorhabdus luminescens*. *J. Gen. Microbiol.* **132**, 1917-1922.
- Akhurst, R. J. & Boemare, N. E. (1988). A numerical taxonomic study of the genus *Xenorhabdus* (Enterobacteriaceae) and proposed elevation of the subspecies of *X. nematophilus* to species. *J. Gen. Microbiol.* **134**, 1835-1845.
- Akhurst, R. J. & Boemare, N. E. (1990). Biology and taxonomy of *Xenorhabdus*. In *Entomopathogenic Nematodes in Biological Control*, pp. 75-90. Edited by R. Gaugler & H. K. Kaya. Boca Raton: CRC Press Florida.

- Akhurst, R. J. & Dunphy, G. B. (1993).** Tripartite Interactions between Symbiotically Associated Entomopathogenic Bacteria, Nematodes, and Their Insect Hosts. In *Parasites and Pathogens of Insects*, pp. 1-23. Edited by N. Beckage, S. Thompson & B. Federici. New York: Academic Press Inc.
- Akhurst, R. J., Mourant, R. G., Baud, L. & Boemare, N. E. (1996).** Phenotypic and DNA relatedness between nematode symbionts and clinical strains of the genus *Photorhabdus* (Enterobacteriaceae). *Int. J. Syst. Bacteriol.* **46**, 1034-41.
- Alatorre-Rosas, R. & Kaya, H. K. (1990).** Interspecific competition between entomopathogenic nematodes in the genera *Heterorhabditis* and *Steinernema* for an insect host in sand. *J. Invert. Pathol.* **55**, 179-188.
- Alexejev, M. F. (1995).** Three kanamycin resistant gene cassettes with different polylinkers. *Bio Techniques* **18**, 52-53.
- Altschul, S. F., Gish, W., Miller, W., Myers, E. W. & Lipman, D. J. (1990).** Basic local alignment search tool. *J. Mol. Biol.* **215**, 403-10.
- Awise, J. C., Arnold, J., Ball, R. M., Bermingham, E., Lamb, T., Niegel, J. E., Reeb, C. A. & Saunders, N. C. (1987).** Intraspecific phylogeography: the mitochondrial DNA bridge between population genetics and systematics. *Ann. Rev. Ecol. Syst.* **18**, 489.
- Baghdigian, S., Boyergiglio, M. H., Thaler, J. O., Bonnot, G. & Boemare, N. (1993).** Bacteriocinogenesis in Cells of *Xenorhabdus nematophilus* and *Photorhabdus luminescens* - Enterobacteriaceae Associated With Entomopathogenic Nematodes. *Biology of the Cell* **79**, 177-185.
- Ball, T. K., Wasmuth, C. R., Braunagel, S. C. & Benedik, M. J. (1990).** Expression of *Serratia marcescens* extracellular proteins requires *recA*. *J. Bacteriol.* **172**, 342-9.
- Bedding, R. A. & Miller, L. A. (1981).** Disinfecting Blackcurrant Cuttings of *Synanthedon tipuliformis*, Using the Insect Parasitic Nematode, *Neoaplectana bibionis*. *Environ. Entomol.* **10**.
- Bedding, R. A. & Molyneux, A. S. (1982).** Penetration of insect cuticle by infective juveniles of *Heterorhabditis* spp. (Heterorhabditidae: Nematoda). *Nematologica.* **28**, 354-359.
- Belshaw, P. J., Walsh, C. T. & Stachelhaus, T. (1999).** Aminoacyl-CoAs as probes of condensation domain selectivity in nonribosomal peptide synthesis. *Science.* **284**, 486-489.
- Berg, C. M., Berg, D. E. & Groisman, E. A. (1989).** Transposable elements and the genetic engineering of bacteria. In *Mobile DNA*, pp. 879-926. Edited by D. E. Berg & M. M. Howe. Washington, D.C.: American Society for Microbiology.
- Berg, D. E. (1989).** Transposon Tn5. In *Mobile DNA*, pp. 185-210. Edited by D. E. Berg & M. M. Howe. Washington, DC: American Society for Microbiology.
- Bernhard, F., Demel, G., Soltani, K., Dohren, H. V. & Blinov, V. (1996).** Identification of genes encoding for peptide synthetases in the gram-negative bacterium *Lysobacter* sp. ATCC 53042 and the fungus *Cylindrotrichum oligospermum*. *DNA Sequence.* **6**, 319-330.
- Bignon, C., Daniel, N. & Djiane, J. S. O. (1993).** Beta-galactosidase and chloramphenicol acetyltransferase assays in 96-well plates. *Biotechniques.* **15**, 243-246.

- Binnington, K. & Brooks, L. (1993).** Fimbrial attachment of *Xenorhabdus nematophilus* to the intestine of *Steinernema carpocapsae*. In *Nematodes and the biological control of insect pests*, pp. 147-155. Edited by R. Bedding, R. Akhurst & H. Kaya. Melbourne Australia: CSIRO Publications.
- Bintrim, S. (1995).** A study of the crystalline inclusion proteins of *Photorhabdus luminescens*. Madison: University of Wisconsin.
- Bintrim, S. B. & Ensign, J. C. (1998).** Insertional inactivation of genes encoding the crystalline inclusion proteins of *Photorhabdus luminescens* results in mutants with pleiotropic phenotypes. *J. Bacteriol.* **180**, 1261-9.
- Bird, A. F. & Akhurst, R. J. (1983).** The nature of the intestinal vesicle in nematodes of the family Steinernematidae. *Int. J. Parasitol.* **13**, 599.
- Bleakley, B. & Neelson, K. H. (1988).** Characterization of primary and secondary form of *Xenorhabdus luminescens* strain Hm. *FEMS Microbiol. Ecol.* **53**, 241-250.
- Blomfield, L. C., Vaughn, V., Rest, R. F. & Eisenstein, B. L. (1991).** Allelic exchange in *Escherichia coli* using the *Bacillus subtilis sacB* gene and the temperature-sensitive pSC101 replicon. *Mol. Microbiol.* **5**, 1447-1457.
- Boemare, N. & Akhurst, R. J. (1988).** Biochemical and physiological characterization of colony form variants in *Xenorhabdus* spp. (Enterobacteriaceae). *J. Gen. Microbiol.* **134**, 751-761.
- Boemare, N. & Akhurst, R. J. (1990).** Physiology of phase variation in *Xenorhabdus* spp. In *Vth International Colloquium on Invertebrate Pathology and Microbial Control*, pp. 208-212. Adelaide: Society for Invertebrate Pathology.
- Boemare, N., Givaudan, A., Brehelin, M. & Laumond, C. (1997).** Symbiosis and Pathogenicity of Nematode-Bacterium Complexes. *Symbiosis.* **22**, 21-45.
- Boemare, N., Thaler, J. O. & Lanois, A. (1997a).** Simple Bacteriological Tests For Phenotypic Characterization of *Xenorhabdus* and *Photorhabdus* Phase Variants. *Symbiosis.* **22**, 167-175.
- Boemare, N. E., Akhurst, R. J. & Mourant, R. G. (1993).** DNA relatedness between *Xenorhabdus* spp. (Enterobacteriaceae), symbiotic bacteria of entomopathogenic nematodes, and a proposal to transfer *Xenorhabdus luminescens* to a new genus, *Photorhabdus*. *Int. J. Syst. Bacteriol.* **43**, 249-255.
- Boemare, N. E., Boyer Giglio, M. H., Thaler, J. O., Akhurst, R. J. & Brehelin, M. (1992).** Lysogeny and bacteriocinogeny in *Xenorhabdus nematophilus* and other *Xenorhabdus* spp. *Appl. Environ. Microbiol.* **58**, 3032-7.
- Boman, H. G. & Hultmark, D. (1987).** Cell-free immunity in insects. *Ann. Rev. Microbiol.* **41**, 103.
- Bowan, D. (1995).** Characterization of a high molecular weight insecticidal protein complex produced by the entomopathogenic bacterium *Photorhabdus luminescens*. Madison: University of Wisconsin.

- Bowen, D., Rocheleau, T.A., Blackburn, M., Andreev, O., Golubeva, E., Bhartia, R. & French-Constant, R.H. (1998).** Insecticidal toxins from the bacterium *Photorhabdus luminescens*. *Science* **280**(5372), 2129-32.
- Bowen, D., Blackburn, M., Rocheleau, T., Grutzmacher, C. & French-Constant, R.H. (2000).** Secreted proteases from *Photorhabdus luminescens*: separation of the extracellular proteases from the insecticidal Tc toxin complexes. *Insect Biochem Mol Biol* **30**(1), 69-74.
- Braun, V. (1999).** Active transport of siderophore-mimicking antibacterials across the outer membrane. *Drug Resistance Update* **2**, 363-369.
- Brehelin, M., Drif, L. & Boemare, N. (1990).** Depression of defence reactions in insects by Steinernematidae and their associated bacteria. In *Proceedings and Abstracts, Vth International Colloquium on Invertebrate Pathology and Microbial Control*, pp. 213-217. Adelaide.
- Brehelin, M. A., Cherqui, A., Drif, L., Luciani, J., Akhurst, R. & Boemare, N. (1993).** Ultrastructural study of surface components of *Xenorhabdus* sp. in different cell phases and culture conditions. *J. Invert. Pathol.* **61**, 188-191.
- Brock, T. D. & Madigan, M. T. (1988).** *Biology of Microorganisms*, Fifth edition: Prentice-Hall, New Jersey.
- Brookman, J. L., Ratcliffe, N. A. & Rowley, A. F. (1988).** Optimization of a monolayer phagocytosis assay and its application for studying the role of the prophenoloxidase system in the wax moth, *Galleria mellonella*. *J. Insect Physiol.* **34**, 337-345.
- Buchanan, R. E. & Gibbons, N. E. (1974).** Bergy's manual of determinative bacteriology. Baltimore: The Williams and Wilkins Co.
- Cane, D. E., Walsh, C. T. & Khosla, C. (1998).** Harnessing the biosynthetic code: combinations, permutations and mutations. *Science*. **282**, 63-68.
- Casadaban, M. J. & Cohen, S. M. (1980).** Analysis of gene control signals by DNA fusion and cloning in *Escherichia coli*. *J. Mol. Biol.* **179**, 179-208.
- Chain, B. M., Leyshon-Sorland, K. & Siva-Jothy, M. T. (1992).** Haemocyte heterogeneity in the cockroach *Periplaneta americana* analysed using monoclonal antibodies. *J. Cell Sci.* **103**, 1261-1267.
- Challis, G. L. & Ravel, J. (2000).** Coelichelin, a new peptide siderophore encoded by the *Streptomyces coelicolor* genome: structure prediction from the sequence of its non-ribosomal peptide synthetase. *FEMS Microbiol. Lett.* **187**, 111-114.
- Challis, G. L., Ravel, J. & Townsend, C. A. (2000).** Predictive, structure-based model of amino acid recognition by nonribosomal peptide synthetase adenylation domains. *Chem. Biol.* **7**, 211-224.
- Chapman, R. F. (1998).** *The insects; structure and function*. Cambridge: Cambridge University Press.
- Charette, M. F., Henderson, G. W., Kezdy, F. J. & Markovitz, A. (1982).** Molecular mechanism for dominance of a mutant allele of an ATP-dependent protease. *J. Mol. Biol.* **162**, 503-510.

- Chen, G., Dunphy, G. B. & Webster, J. M. (1994).** Antifungal Activity of 2 *Xenorhabdus* Species and *Photorhabdus luminescens*, Bacteria Associated With the Nematodes *Steinernema* Species and *Heterorhabditis megidis*. *Biological Control* **4**, 157-162.
- Chiu, H. T., Hubbard, B. K., Shah, A. N., Eide, J., Fredenburg, R. A., Walsh, C. T. & C., K. (2001).** Molecular cloning and sequence analysis of the complestatin biosynthetic gene cluster. *Pro. Nat. Acad. Sci. USA.* **98**, 8548-8543.
- Ciche, T. A., Bintrim, S. B., Horswill, A. R. & Ensign, J. C. (2001).** A Phosphopantetheinyl Transferase Homolog Is Essential for *Photorhabdus luminescens* To Support Growth and Reproduction of the Entomopathogenic Nematode *Heterorhabditis bacteriophora*. *J. Bac.* **183(10)**, 3117-3126.
- Clark, A. J. (1973).** Recombination deficient mutants of *E. coli* and other bacteria. *Ann. Rev. Genetics.* **7**, 67-86.
- Conti, E., Stachelhaus, T., Marahiel, M. A. & Brick, P. (1997).** Structural basis for the activation of phenylalanine in the non-ribosomal biosynthesis of gramicidin S. *EMBO J.* **16**, 4174-4183.
- Coplin, D. L. (1989).** Plasmids and their role in the evolution of plant pathogenic bacteria. *Ann. Rev. Phytopathol.* **27**, 187-212.
- Cosmina, P., Rodriguez, F., de Ferra, F., Perego, M., Venema, G. & van Sinderen, D. (1993).** Sequence and analysis of the genetic locus responsible for surfactin synthesis in *Bacillus subtilis*. *Mol. Microbiol.* **8**, 821-831.
- Cotteril, S. M., Satterthwait, A. C. & Fersht, A. R. (1982).** RecA protein from *Escherichia coli*. A very rapid and simple purification procedure: binding of adenosine 5'-triphosphate and adenosine 5'-diphosphate by the homogenous protein. *Biochemistry.* **21**, 4332-4337.
- Couche, G. A. & Gregson, R. P. (1987).** Protein inclusions produced by the entomopathogenic bacterium *Xenorhabdus nematophilus* subsp. *nematophilus*. *J. Bacteriol.* **169**, 5279-88.
- Couche, G. A., Lehbach, P. R., Forage, R. G., Cooney, G. C., Smith, D. R. & Gregson, R. P. (1987).** Occurrence of intracellular inclusions and plasmids in *Xenorhabdus* spp. *J. Gen. Microbiol.* **133**, 967-973.
- Curran, J. (1989).** Chromosome numbers of *Steinernema* and *Heterorhabditis* species. *Rev. Nematol.* **12**, 145.
- Dadd, R. H. (1971).** Size limitation on the infectivity of mosquito larvae by nematodes during filter feeding. *J. Invert. Pathol.* **18**, 246-251.
- de ferra, F., Rodriguez, F., Tortora, O., Tosi, C. & Grandi, G. (1997).** Engineering of Peptide Synthetases. *J. Biological Chem.* **272**, 25304-25309.
- De Kievit, T. R. & Iglewski, B. H. (2000).** Bacterial Quorum Sensing in Pathogenic Relationships. *Infec. Immun.* **68**, 4839-4849.
- De Lorenzo, V., Herrero, M., Jakubzik, U. & Timmis, K. N. (1990).** Mini-Tn5 Transposon Derivatives for Insertion Mutagenesis, Promoter Probing, and Chromosomal Insertion of Cloned DNA in Gram-Negative Eubacteria. *J. Bacteriol.* **172**, 6568-6572.

- de Lucca, A. J., Jacks, T. J., Takemoto, J., Vinyrad, B., Peter, J., Navarro, E. & Walsh, T. J. (1999). Fungal Lethality, Binding, and Cytotoxicity of Syringomycin-E. *Antimicrobial Agents and Chemotherapy* **43**, 371-373.
- Donnenberg, M. S. & Kaper, J. B. (1991). Construction of an *eae* deletion mutant of enteropathogenic *Escherichia coli* using a positive-selection suicide vector. *Infect. Immun.* **59**, 4310-4317.
- Dowds, B. C. A. (1997). *Photorhabdus* and *Xenorhabdus* - Gene Structure and Expression, and Genetic Manipulation. *Symbiosis*. **22**, 67-83.
- Dunn, P. E. (1986). Biochemical aspects of insect immunology. *Ann. Rev. Entomol.* **31**, 321.
- Dunphy, G., Miyamoto, C. & Meighen, E. (1997). A homoserine lactone autoinducer regulates virulence of an insect-pathogenic bacterium, *Xenorhabdus nematophilus* (Enterobacteriaceae). *J. Bacteriol.* **179**, 5288-91.
- Dunphy, G. B. (1994). Interaction of mutants of *Xenorhabdus nematophilus* (Enterobacteriaceae) with antibacterial systems of *Galleria mellonella* larvae (Insecta: Pyralidae). *Can. J. Microbiol.* **40**, 161-8.
- Dunphy, G. B. (1995). Physicochemical Properties and Surface Components of *Photorhabdus luminescens* Influencing Bacterial Interaction With Non-Self Response Systems of Nonimmune *Galleria mellonella* Larvae. *J. Invert. Pathol.* **65**, 25-34.
- Dunphy, G. B. & Hurlbert, R. E. (1995). Interaction of Avirulent Transpositional Mutants of *Xenorhabdus nematophilus* ATCC 19061 (Enterobacteriaceae) With the Antibacterial Systems of Non-Immune *Galleria mellonella* (Insecta) Larvae. *J. Gen. Appl. Microbiol.* **41**, 409-427.
- Dunphy, G. B., Rutherford, T. A. & Webster, J. M. (1985). Growth and virulence of *Steinernema glaseri* influenced by different subspecies of *Xenorhabdus nematophilus*. *J. Nematol.* **17**, 476.
- Dunphy, G. B. & Thurston, G. S. (1990). Insect immunity. In *Entomopathogenic Nematodes in Biological Control*, pp. 301-323. Edited by R. Gaugler & H. K. Kaya. Boca Raton, Florida: CRC Press.
- Dunphy, G. B. & Webster, J. M. (1984). Interaction of *Xenorhabdus nematophilus* subsp. *nematophilus* with the haemolymph of *Galleria mellonella*. *J. Insect Physiol.* **30**, 883.
- Dunphy, G. B. & Webster, J. M. (1985). Influence of *Steinernema feltiae* (Filipjev) Wouts, Mracek, Gerdin and Bedding DD136 strain on the humoral and haemocytic responses of *Galleria mellonella* (L.) larvae to selected bacteria. *Parasitol.* **91**, 365-380.
- Dunphy, G. B. & Webster, J. M. (1988). Lipopolysaccharides of *Xenorhabdus nematophilus* (Enterobacteriaceae) and their haemocyte toxicity in nonimmune *Galleria mellonella* (Insecta: Lepidoptera) larvae. *J. Gen. Microbiol.* **134**, 1017.
- Dunphy, G. B. & Webster, J. M. (1988a). Virulence mechanisms of *Heterorhabditis heliothidis* and its bacterial associate, *Xenorhabdus luminescens*, in nonimmune larvae of the greater wax moth, *Galleria mellonella*. *Int. J. Parasitol.* **18**, 729.

- Dunphy, G. B. & Webster, J. M. (1991).** Antihemocytic surface components of *Xenorhabdus nematophilus* var *dutki* and their modification by serum of nonimmune larvae of *Galleria mellonella*. *J. Invert. Pathol.* **58**, 40-51.
- Dutky, S. R. (1959).** Insect microbiology. *Adv. Appl. Microbiol.* **1**, 175-200.
- Ehlers, R., Wyss, U. & Stackebrandt, E. (1988).** 16s rRNA cataloging and the phylogenetic position of the genus *Xenorhabdus*. *Syst. Appl. Microbiol.* **10**, 121-125.
- Eisen, J. A. (1995).** The RecA Protein As A Model Molecule For Molecular Systematic Studies Of Bacteria - Comparison Of Trees Of RecAs And 16S rRNAs From The Same Species [Review]. *J. Mol. Evolution* **41**, 1105-1123.
- Farmer, J. J., Jorgensen, J. H., Grimont, P. A. D., Akhurst, R. J., Poinar, G. O., Pierce, G. V., Smith, J. A., Carger, G. P., Wilson, K. & Hickman-Brenner, F. W. (1989).** *Xenorhabdus luminescens* (DNA hybridisation group 5) from human clinical specimens. *J. Clin. Microbiol.* **27**, 1594-1600.
- Farmer, J. J. I. (1984).** Genus *Xenorhabdus*: The Williams & Wilkins Co., Baltimore.
- Fath, M. J. & Kolter, R. (1993).** ABC Transporters: Bacterial Exporters. *Microbiol. Rev.* **57**, 995-1017.
- Feinberg, A. P. & Vogelstein, B. S. O. (1983).** A technique for radiolabeling DNA restriction endonuclease fragments to high specific activity. *Analytical Biochemistry* **132**, 6-13.
- Fellay, R., Frey, J. & Krisch, H. (1987).** Interposon mutagenesis of soil and water bacteria: a family of DNA fragments designed for in vitro insertional mutagenesis of Gram-negative bacteria. *Gene.* **52**, 147-154.
- Ffrench-Constant, R. H., Waterfield, N., Burland, V., Perna, N. T., Daborn, P. J., Bowen, D. & Blattner, F. R. (2000).** A Genomic Sample Sequence of the Entomopathogenic Bacterium *Photorhabdus luminescens* W14: Potential Implications for Virulence. *Appl. Environ. Microbiol.* **66**, 3310-3329.
- Fischer-Le Saux, M., Viillard, V., Brunel, B., Normand, P. & Boemare, N.E. (1999).** Polyphasic classification of the genus *Photorhabdus* and proposal of new taxa: *P. luminescens* subsp. *luminescens* subsp. nov., *P. luminescens* subsp. *akhurstii* subsp. nov., *P. luminescens* subsp. *laumondii* subsp. nov., *P. temperata* sp. nov., *P. temperata* subsp. *temperata* subsp. nov. and *P. asymbiotica* sp. nov. *Int J Syst Bacteriol.* **49**(4), 1645-56.
- Forst, S., Dowds, B., Boemare, N. & Stackebrandt, E. (1997).** *Xenorhabdus* and *Photorhabdus* spp. - BUGS THAT KILL BUGS [Review]. *Ann. Rev. Microbiol.* **51**, 47-72.
- Forst, S. & Neelson, K. (1996).** Molecular Biology of the symbiotic pathogenic bacteria *Xenorhabdus* spp. and *Photorhabdus* spp. [Review]. *Microbiological Reviews* **60**, 21 ff.
- Forst, S. A. & Tabatabai, N. (1997).** Role of the Histidine Kinase, Envz, in the Production of Outer Membrane Proteins in the Symbiotic-Pathogenic Bacterium *Xenorhabdus nematophilus*. *Appl. Environ. Microbiol.* **63**, 962-968.
- Frackman, S., Anhalt, M. & Neelson, K. H. (1990).** Cloning, organization, and expression of the bioluminescence genes of *Xenorhabdus luminescens*. *J. Bacteriol.* **172**, 5767-73.

- Frackman, S. & Neilson, K. H. (1990).** The molecular genetics of *Xenorhabdus*. In *Entomopathogenic Nematodes in Biological Control*, pp. 285-300. Edited by R. Gaugler & H. K. Kaya. Boca Raton, Florida: CRC Press.
- Francis, M. S., Parker, A. F., Morona, R. & Thomas, C. J. (1993).** Bacteriophage Lambda As a Delivery Vector For Tn10-Derived Transposons in *Xenorhabdus bovienii*. *Appl. Environ. Microbiol.* **59**, 3050-3055.
- Freitag, N. & McEntee, K. (1988).** Affinity chromatography of RecA protein and RecA nucleoprotein complexes on RecA protein-agarose columns. *J. Biol. Chem.* **263**, 19525-34.
- Fridovich, I. (1978).** The biology of oxygen radicals. The superoxide radical is an agent of oxygen toxicity; superoxide dismutases provide an important defence. *Science.* **201**, 875-880.
- Fyfe, J. A. M. & Davies, J. K. (1990).** Nucleotide sequence and expression in *Escherichia coli* of the *recA* gene of *Neisseria gonorrhoeae*. *Gene.* **93**, 151-156.
- Gaugler, R. (1999).** Nematodes (Rhabditida : Steinernematidae and Heterorhabditidae): Cornell University.
- Gaugler, R. & Molloy, D. (1981).** Instar susceptibility of *Simulium vittatum* (Diptera: Simuliidae) to the entomogenous nematode *Neoplectana carpocapsae*. *J. Nematol.* **13**, 1-5.
- Gehring, A. M., DeMoll, E., Fetherston, J. D., Mori, I., Hayhew, G. F., Blattner, F. R., Walsh, C. T. & Perry, R. D. (1998).** Iron acquisition in plague: modular logic in enzymatic biogenesis of yersiniabactin by *Yersinia pestis*. *Chem. Biol.* **5**, 573-586.
- Gerritsen, L. J., de Raay, G. & Smits, P. H. (1992).** Characterization of form variants of *Xenorhabdus luminescens*. *Appl. Environ. Microbiol.* **58**, 1975-9.
- Gerritsen, L. J. M. & Smits, P. H. (1993).** Variation in Pathogenicity of Recombinations of *Heterorhabditis* and *Xenorhabdus luminescens* Strains. *Fund. Appl. Nematol.* **16**, 367-373.
- Givaudan, A., Baghdiguan, S., Lanois, A. & Boemare, N. (1995).** Swarming and Swimming Changes Concomitant With Phase Variation in *Xenorhabdus nematophilus*. *Appl. Environ. Microbiol.* **61**, 1408-1413.
- Givaudan, A. & Lanois, A. (2000).** *flhDC*, the Flagellar Master Operon of *Xenorhabdus nematophilus*: Requirement for Motility, Lipolysis, Extracellular Hemolysis, and Full Virulence in Insects. *J. Bacteriol.* **182**, 107-115.
- Givaudan, A., Lanois, A. & Boemare, N. (1996).** Cloning and nucleotide sequence of a flagellin encoding genetic locus from *Xenorhabdus nematophilus*: phase variation leads to differential transcription of two flagellar genes (*fliCD*). *Gene.* **183**, 243-53.
- Gonzalez, J. M., Brown, B. J. & Carlton, B. C. (1982).** Transfer of *Bacillus thuringiensis* plasmids coding for endotoxin among strains of *B. thuringiensis* and *B. cereus*. *Proc. Nat. Acad. Sci. USA.* **79**, 6951-6955.
- Granger, K. (2000).** Partial Purification of Putative Peptide Antimicrobials Expressed by *Xenorhabdus bovienii* T228/1 and Mutation of a Putative ABC Transport Protein. Adelaide: Adelaide University.

- Gray, K. M. (1997).** Intercellular communication and group behavior in bacteria. *Trends in Microbiol.* **5**, 184-188.
- Grimont, P. A., Stegerwalt, A. G., Boemare, N. E., Hickman-Brenner, F. W., Deval, C., Grimont, F. & Brenner, D. (1984).** Deoxyribonucleic acid relatedness and phenotypic study of the genus *Xenorhabdus*. *Int. J. Syst. Bacteriol.* **34**.
- Gross, D. C. (1985).** Regulation of syringomycin synthesis in *Pseudomonas syringae* pv. *syringae* and defined conditions for its production. *J. Appl. Bacteriol.* **58**, 167-174.
- Guenzi, E., Galli, G., Grgurina, I., Gross, D. C. & Grandi, G. (1998).** Characterization of the syringomycin synthetase gene cluster. A link between prokaryotic and eukaryotic peptide synthetases. *J. Biol. Chem.* **273**, 32857-32863.
- Guenzi, E., Galli, G., Grgurina, I., Pace, E., Ferranti, P. & Grandi, G. (1998a).** Coordinate transcription and physical linkage of domains in surfactin synthetase are not essential for proper assembly and activity of the mutlienzyme complex. *J. Biol. Chem.* **273**, 14403-14410.
- Gupta, A. P. (1985).** Hemocytes. In *Comprehensive Insect Physiology, Biochemistry and Pharmacology*, pp. 453-485. Edited by G. A. Kerkut & L. I. Gilbert. Oxford: Pergamon Press.
- Gupta, A. P. (1991).** Insect immunocytes and other hemocytes: roles in cellular and humoral immunity. In *Immunology of Insects and other Arthropods*, pp. 19-118. Edited by A. P. Gupta. Boca Raton: CRC Press.
- Gussow, D. & Clackson, T. S. O. (1989).** Direct clone characterization from plaques and colonies by the polymerase chain reaction. *Nucleic Acids Res.* **17**, 4000.
- Han, R., Wouts, W. M. & Liying, L. (1991).** Development and virulence of *Heterorhabditis* spp. strains associated with different *Xenorhabdus luminescens* isolates. *J. Invert. Pathol.* **58**, 27-32.
- Hartman, P. S. & Eisenstark, A. (1980).** Killing of *Escherichia coli* K-12 by near-ultraviolet radiation in the presence of hydrogen peroxide: role of double-stranded DNA breaks in absence of recombinational repair. *Mutation Res.* **72**, 31-42.
- Herrero, M., de Lorenzo, V. & Timmis, K. N. (1990).** Transposon vectors containing non-antibiotic resistance selection markers for cloning and stable chromosomal insertion of foreign genes in gram-negative bacteria. *J. Bacteriol.* **172**, 6557-6567.
- Hing Hew, F. (1997).** Cloning and characterisation of *recA* from *Xenorhabdus nematophilus* AN6 Adelaide: The University of Adelaide.
- Hoffman, P. S., Pine, L. & Bell, S. (1983).** Production of superoxide and hydrogen peroxide in medium used to culture *Legionella pneumophila*: catalytic decomposition by charcoal. *Appl. Environ. Microbiol.* **45**, 784-791.
- Holmes, D. S. & Quigley, M. S. O. (1981).** A rapid boiling method for the preparation of bacterial plasmids. *Analytical Biochem.* **114**, 193-197.
- Hori, K., Yamamoto, Y., Tokita, K., Saito, F., Kurotsu, T., Kanda, M., Okamura, K., Furuyama, J. & Saito, Y. (1991).** The Nucleotide Sequence for a Proline-Activating Domain of Gramicidin S Synthetase 2 Gene from *Bacillus brevis*. *J. Biochem.* **110**, 111-119.

- Hosseini, P. K. & Neilson, K. H. (1995).** Symbiotic Luminous Soil Bacteria - Unusual Regulation For an Unusual Niche. *Photochemistry & Photobiology*. **62**, 633-640.
- Hultmark, D., Engström, Å., Andersson, K., Bennisch, H., Kapur, R. & Boman, H. G. (1982).** Insect Immunity. Isolation and structure of cecropin D and four minor antibacterial components from cecropia pupae. *Eur. J. Biochem.* **127**, 207-217.
- Hultmark, D., Steiner, H., Rasmuson, T. & Boman, H. G. (1980).** Insect Immunity. Purification and properties of three inducible bactericidal proteins from hemolymph of immunized pupae of *Hyalophora cecropia*. *Eur. J. Biochem.* **106**, 7-16.
- Hurlbert, R. E., Xu, J. & Small, C. L. (1989).** Colonial and cellular polymorphism in *Xenorhabdus luminescens*. *Appl. Environ. Microbiol.* **55**, 1136-1143.
- Jarosz, J. (1996).** Do Antibiotic Compounds Produced *in vitro* By *Xenorhabdus nematophilus* Minimize the Secondary Invasion of Insect Carcasses By Contaminating Bacteria. *Nematologica*. **42**, 367-377.
- Jarosz, J. (1998).** Active Resistance of Entomophagous Rhabditid *Heterorhabditis bacteriophora* to Insect Immunity. *Parasitol.* **117**, 201-208.
- Jhang, J., Wolfe, S. & Demain, A. L. (1989).** Phosphate regulation of ACV synthetase and cephalosporin biosynthesis in *Streptomyces clavuligerus*. *FEMS Microbiol. Lett.* **57**, 145-150.
- Klein, M. G. (1990).** Efficacy against soil-inhabiting insect pests. In *Entomopathogenic Nematodes in Biological Control*, pp. 195-214. Edited by R. Gaugler & H. K. Kaya. Boca Raton, Florida: CRC Press.
- Kleinkauf, H. & von Döhren, H. (1990).** Nonribosomal biosynthesis of peptide antibiotics. *Eur. J. Biochem.* **192**, 1-15.
- Knight, K. L. & McEntee, K. (1986).** Nucleotide binding by a 24-residue peptide from the RecA protein of *Escherichia coli*. *Proc. Nat. Acad. Sci. U S A.* **83**, 9289-93.
- Kolter, R., Inuzuka, M. & Helinski, D. R. (1978).** Transcomplementation-dependent replication of a low molecular weight origin fragment from plasmid R6K. *Cell.* **15**, 1199-1208.
- Konz, D. & Marahiel, M. A. (1999).** How do peptide synthetases generate structural diversity? *Chem. Biol.* **6**, R39-R48.
- Koomey, M., Gotschlich, E. C., Robbins, K., Bergstrom, S. & Swanson, J. (1987).** Effects of *recA* mutations on pilus antigenic variation and phase transitions in *Neisseria gonorrhoeae*. *Genetics.* **117**, 391-8.
- Kowalczykowski, S. C., Dixon, D. A., Eggleston, A. K., Lauder, S. D. & Rehrauer, W. M. (1994).** Biochemistry of Homologous Recombination in *Escherichia coli*. *Microbiol. Rev.* **58**, 401-465.
- Kramer, G. F. & Ames, B. N. (1987).** Oxidative mechanisms of toxicity of low-intensity near-UV light in *Salmonella typhimurium*. *J. Bacteriol.* **169**, 2259-2266.
- Krasomil-Osterfeld, K. C. (1995).** Influence of Osmolarity On Phase Shift in *Photorhabdus luminescens*. *Appl. Environ. Microbiol.* **61**, 3748-3749.

- Krasomil-Osterfield, K. & Ehlers, R.-U. (1994).** Influence of environmental factors on phase variation in *Photobacterium luminescens*. In *VIIth International Colloquium on Invertebrate Pathology*, pp. 101-106. Montpellier.
- Kratzschmar, J., Krause, M. & Marahiel, M. A. (1989).** Gramicidin S biosynthesis operon containing the structural genes *grsA* and *grsB* has an open reading frame encoding a protein homologous to fatty acid thioesterases. *J. Bacteriol.* **171**, 5422-9.
- Kushner, S. R. (1978).** Improved method for transformation of *E. coli* with colE1 derived plasmids. In *Genetic Engineering*. Edited by H. B. Boyer. Amsterdam: Elsevier.
- Kyte, J. & Doolittle, F. R. (1982).** A simple method for displaying the hydropathy character of a protein. *J. Mol. Biol.* **157**, 105-132.
- Landick, R., Turnbough, JR, C. L. & Yanofsky (1996).** Transcription Attenuation. In *Escherichia coli and Salmonella Cellular and Molecular Biology*, pp. 1263-1286. Edited by F. C. Neidhardt. Washington: ASM Press.
- Leclerc, M. C. & Boemare, N. E. (1991).** Plasmids and phase variation in *Xenorhabdus* spp. *Appl. Environ. Microbiol.* **57**, 2597-601.
- Lee, Y. J., Bowman, A., Chuaxin, S., Anderson, M., Mutt, H., Jörnvall, V., Mutt, V. & Boman, H. G. (1989).** Antibacterial peptides from pig intestine: isolation of a mammalian cecropin. *Proc. Nat. Acad. Sci. USA.* **86**, 9159-9162.
- Leisman, G. B., Waukau, J. & Forst, S. A. (1995).** Characterization and environmental regulation of outer membrane proteins in *Xenorhabdus nematophilus*. *Appl. Environ. Microbiol.* **61**, 200-4.
- Li, J., Chen, G., Wu, H. & Webster, J. M. (1995).** Identification of two pigments and a hydroxystilbene antibiotic from *Photobacterium luminescens*. *Appl. Environ. Microbiol.* **61**, 4329-33.
- Lindum, P. W., Anthoni, U., Christophersen, C., Eberl, L., Molin, S. & Givskov, M. (1998).** N-Acyl-L-Homoserine Lactone Autoinducers Control Production of an Extracellular Lipopeptide Biosurfactant Required for Swarming Motility of *Serratia liquefaciens* MG1. *J. Bacteriol.* **180**, 6384-6388.
- Lipmann, F. (1980).** Bacterial production of antibiotic polypeptides by thiol-linked synthesis on protein templates. *Adv. Microbial Physiol.* **21**, 227-266.
- Liu, J., Berry, R., Poinar, G. & Moldenke, A. (1997).** Phylogeny of *Photobacterium* and *Xenorhabdus* species and strains as determined by comparison of partial 16S rRNA gene sequences. *Int. J. Syst. Bacteriol.* **47**, 948-51.
- Lugtenberg, B., Meijers, J., Peters, R., van der Hoek, P. & van Alphen, L. (1975).** Electrophoretic resolution of the major outer membrane protein of *Escherichia coli* K-12 into four bands. *FEBS Lett.* **58**, 254-258.
- Luo, N. & Cella, R. (1994).** A reliable amplification technique with single-sided specificity for the isolation of 5' gene regulating regions. *Gene.* **140**, 59-62.

- Manning, P. A., Heuzenroeder, M. W., Yeadon, J., Leavesley, D. I., Reeves, P. R. & Rowley, D. (1986).** Molecular cloning and expression in *Escherichia coli* K-12 of the O antigens of the Inaba and Ogawa serotypes of the *Vibrio cholera* O1 lipopolysaccharides and their potential for vaccine development. *Infect. Immun.* **53**, 272-277.
- Marahiel, M. A. (1992).** Multidomains involved in peptide synthesis. *FEBS Lett.* **307**, 40-43.
- Marahiel, M. A. (1997).** Protein templates for the biosynthesis of peptide antibiotics. *Chem. Biol.* **4**, 561-567.
- Marahiel, M. A., Nakano, M. M. & Zuber, P. (1993).** Microreview - Regulation of peptide antibiotic production in *Bacillus*. *Mol. Microbiol.* **7**, 631-636.
- Marahiel, M. A., Stachelhaus, T. & Mootz, H. D. (1997).** Modular peptide synthetases involved in nonribosomal peptide synthesis. *Chem. Rev.* **97**, 2651-2673.
- Matha, V. & Mracek, Z. (1984).** Changes in haemocyte counts in *Galleria mellonella* (L.) (Lepidoptera: Galleriidae) larvae infected with *Steinernema* sp. (Nematoda: Steinernematidae). *Nematologica* **30**, 86.
- Maxwell, P. W., Dunphy, G. B. & Niven, D. F. (1995).** Effects of Bacterial Age and Method of Culture On the Interaction of *Xenorhabdus nematophilus* (Enterobacteriaceae) With Hemocytes of Nonimmune *Galleria mellonella* (Insecta) Larvae. *J. Gen. Appl. Microbiol.* **41**, 207-220.
- McClelland, M. & Wilson, R. K. (1998).** Comparison of sample sequences of the *Salmonella typhi* genome to the sequence of the complete *Escherichia coli* K-12 genome. *Infect. Immun.* **66**, 4305-4312.
- McInerney, B. V., Gregson, R. P., Lacey, M. J., Akhurst, R. J., Lyons, G. R., Rhodes, S. H., Smith, D. R., Engelhardt, L. M. & White, A. H. (1991).** Biologically active metabolites from *Xenorhabdus* spp., Part 1. Dithiolopyrrolone derivatives with antibiotic activity. *J Nat Prod* **54**, 774-84.
- McInerney, B. V., Taylor, W. C., Lacey, M. J., Akhurst, R. J. & Gregson, R. P. (1991a).** Biologically active metabolites from *Xenorhabdus* spp., Part 2. Benzopyran-1-one derivatives with gastroprotective activity. *J Nat Prod* **54**, 785-95.
- Meighen, E. A. & Szittner, R. B. (1992).** Multiple repetitive elements and organization of the *lux* operons of luminescent terrestrial bacteria. *J. Bacteriol.* **174**, 5371-81.
- Miller, J. (1972).** *Experiments in Molecular Genetics*: Cold Spring Harbor, NY. USA.
- Miller, V. L. & Mekalanos, J. J. (1998).** A novel suicide vector and its use in construction of insertion mutants: osmoregulation of outer membrane proteins and virulence determinants in *Vibrio cholerae* requires *toxR*. *J. Bacteriol.* **170**, 2575-2583.
- Mootz, H. D. & Marahiel, M. (1997).** Modular Peptide Synthetases Involved in Nonribosomal Peptide Synthesis. *Chem. Rev.* **97**, 2651-2674.
- Mootz, H. D. & Marahiel, M. A. (1997a).** Biosynthetic systems for nonribosomal peptide antibiotic assembly. *Curr. Opin. Chem. Biol.* **1**, 543-551.

- Mootz, H. D. & Marahiel, M. A. (1997b).** The tyrocidine biosynthesis operon of *Bacillus brevis*: complete nucleotide sequence and biochemical characterization of functional internal adenylation domains. *J. Bacteriol.* **179**, 6843-50.
- Mootz, H. D., Schwarzer, D. & Marahiel, M. A. (2000).** Construction of hybrid peptide synthetases by module and domain fusions. *Proc. Nat. Acad. Sci. USA.* **97**, 5848-5853.
- Morgan, J.A., Sergeant, M., Ellis, D., Ousley, M. & Jarrett, P. (2001).** Sequence analysis of insecticidal genes from *Xenorhabdus nematophilus* PMFI296. *Appl Environ Microbiol.* **67**(5), 2062-9.
- Moureaux, N., Karjalainen, T., Givaudan, A., Bourlioux, P. & Boemare, N. (1995).** Biochemical Characterization and Agglutinating Properties of *Xenorhabdus nematophilus* F1 Fimbriae. *Appl. Environ. Microbiol.* **61**, 2707-2712.
- Müller, R. V. & Kokjohn, T. A. (1990).** General microbiology of *recA*: environmental and evolutionary significance. *Ann. Rev. Microbiol.* **44**, 365-391.
- Muller-Hill, B., Crapo, L. & Gilbert, W. (1968).** Mutants that make more *lac* repressor. *Proc. Nat. Acad. Sci. USA.* **59**, 1259-1264.
- Nappi, A. J. & Christensen, B. M. S. O. (1986).** Hemocyte cell surface changes in *Aedes aegypti* in response to microfilariae of *Dirofilaria immitis*. *J. Parasitol.* **72**, 875-879.
- Nealson, K. H. & Hastings, J. W. (1979).** Bacterial bioluminescence: its control and ecological significance. *Microbiol. Rev.* **43**, 496.
- Nealson, K. H., Schmidt, T. M. & Bleakley, B. (1990).** Physiology and biochemistry of *Xenorhabdus*. In *Entomopathogenic nematodes in biological control*, pp. 271-284. Edited by R. Gaugler & H. Kaya. Boca Raton, Florida: CRC Press Inc.
- Neidhardt, F. C. (1996).** *E. coli and Salmonella: Cellular and Molecular Biology*, Second edn. Washington D.C: ASM Press.
- Nishimura, Y., Hagiwara, A., Suzuki, T. & Yamanaka, S. (1994).** *Xenorhabdus japonicus* Sp Nov Associated With the Nematode *Steinernema kushidai*. *World Journal of Microbiology & Biotechnology.* **10**, 207-210.
- Ogawa, T., Wabiko, H., Tsurimoto, T., Horii, T., Masukata, H. & Ogawa, H. (1978).** Characteristics of purified *recA* protein and the regulation of its synthesis *in vivo*. *Cold Spring Harbor Symposium on Quantitative Biology.* **43**, 909-915.
- Paul, V. J., Frautschy, S., Fenical, W. & Nealson, K. H. (1981).** Antibiotics in microbial ecology: isolation and structure assignment of several new antibacterial compounds from the insect-symbiotic bacteria *Xenorhabdus* spp. *J. Chem. Ecol.* **7**, 588-597.
- Payne, S. M. & Finkelstein, R. A. (1977).** Detection and differentiation of iron-responsive mutants on Congo red agar. *Infect. Immun.* **18**, 94-98.
- Phizicky, E. M. & Roberts, J. W. (1981).** Induction of SOS functions: regulation of proteolytic activity of *E. coli* RecA protein by interaction with DNA and nucleoside triphosphate. *Cell.* **25**, 259-67.

- Pinyon, R. A., Hing Hew, F. & Thomas, C. J. (2000).** *Xenorhabdus bovienii* T228 phase variation and virulence are independent of RecA function. *Microbiol.* **146**, 2815-2824.
- Pinyon, R. A., Linedale, E. C., Webster, M. A. & Thomas, C. J. (1996).** Tn5-Induced *Xenorhabdus bovienii* Lecithinase Mutants Demonstrate Reduced Virulence For *Galleria mellonella* Larvae. *J. Appl. Bacteriol.* **80**, 411-417.
- Poinar, G. (1990).** Biology and taxonomy of Steinernematidae and Heterorhabditidae. In *Entomopathogenic nematodes in biological control*, pp. 23-62. Edited by R. R. Gaugler & H. K. Kaya. Boca Raton, Florida: CRC Press Inc.
- Poinar, G. O., Jr. (1979).** *Nematodes for Biological Control of Insects*: CRC Press, Boca Raton, Florida.
- Poinar, G. O., Jr. (1985).** *Neoaplectana intermedia* n. sp. (Steinernematidae: Nematoda) from South Carolina. *Rev. Nematol.* **8**, 321.
- Poinar, G. O., Jr., Jackson, T. & Klein, M. (1987).** *Heterorhabditis megidis* sp. n. (Heterorhabditidae: Rhaditida), parasitic in the Japanese beetle, *Popillia japonica* (Scarabaeidae: Coleoptera), in Ohio. *Proc. Helminthol. Soc. Wash.* **54**, 53.
- Poinar, G. O., Jr., Mracek, Z. & Doucet, M. M. A. (1988).** A re-examination of *Neoaplectana rara* Doucet, 1986 (Steinernematidae: Rhabditida). *Rev. Nematol.* **11**, 447.
- Poinar, G. O. & Thomas, G. M. (1966).** Significance of *Achromobacter nematophilus* Poinar and Thomas (Achromobacteraceae: Eubacteriales) in the development of the nematode, DD136 (*Neoaplectana* sp. : Steinernematidae). *Parasitol.* **56**, 385-390.
- Poinar, G. O. & Thomas, G. M. (1967).** The nature of *Achromobacter nematophilus* as an insect pathogen. *J. Invert. Pathol.* **9**, 510-514.
- Praszkier, J., Bird, P., Nikoletti, S. & Pittard, J. (1989).** Role of Countertranscript RNA in the Copy Number Control System of an IncB Miniplasmid. *J. Bacteriol.* **171**, 5056-5064.
- Pye, F. C. (1974).** Microbial activation of prophenol oxidase from immune insect larvae. *Nature.* **251**, 610-613.
- Quadri, L. E., Weinreb, P. H., Lei, M., Nakano, M. M., Zuber, P. & Walsh, C. T. (1998).** Characterization of Sfp, a *Bacillus subtilis* phosphopantetheinyl transferase for peptidyl carrier protein domains in peptide synthetases. *Biochemistry.* **37**, 1585-1595.
- Quadri, L. E. N., Sello, J., Keating, T. A., Weinreb, P. H. & Walsh, C. T. (1988).** Identification of a *Mycobacterium tuberculosis* gene cluster encoding the biosynthesis enzymes for assembly of the virulence-conferring siderophore mycobactin. *Chem. Biol.* **5**, 631-645.
- Quigley, N. B. & Gross, D. C. (1994).** Syringomycin production among strains of *Pseudomonas syringae* pv. *syringae*: conservation of the *syrB* and *syrD* genes and activation of phytotoxin production by plant signal molecules. *Mol. Plant Microbe Interact.* **7**, 78-90.
- Quigley, N. B., Mo, Y. Y. & Gross, D. C. (1993).** SyrD is required for syringomycin production by *Pseudomonas syringae* pathovar *syringae* and is related to a family of ATP-binding secretion proteins. *Mol Microbiol.* **9**, 787-801.

- Radding, C. M. (1982).** Homologous pairing and strand exchange in genetic recombination. *Ann. Rev. Genetics* **16**, 405-437.
- Rainey, F. A., Ehlers, R. U. & Stackebrandt, E. (1995).** Inability of the polyphasic approach to systematics to determine the relatedness of the genera *Xenorhabdus* and *Photorhabdus*. *Int. J. Syst. Bacteriol.* **45**, 379-81.
- Ramia, S., Neter, E. & Brenner, D. J. (1982).** Production of enterobacterial common antigen as an aid to classification of newly identified species of the families Enterobacteriaceae and *Vibrionaceae*. *Int. J. Syst. Bacteriol.* **32**, 395-398.
- Ratcliffe, N. A. S. O. (1985).** Invertebrate Immunity- a primer for the non-specialist. *Immunol. Lett.* **10**, 253-270.
- Ratcliffe, R. A. & Gagen, S. J. (1977).** Studies on the *in vivo* cellular reactions of insects: An ultrastructural analysis of nodule formation in *Galleria mellonella*. *Tissue and Cell.* **9**, 73-85.
- Reed, K. (1990).** Basic blotting - a quick fix. *Today's Life Science* **2**, 52-60.
- Reed, L. J. & Muench, H. (1938).** A simple method of estimating fifty percentage endpoints. *Am. J. Hygiene* **27**, 493-497.
- Reeves, P. (1993).** Evolution of *Salmonella* O antigen variation by interspecific gene transfer on a large scale. *Trends in Genetics* **9**, 17-22.
- Revilla, G., Ramos, F. R., Lopez-Nieto, M. J., Alvarez, E. & Martin, J. F. (1986).** Glucose Represses Formation of D-(L- α -Amino adipyl)-L-Cysteinyl-D-Valine and Isopenicillin N synthetase but Not Penicillin Acyltransferase in *Penicillium chrysogenum*. *J. Bacteriol.* **168**, 947-952.
- Richardson, W. H., Schmidt, T. M. & Nealson, K. H. (1988).** Identification of an anthraquinone pigment and a hydroxystilbene antibiotic from *Xenorhabdus luminescens*. *Appl. Environ. Microbiol.* **54**, 1602-5.
- Rood, J. I. & Gawthorne, J. M. S. O. (1984).** Apple software for analysis of the size of restriction fragments. *Nucleic Acids Res.* **12**, 689-694.
- Rowley, A. F. & Ratcliffe, N. A. (1981).** Insects. In *Invertebrate Blood Cells*, pp. 421-488. Edited by N. A. Ratcliffe & A. F. Rowley. London: Academic Press.
- Rowley, A. F. & Ratcliffe, R. A. (1976).** The granular cells of *Galleria mellonella* during clotting and phagocytic reaction *in vitro*. *Tissue and Cell.* **8**, 437-446.
- Sambrook, J., Fritsch, E. F. & Maniatis, T. (1989).** *Molecular cloning: A laboratory manual*: Cold Spring Harbor Laboratory Press, Cold Spring Harbor, New York.
- Schell, M. A. (1993).** Molecular biology of the LysR family of transcriptional regulators. *Ann. Rev. Microbiol.* **47**, 597-626.
- Schmidt, A. R. & Ratcliffe, N. A. (1977).** The encapsulation of foreign tissue implants in *Galleria mellonella* larvae. *J. Insect. Physiol.* **23**, 175-184.

- Schmidt, T. M., Bleakley, B. & Neilson, K. H. (1988). Characterization of an extracellular protease from the insect pathogen *Xenorhabdus luminescens*. *Appl. Environ. Microbiol.* **54**, 2793-2797.
- Schneider, E. & Sabine, H. (1998). ATP-binding-cassette (ABC) transport systems: Functional and structural aspects of the ATP-hydrolyzing subunits/domains. *FEMS Microbiol. Rev.* **22**, 1-20.
- Simon, R., Priefer, U. & Puhler, A. (1983). A broad host range mobilization system for *in vivo* genetic engineering: transposon mutagenesis in gram negative bacteria. *Biotechnology.* **1**, 784-791.
- Smart Jr, G. C. (1995). Entomopathogenic Nematodes for the Biological Control of Insects. *J. Nematol.* **27**, 529-534.
- Smigielski, A. J. & Akhurst, R. J. (1994). Megaplasmiids in *Xenorhabdus* and *Photorhabdus* spp, Bacterial Symbionts of Entomopathogenic Nematodes (Families Steinernematidae and Heterorhabditidae). *J. Invert. Pathol.* **64**, 214-220.
- Smigielski, A. J., Akhurst, R. J. & Boemare, N. E. (1994). Phase Variation in *Xenorhabdus nematophilus* and *Photorhabdus luminescens* - Differences in Respiratory Activity and Membrane Energization. *Appl. Environ. Microbiol.* **60**, 120-125.
- Soderhall, K. & Smith, V. J. (1986). The Prophenoloxidase Activating System: The Biochemistry of its Activation and Role in Arthropod Cellular Immunity, with Special Reference to Crustaceans. In *Immunity in Invertebrates: Cells, Molecules and Defence Reactions*, pp. 208-223. Edited by M. Brehelin. New York: Springer-Verlag.
- Southern, E. M. (1975). Detection of specific sequence among DNA fragments separated by gel electrophoresis. *J. Mol. Biol.* **98**, 503-517.
- Stachelhaus, T. & Marahiel, M. A. (1995). Modular structure of genes encoding multifunctional peptide synthetases required for non-ribosomal peptide synthesis. *FEMS Microbiol. Lett.* **125**, 3-14.
- Stachelhaus, T., Mootz, H. D., Bergendahl, V. & Marahiel, M. A. (1998). Peptide-bond formation in non-ribosomal peptide biosynthesis: catalytic role of the condensation domain. *J. Biol. Chem.* **273**.
- Stachelhaus, T., Mootz, H. D. & Marahiel, M. A. (1999). The specificity-conferring code of adenylation domains in nonribosomal peptide synthetases. *Chem. Biol.* **6**, 493-505.
- Stackebrandt, E. & Goebel, B. M. (1994). Taxonomic note: a place for DNA-DNA reassociation and 16S rRNA sequence analysis in the present species definition in bacteriology. *Int. J. Syst. Bacteriol.* **44**, 846-849.
- Stein, T. & Morris, H. R. (1996). The multiple carrier model of nonribosomal peptide biosynthesis at modular multienzymatic templates. *J. Biol. Chem.* **271**, 15428-15435.
- Stintzi, A., Johnson, Z., Stonehouse, M., Ochsner, U., Meyer, J. M., Vasil, M. L. & Poole, K. (1999). The *pvc* gene cluster of *Pseudomonas aeruginosa*: role in synthesis of the pyoverdine chromophore and regulation by PtxR and PvdS. *J. Bacteriol.* **181**, 4118-4124.

- Stroehner, U. H., Lech, A. J. & Manning, P. A. (1994).** Gene Sequence of *recA* and Construction of RecA Mutants of *Vibrio Cholerae*. *Mol. Gen. Genetics*. **244**, 295-302.
- Subbaraju, G. V., Golakoti, T., Patterson, G. M. & Moore, R. E. (1997).** Three new cryptophycins from *Nostoc* sp. GSV 224. *J. Nat. Prod.* **60**, 302-305.
- Sundar, L. & Chang, F. N. (1992).** The role of guanosine-3',5'-bis-pyrophosphate in mediating antimicrobial activity of the antibiotic 3,5-dihydroxy-4-ethyl-trans-stilbene. *Antimicrob. Agents Chemother.* **36**, 2645-51.
- Sundar, L. & Chang, F. N. (1993).** Antimicrobial activity and biosynthesis of indole antibiotics produced by *Xenorhabdus nematophilus*. *J. Gen. Microbiol.* **139**, 3139-48.
- Suzuki, T., Yamanaka, S. & Nishimura, Y. (1990).** Chemotaxonomic study of *Xenorhabdus* species - cellular fatty acids, ubiquinone and DNA-DNA hybridization. *J. Gen. Appl. Microbiol.* **36**, 393-401.
- Symmank, H., Saenger, W. & Bernhardt, F. (1999).** Analysis of Engineered Multifunctional Peptide Synthetases: enzymatic characterisation of surfactin synthetase domains in hybrid bimodular systems. *J. Biol. Chem.* **274**, 21581-21588.
- Szittner, R. & Meighen, E. (1990).** Nucleotide sequence, expression, and properties of luciferase coded by lux genes from a terrestrial bacterium. *J. Biol. Chem.* **265**, 16581-7.
- Taylor, R. L. (1969).** A suggested role for the polyphenol-phenoloxidase system in invertebrate immunity. *J. Invert. Pathol.* **14**, 427-428.
- Thaler, J. O., Baghdiguian, S. & Boemare, N. (1995).** Purification and characterization of xenorhabdinin, a phage tail-like bacteriocin, from the lysogenic strain F1 of *Xenorhabdus nematophilus*. *Appl. Environ. Microbiol.* **61**, 2049-52.
- Thaler, J. O., Boyergiglio, M. H. & Boemare, N. E. (1997).** New Antimicrobial Barriers Produced By *Xenorhabdus* spp. and *Photorhabdus* spp. to Secure the Monoxenic Development of Entomopathogenic Nematodes. *Symbiosis*. **22**, 205-215.
- Thaler, J. O., Duvic, B., Givaudan, A. & Boemare, N. (1998).** Isolation and entomotoxic properties of the *Xenorhabdus nematophilus* F1 lecithinase. *Appl. Environ. Microbiol.* **64**, 2367-73.
- Thomas, G. M. & Poinar, G. M. (1979).** *Xenorhabdus* gen. nov., a genus of entomopathogenic bacteria of the family Enterobacteriaceae. *Int. J. System. Bacteriol.* **29**, 352-360.
- Thompson, J. D., Higgins, D. G. & Gibson, T. J. (1994).** CLUSTAL W: improving the sensitivity of progressive multiple sequence alignment through sequence weighting position gap penalties and weight matrix choice. *Nucleic Acids Res.* **22**, 4673-4680.
- Tillett, D., Dittmann, E., Erhard, M., von-Doehren, H., Boerner, T. & Neilan, B. A. (2000).** Structural organization of microcystin biosynthesis in *Microcystis aeruginosa* PCC7806: An integrated peptide-polyketide synthetase system. *Chem. Biol.* **7**, 753-764.
- Tognoni, A., Franchi, E., Magistrelli, C., Colombo, E., Cosmina, P. & Grandi, G. (1995).** A putative new peptide synthetase operon in *Bacillus subtilis*: partial characterisation. *Microbiol.* **141**, 645-648.

- Towbin, H., Staehlin, T. & Gordon, J. (1979).** Electrophoretic transfer of proteins from polyacrylamide gels to nitrocellulose sheets: procedure and some applications. *Proc. Nat. Acad. Sci. USA.* **90**, 5267-5271.
- Tsuda, M., Miyazaki, H. & Nakazawa, T. (1995).** Genetic and physical mapping of genes involved in pyoverdinin production in *Pseudomonas aeruginosa* PAO. *J. Bacteriol.* **177**, 423-431.
- Unestam, T. & Soderhall, K. S. O. (1977).** Soluble fragments from fungal cell walls elicit defence reactions in crayfish. *Nature.* **267**, 45-46.
- Volgyi, A., Fodor, A., Szentirmai, A. & Forst, S. (1998).** Phase Variation in *Xenorhabdus nematophilus*. *Appl. Environ. Microbiol.* **64**, 1188-1193.
- Volgyi, A., Fodor, A. & Forst, S. (2000).** Inactivation of a novel gene produces a phenotypic variant cell and affects the symbiotic behavior of *Xenorhabdus nematophilus*. *Appl Environ Microbiol.* **66**(4), 1622-8.
- von Döhren, H., Keller, U., Vater, J. & Zocher, R. (1997).** Multifunctional peptide synthetases. *Chem. Rev.* **97**, 2675-2705.
- Wang, H. & Dowds, B. C. (1991).** Molecular cloning and characterization of the *lux* genes from the secondary form of *Xenorhabdus luminescens* K122. *Biochem. Soc. Trans.* **20**, 68S.
- Wang, H. & Dowds, B. C. (1993).** Phase variation in *Xenorhabdus luminescens*: cloning and sequencing of the lipase gene and analysis of its expression in primary and secondary phases of the bacterium. *J. Bacteriol.* **175**, 1665-73.
- Wang, R. F. & Kushner, S. R. (1991).** Construction of versatile low-copy-number vectors for cloning, sequencing and gene expression in *Escherichia coli*. *Gene.* **100**, 195-199.
- Waterworth, P. M. (1969).** The action of light on culture media. *J. Clin. Pathol.* **22**, 273-277.
- Webb, R. B. & Lorenz, J. (1972).** Toxicity of irradiated medium for repair-deficient strains of *Escherichia coli*. *J. Bacteriol.* **112**, 649-652.
- Weber, G., Schorgendorfer, K., Schneider-Scherzer, E. & Leitner, E. (1994).** The peptide synthetase catalyzing cyclosporin production in *Tolypocladium niveum* is encoded by a giant 45.8-kilobase open reading frame. *Curr. Genetics.* **26**, 120-125.
- Weinreb, P. H., Quadri, L. E., Walsh, C. T. & Zuber, P. (1998).** Stoichiometry and specificity of in vitro phosphopantetheinylation and aminoacylation of the valine-activating module of surfactin synthetase. *Biochemistry* **37**, 1575-1584.
- Weinstock, G. M., McEntee, K. & Lehman, I. R. (1979).** ATP-dependent renaturation of DNA catalyzed by the *recA* protein of *Escherichia coli*. *Proc. Nat. Acad. Sci. U S A* **76**, 126-30.
- Wenming, Z., Arceneaux, J. E. L., Beggs, M. L., Byers, B. R., Eisenach, K. D. & Lundrigan, M. D. (1998).** Exochelin genes in *Mycobacterium smegmatis*: identification of an ABC transporter and two non-ribosomal peptide synthetase genes. *Mol. Microbiol.* **29**, 629-639.
- Wilkinson, T. L. & Hay, D. B. (1997).** Symbiotic Interactions in the Entomopathogenic Nematodes. *Symbiosis.* **22**, 9-19.

- Xi, L., Cho, K. W. & Tu, S. C. (1991).** Cloning and nucleotide sequences of *lux* genes and characterization of luciferase of *Xenorhabdus luminescens* from a human wound. *J. Bacteriol.* **173**, 1399-405.
- Xu, J. & Hurlbert, R. E. (1990).** Toxicity of irradiated media for *Xenorhabdus* spp. *Appl. Environ. Microbiol.* **56**, 815-818.
- Xu, J., Lohrke, S., Hurlbert, I. M. & Hurlbert, R. E. (1989).** Transformation of *Xenorhabdus nematophilus*. *Appl. Environ. Microbiol.* **55**, 806-12.
- Xu, J., Olson, M. E., Kahn, M. L. & Hurlbert, R. E. (1991).** Characterisation of Tn5-induced mutants of *Xenorhabdus nematophilus* ATCC 19061. *Appl. Environ. Microbiol.* **57**, 1173-1180.
- Yarranton, G. T. & Sedgwick, S. G. (1982).** Cloned truncated *recA* genes in *E. coli* II. Effects of truncated gene products on in vivo *recA*+ protein activity. *Mol. Gen. Genet.* **185**, 99-104.
- Yu, S., Fiss, E. & Jacobs, W. R. J. (1998).** Analysis of the exochelin locus in *Mycobacterium smegmatis*: biosynthesis genes have homology with genes of the peptide synthetase family. *J. Bacteriol.* **180**, 4676-4685.
- Zagaglia, C., Casalino, M., Colonna, B., Conti, C., Calconi, A. & Nicoletti, M. (1991).** Virulence plasmids of enteroinvasive *Escherichia coli* and *Shigella flexneri* integrate into a specific site on the host chromosome: integration greatly reduces expression of plasmid-carried virulence genes. *Infect. Immun.* **59**, 792-9.
- Zhang, J., Wolfe, S. & Demain, A. L. (1989).** Ammonium ions repress d-(L- α -aminoadipyl)-L-cysteinyl-D-valine synthetase in *Streptomyces clavuligerus* NRRL 3585. *Can. J. Microbiol.* **35**, 399-402.
- Zioni, L., Glazer, I. & Segal, D. (1992).** Life cycle and reproductive potential of the nematode *Heterorhabditis bacteriophora* strain HP88. *J. Nematol.* **24**, 352-358.
- Zuber, P., Nakano, M. M. & Marahiel, M. A. (1993).** Peptide antibiotics. In *Bacillus subtilis and other Gram-positive bacteria*, pp. 897-916. Edited by A. L. Sonenshein, J. A. Hoch & R. Lobsick. Washington, D.C.: American Society for Microbiology.